

WOODHEAD PUBLISHING SERIES IN CIVIL AND STRUCTURAL ENGINEERING



# ADVANCE UPCYCLING OF BY-PRODUCTS IN BINDER AND BINDER-BASED MATERIALS



Edited by  
**MEHMET SERKAN KIRGIZ**

# **Advance Upcycling of By-products in Binder and Binder-based Materials**

This page intentionally left blank

Woodhead Publishing Series in Civil and  
Structural Engineering

# Advance Upcycling of By-products in Binder and Binder-based Materials

*Edited by*

***Mehmet Serkan Kirgiz***

**Northwestern University, Chicago, IL,  
United States**



ELSEVIER

**WP**

WOODHEAD  
PUBLISHING

An imprint of Elsevier

Woodhead Publishing is an imprint of Elsevier  
50 Hampshire Street, 5th Floor, Cambridge, MA 02139, United States  
The Boulevard, Langford Lane, Kidlington, OX5 1GB, United Kingdom

Copyright © 2024 Elsevier Ltd. All rights reserved.

No part of this publication may be reproduced or transmitted in any form or by any means, electronic or mechanical, including photocopying, recording, or any information storage and retrieval system, without permission in writing from the publisher. Details on how to seek permission, further information about the Publisher's permissions policies and our arrangements with organizations such as the Copyright Clearance Center and the Copyright Licensing Agency, can be found at our website: [www.elsevier.com/permissions](http://www.elsevier.com/permissions).

This book and the individual contributions contained in it are protected under copyright by the Publisher (other than as may be noted herein).

### Notices

Knowledge and best practice in this field are constantly changing. As new research and experience broaden our understanding, changes in research methods, professional practices, or medical treatment may become necessary.

Practitioners and researchers must always rely on their own experience and knowledge in evaluating and using any information, methods, compounds, or experiments described herein. In using such information or methods they should be mindful of their own safety and the safety of others, including parties for whom they have a professional responsibility.

To the fullest extent of the law, neither the Publisher nor the authors, contributors, or editors, assume any liability for any injury and/or damage to persons or property as a matter of products liability, negligence or otherwise, or from any use or operation of any methods, products, instructions, or ideas contained in the material herein.

ISBN: 978-0-323-90791-0 (print)

ISBN: 978-0-323-99804-8 (online)

For information on all Woodhead Publishing publications  
visit our website at <https://www.elsevier.com/books-and-journals>

*Publisher:* Matthew Deans  
*Acquisitions Editor:* Gwen Jones  
*Editorial Project Manager:* Toni Louise Jackson  
*Production Project Manager:* Prem Kumar Kaliamoorthi  
*Cover Designer:* Mark Rogers

Typeset by MPS Limited, Chennai, India



# Contents

<b>List of contributors</b>	<b>xv</b>
<b>Preface</b>	<b>xix</b>
<b>Introduction</b>	<b>xxi</b>
<b>1. Wheat straw ash as hydraulic binder substitution in binder-based materials made of an admixture superplasticizer</b>	<b>1</b>
<i>Mehmet Serkan Kirgiz and Hasan Biricik</i>	
1.1 Introduction	1
1.2 Materials and methods	3
1.2.1 Materials—mixing, handling, placing, and forming	3
1.3 Methods used for measuring the physical and mechanical properties of mortar	5
1.4 Physical tests	5
1.4.1 Measurement of air pore	5
1.4.2 Measurement of unit weight	6
1.4.3 Measurement of water absorption in volume	6
1.4.4 Measurement of capillary water absorption	7
1.4.5 Measurement of change of mass	7
1.5 Mechanical tests	8
1.5.1 Flexural strength	8
1.5.2 Compressive strength	9
1.6 Results and discussion and mathematical models for strength estimation	9
1.6.1 Air pore of fresh mortar	9
1.6.2 Unit weight of fresh mortar	11
1.6.3 Water absorption	12
1.6.4 Capillary water absorption	13
1.6.5 Change of mass	14
1.6.6 Flexural strength	16
1.6.7 Compressive strength	17
1.7 Conclusions	19
Acknowledgement	19
Conflict of interest	19
References	20

<b>2. Class C fuel ash as hydraulic binder substitution in binder-based materials fortified with the high-technology additive of graphite nanoparticles</b>	<b>25</b>
<i>Mehmet Serkan Kirgiz</i>	
2.1 Introduction and background of pulverized fuel ash-cement system	25
2.2 Environmental assessment of usage of the pulverized fuel ash in the cement-based materials	27
2.3 Synthetic graphite nanoparticles	28
2.4 Class C pulverized fuel ash	31
2.5 Upcycling process and tests performed	32
2.6 Nature of strength	33
2.6.1 Strength in flexure	33
2.6.2 Strength in splitting tension	35
2.6.3 Strength in compression force	37
2.7 Conclusions	41
Acknowledgments	41
Data availability	41
Funding	41
References	41
<b>3. Class F fuel ash as hydraulic binder substitution in binder-based material fortified with high-technology additive of graphite nanoparticle and admixture of superplasticizer</b>	<b>47</b>
<i>Mehmet Serkan Kirgiz</i>	
3.1 Introduction	47
3.2 Materials and methods	48
3.2.1 Materials	48
3.3 Cement binder and its types	49
3.4 Class F pulverized fuel ash	50
3.5 High-technology additive of graphite nanoparticles	52
3.6 Admixture of a superplasticizer	52
3.6.1 Mixing, handling, placing, and forming processes for upcycling of class F pulverized fuel ash	53
3.6.2 Test program	53
3.7 Properties related to strength	55
3.7.1 Splitting tensile strength	55
3.7.2 Flexural strength	56
3.7.3 Compressive strength	57
3.7.4 Strength gain index at an early age	58
3.7.5 Strength variation in binders used commonly	59
3.8 Conclusion	61
References	62

---

<b>4. Oil shale ash as hydraulic binder substitution in binder-based material with additive of superplasticizer and roller compaction method</b>	<b>67</b>
<i>Ahmed M. Ashteyat, Amani Smadi, Yousef S. Al Rjoub and Mehmet Serkan Kirgiz</i>	
4.1 Introduction	67
4.2 Materials and methods	70
4.2.1 Mix design of the roller-compacted concrete and the roller-compacted green concrete	70
4.2.2 Preparation of the roller-compacted concrete and the roller-compacted green concrete	71
4.2.3 Analysis methods	71
4.3 Results and discussions	73
4.3.1 Chemical and physical properties of mixing materials	73
4.3.2 Physical properties of the roller-compacted concrete and roller-compacted green concrete	76
4.3.3 Durability properties of the roller-compacted concrete and roller-compacted green concrete	79
4.3.4 Mechanical properties of the roller-compacted concrete and the roller-compacted green concrete	82
4.3.5 Microstructure analysis of the roller-compacted concrete and roller-compacted green concrete	93
4.4 Conclusion	96
Availability of data and materials	97
Funding	97
References	97
<b>5. Natural pozzolan as hydraulic binder substitution in combination with recycled aggregates in concrete</b>	<b>101</b>
<i>S. Kenai, M. Ghrici and J. Khatib</i>	
5.1 Introduction	101
5.2 Rheological properties	101
5.3 Mechanical properties	103
5.3.1 Compressive and flexural strength	103
5.3.2 Flexural strength	104
5.3.3 Elastic modulus	105
5.3.4 Shrinkage	105
5.4 Durability	106
5.4.1 Permeability	106
5.4.2 Carbonation	107
5.4.3 Resistance to chloride attack	110
5.4.4 Resistance to sulfate attack	112
5.4.5 Alkali–silica reaction	114
5.5 Microstructure	116
5.6 Environmental and economical aspects	117



5.7	Conclusion	117
	References	118
<b>6.</b>	<b>New hydraulic binder and binder based material with burning pulverised coal ash, household waste, Mediterranean soil, and calcined clay waste</b>	<b>123</b>
	<i>Mehmet Serkan Kurguz and Muhammad Syarif</i>	
6.1	Introduction	123
6.2	Research methodology	128
6.2.1	Tools and materials used	128
6.2.2	Research procedures	129
6.3	Results and discussion	133
6.3.1	Chemical composition of the wastes	133
6.3.2	Chemical composition of new cement	135
6.3.3	X-ray powder diffraction analysis of new cement	136
6.3.4	Physical properties	136
6.4	Conclusions	139
	References	140
<b>7.</b>	<b>Alkali-activated hydraulic binder geopolymer with ground granulated blast furnace slag</b>	<b>143</b>
	<i>Mehmet Serkan Kurguz and Hasan Biricik</i>	
7.1	Introduction	143
7.2	Materials and methods	144
7.2.1	Materials	144
7.2.2	Mixing, handling, placing, and molding of high-performance geopolymers	145
7.2.3	Methods	145
7.3	Results and discussion	146
7.3.1	Capillary water absorption	146
7.3.2	Coefficient of capillarity	147
7.3.3	Flexural capacity	148
7.3.4	Uniaxial compression strength	148
7.4	Conclusions	149
	References	150
<b>8.</b>	<b>Natural rubber latex-substituted-bitumen binder and bitumen binder-based materials used in highway</b>	<b>153</b>
	<i>Theresah Osei, Trinity Ama Tagbor, Johannes A.M. Awudza and Mehmet Serkan Kurguz</i>	
8.1	Introduction	153
8.1.1	Objective	154
8.2	Materials and method	155
8.2.1	Bitumen-based binder	155
8.3	Results and discussion	159
8.3.1	Penetration point	159

---

8.3.2	Softening point temperature (°C)	160
8.3.3	Viscosity analysis	161
8.3.4	Specific gravity test	162
8.3.5	Temperature susceptibility and penetration index	162
8.3.6	Flash point, aging, and viscosity of selected blends	163
8.3.7	Fourier-transform infrared analysis	164
8.4	Conclusions	164
	References	165
<b>9.</b>	<b>Marble powder as hydraulic binder substitution</b>	<b>167</b>
	<i>S. Kenai, B. Benabed and H. Soualhi</i>	
9.1	Introduction	167
9.2	Advantages of marble powder	167
9.3	Applications of marble powder	168
9.4	Properties of marble powder	168
9.4.1	Particle size	168
9.4.2	Physical properties	169
9.4.3	Chemical properties	170
9.5	Effect of marble powder on fresh properties of cement/mortar/concrete	171
9.5.1	Workability	171
9.5.2	Setting time	172
9.5.3	Rheological behavior	173
9.5.4	Hydration heat	174
9.6	Effect of marble powder on the hardened properties	175
9.6.1	Strength activity index of mixtures incorporating marble powder	175
9.6.2	Thermal analysis of mixtures incorporating marble powder	175
9.6.3	Compressive strength	176
9.6.4	Flexural tensile strength	176
9.6.5	Splitting tensile strength	176
9.6.6	Modulus of elasticity	177
9.7	Microstructure	178
9.8	Durability properties of concrete made with marble powder	181
9.8.1	Permeability	181
9.8.2	Water absorption	182
9.8.3	Porosity	183
9.8.4	Shrinkage	184
9.8.5	Sulfate resistance	185
9.8.6	Acid resistance	186
9.8.7	Alkali–silica reaction	186
9.8.8	Carbonation	187
9.8.9	Chloride permeability	188
9.8.10	Corrosion	189
9.8.11	Fire resistance (high temperature resistance)	190

9.8.12	Resistance to freeze and thaw cycling	191
9.8.13	Abrasion resistance	191
9.9	Economic aspect	192
9.10	Environmental performance	193
9.11	Conclusion	194
	References	194
<b>10.</b>	<b>Gray cement, white cement, gypsum, and lime modified with graphite nanoparticles</b>	<b>203</b>
	<i>Mehmet Serkan Kirgiz</i>	
10.1	Introduction	203
10.2	Materials and methods	204
10.2.1	Transforming of conventional binder into binder and mortar including graphite nanoparticles	204
10.3	Casting, mixing, and specimen preparation	205
10.4	Characterization	206
10.5	Results and discussion	206
10.5.1	Compressive strength	206
10.6	Mathematical model for estimation of compressive strength	208
10.7	Bending moment	209
10.8	Mathematical model for prediction of bending moment	212
10.9	Splitting tensile strength	214
10.10	Mathematical model for estimation of splitting tensile strength	216
10.11	Conclusion	217
	References	217
<b>11.</b>	<b>Calcined clay as hydraulic binder substitution</b>	<b>221</b>
	<i>S. Kenai, J. Khatib and M. Ghrici</i>	
11.1	Introduction	221
11.2	Materials	222
11.3	Fresh concrete properties	224
11.3.1	Consistency	224
11.3.2	Setting time	225
11.3.3	Workability	226
11.4	Mechanical properties	227
11.4.1	Effect of type and content of clay minerals	227
11.4.2	Compressive strength	227
11.4.3	Splitting tensile and flexural strengths	230
11.4.4	Elastic and dynamic moduli	231
11.5	Shrinkage	231
11.6	Durability properties	232
11.6.1	General	232
11.6.2	Absorption, porosity, and pore structure	232
11.6.3	Permeability, chloride ingress, and carbonation	234
11.6.4	Sulfate resistance	235

11.6.5	Abrasion and skid resistance	236
11.6.6	Fire resistance	236
11.7	Economic and environmental aspects	236
11.8	Conclusions	237
	References	237
<b>12.</b>	<b>Properties of concrete containing coal bottom ash as hydraulic binder substitution</b>	<b>243</b>
	<i>Khairunisa Muthusamy, Wang Hui Wong, Nabilla Mohamad, Jose Rajan, Ahmed Mokhtar Albshir Budiea, Anwar P.P. Abdul Majeed and Mehmet Serkan Kirgiz</i>	
12.1	Introduction	243
12.2	Methodology	244
12.2.1	Preparation of raw materials	244
12.2.2	Preparation of concrete and testing	246
12.3	Result and discussion	246
12.3.1	Workability	246
12.3.2	Compressive strength	247
12.3.3	Splitting tensile strength	248
12.4	Conclusion	248
	References	249
<b>13.</b>	<b>Upcycling of recycled asphalt pavement aggregate and recycled concrete aggregate and silica fume in roller-compacted concrete</b>	<b>251</b>
	<i>Ahmed M. Ashteyat, Ala' Taleb Obaidat, Baenah Al Tawalbeh and Mehmet Serkan Kirgiz</i>	
13.1	Introduction	251
13.2	Experimental work	255
13.2.1	Materials	255
13.2.2	Testing procedure	259
13.3	Results and discussion	262
13.3.1	Compressive strength	262
13.3.2	Splitting tensile strength	264
13.3.3	Flexural strength	266
13.3.4	Modulus of elasticity	268
13.3.5	Water absorption	270
13.3.6	Density	272
13.4	Conclusions	273
	References	273
<b>14.</b>	<b>Clay and natural latex as admixture in binary and ternary bitumen binder system for transportation and geotechnical applications</b>	<b>277</b>
	<i>Theresah Osei, Trinity Ama Tagbor, Johannes A.M. Awudza and Mehmet Serkan Kirgiz</i>	
14.1	Introduction	277

14.2	Materials and method	278
14.2.1	Bitumen	278
14.2.2	Natural rubber latex	278
14.2.3	Clay samples	278
14.2.4	Sample preparation	279
14.2.5	Absorption test	279
14.3	Particle size distribution	279
14.3.1	Compaction	279
14.3.2	Atterberg limit (plastic and liquid limit)	279
14.4	Hydrogen ion concentration (pH)	279
14.5	Preparation of blends	279
14.5.1	Laboratory analysis	280
14.5.2	Penetration point	280
14.5.3	Softening point temperature	280
14.5.4	Kinematic viscosity	280
14.5.5	Specific gravity	280
14.5.6	Short-term aging test	280
14.5.7	Flash point	280
14.6	Results	281
14.6.1	Atterberg limit and pH	281
14.6.2	Compaction, moisture content, and specific gravity	282
14.6.3	Particle size distribution	282
14.6.4	Penetration point	283
14.6.5	Softening point	284
14.7	Kinematic viscosity	284
14.8	Specific gravity	285
14.8.1	Aging and flash point	286
14.9	Conclusions	287
	References	287
<b>15.</b>	<b>A clean approach through recycling of brick kiln dust and crumb waste rubber tires in the manufacturing of clayey bricks and cementitious composites</b>	<b>291</b>
	<i>Abdul Qadir Bhatti and Anwar Khitab</i>	
15.1	Introduction	291
15.2	Concrete	292
15.2.1	Ingredients	292
15.2.2	Environmental hazards	293
15.2.3	Greenization	293
15.2.4	Replacement of natural aggregates	293
15.3	Waste rubber tires	295
15.3.1	Crumb rubber	295
15.4	Rubberized concrete	296
15.4.1	Untreated rubber particles as replacement of fine aggregates	296

---

15.4.2	Treated rubber particles as replacement of fine aggregates	298
15.4.3	Rubber powder as an admixture	298
15.5	Waste brick powder	299
15.5.1	Use in concrete	299
15.5.2	Use in clayey bricks	302
15.6	Conclusion	303
	References	303
<b>16.</b>	<b>Self-compacting concrete blended with fly ash and ground granulated blast furnace slag</b>	<b>309</b>
	<i>Naraindas Bheel, Paul Awoyera, Irfan Ali Shar and Mehmet Serkan Kirgiz</i>	
16.1	Introduction	309
16.2	Materials and methodology	311
16.2.1	Materials	311
16.3	Mix proportion	312
16.4	Testing methods	313
16.4.1	Fresh properties of self-compacting concrete mixture	313
16.4.2	Hardened properties of self-compacting concrete mixture	314
16.5	Results and discussion	314
16.5.1	Fresh concrete results	314
16.6	Hardened concrete results	319
16.6.1	Compressive strength of self-compacting concrete mixture	319
16.6.2	Splitting tensile strength of self-compacting concrete mixture	321
16.6.3	Flexural strength of self-compacting concrete mixture	324
16.6.4	Water penetration depth of self-compacting concrete mixture	325
16.7	Conclusion	327
	References	330
<b>17.</b>	<b>Use of alternative recycled fillers in bituminous mixtures: a review</b>	<b>335</b>
	<i>R. Joublat, H. Kassem, A. Elkordi and J. Khatib</i>	
17.1	Introduction	335
17.2	Management practices of municipal solid waste incineration ashes	337
17.3	Municipal solid waste incineration ashes as road construction material	339
17.3.1	Municipal solid waste incineration bottom ash	339
17.3.2	Application of bottom ash in bituminous mixtures	340
17.3.3	Municipal solid waste incineration fly ash	342
17.4	Environmental effect of municipal solid waste incineration ashes as a road construction material	345
17.4.1	Leaching characteristics of municipal solid waste incineration ashes	345

17.4.2	Municipal solid waste incineration ash leaching reduction and treatments	347
17.5	Conclusions and recommendations	348
	References	348
<b>18.</b>	<b>Ecology-based green clay–hemp brick material made with ground granulated blast-furnace slag</b>	<b>357</b>
	<i>Jonathan Oti, John Kinuthia and Mehmet Serkan Kirgiz</i>	
18.1	Introduction	357
18.2	Methodology	358
	18.2.1 Materials	358
	18.2.2 Mix composition, sample preparation, and testing	360
18.3	Result and discussion	364
	18.3.1 Strength development of the lime–GGBS and PC–GGBS stabilized systems	364
	18.3.2 Linear expansion	365
	18.3.3 Laboratory stabilized clay–hemp brick manufacture	368
	18.3.4 Cost analysis hemp–clay brick	369
18.4	Conclusions	370
	References	371
<b>19.</b>	<b>Innovative and sustainable concrete materials</b>	<b>373</b>
	<i>Antonella D’Alessandro and Filippo Ubertini</i>	
19.1	Introduction	373
19.2	State-of-art concrete materials	374
19.3	New binders	376
	19.3.1 Mixing ground granulated blast furnace slag (GGBFS) and geopolymers	377
	19.3.2 Earth-concretes	377
	19.3.3 Fine recycled fillers: fly ash and silica fume	379
	19.3.4 New efficient cements	380
19.4	Recycled components	380
	19.4.1 Recycled aggregates	380
	19.4.2 Recycled tires	383
	19.4.3 Recycled glass	384
	19.4.4 Recycled plastic	385
	19.4.5 Organic waste	387
19.5	Multifunctional properties	388
19.6	New additives	389
19.7	Novel sustainable processes	389
19.8	Conclusion	390
	Funding	390
	References	391
	<b>Index</b>	<b>397</b>

# List of contributors

**Yousef S. Al Rjoub** Department of Civil Engineering, Jordan University of Science and Technology, Amman, Jordan

**Ahmed M. Ashteyat** Department of Civil Engineering, University of Jordan, Amman, Jordan

**Paul Awoyera** Department of Civil Engineering, Covenant University, Ota, Nigeria

**Johannes A.M. Awudza** Department of Chemistry, Kwame Nkrumah University of Science and Technology, Kumasi, Ghana

**B. Benabed** Civil Engineering Department, University of Laghouat, Laghouat, Algeria

**Abdul Qadir Bhatti** Department of Civil Engineering, Faculty of Engineering, Islamic University of Madinah, Madinah, Saudi Arabia

**Naraindas Bheel** Department of Civil and Environmental Engineering, Universiti Teknologi Petronas, Bandar Seri Iskandar, Tronoh, Perak, Malaysia

**Hasan Biricik** Department of Civil Engineering, Construction Materials Laboratory, Yıldız Teknik University, Bakırköy, İstanbul, Turkey

**Ahmed Mokhtar Albshir Budiea** Faculty of Industrial Management, University Malaysia Pahang, Pahang, Malaysia

**Antonella D'Alessandro** Department of Civil and Environmental Engineering, University of Perugia, Perugia, PG, Italy

**A. Elkordi** Faculty of Engineering, Department of Civil and Environmental Engineering, Beirut Arab University, Beirut, Lebanon; Faculty of Engineering, Department of Civil Engineering, Alexandria University, Alexandria, Egypt

**M. Ghrici** Civil Engineering Department, University of Chlef, Algeria



**R. Joumblat** Faculty of Engineering, Department of Civil and Environmental Engineering, Beirut Arab University, Beirut, Lebanon

**H. Kassem** Faculty of Engineering, Department of Civil and Environmental Engineering, Beirut Arab University, Beirut, Lebanon

**S. Kenai** Civil Engineering Department, University Blida 1, Blida, Algeria

**J. Khatib** Faculty of Engineering, Department of Civil and Environmental Engineering, Beirut Arab University, Beirut, Lebanon; Faculty of Science and Engineering, University of Wolverhampton, Wolverhampton, United Kingdom

**Anwar Khitab** Civil Engineering, Mirpur University of Science and Technology, Mirpur, AJ&K, Pakistan

**John Kinuthia** School of Engineering, Faculty of Computing, Engineering and Science, University of South Wales, Pontypridd, United Kingdom

**Mehmet Serkan Kirgiz** Northwestern University, Chicago, IL, United States

**Nabilla Mohamad** Faculty of Civil Engineering Technology, University Malaysia Pahang, Pahang, Malaysia

**Khairunisa Muthusamy** Faculty of Civil Engineering Technology, University Malaysia Pahang, Pahang, Malaysia

**Ala' Taleb Obaidat** Civil Engineering Department, Philadelphia University, Amman, Jordan

**Theresah Osei** Council for Scientific and Industrial Research, Building and Road Research Institute, Kumasi, Ghana

**Jonathan Oti** School of Engineering, Faculty of Computing, Engineering and Science, University of South Wales, Pontypridd, United Kingdom

**Anwar P.P. Abdul Majeed** Faculty of Manufacturing and Mechatronics Engineering Technology, University Malaysia Pahang, Pahang, Malaysia

**Jose Rajan** Faculty of Industrial Science and Technology, University Malaysia Pahang, Pahang, Malaysia

**Irfan Ali Shar** Department of Civil Engineering, ISRA University Hyderabad, Sindh, Pakistan

---

**Amani Smadi** Department of Civil Engineering, Jordan University of Science and Technology, Amman, Jordan

**H. Soualhi** Civil Engineering Department, University of Laghouat, Laghouat, Algeria

**Muhammad Syarif** Department of Architecture, Faculty of Engineering, University of Muhammadiyah Makassar, Makassar, Indonesia

**Trinity Ama Tagbor** Council for Scientific and Industrial Research, Institute of Industrial Research, Accra, Ghana

**Baenah Al Tawalbeh** Department of Civil Engineering, University of Jordan, Amman, Jordan

**Filippo Ubertini** Department of Civil and Environmental Engineering, University of Perugia, Perugia, PG, Italy

**Wang Hui Wong** Faculty of Civil Engineering Technology, University Malaysia Pahang, Pahang, Malaysia

This page intentionally left blank

# Preface

Construction materials—concrete, geopolymer material, cement, and mortar—are the most manufactured structural materials. Sometimes, they substitute one another, and sometimes, they contest with one another so that similar structure types and functions could be built by any of the materials. However, scientists often focus more on advanced upcycling processes, in which by-products are made in various industrial manufacturing.

Today's building construction is totally different because the point the construction technology has reached involves the constructions printed with three-dimension printers using either cement paste or cement mortar, water and sand and binder. It is clearly true that manufacturers give guarantee regarding binder quality in a manner similar to that of other construction materials—tiles, brick, steel, wood, and so on. Nevertheless, the topic of advanced upcycling of byproducts in binder and binder-based materials is not limited to cement since there appear a number of novel binders everyday, such as geopolymer binder systems. The disparity in the methods of upcycling making is, therefore, unique, and the significance of the control of the quality of materials work on the site is apparent. Furthermore, since the trade of a materialist has not yet become the education and the convention of a number of other building trades, a scientist supervision is essential on the site. These facts must be considered in mind by the researcher and scientist as careful and intricate design could be easily vitiated if the properties of the actual materials differ from those assumed in the design calculation.

From the above points mentioned, it must not be inferred that making good upcycling of by-products is difficult. Good upcycling is often related to a substance of suitable constituents, mixing, hardening into a formwork, and homogeneous mass. Unfortunately the constituents of a bad upcycling process are also related to the same functions. Therefore the difference is obtained in terms of know-how and cost of labor.

What, then, is the advanced upcycling of by-products? There are two overall criteria: The method has to be satisfactory in its hardened state as well as its fresh state while being moved from the mixer and put in the formwork. The rules in the fresh state of upcycled materials are that there should be consistency in the mix and that it should be compacted by the means desired without excessive effort and also that the mix should be cohesive enough for the method of putting used not to make segregation with a consequent lack of homogeneity of the finished material.

Because the book will be used in so many countries, I thought it is best to use SI units of measurement. All the data, figures, and tables are therefore conveniently presented for readers, progressive or traditionalist, in all countries.

In a book of this size, it is not possible to cover the whole field of upcycling of by-products. The editor and author choose what they take into account as the most important or most interesting or simply what they know most about, but the emphasis is on an integrated view of the properties of materials containing by-products and on the underlying scientific reasons.

**Mehmet Serkan Kirgiz**

# Introduction

Upcycling can be described as transforming a by-product into a useful material which will be used in mainstream. In other words, it is also known as creative reuse, which is the process of transforming byproducts, remnants, and wastes into novel materials or products with a greater quality.

For constructional purposes, the meaning of the term upcycling is restricted to the bonding materials used with stone, steel, sand, brick, building blocks, and so on. The principal content of the book includes binders, byproducts, testing, and conclusions at the same time. Upcycling is used in many applications – art, music, industry, clothes, foods, design processes, and so on. The built environment is an indicator for overcoming climate change and transforming CO<sub>2</sub> emission in manufacturing to a net-zero emission in near future. The promotion of management of upcycling for sustainable purposes should use the pressure in demand for the adoption of proper methods to make cement more durable. Since construction by nature is not an ecofriendly activity and even if construction provides life for human generation, construction generates demolition waste whenever any development environment activity takes place, for example, building roads, bridges, fly-over, subway, and remodeling. It includes mostly inert and nonbiodegradable materials such as concrete, plaster, metal, wood, plastics, and so on. Apart from industrial byproducts, some of this waste comes to the municipal stream. These wastes are heavy, having a grand unit volume weight, are often massive, and have considerable storage space either on the road/agricultural land or in common waste. Considering all information mentioned above, this book presents efficient upcycling examples for wheat straw ash; fuel ash, both class C and class F; oil shale ash; household waste; calcined clay; ground granulated blast furnace slag; natural rubber latex; recycled asphalt pavement aggregate; recycled concrete aggregate; silica fume; limestone; brick kiln dust; and crumb waste rubber tire in either cement-based systems or bitumen-based systems.

**Mehmet Serkan Kirgiz**

*Northwestern University, Chicago, IL, United States*

This page intentionally left blank

# Wheat straw ash as hydraulic binder substitution in binder-based materials made of an admixture superplasticizer

1

Mehmet Serkan Kırgız<sup>1</sup> and Hasan Biricik<sup>2</sup>

<sup>1</sup>Northwestern University, Chicago, IL, United States, <sup>2</sup>Department of Civil Engineering, Construction Materials Laboratory, Yıldız Teknik University, Bakırköy, İstanbul, Turkey

## 1.1 Introduction

According to a global agricultural supplying and demand estimating report published by United States Department of Agriculture in January 2021 the consumption of wheat reached 759.5 million tons (mt) because of the making of food and feedstock from it and its use in nonfood applications, including biodegradable binders (Perdue, 2021). Considering the wheat plant, there is lignin, a class of organic polymers, and holocellulose carbohydrate-based biopolymer fiber in the renewable wheat straw (Biricik et al., 1999, 2000). Since this renewable resource emerges in the wheat plant every year, people take advantages such as cheapness, abundance, and biodegradability of the wheat straw into account. Therefore wheat straw is known as an alternative material required, and the practice of it is seen in various industries where it has been commonly used in energy manufacturing as biomass (Gadde et al., 2009; Yadvinder & Bijay, 2008), in cattle farming as feed (Kadam et al., 2000), and in cement-based materials (CBMs) as an additive for durability demand (Ataie et al., 2015; Biricik et al., 1999, 2000; Juenger & Siddique, 2015; Martirena & Monzó, 2018; Nehdi et al., 2003). In addition to the use of the wheat straw mentioned above, wheat straw-based ash has been evaluated in portland cement (PC) and the CBMs as artificial pozzolana, either a supplementary material for CBM or a substitution material for cement since the last two decades because of its reactive silica component, over 83.5% (Biricik et al., 1999, 2000). Al-Akhras and Abu-Alfoul carried out a study on the influence of wheat straw ash (WSA) on the mechanical properties of cement mortar autoclaved in 2002. In the study, WSA of 3.6%, 7.3%, and 10.9% was replaced with mortar sand. The autoclaved mortar including 10.9% WSA and 89.1% limestone sand increased in the bending moment; the strength of compression force and the strength of splitting tensile force changed by over 71%, 87%, and 67%, respectively, when compared to the mortar without the WSA (Al-Akhras & Abu-Alfoul, 2002). Similarly, Martirena and Monzó worked on the ash in 2018. They achieved to reach out important findings that explain the benefit of using vegetable ash as



supplementary cementitious material (SCM) in the CBMs. Their working unveiled that the vegetable ash showed a certain compatibility with CBM once the agricultural renewable resources were burned at temperatures of 600°C and 700°C (Martirena & Monzó, 2018). In 2015, Ataie et al. performed one of the last significant studies related to the effect of zinc oxide (ZnO) and sugar on cement hydration and showed how they interact with the WSA, rice husk ash, silica fume, metakaolin, and pulverized fuel ash in the CBMs. It concluded from the experimental results that the effect of ZnO was the retarder for the hydration process because it led to agglomeration of the C-S-H gel (Ataie et al., 2015). Juenger and Siddique performed the last important study on recent advances in understanding the role of SCMs in concrete in 2015. They revealed that this application of SCM was compatible with the industry, currently working on the sustainability of concrete in terms of cost-effectiveness, environmental friendliness, the long-term strength, and the long-term durability developed (Juenger & Siddique, 2015).

On the contrary to the studies of common cement and the WSA mentioned above, construction binder-based mortars, for example, lime mortar, cement mortar, and gypsum mortar, have been used without any innovation in the world since the invention of the cement. All mortars were prepared with nonrenewable materials, such as aggregate, cement, lime, and gypsum. Therefore there is a need to enable the sustainability of construction binders. Because of the highly reactive silica component in the WSA, like in other artificial pozzolanic materials, research studies regarding on WSA try to find a holistic answer for the need properly. However, today's constructions had the load carrying systems; for example, the masonry building and the reinforced concrete building contain the CBMs. Since various sections of a construction can be placed in the atmosphere, on the floor, or within water, the water repelling force affects these sections negatively. If the sections are not covered with a water/heat-repelling insulator, the gap between cement and aggregate gains importance in the CBM, which is used in water constructions, such as dam bodies, water reservoirs, water channels, and flumes, because of capillary water absorption (Auskern & Horn, 1973; Postacioğlu, 1969; Powers, 1956; Troxell et al., 1968; Uyan, 1975). Moreover the water absorption of cement matrix, which turns out to be the interfacial transition zone among aggregates in the CBM, is a certain agent in the durability of the CBM (Kırgız, 2019, 2020). The water absorption percent of cement matrix is a function of not only the gap but also the surface area of the hydrated binder products and free energy for capillarity (Powers, 1979). Additionally the bulk cement stack, whose Blaine area is greater than that of today's binder, can be in a need for much more quantity of water to develop the hydration products. Thereby the velocity of capillary water absorption could be slowed (Hogan & Meusel, 1981). Considering the mechanism regarding strength behavior in PC, which is made of artificial pozzolana, an important property, such as durability, is monitored in the cement matrix. As the ash particle of artificial pozzolana provides fast and easy nucleation of cement hydration products in the matrix, these products may intervene between the ashes. Because of the change in porosity and strength and pozzolanic reactions in the matrix, the strength increases and the porosity decreases (Montgomery et al., 1981). The PC-added artificial

pozzolana is being more durable in an aggressive environment. This is attributed to the portlandite ( $\text{Ca}(\text{OH})_2$ ) being decreased, low porosity of the products, various components of cement gel, and instability of the ettringite crystal formed in the pozzolanic cement (Massazza, 1989).

In the practical light of the scientific information mentioned, this chapter aims at evaluating such significant properties as the unit weight of fresh mortar containing WSA, water absorption, capillary water absorption, the change of mass, flexural strength, and the compressive strength of hardened mortar containing the WSA. It also presents forceful correlations and regression equations between the mixing features of mortar and the physical and mechanical properties of the mortar to estimate the properties through the mathematical models previously.

## 1.2 Materials and methods

### 1.2.1 Materials—mixing, handling, placing, and forming

In this study, mortar samples were produced according to the rules specified in the BS EN 197–1 (BS EN 197–1:2011, 2019) standard method. Standard RILEM sand, PC (CEM I 42.5N)—common construction binder and WSA—artificial pozzolanic substitution material, whose physical and chemical properties are presented in Table 1.1, and a plasticizer were used to mix the samples.

**Table 1.1** Physical and chemical properties of the Portland cement and the wheat straw ash.

Physical properties	Cement	Wheat straw ash
Specific weight ( $\text{g}/\text{cm}^3$ )	3.05	2.41
Initial set (min)	110	—
Final set (min)	215	—
Expansion (mm)	3	—
Specific surface (blaine) ( $\text{cm}^2/\text{g}$ )	3204	5520
200 ( $\mu\text{m}$ ) (900 meshes) sieve residue (%)	0.2	1.6
90 ( $\mu\text{m}$ ) (4700 meshes) sieve residue (%)	5.2	2.6
Chemical compounds (%)	Cement	Wheat straw ash
$\text{SiO}_2$ (dissolved)	20.6	54.24
$\text{SiO}_2$ (nondissolved)	0.38	29.56
$\text{Al}_2\text{O}_3$	6.1	4.55
$\text{Fe}_2\text{O}_3$	3.72	1.05
CaO	63.65	12.54
MgO	1.29	2.39
$\text{SO}_3$	2.55	1.49
Loss on ignition (LOI)	1.42	—
Insoluble residue	0.25	—
Free CaO	2.08	—

**Table 1.2** Physical and chemical properties of wheat straw ash initially.

Physical properties	Wheat straw ash	Chemical properties	Wheat straw ash
Humidity (%)	9.54	Extractive material (%)	4.23
Ash content (%)	8.6	Ash (%)	8.6
Specific weight (gr/cm <sup>3</sup> )	2.31	Lignin (%)	15.03
Density (gr/cm <sup>3</sup> )	0.07	Holocellulose in carbohydrate (%)	45.13

**Table 1.2** presents the initial physical and chemical properties of the WSA used.

The mixing, handling, placing, and forming of the sample depend on four stages. The first stage is the preparation of the WSA-substituted cement (WSA-SC). The cement series were prepared by replacing 8%, 16%, and 24% of WSA with weights of 8%, 16%, and 24% of common PC, respectively. To maintain the homogeneity and nonagglomeration of the WSA-SC series the following steps were carried out with an automatic mixer at 4 minutes: (1) the CEM I 42.5N type PC and the WSA are put into the bowl, (2) the mixture is blended for 90 (seconds) at a high speed, (3) it is blended again for 150 seconds at a low speed, and (4) the homogenized cement mixture is packed to prevent humidity. The second stage consists of the preparations of the WSA-SC mortar containing a plasticizer to measure fresh and hardened properties of it. The plasticizer, which is a blending aid material, provides self-consolidation for mortar; thus it saves time in the mixing of mortar. Additionally, it does not lead to segregation and to ensure equal workability with mortars with each other, including the WSA-SC and the PC. The mortar of 8% WSA-92%SC, 16% WSA-84%SC, and 24% WSA-76%SC was prepared with a distilled water:WSA-SC:sand:plasticizer ratio of 1:2.01:6.06:0.010. The mortar of 16% WSA-84%SC was prepared with a distilled water:WSA-SC:sand:plasticizer ratio of 1:2.04:6.12:0.018. The mortar of 24% WSA-76%SC was prepared with a distilled water:WSA-SC:sand:plasticizer ratio of 1:2.09:6.26:0.041. The control mortar of 100%PC was prepared with a distilled water:PC:sand ratio of 1:2:6. The mixing of the constituent ratio provides constant flow, 1.2 Y-R/100, for the mortar samples.

The third stage deals with placing the mortar samples into the mold, with a prismatic size of 40 × 40 × 160 (mm). The following steps were applied for mortar molding at 2 minutes: (1) The mold is placed on the jolting machine, (2) the mold is filled up to half with mortar, (3) the mold is jolted with BS EN 196-2 standard method, (4) the mold is filled wholly with mortar, (5) the mold is jolted through a similar method as step 3, and (6) the mold with the filled mortar sample is placed in a calcereous water curing cabinet, where both the heat and the humidity are controlled by a computer. The fourth stage is the forming of the mortar sample. The WSA-SC and PC mortar samples were placed within water at 20°C ± 2°C for 27 days by removing off the mold in 24 hours after preparing.

The test of the unit weight of fresh mortar was carried out after the mortar mixing. The tests of the water absorption by volume, the capillary water absorption, the flexural strength, and the compressive strength of hardened mortar were carried out at 0th day, 28th day, 56th day, 90th day, and 208th day. Once mortar was removed from the mold the change in unit mass was performed so as to reach out the time-dependent change in mass relatively. After that measurement of the change in mass initially the regular test of change in mass was conducted at 0th day, 28th day, 56th day, 90th day, and 208th day.

### **1.3 Methods used for measuring the physical and mechanical properties of mortar**

To evaluate the effect of WSA, which was obtained from burning of the wheat straw at 670°C and fast cooling, on the properties of mortar the unit weight, the water absorption, the capillary water absorption, the change of mass, the flexural strength, and the compressive strength were measured with international current standard methods. The chapter also presents a number of important correlations and regressions between the properties to estimate the time-dependent properties of mortar, such as the flexural strength and the compressive strength, from the mixing features of mortar and the fresh properties of mortar (Biricik et al., 1999).

### **1.4 Physical tests**

To better explain, physical tests were carried out in two different stages: the physical experiments for the fresh state of mortar and the physical experiments for the hardened state of mortar. In the first stage the unit weight was measured from the fresh state of mortar with and without the WSA. In the second stage the unit mass, water absorption in volume, capillary water absorption, and mass change tests were performed to determine the change in physical properties of hardened mortar with and without the WSA. Unless otherwise stated the physical tests were repeated five times in the book chapter, and the results are presented as either the average of arithmetic with standard deviation or relative data which were found through dividing one property to another.

#### **1.4.1 Measurement of air pore**

The air content of the fresh mortar sample was determined according to the specifications in the ASTM C185-20 and BS EN 413-2 (ASTM C185-20, 2020; BS EN413, 2016). The following steps were performed to measure the air pore: (1) The fresh sample of the mortar is put into 1 L capacity cylinder of the air meter (V)

in three thicknesses; (2) each thickness is compressed by tamping or by a vibrator; (3) the cover of the cylinder is clipped; (4) water is put into the upper section of the cylinder to allow air exit through the valve; (5) the valve is locked, and the inner pressure is increased with a bike pump; (6) the falling of water level in the cylinder is followed up; (7) before the bar level exceeds 2.5 the water level is written down; (8) the pressure is dropped to allow the rise of water level; (9) the distinction among two water levels ( $V_a$ ) as air pore (A) is written down (ASTM C185-20, 2020; BS EN413, 2016). In fresh mortar the air pore was calculated by using Eq. (1.1) below.

$$A = \frac{V_a}{V} \times 100 \quad (1.1)$$

### 1.4.2 Measurement of unit weight

Unit weight measurement of fresh mortar was carried out within 240 (seconds) as soon as cement, sand, and water were contacted with each other. The unit weight experiment is performed on the fresh stance of the mortar so that the load caused by the mortar in the construction could be taken into account. The following steps were performed to measure the unit weight: (1) A 10 L capacity steel bowl ( $v$ ) is weighed with a precision of 0.01 g; (2) the weight of the bowl is recorded as  $sd$ ; (3) the fresh sample of the mortar is filled into the bowl in three layers; (4) the steel bowl with the filled sample is weighed in the same scale; (5) the weight of the steel bowl with the filled sample is recorded as  $pd$ ; (6) the mass of the fresh sample in the bowl is calculated as  $pd-sd$ ; (7) the mass of the fresh sample is recorded as  $m_d$  (Kirgiz, 2016). The unit weight of the fresh mortar ( $\gamma_{UW}$ ) is provided by using Eq. (1.2) below.

$$\gamma_{UW} = \frac{m_d}{v} \quad (1.2)$$

### 1.4.3 Measurement of water absorption in volume

Water absorption is used to measure the quantity of water absorbed by the mortar under environments of water and vapor. For the water absorption test the sample is dried in an oven at  $50^\circ\text{C} \pm 5^\circ\text{C}$  until a constant mass is reached out. Then, it is placed in a desiccator to cool. Immediately upon cooling the sample is weighed and the constant mass is recorded as the dry weight of mortar ( $W_k$ ). The sample is, then, dipped within the distilled water, whose height exceeds the height of the sample above  $5 \pm 1$  cm, often  $23^\circ\text{C}$  for 24 hours or until equilibrium. The sample is removed, patted dry with a lint-free cloth, and weighed in air. The water-saturated weight of mortar is recorded as the weight in air of the water-saturated sample ( $W_{sh}$ ). To measure the weight in water of the water-saturated sample the

Archimedes weighing scale is used. The weight in water of the water-saturated sample is recorded as  $W_{ss}$ . The test of water absorption of mortar is repeated for different ages, including the 28th day, the 56th day, the 90th day, and the 208th day, like in the study. The equation of (5.3) was used to calculate the water absorption in volume ( $h_s$ ) in all groups in samples with dimensions of  $40 \times 40 \times 50$  mm.

$$h_s = \frac{W_{sh} - W_k}{W_{sh} - W_{ss}} \times 100 \quad (1.3)$$

#### 1.4.4 Measurement of capillary water absorption

The water transport in porous media is dealt with the hygrothermal property of the mortar. The capillary water absorption is a key factor for characterizing the capability of the water absorption of porous material, which is important to better explain the simulation of humidity transport. In the measurement of capillary water absorption a sample with dimensions of  $40 \times 40 \times 50$  mm was used on the 28th day, the 56th day, the 90th day, and the 208th day. The measurement includes the following processes: (1) The mortar is dried in an oven at  $50^\circ\text{C} \pm 5^\circ\text{C}$  until the constant weight is achieved; (2) the mortar is cooled in a desiccator up to room temperature; (3) the mortar is weighed in a scale with a precision of 0.01 g, and this weight is recorded as  $W_k$  of the dried sample; (4) the  $40 \times 40$  mm surface ( $F$ ,  $\text{cm}^2$ ) of the mortar is dipped within the distilled water; (5) the height of the distilled water is maintained constant at  $7 \pm 2$  mm from the bottom surface of the mortar; (6) the height of distilled water is measured with a vernier calliper from the bottom surface of the mortar; (7) the mortar mass subjected to the capillary water absorption is weighed; (8) the distilled water quantity of mortar absorbed is recorded as  $Q$  ( $\text{cm}^3$ ) at the 1st minute, 4th minute, 9th minute, 16th minute, 25th minute, 36th minute, 49th minute, and 64th minute ( $t$ ) after the beginning. The capillary water absorption coefficient ( $K$ ) is found from the equation of (4); the  $K$  was computed as the capillary coefficient ( $\text{cm}^2/\text{seconds}$ ).

$$K = \frac{Q^2}{F^2 \times t} \quad (1.4)$$

#### 1.4.5 Measurement of change of mass

The conservation of mass is commonly used in a number of broad fields, for example, chemistry, mechanics, and fluid dynamics. First, it was referred to as the chemical reactions, and later, it was rediscovered for the progress from alchemy to the contemporary natural science of chemistry. As a consequence of its importance the conservation of mass is modified to comply with the laws of quantum mechanics and special relativity under the principle of mass–energy equivalence, which explains that the conserved quantity is formed by energy and mass. Therefore the

measurement of the change of mass was performed on solid samples such as hardened mortar. Three prism samples,  $40 \times 40 \times 50$  mm, were used in the test of the change of mass ( $W$ ). Performing the test includes the following steps: (1) The sample is removed from water curing on the 28th day; (2) the sample is weighed in a 0.01 gram precision scale ( $W_{sh}$ ); (3) the samples are cured in water and weighed in the same way on the 56th day, 90th day, and 208th day ( $W_k$ ). The change of mass was calculated from Eq. (1.5) below. The relative change of mass was computed with proportioning the change of mass of the ash-substituted mortar to the 28th day change of mass of reference mortar.

$$W = \frac{W_{sh} - W_k}{W_k} \times 100 \quad (1.5)$$

## 1.5 Mechanical tests

As the hardened stance of mortar with and without the WSA was used in the section, the mechanical tests were performed at one stage. The one-stage tests include the measurement of the flexural moment and the compressive strength. To better explain the effect of the WSA on the properties of mortar the chapter presents the relative change in the properties of mortar. Unless otherwise stated the mechanical tests were repeated five times in the book chapter. The relative data which were found through dividing one property to another are presented in the results and discussion section.

### 1.5.1 Flexural strength

Flexural strength is commonly measured in two stances. A beam flexing that is on two structural supportings, where one of them is rigid and the other is bustling, is known as a simple bending stance, and the second bending stance, where a side of the beam is jointed and another side is free, is known as the cantilever flexing. For the simple flexing the upper surface of the beam is subjected to compression force and the bottom surface is subjected to tension force. An axis that is at a region of zero strength of the beam is known as neutral axis (NA). The chapter uses the simple flexing method to measure the flexural moment. The test was performed on the mortar  $40 \times 40$  (b)  $\times 160$  (L) mm on the 28th day, 56th day, 90th day, and 208th day. The test includes the following steps: (1) The mortar sample is placed within water curing until the test day; (2) the mortar sample is placed in the flexural set; (3) the flexing force ( $P_k$ ) is applied until the mortar sample was failed. Flexural strength ( $f_{ce}$ ) was calculated through using Eq. (1.6) below. The time-dependent change of relative flexural strength, which was found by proportioning the flexural

strength of the ash-substituted mortar to the 28th day flexural strength of reference mortar, is presented in the results and discussion section.

$$f_{ce} = 1.5 \times \frac{P_k \times L}{b^3} \quad (1.6)$$

### 1.5.2 Compressive strength

Compressive strength is an essential property in structural materials, for example, mortar, which comprises the interfacial transition zone in concrete, stone, and steel, since material design is normally evaluated in terms of the risk of compression failure. In addition the CBM is known as having strength for compression force. Therefore plenty of standard tests exist to measure the compressive strength of structural materials. As the standards the following steps were applied to measure the compressive strength of mortar, dimensions  $40 \times 40$  ( $b$ ) mm: (1) The mortar is placed within the water curing cabinet, which controls the heat of water and humidity, until the test day; (2) the mortar sample is placed in the compression load cell; (3) the compression force ( $P_k$ ) is applied until the mortar sample fails. The compressive strength ( $f_{cb}$ ) was calculated from Eq. (1.7). The time-dependent change of relative compressive strength, which was found by proportioning the compressive strength of the ash-substituted mortar to the 28th day compressive strength of reference mortar, is presented in the results and discussion section.

$$f_{cb} = \frac{P_k}{b^2} \quad (1.7)$$

## 1.6 Results and discussion and mathematical models for strength estimation

### 1.6.1 Air pore of fresh mortar

The air pore structure of a CBM is a fundamental property influencing the durability of the CBM. The air pore is influenced by the mixing constituent of the CBM, the water-to-cement ratio, the aeration, and the cracking (Kucharczyková et al., 2010). The detrimental effect regarded on the durability of the CBM is of high significance in the broad practice of pavement, dam, foundation, and bridge (Mindess et al., 2002). The durability of the CBM under various climate conditions is pretty dependent on its air pore structure. Additionally, its content, size, and distribution are significantly related to not only the durability but also the physical and the mechanical properties of the CBM (Moravcova et al., 2016). Fig. 1.1 also shows an important relationship between air pore and water-to-cement ratio of fresh mortar made of WSA-SC and common CEM I 42.5N cement, including a mathematical equation and its relationship degree as  $R^2$ , which equals to 1, meaning that it is the most important equation suggested for estimating the air pore of fresh mortar from the water-to-cement ratio.



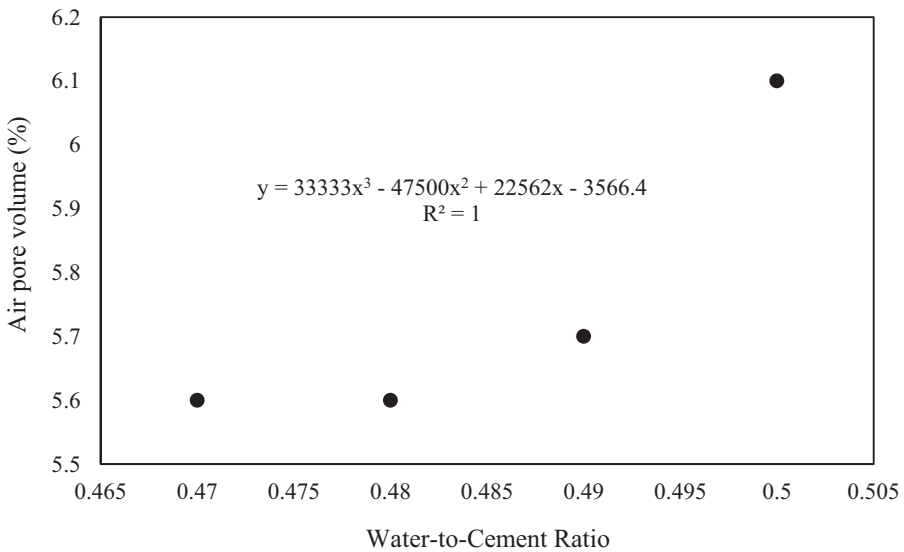


**Figure 1.1** An important relationship between air pore and water-to-cement ratio of fresh mortar made of WSA-substituted cement and common CEM I 42.5N cement and a mathematical equation and its relationship degree. Since the water-to-cement ratio increases, the air pore volume of fresh mortar increases.

As the water-to-cement ratio increased from 47% to 50% in the fresh mortar, the air pore property did rise proportionally with it. It was noticed that the average air pore of WSA-substituted mortar is different from the average air content of non-WSA-substituted mortar. In addition, as expected, the air pore of fresh mortar was found to be polynomially correlated to the water-to-cement ratio. As the water-to-cement ratio increased, the air pore of fresh mortar increased as well. This increase (6.3%) in water-to-cement ratio, from 47% to 50%, also led to an increase (8.9%) in air pore content. In comparison to the control mortar the WSA leads to a higher water-to-cement ratio and air content in the WSA-substituted mortar. Research results were in good agreement with the air pore content of fresh mortar presented. Results from the science literature state a similar conclusion for the air pore content of WSA-substituted mortar (Khushnood et al., 2014). During burning, internal moisture of the WSA was extracted, resulting in a larger surface area. Therefore the larger surface area required much more water demand in the WSA-substituted mortar. It is possible to clearly understand from the results of WSA-substituted mortar that since the WSA was burned at 670°C, the water demand increased tangibly. This could be referred to the fact that the water demand of the WSA-substituted mortar increased the air content of it. In Fig. 1.1 a polynomial equation is adopted to show the relationship between air pore and water-to-cement ratio of fresh mortar made of WSA-SC and common CEM I 42.5N cement. The relationship degree of  $R^2$  is also provided in Fig. 1.1 and shows a good compatibility between the two specified properties. As the relationship degree of  $R^2$  equals to 1, the air pore content could be estimated with the math equation in Fig. 1.1 by preparing at least one of the fresh mortar specimens.

### 1.6.2 Unit weight of fresh mortar

The unit weight of CBM is defined by three density classes: A lightweight one has an average density less than  $1680 \text{ kg/m}^3$ , a middle-weight one has an average density greater than  $1680 \text{ kg/m}^3$  and lower than  $2000 \text{ kg/m}^3$ , and a heavy weight one has an average density greater than  $2000 \text{ kg/m}^3$  (Samui et al., 2020). The mixing constituent of aggregate stack density can be found afterward even if it is not measured. However, the unit weight of fresh mortar, which is the bonding zone among aggregates within the CBM, is necessary to define in terms of the calculation of hydrostatic pressure in the framework (Rajapakse, 2017), the elastic modulus of CBM (McCarthy & Dyer, 2017), the entire mass of load-bearing elements in construction (Rajapakse, 2017), and so on. Evaluating the unit weight data measured a regression analysis was conducted on the relationship between the unit weight and water-to-cement ratio. Among the different types of regression equations conducted the polynomial equation type was found to be the most suitable. Since the coefficient was high, it could be ideal to use the water-to-cement ratio for estimating the unit weight of fresh mortar. Fig. 1.2 also shows an important relationship between unit weight and water-to-cement ratio in the fresh mortar made of WSA-SC and common CEM I 42.5N cement, a mathematical equation, and the relationship degree as  $R^2$ , which is equal to 1, standing for that there is an important indicator for a forceful relationship between the two properties.

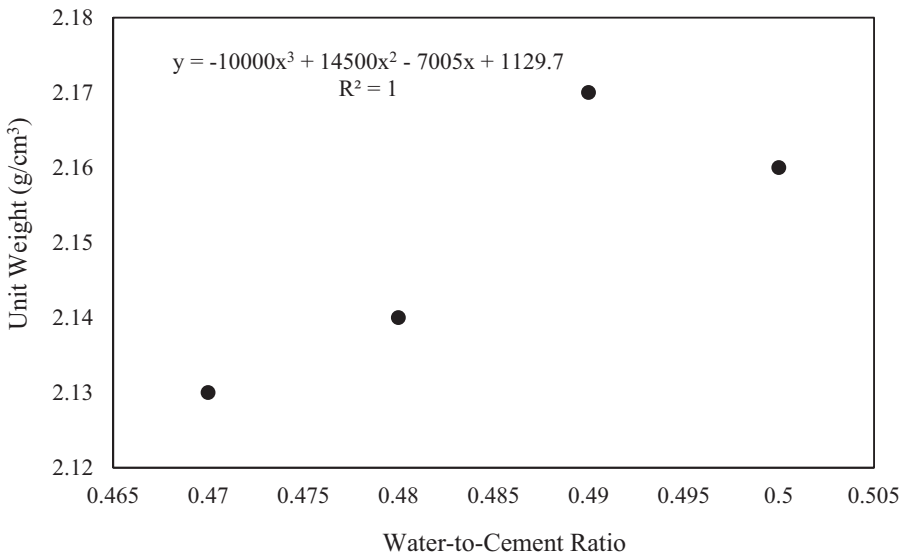


**Figure 1.2** An important relationship between unit weight and water-to-cement ratio for the fresh mortar made of WSA-substituted cement and common CEM I 42.5N cement, a mathematical equation, and relationship degree. Since the water-to-cement ratio increases in the CBM, the unit weight of fresh mortar increases.

Moreover the unit weight is another quality control parameter for the CBM, which may be important for construction projects, for example, constructing of tall buildings, reinforced-concrete walls of dams, and highway concreting (Tyagi et al., 2019). In most cases the unit weight of the CBM may increase depending upon the type of binder, aggregate gradation (Tasong et al., 1998), type of chemical admixture (Lea, 1970), and content and unit weight of substitution materials (Kirgiz, 2014; Kirgiz, 2015). However, this may be strictly true because cement absorbs from mixing water during the hydration reaction and many cementitious substitution materials undergo pozzolanic reaction with cement, which changes the mineralogical constitution of the CBM. A report was presented for the fact that the unit weight of the CBM increases with the content of cement and ageing (Uddin et al., 1997). However, until now, there is still no equation established for estimating the unit weight of the mortar. The chapter filled the gap in the science literature. Fig. 1.2 shows a good compatibility between the two specified properties. As the relationship degree of  $R^2$  is equal to 1, standing for the unit weight could be estimated with the equation. Comparison with regression equations for estimating unit weight indicates that the calculated unit weight agrees well with the range of unit weight measurements for the mortar.

### 1.6.3 Water absorption

In addition to durability-related properties, there are important properties such as permeability (Neithalath et al., 2010), compressive strength (Nguyen et al., 2017), and thermal conductivity (Chung et al., 2016), which are strongly affected by the water absorption ability of the CBM. Valid measurement of water absorption is therefore necessary for selecting the mixing materials properly and evaluating the performance and durability of mortar in different climate environments. As explained in the subtitle of air pore of fresh mortar, mixing materials are important to not to turn out porosity in mortar. In comparison to the control the WSA showed a decrease in water absorption. It is due to the fact that the reaction between the pozzolan and calcium hydroxide during hydration of cement paste is a lime-consuming process. Additionally, it would be shown later that this pozzolan is effective in reducing the porosity of the mortar, which, in turn, improves the durability of the CBM. Examining Fig. 1.3, in which the water-to-sand ratio-dependent change of relative water absorption in percent is given, it was understood that the water absorption of all groups displayed an increase depending on the increase in water-to-sand ratio. Fig. 1.3 also gives an equation to estimate water absorption in percentage from the water-to-sand ratio as well as regression degree  $R^2$ , which is equal to 1, meaning that there is an important indicator for a forceful relationship between the two properties.

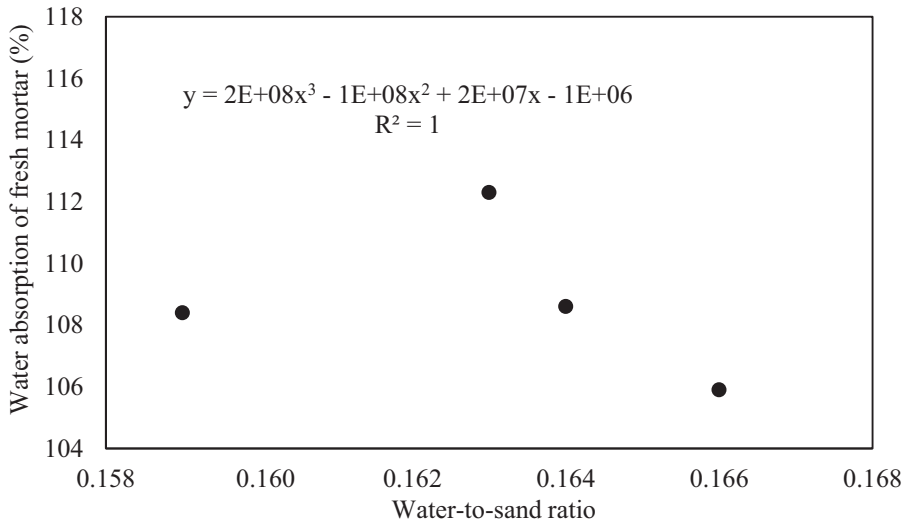


**Figure 1.3** A forceful relationship between relative water absorption and water-to-sand ratio of the fresh mortar made of WSA-substituted cement and common CEM I 42.5N cement, a mathematical equation, and a relationship degree. Since the water-to-sand ratio increases, the water absorption of fresh mortar increases.

### 1.6.4 Capillary water absorption

Water would be imbibed by even a dense mortar because of the capillary pores. Nevertheless, if the water-to-cement ratio can be lessened under about 0.45 for each cubic meter, the capillary pore system which has continuity between each other loses its effect and the pressure of water permeability is significantly retarded. The best process of reaching this retarded degree of water is to use an admixture of water reduction. The process can also enable a sufficient workability for full compaction of mortar and reduce shrinkage cracking in mortar (Dransfield, 2003). Fig. 1.4 also shows five important relationships between relative capillary water absorption and relative water absorption of mortar made of WSA-SC and common CEM I 42.5N cement, five mathematical equations, and five degrees of relationship as  $R^2$ , which is equal to 1, meaning that there is an important indicator for a forceful relationship between the two properties. Examining Fig. 1.4, it can be understood that capillary water absorption of mortar including 8% and 24% WSA is lower than that of the control mortar at the 28th day and 56th day, and capillary water absorption of mortar including 8% and 16% WSA is lower than that of the control mortar at the 90th day, 180th day, and 208th day.

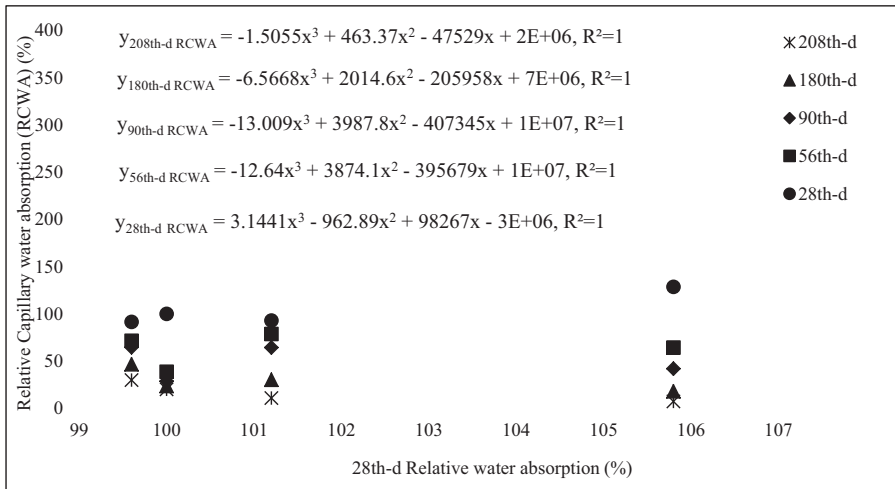


**Figure 1.4** Five important relationships between relative capillary water absorption and relative water absorption of mortar made of WSA-substituted cement and common CEM I 42.5N cement, five mathematical equations, and five degrees of relationship.

Additionally, it can be concluded that the WSA bars the continuity of capillary pores. It can also be understood from the findings that the active ash ratio for capillarity was 8% and 16% since the capillarity was decreased by the content. However, the chapter revealed that the total capillarity of the CBM is decreased as the substitution of WSA for cement is increased up to 24%, and the most probable pore diameter of the CBM is reduced, from which is a bigger pore through a smaller one. In Fig. 1.4, five polynomial equations are given to calculate the relationship between the relative capillary water absorption of the CBM and the 28th day relative water absorption of the CBM. The degrees of  $R^2$  are also provided in Fig. 1.4 and show a good compatibility between the two properties specified. As the figure exhibits equations for the CBM, the relative capillary water absorption up to 208 days could be estimated from 28th day water absorption testing.

### 1.6.5 Change of mass

The progress of change of mass depends on superplasticizer content used for the mixture of mortar. The change of mass of mortar without a superplasticizer is higher than that of mortar prepared with a superplasticizer. This progress could be related to the modification of water content closely in the mortar mixture. If a sufficient superplasticizer is added, the water content is reduced in the process of change of mass. Actually the water-to-cement ratio of the mortar without a superplasticizer is rather high. With a superplasticizer, any mixing component segregation was not observed in the fresh mixture of mortar, either during the mixing or

during the manufacturing of the mortar. Using the change of mass data measured a regression analysis was conducted on the relationship between the relative of changes of masses. Among the different types of regression equations evaluated the power and polynomial equation types were found to be the most suitable. Since the coefficients were high, they could be ideal to use the 28th day relative change of mass for estimating the relative change of mass on the 56th day, 90th day, 180th day, and 208th day. Fig. 1.5 presents four important relationships between the changes of masses of mortar made of WSA-SC and common CEM I 42.5N cement.

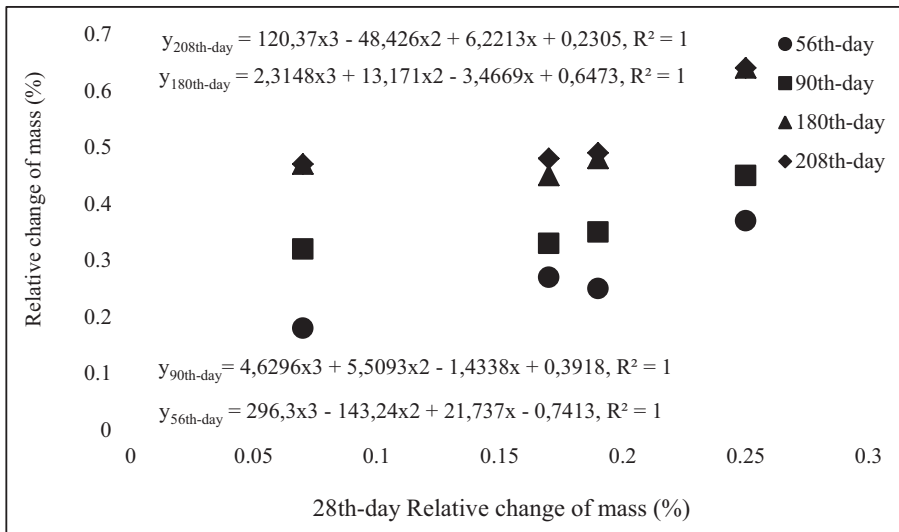


**Figure 1.5** Four important relationships between the changes of masses of mortar made of WSA-substituted cement and common CEM I 42.5N cement.

It also gives four mathematical equations and four degrees of relationship  $R^2$ , which is very close to 1, standing for that there is an important indicator for a forceful relationship between the two properties specified. Except the group made of 8% WSA substitution for cement, other two ash-substituted mortar groups' change of mass is much lower than that of nonash-added mortar. Increases in mass in all groups showed the tendency to be stable after the 90 days. Considering the initial quantity, it is seen that mass of change depends on ash ratio in mortar. The change toward the decline in mass increase is connected to new chemical formations during hydration process (Montgomery et al., 1981). The four polynomial equations are given to calculate the relative change of mass from the 28th day relative change of mass. The degrees of  $R^2$  are also provided in Fig. 1.5 for showing a good compatibility between the two properties specified. As the figure exhibits equations for the CBM, the relative change of mass could be estimated through mathematical equations in Fig. 1.5 by testing a fresh sample.

### 1.6.6 Flexural strength

A study on strength estimation equation found that the relationship between the compressive strength and flexural strength of roller compacted concrete (RCC) is similar to that of the conventional concrete. This result could be referred to the fact that the compaction and aggregate interlock can play an improving role in not only the compressive strength of the RCC but also its flexural strength. If the fact was not valid, researchers would have established a greater flexural strength for the same compressive strength and properties of the RCC than the conventional CBM (Chhorn et al., 2018). For conventional CBM the type of power equation is known to determine the flexural strength by measuring the compressive strength. Mohd et al. explain that their relationship is dependent on many factors, for example, strength level, aggregate gradation and mineralogy, types of admixture used, moisture content of sample, compaction and curing conditions, dimension of sample, and age of CBM (Mohd et al., 2014). Using the flexural strength data measured a regression analysis was conducted on the relationship between the flexural and compressive strengths. Among the different types of regression equations evaluated the polynomial equation type was found to be the most suitable. Since the coefficients were high, they could be ideal to use the compressive strength for estimating the flexural strength of the mortar. Fig. 1.6 shows five important relationships between the flexural strength and the 28th day compressive strength as well as their mathematical models and regression degrees.

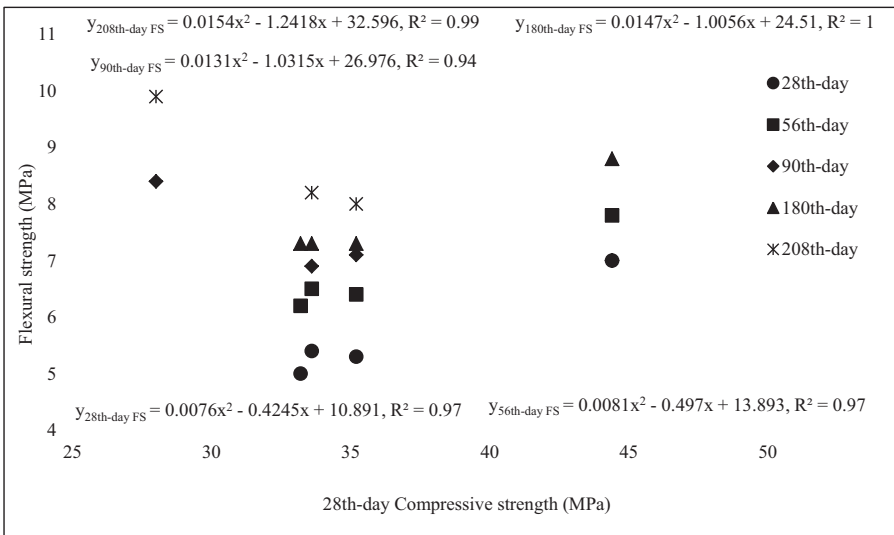


**Figure 1.6** Five important relationships between the flexural strength and the 28th day compressive strength as well as their mathematical models and regression degrees.

As will be seen in Fig. 1.6, five polynomial equations show the relationship between the flexural strength and the compressive strength. The forceful  $R^2$  degrees, which show a good compatibility between the two properties specified, are also provided in Fig. 1.6. As the figure exhibits equations for the CBM, one could use the 28th day compressive strength for estimating the flexural strength up to 208 days by performing only the compressive strength testing at 28 days. A few studies have shown the relationship which used the compressive strength for estimating the flexural strength because science society has thought that as the age and strength increase, the ratio of the flexural strength to the compressive strength decreases (Ahmad & Shah, 1985). Nevertheless, a study of Legeron and Paultre was the one that suggested an equation for estimating the flexural strength ( $f_c$ ) from the compressive strength in 2000, as in the chapter. Their equation was  $f_c \text{ min. } 0.68f_c^{0.5}$  (Legeron & Paultre, 2000), and it can be used today. The five polynomial equations show that the relationship between the flexural strength and compressive strength of mortar is nonlinear in the chapter.

### 1.6.7 Compressive strength

To better explain how the compressive strength develops, there is a need for evaluating the mixing materials and their fractals in the CBM. There was plenty of comprehensive studies carried out on the fractals of mixing materials of the CBM by a number of researchers previously. Rafeet et al. revealed that both compressive strength and setting time were influenced by a low water-to-cement ratio positively in the CBM (Rafeet et al., 2017). Another study performed by Kim unveiled an important result that for a water-to-waste concrete powder ratio of 15% the compressive strength of CBM was a bit over 30 (MPa) on the 28th day (Kim, 2017). Vurst et al. determined yield strength, robustness, viscosity, and rheology of paste and scrutinize the influence of paste volume and water-to-powder volumetric ratio. As a result the increase in water content leads to retard yield strength. On the contrary to the current result the robustness of paste was improved by an increase in the water-to-powder volumetric ratio (Vurst et al., 2017). The fact that the mixing ratio of the CBM has a powerful effect on development of the compressive strength was presented by Šipos̆ et al. (2017). Sassani et al. worked on the mixing raw material ratio of the CBM, for example, carbon fiber dosage, fiber length, coarse-to-fine aggregate volume ratio, conductivity enhancing agent dosage, and fiber dispersive agent dosage. The result of compressive strength was influenced by the dosage of fiber, conductivity enhancing agent, and fiber dispersive agent positively. Additionally the flexural strength is dependent on the coarse-to-fine aggregate volume ratio and the dosage of fiber dispersive agent (Sassani et al., 2017). Fig. 1.7 shows five important relationships between the compressive strength and the 28th day flexural strength as well as their mathematical models and regression degree.



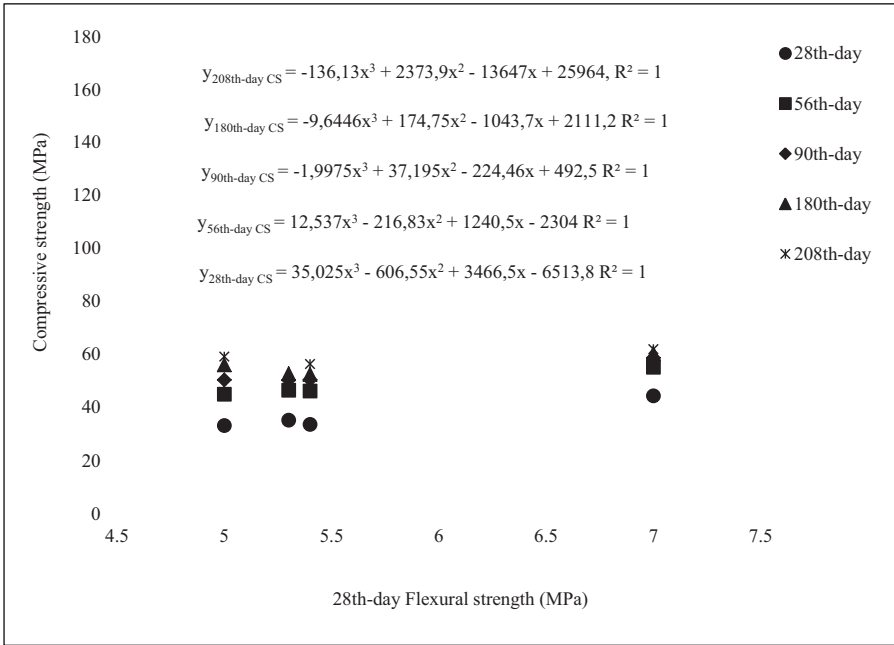


**Figure 1.7** Five important relationships between the compressive strength and the 28th day flexural strength as well as their mathematical models and regression degrees.

However, the relationship between compressive strength and flexural strength is a very popular title for the CBM, especially forecasting the compressive strength from flexural strength, and vice versa. This use of relationship has plenty of advantages if it is merged with the mixing constituent of the CBM. It will allow researchers to forecast the compressive strength before the CBM is prepared in a laboratory. The main aim for the suggestion of relationship between compressive strength and flexural strength is to help reduce the workload in the laboratory. For that aim, there are a number of comprehensive studies in the current science literature. One of them was carried out by American Concrete Institute (ACI) in 1997 to forecast the compressive strength of conventional concrete from the flexural strength (ACI Committee 363, 1997). Mindness et al. did perform another study related to the forecasting of compressive strength. Their equation was  $0.11 f_c \leq f_{\zeta} \leq 0.23 f_c$  (Mindness et al., 2002). Because the most precious datum is the compressive strength for the CBM, the people would like to find an equation which includes the entire type of the CBMs. A similar study of Mindness et al. was conducted by Ahmed et al. in 2008. Their equation included a broad range for the forecasting of compressive strength, for example,  $0.35 f_c \leq f_{\zeta} \leq 0.23 f_c \leq 0.5$  (Ahmed et al., 2008). Examining the

studyings, there is a need for estimating the compressive strength in mortar, having either SCM or not. A regression analysis was performed on the relationship which used the flexural strength for estimating the compressive strength. Between the different types of regression equations found the polynomial equation gave the best results. The effect of difference of curing age on the regression analysis was also studied; nevertheless, it was established that it was insignificant. With compressive strength data measured, it can be concluded that age is not an essential factor in estimating the compressive strength of the mortar. Fig. 1.7 would fill the gap between the studies because the chapter presents both the properties of mixing materials of mortar and the mechanical properties of mortar. In Fig. 1.7, five polynomial equations are presented to show the relationship between the compressive strength and the flexural strength. The R square degrees, which show a good compatibility between the two properties, are also provided in Fig. 1.7. As the figure exhibits estimation equations with 95% reliability for the CBM, one could use it to estimate the compressive strength up to 208 days from the 28th day flexural strength by performing the flexural strength testing on the 28th day.

## 1.7 Conclusions

Based on the test results, WSA is a favorable substitution material of hydraulic binder and hydraulic binder-based construction materials for improving the durability feature for harmful climatic conditions and the physical and mechanical features for static and dynamic loads in construction once it is grounded as fine as cement. The estimating models for the properties of the CBM with and without WSA are suggested in the book chapter. Also the models were useful for estimating one property from another. Additionally the mathematical models presented in the book chapter are expected to a leading method for such studies, including cementitious substitution materials for hydraulic binders.

## Acknowledgement

The authors declare that they have no fund for the book chapter.

## Conflict of interest

The authors declare that they have no conflict of interest.

## References

- ACI Committee 363. (1997). State-of-the-art report on high-strength concrete-ACI 363R-92. American Concrete Institute. Retrieved from <https://www.concrete.org/publications/internationalconcreteabstractsportal/m/details/id/5194>.
- Al-Akhras, N. M., & Abu-Alfoul, B. A. (2002). Effect of wheat straw ash on mechanical properties of autoclaved mortar. *Cement and Concrete Research*, 32(6), 859–863. Available from [https://doi.org/10.1016/S0008-8846\(02\)00716-0](https://doi.org/10.1016/S0008-8846(02)00716-0).
- Ahmed, M., Dad Khan, M. K., & Wamiq, M. (2008). Effect of concrete cracking on the lateral response of RCC buildings. *Asian Journal of Civil Engineering Building and Housing*, 9(1), 25–34.
- Ataie, F. F., Juenger, M. C. G., Taylor-Lange, S. C., & Riding, K. A. (2015). Comparison of the retarding mechanisms of zinc oxide and sucrose on cement hydration and interactions with supplementary cementitious materials. *Cement and Concrete Research*, 72, 128–136. Available from <https://doi.org/10.1016/j.cemconres.2015.02.023>.
- Ahmad, S. H., & Shah, S. P. (1985). Structural properties of high strength concrete and its implications for precast prestressed concrete. *PCI Journal*, 30(6), 92–119.
- ASTM C185-20. (2020). *Standard test method for air content of hydraulic cement mortar*. ASTM International.
- Auskern, A., & Horn, W. (1973). Capillary porosity in hardened cement paste. *Journal of Testing and Evaluation*, 1(1), 74–79.
- Biricik, H., Aköz, F., Berktaş, I., & Tulgar, A. N. (1999). Study of pozzolanic properties of wheat straw ash. *Cement and Concrete Research*, 29(5), 637–643.
- Biricik, H., Aköz, F., Türker, F., & Berktaş, I. (2000). Resistance to magnesium sulfate and sodium sulfate attack of mortars containing wheat straw ash. *Cement and Concrete Research*, 30(8), 1189–1197. Available from [https://doi.org/10.1016/S0008-8846\(00\)00314-8](https://doi.org/10.1016/S0008-8846(00)00314-8).
- BS EN 197–1:2011. (2019). *Cement composition, specifications and conformity criteria for common cements*. British Standards Institution (BSI).
- BS EN413. (2016). *Masonry cement: Test methods*. British Standard Institute.
- Chhorn, C., Hong, S. J., & Lee, S. W. (2018). Relationship between compressive and tensile strengths of roller-compacted concrete. *Journal of Traffic and Transportation Engineering*, 5(3), 215–223. Available from <https://www.sciencedirect.com/science/article/pii/S2095756417301253#bib3>.
- Chung, S.-Y., Han, T.-S., Kim, S.-Y., Kim, J.-H. J., Youm, K. S., & Lim, J.-H. (2016). Evaluation of effect of glass beads on thermal conductivity of insulating concrete using micro CT images and probability functions. *Cement and Concrete Composites*, 65, 150–162.
- Dransfield, J. (2003). Constituent materials: Part 3 admixtures-4. Admixtures for concrete, mortar and grout. In J. Newman, & B. S. Choo (Eds.), *Advanced concrete technology*. Butterworth-Heinemann. Available from <https://doi.org/10.1016/B978-0-7506-5686-3.X5246-X>.
- Gadde, B., Menke, C., & Wassmann, R. (2009). Rice straw as a renewable energy source in India, Thailand, and the Philippines: Overall potential and limitations for energy contribution and greenhouse gas mitigation. *Biomass and Bioenergy*, 33(11), 1532–1546. Available from <https://doi.org/10.1016/j.biombioe.2009.07.018>.
- Hogan, F. J., & Meusel, J. W. (1981). Evaluation of ground granulated blast-furnace slag. *Cement, Concrete and Aggregates Journal*, 3, 40–52.

- Juenger, M. C. G., & Siddique, R. (2015). Recent advances in understanding the role of supplementary cementitious materials in concrete. *Cement and Concrete Research*, 78, 71–80. Available from <https://doi.org/10.1016/j.cemconres.2015.03.018>.
- Kadam, K. L., Forrest, L. H., & Jacobson, W. A. (2000). Rice straw as a lignocellulosic resource: Collection, processing, transportation, and environmental aspects. *Biomass and Bioenergy*, 18(5), 369–389. Available from [https://doi.org/10.1016/S0961-9534\(00\)00005-2](https://doi.org/10.1016/S0961-9534(00)00005-2).
- Khushnood, R. A., Rizwan, S. A., Memon, S. A., Tulliani, J.-M., & Ferro, G. A. (2014). Experimental investigation on use of wheat straw ash and bentonite in self-compacting cementitious system. *Advances in Materials Science and Engineering*, 2014. Available from <https://doi.org/10.1155/2014/832508>.
- Kim, Y.-J. (2017). Quality properties of self consolidating concrete mixed with waste concrete powder (WCP). *Construction and Building Materials*, 135, 177–185.
- Kirgiz, M. S. (2014). Advances in physical properties of C class fly ash cement systems blended nanographite—Part 1. *ZKG International*, 12, 42–48. Available from <http://www.zkg-online.info/en/index.html>.
- Kirgiz, M. S. (2015). Advances in physical properties of C class fly ash–cement systems blended nanographite (Part 2). *ZKG International*, 1–2, 60–67.
- Kirgiz, M. S. (2016). Advancements in mechanical and physical properties for marble powder-cement composites strengthened by nanostructured graphite particles. *Mechanics of Materials*, 92, 223–234. Available from <https://doi.org/10.1016/j.mechmat.2015.09.013>.
- Kirgiz, M. S. (2019). Specifications effected in durability of construction materials. *Journal of Advanced Composite Materials, Construction*, 2019, 1–7.
- Kirgiz, M. S. (2020). Nano size particle packing for nanoconcretes and cement based materials: Mathematical models, theory, and technology. In M. S. Liew, P. Nguyen-Tri, T. A. Nguyen, & S. Kakooei (Eds.), *Smart nanoconcretes and cement-based materials*. Elsevier. Available from <https://doi.org/10.1016/C2018-0-02596-7>.
- Kucharczyková, B., Misák, P., & Vymazal, T. (2010). Determination and evaluation of the air permeability coefficient using torrent permeability tester. *Russian Journal of Nondestructive Testing*, 46, 226–233. <https://doi.org/10.1134/s1061830910030113>.
- Lea, F. M. (1970). *The chemistry of cement and concrete*, 1–442.
- Legeron, F., & Paultre, P. (2000). Prediction of modulus of rupture of concrete. *ACI Material Journal*, 97(2), 193–200.
- Martirena, F., & Monzó, J. (2018). Vegetable ashes as supplementary cementitious materials. *Cement and Concrete Research*, 114, 57–64. Available from <https://doi.org/10.1016/j.cemconres.2017.08.015>.
- Massazza, F. (1989). Puzolanlı Çimentolar ve Kullanım Alanları (English Title: Cements with Pozzolan and their Usage Areas), Türkiye Çimento Müstahsilleri Birliği Dergisi-Çimento ve Beton Dünyası (Magazine of The Turkish Cement Manufacturers' Association- Cement and Concrete World).
- McCarthy, M. J., & Dyer, T. D. (2017). Pozzolanas and pozzolanic materials. In P. C. Hewlett, & M. Liska (Eds.), *Lea's chemistry of cement and concrete* (5th ed., pp. 363–467). Butterworth-Heinemann. Available from <https://doi.org/10.1016/C2013-0-19325-7>.
- Mindess, S., Young, J. F., & Darwin, D. (2002). *Concrete* (2nd ed.). Prentice Hall.
- Mohd, A., Javed, M., & Mohd, A. H. (2014). A study of factors affecting the flexural tensile strength of concrete. *Journal of King Saud University Engineering Sciences*, 28(2), 147–156.

- Montgomery, D. G., Hughes, D. C., & Williams, R. I. T. (1981). Fly ash in concrete—a microstructure study. *Cement and Concrete Research*, 11(4), 591–603. Available from [https://doi.org/10.1016/0008-8846\(81\)90089-2](https://doi.org/10.1016/0008-8846(81)90089-2).
- Moravcova, B., Possl, P., Misak, P., & Blazek, M. (2016). Possibilities of determining the air-pore content in cement composites using computed tomography and other methods. *Materials and Technology*, 50, 491–498.
- Nguyen, T. T., Bui, H. H., Ngo, T. D., & Nguyen, G. D. (2017). Experimental and numerical investigation of influence of air-voids on the compressive behaviour of foamed concrete. *Materials and Design*, 130, 103–119.
- Nehdi, M., Duquette, J., & El Damatty, A. (2003). Performance of rice husk ash produced using a new technology as a mineral admixture in concrete. *Cement and Concrete Research*, 33(8), 1203–1210. Available from [https://doi.org/10.1016/S0008-8846\(03\)00038-3](https://doi.org/10.1016/S0008-8846(03)00038-3).
- Neithalath, N., Sumanasooriya, M. S., & Deo, O. (2010). Characterizing pore volume, size, and connectivity in pervious concretes for permeability prediction. *Materials Characterization*, 61, 802–813.
- Perdue, S. (2021). World agricultural supply and demand estimates. WASDE–608, Secretary of Agriculture, United States Department of Agriculture. <https://www.usda.gov/oce/commodity/wasde/wasde0121.pdf>.
- Postacıoğlu, B. (1969). Yapı Malzemesi Ders Notları (*English Title: Lecture Notes of Construction Materials*). Istanbul Technic University Publisher.
- Powers, T. C. (1956). The physical structure of cement and concrete. *Cement and Lime Manufacture*, 29, 13–24.
- Powers, T. C. (1979). The specific surface area of hydrated cement obtained from permeability data. *Matériaux et Constructions*, 12(3), 159–168. Available from <https://doi.org/10.1007/BF02494246>.
- Rafeet, A., Viani, R., Soutos, M., & Sha, W. (2017). Guidelines for mix proportioning of fly ash/GGBS based alkali activated concretes. *Construction and Building Materials*, 147, 130–142.
- Rajapakse, R. (2017). *Construction engineering calculations and rules of thumb*. Butterworth-Heinemann. <https://doi.org/10.1016/C2015-0-02096-2>.
- Samui, P., Iyer, N.R., Kim, D., & Chaudhary, S. (2020). *New materials in civil engineering*. Butterworth-Heinemann. <https://doi.org/10.1016/C2018-0-04445-X>.
- Sassani, A., Ceylan, H., Kim, S., Gopalakrishnan, K., Arabzadeh, A., & Taylor, P. C. (2017). Influence of mix design variables on engineering properties of carbon fiber modified electrically conductive concrete. *Construction and Building Materials*, 152, 168–181.
- Špišoš, T. K., Milicevic, I., & Siddique, R. (2017). Model for mix design of brick aggregate concrete based on neural network modelling. *Construction and Building Materials*, 148, 757–769.
- Tasong, W. A., Lynsdale, C. J., & Cripps, J. C. (1998). Aggregate-cement paste interface. II: Influence of aggregate physical properties. *Cement and Concrete Research*, 28(10), 1453–1465. Available from [https://doi.org/10.1016/S0008-8846\(98\)00126-4](https://doi.org/10.1016/S0008-8846(98)00126-4).
- Troxell, G., Davis, H., & Kelley, J. (1968). Composition and properties of concrete. In *Civil engineering series*. Mc Graw-Hill.
- Tyagi, A., Xia, H. W., Chin, K.-G., & Lee, F.-H. (2019). Model for predicting the unit weight of cement-treated soils. *Soils and Foundations*, 59(6), 1921–1932. Available from <https://doi.org/10.1016/j.sandf.2019.09.002>.
- Uddin, K., Balasubramaniam, A. S., & Bergado, D. T. (1997). Engineering behavior of cement-treated bangkok soft clay. *Geotechnic Engineering*, 28(1), 89–119.

- 
- Uyan, M. (1975). Beton ve Harçlarda Kılcallık Olayı (English Title: Capilarity in Concrete and Mortars), PhD Thesis, Istanbul Technical University.
- Vurst, F. V. D., Grünewald, S., Feys, D., Lesage, K., Vandewalle, L., Vantomme, J., & Schutter, G. D. (2017). Effect of the mix design on the robustness of fresh self-compacting. *Cement and Concrete Composites*, 82, 190–201.
- Yadvinder, Singh, & Bijay, Singh (2008). Efficient management of primary nutrients in the rice-wheat system. *Journal of Crop Production*, 23–85. Available from [https://doi.org/10.1300/J144v04n01\\_02](https://doi.org/10.1300/J144v04n01_02).

This page intentionally left blank

# Class C fuel ash as hydraulic binder substitution in binder-based materials fortified with the high-technology additive of graphite nanoparticles

2

*Mehmet Serkan Kirgiz*

Northwestern University, Chicago, IL, United States

## 2.1 Introduction and background of pulverized fuel ash-cement system

In today's world, it is common that a portion of cement in cement-based materials (CBMs), such as grout, stucco, concrete, and so on, is substituted with one or more byproducts. Once it is substituted with byproducts partially the cement is known as composite or substituted cement (Ingham, 2013). The substituted cement is suggested in terms of improving the durability, the physical features, and the mechanical features of CBMs, but there are also cementless binder systems for construction technology instead (Kuo et al., 2014). One of the original reasons for popularization the substituted cement is the aim for cost saving (S. Ahmad et al., 2014; Alsalman et al., 2017; Azmee et al., 2021; Li, 2016; Liu et al., 2018) in the construction technology. Azmee et al. revealed that the CBM containing 10% ultrafine calcium carbonate with a mean particle size of 3.5  $\mu\text{m}$  blended with 40% pulverized fuel ash (PFA) showed the best performance, with an improvement of 25% in the compressive strength in the early age (Azmee et al., 2021). The latter is an aim to reduce the carbon footprint that the cement manufacturing led to. The last one is a desire to help develop a much durable binder material for construction technology (Ingham, 2013). Among the byproducts used for that aim the most known one is the coal combustion byproduct because it is abundant, useful, and one of the byproducts which consist of PFA, bottom ash, boiler slag, flue-gas desulfurization, and fluidized bed combustion waste (Suárez-Ruiz & Crelling, 2008). The mineralogical structure of the PFA represents the mineralogical component of the charcoal, the method and condition of burning, and the environmental control technology used by the power plant. The PFA includes oxides of silica and aluminum ( $\text{SiO}_2$ ,  $\text{Al}_2\text{O}_3$ ) mostly and normally lower oxides of iron ( $\text{Fe}_2\text{O}_3$ ), calcium ( $\text{CaO}$ ), magnesium ( $\text{MgO}$ ), potassium ( $\text{K}_2\text{O}$ ), and sodium ( $\text{Na}_2\text{O}$ ), although the oxide of silica and aluminum varies inversely with oxide of calcium. Some of these components are



insoluble solids ( $\text{SiO}_2$ ,  $\text{Al}_2\text{O}_3$ ), some are water-soluble (e.g., metal sulfates), and some are water-reactive metal oxides (e.g.,  $\text{CaO}$ ,  $\text{MgO}$ ,  $\text{K}_2\text{O}$ ,  $\text{Na}_2\text{O}$ ) (Suárez-Ruiz & Crelling, 2008). A similar chemical component of the PFA mentioned above is in Portland cement as well. The major chemical component of Portland cement is a mixture of the oxides of calcium ( $\text{CaO}$ ), silicon ( $\text{SiO}_2$ ), aluminum ( $\text{Al}_2\text{O}_3$ ), and iron ( $\text{Fe}_2\text{O}_3$ ). Additionally, it also contains the minor component of magnesium oxide ( $\text{MgO}$ ) and oxides of the alkali metals potassium ( $\text{K}_2\text{O}$ ) and sodium ( $\text{Na}_2\text{O}$ ) (Hurley & Pritchard, 2005). As a result of the similarity in the chemical components of both the PFA and the Portland cement, PFA is useful for CBMs in terms of durability (Chen et al., 2021; Park et al., 2021), strength (Nikoloutsopoulos et al., 2021), and elasticity (Guo et al., 2019). A manuscript presented by Chen et al. unveiled that the ultrafine PFA additive improved the entire erosion capability for the CBM against the environment of  $\text{Na}_2\text{SO}_4$  and  $\text{MgSO}_4$  (Chen et al., 2021). Nikoloutsopoulos et al. determined that the CBM including the PFA indicated competitive compressive strength when compared to conventional CBM and its splitting tensile strength within the limits specified by Eurocode 2 (EN 1992-1-1, 2004; Nikoloutsopoulos et al., 2021).

Recently the ongoing development of nanomaterials allowed to obtain CBMs with superior properties (Mostafa et al., 2020). Nanomaterials also have a greater Blaine surface area than conventional cement as well as a nucleation effect on cement hydration (Shi et al., 2015; Wu, Khayat, et al., 2017). Additionally, supplementing of nanomaterials into mixing of the CBM increases compacity, which makes the microstructure of CBM denser and homogeneous and enhances the bond structure between aggregate and hydration compounds of cement (Norhasri et al., 2016; Wu, Khayat, et al., 2017). Heikal et al. presented that the supplementing of 1% nanoclay for cement shortened both the initial and final setting times of the CBM and increased the 1 day strength, up to 80% (Heikal & Ibrahim, 2016). The results of Ghafari et al. indicated that nanometakaolin increased the strength, about 20%, at the age of 91 days. It can act as a latent hydraulic strength increaser to densify the cement matrix and to fortify the transition zone in the CBM (Ghafari et al., 2015). Wu et al. found that the supplementing of nanometakaolin is effective in reducing the total porosity and diameter of pores in cement mortar due to its effect of latent hydraulic supplementing (Wu, Khayat, et al., 2017). Additionally, nanoclay showed that it also has a healing capacity for the microstructure of cement matrix and mitigates drawbacks leading to the chloride attack in the CBM (Ghafari et al., 2015). Balapour et al. revealed that the supplementing of nano-rice husk ash improved the compressive strength at early and later ages. Additionally, it reduced the chloride migration coefficient significantly (Balapour et al., 2017). Similarly, Xiao et al. reported that the supplementing of waste glass powder enhanced the strength development due to its high content of amorphous silica (Xiao et al., 2020). In addition to the aforementioned nanomaterials, graphite nanoparticles (nGs) were studied by Kirgiz in the CBM. The nGs provided grand advancement for marble powder-cement system and Portland PFA-cement system, both class C PFA-cement and class F PFA-cement. In all these studies the nGs improved flexural and compressive strengths of the CBM at both the early age and later age; lessened

the setting time, fluidity, water absorption, and porosity; and helped increase compacity and unit weight of the CBM (Kirgiz, 2015, 2016, 2018a,b,c). Nevertheless, research studies do not show a desirable interest for the nGs.

Therefore the aim of this chapter is to explain upcycling of class C fuel ash as hydraulic binder substitution in binder-based materials fortified with the high-technology additive of nGs and the admixture of a superplasticizer.

## 2.2 Environmental assessment of usage of the pulverized fuel ash in the cement-based materials

The aim of the utilization of PFA in the CBM is mainly to lessen both material cost and harmful environmental impacts. Considering different industrial situations among regions the measurement and comparison of construction material costs are unfeasible. Thus this section presents an environmental impact summary of construction materials and byproducts used in construction industry. This summary is based on previous papers published (Long et al., 2015; Turner & Collins, 2013). As shown in Table 2.1 the CO<sub>2</sub> emission and the energy consumption are referred to the footprint of carbon per unit (kg/kg) of each construction material and byproduct and the quantity of energy based on fossil resources per unit (MJ/kg) of each construction material and byproduct, respectively. In Table 2.2 the comparison of CO<sub>2</sub> emission and energy consumption between the mortars made of ASTM type I cement and PFA-cement per unit weight of cubic meter is shown as the sum of the quantity obtained by multiplying the footprint of carbon quantity in Table 2.1 and the mass ratio of each construction material and byproduct; the computing method of the energy consumption of mortar is similar to that of CO<sub>2</sub> emission except using the energy consumption in Table 2.1.

**Table 2.1** The carbon dioxide emission and energy consumption of the constituent materials.

Types of constituent materials	Carbon dioxide emission (kg/kg)	Energy consumption (MJ/kg)
Cement	0.83	4.727
Water	0.0003	0.006
River aggregate	0.001	0.022
Aggregate crushed	0.007	0.113
Ground granulated blast furnace slag	0.019	1.588
Pulverized fuel ash	0.009	0.833
Marble powder	0.017	0.35
Metakaolin	0.4	3.48
Silica fume	0.014	0.1
Sodium silicate	1.514	18.3

**Table 2.2** The comparison of the carbon dioxide (CO<sub>2</sub>) emission and energy consumption of ASTM type I cement mortar and PFA-cement mortar mixings for 1 cubic meter.

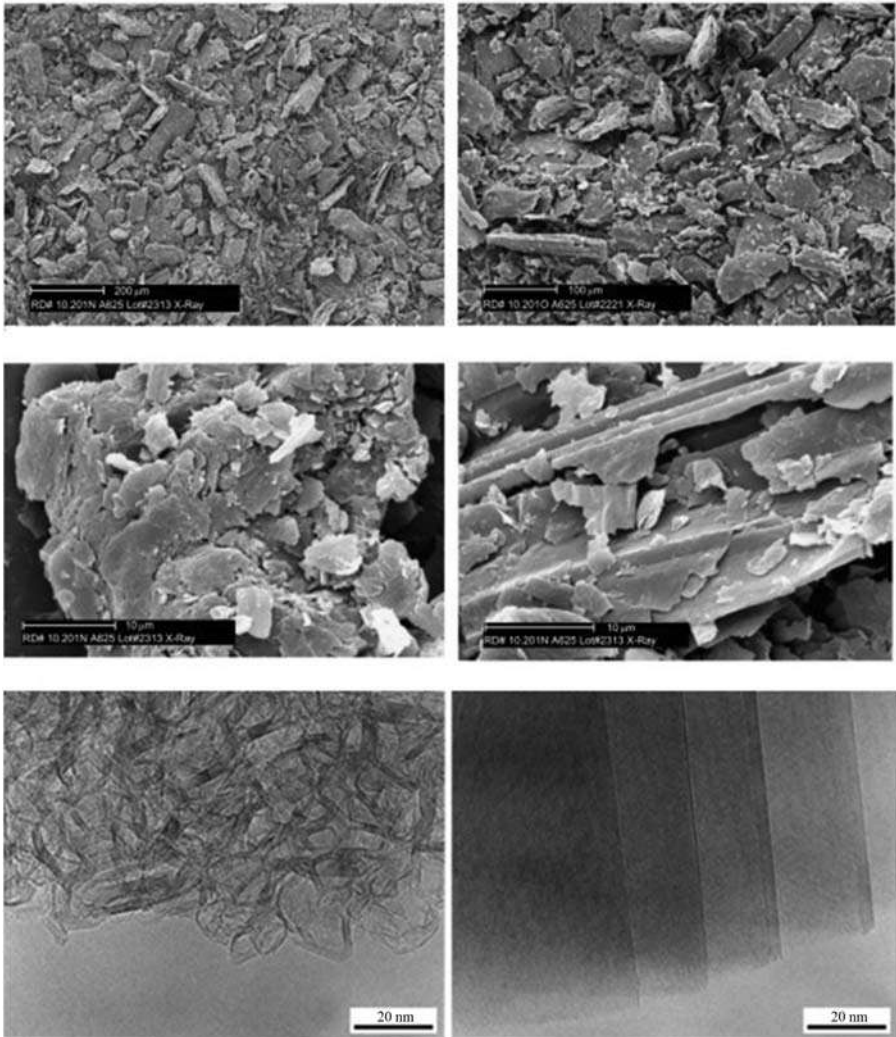
Types of materials prepared	Constituent materials (wt.%)				Carbon dioxide emission (kg/kg)	Energy consumption (MJ/kg)	References
	Cement	Fine aggregate	Water	PFA			
ASTM type I cement mortar	15.6	72.3	12.1	0	0.134	0.80	Kirgiz (2018a,b,c)
PFA-cement mortar	14.4	66.6	11.3	7.7	0.1146	0.75	Kirgiz (2015)

From a practical point of view, it is expected that the compound growth annual rate of using of fuel ash will reach 7.9% by the beginning of 2027. Now this is US\$ 13.6 mn worth. In 2018 its worth was US\$ 6.8 mn (Anonymous, 2023). Considering the cement manufacture of 5.5 million tons in 2018, if the PFA were replaced with cement, up to 35%, approximately 2 million tons of cement would be saved. Owing to the compound impact of saving natural raw materials and energy, both cement industry and energy industry based on use of the fossil coal combustion would have multiplied their income double times.

## 2.3 Synthetic graphite nanoparticles

Synthetic nGs are an artificial material including graphitic carbon, which has also been made of graphitizable carbon by chemical vapor deposition from hydrocarbons at a temperature above 2226.8°C by decomposition of unsteady carbide thermally or by crystallization of metal melting and saturated with carbon superbly (Marsh & Rodríguez-Reinoso, 2006). Activated carbon, known as nongraphitizable carbon, could also be produced with nongraphitizable carbons manufactured by the pyrolysis of sucrose and polyvinylidene chloride; heat treatment could not transform it into graphite solely. As understood from knowledge above the physical properties of the graphitizable carbons and the nongraphitizable carbons are very different from each other. The graphitizable carbons had quite soft and nonporous physical structures, while the nongraphitizable carbons had hard and microporous structures (Harris, 2016). The resource of synthetic graphitic carbon is nearly all types of organic components, for example, sugar, coal-tar pitch and petroleum coke (Dante, 2016), oil, wood, sawdust, nutshells, fruit stones, peat, lignite, and coal

(Marsh & Rodríguez-Reinoso, 2006). Fig. 2.1 shows the scanning electron microscopy (SEM) image of synthetic nGs and the transmission electron microscopy (TEM) image of activated carbon.



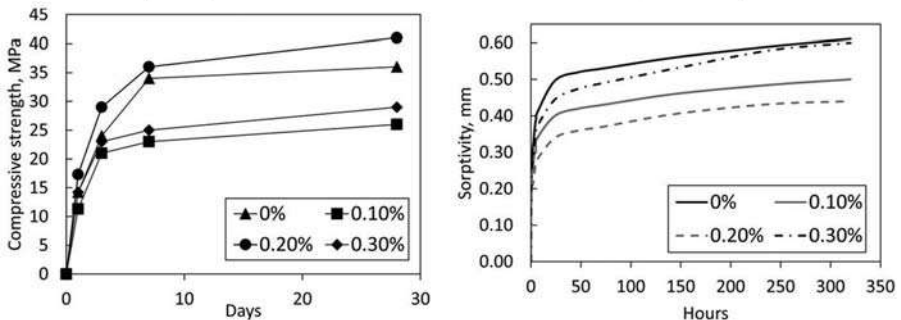
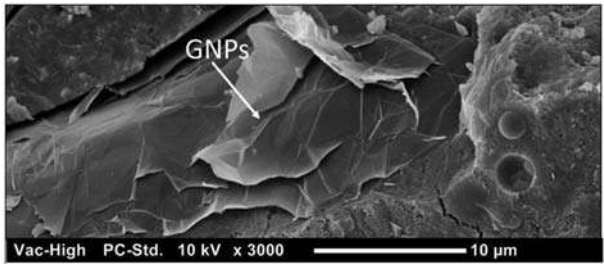
**Figure 2.1** SEM image of synthetic graphite nanoparticles and TEM image of activated carbon; the 200 μm SEM image of synthetic graphite nanoparticles in the first row, the 10 μm SEM image of synthetic graphite nanoparticles in the second row, the 20 nm TEM image of sucrose carbon in the third row and the first column, and the 20 nm TEM image of anthracene carbon in the third row and the second column including heat treatment at 2300°C.

Table 2.3 shows the effect of high heat treatment on surface area and density of carbon made of polyvinyl chloride (PVC) and cellulose.

**Table 2.3** The effect of high heat treatment on surface area and density of carbon made of polyvinyl chloride and cellulose.

Material	Specific surface area (m <sup>2</sup> /g)				
	700°C	1500°C	2000°C	2700°C	3000°C
Carbon from PVC	0.58	0.21	0.21	0.71	0.56
Carbon from cellulose	408	1.6	1.17	2.23	2.25
Material	Density (g/cm <sup>3</sup> )				
	700°C	1500°C	2000°C	2700°C	3000°C
Carbon from PVC	1.85	2.09	2.14	2.21	2.26
Carbon from cellulose	1.9	1.47	1.43	1.56	1.7

Examples of use of the nG in binder and binder-based materials are very few and also have attractive results. One of the very few nG studies in construction materials was performed by Matalkah and Soroushian in 2020. Their results demonstrated the fact that addition of 0.20% nG by mass of the binder resulted in over 40 MPa compressive strength at the age of 28 days and provided gain for abrasion resistance and moisture sorptivity. Moreover the heat of hydration test unveiled that the addition of nG boosted the hydration process and led to an increase in the hydration product at an early age, and the analysis of SEM on the binder paste-added nGs confirmed the lack of microcracks in binder paste and escalating the microcrack propagation within binder matrix and a very good bond between binder paste with nGs and aggregate stack (Matalkah & Soroushian, 2020). Fig. 2.2 shows the SEM analysis of binder paste-added nGs, where the development of compressive strength led to nG addition, and the gain in moisture sorptivity of binder paste-added nGs.



**Figure 2.2** The SEM analysis of binder paste-added nGs, where the development of compressive strength led to nG addition, and the gain in moisture sorptivity of binder paste-added nGs.

In Fig. 2.2, GNP stands for the nG used in the chapter. Medina et al. reported a study on advancement of mechanical and physical properties of cement paste and mortar-added isostatic nGs in 2018. The study shared such details as nGs, as carbon, has great purity and has a crystalline structure, addition of nG increases the compressive and flexural strengths and thermal conductivity, and nG also has the ability of CO<sub>2</sub> entrapping (Medina et al., 2018). One of the most important studies proved that nGs reduce the quantity of calcium hydroxide (Ca(OH)<sub>2</sub>) and increase the quantity of C-S-H; the study was carried out by Yanturina et al. in 2017. With thermogravimetric analysis, they calculated the quantity of Ca(OH)<sub>2</sub> and C-S-H, that is, 5.3% and 9.6% in the cement paste containing no nGs, respectively, and 4.1% and 13.6% in the cement paste containing nGs, respectively. The reduction in the quantity of Ca(OH)<sub>2</sub> was observed in the cement paste containing 0.01% of nG addition by mass of cement. Moreover the addition of 0.01% nG by mass of cement developed a compressive strength of CBM up to 15%, a frost resistance up to 2 times, a heat resistance up to 4.5 times, and a thermofrost resistance up to 5 times. The developments can be attributed to the binding effect of Ca(OH)<sub>2</sub> on the phase of C-S-H partially (Yanturina et al., 2017). Lin and Du reported the fact that the nG-reinforced cement composite also has great potential to construct smart and sustainable settlement (Lin & Du, 2020).

## 2.4 Class C pulverized fuel ash

PFA-cement system, known as Portland fly ash cement, CEM II A-V/B-V, CEM II A-W/B-W to standard (BS EN 197-1, 2011), has been used in the world since the beginning of 1940. There were comprehensive restrictions of the types of fuel ash allowed in substituting for cement partially: The reactive silica content shall not be less than 25% by mass, the loss on ignition for fuel ash shall not exceed 5%, reactive oxide of calcium (CaO) shall be less than 10% with free CaO less than 1%, and the fuel ash shall be proven to have pozzolanic activity once tested in accordance with BS EN 196-5 (Lindon, 2001). Maybe the most important development was the acceptance of the pozzolanic PFA cement in 1996. This meant that the compressive strength of pozzolanic PFA-cement system shall not be less than 12 MPa at the age of 7 days and 22.5 MPa at the age of 28 days (BS6610, 1996). The chemical component and particle size of PFA differ from plant to plant. However, it is usually known as a fine spherical powder, which improves the workability of CBM. As a result of pozzolanic reaction of it with binder the PFA increases the late age strength of CBM. The usage of PFA can reduce carbon dioxide (CO<sub>2</sub>) emission (Li, 2016; Van Tuan et al., 2011) and the production cost and energy of CBM (S. Ahmad et al., 2014; Li, 2016; Wu, Shi, et al., 2017). Recently, many research studies have focused on improving new CBM mixtures with PFA because substituting cement with PFA can help reduce harmful environmental impacts.

As a consequence of the importance of the PFA the compressive strength of CBM with PFA is about 95 MPa at 3 days, 110–185 MPa at 28 days, and 152–202 MPa at 91 days, with a replacement of binder material between 10% and 20%. It has been concluded that the CBM with PFA also exhibits the minimum ultra-high-strength property requirement. This meant that the PFA could enhance

the properties of the CBM, while it helps reduce harmful environmental impacts of CO<sub>2</sub> release, the cost of CBM manufacturing, and consuming natural raw materials and nonrenewable energy (Park et al., 2021).

## 2.5 Upcycling process and tests performed

The main scope of this section is to present the upcycling process and testing performance of class C PFA along with nGs and a superplasticizer. To achieve this scope, eight mixes were prepared and tested. The reference mixture was prepared with ASTM type I cement. Table 2.4 shows relative mixing components of the eco-friendly green binder and the binder-based materials for one cubic meter and nG/ASTM type I cement ratio and nG/class C PFA-cement ratio. Unless otherwise stated the relative content of mixing materials used was calculated with water quantity to ASTM type I cement quantity, water quantity to class C PFA-cement quantity, water quantity to class C PFA quantity, water quantity to fine aggregate quantity, and water quantity to nG quantity for one cubic meter in Table 2.4. The dosages of nGs added were 0.34%, 0.84%, and 1.7% of the mass of the cement quantity in the green binder materials prepared.

**Table 2.4** Relative component of mixing materials for one cubic meter, nG/ASTM type I cement ratio, and nG/class C PFA-cement ratio.

Types of materials	Relative content of conventional cement and cement-based materials			nG/ASTM type I cement ratio		
	Water	ASTM type I cement	Fine aggregate (<2 mm)			
Reference	1	1.3	6	0		
Types of materials	Relative content of conventional cement and cement-based materials along with nGs					
	Water	ASTM type I cement	Fine aggregate (<2 mm)	nG	nG/ASTM type I cement ratio	
100%ASTM&0.34%nG	1	1.3	6	0.0044	0.003	
100%ASTM&0.84%nG	1	1.3	6	0.0109	0.009	
100%ASTM&1.7%nG	1	1.3	6	0.0221	0.017	
Types of materials	Relative content of conventional class C PFA binder and binder-based materials					
	Water	ASTM type I cement	Fine aggregate (<2 mm)	Class C PFA	nG/class C PFA-cement ratio	
65%ASTM&35%CPFA	1	1.3	6	0.699	0	
Types of materials	Relative content of class C PFA binder and binder-based materials along with nGs					
	Water	ASTM type I cement	Fine aggregate (<2 mm)	Class C PFA	nG	nG/class C PFA-cement ratio
65%ASTM&35%CPFA&0.34%nG	1	1.3	6	0.699	0.0044	0.003
65%ASTM&35%CPFA&0.84%nG	1	1.3	6	0.699	0.0109	0.009
65%ASTM&35%CPFA&1.7%nG	1	1.3	6	0.699	0.0221	0.017

The test of compressive strength for all eco-friendly green binder-based CBMs was performed according to EN 196-1 on cubic samples with dimensions of  $50 \times 50 \times 50 \pm 0.8$  mm. The test of splitting tensile strength was carried out according to ASTM C1006/C1006M-20a. Three samples were tested, and the average value was considered. In flexural strength testing, beams of eco-friendly green binder-based CBMs with a size of  $25 \times 44 \times 100 \pm 0.4$  mm were used according to EN 196-1 (ASTM C1006/C1006M-20a, 2020; EN 196-1:2002, 2002). The force loading rate was 0.008 mm/sn in all tests. The average quantity of sample derived is used in regression analysis to predict strength from mixing materials property, nG/ASTM type I cement and nG/class C PFA-cement.

## 2.6 Nature of strength

### 2.6.1 Strength in flexure

The paramount influence of mineralogical addition-to-cement ratio in the mixing of CBM on its gain of strength has not been explained comprehensively, and it should be possible to relate this ratio to the authentic fracture (Kırgız, 2018b). For that reason the CBMs are considered as a fragile material (Figmig et al., 2021; Neville, 1993), although it displays a small amount of flexing action, as cracking under static loading occurs at a quite low total straining; a straining of 0.001–0.005 at cracking has been recommended as the limit of flexing action (Neville, 1993). Fig. 2.3 shows regression relationships between the flexural strength and nG/ASTM type I cement in different curing times of the mortar samples and prediction equations for flexural strength and its r squares.

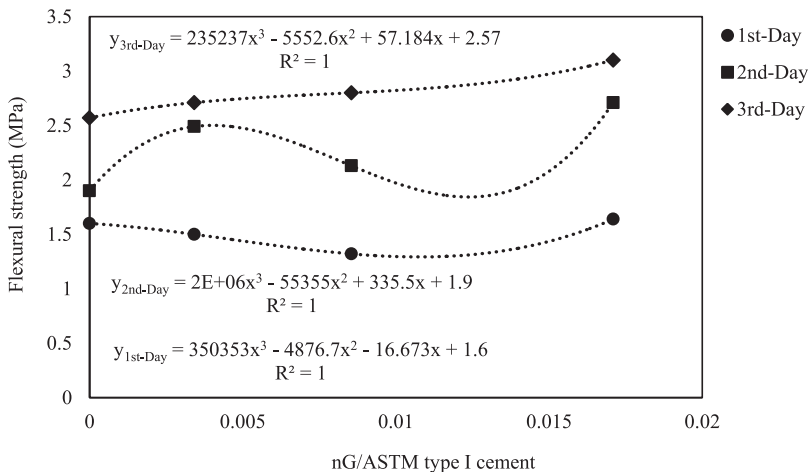


**Figure 2.3** Regression relationships between the flexural strength and nG/ASTM type I cement in different curing times of the mortar samples and prediction equations for flexural strength and its r square regression analysis.



Fig. 2.4 shows regression relationships between the flexural strength and nG/class C PFA-cement in different curing times of the mortar samples and prediction equations for flexural strength and its r squares. While we do not know the certain mechanism of flexural strength of the CBM, this possibly depends upon micro- and nanocracks within cement paste and bond structures among cement paste and aggregate. To better explain this phenomena, Griffith reported a hypothesis in 1921 (Griffith, 1921). This hypothesis recommends microscopic cracking at the region of a fault, and it is usually responsible for the strength of the whole sample, where the volume unit contains the weakest fault. This could be attributed to the fact that the weakest chain of the strength is the fault which could spread throughout the section of the sample (Griffith, 1921; Neville, 1993). A uniform distribution of nG is probably a remedy to bar the fault's spreading in the CBM. Additionally, Mostafa et al. showed that nanomaterials could improve strength properties, healing the microstructure and retarding the absorption of the CBM (Mostafa et al., 2020).

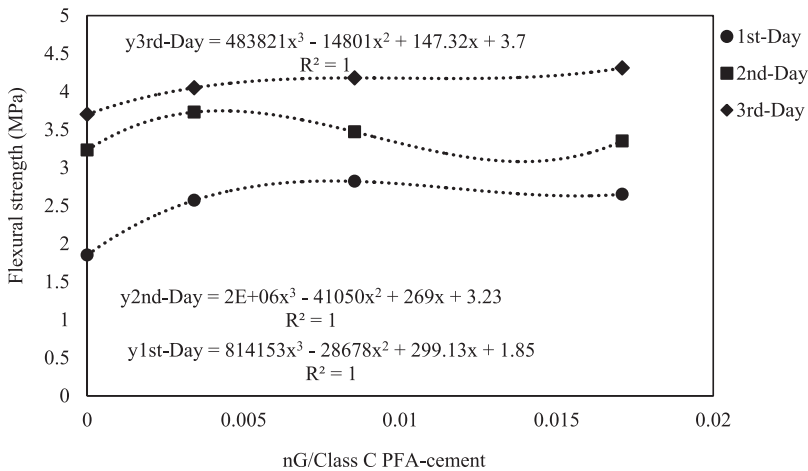


**Figure 2.4** Regression relationships between the flexural strength and nG/class C PFA-cement in different curing times of the mortar samples and prediction equations for flexural strength and its r square regression analysis.

It is concluded from the results that the flexural strength of all mixes, conventional cement-based materials and class C PFA-cement-based materials along with the nGs, was developed when compared to the reference mix. In addition to the conclusion, it is also concluded from the science literature that the supplementing of nanoparticles into binder-based materials densifies the microstructure of CBM and refines the interfacial transition zone between the cement matrix and aggregate stack (Kırgız, 2018c). In addition, because of

the high pozzolanic reaction effect of nGs, it saturates the volume of weak calcium hydroxide and replaces it with C-nG-H, which shows a higher strength (Kırgız, 2018a). The nGs seem to have the best influence on the flexural strength gain for both ASTM type I cement material and class C PFA-cement material when 1.7% is added by mass of cement. With less dosages the flexural strength tends to increase. Nevertheless, the velocity of the flexural strength gain is slow when compared to both 100%ASTM&1.7%nG and 65% ASTM&35%CPFA&1.7nG. The performance of nGs with the results of compressive strength and splitting tensile strength of the ASTM type I cement material and class C PFA-cement material is the same with its flexural strength results. Moreover the chapter would fill the gap in relating to predicting strength and strength-related properties from the ratios of material mixing prepared. For that aim, Figs. 2.3 and 2.4 are presented in the subsection. These figures contain both polynomial mathematical equations and r squares. The meaning of the equations given is that a normal trend can be found for the strength relationships. The one worth for all r squares of the equations derived in Figs. 2.3 and 2.4 confirms that the relationship between the flexural strength and the nG/ASTM type I cement the and nG/class C PFA-cement is powerful, valid, and useful to predict strength and strength-related properties. These equations and r squares also provide an opportunity for using the sample nondestructively and the data reached in the artificial neural network software.

## 2.6.2 Strength in splitting tension

Usually the indirect test is accepted for use in determining the splitting tensile strength of CBM since the direct splitting tensile test is difficult to perform. The most known indirect splitting tensile tests are the flexure and splitting tensile tests. One of them is flexural strength, which is determined by failure of beam sample in bending test, performed with either compression force or tensile force until cracking. The other one is determined at a point where cracking is due to the compression force, instead. For CBMs, there were plenty of power-type equations to predict the flexural-based splitting tensile strength from the compressive strength of the sample. Mohd et al. in 2014 confirmed that there are many factors which influence the relationship between flexural and compressive and splitting tensile strengths, such as level of strength, properties and mineralogy of aggregate, types of admixture, moisture percent of sample, conditions of mixing and curing of sample, geometry of sample, age of sample, and so on (Mohd et al., 2014). Research studies presented many relationships between the splitting tensile strength and compressive strength (Raphael, 1984). Table 2.5 shows the relationship between the splitting tensile strength and the compressive strength of the CBM, where  $f_{sp}$  stands for the splitting tensile strength (MPa) and  $f_c$  stands for the compressive strength (MPa).

**Table 2.5** Relationship between splitting tensile strength and compressive strength of the CBM.

References	Equations
ACI Committee 318 (1999)	$f_{sp} = 0.56 f_c^{0.5}$
Carneiro and Barcellos (1953)	$f_{sp} = 0.34 f_c^{0.735}$
Carino and Lew (1982)	$f_{sp} = 0.272 f_c^{0.71}$
Oluokun et al. (1991)	$f_{sp} = 0.294 f_c^{0.69}$
CEB-FIP Model Code for Concrete Structure (1990)	$f_{sp} = 0.3 f_c^{2/3}$
Raphael (1984)	$f_{sp} = 0.313 f_c^{0.667}$
Gardner et al. (1988)	$f_{sp} = 0.47 f_c^{0.59}$
	$f_{sp} = 0.466 f_c^{0.66}$

However, a few relationships between the mineralogical supplementing and the strength-related properties were presented. The chapter would like to fill the gap, which is predicting strength-related properties from mineralogical supplementing. Fig. 2.5 shows regression relationships between the splitting tensile strength and nG/ASTM type I cement in different curing times of the mortar samples and prediction equations for splitting tensile strength and its r squares.

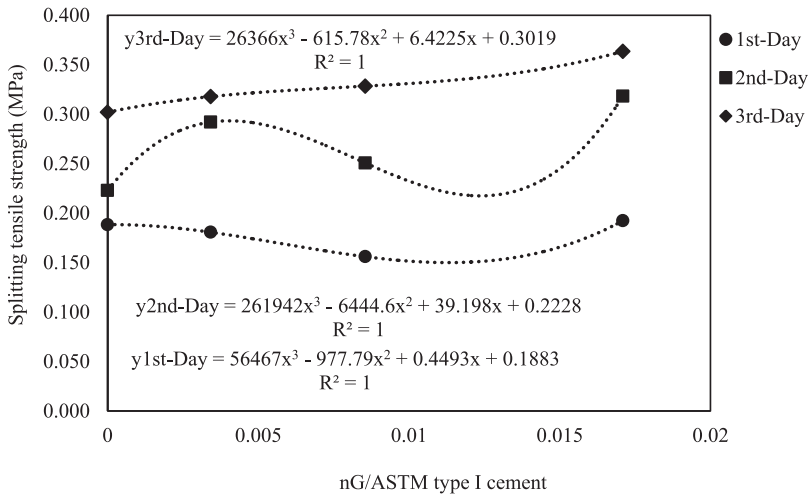
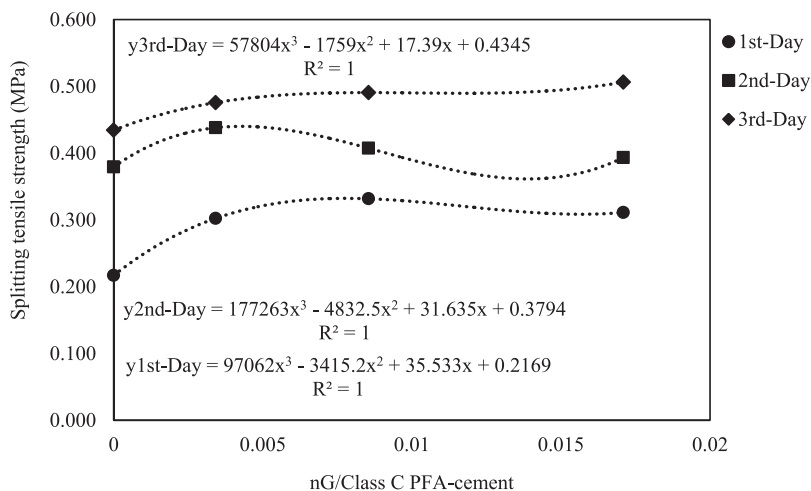
**Figure 2.5** Regression relationships between the splitting tensile strength and nG/ASTM type I cement in different curing times of the mortar samples and prediction equations for splitting tensile strength and its r square regression analysis.

Fig. 2.6 shows regression relationships between the splitting tensile strength and nG/class C PFA-cement in different curing times of the mortar samples and prediction equations for splitting tensile strength and its r squares.



**Figure 2.6** Regression relationships between the splitting tensile strength and nG/class C PFA-cement in different curing times of the mortar samples and prediction equations for splitting tensile strength and its  $r$  square regression analysis.

It is concluded from the results that the splitting tensile strength of all mixes, conventional cement-based materials and class C PFA-cement-based materials along with the nGs, was developed when compared to the reference mix. The nG seems to have the best influence on the splitting tensile strength gain for both ASTM type I cement material and class C PFA-cement material when 1.7% is added by mass of cement. With less dosages the splitting tensile strength tends to increase; however, the velocity of the splitting tensile strength gain is slow when compared to both 100%ASTM&1.7%nG and 65%ASTM&35%CPFA&1.7nG. Moreover, because the age and strength of the CBM increase, the percent of determining the splitting tensile strength from the compressive strength result decreases (S. H. Ahmad & Shah, 1985). Precisely, regression analysis was carried out for the relationship between the mineralogical supplementing and the splitting tensile strength which was absent previously. In the regression analysis of the relationship performed the polynomial equations gave the best results. The effect of changing ratio of nG by mass of cement binder was studied, and this was found to be the most significant factor. The meaning of the one worth for all  $r$  squares in the equations derived in Figs. 2.5 and 2.6 proves that the relationship between the splitting tensile strength and the nG/ASTM type I cement and nG/class C PFA-cement is useful to predict strength and strength-related properties of the CBM repeatedly.

### 2.6.3 Strength in compression force

The cement hydration influences the compressive strength of the CBM significantly. In the CBM with ultra-high-strength properties, both the cement hydration

and compaction applied influence the compressive strength gain. The packing of CBM activates the interaction between the nanoparticle and binder particle. Therefore the CBM also has an initial force carrying ability and strength. Without sufficient compaction or unit weight in volume the maximum compressive strength cannot be reached. Although the compressive strength of the CBM can be improved using internal and external compaction, the advancement of splitting tensile strength may not be succeeded. The guide for CBM of roller-compacted concrete is that the compressive strength and the flexural strength respectively vary in a broad range from 28 to 41 MPa and from 3.5 to 7 MPa at the age of 28 days (Harrington et al., 2010). In addition to the fact of compaction the performance of nGs with the results of compressive strength of the ASTM type I cement material and class C PFA-cement material is the same with its other strength results. Table 2.6 shows the existing relationship between compressive strength and flexural strength of the CBM, where  $f_r$  stands for the flexural strength (MPa). It is concluded from the results that the compressive strength of all mixes, conventional cement-based materials and class C PFA-cement-based materials along with the nGs, was developed when compared to the reference mix. The nG seems to have the best influence on the compressive strength gain for both ASTM type I cement material and class C PFA-cement material when 1.7% is added by mass of cement because of its reaction effect with calcium oxide-based components in binder and binder-based materials. With less dosages the compressive strength tends to increase; however, the velocity of the compressive strength gain is slow when compared to both 100%ASTM&1.7%nG and 65%ASTM&35%CPFA&1.7nG.

**Table 2.6** Relationship between compressive strength and flexural strength of the CBM.

References	Equations
Ahmed et al. (2008)	$0.3 f_c^{0.5} \leq f_r \leq f_c^{0.5}$
Legeron and Paultre (2000)	$f_{r_{avg}} = 0.94 f_c^{0.5}$
ACI Committee 363 (1997)	$f_r = 0.94 f_c^{0.5}$
Mindess et al. (2003)	—

Chhorn and Lee reported that distribution of aggregate size, effort of compaction, and setting of curing conditions can also improve the compressive strength of CBM (Chhorn & Lee, 2016). Gouvas and Orfanos also recommended the fact that the prediction of compressive strength of CBM would depend upon such different factors as humidity of aggregate, quality of aggregate source, and so on (Gouvas & Orfanos, 2014). Ahmad et al. substituted a part of silica fume (SF) with PFA and reported that replacement of PFA with the SF, up to 11.8% of the mass of binder, slightly led to greater compressive strength than the minimum requirement of 150 MPa at 28 days. This meant that the usage of PFA can reduce the cost of CBM

slightly. It has been concluded that PFA can also improve many characteristics of high-strength mortar (S. Ahmad et al., 2014). However, Pyo et al. unveiled that substitution of 12.8% cement with PFA retarded the compressive strength in conventional CBM at 1 day and 3 days (Pyo & Kim, 2017). Wu et al. also evaluated the effect of PFA as an additive for the CBM and confirmed that the PFA has influenced the compressive strength negatively (Wu, Shi, et al., 2017). The 15% substitution ratio of cement with PFA led to 13.5% and 8% lesser compressive strength when compared with the compressive strength of reference samples at 3 days and 28 days, respectively. Randl et al. reported that the 38.5% substitution ratio of cement with PFA retarded the compressive strength by 24.9% compared to that of the reference sample at 28 days, although the packing unit weight in volume of PFA is greater (Randl et al., 2014). Thus it is concluded that the pozzolanic reaction effect of PFA is slow for the compressive strength of the CBM. In contrast to the results mentioned above, there were comprehensive studies reporting nonidentical trends. For example, Šeps et al. substituted the cement of 30% with PFA and the substitution led to over 19% greater compressive strength compared to the reference specimen containing SF only at 28 days (Šeps et al., 2019). Fig. 2.7 shows regression relationships between the compressive strength and nG/ASTM type I cement in different curing times of the mortar samples and prediction equations for compressive strength and its r squares.

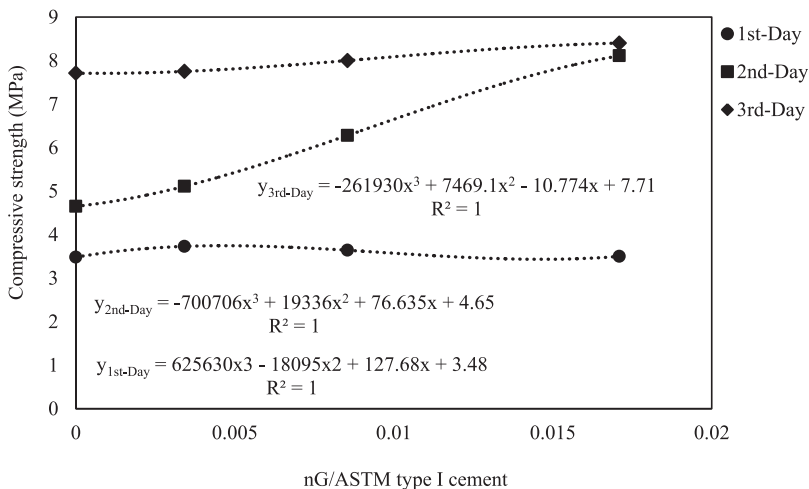


**Figure 2.7** Regression relationships between the compressive strength and nG/ASTM type I cement in different curing times of the mortar samples and prediction equations for compressive strength and its r square regression analysis.

Fig. 2.8 shows regression relationships between the compressive strength and nG/class C PFA-cement in different curing times of the mortar samples and prediction equations for compressive strength and its r squares.

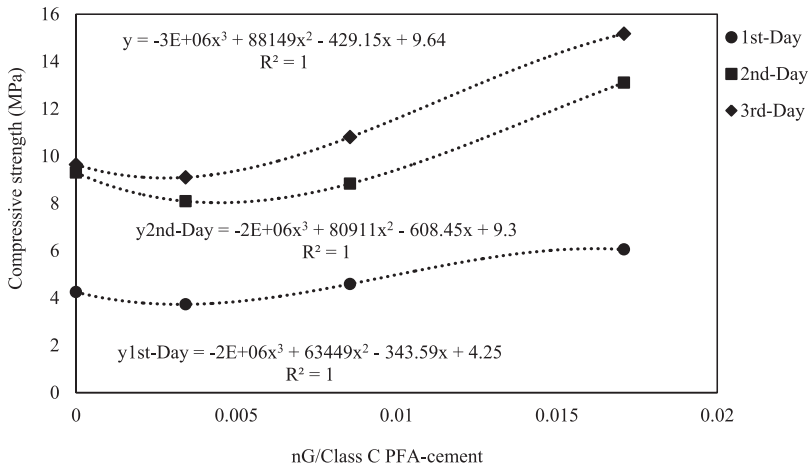


**Figure 2.8** Regression relationships between the compressive strength and nG/class C PFA-cement in different curing times of the mortar samples and prediction equations for compressive strength and its r square regression analysis.

Additionally, Ferdosian and Camões presented a way of how to optimize the CBM mixture design that satisfies the requirements of the compressive strength and the flowability using PFA in which the average particle size is  $4.48 \mu\text{m}$  (Ferdosian & Camões, 2017). They called the design as both an eco-efficient mixture and a cost-efficient mixture that releases the lowest  $\text{CO}_2$  emission and maximizes the usage of PFA and sand quantity as well as minimizes the quantity of SF. The eco-efficient mix and cost-efficient mixture design led to over 6.8% greater compressive strength than reference samples prepared with PFA of 34.1% within the cement. The ternary usage of SCMs including PFA can also be a feasible remedy to reduce the quantity of cement and SF in the CBM. Li reported that the ternary usage of PFA, metakaolin (MK), and cement can provide a better compressive strength for the CBM than the CBM prepared with the binary usage of SF and cement. As 20% and 3.8% of cement were substituted with PFA and MK, respectively, the compressive strength developed up to 26% at 28 days (Li, 2016). With a better understanding of the relationship the more reliable structural design of both ASTM type I cement material and the class C PFA-cement material was achieved. Figs. 2.7 and 2.8 include both polynomial mathematical equations and r squares. The meaning of the equations given is that with various supplementing ratios of nGs a normal relationship trend can be found for the strength and strength-related properties. The one worth for all r squares of the equations derived in Figs. 2.7 and 2.8 verifies that the relationship between the compressive strength and the nG/ASTM type I cement and nG/class C PFA-cement is necessary to predict strength and strength-related properties. These equations and r squares also provide an opportunity for researchers to help their data use repeatedly.

## 2.7 Conclusions

Results support the following conclusions:

- The constructional efficiency of the nGs increases the strength and strength-related properties of PFA-cement system. In the light of results, it is concluded that the use of the nGs and class C PFA is necessary for developing eco-friendly green binder and green binder-based materials.
- Additionally, in view of the positive contribution of the nGs and class C PFA, such construction technology practices as the green construction building, the infrastructure building and infrastructure renewal, the construction retrofit, and the construction reinforcement could be used.
- As confirmed in this chapter the nGs are the best supplementing material to make upcycling the class C PFA as a hydraulic binder and binder-based material for saving natural raw material, environment, and energy.

## Acknowledgments

This study does not include a research budget obtained from either nonprofit organizations or profit organizations.

## Data availability

The “Experimental Research” data used to support the findings of this study are available from the corresponding author upon request.

## Funding

The authors declare no funding property in the work.

## References

- ACI Committee 318 (1999). Building Code Requirements for Structural Concrete (ACI 318-99) and Commentary. 318R-99. American Concrete Institute, Farmington Hills.
- ACI Committee 363 (1997). State-of-the-Art Report on Highstrength Concrete. ACI 363R-92. American Concrete Institute, Farmington Hills.
- Ahmad, S. H., & Shah, S. P. (1985). Structural properties of high strength concrete and its implications for precast prestressed concrete. *PCI Journal*, 30(6), 92–119.
- Ahmad, S., Hakeem, I., & Maslehuddin, M. (2014). Development of UHPC mixtures utilizing natural and industrial waste materials as partial replacements of silica fume and sand. *Scientific World Journal*, 2014. Available from <https://doi.org/10.1155/2014/713531>.



- Ahmed, M., Dad Khan, M. K., & Wamiq, M. (2008). Effect of concrete cracking on the lateral response of RCC buildings. *Asian Journal of Civil Engineering Building and Housing*, 9(1), 25–34.
- Alsalmán, A., Dang, C. N., & Micah Hale, W. (2017). Development of ultra-high performance concrete with locally available materials. *Construction and Building Materials*, 133, 135–145. Available from <https://doi.org/10.1016/j.conbuildmat.2016.12.040>.
- Anonymous. Fly ash market size is likely to experience a tremendous growth of USD 12.46 Billion by 2029, share, growth, regional outlook, challenges and competitive analysis. Data Bridge Market Research, 2023. <https://www.globenewswire.com/news-release/2023/01/26/2596404/0/en/Fly-Ash-Market-Size-Is-Likely-to-Experience-a-Tremendous-Growth-of-USD-12-46-Billion-by-2029-Share-Growth-Regional-Outlook-Challenges-and-Competitive-Analysis.html>.
- ASTM C1006/C1006M-20a. (2020). *Standard test method for splitting tensile strength of masonry units*. ASTM International.
- Azmeel, N., Abbas, Y. M., Shafiq, N., Fares, G., Osman, M., & Iqbal Khan, M. (2021). Enhancing the microstructure and sustainability of ultra-high-performance concrete using ultrafine calcium carbonate and high-volume fly ash under different curing regimes. *Sustainability*, 13(7), 3900. Available from <https://doi.org/10.3390/su13073900>.
- Balapour, M., Ramezani-pour, A. A., & Hajibandeh, E. (2017). An investigation on mechanical and durability properties of mortars containing nano and micro RHA. *Construction and Building Materials*, 132, 470–477. Available from <https://doi.org/10.1016/j.conbuildmat.2016.12.017>.
- BS EN 197-1. (2011). *Cement-composition, specification and conformity criteria for common cements*. British Standard Institute.
- BS6610. (1996). *Specification of pozzolanic pulverised fuel ash cement*. British Standard Institute.
- Carino, N. J., & Lew, H. S. (1982). Re-examination of the relation between splitting tensile and compressive strength of normal weight concrete. *ACI Journal Proceedings*, 79(3), 214–219.
- Carneiro, F. L. L., & Barcellos, A. (1953). Tensile Strength of Concrete. RILEM Bulletin No. 13. Union of Testing and Research Laboratories for Materials and Structures, Paris.
- CEB-FIP Model Code for Concrete Structures. (1990). Evaluation of the Time Dependent Behaviour of Concrete. Bulletin d'Information No. 199. Comité Européen du Béton/ Federation Internationale de la Précontrainte, Lausanne.
- Chen, X., Sun, Z., & Pang, J. (2021). A research on durability degradation of mineral admixture concrete. *Materials*, 14(7), 1752. Available from <https://doi.org/10.3390/ma14071752>.
- Chhorn, C., & Lee, S. W. (2016). Influencing compressive strength of roller-compacted concrete. *Construction Materials*, 171(1), 1–8.
- Dante, R. C. (2016). *Handbook of friction materials and their applications- carbon materials*. Elsevier. Available from <https://doi.org/10.1016/B978-0-08-100619-1.00007-9>.
- EN 196–1:2002. (2002). *Methods of testing cement—part 1: Determination of strength*. British Standard Institute.
- EN 1992-1-1. (2004). Eurocode 2: Design of concrete structures—Part 1-1: General rules and rules for buildings. In *Regulation 305/2011, Directive 98/34/EC, Directive 2004/18/EC*. The European Union.
- Ferdosian, I., & Camões, A. (2017). Eco-efficient ultra-high performance concrete development by means of response surface methodology. *Cement and Concrete Composites*, 84, 146–156.

- Figmig, R., Estokova, A., & Luptak, M. (2021). Concept of evaluation of mineral additives' effect on cement pastes' durability and environmental suitability. *Materials*, 14(6), 1448. Available from <https://doi.org/10.3390/ma14061448>.
- Gardner, N. J., Sau, P. L., & Cheung, M. S. (1988). Strength development and durability of concretes cast and cured at 0 C. *ACI Materials Journal*, 85(6), 529–536.
- Ghafari, E., Costa, H., & Júlio, E. (2015). Critical review on eco-efficient ultra high performance concrete enhanced with nano-materials. *Construction and Building Materials*, 101, 201–208. Available from <https://doi.org/10.1016/j.conbuildmat.2015.10.066>.
- Gouvas, H., & Orfanos, C. (2014). Determination of factors affecting compressive strength of lean RCC mixtures: The experience of Filiatrinos dam. *Geotechnical and Geological Engineering*, 32(5), 1317–1327. Available from <https://doi.org/10.1007/s10706-014-9807-y>.
- Griffith, A. A. (1921). VI. *The phenomena of rupture and flow in solids*. Philosophical Transactions of the Royal Society of London. Series A, Containing Papers of a Mathematical or Physical Character. <https://doi.org/10.1098/rsta.1921.0006>.
- Guo, J. Y., Wang, J. Y., & Wu, K. (2019). Effects of self-healing on tensile behavior and air permeability of high strain hardening UHPC. *Construction and Building Materials*, 204, 342–356. Available from <https://doi.org/10.1016/j.conbuildmat.2019.01.193>.
- Harrington, D., Abdo, F., Adaska, W., Hazaree, C.V., & Ceylan, H. (2010). *Guide for roller-compacted concrete pavements*. National Concrete Pavement Technology Center. Institute for Transportation, Iowa State University. [https://lib.dr.iastate.edu/cgi/viewcontent.cgi?referer=&httpsredir=1&article=1100&context=intrans\\_reports](https://lib.dr.iastate.edu/cgi/viewcontent.cgi?referer=&httpsredir=1&article=1100&context=intrans_reports).
- Harris, P. J. F. (2016). *Non-graphitizing carbons: Structure. Reference module in materials science and materials engineering*. Elsevier. Available from <https://doi.org/10.1016/B978-0-12-803581-8.02293-1>.
- Heikal, M., & Ibrahim, N. S. (2016). Hydration, microstructure and phase composition of composite cements containing nano-clay. *Construction and Building Materials*, 112, 19–27. Available from <https://doi.org/10.1016/j.conbuildmat.2016.02.177>.
- Hurley, P. W., & Pritchard, R. G. (2005). *Cement: Encyclopedia of Analytical Science* (pp. 458–463). Elsevier BV. Available from <https://doi.org/10.1016/b0-12-369397-7/00062-5>.
- Ingham, J. (2013). *Geomaterials under the microscope* (pp. 1–192). Manson: Elsevier. Available from <https://doi.org/10.1016/C2012-0-01197-0>.
- Kırgız, M. S. (2015). Advance treatment by nanographite for Portland pulverised fly ash cement (the class F) systems. *Composites Part B: Engineering*, 82, 59–71. Available from <https://doi.org/10.1016/j.compositesb.2015.08.003>.
- Kırgız, M. S. (2016). Advancements in mechanical and physical properties for marble powder-cement composites strengthened by nanostructured graphite particles. *Mechanics of Materials*, 92, 223–234. Available from <https://doi.org/10.1016/j.mechmat.2015.09.013>.
- Kırgız, M. S. (2018a). Green cement composite concept reinforced by graphite nano-engineered particle suspension for infrastructure renewal material. *Composites Part B: Engineering*, 154(12), 423–429.
- Kırgız, M. S. (2018b). Effect of mineralogical substitution raw material mixing ratio on mechanical properties of concrete. *ZKG International*, 30–41.
- Kırgız, M. S. (2018c). Pulverized fuel ash cement activated by nanographite. *ACI Materials Journal*, 115(6), 803–812. Available from <https://doi.org/10.14359/51689101>.
- Kuo, W.-T., Wang, H.-Y., & Shu, C.-Y. (2014). Engineering properties of cementless concrete produced from GGBFS and recycled desulfurization slag. *Construction and Building Materials*, 63, 189–196. Available from <https://doi.org/10.1016/j.conbuildmat.2014.04.017>.
- Legeron, F., & Paultre, P. (2000). Prediction of modulus of rupture of concrete. *ACI Material Journal*, 97(2), 193–200.

- Li, Z. (2016). Drying shrinkage prediction of paste containing meta-kaolin and ultrafine fly ash for developing ultra-high performance concrete. *Materials Today Communications*, 6, 74–80. Available from <https://doi.org/10.1016/j.mtcomm.2016.01.001>.
- Lin, Y., & Du, H. (2020). Graphene reinforced cement composites: A review. *Construction and Building Materials*, 265.
- Lindon, K. A. S. (2001). Fly ash standards, market strategy, and UK practice. In *2001 International Ash Utilization Symposium*. Center for Applied Energy Research, University of Kentucky. <http://www.flyash.info>.
- Liu, Z., El-Tawil, S., Hansen, W., & Wang, F. (2018). Effect of slag cement on the properties of ultra-high performance concrete. *Construction and Building Materials*, 190, 830–837. Available from <https://doi.org/10.1016/j.conbuildmat.2018.09.173>.
- Long, G., Gao, Y., & Xie, Y. (2015). Designing more sustainable and greener self-compacting concrete. *Construction and Building Materials*, 84, 301–306. Available from <https://doi.org/10.1016/j.conbuildmat.2015.02.072>.
- Medina, N. F., Barbero-Barrera, M. M., & Jové-Sandoval, F. (2018). Improvement of the mechanical and physical properties of cement pastes and mortars through the addition isostatic graphite. *Construction and Building Materials*, 189, 898–905.
- Marsh, H., & Rodríguez-Reinoso, F. (2006). *Chapter 9: Production and reference material. Activated carbon*. Elsevier. Available from <https://doi.org/10.1016/B978-008044463-5/50023-6>.
- Matakah, F., & Soroushian, P. (2020). Graphene nanoplatelet for enhancement the mechanical properties and durability characteristics of alkali activated binder. *Construction and Building Materials*, 249. Available from <https://www.sciencedirect.com/science/article/abs/pii/S0950061820307789#!>.
- Mindess, S., Young, J., & Darwin, D. (2003). *Concrete* (second ed.). Upper Saddle River: Pearson Education, Inc.
- Mohd, A., Javed, M., & Mohd, A. H. (2014). A study of factors affecting the flexural tensile strength of concrete. *Journal of King Saudi University Engineering Sciences*, 28 (2), 147–156.
- Mostafa, S. A., Faried, A. S., Farghali, A. A., El-Deeb, M. M., Tawfik, T. A., Majer, S., & Elrahman, M. A. (2020). Influence of nanoparticles from waste materials on mechanical properties, durability and microstructure of uhpc. *Materials*, 13(20), 1–22. Available from <https://doi.org/10.3390/ma13204530>.
- Neville, A. M. (1993). *Properties of concrete* (pp. 1–779). Longman Scientific & Technical.
- Nikoloutsopoulos, N., Sotiropoulou, A., Kakali, G., & Tsvililis, S. (2021). Physical and mechanical properties of fly ash based geopolymer concrete compared to conventional concrete. *Buildings*, 11(5), 178. Available from <https://doi.org/10.3390/buildings11050178>.
- Norhasri, M. S. M., Hamidah, M. S., Mohd Fadzil, A., & Megawati, O. (2016). Inclusion of nano metakaolin as additive in ultra high performance concrete (UHPC). *Construction and Building Materials*, 127, 167–175. Available from <https://doi.org/10.1016/j.conbuildmat.2016.09.127>.
- Oluokun, F. A., Burdette, E. G., & Deatherage, J. H. (1991). Splitting tensile strength and compressive strength relationships at early ages. *ACI Materials Journal*, 88(2), 115–121.
- Park, S., Wu, S., Liu, Z., & Pyo, S. (2021). The role of supplementary cementitious materials (SCMs) in ultra high performance concrete (UHPC): A review. *Materials*, 14(6), 1472. Available from <https://doi.org/10.3390/ma14061472>.
- Pyo, S., & Kim, H. K. (2017). Fresh and hardened properties of ultra-high performance concrete incorporating coal bottom ash and slag powder. *Construction and Building Materials*, 131, 459–466. Available from <https://doi.org/10.1016/j.conbuildmat.2016.10.109>.

- Randl, N., Steiner, T., Ofner, S., Baumgartner, E., & Mészöly, T. (2014). Development of UHPC mixtures from an ecological point of view. *Construction and Building Materials*, 67, 373–378.
- Raphael, J. M. (1984). Tensile strength of concrete. *Journal of the American Concrete Institute*, 81(2), 158–165.
- Šeps, K., Broukalová, I., & Chylík, R. (2019). Cement substitutions in UHPC and their influence on principal mechanical-physical properties. In *IOP conference series materials science engineering*, 522.
- Shi, C., Wu, Z., Xiao, J., Wang, D., Huang, Z., & Fang, Z. (2015). A review on ultra high performance concrete: Part I. Raw materials and mixture design. *Construction and Building Materials*, 101, 741–751. Available from <https://doi.org/10.1016/j.conbuildmat.2015.10.088>.
- Suárez-Ruiz, I., & Crelling, J. (2008). *Applied coal petrology*. Applied coal petrology. Elsevier Ltd. Available from <https://doi.org/10.1016/B978-0-08-045051-3.X0001-2>.
- Turner, L. K., & Collins, F. G. (2013). Carbon dioxide equivalent (CO<sub>2</sub>-e) emissions: A comparison between geopolymer and OPC cement concrete. *Construction and Building Materials*, 43, 125–130. Available from <https://doi.org/10.1016/j.conbuildmat.2013.01.023>.
- Van Tuan, N., Ye, G., Van Breugel, K., Fraaij, A. L. A., & Bui, D. D. (2011). The study of using rice husk ash to produce ultra high performance concrete. *Construction and Building Materials*, 25(4), 2030–2035. Available from <https://doi.org/10.1016/j.conbuildmat.2010.11.046>.
- Wu, Z., Khayat, K. H., & Shi, C. (2017). Effect of nano-SiO<sub>2</sub> particles and curing time on development of fiber-matrix bond properties and microstructure of ultra-high strength concrete. *Cement and Concrete Research*, 95, 247–256. Available from <https://doi.org/10.1016/j.cemconres.2017.02.031>.
- Wu, Z., Shi, C., & He, W. (2017). Comparative study on flexural properties of ultra-high performance concrete with supplementary cementitious materials under different curing regimes. *Construction and Building Materials*, 136, 307–313. Available from <https://doi.org/10.1016/j.conbuildmat.2017.01.052>.
- Xiao, R., Polaczyk, P., Zhang, M., Jiang, X., Zhang, Y., Huang, B., & Hu, W. (2020). Evaluation of glass powder-based geopolymer stabilized road bases containing recycled waste glass aggregate. *Transportation Research Record*, 2674(1), 22–32. Available from <https://doi.org/10.1177/0361198119898695>.
- Yanturina, R. A., Trofimov, B., Ya., & Ahmedjanov, R. M. (2017). The influence of graphite-containing nano-additives on thermofrost resistance of concrete. *Procedia Engineering*, 206, 869–874.

This page intentionally left blank

# Class F fuel ash as hydraulic binder substitution in binder-based material fortified with high-technology additive of graphite nanoparticle and admixture of superplasticizer

*Mehmet Serkan Kirgiz*

Northwestern University, Chicago, IL, United States

## 3.1 Introduction

At nanoscale and microscale, binder-based materials (BBMs) can be separated into three sections: aggregate stack, bulk binder matrix, and the interfacial transition zone (ITZ) (Elsharief et al., 2003). Between the sections the ITZ, as a grout material, is the most fragile section of BBM under static and dynamic forces because the ITZ has the most calcium hydroxide (CH) content (Liao et al., 2004). Thus the development of the micro- and the nanostructures of the ITZ can potentially advance strength and strength-related properties of BBM. The most effective way to advance the structural properties of the ITZ is to add a mineral additive, a plasticizer, and nanomaterials into the BBM. For instance, in 1991 Bentz and Garboczi reported that the silica fume (SF), which is as a mineral addition, could be used for the strength and strength-related properties of the BBM to make the ITZ be stronger ever (Bentz & Garboczi, 1991). Gao et al., in 2005, recommended that the ground granulated blast furnace slag (GGBFS) not only healed the CH mass in the ITZ but also lessened its content (Gao et al., 2005). In 2000 Kuroda et al. presented a study related to fly ash, which had a high CaO and low SiO<sub>2</sub> content and could also improve the micro- and nanostructures of the ITZ and thus growth the whole strength of the BBM system (Kuroda et al., 2000). In addition to the fact mentioned previously, graphite nanoparticles (nGs) are also expected to heal the structure of the ITZ along with strength and strength-related properties in the BBM because it is a reactive nanomaterial.

Formerly, research studies have only evaluated the effect of nGs on the properties of bulk binder matrix (Hu et al., 2019). However, the strength and strength-related properties of grout, as an ITZ material, have not been evaluated once the

nGs and class F fuel ash are incorporated. The component of ITZ is different from the bulk binder matrix in factors of mineral additive-to-cement ratio (Kırgız, 2023), water-to-cement ratio, mineral additive-to-fine aggregate ratio, nanomaterials-to-cement ratio (Kırgız, 2018), and products of hydration, and the nGs can effect these factors significantly (Li et al., 2018).

On the other hand the elastic modulus and splitting tensile strength of nGs are a little over 1100 and 125 GPa, respectively, and they also have a high specific surface between 220 and 1200 m<sup>2</sup>/g (Yang et al., 2017). Such strength and fineness properties enable the nGs to act as a reinforcement material in the BBM to make its mechanical properties greater. The advances of the mechanical properties in the nG-based binder materials have been also presented (Peng et al., 2019). For instance, Kırgız revealed that addition of 0.2% nG by weight of binder enhanced the bending strength of cement matrix by 92%. The development of mechanical properties was attributed to the healing effect of the nGs on the strength and strength-related properties of the cement matrix (Kırgız, 2014, 2015). In 2015, Pan et al. reported that the nGs can reduce the porosity in binder matrix. It increased the ratio of gel structure, which varies between 1 and 45 μm, while it reduced the ratio of micro- and macroporosity. The distribution of porosity and its size in cement matrix happened to be more uniform because the nGs were incorporated (Pan et al., 2015). Research studies also have findings that confirmed that the nGs could heal the crystal structure, such as CH, in hydration products of cement (Peng et al., 2019). This healing helped the splitting tensile, compressive, and flexural strengths increase by 78.6%, 38.9%, and 60.7%, respectively (Peng et al., 2019).

In the light of explanation above the effect of nG/ASTM type I cement and nG/Class F PFA–cement on the strength properties of grout, such as splitting tensile strength, flexural strength, and compressive strength, was determined through the strength monitoring method in the chapter. Based on the result, various models were presented to estimate these strengths of materials from nanomaterial-to-binder ratio. It is expected that the study would contribute to the development of relationships between nanomaterial-to-binder ratio and strength properties in the ASTM type I binder grout and the class F PFA–binder along with the nGs.

## 3.2 Materials and methods

### 3.2.1 Materials

Table 3.1 demonstrates the characteristic components of the used bulk material of nGs, class F PFA, and common cement, and components of fuel ashes from various macs of coal.

**Table 3.1** Characteristic components of the nGs, the class F PFA used, common cement used, and components of fuel ashes from various macs of coal; chemical components of the nGs, the class F PFA, cement, and fuel ashes generated from different macs of coal combustion.

Component	nG	PFA used	Bituminous mac fuel ash	Subbituminous mac fuel ash	Lignite mac fuel ash	Cement used
SiO <sub>2</sub> (%)	0	44	20–60	40–60	15–45	20
Al <sub>2</sub> O <sub>3</sub>	0	22	5–35	20–30	20–25	4
Fe <sub>2</sub> O <sub>3</sub>	0	17	10–40	4–10	4–15	3
CaO	0	5	1–12	5–30	15–40	62
C	99.9	0	0	0	0	0
Loss on ignition (LOI)	0.1	2.8	0–15	0–3	0–5	1.1

### 3.3 Cement binder and its types

Cement is a complex chemical component of oxide of silicon, calcium, iron, aluminum, and other raw materials. Once the product is out from rotary kiln, it is defined as a clinker. Cement is produced through grinding of the clinker along with gypsum (calcium sulfate). The ratio of clinker to gypsum varies from plant to plant. Because gypsum influences the hardening time of cement, each plant mixes the clinker and gypsum at different ratios. There are principally two different classifications for cement used commonly (Cottis et al., 2010). According to ASTM C150 and AASHTO M 85, there are five common cement types as follows:

- Type I defines a cement binder for regular goal in construction. Type I has the same properties as CEM I cement classified by EN 197-1:2000 standard.
- Type II is known as a durable cement binder for a moderate quantity of sulfate in air, soil, and water.
- Type II (MH) is also a durable cement binder for sulfate moderately and leads to low heat during curing of BBM.
- Type III defines a cement binder for the high strength aim at an early age, usually at the first 3 days.
- Type IV is a cement binder type that provides low heat in hydration process and is preferred for use in massive concrete constructions, for example, dams, highway roads, and airport runways.
- Type V is known as a durable cement binder for harmful chemical effects because of high sulfate in air, water, and soil.

Types IA, IIA, II (MH)A, and IIIA are the combinations of cement binders of types I, II, II (MH), and III, including a small quantity of air-entraining admixture. On the contrary to types I, II, II(MH), and III, types IA, IIA, II (MH)A, and IIIA are used to produce air-entrapped concrete (AASHTO M 85, 2020; ASTM C150/C150M-20, 2020).

According to burnt shale (BS) EN 197-1:2011 a cement binder is defined as “a hydraulic binder”, that is, an inorganic material which is ground finely. Once it contacts water, it makes up a matrix which starts setting and hardening in terms of reaction of hydration even



under water. After its hardening, it keeps its strength, rigidity, and durability in air and under water and soil. The hydration of oxide of calcium and silicon and the heat of oxide of aluminum released mainly lead to the hardening of cement binder matrix (BS EN 197-1:2011, 2019). The classification of cement in BS EN 197-1:2000 differs from that in ASTM C150 and AASHTO M 85. BS EN 197-1:2000 accepts various supplementary components as well as cement clinkers in cement binder production. These supplementary components can be GGBFS, natural pozzolan, industrial byproducts such as pozzolanic materials, BS, limestone powder like marble cutting remnant, SF as a latent hydraulic additive, and gypsum (calcium sulfate). As a consequence of various supplementary materials used in BS EN 197-1:2000, 27 common cements are collected into five main types as follows:

- CEM I—Portland cement
- CEM II—Portland—composite cement
- CEM III—Blast furnace cement
- CEM IV—Pozzolanic cement
- CEM V—Composite cement.

### 3.4 Class F pulverized fuel ash

The burning process of natural raw materials in the production of Portland cement (PC) releases plenty of much greenhouse gas. This means that it led to the release of carbon dioxide (CO<sub>2</sub>) between 800 and 1000 kg for each ton of the PC produced (Flower & Sanjayan, 2007; Han et al., 2003). In other words the production of PC causes approximately 7% of carbon dioxide released worldwide. Due to the chemistry of fuel ash, which includes reactive amorphous silica and quartz, the fuel ash could be one of the raw materials in the production of PC, instead of the pozzolanic character of the fuel ash in BBMs (Han et al., 2003). Fig. 3.1 shows the back-scattered electron (BSE) image of fuel ash.

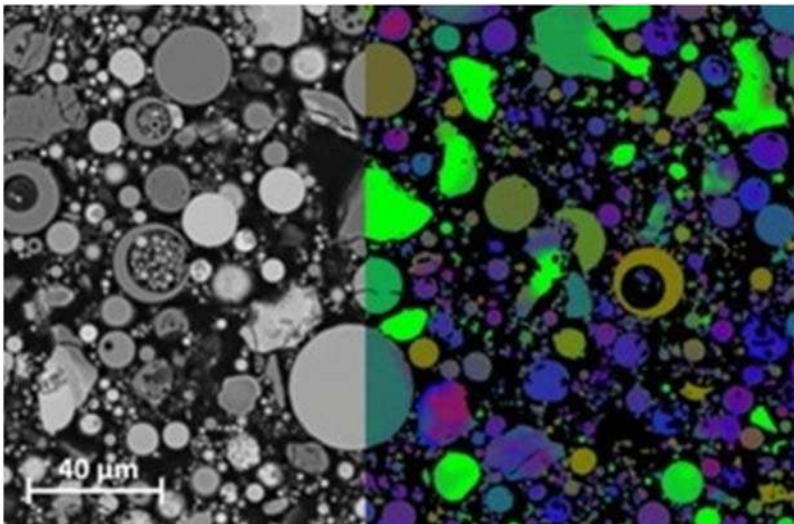


**Figure 3.1** The BSE image of fuel ash in the binder material.

Additionally, it also has spherical shape particles as well as dispensation of particle dimensions of fly ash as it provides a lower water demand (Abel & Rancitelli, 1975; Provis et al., 2009) and a greater particle packing density (Kırgız, 2020). Therefore with an enterprise for transforming the byproducts into construction materials and mitigating the CO<sub>2</sub> release globally a large amount of work has been done on surface precipitation modeling of fuel ash (Apul et al., 2005), high-strength BBMs containing fuel ash (Cobb et al., 1992), and structural evaluation of fuel ash (Sindhunata et al., 2008). Approximately 395 million tons of fuel ash is generated each year in the globe, and its disposal cost is among \$120 and \$140 for each ton (Lokeshappa & Dikshit, 2011). In 2009, Piispanen et al. confirmed that there could be a higher capacity for using fuel ash in various applications, including manufacture of construction binders (Piispanen et al., 2009). McCarthy et al. stated on the current advancement that fuel ash could minimize sulfate heave in lime-stabilized soils (McCarthy et al., 2012). In addition to the fact, high-volume fuel ash could be added/substituted in the BBM and also helps increase the durability capacity (Glasser et al., 2008) and the strength gain (Malhotra, 1990) of binder-based construction materials, without capturing CO<sub>2</sub>. In spite of the broad application opportunity and growth in requirement of reuse of fuel ash, plenty of studies have been made on the properties of fuel ash because of variability of the fuel ash generated. Miscellaneousness of chemical compositions and microstructures, for example, spherical glass structures and crystalline structures, have been determined simultaneously in the fuel ash. Table 3.2 presents the properties of class F PFA and class C PFA (Kırgız, 2023) used for comparison with the properties of high-loss-on-ignition (LOI) PFA (Locum et al., 2017) and the requirements of class F PFA, class C PFA, and class N PFA sorted by AASHTO M295 (AASHTO M 295, 2019).

**Table 3.2** The properties of the class F PFA and class C PFA used for comparison with the properties of high-LOI PFA and the requirements of class F PFA, class C PFA, and class N PFA sorted by AASHTO M295 PFA and requirements as AASHTO M 295.

Chemical component (%)	Class F PFA used in section 6	Class C PFA used in section 5	High-LOI PFA used by Locum et al. in 2017	Class F PFA sorted by AASHTO M 295	Class C PFA sorted by AASHTO M 295	Class N PFA sorted by AASHTO M 295
Silicon dioxide	44.4	38.4	47.8	—	—	—
Aluminum oxide	22.6	21.8	21.5	—	—	—
Iron oxide	17.3	5.2	8.7	—	—	—
SiO <sub>2</sub> + Al <sub>2</sub> O <sub>3</sub> + Fe <sub>2</sub> O <sub>3</sub>	84.3	65.4	78	≥ 70	≥ 50	≥ 70
Calcium oxide	5.1	21.3	7.9	—	—	—
Magnesium oxide	1	4.4	1.7	—	—	—
Sulfur trioxide	1.6	1.7	0	≤ 5	≤ 5	≤ 4
Alkali (Na <sub>2</sub> O + 0.66 K <sub>2</sub> O)	1.7	2	1.1	≤ 1.5	≤ 1.5	≤ 1.5
Loss on ignition (LOI)	2.88	0.7	11.1	≤ 5	≤ 5	≤ 5

### 3.5 High-technology additive of graphite nanoparticles

Despite a well-known preparation process of the high-technology additive material of nGs since a century, today's comprehensive studies also show a great effort to better understand their microstructures/nanostructures; components; and electrical, thermal, and optical properties in accordance with desirable applications as artificial nGs (Dreyer et al., 2010). Metal-based graphite exhibits excellent interconnection behavior, which is very similar to the property of calcined clay minerals found. On the contrary to the studies on silicate (Giannelis et al., 1999) a few science literature studies have focused on the use of nGs for binders.

The nGs are significantly hydrophobic, as is known from the grand carbon component in the field of lamination. They can be placed between water and other solvent molecules along with a surprisingly high level of lengthy span structure (Barroso-Bujans et al., 2010; Cerveny et al., 2010). nGs can also lodge surfactants which have cationic properties (Matsuo et al., 1999), alkylchlorosilanes (Matsuo et al., 2005), and alkylamines (Matsuo et al., 2007).

### 3.6 Admixture of a superplasticizer

The superplasticizer (SP) manufactured by chemical industry is an admixture for adjustment of workability in the BBM and could demonstrate the same effect as the air-entrainment admixture, which also has air formation entrapped (Massana et al., 2018). The SPs used in BBMs are of four major types: vinyl copolymers, sulfated naphthalene formaldehyde, polycarboxylic ethers, and sulfated melamine formaldehyde (Aicha, 2020). Research studies in the science literature focus on their type and dosage to obtain the most constant workability through flow. For various dosages of SPs used as binder weights in BBMs the relation between flow time and SP dosage is reported by Benaicha et al. in 2019, as seen in Fig. 3.2 (Benaicha et al., 2019).

As will be understood from Fig. 3.2 the SP lessened the flow time of BBM, using a Marsh cone for measurement, even depending upon the dosage of SP. The relationship specifies two major factors that manage the rheology of the synthesis of BBM-SP in Fig. 3.2: (1) the critical saturation degree of SP dosage in the BBM related to the standard deviation of the relationship, 1% SP by the binder mass; (2) in the critical saturation dosage of SP the optimum flow time is at 22 seconds. It should be noted that the degree of saturation of SP and the flow time could be different because of components of BBM mixing. In other words, this depends upon the mixing method and the component in the BBM in which the materials are incorporated. After the saturation degree the addition of SP does not maintain the flow of mortar constant (Fig. 3.2). However, the abundance of addition of SP could retard the setting time of binder and lead to the risk of segregation between binder matrix and aggregate stack.

The advances are because of the tight connections between the SP and the binder particle. Therefore mixing water entrapped between the fine aggregates may spread

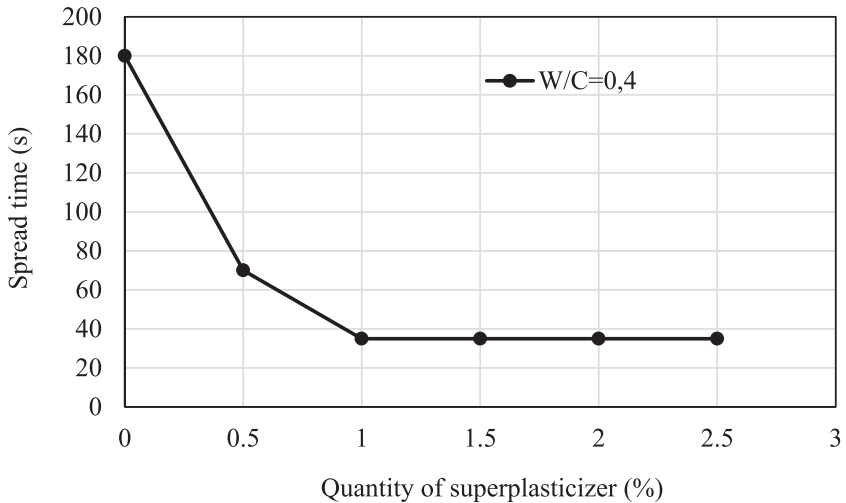


**Figure 3.2** The relation between flow time and superplasticizer dosage.

freely, which eases the flow and workability of the BBM. This could be attributed to the fact that it retards the yield stress of the BBM (Fig. 3.2). At the same stage the reduction in the tight connection efficiency led to the increase in the dosage of SP. The advancement of yield stress (Fig. 3.2) is similar to the flow time of BBM (Fig. 3.2). In spite of the growth of dosage of SP, it could not change constancy of all these factors.

### 3.6.1 *Mixing, handling, placing, and forming processes for upcycling of class F pulverized fuel ash*

Table 3.3 shows the mixing proportion of constituent materials for one cubic meter of ASTM type I binder grout, nG-added ASTM type I binder grout, class F PFA–binder grout, and nG-added class F PFA–binder grout along with SP or without SP relatively.

### 3.6.2 *Test program*

The test of compression force for all ecofriendly grout materials was performed on cubic samples with dimensions of  $50 \times 50 \times 50 \pm 0.8$  mm according to BS EN 196-1 standard rules. The test of splitting tensile force was performed according to ASTM C1006/C1006M-20a standard specifications. The EN 196-1 standard specifications were followed to measure the failure of all ecofriendly grout materials in the flexure force. In all tests the force loading velocity was 0.008 mm/sn. The average quantity of sample obtained is utilized in regression analysis to estimate strength from mixing materials properly, nG/ASTM type I cement and nG/class F PFA–cement.

**Table 3.3** The mixing proportion of constituent materials for one cubic meter of ASTM type I binder grout, nG-added ASTM type I binder grout, class F PFA–binder grout, and nG-added class F PFA–binder grout along with SP or without SP relatively.

Types of mixing materials	Relative content of the conventional binder and binder-based material					nG/ASTM type I binder	
	Water	ASTM type I binder	Fine aggregate (<2 mm)				
Reference	1	1.3	6			0	
Types of mixing materials	Relative content of the conventional binder and binder-based material along with nGs					nG/ASTM type I binder	
	Water	ASTM type I binder	Fine aggregate (<2 mm)	nG	Superplasticizer		
100%ASTM&0.34%nG	1	1.3	6	0.0044	0	0.003	
100%ASTM&0.84%nG	1	1.3	6	0.0109	0	0.009	
100%ASTM&1.7%nG	1	1.3	6	0.0221	0	0.017	
Types of mixing materials	Relative content of conventional class F PFA–binder and binder-based material along with SP					nG/class F PFA–binder ratio	
	Water	ASTM type I binder	Fine aggregate (<2 mm)	Class F PFA	nG		Superplasticizer
65%ASTM&35%FPFA	1	1.3	6	0.699	0	0	0
Types of mixing materials	Relative content of conventional class F PFA–binder and binder-based material along with nGs and SP					nG/class F PFA–binder ratio	
	Water	ASTM type I binder	Fine aggregate (<2 mm)	Class F PFA	nG		Superplasticizer
65%ASTM&35%FPFA&0.34%nG	1	1.3	6	0.699	0.0044	0	0.003
65%ASTM&35%FPFA&0.84%nG	1	1.3	6	0.699	0.0109	0	0.009
65%ASTM&35%FPFA&1.7%nG	1	1.3	6	0.699	0.0221	0	0.017
65%ASTM& 35%FPFA&1.7% nG&1.52%SP	1	1.3	6	0.699	0.0221	0.0198	0.017

## 3.7 Properties related to strength

### 3.7.1 Splitting tensile strength

Fig. 3.3 shows the relationship between nG/class F PFA–binder and splitting tensile strength in BBMs made of class F fuel ash, which is a latent hydraulic substitution, and ASTM type I cement and water and fine aggregate along with the high-technology additive of nGs and the admixture of an SP. Since the splitting tensile strength results of reference grout and ASTM type I binder with nG grout and relationships between the splitting tensile strength and nG/ASTM type I binders are given in Chapter 5, Natural pozzolan as hydraulic binder substitution in combination with recycled aggregates, this subsection only depends on the splitting tensile strength results of class F PFA–binder, class F PFA–binder with nGs, and class F PFA–binder with nGs and SP.

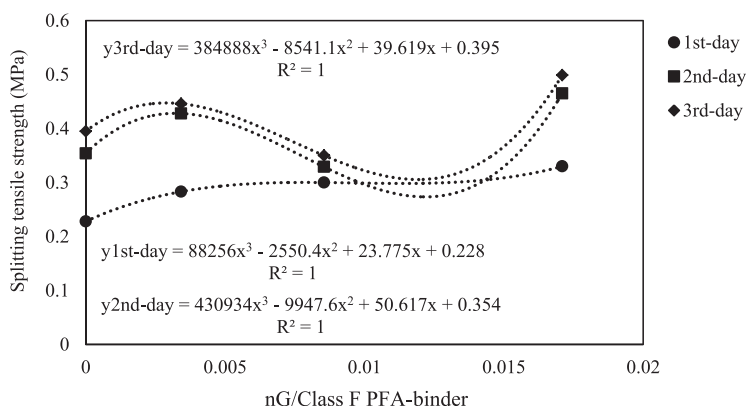


**Figure 3.3** Relationship between nG/class F PFA–binder and splitting tensile strength in binder-based materials.

Strength of BBM is an intrinsic property. Nevertheless, as a practical point of view, it is also a factor of the physical and mechanical system which helps the BBM develop (Neville, 1993). Normally, it has to be a solution to better explain the criteria of failure under whole practicable strength combinations through a single strength property, for example, strength in uniaxial tensile. This chapter also presents such a solution to estimate the splitting tensile strength properties of BBM from the mixing component of the BBM, as seen in Fig. 3.3. In addition to the numerical estimation studies for one property from another, a few interesting studies focused on the splitting tensile strength of grout containing high-volume PFA. For instance, Sampaio and Cabral indicated that at 28 days the whole PFA grouts show greater splitting tensile strength than the reference grout and the greatest splitting tensile strength is in grout mixes with binder 50% and lime 12.5% and PFA 37.5%. To achieve this splitting tensile strength development, Sampaio and Cabral used the PFA in which the total oxides of silicon, aluminum, and iron are more than 84%;

the specific mass is  $2360 \text{ kg/m}^3$ ; and the maximum grain size is  $5.01 \mu\text{m}$  (Sampaio & Cabral, 2017). To develop equations for BBM strength, it should be considered that such factors as strength at the initiation of failure, BBM mixing properties, and age of test are a preliminary point. The equations presented can be used for a numerical evaluation of the failure of BBM under splitting tensile strength with the parameters of mixing that helped prepare the BBM. Some experimental data for samples of various types are shown in Fig. 3.3. The application of equations has to be ceased since the nG-to-binder ratio has quantities such that the nG-to-binder ratio can exceed 0.017. The behavior of BMM is than no longer elastic but plastic.

### 3.7.2 Flexural strength

Fig. 3.4 shows the relationship between nG/class F PFA–binder and flexural strength in BBMs made of class F fuel ash, which is a latent hydraulic substitution, and ASTM type I cement and water and fine aggregate along with the high-technology additive of nGs and the admixture of an SP. Since the flexural strength results of reference grout and ASTM type I binder with nG grout and relationships between the flexural strength and nG/ASTM type I binders are given in Chapter 5, Natural pozzolan as hydraulic binder substitution in combination with recycled aggregates, this subsection only depends on the flexural strength results of class F PFA–binder, class F PFA–binder with nGs, and class F PFA–binder with nGs and SP.

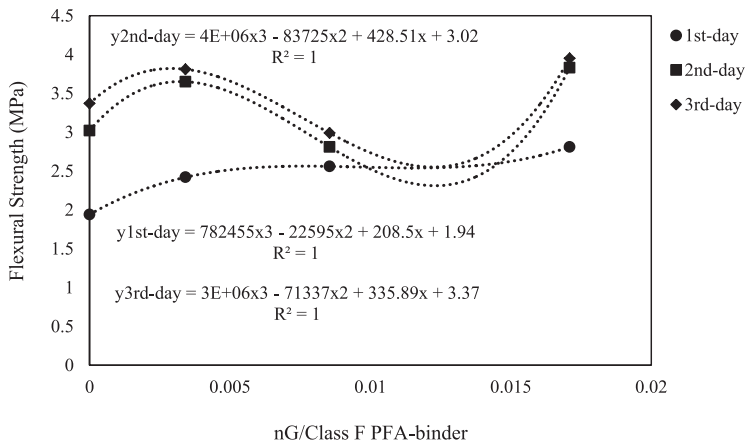


**Figure 3.4** Relationship between nG/class F PFA–binder and flexural strength in binder-based materials.

There are also a number of studies related to BBMs made of high-volume fuel ash, low-volume cement binder, SP, gypsum, and CH. Such a study conducted by Drury et al. replaces 47% and 70% cement binder with the fuel ash in the BBM. They apply regular water curing for their samples and make their flexural strength increase more than over 3% when compared with control BBM (Drury et al., 2017). To save natural

raw materials and the environment and to reduce the construction cost and CO<sub>2</sub> release, plenty of studies on replacement of cement binder with fuel ash in the BBM could also be found. However, this chapter also depends on reaction between the nGs and the class F PFA in the BBM because the class F PFA is a byproduct which is an artificial pozzolanic material as well as has latent hydraulic activity, and the nGs are an active strength-increasing nanomaterial for binder-based construction materials containing a high ratio of calcium oxide (CaO) and calcium hydroxide (Ca(OH)<sub>2</sub>). Additionally, this chapter uses the data obtained from experimental flexure test; a regression analysis was carried out on the relationship between the flexural strength and the mixing component of BBM. Between various types of linear regression equations found the polynomial equations were found to be the most suitable in Fig. 3.4 because the coefficients of determination were great. Thus it may be ideal to use the mixing components of BBM for estimating the flexural strength of BBM.

### 3.7.3 Compressive strength

Fig. 3.5 shows the relationship between nG/class F PFA binder and compressive strength in BBMs made of class F fuel ash, which is a latent hydraulic substitution, and ASTM type I cement and water and fine aggregate along with the high-technology additive of nGs and the admixture of an SP. Since the compressive strength results of reference grout and ASTM type I binder with nGs and relationships between the compressive strength and nG/ASTM type I binders are given in Chapter 5, Natural pozzolan as hydraulic binder substitution in combination with recycled aggregates, this subsection only depends on the compressive strength results of class F PFA–binder, class F PFA–binder with nGs, and class F PFA–binder with nGs and SP.

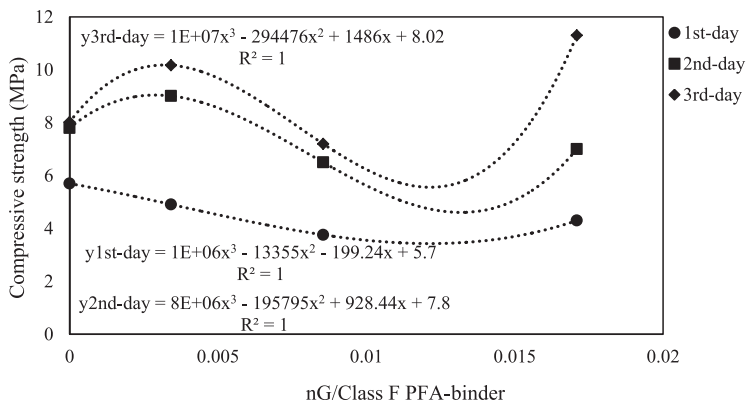


**Figure 3.5** Relationship between nG/class F PFA–binder and compressive strength in binder-based materials.

In 2017 Cohen et al. reported a significant study on the class F PFA using concrete as sand substitution. They determined that class F PFA used contains mainly mullite ( $3\text{Al}_2\text{O}_3-2\text{SiO}_2$ ) and quartz ( $\text{SiO}_2$ ) with X-ray diffraction analysis. Its trace



elements are hematite ( $\text{Fe}_2\text{O}_3$ ), calcite ( $\text{CaCO}_3$ ), lime ( $\text{CaO}$ ), magnetite ( $\text{Fe}_3\text{O}_4$ ), and anhydrite ( $\text{CaSO}_4$ ). In concrete, class F PFA, as a sand substitution material, is very active according to the results of compressive strength measured by Cohen et al. The high compressive strength gain because of the activation of class F PFA was attributed by them to a reaction between calcium hydroxide ( $\text{Ca}(\text{OH})_2$ ) and particles of class F PFA to result in new C-S-H formation (Cohen et al., 2017). Additionally, Sampaio and Cabral reported that at 28 days, whole PFA mortars show greater compressive strength than reference mortar and the greatest compressive strength is in mortar mixes with cement 50% and lime 12.5% and PFA 37.5%. To achieve this compressive strength development, Sampaio and Cabral used the PFA whose properties were explained in the section of splitting tensile strength (Sampaio & Cabral, 2017). On the contrary to class F PFA and class C PFA and class N PFA specified by AASHTO M295 (AASHTO M 295, 2019) a research study conducted by Locum et al. used the limestone screening with a PFA supplement which also has a high-LOI component, 11.1%, as well as the total of 78% of  $\text{SiO}_2 + \text{Al}_2\text{O}_3 + \text{Fe}_2\text{O}_3$ . They demonstrated that although the PFA used has 91.7% greater LOI than the PFA known as class C, F, and N, the limestone screening with high-LOI PFA meets the whole criteria of TDOT 204.06B (TDOT 204.06B, 2015) for compressive strength (Locum et al., 2017). They sincerely hoped that the controlled low-strength materials provide an important way of outlet for the PFA containing a high ratio of LOI and the limestone screening used. Additionally, this chapter uses the data obtained from experimental compression test; a regression analysis was carried out on the relationship between the compressive strength and the mixing component of BBM. Between various types of linear regression equations found the polynomial equations were found to be the most suitable in Fig. 3.5 because the coefficients of determination were high. Thus it could be ideal to use the mixing component of BBM for estimating the compressive strength of BBM.

### 3.7.4 Strength gain index at an early age

Since recent studies, like class F PFA–binder, which replaces a great quantity of cement with PFA, there is a need for strength gain index (SGI). There is not enough to keep flow constant at the same level in materials containing PFA because the PFA, which does not react with cement during hydration, leads to the flocculation within the material hardened. To protect the material from the flocculation, there is a need for SGI. In current studies, SGI has been calculated as the ratio of the compressive strength of PFA–BBM to the compressive strength of the reference material at the age of 28 days curing time. In this chapter, there is a certain difference that the SGI of BBMs depends principally on the tensile strength, the flexural strength, and the compressive strength at an early age of curing time. This index could be used as pozzolanic activity index in the hydraulic binder studies containing PFA and other byproducts as substitution materials. Fig. 3.6 shows the SGI for the flexural strength, the compressive strength, and the splitting tensile strength of grout made of ASTM type I binder, ASTM type I binder and nGs, class F PFA–binder, class F PFA–binder and nGs, and class F PFA–binder and nGs and SP.

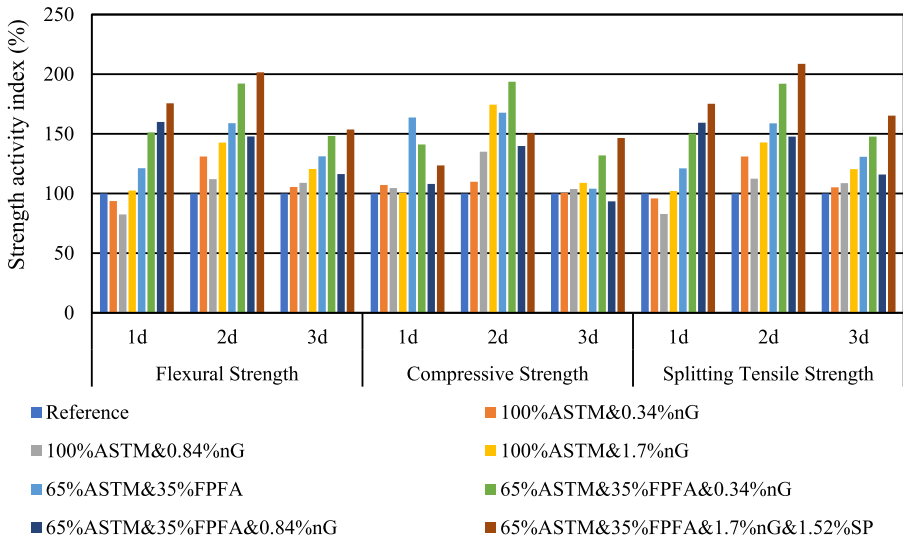


**Figure 3.6** Strength activity index for the flexural strength, the compressive strength, and the splitting tensile strength of grout made of ASTM type I binder, ASTM type I binder and nGs, class F PFA–binder, class F PFA–binder and nGs, and class F PFA–binder and nGs and SP.

SGI was calculated using Formula 3.1. Formula 3.2 was used to compute the strength that was because of the pozzolanic reaction (SPR). The SPR is the difference between the SGI with the PFA and nGs and SP ( $SGI_{PFA\&nG\&SP}$ ) and the SGI with nGs and SP PFA ( $SGI_{nG\&SP}$ ).

$$SGI = \frac{\text{The strength of the grout with PFA binder and nG and superplasticizer}}{\text{The strength of the reference grout}} \quad (3.1)$$

$$SPR = SPR_{PFA\&nG\&SP} - SPR_{nG\&SP} \quad (3.2)$$

### 3.7.5 Strength variation in binders used commonly

Strength variation in PC used depends upon the lack of conformity in the natural raw materials extracted in its production, either various resources of supply or resources of mining (Neville, 1959). Moreover, diversity in steps of cement production, variation of ash component of coal used to burn farin of cement, and calculation variation in mixing of raw materials to obtain the target chemical component of cement contribute to the strength variation in commercial cements (Kırgız, 2007). A magnitude of the strength variation in commercial cement is presented in Fig. 3.7, which demonstrates the compressive strength results of tests on CEM I N 32.5N cement mortar and ASTM type I cement mortar made of samples of cement obtained from the same plant in Turkey and the United States at intervals of 2 weeks.

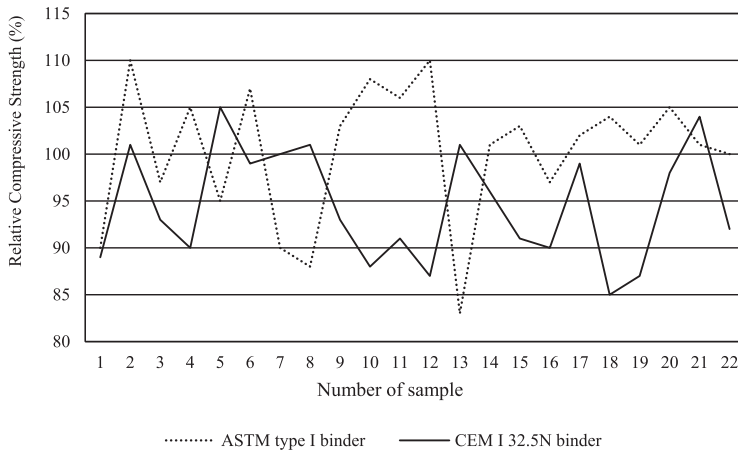


**Figure 3.7** A magnitude of the strength variation in commercial cement. The compressive strength variations of CEM I N 32.5N cement mortar and ASTM type I cement mortar.

The strength is stated as a percentage of the mean strength of whole samples from studies given, and each curve is an average of strength ratios measured at 28 days. BS EN 197–1 standard (BS EN 197–1:2011, 2019) gives a way of assessing the conformity of cement, which accepted  $\pm 10\%$  increase and decrease in the target compressive strength, while ASTM Standard C917/C917M-18 uses a method of assessing the uniformity of cement from one single resource (ASTM C917/C917M–18, 2018). The standard deviation of the compressive strength of BBM because of the variation in cement does not rise with aging of BBM; truly, plenty of data obtained from German cement manufacturing experiments recommend that there was a certain decrease of up to 1 MPa (Wright, 1958). As compressive strength increases with aging, the coefficient of variation of compressive strength suits smaller once the BBM is older. Table 3.4 presents data of the variability of strength in binders at different ages at test.

**Table 3.4** Strength variation of BBMs made of different silos of cement in a plant. Strength variation of BBMs made of different silos of cement in a plant.

Material	Property	Age at test day					
		1	3	7	28	91	365
BS EN 196-1 standard grout	Mean strength (MPa)	6.1	22	34.8	50.7	60.4	69.4
	Standard deviation	3.2	5.5	5	3.9	4.2	4.4
	Coefficient of strength variation (%)	52	25	14	8	7	6
	Standard deviation between silos	3.2	5.7	5	3.6	3.6	4
	Standard deviation within silos	0.5	1	1.2	1.9	3.4	3.3

(Continued)

**Table 3.4** (Continued)

Material	Property	Age at test day					
		1	3	7	28	91	365
BBM with a water-to-binder ratio of 0.5	Mean strength (MPa)	15.4	27.2	30.7	39.7	49.8	57.4
	Standard deviation	4.6	4.3	3.9	4.8	4.6	4.6
	Coefficient of strength variation (%)	30	16	13	12	9	8
	Standard deviation between silos	4.5	4.3	3.8	4.8	4.5	4.5
	Standard deviation within silos	0.8	1.1	1.1	1.6	1.7	1.9

This behavior is not expected since a great part of the variation in the compressive strength of cement is because of the changes in fineness of cement and in the calcium hydroxide ( $\text{Ca}(\text{OH})_2$ ) component and in the calcium-silica-hydrate (C-S-H) gel component: The influences of the parameters are the greatest at early ages with the time stop to be important. The standard deviation within a binder batch increases with an increase in average strength. [Table 3.5](#) presents the quantity of standard deviation of strength of BBM made in situ.

**Table 3.5** Quantity of standard deviation of strength of BBM made in situ.

Reasons	Standard deviation	
	Good reference	Fair reference
From strength variation increase in situ	3.1	4.8
From strength variations in binder from the plant	2.7	2.7
Total where the binder is from a plant	4.1	5.5
From strength variations between binder plants	4.8	4.8
Total where the binder is from a number of plants	6.2	7.2

[Fig. 3.7](#) and [Tables 3.4](#) and [3.5](#) illustrate that either the use of a binder from different plants or even the use of a binder from different silos in a plant results in a certain strength variation of the BBM. A vital part of this strength variation can be removed by the use of a binder from a silo at the plant. Ultimately, it should be stated that the strength variation in binder influences early strength gain of BMM negatively, that is, the strength usually established by test; nevertheless, the strength of most application importance is not essential.

### 3.8 Conclusion

Various BBM mixtures were employed in the chapter, which helped obtain a significant trend in the relationship between the mixing component of BBM and the

compressive and flexural and splitting tensile strengths of the BBM. The effect of nG-to-binder ratio on the strengths of BBM is significant as the nGs and SP improved the properties of class F PFA–binder and BBMs, thereby increasing the early compressive strength. The flexural strength of the BBM was greater than that of the conventional BBM and reference grout. This indicated that the compatibility of nGs and SP helps in improving the strength of flexural structures. Additionally the splitting tensile strength of the BBM was found to be greater when compared to both the conventional BBM and reference grout. This result unveils that the compatibility of nGs and SP could be useful in improving the strength of the whole tensile elements. The polynomial-type regressions were found to be suitable in predicting the strengths of BBM. A significant development was observed in the predicting of strengths of flexural, compressive, and splitting tensile when the early day of curing was taken into account. Moreover the chapter presented an innovative SGI for the class F PFA–binder system using the data of flexural, compressive, and splitting tensile strengths and recommended that a research study has to be performed from the same silo of cement in a plant of cement.

## References

- AASHTO M 295. (2019). *Standard specification for coal fly ash and raw or calcined natural pozzolan for use in concrete*. American Association of State Highway and Transportation Officials (AASHTO).
- AASHTO M 85. (2020). *Standard specification for Portland cement*. American Association of State Highway and Transportation Officials (AASHTO).
- Abel, K. H., & Rancitelli, L. A. (1975). *Major, minor, and trace element composition of coal and fly ash, as determined by instrumental neutron activation analysis* (Vol. 141, pp. 118–138). ACS: American Chemical Society. Available from <https://doi.org/10.1021/ba-1975-0141.ch010>.
- Aicha, M. B. (2020). The superplasticizer effect on the rheological and mechanical properties of self-compacting concrete. In P. Samui, N. R. Iyer, D. Kim, & S. Chaudhary (Eds.), *New materials in civil engineering* (pp. 315–331). Elsevier.
- Apul, D. S., Gardner, K. H., Eighmy, T. T., Fällman, A. M., & Comans, R. N. J. (2005). Simultaneous application of dissolution/precipitation and surface complexation/surface precipitation modeling to contaminant leaching. *Environmental Science and Technology*, 39(15), 5736–5741. Available from <https://doi.org/10.1021/es0486521>.
- ASTM C150/C150M-20. (2020). *Standard specification for Portland cement*. ASTM International.
- ASTM C917/C917M–18. (2018). *Standard test method for evaluation of variability of cement from a single source based on strength*. ASTM International. Available from [https://doi.org/10.1520/C0917\\_C0917M-18](https://doi.org/10.1520/C0917_C0917M-18).
- Barroso-Bujans, F., Cervený, S., Alegri, A. A., & Colmenero, J. (2010). Sorption and desorption behavior of water and organic solvents from graphite oxide. *Carbon*, 48(11), 3277–3286.
- Benaïcha, M., Hafidi Alaoui, A., Jalbaud, O., & Burtshell, Y. (2019). Dosage effect of superplasticizer on self-compacting concrete: Correlation between rheology and strength. *Journal of Materials Research and Technology*, 8(2), 2063–2069. Available from <https://doi.org/10.1016/j.jmrt.2019.01.015>.

- Bentz, D. P., & Garboczi, E. J. (1991). Simulation studies of the effects of mineral admixtures on the cement paste-aggregate interfacial zone. *ACI Materials Journal*, 88(5), 518–529.
- BS EN 197-1:2011. (2019). *Cement: Composition, specifications and conformity criteria for common cements*. British Standard Institute.
- Cerveny, S., Barroso-Bujans, F., Alegri'A, A., & Colmenero, J. (2010). Dynamics of water intercalated in graphite oxide. *Journal of Physical Chemistry C*, 114(6), 2604–2612.
- Cobb, J. T., Mangelsdorf, C. P., Blachere, J. R., Banerjee, K., Reed, D., Crouch, C., Miller, C., Li, J., & Trauth, J. (1992). *High-strength Portland cement concrete containing municipal solid waste incinerator ash* (pp. 264–275). ACS: American Chemical Society. Available from <https://doi.org/10.1021/bk-1992-0515.ch021>.
- Cohen, H., Lieberman, R. N., & Knop, Y. (2017). Coal residues: The new golden treasure. In *World of Coal Ash (WOCA) conference*. Lexington, KY, University of Kentucky.
- Cottis, B., Graham, M., Lindsay, R., Lyon, S., Richardson, T., Scantlebury, D., & Stott, H. (2010). *Shreir's corrosion*. Elsevier Science.
- Dreyer, D. R., Park, S., Bielawski, C. W., & Ruoff, R. S. (2010). The chemistry of graphene oxide. *Chemical Society Reviews*, 39(1), 228–240.
- Drury, J. T., Looney, T. J., Arezoumandi, M., & Volz, J. S. (2017). An experimental study on bond strength of reinforcing steel in high-volume fly-ash concrete. In *World of Coal Ash (WOCA) conference*. University of Kentucky.
- Elsharief, A., Cohen, M. D., & Olek, J. (2003). Influence of aggregate size, water cement ratio and age on the microstructure of the interfacial transition zone. *Cement and Concrete Research*, 33(11), 1837–1849. Available from [https://doi.org/10.1016/S0008-8846\(03\)00205-9](https://doi.org/10.1016/S0008-8846(03)00205-9).
- Flower, D. J. M., & Sanjayan, J. G. (2007). Green house gas emissions due to concrete manufacture. *International Journal of Life Cycle Assessment*, 12(5), 282–288. Available from <https://doi.org/10.1065/lca2007.05.327>.
- Gao, J. M., Qian, C. X., Liu, H. F., Wang, B., & Li, L. (2005). ITZ microstructure of concrete containing GGBS. *Cement and Concrete Research*, 35(7), 1299–1304. Available from <https://doi.org/10.1016/j.cemconres.2004.06.042>.
- Giannelis, E., Krishnamoorti, R., & Manias, E. (1999). Polymer-silicate nanocomposites: Model systems for confined polymers and polymer brushes. In K. Binder, P.-G. de Gennes, E. Giannelis, G. Grest, H. Hervet, & S. Granick (Eds.), *Polymers in confined environments, advances in polymer science* (138, pp. 107–147). Springer, 107–147. Available from [https://doi.org/10.1007/3-540-69711-X\\_3](https://doi.org/10.1007/3-540-69711-X_3).
- Glasser, F. P., Marchand, J., & Samson, E. (2008). Durability of concrete—degradation phenomena involving detrimental chemical reactions. *Cement and Concrete Research*, 38(2), 226–246. Available from <https://doi.org/10.1016/j.cemconres.2007.09.015>.
- Han, S. H., Kim, J. K., & Park, Y. D. (2003). Prediction of compressive strength of fly ash concrete by new apparent activation energy function. *Cement and Concrete Research*, 33(7), 965–971. Available from [https://doi.org/10.1016/S0008-8846\(03\)00007-3](https://doi.org/10.1016/S0008-8846(03)00007-3).
- Hu, M., Guo, J., Fan, J., li, P., & Chen, D. (2019). Dispersion of triethanolamine-functionalized graphene oxide (TEA-GO) in pore solution and its influence on hydration, mechanical behavior of cement composite. *Construction and Building Materials*, 216, 128–136. Available from <https://doi.org/10.1016/j.conbuildmat.2019.04.180>.
- Kırğız, M. S. (2007). *Usage of the wastes of marble and brick industries in cement manufacturing as mineralogical additive* (p. 257). Gazi University. <https://tez.yok.gov.tr/UlusalTezMerkezi/giris.jsp>
- Kırğız, M. S. (2014). Advances in physical properties of C class fly ash cement systems blended nanographite—Part 1. *ZKG International*, 67(12), 42–48. Available from <http://www.zkg-online.info/en/index.html>.

- Kirgiz, M. S. (2015). Advances in physical properties of C class fly ash–cement systems blended nanographite. *ZKG International*, 60–67.
- Kirgiz, M. S. (2018). Effect of mineralogical substitution raw material mixing ratio on mechanical properties of concrete. *ZKG International*, 30–41.
- Kirgiz, M. S. (2020). Nano size particle packing for smart nanoconcretes and cement based materials: Theory and technology. In M. S. Liew, P. Nguyen-Tri, T. A. Nguyen, & S. Kakooei (Eds.), *Smart nanoconcretes and cement-based materials* (pp. 41–76). Elsevier. Available from <https://doi.org/10.1016/C2018-0-02596-7>.
- Kirgiz, M. S. (2023). In M. S. Kirgiz (Ed.), *Advance upcycling of by-products in binder and binder based materials: Class C fuel ash as hydraulic binder substitution in binder based material fortified with high technology additive of graphite nano particle*. Elsevier.
- Kuroda, M., Watanabe, T., & Terashi, N. (2000). Increase of bond strength at interfacial transition zone by the use of fly ash. *Cement and Concrete Research*, 30(2), 253–258. Available from [https://doi.org/10.1016/S0008-8846\(99\)00241-0](https://doi.org/10.1016/S0008-8846(99)00241-0).
- Li, X., Li, C., Liu, Y., Chen, S. J., Wang, C. M., Sanjayan, J. G., & Duan, W. H. (2018). Improvement of mechanical properties by incorporating graphene oxide into cement mortar. *Mechanics of Advanced Materials and Structures*, 25(15–16), 1313–1322. Available from <https://doi.org/10.1080/15376494.2016.1218226>.
- Liao, K. Y., Chang, P. K., Peng, Y. N., & Yang, C. C. (2004). A study on characteristics of interfacial transition zone in concrete. *Cement and Concrete Research*, 34(6), 977–989. Available from <https://doi.org/10.1016/j.cemconres.2003.11.019>.
- Locum, J. T., Crouch, L. K., & Badoe, D. (2017). Excavatable and early strength CLSM using high LOI fly ash and limestone screenings. In *World of Coal Ash (WOCA) conference*. Lexington, University of Kentucky.
- Lokeshappa, B., & Dikshit, A. K. (2011). Disposal and management of coal fly ash. In *International conference on life science and technology IPCBEE*. IACSIT Press, 3, pp. 11–14.
- Malhotra, V. M. (1990). Durability of concrete incorporating high-volume of low-calcium (ASTM Class F) fly ash. *Cement and Concrete Composites*, 12(4), 271–277. Available from [https://doi.org/10.1016/0958-9465\(90\)90006-J](https://doi.org/10.1016/0958-9465(90)90006-J).
- McCarthy, M. J., Csetenyi, L. J., Sachdeva, A., & Dhir, R. K. (2012). Identifying the role of fly ash properties for minimizing sulfate-heave in lime-stabilized soils. *Fuel*, 92(1), 27–36. Available from <https://doi.org/10.1016/j.fuel.2011.07.009>.
- Massana, J., Reyes, E., Bernal, J., León, N., & Sánchez-Espinosa, E. (2018). Influence of nano- and micro-silica additions on the durability of a high-performance self-compacting concrete. *Construction and Building Materials*, 165, 93–103. Available from <https://doi.org/10.1016/j.conbuildmat.2017.12.100>.
- Matsuo, Y., Miyabe, T., Fukutsuka, T., & Sugie, Y. (2007). Preparation and characterization of alkylamine-intercalated graphite oxides. *Carbon*, 45(5), 1005–1012.
- Matsuo, Y., Niwa, T., & Sugie, Y. (1999). Preparation and characterization of cationic surfactant-intercalated graphite oxide. *Carbon*, 37(6), 897–901.
- Matsuo, Y., Tabata, T., Fukunaga, T., Fukutsuka, T., & Sugie, Y. (2005). Preparation and characterization of silylated graphite oxide. *Carbon*, 43(14), 2875–2882.
- Neville, A. M. (1959). The relation between standard deviation and mean strength of concrete test cubes. *Magazine of Concrete Research*, 11(32), 75–84. Available from <https://doi.org/10.1680/mac.1959.11.32.75>.
- Neville, A. M. (1993). *Properties of concrete*. Longman Scientific and Technical.
- Pan, Z., He, L., Qiu, L., Korayem, A. H., Li, G., Zhu, J. W., Collins, F., Li, D., Duan, W. H., & Wang, M. C. (2015). Mechanical properties and microstructure of a graphene oxide-

- cement composite. *Cement and Concrete Composites*, 58, 140–147. Available from <https://doi.org/10.1016/j.cemconcomp.2015.02.001>.
- Peng, H., Ge, Y., Cai, C. S., Zhang, Y., & Liu, Z. (2019). Mechanical properties and microstructure of graphene oxide cement-based composites. *Construction and Building Materials*, 194, 102–109. Available from <https://doi.org/10.1016/j.conbuildmat.2018.10.234>.
- Piispanen, M. H., Arvilommi, S. A., Van Den Broeck, B., Nuutinen, L. H., Tiainen, M. S., Perämäki, P. J., & Laitinen, R. S. (2009). A comparative study of fly ash characterization by LA-ICP-MS and SEM-EDS. *Energy and Fuels*, 23(7), 3451–3456. Available from <https://doi.org/10.1021/ef801037a>.
- Provis, J. L., Rose, V., And, S. A. B., & Deventer, J. S. J. V. (2009). High-resolution nanoprobe x-ray fluorescence characterization of heterogeneous calcium and heavy metal distributions in alkali-activated fly ash. *Langmuir: The ACS Journal of Surfaces and Colloids*, 25(19), 11897–11904. Available from <https://doi.org/10.1021/la901560h>.
- Sampaio, K. N. H., & Cabral, A. E. B. (2017). Use of coal ash from thermal power plant in coating mortar. In *World of Coal Ash (WOCA) conference*. Lexington, KY, University of Kentucky.
- Sindhunata, Provis, J. L., Lukey, G. C., Xu, H., & Van Deventer, J. S. J. (2008). Structural evolution of fly ash based geopolymers in alkaline environments. *Industrial and Engineering Chemistry Research*, 47(9), 2991–2999. Available from <https://doi.org/10.1021/ie0707671>.
- TDOT 204.06B. (2015). *Standard specifications for road and bridge construction*. Tennessee Department of Transportation.
- Wright, P. J. F. (1958). Variations in the strength of Portland cement. *Magazine of Concrete Research*, 10(30), 123–132. Available from <https://doi.org/10.1680/macr.1958.10.30.123>.
- Yang, H., Monasterio, M., Cui, H., & Han, N. (2017). Experimental study of the effects of graphene oxide on microstructure and properties of cement paste composite. *Composites Part A: Applied Science and Manufacturing*, 102, 263–272. Available from <https://doi.org/10.1016/j.compositesa.2017.07.022>.



This page intentionally left blank

# Oil shale ash as hydraulic binder substitution in binder-based material with additive of superplasticizer and roller compaction method

Ahmed M. Ashteyat<sup>1</sup>, Amani Smadi<sup>2</sup>, Yousef S. Al Rjoub<sup>2</sup> and Mehmet Serkan Kirgiz<sup>3</sup>

<sup>1</sup>Department of Civil Engineering, University of Jordan, Amman, Jordan, <sup>2</sup>Department of Civil Engineering, Jordan University of Science and Technology, Amman, Jordan,

<sup>3</sup>Northwestern University, Chicago, IL, United States

## 4.1 Introduction

Cement and concrete material consumption are 15 times greater than that of steel in the world. In other words the consumption means that one person consumes more than 3 tons of concrete per year. The most significant mix constituent of concrete is cement, which emits not only carbon dioxide (CO<sub>2</sub>) but also nitrogen oxides (NO<sub>x</sub>) and methane (CH<sub>4</sub>), and the emissions involved are also very high, for example, 33.4 billion metric tons from fossil fuels and cement consumption and 3.3 billion tons from land-use changing with firing. These two examples lead to 100% CO<sub>2</sub> emission in the globe. The atmosphere, the land, and the oceans respectively absorb 50%, 26%, and 24% of CO<sub>2</sub>. Although the greatest emissions are caused by Portland cement manufacturing, the major and common construction binder material is still cement. In near future the manufacture of Portland cement will remain a concern to population growth in the world. In 1880, cement manufacturing was 2 million tons, and it increased to 5 billion tons in 2019 years (Mirza, 2019). To lessen the harmful effects of cement consumption the cement is partially replaced with supplementary cementitious materials (SCMs) such as oil shale ash (OSA), marble powder, rice husk ash (RHA), pulverized fuel ash, calcined clay, ground granulated blast furnace slag, limestone powder (LS), and so on in the cement-based material mixture, like the roller-compacted green concrete (RCGC) in the study. This method of cement replacement with the SCMs provides a clean production, which is an ecofriendly and sustainable green binder in the building industry.

To solve the problems and develop new ecology-based sustainable green cement-based materials the study enables to use OSA in the mixing of roller-compacted concrete (RCC) as the SCM. The RCC also uses Portland cement along

with pulverized fuel ash, which is the most known SCM, in its mixing design, and several other SCMs are also added in its mixing because the SCMs have valuable chemical composition for the growth of the cement hydration, the cement durability, the cement physical properties, and the cement mechanical properties. The demand of green material and reduction of the cost in construction industry has led to a current model for reuse, recycle, and upcycling of various wastes from manufacturing of various goods in the cement-based ecofriendly material system. One of the wastes essentially used is OSA, which contains very valuable chemical oxides and is generated by oil industry, with more than 250 billion tons in the world (Dabbas, 1997). Burning of oil shale for manufacturing the fuel-based energy is the main source of OSA. The environmental problems related to the production of OSA and the high cost of its disposal have attracted most researchers to examine its potential use in the cement and concrete industry (Al-Massaid et al., 1989; Ashteyat et al., 2012).

RCC was identified by ACI as concrete compacted by a roller; it means that a roller squashes the concrete in its fresh stance to form the RCC (Schrader, 2006). The RCC has similar constituents of traditional concrete mixing, with a broad range of materials and a low water-to-cement ratio. Its water-to-cement ratio is between 0.2 and 0.4; the aggregate gradation has different requirements according to normal concrete, and it needs SCMs as additives. RCC consistency requirement is different than traditional concrete in use. Mixing should be dry enough to be compacted by a roller vibrator, and the mixing water should be sufficient to wet aggregate stack and to start the hydration process of its binder during the mixing and compaction (Schrader, 2006). The RCC provides the strength and performance required as being in the conventional concrete as well as reduction of the oil-based asphalt use (Kassem et al., 2018; ACI, 2001).

The RCC used for the purpose of dam mixing usually contains a higher volume of pulverized fuel ash and/or other types of SCMs; RCC is also used for pavement mixing. The maximum quantity of the pulverized fuel ash used in the RCC for pavement mixing is usually 20% of the total binder mass. Regularly, using the pulverized fuel ash in the RCC mixing increases the fine material, leading to higher-yielding homogeneous paste and greater consistency (Marchand et al., 1997). The addition of pulverized fuel ash also provides a higher compressive strength as the microstructure of the RCC for pavement is improved with additional pozzolanic reactions between the Portland cement and the pulverized fuel ash (Kirgiz, 2018). Such byproducts as silica fume, marble powder, limestone dust, brick powder, graphite nanoparticles, OSA, ground granulated blast furnace slag, and RHA could be enumerated among other SCMs used extensively in the RCC mixing, and they enable to improve the strength of RCC, the density of RCC, and the frost resistance of RCC. The maximum quantity of SCM in the mixing of RCC is between 35% and 50% of the total binder mass (Kirgiz, 2018, 2019; Gauthier & Marchand, 2005; Pigeon & Malhotra, 1995).

However, plenty of comprehensive studies summarized plenty of benefits of SCMs used in RCC, as indicated by the following examples: Jingfu et al. (2009)

examined the features of stress and shrinkage of RCC along with tire rubber as a substitution material for sand, and the compressive stress was kept constant at 40 (MPa). Results showed that replacing the same volume of sand with the same volume of tire rubber particles reduced the workability of RCC. In the compression test the RCC specimens presented a higher ductile failure than the RCC with no tire rubber particles. Increasing the rubber tire particle content increased the splitting tensile stress, the flexural moment stress, and ultimate tension elongation. Villena et al. (2011) evaluated the properties of RCC mixing with the addition of RHA used for application in composite pavement. Results of Villena indicated that RHA caused significant improvement in the properties of RCC as the RCC mixing included 5% RHA. The addition increased the compressive stress, the flexural moment stress, and the modulus of elasticity in the RCC as well. This increase is referred to the curing age of the RCC, the RHA content, and the content of cement used. Ashteyat et al. (Madhkhan et al., 2012) investigated the potential use of waste white cement bypass dust (WCBPD) in producing RCC. Cement was replaced by WCBPD at 10%, 20%, 30%, and 40% with addition of polypropylene fiber in two percent values (0.25% and 0.5%). Results have shown that increasing WCBPD to 20%, 30%, and 40% replacement of cement has significantly decreased the mechanical properties of RCC mixes. However, the addition of PPF has improved the mechanical and durability properties of RCC mixes with WCBPD. Debieb et al. (2009) reported the possibility for the replacement of 100% of both coarse and fine natural aggregates (NAs) with the recycled concrete aggregate (RCA) in the mixing of the RCC. The results showed that the RCA has contained more chloride than sulfate, and the harmful content of RCA was leached as it was soaked in water. Significant differences were observed between the properties of original concrete and RCA concrete in the study, and the results showed that the need for considering of the harmful content of RCA was essential. Chafika et al. (Settari et al., 2015) studied the effects of the replacement of various sizes of the recycled asphalt pavement aggregate (RAPA) with the coarse and fine NAs on the mechanical properties and durability of the RCC. The experimental results revealed that it was possible to replace 50% of the RAPA with the NA in the RCC without any loss in the properties. Saeid et al. (Hesami et al., 2016) published a research article related to the effects of coal waste powder (CWP), coal waste ash (CWA), and LS powder on the mechanical properties of RCC pavement. Its test results pointed out that the use of CWP and CWA increased the water-to-cement ratio in the mixing of the RCC pavement. It was also noted that the RCCP mixture containing 5% CWP and/or 5% CWA showed similar performance as in the control of the RCC mixing. On the other hand, as the replacement of SCM with cement increased up to 20%, this replacement growth reduced the strength value and the modulus of elasticity in the RCC pavement at all curing ages.

In the light of the studies, environmental problems, and demand in cost reduction in oil and cement industries mentioned above, it is clear that a comprehensive study on the OSA used in cement-based materials is essential as there is no comprehensive study carried out. Therefore the aim of this research is to evaluate the use of OSA as one of the substitution materials for cement in the RCGC composite

mixing, to reduce the cost of processing of the RCGC and the high cost of disposal of the OSA, and to solve the environmental problems associated with the manufacturing of conventional oil and cement.

## 4.2 Materials and methods

### 4.2.1 Mix design of the roller-compacted concrete and the roller-compacted green concrete

The study designs the mixing contents and proportions of the RCGC according to the method of soil compaction, which is based on a current relationship between the moisture content and the dry density of the RCC. The maximum dry density at optimum water content is determined from a plot manufacturing of the RCGC for each cementitious material content. In this research the water-to-cement ratio is constant at 0.4 for both the RCGC specimens and the RCC specimens. The specimens include different cementitious contents, such as 0%, 13%, 14%, and 15%, along with different water contents, such as 4.5%, 5%, 5.5%, and 6% for each mixing cementitious content. It is clear from pioneer experiment on optimum moisture content (OMC) that the OMC occurred at cement content 13% with water content 5.1% ( $w/c = 0.4$ ). As the RCC is a special concrete, it has zero slump property. These zero slumps do not negatively affect the workability of RCC because the RCC needs a roller compaction for casting in situ. However, ACI identified the RCC and has used it with zero slump since 2000. Table 4.1 gives the RCC and the RCGC mixing that are used in casting specimens for different curing ages and for different tests.

**Table 4.1** Mixing proportion of the roller-compacted concrete (RCC) and the roller-compacted green concrete (RCGC).

Types of mixing		Mixing constituent proportion as kilogram per cubic meter							Ratio of mixing feature	
		Cement	Aggregate		Silica sand	Water	OSA	Water reducer (WR)	W/C	OSA/C
			CA > 4 (mm) <sup>a</sup>	FA < 4 (mm) <sup>a</sup>						
RCC	OSA-0%	266	924.6	1073	57.2	102.75	0	5.32	0.4	0
RCGC	OSA-10%	239.4	924.6	1073	57.2	102.75	26.6	4.78	0.4	0.1
	OSA-20%	212.8	924.6	1073	57.2	102.75	53.2	4.25	0.4	0.2
	OSA-30%	186.2	924.6	1073	57.2	102.75	79.8	3.72	0.4	0.3
	OSA-40%	159.6	924.6	1073	57.2	102.75	106.4	3.2	0.4	0.4

<sup>a</sup>CA stands for coarse aggregate, and FA stands for fine aggregate.

As the RCC needs to compact with a roller in situ, the mixing water content is only responsible for hydrate cement as well. The aggregate in mixing is in the stance that is dry surface and water-saturated. Therefore the water content is sufficient in [Table 4.1](#).

## **4.2.2 Preparation of the roller-compacted concrete and the roller-compacted green concrete**

### **4.2.2.1 Mixing**

For mixing the RCC and the RCGC constituent a tilting drum mixer, with a volume of 0.15 (m<sup>3</sup>), was used. To prepare the RCC and the RCGC, the following steps are applied: (1) Pour a little amount of water in the bowl mixer; (2) add the coarse aggregate; (3) put the cement and fine aggregate gradually; (4) add the water reducer at various percentage by cement weight to provide workability; (5) blend the constituents for about 6 minutes in the mixer to obtain cohesive mixes with the RCC and the RCGC.

### **4.2.2.2 Casting and curing**

Cylindrical steel mold, dimensions of 150 (mm) diameter and 300 (mm) height, was used to prepare the specimens of RCC and the RCGC for testing compressive strength and splitting strength, and cubic steel mold, dimensions of 150 × 150 × 150 (mm), was used for the tests of the freezing and thawing and the loss in weight after freezing and thawing, and prism steel mold, dimensions of 100 × 100 × 300 (mm), was used for testing the flexural stress. After mixing the fresh constituent materials of the RCC and the RCGC were placed as three layers in the mold, and all specimens were compacted according to ASTM C 1435 using a vibrating compaction hammer ([ASTM C1435/C1435M-14, 2014](#)). It has a minimum power input of 900 (W) and should be able to provide at least 2000 impacts per minute. Before all specimens were placed in a water tank to cure until testing at the 7th day, 28th day, and 90th day the casted specimens were covered with wetting burlap for 24 hours to prevent loss in the moisture content of specimens.

## **4.2.3 Analysis methods**

### **4.2.3.1 Chemical and physical properties of mixing materials**

The chemical composition of both the OSA and the conventional cement was identified according to the ASTM C114-07 standard method known as wet chemical analysis ([ASTM C 114-07, 2007](#)). To determine the aggregate granulometry, sieve analysis was carried out along with a sieve set according to ASTM C136 ([ASTM C128-01, 2001](#)). In addition to the analysis of chemistry and granulometry of the OSA, scanning electron microscopy (SEM) was used to analyze the shape of the OSA particles.

### **4.2.3.2 Density of fresh mixing**

The fresh density of the RCC mixing and the RCGC mixing was measured according to the specification in ASTM C138/C138M-09 ([ASTM C128-01, 2001](#); [ASTM C138/C138M-09](#)).

### 4.2.3.3 Density of hardened specimens

The hardened density of the RCC composite and the RCGC composite was measured according to the rules in ASTM C642-13 (ASTM C642-13, 2013).

### 4.2.3.4 Porosity measurement

The void as porosity was measured in the hardened specimens of the RCC and the RCGC according to the specification in ASTM C642-13 (ASTM C642-13, 2013). Porosity is defined as the ratio of the volume of voids to the total volume of the concrete mass. All specimens are dried in an oven at  $105^{\circ}\text{C} \pm 5^{\circ}\text{C}$  at the age of 90 days and then allowed to cool up to room temperature. To determine porosity the dry mass of the specimen is taken; then it is totally immersed in water until it achieves a constant water-saturated mass. To evaluate the porosity of the RCC and the RCGC and its relationship to the material's behavior the porosity of RCC and the RCGC was determined at the age of 90 days according to Eq. (4.1).

$$P = \left( 1 - \left( \frac{W_1 - W_2}{V \times q_w} \right) \right) \times 100\% \quad (4.1)$$

Here,  $P$  is the total porosity of the RCC and/or the RCGC (%),  $V$  is the volume of specimen ( $\text{cm}^3$ ),  $q_w$  is the water density, which equals to  $1000 \text{ (kg/m}^3\text{)}$ ,  $W_2$  is the mass of specimen after drying for 24 hours in an oven at  $105^{\circ}\text{C} \pm 5^{\circ}\text{C}$ , and  $W_1$  is the mass of specimen under water (kg).

### 4.2.3.5 Durability measurement

The freeze–thaw cycle resistance of hardened RCC and RCGC was determined on 150 (mm) cube specimens according to ASTM C666/C666M standard (ASTM C666/C666M-15, 2015). Loss in weight of the RCC and the RCGC was measured with a scale before and after the freezing–thawing cycle. After the freezing and thawing cycle of the RCC and the RCGC the study measured the specimens' weight loss ( $W$ ) using the following equation:

$$W = [(W_2 - W_1)/W_1] \times 100 \quad (4.2)$$

Here  $W_1$  is the initial weight of specimens before freeze–thaw cycles and  $W_2$  is the weight of specimen after  $n$  cycles. Also the compressive stress of the specimens of the RCC and the RCGC during the 38-day period per 300 cycles is determined.

### 4.2.3.6 Mechanical properties

In this research the compressive stress and the splitting tensile stress of the cylinder specimens were determined according to the standards of ASTM C 39 and ASTM C 496 and a universal testing machine (ASTM C39/C39M-18, 2018; ASTM C496/C496M-17, 2017). The compressive stress was determined on both the RCC and the RCGC after

their water curing at 7 days and 28 days. The flexural moment stress of the prism is evaluated according to ASTM C 293 (ASTM C293/C293M-16, 2016). This also presents the bending test of one point loading for the prism specimens of the RCC and the RCGC. The cylindrical composite specimens of RCC and RCGC were also prepared to evaluate the modulus of elasticity according to ASTM C 469 and determined at 90 days (ASTM C469/C469M-14, 2014). The reading of the stress and strain was measured through the help of the LVDT that was connected to the RCC and the RCGC. Then the modulus of elasticity is calculated from the ratios between the stress and the strain in the linear part.

#### 4.2.3.7 Microstructure and mineralogical phase analysis

To observe the chemical compound in the hardened inner structure of the RCC composite and the RCGC at 90 days a current SEM system was used according to the ASTM C1723-16 standard (ASTM C1723-16, 2022). To analyze the proportion of mineral phase in the RCC and the RCGC at 3 days and 14 days and 90 days the study uses the X-ray powder diffraction (XRD) method according to ASTM C1365-18 standard (ASTM C1365-18, 2018). The mineralogy of the RCC composite and the RCGC is evaluated with XRD in regard to the rules of both Bragg's law and the ASTM C1365-18 standard.

## 4.3 Results and discussions

### 4.3.1 Chemical and physical properties of mixing materials

#### 4.3.1.1 Cement

Table 4.2 gives both the chemical properties of conventional Portland cement (ASTM type I) and OSA-substituted ASTM type I cement used in preparing the RCC and the RCGC for experiments carried out in the study.

**Table 4.2** Chemical properties of the ASTM type I cement and the OSA-substituted ASTM type I cement used in the study.

Types of cement	Chemical properties (%)										
	CaO	SiO <sub>2</sub>	Al <sub>2</sub> O <sub>3</sub>	Fe <sub>2</sub> O <sub>3</sub>	MgO	SO <sub>3</sub>	Na <sub>2</sub> O	K <sub>2</sub> O	Alkali	TiO <sub>2</sub>	Loss in ignition
ASTM type I	64	20	4.69	3.78	2.46	2.27	0.02	0.4	0.265	—	0.78
10% OSA + 90% ASTM type I	62.3	19.9	4.8	3.6	2.29	2.8	0.018	0.42	0.248	0.02	1.24
20% OSA + 80% ASTM type I	60.6	19.8	4.95	3.42	2.12	3.41	0.016	0.44	0.220	0.04	1.7
30% OSA + 70% ASTM type I	58.9	19.7	5.08	3.24	1.96	3.98	0.014	0.46	0.193	0.06	2.16
40% OSA + 60% ASTM type I	57.2	19.6	5.21	3.06	1.79	4.56	0.012	0.48	0.165	0.08	2.62



Common cement is the combination of the oxides of calcium, silica, aluminum, sulfate, sodium, and potassium. The alkali and loss on ignition are within chemical components of cement. Apart from common cement the OSA-blended cement contains one more component, which is the oxide of titanium. This OSA blending provides the component of titanium oxide for common cement. Its content varies between 0.02% and 0.08% in the OSA-blended cement (Table 4.2). This means that the oxide of titanium could lead to new hydration compounds, for example, calcium-titanium-hydroxide (C-T-H).

#### 4.3.1.2 Aggregate

The aggregate stack in the RCC mixing and the RCGC mixing is a combination of coarse aggregate and fine aggregate and silica sand (55% coarse aggregate and 40% fine aggregate and 5% silica sand). The determined specific gravity and water absorption, according to ASTM C128, are respectively 2.62 and 1.5% for the coarse aggregate and are respectively 2.58 and 4.5% for the fine aggregate and silica sand (ASTM C128-15, 2015). The analyzed gradation and fineness modulus of aggregate are determined according to the ASTM C136 standard (ASTM C136/C136M-14, 2014), and the fineness modulus of fine aggregate is 2.7. Fig. 4.1 presents the aggregate gradation limits and the design of aggregate gradation used in the RCC mixing and the RCGC mixing.

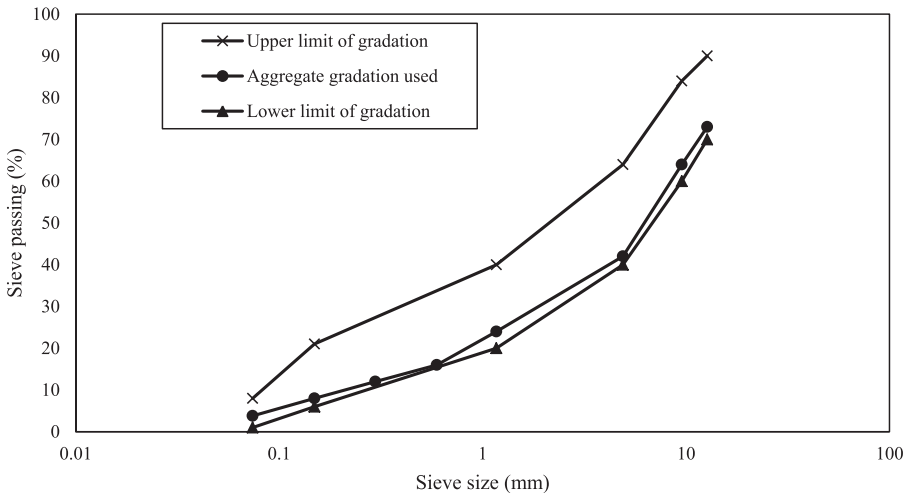


**Figure 4.1** The aggregate gradation limits and the design of aggregate gradation used in the RCC mixing and the RCGC mixing.

#### 4.3.1.3 Oil shale ash

After crushing and burning of oil shale rock at the temperature of 650°C and then again grinding the burned oil shale rock chunk the OSA is obtained for use in the OSA-substituted cement and the RCGC. The OSA particle has a specific gravity of

2.69 (g/cm<sup>3</sup>). Fig. 4.2 presents that the OSA has various amorphous and geometrical shapes such as angular, tetragonal, pentagonal, and hexagonal with rough and porous surfaces as shown in the micrograph from SEM and mineralogy analysis from XRD.

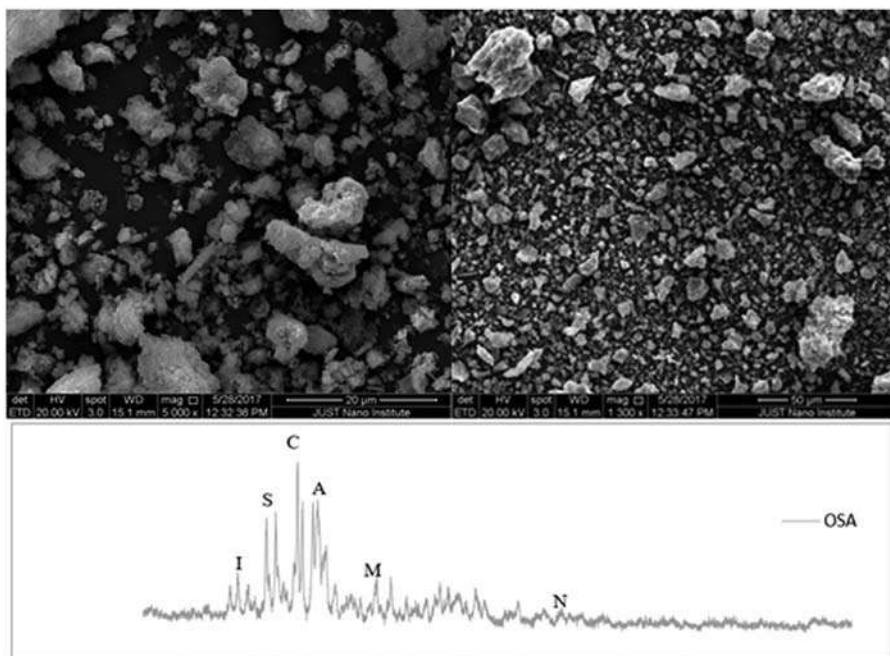


**Figure 4.2** SEM micrograph and XRD analysis of the OSA used in the current study. C: Calcium oxide, S: Silicon oxide, A: Aluminum oxide, I: Ferrite oxide, M: Magnesium oxide, N: Sodium oxide.

SEM and XRD analysis confirm that most of the OSA consisted of the angular geometric particles (Fig. 4.2). It is also apparent that the OSA is composed of various sized particles ranging from several micrometers to dozens of ultrafine micrometers. Additionally the microstructure of the OSA has slightly little amorphous hollows (Fig. 4.2). There is mainly calcite, which is mainly a white and colorless mineral consisting of calcium carbonate as well as silicon and minor other minerals, such as aluminum, ferrite, sodium, titanium, sulfate, and periclase. Table 4.3 gives the chemical composition of the OSA.

**Table 4.3** The chemical composition of the oil shale ash.

Type of supplementary cementitious material	Chemical composition (%)								
	SiO <sub>2</sub>	Al <sub>2</sub> O <sub>3</sub>	Fe <sub>2</sub> O <sub>3</sub>	CaO	MgO	SO <sub>3</sub>	K <sub>2</sub> O	TiO <sub>2</sub>	Loss in ignition
Oil shale ash	19	6	2	47	0.8	8	0.6	0.2	5.4

According to high calcium oxide (CaO) content of the OSA used, this study classified it as a latent hydraulic additive (Table 4.3 and Fig. 4.2). Additionally, since the OSA consists of the content of precious silicon oxide, aluminum oxide, iron oxide, and calcium oxide, totally 74%, as well as titanium oxide, the study does suggest the OSA to be accepted as a SCM in the literature (Table 4.3 and Fig. 4.2).

### 4.3.2 Physical properties of the roller-compacted concrete and roller-compacted green concrete

#### 4.3.2.1 Density of fresh mixing

Fig. 4.3 shows the change in the fresh density of the RCC and the RCGC and the replacement percent of the OSA with cement. The density for the fresh RCC and the fresh RCGC was measured by weighing the specimen in 0.1 (g) precision scale and dividing its determined weight to its volume of the cylinder. The reduction in fresh density reached the lowest quantity in the mixing of O-10% of RCGC. As the 10% OSA is replaced with cement, the reduction equals to 3% in the fresh density. The highest reduction in the fresh density of RCGC is at the mixing of O-40% containing 40% OSA replaced with cement; it equals to 11.1% (Fig. 4.3). Apart from the mixing of O-0% of RCC the second highest fresh density is in the mixing of O-10% of RCGC. The fresh density of O-20% of RCGC is approximately the same as the fresh density of O-30% and O-40% of RCGC. The mixing of O-40% of RCGC demonstrated 10.5% lesser fresh density when compared with the mixing of O-20% and of O-30% of RCGC. This means that the most effective percent for the replacement of OSA with cement is 10% because the replacement ratio provides

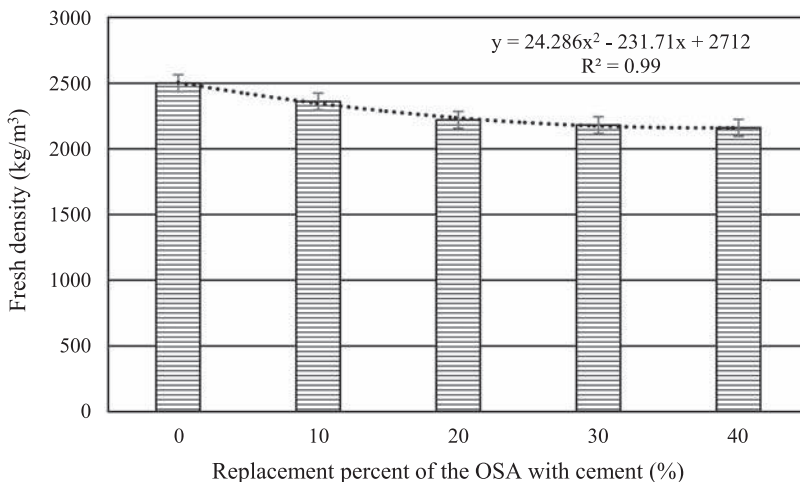


**Figure 4.3** The change in the fresh density for the RCC and the RCGC and the replacement percent of the OSA with cement.

lightweight RCGC for construction industry (Fig. 4.3). Moreover, it is clear to understand that the increase in the OSA content leads to the decrease in the density of fresh RCGC as shown in Fig. 4.6. The other meaning of this decrease is that as the specific gravities of the OSA (2.69) and the cement (3.19) are not equal to each other, the loss in the fresh density occurs in the RCGC.

The equation in Fig. 4.3 estimates the fresh density of RCC and the RCGC with 99% regression integrity. The meaning of this new equation is that if anyone uses the OSA, as the SCM, instead of cement up to 40% in the mixing of the RCC and the RCGC, the fresh density of RCC and the RCGC could be calculated without testing, and the equation gives insight on the fresh density of the RCC and the RCGC and a significant relationship between the OSA content and the cement content and the fresh density (Fig. 4.3).

#### 4.3.2.2 Density of the hardened specimens

Fig. 4.4 shows the relationships between water content and the hardened density for the RCC and the RCGC including different percentage of the OSA. The density and the water content, determined with the soil compaction method, are used for the selection of optimum cementitious content. In the practical start point the optimum cement content was calculated from the cement-to-dry constituent material ratio in the RCC (the optimum cement content for O-0% is 266/2054.8, and it equals 0.12) (Fig. 4.4). A good starting point for optimum cement content in the RCC is between 11 and 13% by weight of its dry constituent material.

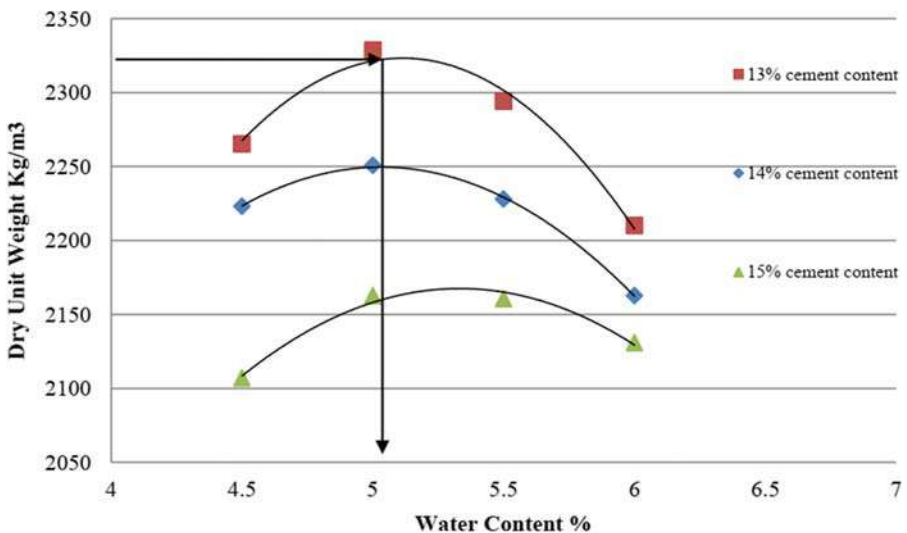


**Figure 4.4** The relationships between water content and the dry density for different percentage of the OSA in the RCGC.

The main factor controlling cement content would be target stress gain requirement and minimum cement material requirement and water content, as seen in Fig. 4.4. Moisture content is described as the weight of water divided by the weight of dry material totally in the RCC. The dry density is then plotted against moisture content, as seen in Fig. 4.4. The total cementitious material content (cement + OSA) was kept constant at 13% and the water-to-cement ratio was kept constant at 0.4 according to Fig. 4.4 and Table 4.1 in the current study.

### 4.3.2.3 Porosity

The effects of the replacement percent of OSA with cement on the porosity of the RCC and the RCGC are evaluated. Fig. 4.5 shows a strong regression relationship between the replacement percent of the OSA with cement and the porosity of RCC and RCGC at the age of 90 days curing. The increase in porosity of RCGC reached the lowest quantity in the mixing of O-10% of RCGC. As the 10% OSA is replaced with cement, the increase in porosity equals to 51%. The highest increase in the porosity of RCGC is at the mixing of O-40% containing 40% OSA replacement with cement; it equals to 63.5% (Fig. 4.5). The study showed the highest porosity in the mixing of the O-40% of RCGC because the cement content is reduced up to 40% in its mixing. The meaning of the porosity in the RCGC is that the most effective percent for the replacement of OSA with cement is 10% in view of the lowest porosity increase (Fig. 4.5). Additionally, it can be seen that the porosity is linearly increased, associated with the decrease of the density in the RCGC. In Fig. 4.5 the results reveal that the OSA leads to obtaining the lightweight RCGC material as effective as regular RCC material. However, in the RCC and the RCGC, water content would be reduced without protecting the reactions between the OSA and cement in the hydration process at the constant water-to-cement ratio of 0.4 used in the study.

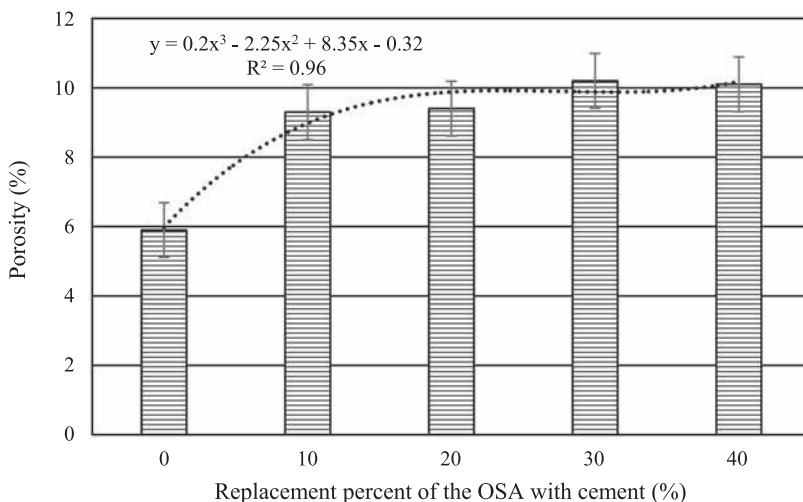


**Figure 4.5** The porosity of RCC and the RCGC at the age of 90-day curing.

Therefore it could increase the percentage of porosity. The results complied with the results of Raado et al. (2014), who reported that the existence of calcium oxide (CaO) and silicon oxide (SiO<sub>2</sub>) caused the porosity based on water demand in the hydration process of the binder. This means that the higher the water demand, the higher the volume of large capillary pores. In addition to the result of porosity of the RCC and the RCGC, it is common to estimate the porosity of hardened concrete material from its design of mixing constituents such as the replacement percent of the OSA with cement, the content of OSA, the water-to-cement ratio, and the content of cement. The equation in Fig. 4.5 estimates the porosity of the RCC and the RCGC with 96% regression integrity. The meaning of this new equation is that if anyone uses the OSA, as the SCM, instead of cement up to 40% in the mixing of RCC and RCGC, the hardened porosity of the RCC and the RCGC could be calculated without testing, and the equation gives insight on the porosity of the hardened state of the RCC and the RCGC and the significant regression relationship between the OSA content and the cement content and the porosity (Fig. 4.5).

### **4.3.3 Durability properties of the roller-compacted concrete and roller-compacted green concrete**

This section is on durability issues of the RCC and the RCGC made of ASTM type I cement and OSA and other mixing constituent materials. The freezing and thawing cycles, the loss in weight after freezing and thawing cycles, and the loss in compressive stress after freezing and thawing cycles of the RCC and the RCGC were evaluated. The following subsections consist of the durability properties of the RCC and the RCGC measured along with regression equations and their discussion and several literature research studies to compare each other.

#### **4.3.3.1 Freezing and thawing**

The 38-day freeze–thaw cycle resistance of the hardened RCC and the hardened RCGC was determined. In the freezing–thawing cycle the loss in weight was measured after the cycles of 0th, 32nd, 64th, 96th, 144th, 216th, and 300th, and the loss in the compressive stress was determined at the 0th, 144th, and 300th cycles.

##### **Change in weight after freezing–thawing cycle**

The adequacy resistance of frost attack in the RCC and the RCGC can be determined by freezing and thawing tests. ASTM has developed two tests for frost resistance in concrete material. In both of these, rapid freezing is applied; one of them takes place during the freezing and thawing in water, while the other takes place during freezing in air and thawing in water. The meaning of the condition is to duplicate the possible practical exposure of the freezing and thawing. The British Standards (BS) also measures the freezing effect in concrete material. The difference between the ASTM and the BS is that the BS prescribes the freezing in water, and frost damage is assessed after several cycles of freezing and thawing by measuring the loss in mass of the specimens, the increase in length of the specimens, and the decrease in durability strength of

the specimens. The study used the freezing and thawing method specified by the ASTM to determine the effect of frost exposure in the RCC and the RCGC (Meddah, 2015). Fig. 4.6 shows the loss on weight after freezing and thawing cycles and vulnerable RCC and RCGC on cooling.

It is clear that the weight decreased when the number of freezing and thawing cycles increased; this is due to the increase in the water absorption of OSA, which means that more capillary pores lead to higher water pressure during the freezing process and to an increase in weight loss in the RCC and the RCGC (Fig. 4.6). The loss in weight of RCGC reached the lowest quantity in the mixing of O-10%. As the 10% OSA is replaced with cement, the reduction equals to 3% only. The highest loss in weight of RCGC is at the mixing of O-40% because it consists of 40% OSA and 60% cement and water and aggregate stack; it equals to 6.7% (Fig. 4.6). The study faced the lowest frost durability in the mixing of the O-40% of RCGC at 300 cycles because the cement content is reduced up to 40% in the mixing of O-40%. Apart from the mixing of O-0% of RCC the second highest frost durability is in the mixing of O-10% of RCGC at all freezing and thawing cycles. The loss in weight of O-20% of RCGC is the same with the loss in weight of O-30% and O-40% of the RCGC at all freezing and thawing cycles (Fig. 4.6). For less severe conditions of frost, good quality of RCC without OSA may not be sufficient. Table 4.1 gives the recommended maximum quantity of the water-to-cement ratio and the minimum content of cementitious material, and Fig. 4.6 also gives the minimum loss in the weight of the RCC and the RCGC after 300 cycles of freezing and thawing cycles. As shown in Table 4.1 and Fig. 4.6 the 10% OSA replacement with cement is useful to slow the effect of frost conditions in the RCGC. Therefore the

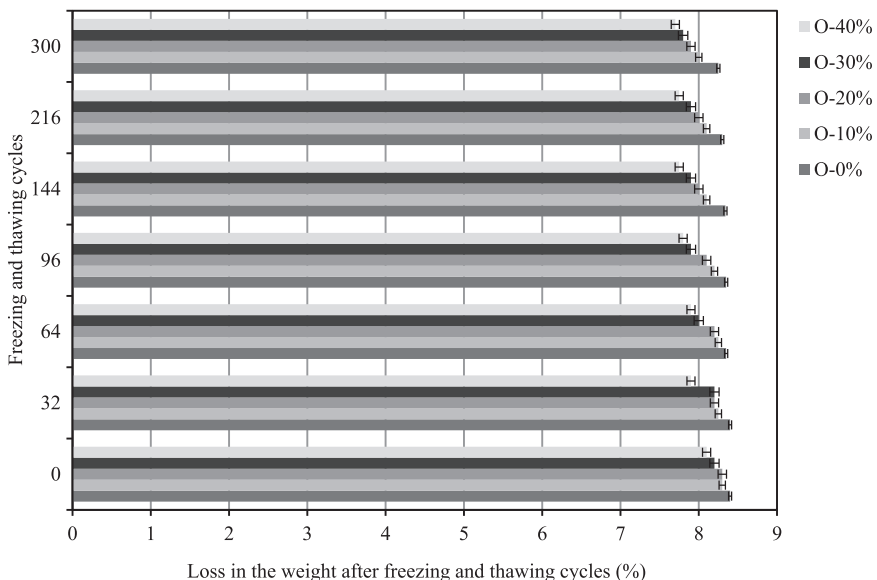


**Figure 4.6** The loss on weight after freezing and thawing cycles for RCC and RCGC.

most effective OSA replacement percent with cement in RCGC is 10%, as determined by the study.

**Compressive stress after freezing–thawing cycle**

Fig. 4.7 shows regression equations between freezing–thawing cycle and compressive stress, regression relationship degree ( $R^2$ ), and the compressive stress feature for each OSA content at each freezing and thawing cycle. The reduction in the compressive stress of RCGC reached the lowest quantity in the mixing of O-10% of RCGC in the frost durability. As the 10% OSA is replaced with cement, the reduction equals to 45%. The highest reduction in the compressive stress of RCGC is at the mixing of O-40% because it contains 40% OSA replacement with cement, and the reduction compressive stress is equal to 70%. Apart from the mixing of O-0% of RCC the second highest compressive stress is in the mixing of O-10% of RCGC at 300 cycles of freezing and thawing. At 300 freezing and thawing cycles the compressive stress of O-20% of RCGC is approximately the same as the compressive stress of O-10% of RCGC. A similar result is valid for the compressive stress of O-30% and O-40% in the RCGC (Fig. 4.7).

Additionally the compressive stress decreases with increasing freezing and thawing cycles. The decrease in the compressive strength can be explained as the increase in porosity with increasing OSA; the freezable water in the cement paste will increase and will cause internal expansive pressure during freezing and will increase cracks and weight loss in the specimens of RCGC. In addition to the result of compressive stress of RCC and RCGC before and after freezing and thawing vulnerability a regression equation is developed to estimate the compressive stress of RCC and the RCGC with 96% regression integrity (Fig. 4.7). The meaning of these new equations is that if anyone replaces the OSA with cement as in the RCC and the RCGC, the compressive stress of the RCC and the RCGC could be calculated

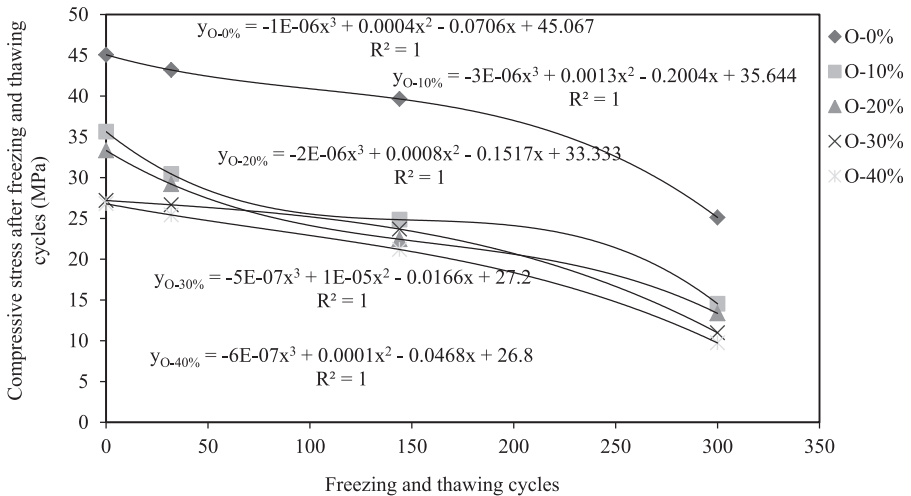


**Figure 4.7** Regression equations between freezing–thawing cycle and compressive stress for each OSA content at each freezing and thawing cycle.



without a need for the freezing and thawing testing, and the equations give insight on the frost resistance of RCC and RCGC and a significant regression relationship between the content of OSA and of cement and the frost resistance.

### 4.3.4 Mechanical properties of the roller-compacted concrete and the roller-compacted green concrete

#### 4.3.4.1 Compressive stress

The study measured the compressive stress at 7th day and 28th day as these periods were sufficient according to national and international standards used. Moreover, other stress tests were continued until 90 days because there were several rules regarding these tests and water curing periods in their national and international standards. The compressive stress of RCC and of RCGC is determined using a testing cylinder, with dimensions of  $150 \times 300$  (mm), according to the procedure described in ASTM C 39 standard (ASTM C39/C39M-18, 2018). Each test was carried out on nine cylinders for each curing day and each group in Table 4.1. Fig. 4.8 shows descriptive results related to the compressive stress at the 7th day and 28th day for the RCC and the RCGC and a number of compressive stress results from in situ applications of conventional RCC.

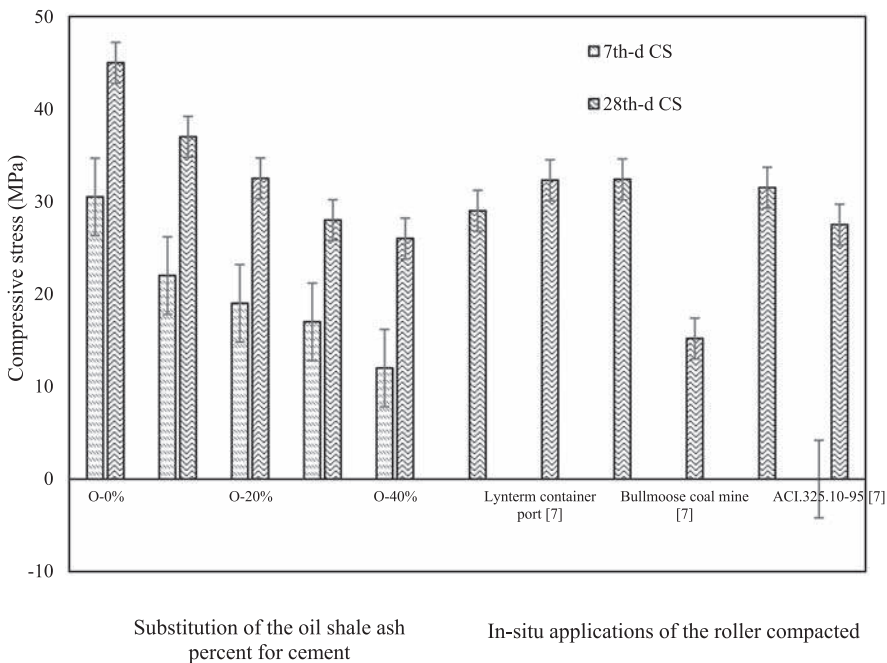


**Figure 4.8** The compressive stress at the 7th day and 28th day for the RCC and the RCGC and the substitution percent of the OSA for cement.

The compressive stress was between 12 and 22 (MPa) at the 7th day and between 26 and 37 MPa at the 28th day. This means that this could be referred as a success for using OSA as a supplementary latent hydraulic cementitious material in the RCGC. In a study conducted by Uibu et al. (2016) for OSA backfilling in concrete and its strength development the compressive stress was between 1 and 5 (MPa) at the 7th-day and the 28th-day compressive stress reached the maximum value of 25 (MPa). As seen in Fig. 4.8 the compressive stress decreased with the replacement of the OSA with cement because there is no activator for the calcium oxide (CaO) in the chemical composition of the OSA (Table 4.3). The decrease in compressive stress does not deal with the replacing percent of the OSA with cement because the mixing of O-10% of RCGC reached the compressive stress of 37 (MPa)—it complies with the compressive stress of CEM I 42.5N cement mortar at the 28th day. Moreover the mixing of RCGC does not demonstrate a higher success against the mixing of RCC because the RCC does not reduce cement content similar to the mixing of RCGC. This means that the control specimens for O-10%, O-20%, O-30%, and O-40% of RCGC should respectively include the cement content of 90%, 80%, 70%, and 60% in a constant water-to-mixing material ratio. According to ACI.325.10-95 the minimum compressive stress for the RCC which would be used for the public traffic depends on the slab thickness (ACI, 2001). The minimum requirement for compressive stress of the RCC for the slab is nearly over 27.5 (MPa) as a main structural layer. However, the 28th-day compressive stress of O-10% and O-20% of RCGC is greater than that of in situ applications of RCC, and the 28th-day compressive stress of RCGC reached the satisfied criteria of ACI (2001) as well. Therefore the study could suggest the mixing of the O-10%, the O-20%, and the O-30% as an upcycling example of the OSA in the cement and RCGC mixing. Fig. 4.9 shows a strong relationship between 7th-day compressive stress and the OSA-to-cement ratio.

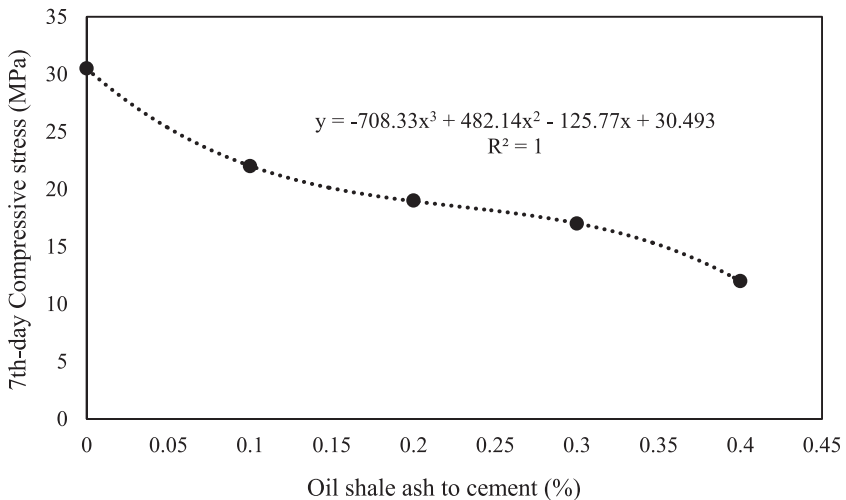


**Figure 4.9** Regression relationship between 7th-day compressive stress and the OSA-to-cement ratio.

A significant study published by [Radwan et al. \(2013\)](#) supports the inference in the current study. They agree with the inference that the OSA is an essential activator for the RCC since it has plenty of chemical compounds such as calcium oxide, silicon dioxide, aluminum oxide, ferrite oxide, and titanium oxide. Therefore they used an alkali activator for the blended cement containing OSA, and in the absence of an alkali activator the blended cement containing OSA showed nearly 20% lesser compressive stress than the Portland cement. With an alkali activator the compressive stress of cement-blended OSA increased as in the Portland cement ([Meddah, 2015](#)). [Fig. 4.10](#) shows a strong regression relationship between 28th-day compressive stress and the OSA-to-cement ratio.

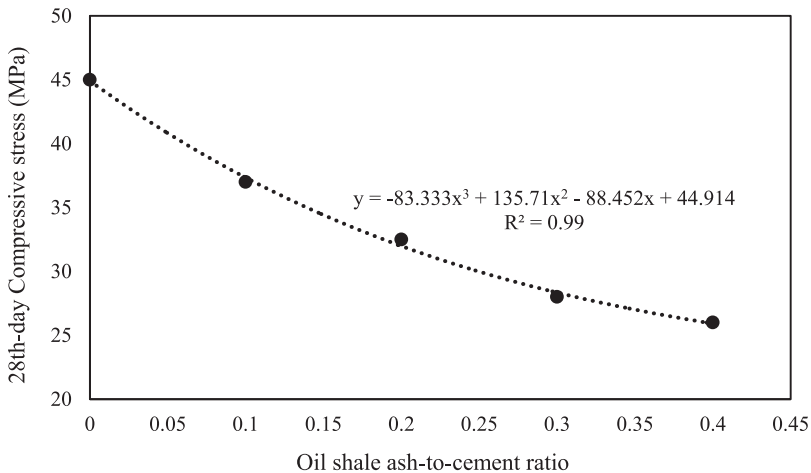


**Figure 4.10** Regression relationship between 28th-day compressive stress and the OSA-to-cement ratio.

Estimating the 7th-day compressive stress from the mixing ratio of concrete material is always great interest in both science community and construction industry because every stress gain process in concrete leans its mixing proportion ([Fig. 4.9](#)). The equation in [Fig. 4.8](#) also estimates the 7th-day compressive stress of the RCC and the RCGC with 100% regression integrity. [Fig. 4.10](#) estimates the 28th-day compressive stress of RCC and of RCGC with 99% regression integrity. The meaning of the new equation is that if anyone replaces the OSA with cement as in the RCC and RCGC, the 28th-day compressive stress of the RCC and the RCGC could be calculated without repeating the compressive stress testing, and the equation gives insight on the resistance of compression force for the RCC and the RCGC and a significant regression relationship between the content of OSA and of cement and the compressive stress at 28d.

Chhaiba et al. reported an important study that the cement paste containing OSA and coal waste provides the highest compressive stress for the green concrete composite (Chhaiba et al., 2018).

#### 4.3.4.2 Splitting tensile stress

Fig. 4.11 shows the change in the splitting tensile stress of RCC and of RCGC. The splitting tensile stress reflects the ability of concrete to resist the tension force since the concrete is a brittle material and it will not be able to face the tensile force significantly. The splitting tensile stress of the RCC reached the highest quantity at the age of 90 days in standard water curing, 4.1 (MPa), because it includes 100% cement content. The reduction quantity of splitting

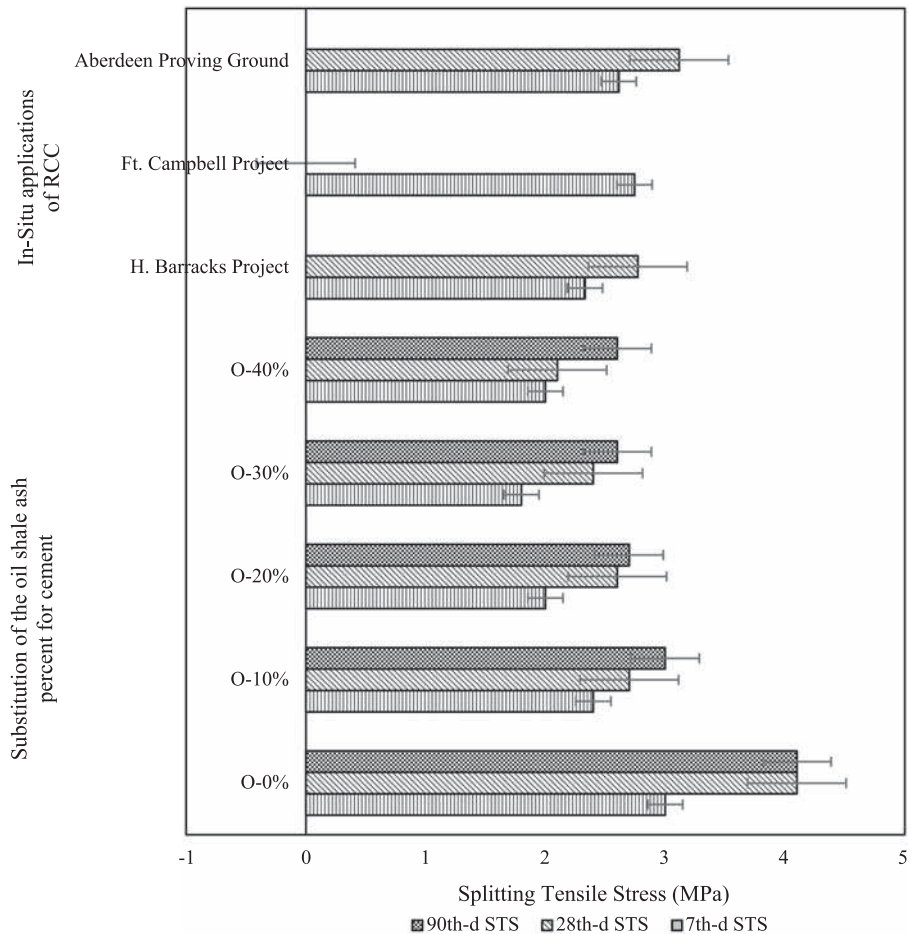


**Figure 4.11** The change in the splitting tensile stress of the RCC and the RCGC.

tensile of RCGC reached the lowest quantity when 10% OSA is replaced with cement; the reduction equals to 26.83%. The highest reduction in the splitting tensile stress of RCGC is at 40% OSA replacement with cement, which is equal to 36.6%, because the cement content was reduced up to 40% in the mixing of O-40%. The second highest splitting tensile stress is in the mixing of O-10% of RCGC at 7d. Its splitting tensile stress is 20% higher than that of other OSA mixing systems in the RCGC (Fig. 4.11).

Similar results, like in the mixing of the O-10% at 7d, were observed in the mixing of the O-10% at 28d and 90d (Fig. 4.11). At the 7th day and 28th day the splitting tensile stress of O-10% of RCGC is also greater than that of in situ applications of RCC used in the projects of H. Barracks and of Ft. Campbell, and the splitting tensile stress of RCGC reached the satisfied quantity as it exceeded the splitting tensile stress measured by the ACI in in situ applications of RCC (ACI, 2001). This means that the most effective percent for the replacement of OSA with cement is 10% in view of stress gain of splitting tensile. Fig. 4.12 shows a strong regression relationship between 7th-day splitting tensile stress and the OSA-to-cement ratio.

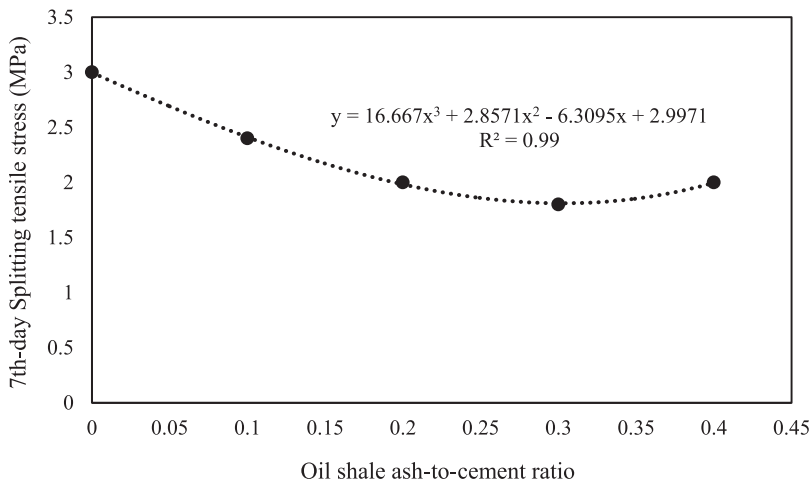


**Figure 4.12** Regression relationship between 7th-day splitting tensile stress and the OSA-to-cement ratio.

The equation in Fig. 4.12 estimates the splitting tensile stress of RCC and RCGC with 99% regression integrity. Figs. 4.13 and 4.14 show a strong regression relationship between 28th-day and 90th-day splitting tensile stresses and the OSA-to-cement ratio.

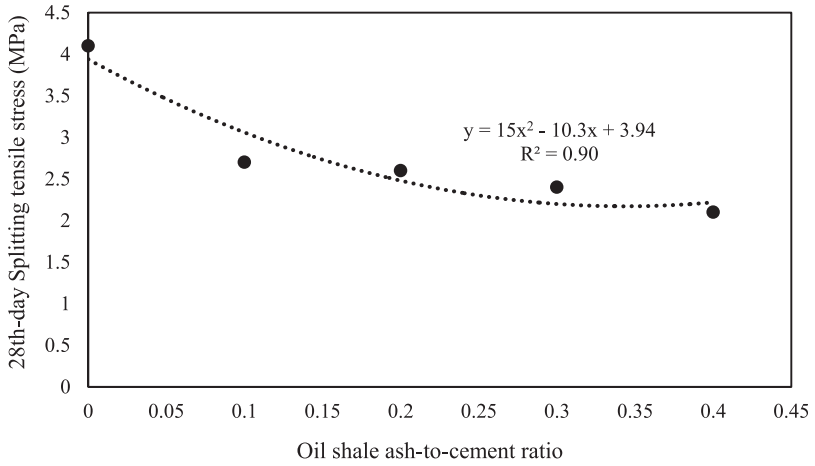


**Figure 4.13** Regression relationship between 28th-day splitting tensile stress and the OSA-to-cement ratio.

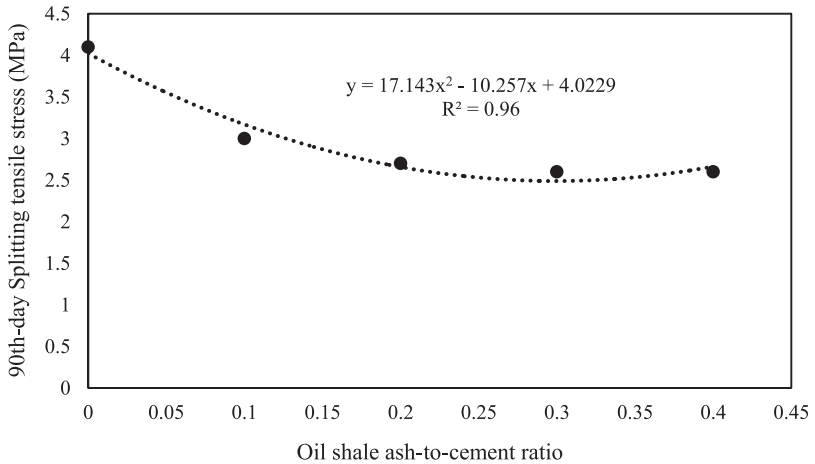


**Figure 4.14** Regression relationship between 90th-day splitting tensile stress and the OSA-to-cement ratio.

The equations in [Figs. 4.13 and 4.14](#) estimate the 28th-day and 90th-day splitting tensile stresses of RCC and RCGC with 90% and 96% regression integrity, respectively.

### 4.3.4.3 Flexural moment stress

One of the most important ways to understand this integrity for the structure is application of the flexure load in the concrete material. The flexural load could help to understand two important properties of concrete, which are the splitting tensile stress and the flexural moment stress. There was little impact of the type of aggregate on the direct and splitting tensile stresses, but the flexural moment stress of RCC was greater as angular crushed aggregate was used compared to that of the rounded natural gravel. The explanation was that the improved bond of crushed aggregate, which has a rough surface, holds the materials together, but this was ineffective in direct and indirect tension. Therefore the RCC and the RCGC must be designed to be able to withstand high flexure load and the repeated load, such as trucks and cars in the RCC pavement, and heavy water load as in the RCC dam. Fig. 4.15 shows the flexural moment stress at the 7th day, 28th day, and 90th day for the RCC and the RCGC and the substitution percent of the OSA for cement.

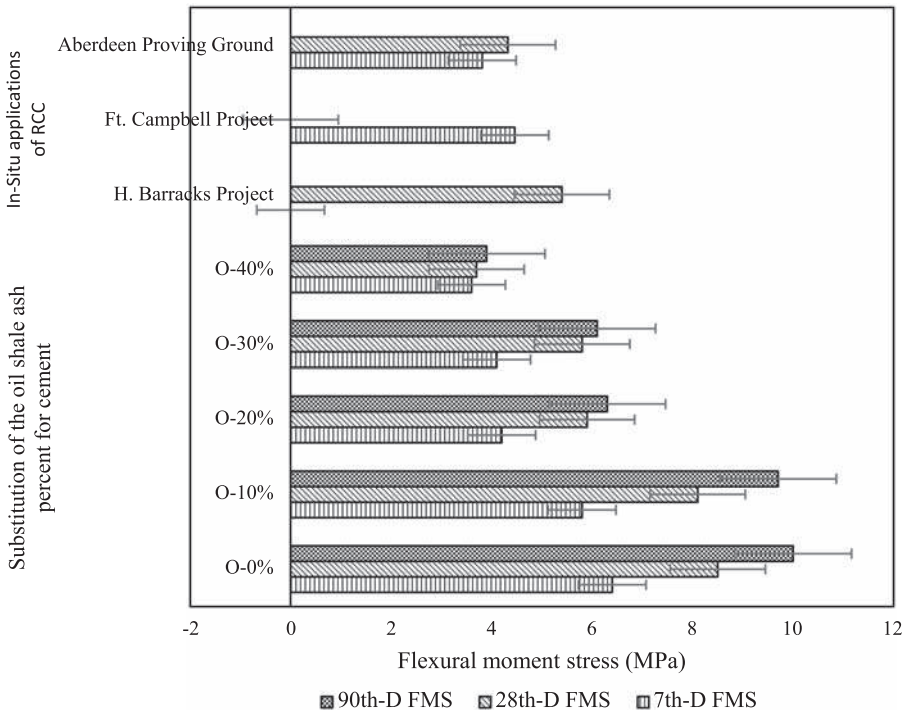


**Figure 4.15** The flexural moment stress at the 7th day, 28th day, and 90th day for the RCC and the RCGC and the substitution percent of the OSA for cement.

The flexural moment stress of RCC reached the highest quantity at the ages of 7 days, 28 days, and 90 days in standard water curing, with 6.4 MPa, 8.5 MPa, and 10 MPa, respectively. The reduction quantity of flexural moment stress of RCGC reached the lowest quantity in the mixing of O-10% of RCGC. As the 10% OSA was replaced with cement, the reduction equals to 10%. The highest reduction in the flexural moment stress of RCGC is at the mixing of O-40% containing 40% OSA replacement with cement; it equals to 43.7%. In this study the lowest flexural moment stress in the mixing of the O-40% of RCGC is at 7d because the cement content was reduced up to 40% in the mixing of O-40%. Apart from the mixing of O-0% of RCC the second highest flexural moment stress is in the mixing of O-10% of RCGC at 7d, 28d, and 90d. Its 7th-day flexural moment stress is 37.9% higher than that of other OSA mixing systems in the RCGC (Fig. 4.15). At 7 days the flexural moment stress of O-20% of RCGC is the same with the flexural moment stress of O-30% of RCGC. The mixing of O-40% of RCGC demonstrated 10.5% lesser 7th-day flexural moment stress when compared with the mixing of O-20% and O-30% of RCGC. At the 7th day and 28th day the flexural moment stress of O-10%, O-20%, and O-30% of RCGC is greater than that of in situ applications of RCC used in the projects of H. Barracks, of Ft. Campbell, and of Aberdeen Proving Ground, and the flexural moment stress of RCGC reached the satisfied quantity as it exceeded the flexural moment stress measured by the ACI in in situ applications of RCC (ACI, 2001). This means that the most effective percent for the replacement of OSA with cement is 10% in view of stress gain of flexural moment. Figs. 4.16–4.18 give a strong regression relationship between 7th-day, 28th-day, and 90th-day flexural moment stresses and the OSA-to-cement ratio.

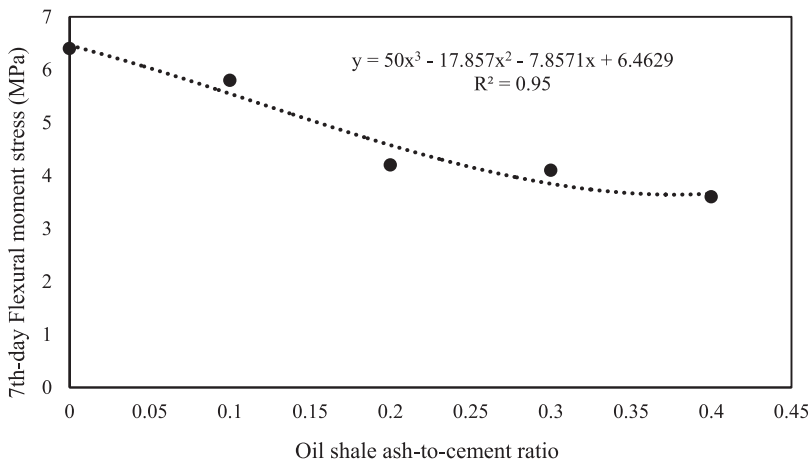


**Figure 4.16** Regression relationship between 7th-day flexural moment stress and the OSA-to-cement ratio.



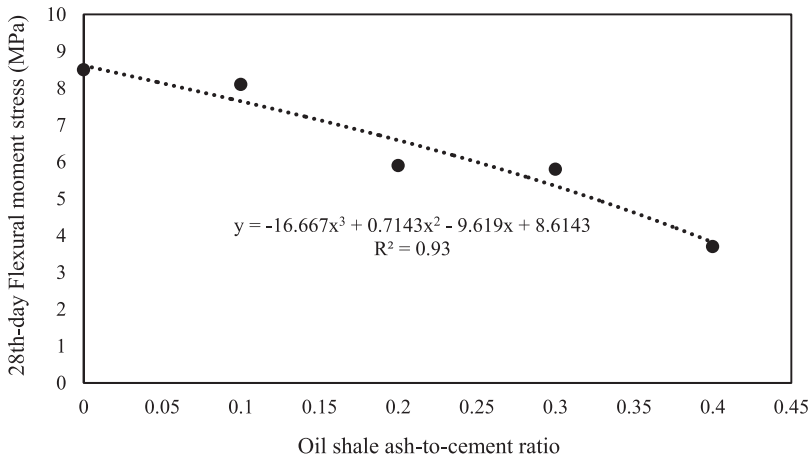


**Figure 4.17** Regression relationship between 28th-day flexural moment stress and the oil shale ash-to-cement ratio.

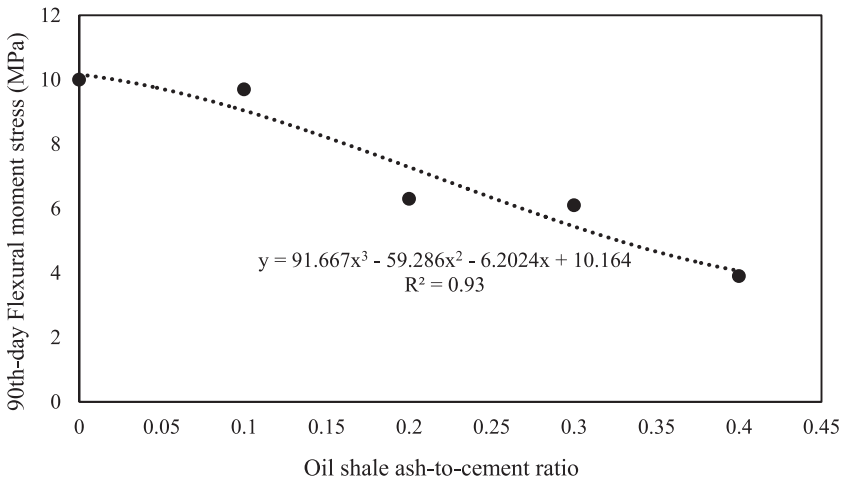


**Figure 4.18** Regression relationship between 90th-day flexural moment stress and the oil shale ash-to-cement ratio.

Rooholamini et al. published an important study in 2019 (Rooholamini et al., 2019). To evaluate the mechanical properties of the RCC, various tests were performed, including the compressive stress, splitting tensile stress, semicircular bending moment stress, and three-point bending moment stress. The results revealed that

fine and coarse steel slag from an electric arc furnace (EAF) as aggregate in the RCC had different impacts on the mechanical properties of the RCC. Moreover, they indicated that the flexural moment stress of RCC including EAF steel slag aggregate was related to the broken aggregate fraction of fracture face exponentially (Rooholamini et al., 2019). Kasu et al. reported an interesting study in 2019, which explained the effect of aggregate size on the flexural moment stress of concrete composites under repeated loading (Kasu et al., 2019). In their study the authors evaluated the effect of nominal maximum aggregate size under different stress levels between 80% and 90% and different loading frequencies between 2 (Hz) and 10 (Hz), and they chose to carry out the flexural moment stress as fatigue test on concrete beam specimens.

The results of the flexural moment stress pointed out that a smaller nominal maximum aggregate size was more beneficial for the flexural moment stress as the fatigue performance of concrete composites in repeated loadings such as traffic and thermal (Kasu et al., 2019). The flexural moment stress reached 10, 9.4, 6.7, 6.2, and 3.9 MPa at 0%, 10%, 20%, 30%, and 40% OSA replacement levels, respectively. After 10% OSA, significant reduction in flexural strength was noticed; it reached maximum 60% at 40% OSA replacement level. The equation in Fig. 4.18 estimates the 90th-day flexural moment stress of RCC and RCGC along with 93% regression integrity. The meaning of the new equation is that if anyone replaces the OSA with cement as in the RCC and the RCGC, the 90th-day flexural moment stress of RCC and RCGC could be calculated without a need for the flexural moment testing, and the equation gives insight on the 90th-day flexural force resistance of RCC and of RCGC, a significant relationship between the content of OSA and cement, and the 90th-day flexural moment stress gain. Zhang et al. published an important study and its results in 2019 (Zhang et al., 2019). According to their study, results pointed out that the use of both polymer latex and an expansive agent in the CA and concrete composite increased the interfacial bonding stress owing to the dense microstructure. Because of the increase in the bonding between interlayers, the failure modes of CA and concrete composite transformed from an incompatible failure to a compatible failure, and their flexural moment stress significantly increased. After careful consideration of its results and making inferences the authors suggested that the use of polymer latex and an expansive agent would be very useful to enhance the mechanical properties and the serviceability of cement and concrete composite in practices, such as slab track (Zhang et al., 2019).

#### 4.3.4.4 Modulus of elasticity

Fig. 4.19 shows the stress–strain curves of elasticity for the RCC and the RCGC, various replacement percent of OSA with cement, and identification of the modulus of elasticity at the 90th day.

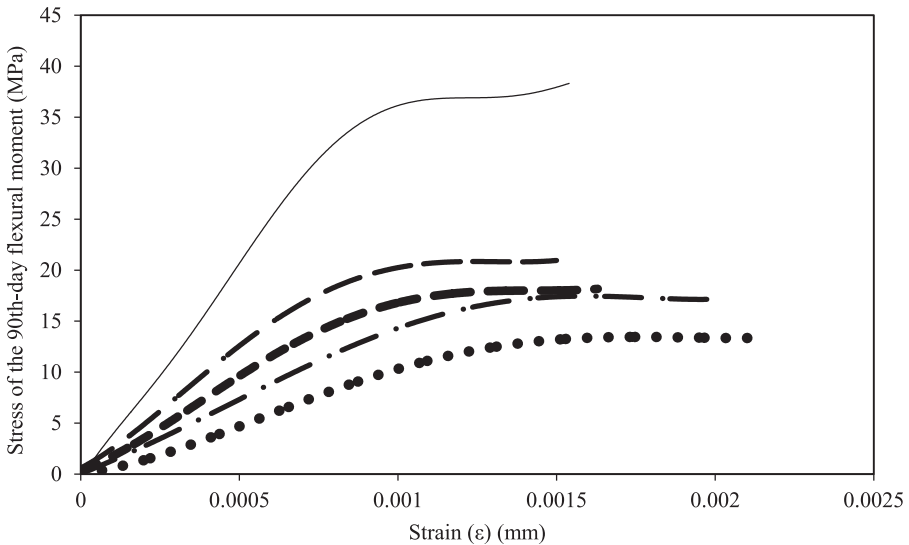


**Figure 4.19** Stress–strain curves for the RCC and the RCGC at various replacement percent of OSA with cement.

The curves in Fig. 4.19 show two stages. The first one is a linear behavior stage; then it is followed by a nonlinear behavior stage due to the brittle behavior of RCC and RCGC. As the OSA replacement content is increased, the linearity in the stress–strain diagram also decreases; it provides nonlinearity for the RCGC through a relatively low stress gain. The decrease in linearity with an increase in the OSA replacement with cement is due to the decrease in ultimate flexural moment stress, which also relates to reduction in modulus of elasticity. In addition to the result, increasing the OSA content in the specimens of the RCGC gives much more ductility, where the brittle failure is obvious in the specimens of RCC. On the other hand, it was observed in the experiment that the specimen of O-40% does not have obvious cracks on its surface until it fails.

The modulus of elasticity of RCC reached the highest quantity at the age of 90 days, 37 (MPa), because it includes 100% cement content. The reduction quantity of modulus of elasticity reached the lowest percent in the O-10% of RCGC as the 10% OSA was replaced with cement; this reduction equals to 41%. The highest reduction in the modulus of elasticity of RCGC is in the specimens containing 40% OSA replacement with cement; it equals to 64% (Fig. 4.19). The study faced the lowest modulus of elasticity in the mixing of the O-40% of RCGC at 90d because the cement content was reduced up to 40% in the mixing of O-40%. Apart from the mixing of O-0% of RCC the second highest modulus of elasticity is in the mixing

of O-10% of RCGC at 90d. Its modulus of elasticity is 40% higher than that of other OSA mixing systems in the RCGC (Fig. 4.19). At 90 days the modulus of elasticity of O-20% of RCGC reached the same quantity with the modulus of elasticity of O-30% of RCGC. The mixing of O-40% of RCGC demonstrated 17% lesser modulus of elasticity when compared with other OSA mixing systems in the RCGC. The meaning of these quantities of elasticity modulus is that the most effective percent for the replacement of OSA with cement is 10% in view of the modulus of elasticity gain (Fig. 4.19).

### **4.3.5 Microstructure analysis of the roller-compacted concrete and roller-compacted green concrete**

#### **4.3.5.1 Microstructure analysis with scanning electron microscopy**

The SEM micrographs in Fig. 4.20, which had been taken at the curing age of the 90th day of the RCC and the RCGC, show the ettringite which was increasing with increasing OSA content; ettringite is formed in the early age of concrete to reduce the flash setting of cement, but its formation means that the hydration of the mix had not been completed, which will lead to expansion and therefore weaken the specimen. It was observed that in hydration of cement with the OSA, angular cement grains were surrounded by radiating fibers of calcium-silicate-hydrate (C-S-H) resembling patterns of C-S-H of ordinary cement. Randomly oriented portlandite (CH) crystals and prismatic ettringite crystals were widely dispersed through paste of O-0%, O-10%, O-20%, O-30%, and O-40% (Fig. 4.20).

However, in the O-40% at the curing age of the 90th day, it was found that the OSA grains were covered with amorphous (with respect to C-S-H) layered CH hydration products. The matrix phase is mainly composed of short radicular outgrowths of C-S-Hs around cement grains and needle-shaped ettringite crystals (Fig. 4.20). The microstructure of hydrated paste of RCGC at the curing age of the 90th day was presented by amorphous gel filling spaces between hydrated particles. In pastes of RCGC, layered accumulations of the CH crystals of about 12  $\mu\text{m}$  in width are intermingled through paste (Fig. 4.20). There is a visible densification around the ordinary cement grain due to partial hydration of the OSA grain, leading to formation of additional C-S-H. At the curing age of 90th day the OSA grains were well located in the matrix and were sunk in a layered CH. Observation of paste based on the RCGC demonstrated that the OSA grains turned out to be amorphous reaction prisms. In CH phase the matrix of RCGC is found to be richer in calcium than the paste of RCC. At the curing age of 90th day the microstructure of RCGC was further densified with respect to RCC paste (Fig. 4.20) (Kırgız, 2014).

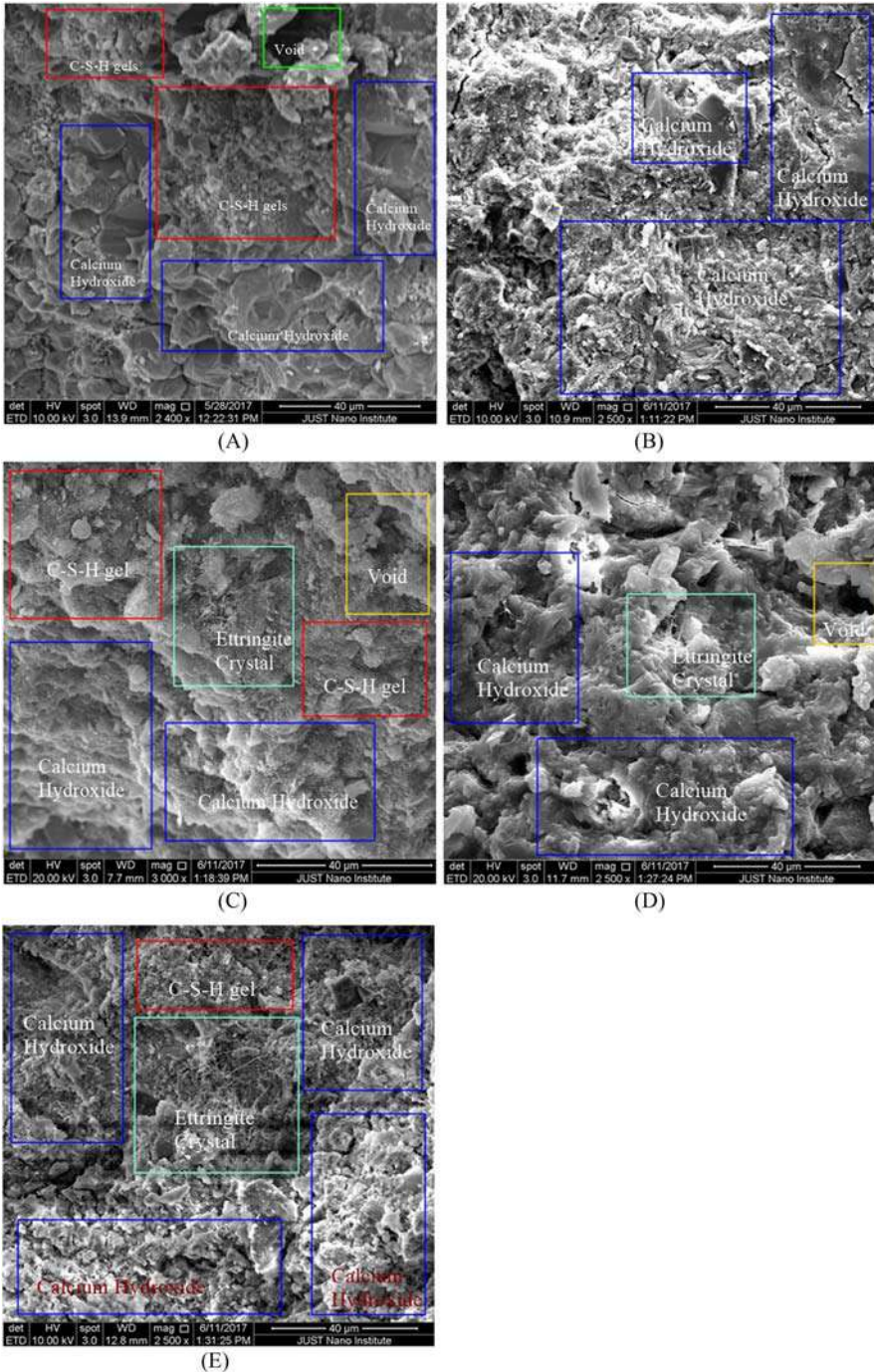


**Figure 4.20** The SEM micrographs for the RCC and the RCGC at the curing age of 90th day; SEM image of O-0% (A), SEM image of O-10% (B), SEM image of O-20% (C), SEM image of O-30% (D), and SEM image of O-40% (E).

### 4.3.5.2 Mineralogical phase analysis with X-ray diffraction

The study had made the XRD analysis for the RCGC specimen containing the 20% OSA at the curing ages of 3rd day, 14th day, and 90th day, as seen in Fig. 4.21.

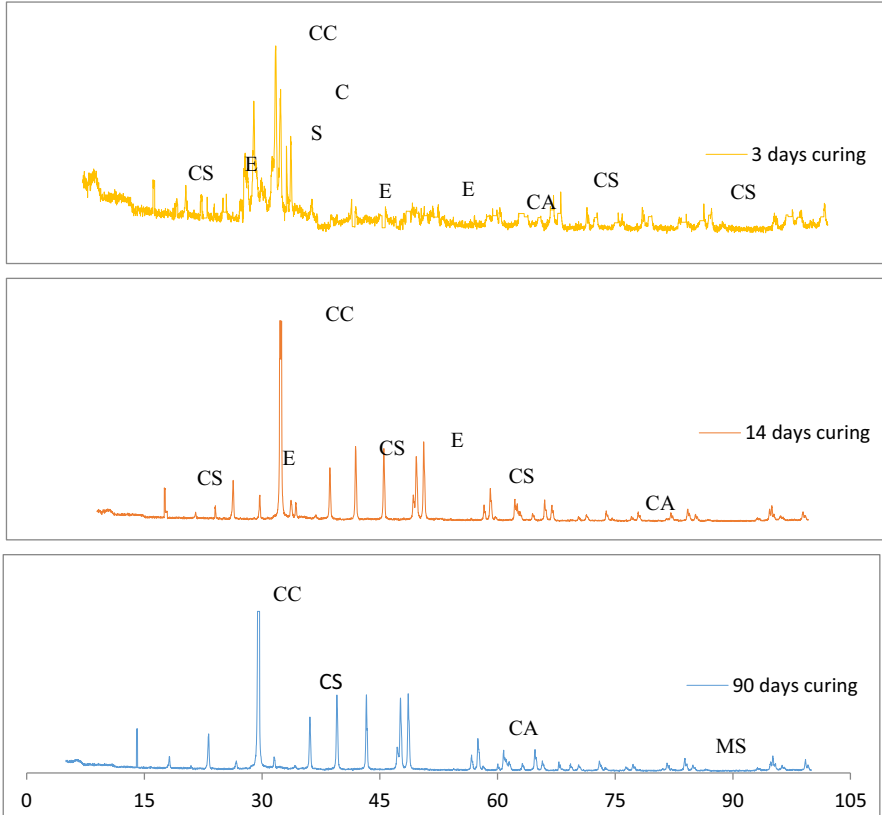


**Figure 4.21** The XRD analysis for O-20% specimen at the curing ages of 3rd day, 14th day, and 90th day. CC stands for calcite ( $\text{CaCO}_3$ ), E means ettringite, S stands for  $\text{SiO}_4$ , C stands for calcium oxide ( $\text{CaO}$ ), CA stands for calcium-aluminate-hydrate ( $\text{CaO} \cdot \text{Al}_2\text{O}_3 \cdot \text{H}_2\text{O}$ ), CS stands for RCGC calcium silicate ( $\text{Ca}_2\text{SiO}_4 \cdot \text{H}_2\text{O}$ ) hydrate, and MS stands for magnesium silicate ( $\text{MgO} \cdot \text{SiO}_2 \cdot \text{H}_2\text{O}$ ) hydrate.

At 3 days, there are the contents of calcite ( $\text{CaCO}_3$ ), calcium oxide ( $\text{CaO}$ ), silicon dioxide ( $\text{SiO}_2$ ), and calcium-silica-hydrate (C-S-H), which is a major compound, as well as the content of ettringite and calcium-aluminate-hydrate (C-A-H) as a minor compound in the O-20% of RCGC paste. Apart from the calcium oxide content, at 14 days, it is analyzed that there are the same major compound and minor compound in the O-20% of RCGC paste. There is a difference between the major compound and minor compound in the O-20% of RCGC paste at 90 days. This difference is due to the magnesium silicate ( $\text{MgO} \cdot \text{SiO}_2 \cdot \text{H}_2\text{O}$ ) hydrate (M-S-H). At 90 days in the O-20% of RCGC paste, all other major and minor compounds are

the same with the major and minor compounds of the O-20% of RCGC paste at 3 days and 14 days.

The mineral composition in the O-20% of RCGC paste is due to the chemical composition of OSA in Fig. 4.2 (Table 4.3). The chemical composition of OSA has a high quantity of silicon oxide ( $\text{SiO}_2$ ) and calcium oxide ( $\text{CaO}$ ) as well as the oxides of aluminum and ferrite, which are very important compounds in the hydration reaction of cement to turn out new hydration products, such as calcium-aluminum-hydrate (Fig. 4.21). It is clear to infer that the  $\text{CaO}$  and the  $\text{SiO}_2$  would be consumed by the CH, which is the biggest hydration product of cement with time to form calcium-silicate-hydrate (Fig. 4.21). It leads to the increase in the demand of water and the ettringite, which enhances strength gain in the RCGC. The increase in the water absorption of the OSA leads to an increase in the water demand of the RCGC, and therefore the study uses a water reducer to prevent being unhydrated cement particles, which results in the decrease in stress gain (Kırgız, 2014, 2018, 2019).

## 4.4 Conclusion

Based on the results of this experimental research the following conclusions are summarized:

- The study suggests that the OSA, which includes the shapes of various amorphous and geometrical particles along with rough and porous surfaces and has a specific gravity of  $2.69 \text{ (g/cm}^3\text{)}$ , is the SCM and the latent hydraulic additive for cement and cement-based materials because of its precious chemical compounds, such as silicon oxide, aluminum oxide, iron oxide, and calcium oxide as well as titanium oxide, which is not within the chemical compound of conventional cement.
- The OSA lightens the fresh and hardened density of RCGC because its specific gravity and the specific gravity of cement are not equal to each other.
- As the OSA increases the porosity of RCGC the study suggests that the OSA is a supplementary material to turn out lightweight RCGC, which is as effective as conventional RCC.
- As the O-10% of RCGC shows the same durability property as the durability property of the O-0% of RCC, the study offers that the OSA is the SCM for protecting the harmful effect of freezing and thawing.
- The O-40% of RCGC mixing prescription shows the least performance among the OSA substitutions for cement evaluated here against strength development as well as freezing and thawing resistance.
- It is also evident that the substitution of OSA with cement produces new hydration products for the RCGC, such as the magnesium-silicate-hydrate, which may increase the strength gain and durability development.
- The study also suggests that the best mixing prescription of RCGC is the mixing proportion of the O-10% of RCGC as the O-10% of RCGC mixing prescription shows the best performance in terms of both the strength gain and durability development and elasticity.
- The effort carried out in the study should be used to find out the possible ways to sustain the manufacturing of RCGC with the OSA and conventional cement. The results of such studies would directly benefit the construction industry as well.

## Availability of data and materials

The “Experimental Research” data used to support the findings of this study are available from the corresponding author upon request.

## Funding

The authors declare no funding property in the work.

## References

- ACI. (2001). *State of the-art report on roller compacted concrete pavement*. American Concrete Institute Report ACI.325.10-95.
- ASTM C114-07. (2007). American Society for Testing and Material, (ASTM). Designation C 114-07, Standard Test Methods For of Chemical Analysis of Hydraulic-Cement. P 1-32, Current Edition Approved, July 15. Published August 2007.
- ASTM C128-01. (2001). *Standard test method for density, relative density (specific gravity), and absorption of fine aggregate*. West Conshohocken, PA: ASTM International, <http://www.astm.org>
- ASTM C128-15. (2015). *Standard test method for relative density (specific gravity) and absorption of fine aggregate*. West Conshohocken, PA: ASTM International, <http://www.astm.org>
- ASTM C1365-18. (2018) *Standard test method for determination of the proportion of phases in Portland cement and Portland-cement clinker using x-ray powder diffraction analysis*. West Conshohocken, PA: ASTM International, <http://www.astm.org>
- ASTM C39/C39M-18. (2018). *Standard test method for compressive strength of cylindrical concrete specimens*, ASTM International, West Conshohocken, PA, <http://www.astm.org>
- ASTM C136/C136M-14. (2014). *Standard test method for sieve analysis of fine and coarse aggregates*, West Conshohocken, PA: ASTM International, <http://www.astm.org>
- ASTM C138/C138M-09. *Standard test method for air content of freshly mixed concrete by the pressure method*.
- ASTM C293/C293M-16. (2016). *Standard test method for flexural strength of concrete (using simple beam with center-point loading)*. West Conshohocken, PA: ASTM International.
- ASTM C469/C469M-14. (2014). *Standard test method for static modulus of elasticity and Poisson’s ratio of concrete in compression*. West Conshohocken, PA: ASTM International, <http://www.astm.org>
- ASTM C496/C496M-17. (2017). *Standard test method for splitting tensile strength of cylindrical concrete specimens*. West Conshohocken, PA: ASTM International, <http://www.astm.org>
- ASTM C642-13. (2013). *Standard test method for density, absorption, and voids in hardened concrete*. West Conshohocken, PA: ASTM International, <http://www.astm.org>.
- ASTM C666/C666M-15. (2015). *Standard test method for resistance of concrete to rapid freezing and thawing*. West Conshohocken, PA: ASTM International, <http://www.astm.org>



- ASTM C1435/C1435M-14. (2014). *Standard practice for molding roller-compacted concrete in cylinder molds using a vibrating hammer*. West Conshohocken, PA: ASTM International, <http://www.astm.org>
- Al-Massaid, H., Khedaywi, T., & Smadi, M. (1989). Properties of asphalt-oil shale ash bituminous mixture under normal and freeze-thaw conditions. *TranspRes Record*, 1228, 54–62.
- Ashteyat, A., Haddad, R. H., & Yamin, M. M. (2012). Production of self-compacting concrete using Jordanian oil shale ash. *Jordan Journal of Civil Engineering*, 6, 202–214.
- ASTM C1723-16. (1723). Standard guide for examination of hardened concrete using scanning electron microscopy. West Conshohocken, PA: ASTM International. Available from <http://www.astm.org>.
- Chhaiba, S., Blanco-Varela, M. T., Diouri, A., & Bougarrani, S. (2018). Characterization and hydration of cements and pastes obtained from raw mix containing Moroccan oil shale and coal waste as a raw material. *Construction and Building Materials*, 189, 539–549, November 20, 2018.
- Dabbas, M.A. (1997). Oil shale: Hopes and ambitions (in Arabic). In *Second Jordanian conference for mechanical engineering, JIMEC '97*, Amman-Jordan, JAE.
- Debieb, F., Courard, L., Kenai, S., & Degeimbre, R. (2009). Roller compacted concrete with contaminated recycled aggregates. *Construction and Building Materials*, 23, 3382–3387.
- Gauthier, P., & Marchand, J. (2005). Design and construction of roller compacted concrete pavements in Quebec. Cement Association of Canada (CAC), the Association béton Québec (ABQ) and Association des constructeurs de routes et grands travaux du Québec (ACRGTO), 111 p.
- Hesami, S., Modarres, A., Soltaninejad, M., & Madani, H. (2016). Mechanical properties of roller compacted concrete pavement containing coal waste and limestone powder as partial replacements of cement. *Construction and Building Materials*, 111, 625–635.
- Jingfu, K., Chuncui, H., & Zhenli. (2009). Strength and shrinkage behaviors of roller-compacted concrete with rubber additives. *International Journal of Computational Engineering Research*, 42(8), 1117–1124.
- Kassem, M., Soliman, A., & Naggat, H. E. (2018). Sustainable approach for recycling treated oil sand waste in concrete: Engineering properties and potential applications. *Journal of Cleaner Production*, 204, 50–59, 10 December.
- Kasu, S. R., Deb, S., Mitra, N., Muppireddy, A. R., & Kusam, S. R. (2019). Influence of aggregate size on flexural fatigue response of concrete. *Construction and Building Materials*, 229116922. Available from <https://doi.org/10.1016/j.conbuildmat.2019.116922>, 30 December 2019.
- Kirgiz, M. S. (2014). Effects of blended-cement paste chemical composition changes on some strength gains of blended-Mortars. *The Scientific World Journal*, 2014, 1–11. Available from <https://doi.org/10.1155/2014/625350>, Article ID 625350.
- Kirgiz, M. S. (2018). Advancements in properties of cement containing pulverised fly ash and nanomaterials by blending and ultrasonication method (review—Part I). *Nano Hybrids and Composites*, 19, 1–11.
- Kirgiz, M. S. (2019). Advancements in properties of cement containing pulverised fly ash and nanomaterials by blending and ultrasonication method (review—Part II). *Nano Hybrids and Composites*, 24, 37–44.
- Madhkhan, M., Azizkhani, R., & Torki Harchegani, M. E. (2012). Effects of pozzolans together with steel and polypropylene fibers on mechanical properties of RCC pavements. *Construction and Building Materials*, 26(1), 102–112.

- Marchand, J., Gagne, R., Ouellet, E., & Lepage, S. (1997). Mixture proportioning of roller compacted concrete: A review. *Advanced Concrete Technology*, 457–486, [ACI Special Publication, SP-171].
- Meddah, M. S. (2015). Durability performance and engineering properties of shale and volcanic ashes concretes. *Construction and Building Materials*, 79, 73–82, 15 March 2015.
- Mirza, J. (2019). Reduction in ecology, environment, economy and energy in concrete industry using waste materials. In M. S. Kirgiz (Ed.), *The proceedings of abstracts book of the third annual international conference on eco-sustainable construction materials*, August 26–29, 2019, p.16, İstanbul, TR, ISBN: 978-605-031-179-2.
- Pigeon, M., & Malhotra, M. (1995). Frost resistance of roller compacted high-volume fly ash concrete. *Journal of Materials in Civil Engineering*, 7(4), 208–211.
- Raado, L.-M., Kuusik, R., Hain, T., Uibu, M., & Somelar, P. (2014). Oil shale ash based stone formation hydration, hardening dynamics and phase transformations. *Oil Shale*, 31(1), 91–101. Available from <https://doi.org/10.3176/oil.2014.1.09>.
- Radwan, M. M., Farag, L. M., Abo-El-Enein, S. A., Abd., & El-Hamida, H. K. (2013). Alkali activation of blended cements containing oil shale ash. *Construction and Building Materials*, 40, 367–377, March 2013.
- Rooholamini, H., Sedghi, R., Ghobadipour, B., & Adresi, M. (2019). Effect of electric arc furnace steel slag on the mechanical and fracture properties of roller-compacted concrete. *Construction and Building Materials*, 211, 88–98, 30 June 2019.
- Schrader, E. K. (2006). Building roller-compacted-concrete dams on unique foundations. *HydroReview (HRW)*, 14(1), 28–33.
- Settari, C., Debieb, F., Kadri, E. H., & Boukendakdji, O. (2015). Assessing the effects of recycled asphalt pavement materials on the performance of roller compacted concrete. *Construction and Building Materials*, 101, 617–621.
- Uibu, M., Somelar, P., Raado, L.-M., Irha, N., Hain, T., Koroljova, A., & Kuusik, R. (2016). Oil shale ash based backfilling concrete—Strength development, mineral transformations and leachability. *Construction and Building Materials*, 102(1), 620–630.
- Villena, J., Trichês, G., & Prudêncio, L. R., Jr (2011). *Replacing the aggregate by rice husk ash in roller compacted concrete for composite pavements* (pp. 19–27). American Society of Civil Engineers.
- Zhang, Y., Cai, X., Gao, L., & Wu, K. (2019). Improvement on the mechanical properties of cement asphalt mortar (CA) and concrete composite specimens in high-speed railway by modification of interlayer bonding. *Construction and Building Materials*, 228116758. Available from <https://doi.org/10.1016/j.conbuildmat.2019.116758>, 20 December 2019.

This page intentionally left blank

# Natural pozzolan as hydraulic binder substitution in combination with recycled aggregates in concrete

*S. Kenai<sup>1</sup>, M. Ghrici<sup>2</sup> and J. Khatib<sup>3</sup>*

<sup>1</sup>Civil Engineering Department, University Blida 1, Blida, Algeria, <sup>2</sup>Civil Engineering Department, University of Chlef, Algeria, <sup>3</sup>Faculty of Engineering, Department of Civil and Environmental Engineering, Beirut Arab University, Beirut, Lebanon

## 5.1 Introduction

Various mineral additions have been used as partial substitution of cement to reduce the environmental impact of cement production by decreasing energy consumption and CO<sub>2</sub> emissions during clinker manufacture and consequently reducing the cost of cement production. These include fly ash (FA), ground granulated blast furnace slag (GGBS), silica fume or microsilica, desulphurised waste, ground glass and calcined clay. Also, natural pozzolan (NP) which is available in some regions of the world in large quantities and could be used as a cement replacement material. Recycled aggregate, derived from various processes such as demolition waste, can be used instead of natural/virgin aggregate in the production of concrete. Recycled aggregates include recycled concrete, recycled brick, recycled glass, recycled polystyrene, recycled plastic, bottom ash, and waste granular cork. This chapter reviews the effect of NP on the rheological, mechanical, and durability properties of mortar and concrete.

## 5.2 Rheological properties

There is noticeable change in the rheological properties of NP in concrete including slump flow and the resistance to segregation. The reduction in workability is probably because of the lower density of NP compared to cement, the angular shape and rough surface structure of NP particles, the higher water absorption on the surface of the more porous NP particles, and its reactivity, which might increase the cohesiveness of the mix (Belaidi et al., 2012; Juenger & Siddique, 2015). This is contrary to the positive effect at 15% and 30% substitution of cement by slag which was found to increase the workability of self-compacting concrete (SCC) mixes

with and without recycled aggregates (Boukhelkhal et al., 2018; Kouider-Djelloul et al., 2018). SCC mixes with 15% NP showed higher stability with laitance of only 2.3% and hence higher resistance to segregation and bleeding as compared to mixes with 15% slag or 15% of limestone (Boukhelkhal et al., 2018).

Slump flow is usually reduced in comparison to control concrete. A slump flow reduction from 755 to 654 mm is reported when the NP content increases from 0% to 25% as can be seen in (Table 5.1) (Guettaf et al., 2020), whereas comparable slump flow is reported for up to 15% NP (Omrane et al., 2017).

The increase in plastic viscosity and yield stress with the increase in NP content has been reported by other researchers with good correlation between viscosity and yield stress on one side and slump flow on the other side (Adjoudj et al., 2014; Guettaf et al., 2020). The combination of NP and marble powder (MP) has a beneficial effect on slump flow, which is increased for a mixture with 10% of mineral addition. The flow time is also reduced, and the viscosity and the sieve stability are improved (Belaidi et al., 2016).

Hammat et al. (2021) investigated the effect of fineness of natural pozzolan by grinding it to three different finenesses of 350, 420, and 500 m<sup>2</sup>/kg with a substitution rate of 15% and 20 % (by weight). They concluded that NP affects negatively the rheological properties of self-compacting mortar regardless of the fineness. The V-funnel and plastic viscosity were almost doubled at the highest fineness used of 500 m<sup>2</sup>/kg (Table 5.2).

The use of 15%–20% of NP, as partial cement replacement, in mixes with 50% recycled aggregates gave comparable slump flow to the control mix, however, for 25% NP replacement, the slump flow was slightly reduced (Fig. 5.1). The V-funnel

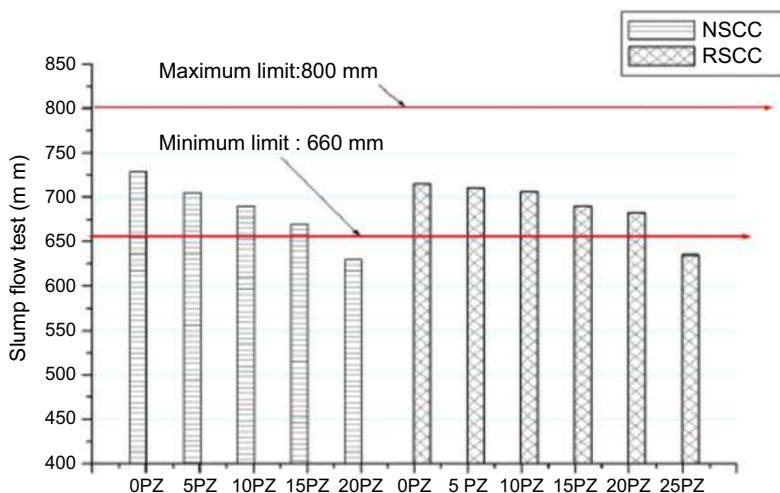
**Table 5.1** Fresh properties of SCC mixtures with various NP replacements.

		SCC-0	SCC-15	SCC-25	ENFRAC guidelines
Slump flow test	Diameter (mm)	755	732	654	550–850
	Time T <sub>500</sub> (s)	2.86	3.52	4.15	SF2 660–750 2–5
J-ring test	Diameter (mm)	745	729	651	550–850
V-funnel test	Time T <sub>Vf</sub> (s)	7.86	8.16	9.65	6–12
L-box test	H <sub>2</sub> /H <sub>1</sub> ratio	0.88	0.84	0.81	0.80–1.00
	T <sub>200</sub> (s)	0.68	0.86	1.10	–
	T <sub>400</sub> (s)	1.22	1.43	2.13	–
Sieve stability test	Laitance (%)	9.22	6.15	4.11	0–15
Rheometer test	Yield stress ( $\tau$ ) (Pa)	09.21	20.54	25.14	–
	Plastic viscosity ( $\mu$ ) (Pa.s)	06.26	09.93	11.55	–

Reprinted from Guettaf, Y., Kenai, S., Khatib, J., & Yahiaoui, W. (2020). Effect of wet curing and hot climate on strength and durability of SCC with natural pozzolan. *Current Materials Science*, 13(1), 58-73. Copy right (2023), with permission from Bentham.

**Table 5.2** Results of fresh mortars tests (SCM with NP) [Hammat et al. \(2021\)](#).

Fineness of natural pozzolan ( $m^2/kg$ )						
	350		420		500	
Content (%)	Slump flow (mm)	V-Funnel time (s)	Slump flow (mm)	V-Funnel time (s)	Slump flow (mm)	V-Funnel time (s)
NP0	296.5	2.52	296.5	2.52	296.5	2.52
NP15	296.0	3.65	283.5	3.86	279.0	4.88
NP30	281.5	4.20	278.0	4.25	273.0	9.93

**Figure 5.1** Slump flow on natural and recycled aggregate concrete with various NP contents ([Omrane et al., 2017](#)).

flow time increases with the NP content, and J-ring decreases for both mixes with natural and recycled aggregates ([Omrane et al., 2017](#)). [Debbih et al. \(2020\)](#) confirmed the reduction in slump flow and the increase of segregation resistance of 15% NP on mixes with 50% of recycled aggregates.

## 5.3 Mechanical properties

### 5.3.1 Compressive and flexural strength

The compressive strength of NP mortar and concrete mixes is usually lower at an early age because the pozzolanic reaction is slow but becomes comparable in the

long term as is the case with other mineral admixtures such as slag and fly ash. [Hammat et al. \(2021\)](#) reported a reduction of compressive strength at 1, 7, and 28 days of 49%, 39%, and 6%, respectively. At 90 days the highest strength was obtained for mixes with 15% NP whereas at 180 days an increase of 3 MPa was obtained for mortar with 15% and 30% NP. The increase was higher with the increase of the fineness of NP ([Fig. 5.2](#)). The enhancement of the long term compressive strength has been confirmed by other researchers ([Guettaf et al., 2020](#)).

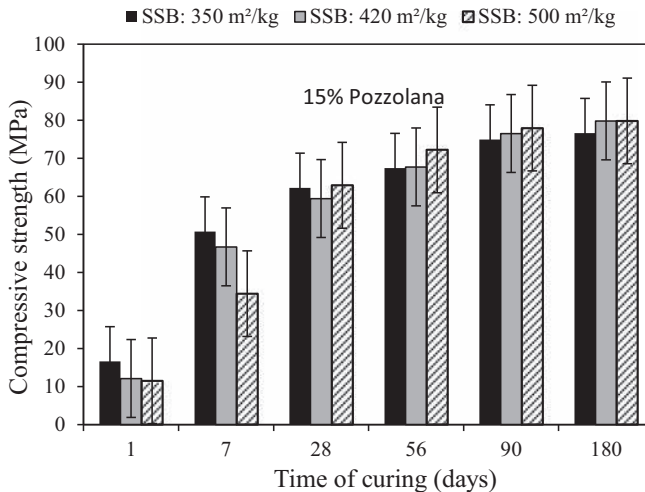


**Figure 5.2** Effect of natural pozzolan fineness on compressive strength of SCM at 15% replacement level.

The compressive strength could be improved the short term and long term through the combination of NP with other admixtures such as limestone ([Ghrici et al., 2007](#)). [Belaidi et al. \(2016\)](#) combined NP with MP with a ratio of MP/NP of 3 and obtained a comparable compressive strength of SCC with OPC at 90 days with 40% of NP and MP. The beneficial effect of NP under hot climate conditions was proved if proper humid curing is provided ([Guettaf et al., 2020](#)). The strength for SCC concrete is satisfactory even at higher temperatures curing of 40°C and 80°C ([Boukhelkhal et al., 2018](#)). [Omrane et al. \(2017\)](#) combined 50% of recycled coarse and fine aggregates and NP in SCC mixes and showed the beneficial effect of NP on the 120 days compressive strength and hence the possibility of producing concrete with less environmental impact.

### 5.3.2 Flexural strength

The flexural strength development of self compacting concrete with NP is similar to that of the control. A reduction of 39% at 3 days of curing for SCC mixes with 15% NP has been reported, but at 90 days the decrease was only 4% indicating more pozzolanic reaction in the presence of NP ([Boukhelkhal et al., 2018](#)). The same authors

indicated that at high temperature curing of 40°C, the reduction in flexural strength for NP mixes is reduced and the flexural strength is comparable to that of the control mixes.

### 5.3.3 Elastic modulus

Due to the slow pozzolanic reaction, the elastic modulus is slightly reduced for NP mixes as compared to ordinary cement mixes. The 28 days modulus of elasticity was reduced by 6% for NP mixes as compared to reference mixtures at 20°C of curing, and no negative effect was noticed for a temperature curing of 40°C and 80°C (Boukhelkhal et al., 2018).

### 5.3.4 Shrinkage

Total shrinkage increases slightly with the NP content at early age, probably because of the formation of capillary porosity due to the slow pozzolanic reaction. The long term shrinkage is lower than that of reference mortar due to the densification of the hydrated cement paste in the presence of NP, which slows the water evaporation. Hammat et al. (2021) reported an increase of about 14% of the total shrinkage for mixes with 30% NP at 10 days, but beyond 14 days the shrinkage was lower compared to reference mortar (Fig. 5.3). The increase in NP fineness increases the total and autogenous shrinkage as compared to control mortar.

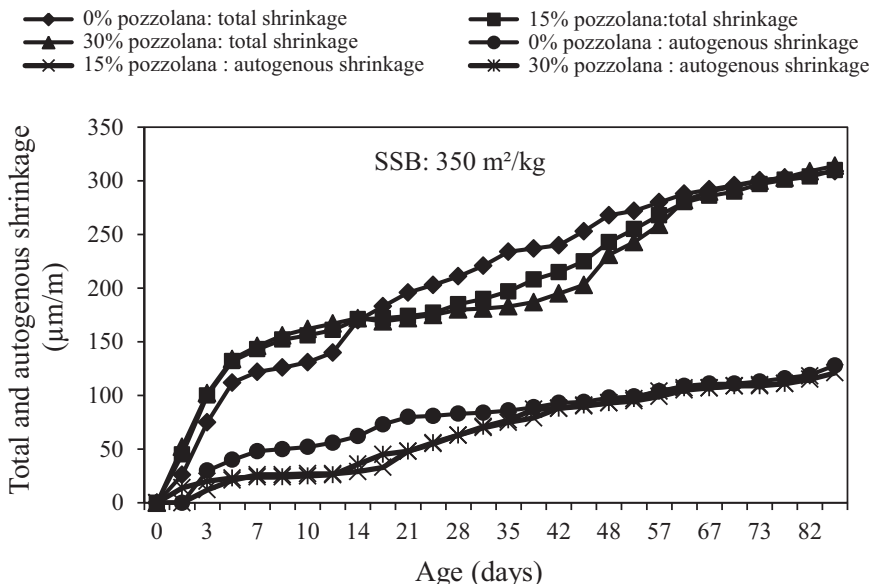


**Figure 5.3** Total and autogenous shrinkage of SCM with natural pozzolan (SSB: 350 m<sup>2</sup>/kg).



## 5.4 Durability

### 5.4.1 Permeability

Several studies reported the beneficial effects of NP on the permeability of concrete compared to control mixtures depending on many parameters, including quality and quantity of pozzolan, time of curing, and concrete constituents (Cyr, 2013). The reduction of permeability is mainly attributed to the pore structure refinement due to the pozzolanic reaction and the pore continuity (Mehta, 1981). In this context, Ramezaniapour et al. (2015) investigated the use of natural zeolite (NZ) on the concrete permeability. Concretes with water-to-cementitious material (w/cm) ratios of 0.35, 0.40, 0.45, and 0.50 were prepared, and cement was replaced with up to 15% NZ. Use of NZ led to considerable reduction in water permeability and capillary absorption regardless of the w/cm ratio. An increase in the w/cm ratio led to an increase in both the permeability and the rate of absorption by capillary action. Likewise, Samimi et al. (2018) found an improved durability performance of SCC with NPs. Zeyad et al. (2020) showed that the high-strength concrete produced by partially replacing the cement with volcanic pumice powder(PC) exhibited higher durability indicated by the low water absorption and initial surface absorption compared with the control mixture. In addition, Najimi et al. (2012) studied the properties of concrete containing the same NZ from Iran, with 15% and 30% replacement of cement, and reported lower water penetration depths at 28 and 90 days for higher replacement levels. On the other hand, water absorption of the concrete mixtures containing NZ was higher than that of the control concrete (Table 5.3). This was attributed to the finer pore structure in the presence of NZ.

**Table 5.3** Effect of natural zeolite on the transport properties (Najimi et al., 2012).

Mixture identification	Water penetration depth (mm)		24 h water absorption (%)	
	28 days	90 days	28 days	90 days
NZ0 (control)	15	15	6.88	6.50
NZ15	13	11	7.97	7.95
NZ30	9	10	7.75	7.60

Ghrici et al. (2007) reported on the efficiency of an Algerian NP on the sorptivity of mortar. They found that at 28 days of curing the sorptivity coefficient of concrete containing 30% of natural pozzolan diminished by 29% and 56% compared with the control concrete for water-to-binder (w/b) ratios of 0.4 and 0.6, respectively. Similarly and at 90 days of age the sorptivity coefficient was 34% lower than that of the corresponding OPC mortar for both (w/b) ratios of 0.4 and 0.6. In this case, there are pores in the bulk paste or in the interfacial zone between aggregate and cement paste. The capillary pores are reduced by the formation of secondary C–S–H gel due to the pozzolanic reaction and hence the reduction in the capillary sorption of concrete. The reduction of water permeability and water

capillary absorption have been confirmed by other researchers as NP refines the pore structure if humid curing is applied for at least 7 days and the lowest water permeability was obtained for 15% NP mixtures (Guettaf et al., 2020).

Masood et al. (2020) reported that water absorption of recycled aggregate concrete (RAC) was higher than that of natural aggregate concrete (NAC) by more than 23% due to the higher water absorption capacity of recycled aggregates. This increase in absorption could be due to porous/permeable matured cement paste in RCA. In addition, bentonite (low-calcium pozzolan) addition by up to 20% in both NAC and RAC decreased the water absorption. For both types of concrete, NAC and RAC, the maximum reduction was observed for the replacement level of 20% bentonite. They concluded that bentonite is beneficial for both NAC and RAC in terms of reducing the water absorption.

Mehrabi et al. (2021) investigated the feasibility of using RCA and supplementary cementitious materials (SCMs) including PC and nanoclay (NC) as a partial replacement of natural coarse aggregate and Portland cement in pervious concrete, respectively. For this purpose the normal coarse aggregate (NCA) was replaced with 10%, 25%, 50%, and 100% RCA and the Portland cement was replaced with 10%, 25%, and 50% pumice in addition to 1% to 3% NC. They reported that PC incorporating recycled aggregates exhibits higher water permeability compared to the control mix. Generally, adding pumice and NC densifies the pore system due to their pozzolanic reactivity and microfilling ability. However, the permeability coefficient of PC mixes incorporating pumice increased with the increase in pumice content due to the porous and rough texture of the pumice stone, which has increased air trapped in the matrix. Moreover the use of NC in mixtures prepared with RCA and pumice resulted in a marginal reduction in the void content and the permeability coefficient.

## 5.4.2 Carbonation

The presence of carbon dioxide levels in the atmosphere above 0.04% by volume diffuses through the unsaturated concrete open pores or cracks, dissolves in the pore water, and then reacts with the hydrates of cement to form calcium carbonate ( $\text{CaCO}_3$ ) and silica gels (Dunster, 1989). The main carbonation reaction is that of calcium hydroxide and can be described as shown in Eq. (5.1):



Other constituents in the concrete can also carbonate, particularly calcium–silicate hydrates (C–S–H), which are the major constituents of hydrated cement paste. Peter et al. (2008) suggest that the C–S–H phases start carbonating as soon as the available calcium hydroxide has been depleted. Carbonation reactions have two main functions (Cyr, 2013):

- A reduction of global concrete porosity and a modification of the pore size distribution. The decrease of the porosity can lead to the improvement of some mechanical performances.

- The consumption of portlandite, causing a decrease in the pore solution pH, from 12.5 or 13.5 to around 9. At that level of pH the passivating layer is not stable and dissolves, causing corrosion to start. This generally leads to a strong reduction in the durability of the structure.

The depth of carbonation is usually proportional to the square root of time, which means that it is driven by the process of gas diffusion (Cyr, 2013). Thomas (2013) reported that carbonation of mortar and concrete increases as SCM increases, w/cm increases, strength decreases and curing decreases.

In addition to the parameters, the depth of carbonation attains maximum values at relative humidity (RH) levels of between 50% and 70% (Hewlett & Liska, 2019) because RH must be sufficiently low to allow the permeation of CO<sub>2</sub> into the concrete but also sufficiently high for the carbonation reaction to be achieved in an aqueous phase.

It should be noted that SCMs influence the carbonation of mortar and concrete by the consumption of portlandite due to the pozzolanic reaction, which implies that a smaller amount of CO<sub>2</sub> is required to carbonate the remaining hydrates. On the other hand, Bier (1986) has shown that the depth of carbonation increased as the portlandite content in the cementitious material (CM) decreased. Consequently, the presence of SCMs could result in more rapid carbonation. The overall trend found in the literature is that the depth of carbonation increases with the use of pozzolan in concretes (Neville, 2011).

Ramezaniapour et al. (2015) investigated the use of NZ on the concrete carbonation. In this study, for w/cm ratios of 0.35, 0.40, 0.45, and 0.50, concrete mixtures containing 0%, 10%, and 15% replacement of cement with NZ were made. The results showed that the carbonation depth of specimens measured at different ages of 28, 90, and 270 days increased with the increase in w/c and NZ replacement level. However, the depth of carbonation decreased by increasing the curing time due to the continuation of the hydration process, thus improving pore structures as presented in Table 5.4.

**Table 5.4** Results of accelerated carbonation test on the selected concrete mixtures (Ramezaniapour et al., 2015).

Mixture ID	w/c	Natural zeolite replacement level (%)	Carbonation depth (cm)		
			28 days	90 days	270 days
A0	0.35	0	1.5	1.2	0.1
A10	—	10	2.5	3.2	0.3
A15	—	15	2.5	3.7	1.4
B0	0.40	0	2.1	1.4	0.3
B10	—	10	5.2	3.9	1.6
B15	—	15	6.0	4.2	2.9
C0	0.45	0	3.0	3.1	0.9
C10	—	10	6.9	5.1	2.8
C15	—	15	8.3	5.2	3.0
D0	0.55	0	3.3	3.3	1.0
D10	—	10	7.1	5.4	3.9
D15	—	15	8.8	6.0	5.1

Recently, [Al-Amoudi et al. \(2019\)](#) measured the accelerated carbonation for a period of 90 and 180 days on mortars containing NPs obtained from three different sources in Saudi Arabia. They showed that after both exposure periods the depth of carbonation was relatively higher in the specimens prepared with NP-concrete mixtures as compared with that of OPC concrete. This is in agreement with the fact that concretes containing pozzolanic admixtures possess lower resistance to carbonation as compared to the concrete mixtures containing Portland cement alone due to the fact that the amount of available  $\text{Ca}(\text{OH})_2$  is reduced because of the lower cement content and its consumption in the pozzolanic reaction. Furthermore, C-S-H gel as a result of the pozzolanic reaction is more prone to carbonation compared with C-S-H gel from cement hydration ([Thomas et al., 2014](#)). In this way the C-S-H gel in pozzolanic concrete will be easily carbonated.

According to many studies the carbonation depth of RAC increased with the increase in coarse and fine RA content as a consequence of higher porosity of RA as well as an increase in effective w/c ratio, as shown in [Fig. 5.4 \(Tam et al., 2021\)](#). This may be attributed to the higher adhered mortar of RA, which increases the total cement content and slows down the carbonation rate. [Silva et al. \(2015\)](#) found that the relative carbonation depth of RAC with 100% coarse RA was 2.5 times higher than that of NAC. For the concrete with the same incorporation of fine RA the carbonation depth was 8.7 times, probably due to the higher water absorption capability of fine RA. When the replacement ratio of coarse RA increased the RAC can achieve similar strength and carbonation depth as NAC by lowering the w/c ratio of RAC ([Silva et al., 2015](#)).

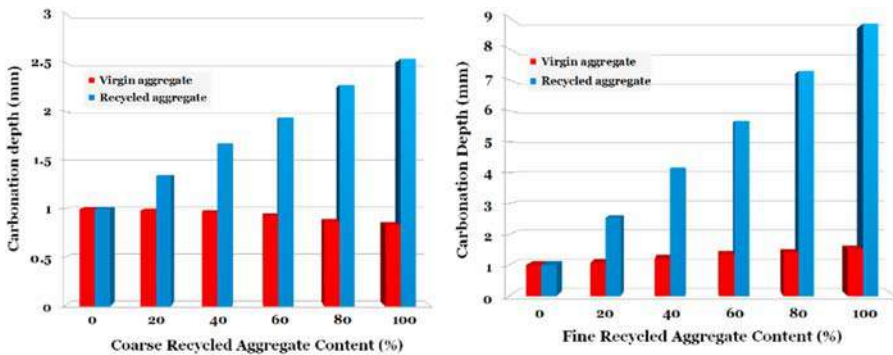


**Figure 5.4** Carbonation depth relative to coarse and fine RA content ([Tam et al., 2021](#)).

Based on the literature, [Guo et al. \(2018\)](#) summarized the influence of different parameters on the carbonation resistance of RAC as presented in [Table 5.5](#).

**Table 5.5** Influence of different parameters on the carbonation resistance of RAC (Guo et al., 2018).

Parameter	Change	Effect
RA content	↑	Strong negative
w/c ratio	↑	Strong negative
Size of RA	↓	Mild negative
Adhered mortar	↑	Strong negative
Exposure time	↑	Negative
Pozzolanic materials	↑	Negative
Superplasticizers	—	Positive
Pretreatment RA	—	Mild positive
Mixing method	—	Mild positive

Remarks: ↑—increase, ↓—decrease.

Chakkamalayath et al. (2020) carried out an accelerated carbonation test, according to BS 1881–210 (2013), after 28 days of curing in water, on six concrete mixes with different compositions, including the replacement of ordinary Portland cement and NCAs with 30% volcanic ash (VA) and 30% RCA, respectively. The control mixes (VCC and SCC) were not affected by carbonation. Also, the carbonation was not affected by the replacement of natural aggregates with RCA as in the case of SR30 (mix containing 30% RCA), maybe because the old mortar adhered to recycled aggregates causes higher alkaline content, which may be shielding the concrete surface against carbonation. However, the carbonation depth was increased with the replacement of OPC with VA and granulated glass blast furnace slag (GGBS). The reduction in carbonation resistance for binary and ternary mixes containing VA and GGBS may have been due to the predominant effect of reduction in calcium hydroxide because of the pozzolanic nature, more than the effect due to pore refinement.

### 5.4.3 Resistance to chloride attack

Chloride binding by cement-based materials is very complex and influenced by many factors. Also it is a function of the amount of C-S-H gel in the concrete. NP increases the formation of more gel, thus providing more surface area available for adsorption. In addition, chloride binding capacity depends on the pH value or OH<sup>-</sup> concentration in the pore solution of concrete. In fact the higher the pozzolanic activity, the higher the decrease in OH<sup>-</sup> and the lower the rapid chloride penetration value.

Ramezaniyanpour et al. (2015) measured the rapid chloride penetrability according to ASTM C1202 (2010) at different ages of 28, 90, and 270 days. The concrete mixes were designed with four w/cm ratios, 0.35 (A), 0.40 (B), 0.45 (C), and 0.50 (D), and the replacements of 10% and 15% in Portland cement weight per NZ. Their results are presented in Fig. 5.5. As can be seen that the use of NZ led to considerable reduction in chloride ion penetration, measured as passing charge through

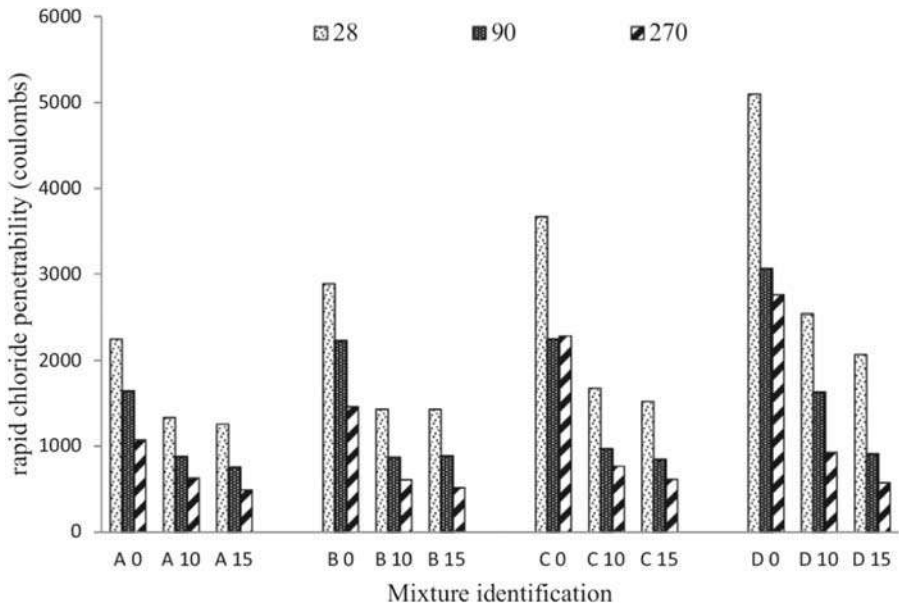


**Figure 5.5** Rapid chloride penetrability test results of the selected concrete mixtures (Ramezaniapour et al., 2015).

the specimens. In addition, these improvements were more significant for mixtures having a higher w/cm ratio.

Ahmadi and Shekarchi (2010) reported that concretes made with 10%–20% NZ showed a significant decrease in diffusion coefficient compared to control concrete. However, silica fume (SF) concretes had a better effect on improving diffusion characteristics of concrete than NZ concretes at the same level of replacement. This confirms the results obtained by Chan and Ji (1999), which indicate that the NZ was more effective than pulverized fuel ash in terms of chloride diffusion into concrete, but it was less effective than SF. Several researchers (Celik et al., 2014; Hossain & Lachemi, 2004; Najimi et al., 2012; Uzal et al., 2007) also found higher reduction in chloride ion penetration with NPs. Recently, Al-Amoudi et al. (2019) investigated the chloride profiles obtained by testing the powdered samples collected at different depths from the specimens of OPC and NP concretes after six months of exposure of the specimens to the 5% NaCl solution. They found that with the incorporation of NPs into the mixtures as a partial replacement of the OPC the coefficient of chloride diffusion has clearly decreased by about more than two times.

There is a consensus in the literature that RAC tends to exhibit greater chloride ion penetration than the corresponding NAC and that the magnitude of the difference depends on several factors related to the use of RA which are discussed by several researchers.

Jalilifar et al. (2020) studied the durability of recycled concrete made of coarse RAC containing silica fume and NP. They found that the rapid penetration of chloride ions remained nearly constant up to 50% RAC, whereas it increased dramatically when the RAC incorporation levels increased to 100%. Masood et al. (2020) studied the chloride migration coefficient in concretes made with 0%–20% of bentonite (i.e. low-calcium pozzolan) by mass replacement of Portland cement in both NAC and RAC. A decrease in resistance to chloride migration was observed by replacing RCA with NAC in concrete mixes. Due to the poor interfacial transition zone (ITZ) and the high pore volume, RAC had a significantly higher chloride migration coefficient than NAC. RAC mixes resulted in a 27% less resistance to chloride penetration as compared with that of mixes of NAC. On the other hand, increasing the dosage of bentonite improved the resistance to chloride penetration in NAC and RAC mixtures. In another study, Chakkamalayath et al. (2020) reported that the mixture with 30% RCA (SR30) showed a higher passing charge at 90 days when conducting the rapid chloride ingress test. The conductivity decreased with the increase of the curing time. On the other hand the higher conductivity at 90 days was also compensated by the incorporation of VA. In addition, it was confirmed that the incorporation of GGBS resulted in finer microstructures as mixes containing GGBS showed very low permeability at 90 and 180 days. It should be noted that the same findings were obtained by other researchers (Al-Swaidani & Al-Hajeh, 2017; Soldado et al., 2021).

#### 5.4.4 Resistance to sulfate attack

Sulfate salts are harmful to concrete as they can cause expansion, loss of strength, and eventually transform the material into a mushy mass (Hewlett & Liska, 2019). The sulfates can come from different sources and are found in the form of sodium sulfate ( $\text{Na}_2\text{SO}_4$ ), potassium sulfate ( $\text{K}_2\text{SO}_4$ ), magnesium sulfate ( $\text{MgSO}_4$ ), and calcium sulfate ( $\text{CaSO}_4$ ), and these salts are highly soluble. The sulfate attack is generally attributed to the formation of gypsum ( $\text{CaSO}_4 \cdot 2\text{H}_2\text{O}$ ) and delayed ettringite formation, which must be distinguished from primary Aft resulting from the reaction of  $\text{C}_3\text{A}$  with calcium sulfate. Ettringite eventually transforms to monosulfate hydrate,  $\text{C}_4\text{ASH}_{18}$ , which makes the concrete vulnerable to sulfate attack. The rate of sulfate attack depends on the permeability and the amount of calcium hydroxide and reactive alumina phases present (Mehta & Monteiro, 2006).  $\text{C}_3\text{A}$  is the main compound of cement responsible for the sulfate resistance, whereas  $\text{C}_4\text{AF}$  and CH can also affect the sulfate resistance of low  $\text{C}_3\text{A}$  (González & Irassar, 1998).

Several studies have shown that the partial replacement of Portland cement by SCMs improves the sulfate resistance of mortar and concrete by a number of mechanisms (Thomas, 2013). Kasaniya et al. (2021a, 2021b) studied the effect of several cementitious additions on the sulfate resistance of mortar according to the ASTM C1012 standard. The obtained results indicate that all raw NPs (five pumices and one perlite) and three ground glasses demonstrated a significant improvement in sulfate resistance (Fig. 5.6). Also it can be seen in Fig. 5.6 that all mortars produced with these cementitious additions behaved in a similar manner upon exposure

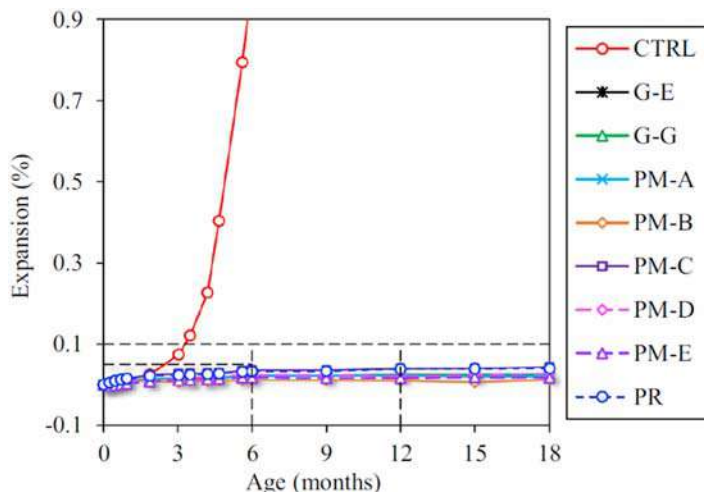


**Figure 5.6** Sulfate attack-induced expansion results for ground glasses, pumices, and perlite (note: 25% PC replacement level unless otherwise specified) (Kasaniya et al., 2021a, 2021b).

to the sodium sulfate solution and the pozzolanic reactivity of these materials did not indicate their contribution to the enhancement of sulfate resistance.

Shahmansouri et al. (2021) conducted an experimental investigation on the effect of NZ as cement replacement on durability of mortars under sulfate attack. The deterioration level was determined by measuring the compressive strength loss of mortar specimen after 90 and 180 days of immersion in the 5%  $\text{Na}_2\text{SO}_4$  solution at 20°C. Several mix designs cover an extensive range of w/cm ratios, different CM contents, and different rates of NZ (0, 5, 7, 5, 10, 15, and 20%). The incorporation of NZ in the mixtures increases the sulfate resistance of the concrete. As the percentage of NZ increases, the sulfate resistance is improved. However, an increase in the CM content and the w/cm ratio reduces the sulfate resistance of concrete.

Some researchers (Ghrici et al., 2006; Martínez-Rosales et al., 2020) reported that the strength of the mortar samples containing NPs usually increases at early ages in sodium sulfate solution but reduces at longer ages. In addition the sulfate attack of magnesium sulfate is considered to be more severe than that of sodium sulfate. Ramezaniapour (2014) reported that the use of different amounts of NPs usually increases the resistance of concretes and mortars in sodium sulfate exposure, but they may worsen the performance of sulfate resisting Portland cements in magnesium sulfate solutions. This opposite action depends on the type and properties of NPs.

Boudali et al. (2016) investigated the performance of SCC and self-compacting sand concrete incorporating recycled concrete aggregate and fine recycled concrete in different sulfate environments. Similar mixtures incorporating natural aggregates and natural pozzolan were also tested for comparison. The obtained results indicated that mixtures incorporating recycled concrete aggregate and fine recycled



concrete exhibited a better sulfate resistance behavior than those with natural aggregates and natural pozzolan.

Omrane et al. (2017) reported that the incorporation of 15% and 20% of NP in NSCC and RSCC, respectively, has a beneficial effect on the resistance to sulfuric acid ( $\text{H}_2\text{SO}_4$ ) attack. The comparison between NSCC and RSCC confirms that the mass loss of RSCC is less than 23% compared to NSCC, which shows the beneficial use of recycled aggregates. Recently, Masood et al. (2020) studied the effect of various levels of bentonite (0, 5, 10, 15, and 20%) on the sulfuric acid attack resistance of both NAC and RAC. It was concluded that the significant improvement in the acid attack resistance of RAC was noticed with the inclusion of bentonite. Moreover, improvement in acid attack resistance was observed to be enhanced for both NAC and RAC mixes with increasing level of bentonite.

#### 5.4.5 Alkali–silica reaction

Alkali-silica reaction (ASR) is one of the major durability concerns of concrete structure. ASR gels are formed when reactive silica in the aggregate reacts with hydroxyl ions ( $\text{OH}^-$ ) in the pore solution of cement paste. Alkali metal ions ( $\text{Na}^+$  and  $\text{K}^+$ ) contribute toward the high concentration of hydroxyl ion and then the formation of expansive alkali-silica gel (Mo et al., 2021). This can cause volume expansion internally within concrete and in severe cases can cause cracking and spalling of concrete. The three essential conditions for the formation of ASR gels are the presence of reactive silica, high alkali content, and sufficient moisture.

One possible measure of controlling expansion due to ASR is the use of SCMs to partially replace the Portland cement in the mixture. SCMs can mitigate ASR mainly by reducing the amount of alkalis available for the reaction with the aggregate, and the ability of SCMs to bind alkalis appears to be strongly related to the  $\text{CaO/SiO}_2$  ratio of the SCM (Thomas, 2011).








A research study on the ASR showed a reduction in the expansion at 1 year of age from 0.28% to 0.02% with a 30% replacement of OPC with NP by mass (Saad et al., 1982). Moreover, Bektas et al. (2005) investigated the influence of calcined perlite powder (CPP) in suppressing the expansion resulting from ASR. They found that CPP can effectively limit the expansion of mortars.

Seraj (2014) studied the ability of NPs to control expansion due to ASR by performing tests in accordance with ASTM C 1567 (2013) with reactive sand. The replacement amount of cement with SCM was varied to determine the minimum amount of SCM necessary to control expansion. The minimum amount of SCM needed to control expansion varied between 15% and 25%.

Mahyar et al. (2018) studied the ASR expansion of mortars prepared using one of two different Portland cements, a reactive siliceous fine aggregate, and SCMs. The SCMs comprised six fly ashes, two ground granulated blast furnace slags, and three NPs. They found that all tested SCMs are able to mitigate the ASR expansion of cement mortars. They concluded that about 15%–27% replacement with any of the three NPs was needed to reduce 14-day expansion to 0.1% according to ASTM C 1567 (2013). These results corroborate those found by Seraj (2014).

In the study conducted by [Kasaniya et al. \(2021a, 2021b\)](#) a high-alkali Portland cement and a highly alkali–silica reactive borosilicate glass aggregate were used to prepare mortar prisms in accordance with the ASTM C441 ASR test. They found that all the pozzolans tested (pumice and perlite) reduced the expansion of mortar bars containing reactive Pyrex glass. The reduction in expansion due to ASR by the incorporation of pozzolans is due to the decrease in the concentration of alkali hydroxides ( $\text{Na}^+$ ,  $\text{K}^+$ , and  $\text{OH}^-$ ) in the interstitial solution and the increase in binding alkaline by C-S-H, which has a higher calcium-to-silica (Ca/Si) ratio than the C-S-H produced by PC alone ([Glasser & Marr, 1985](#)). According to [Guo et al. \(2018\)](#), since the microstructure and interface characteristics of RAC are more complex than those of NAC, it becomes more difficult to quantify and clearly understand the ASR mechanism in the RAC system. [Cassiani et al. \(2021\)](#) summarized the main factors affecting the ASR in RCA as presented in [Table 5.6](#).

**Table 5.6** Factors affecting the alkali–silica reaction in recycled concrete aggregates (RCAs) ([Cassiani et al., 2021](#)).

Factor	Factor description	Result in ASR expansions
Natural aggregate reactivity	More reactive	
Reactive RCA proportion	More content	
Crushing process	Recrushing	
Extent of ASR damage demolition	More damage	
Residual mortar amount	More content	
RCA—water absorption	High	
SCM addition	Higher	

[McCarthy et al. \(2015\)](#) pointed out that the expansion of fine RA was slightly greater than that of coarse RA when mixed with reactive aggregate in a new concrete in high-alkaline environment. It should be noted that there is a lack of studies on the effect of NP on ASR of RAC. However, the study conducted by [Adams and Ideker \(2020\)](#) demonstrated that ASR in concrete made with RCA can be effectively reduced using SCMs. Ternary blends containing Portland cement, a class F fly ash, and metakaolin were most effective in reducing expansions for RCAs used in this study. The amount of a particular SCM replacement needed in a mixture to reduce expansions to acceptable amounts depends on several factors. These include (1) the replacement level of RCA, (2) whether the coarse or the fine original natural aggregate was the reactive component in the RCA, and (3) access to the reactive component. The amount of adhered mortar in a particular RCA may also play an important

role. It was found that the use of SCMs has the ability to reduce the alkalinity of pore solution, and the amount of SCMs needed for RAC with ASR-affected RA was higher than that of concrete prepared with the virgin reactive aggregate.

## 5.5 Microstructure

The microstructure and porosity of mortars and concretes are closely correlated with strength. They mainly depend on the degree of hydration and the w/c ratio. [Cyr \(2013\)](#) reported that the microstructure of the cementitious paste plays an important role in determining the properties of mortars and concretes under certain conditions (e.g., active pozzolan, a long curing time). [Mehta \(1981\)](#) found that the addition of NP to Portland cement causes pore refinement by transformation of larger pores into fine pores ([Fig. 5.7](#)).

From [Fig. 5.7](#), one may observe that there is a great difference between the characteristics of the pore system of a pozzolanic cement paste compared to that of a Portland cement. Hence mortar with Portland cement generally has a higher total porosity than that with blended cement. Within the hydration process the reduction of larger volume pores is more pronounced for mortar containing NP than for mortar with Portland cement. Furthermore, this reduction is more significant at a later age. It was also found that the incorporation of NP considerably reduces the average pore radius and increases the number of smaller pores, especially for a high amount of NP.

The microstructure of concrete has three phases: bulk hydrated cement paste phase, aggregate phase, and the ITZ between aggregate particles and cement mortar. Due to the higher porosity of the matrix formed near the aggregates the ITZ is usually known

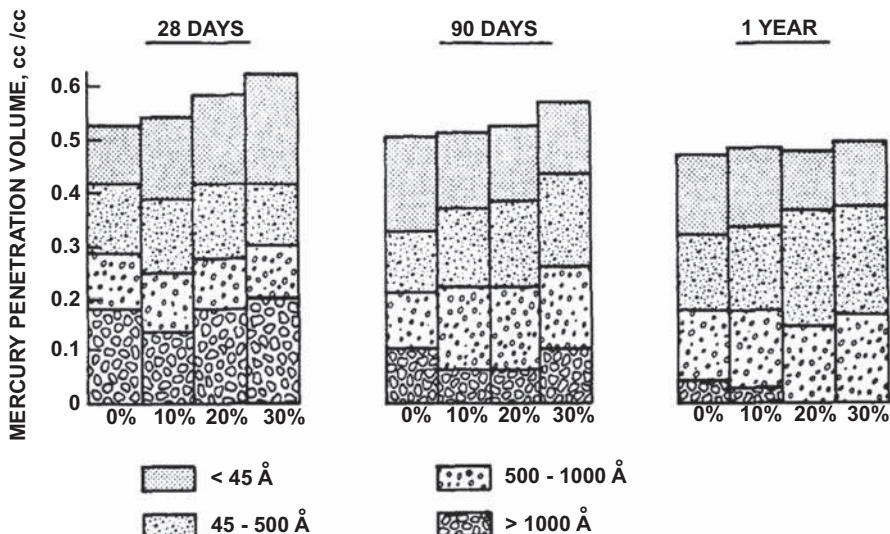


**Figure 5.7** Pore size distribution of hydrated cement pastes ([Mehta, 1981](#)).

to be the weakest zone of the concrete associated with negative impacts on mechanical and durability characteristics of concrete. In comparison with natural aggregates, recycled aggregates are more porous and usually partially carbonated due to the adhesion of old cement pastes on the aggregate surface. Poon et al. (2004) indicated that the ITZ microstructure of the RAC will be different from that of the NAC. However, Medina et al. (2012) found that the ITZ between RCA and new cement mortars is denser with fewer pores than the ITZ between natural aggregates and cement mortars. Some researchers believe that the water absorbed in RCA during the hydration process leads at a later age to internal curing in RC which will eventually improve the quality of the ITZ in this area (Jalilifar & Sajedi, 2021). In addition the use of a mineral admixture is an effective method to improve the interface structure and the performances of RAC. This is because in an alkaline environment, mineral admixtures could promote pozzolanic reaction to generate secondary C-S-H gel and refine pore structures.

Recently, Jalilifar and Sajedi (2021) investigated the microstructure of 100% recycled concrete (RC) containing recycled coarse concrete aggregates (RCA). After 180 days of hydration the results showed that there was still a large amount of pores and discontinuities at the mortar surface and the ITZ of RC without pozzolan. In contrast the use of 10% of SF in RC significantly reduced the pores and compressed the ITZ by bridging the hydration products, and the ITZ of this concrete was very close to that of conventional concrete (CC). The slow pozzolanic reactions in the fly ash as well as the low reactive capacity of the NZ resulted in the RC containing these two pozzolans with relatively porous and less dense microstructures.

## 5.6 Environmental and economical aspects

Cement manufacture is an energy-intensive process. For every ton of cement produced, there is up to 1 ton of carbon dioxide emitted into the atmosphere, partly due to the energy input for the calcination temperature and partly due to the decomposition of calcium carbonate. Therefore any reduction in the amount of cement in the production of concrete, through partial replacement of cement with naturally occurring material, is highly advantageous in that it reduces the amount of carbon dioxide emitted into the atmosphere and the unit cost of concrete. NPs are one of these natural materials, and their usage in concrete can offer environmental and economic benefits. Also replacing cement with NP can improve the durability of the structures, thus extending their lifespan, and further contribute to the reduction in cost and economy. Government legislations are a key to allowing construction professionals to a wider utilization of cement replacement materials including natural pozzolan.

## 5.7 Conclusion

Using NP in concrete to partially replace the cement can offer adequate fresh, mechanical, and durability properties. For example, using natural pozzolan to

partially replace cement can increase the resistance to sulfate attack and alkali aggregate reaction, thereby improving the long-term performance of concrete subjected to sulfate environment or concrete containing reactive aggregate. Also, the compressive strength of concrete containing natural pozzolan is acceptable which allows its usage in many concrete applications. Therefore where NP is present, it is important to use it in concrete production.

## References

- Adams, M. P., & Ideker, J. H. (2020). Using supplementary cementitious materials to mitigate alkali-silica reaction in concrete with recycled-concrete aggregate. *Journal of Materials in Civil Engineering*, 32(8), 04020209.
- Ahmadi, B., & Shekarchi, M. (2010). Use of natural zeolite as a supplementary cementitious material. *Cement & Concrete Composites*, 32, 134–141.
- Adjoudj, M., Ezziane, K., Kadri, E., Ngo, T., & Kaci, A. (2014). Evaluation of rheological parameters of mortar containing various amounts of mineral addition with polycarboxylate superplasticizer. *Construction and Building Materials*, 70, 546–559.
- Al-Amoudi, O. S. B., Ahmad, S., Khan, S. M. S., & Maslehuddin, M. (2019). Durability performance of concrete containing Saudi natural pozzolans as supplementary cementitious material. *Advances in Concrete Construction*, 8(2), 119–126.
- Al-Swaidani, A. M., & Al-Hajeh, T. (2017). Production of greener recycled aggregate concretes using local supplementary cementing materials. *MOJ Civil Engineering*, 2(1), 12–18.
- ASTM C1202. (2010). *Standard test method for electrical indication of concrete's ability to resist chloride ion penetration*.
- ASTM C 1567. (2013). *Standard test method for determining the potential alkali-silica reactivity of combinations of cementitious materials and aggregate (accelerated mortar-bar method)*.
- Bektas, F., Turanlia, L., & Monteirob, P. J. M. (2005). Use of perlite powder to suppress the alkali-silica reaction. *Cement and Concrete Research*, 35, 2014–2017.
- Belaidi, A. S. E., Azzouz, L., Kadri, E. H., & Kenai, S. (2012). Effect of natural pozzolana and marble powder on the properties of self-compacting concrete. *Construction and Building Materials*, 31, 251–257.
- Belaidi, A. S., Kenai, S., Kadri, E., Soualhi, H., & Benchaâ, B. (2016). Effects of experimental ternary cements on fresh and hardened properties of self-compacting concretes. *Journal of Adhesion Science and Technology*, 30(3), 247, 26. Available from <http://doi.org/10.1080/01694243.2015.1099864>.
- Bier, T.A. (1986). Influence of type of cement and curing on carbonation progress and pore structure of hydrated cement paste. In *Symposium microstructural development during hydration of cement* (pp. 85, 123–134).
- Boudali, S., Kerdal, D. E., Ayed, K., Abdulsalam, B., & Soliman, A. M. (2016). Performance of self-compacting concrete incorporating recycled concrete fines and aggregate exposed to sulphate attack. *Construction and Building Materials*, 124, 705–713.
- Boukhelkhal, D., Boukendakdji, O., Kenai, S., & Kadri, E. (2018). Combined effect of mineral admixture and curing temperature on mechanical behavior and porosity of SCC. *Advances in Concrete Construction*, 6(1), 69–85. Available from <https://doi.org/10.12989/acc.2018.6.1.069>, 2018.

- Cassiani, J., Martinez-Arguelles, G., Penabaena-Niebles, R., Keßler, S., & Dugarte, M. (2021). Sustainable concrete formulations to mitigate alkali-silica reaction in recycled concrete aggregates (RCA) for concrete infrastructure. *Construction and Building Materials*, *307*, 124919.
- Celik, K., Jackson, M. D., Mancio, M., Meral, C., Emwas, A.-H., Mehta, P. K., & Monteiro, P. J. M. (2014). High-volume natural volcanic pozzolan and limestone powder as partial replacements for Portland cement in self-compacting and sustainable concrete. *Cement & Concrete Composites*, *45*, 136–147.
- Chakkamalayath, J., Joseph, A., Al-Baghli, H., Hamadah, O., & Dashti, D. (2020). Performance evaluation of self-compacting concrete containing volcanic ash and recycled coarse aggregates. *Asian Journal of Civil Engineering*, *21*, 815–827.
- Chan, S. Y. N., & Ji, X. (1999). Comparative study of the initial surface absorption and chloride diffusion of high performance zeolite, silica fume and PFA concretes. *Cement & Concrete Composites*, *21*, 293–300.
- Cyr, M. (2013). Influence of supplementary cementitious materials (SCMs) on concrete durability. In F. Pacheco-Torgal, S. Jalali, J. Labrincha, & V. M. John (Eds.), *Eco-efficient concrete* (pp. 153–197). Woodhead publishing.
- Debbih, A., Kenai, S., Kaci, A., Kadri, E., & Kirgiz, M. S. (2020). Assessment of the effect of fine and coarse recycled aggregates and natural pozzolan on various properties of self-compacting concrete. *Cement, Clinker and Gypsum (ZKG)*, *9*, 36–45.
- Dunster, A. M. (1989). An investigation of the carbonation of cement paste using trimethylsilylation. *Advances in Cement Research*, *2*(7), 99–106.
- Ghrici, M., Kenai, S., & Meziane, E. (2006). Mechanical properties and durability of cement mortar with Algerian natural pozzolana. *Journal of Materials Science*, *41*(21), 6965–6972.
- Ghrici, M., Kenai, S., & Said-Mansour, M. (2007). Mechanical properties and durability of mortar and concrete containing natural pozzolana and limestone blended cements. *Cement & Concrete Composites*, *29*(7), 542–549.
- Glasser, F. P., & Marr, J. (1985). The alkali binding potential of OPC and blended cements. *Cemento*, *82*, 85–94.
- González, M. A., & Irassar, E. F. (1998). Effect of limestone filler on the sulfate resistance of low C<sub>3</sub>A Portland cement. *Cement and Concrete Research*, *28*(11), 1655–1667.
- Guettaf, Y., Kenai, S., Khatib, J., & Yahiaoui, W. (2020). Effect of wet curing and hot climate on strength and durability of SCC with natural pozzolan. *Current Materials Science, Formerly: Recent Patents on Materials Science*, *13*(1), 58–73. Available from <https://doi.org/10.2174/2666145413666200207123935>, 2020.
- Guo, H., Shi, C., Guan, X., Zhu, J., Ding, Y., Ling, T.-C., Zhang, H., & Wang, Y. (2018). Durability of recycled aggregate concrete: A review. *Cement and Concrete Composites*, *89*, 251–259.
- Hammam, S., Menadi, B., Kenai, S., Thomas, C., Kirgiz, M. S., & Sousa-Galdino, A. G. (2021). The effect of content and fineness of natural pozzolana on the rheological, mechanical and durability properties of self-compacting mortar. *Journal of Building Engineering*, *44*(2021), 103276.
- Hewlett, P., & Liska, M. (2019). *Lea's chemistry of cement and concrete* (5th ed.). Elsevier Science & Technology Books.
- Hossain, K. M. A., & Lachemi, M. (2004). Corrosion resistance and chloride diffusivity of volcanic ash blended cement mortar. *Cement and Concrete Research*, *34*, 695–702.
- Jalilifar, H., & Sajedi, F. (2021). Micro-structural analysis of recycled concretes made with recycled coarse concrete aggregates. *Construction and Building Materials*, *267*, 121041.

- Jalilifar, H., Sajedi, F., & Toosi, V. R. (2020). Evaluating the durability of recycled concrete made of coarse recycled aggregate concrete containing silica-fume and natural zeolite. *Revista de la Construcción*, 19(3), 457–473.
- Juenger, M. C. G., & Siddique, R. (2015). Recent advances in understanding the role of supplementary cementitious materials in concrete. *Cement Concrete Research*, 78, 71–80.
- Kasaniya, M., Thomasa, M. D. A., & Moffatt, E. G. (2021a). Efficiency of natural pozzolans, ground glasses and coal bottom ashes in mitigating sulfate attack and alkali-silica reaction. *Cement and Concrete Research*, 139, 106551.
- Kasaniya, M., Thomasa, M. D. A., & Moffatt, E. G. (2021b). Pozzolanic reactivity of natural pozzolans, ground glasses and coal bottom ashes and implication of their incorporation on the chloride permeability of concrete. *Cement and Concrete Research*, 139, 106259.
- Kouider-Djelloul, O., Menadi, B., Wardeh, G., & Kenai, S. (2018). Performance of self-compacting concrete made with coarse and fine recycled aggregates and ground blast furnace slag. *Advances in Concrete Construction*, 6(2), 103–121. Available from <https://doi.org/10.12989/acc.2018.6.2.103>.
- Mahyar, M., Erdogan, S. T., & Tokyay, M. (2018). Extension of the chemical index model for estimating alkali-silica reaction mitigation efficiency to slags and natural pozzolans. *Construction and Building Materials*, 179, 587–597.
- Martínez-Rosales, R. I., Miranda-Vidales, J. M., Narváez-Hernández, L., & Lozano de Poo, J. M. (2020). Strength and corrosion studies of mortars added with pozzolanin sulphate ions environment. *KSCE Journal of Civil Engineering*, 24(12), 3810–3819.
- Masood, B., Elahi, A., Barbhuiya, S., & Ali, B. (2020). Mechanical and durability performance of recycled aggregate concrete incorporating low calcium bentonite. *Construction and Building Materials*, 237, 117760.
- McCarthy, M. J., Csetenyi, L. J., Halliday, J. E., & Dhir, R. K. (2015). Evaluating the effect of recycled aggregate on damaging AAR in concrete. *Magazine of Concrete Research*, 67(11), 598–610.
- Medina, C., Frías, M., & Sánchez de Rojas, M. I. (2012). Microstructure and properties of recycled concretes using ceramic sanitary ware industry waste as coarse aggregate. *Construction and Building Materials*, 31, 112–118.
- Mehrabi, P., Shariati, M., Kabirifar, K., Jarrah, M., Rasekh, H., Trung, N. T., Shariati, A., & Jahandari, S. (2021). Effect of pumice powder and nano-clay on the strength and permeability of fiber-reinforced pervious concrete incorporating recycled concrete aggregate. *Construction and Building Materials*, 287, 122652.
- Mehta, P. K. (1981). Studies on blended Portland cements containing Santorin earth. *Cement and Concrete Research*, 11(4), 507–518.
- Mehta, P. K., & Monteiro, P. J. M. (2006). *Concrete—microstructure, properties, and materials* (3rd ed.). New York: McGraw-Hill Professional.
- Mo, K. H., Ling, T.-C., Tan, T. H., Leong, G. W., Yuen, C. W., & Shah, S. N. (2021). Alkali-silica reactivity of lightweight aggregate: A brief overview. *Construction and Building Materials*, 270, 121444.
- Najimi, M., Sobhani, J., Ahmadi, B., & Shekarchi, M. (2012). An experimental study on durability properties of concrete containing zeolite as a highly reactive natural pozzolan. *Construction and Building Materials*, 35, 1023–1033.
- Neville, A. M. (2011). *Properties of concrete* (5th ed.). Essex, UK: Pearson Education Limited.
- Omrane, M., Kenai, S., Kadri, E.-H., & Ait-Mokhtar, A. (2017). Performance and durability of self-compacting concrete using recycled concrete aggregates and natural pozzolan. *Journal of Cleaner Production*, 165, 415–430.

- Peter, M., Munteen, A., Meier, S., & Bohm, M. (2008). Competition of several carbonation reactions in concrete: A parametric study. *Cement and Concrete Research*, *38*, 1385–1393.
- Poon, C. S., Shui, Z. H., & Lam, L. (2004). Effect of microstructure of ITZ on compressive strength of concrete prepared with recycled aggregates. *Construction and Building Materials*, *18*, 461–468.
- Ramezaniyanpour, A. A. (2014). *Cement replacement materials: Properties, durability, sustainability*. Springer.
- Ramezaniyanpour, A. A., Mousavi, R., Kalhori, M., Sobhani, J., & Najimi, M. (2015). Micro and macro level properties of natural zeolite contained concretes. *Construction and Building Materials*, *101*, 347–358.
- Saad, M. N., Andrade, W., & Paulon, V. A., W. P. (1982). Properties of mass concrete containing an active pozzolan made from clay. *Concrete International*, *4*(7), 59–65.
- Samimi, K., Kamali-Bernard, S., & Maghsoudi, A. A. (2018). Durability of self-compacting concrete containing pumice and zeolite against acid attack, carbonation and marine environment. *Construction and Building Materials*, *165*, 247–263.
- Seraj, S. (2014). *Evaluating natural pozzolans for use as alternative supplementary cementitious materials in concrete*. PhD thesis, The University of Texas at Austin.
- Shahmansouri, A. A., Bengar, H. A., & AzariJafari, H. (2021). Life cycle assessment of eco-friendly concrete mixtures incorporating natural zeolite in sulfate-aggressive environment. *Construction and Building Materials*, *268*, 121136.
- Silva, R. V., Neves, R., de Brito, J., & Dhir, R. K. (2015). Carbonation behaviour of recycled aggregate concrete. *Cement & Concrete Composites*, *62*, 22–32.
- Soldado, E., Antunes, A., Costa, H., Do Carmo, R., & Júlio, E. (2021). Influence of pozzolan, slag and recycled aggregates on the mechanical and durability properties of low cement concrete. *Materials*, *14*, 4173.
- Tam, V. W. Y., Soomro, M., Evangelista, A. C. J., & Haddad, A. (2021). Deformation and permeability of recycled aggregate concrete—A comprehensive review. *Journal of Building Engineering*, *44*, 103393.
- Thomas, M. (2011). The effect of supplementary cementing materials on alkali-silica reaction: A review. *Cement and Concrete Research*, *41*, 1224–1231.
- Thomas, M. (2013). *Supplementary cementing materials in concrete*. CRC Press, Taylor & Francis Group.
- Thomas, J. J., Chen, J. J., Allen, A. J., & Jennings, H. M. (2014). Effects of decalcification on the microstructure and surface area of cement and tricalcium silicate pastes. *Cement and Concrete Research*, *34*, 2297–2307.
- Uzal, B., Turanli, L., & Mehta, P. K. (2007). High-volume natural pozzolan concrete for structural applications. *ACI Materials Journal*, *104*(5), 535–538.
- Zeyad, A. M., Khan, A. H., & Tayeh, B. A. (2020). Durability and strength characteristics of high-strength concrete incorporated with volcanic pumice powder and polypropylene fibers. *Journal of Materials Research and Technology*, *9*(1), 806–818.



This page intentionally left blank

# New hydraulic binder and binder based material with burning pulverised coal ash, household waste, Mediterranean soil, and calcined clay waste

Mehmet Serkan Kirgiz<sup>1</sup> and Muhammad Syarif<sup>2</sup>

<sup>1</sup>Northwestern University, Chicago, IL, United States, <sup>2</sup>Department of Architecture, Faculty of Engineering, University of Muhammadiyah Makassar, Makassar, Indonesia

## 6.1 Introduction

Waste is a remnant of production that does not contribute to human life. In particular, waste is seen as something that does not have a positive impact on people, but it has a huge influence on the continuation of human life. Improper waste handling would lead to unhealthy environmental patterns and damage the ecosystem. At present the problem of waste becomes a world problem, and since two decades, various ways have been tried by people as a step to save the environment from negative effects that can be caused by waste. About 60% of the waste production is estimated to be human-based household waste (HW) in Indonesia. Integrated waste management from the source to downstream could minimize the impacts arising from waste, such as the emergence of various diseases and environmental contamination, including in water, air, and soil. With its good management the waste would actually be a useful resource of raw material for various industries such as cement, tile, brick, and also energy (Yustikarini, 2017). Makassar, as one of the major cities in Indonesia, has generated waste of 4000 m<sup>3</sup>/d (Oktavianus, 2015). Another material that does not contribute to human life is the Mediterranean soil, which is often known as rocky soil. This is due to its lime content that is high enough to make it very difficult for plants to grow. Increased demand for housing and infrastructure automatically increases the need for building materials. Growth related to building material demand requires to be addressed by conducting research on the utilization and development of new building materials that are capable of being alternative materials. The current experimental research relates to this matter by substituting Mediterranean and clay soils with waste in a recycling system of waste that uses HW and coal waste (fly ash and bottom ash) to form new cement and new cement paste composites, which would be alternatives to Portland cement. The following

paragraphs summarize the aforementioned wastes and materials as constituent materials for new cement and paste composites.

Mediterranean soils, forming under a Mediterranean climate, are variously called the Terra Rossa Soil on hard limestone and Red Mediterranean Soil. However, whole soils are not classified as such in a Mediterranean environment because significant erosion, the lack of clean water, unfavorable mineral characteristics, coherence, and permeability may hamper the development of regular Mediterranean soil formation process (Verheye & Rosa, 2005). The variety of soils is very wide in the Mediterranean region, but the carbonaceous soils seem to be the most common land materials. Throughout the Mediterranean Sea the calcareous sedimentary soils such as limestone soils, dolomitic soils, and marl soils have various features in terms of hardness, mineralogical composition, and permeability. In South Africa and Australia, noncalcareous sedimentary soils including sandstone, mudstone, and shale are well known. In addition, granite as plutonic mac, basalt as volcanic mac, and quartzite and gneiss as metamorphic macs are abundant in the region. The soils have various chemical structures, and each behaves differently in terms of solubility when subject to disintegration and weathering (Verheye & Rosa, 2005). The mineralogical structures in carbonaceous soil start with a chemical attack and dissolution of calcium carbonate by penetrating rain water and freeze-thawing cycles, especially when enriched by CO<sub>2</sub> and the plant root system:



The insoluble calcium carbonate (CaCO<sub>3</sub>) first meets with carbonic acid (H<sub>2</sub>CO<sub>3</sub>) in the environment, and the carbonate is converted into soluble calcium bicarbonate (Ca(HCO<sub>3</sub>)<sub>2</sub>), which is then removed by drainage water in the foundation, as shown in Eq. (6.1). The dissolution of the soil leaves behind a fresh product from the CaCO<sub>3</sub>, whose properties depend on the natural environment, the hardness of the substrate, and the level of chemical aggressiveness of the water that leaches through the soil (Verheye & Rosa, 2005). This would be referred to as decrease of soil pH from 8–8.2 range to 7–7.2 range, and a reduction tendency towards a desaturation of the cation exchange complex. On non-carbonaceous and acid layer, like granites, gneiss or sandstones, as natural leaching and plant acid root system escalate the acidity and desaturation during the winter period, the soil pH is between 6 and 7 (Verheye & Rosa, 2005). Fig. 6.1 illustrates various materials—for example, the Mediterranean pozzolanic soil, the HW, the calcined clay, the fly ash, and the bottom ash, and the scheme of the plot manufacturing of new clinker and cement.

In addition to the Mediterranean soil, the amount of HW increased very rapidly because of rapid growth in urbanization and industrialization. In addition to the growth, in near future, since people continue to increasingly generate the HW and because of the lack of landfill regions for the HW, together with the increase of cost for landfill operation of the HW, its disposal is becoming a very significant problem

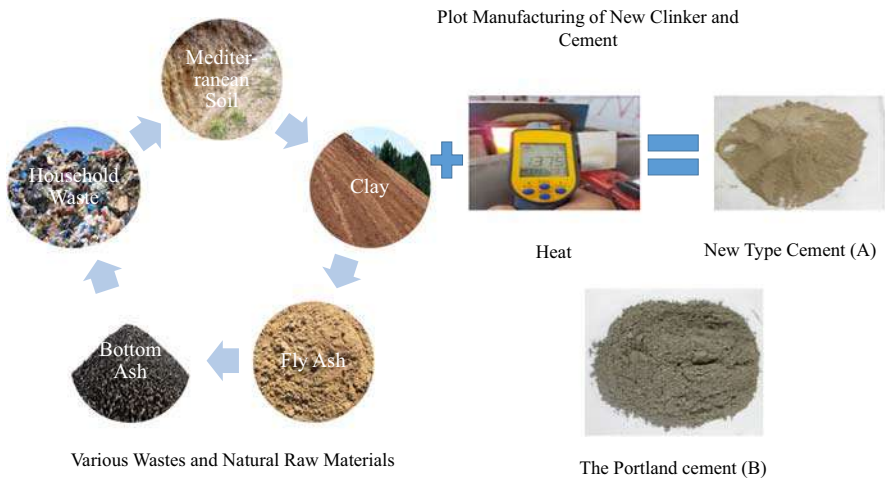


**Figure 6.1** A process of plot manufacturing of new cement from various wastes and natural raw materials; new type cement (A) and the Portland cement (B).

for most communities. With the increase of environmental awareness and the potential hazardous effect of the HW the recycling of HW is gaining immense interest, instead of the disposal of HW. Ash from energy power stations (EPSs) could possibly be used in concrete manufacturing. There are plenty of paper reports with further details about the physical, chemical, and mineralogical compositions and elemental analysis of the ash of EPS. They include the effect of EPS ash on the compressive strength, chloride resistance, and shrinkage of concrete. They also deal with the leachate analysis of ash of EPS (Siddique, 2010). A study, entitled “Recycling of municipal solid waste for cement production: pilot-scale test for transforming incineration ash of solid waste into cement clinker,” carried out by Kikuchi in 2001 showed that the quality of the resulting cement is sufficient to enable the cement to be put to practical use in construction. Furthermore the tested process does not result in secondary pollution. Consequently the study reported that approximately 50% of the raw material used in cement manufacturing would be obtained from the incineration ash of HW (Kikuchi, 2001). Another study published by Joseph et al. in 2018 explained that huge amounts of HW were being generated, and even though the incineration process reduced the mass and volume of the HW to a large extent, a massive quantity of residue of HW still remained. On average, out of 1.3 billion tons of HW generated per year, around 130 million tons were incinerated in the world. About 400 kT of bottom ash residues was generated in Flanders the previous year, out of which only 102 kT was utilized, and the rest was exported or landfilled due to nonconformity to environmental regulations. The landfilling makes the valuable resources in the HW unavailable and results in large quantities of primary raw material being used, increasing mining activities and related hazards. Identifying and employing the right

pretreatment techniques for HW are the key to attaining a circular economy. Uses of HW in the cement industry as a binder and cement raw meal replacement are identified as possible effective utilization options for large quantities of bottom ash of HW. With all the research evidence available, there is now a need for combined efforts from incineration and the cement industry for technical and economic optimization of the process flow of HW (Joseph et al., 2018).

However, there are many reports on the use of the calcined clay for cement manufacturing. It is reported that the cement industry could substitute the pozzolanic and latent hydraulic cementitious constituents for Portland cement clinker to provide a holistic approach for reduction of CO<sub>2</sub> emission effect on the environment. It is clear that due to a significant increase in demand for cement, calcined clay is becoming more important for the cement manufacturing as a valuable pozzolanic constituent. It is possible to use calcined clay in cement as the main constituent in regard to EN 197-1 if the percent of the reactive silicon dioxide is not lower than 25% by mass. Particularly the effect of the chemical and mineralogical compositions of the clay on their suitability as a main constituent in cement has not yet been sufficiently evaluated. The compressive strength tests on CEM II/A-Q were carried out with a water-to-cement ratio of 0.5 and on CEM IV/B (Q) with a water-to-cement ratio of 0.6 for process-related reasons. The strengths of CEM II/A-Q were between approximately 21 MPa and approximately 29 MPa at the age of 2 days and between approximately 48 MPa and approximately 66 MPa at the age of 28 days. The strengths of CEM IV/B (Q) were between approximately 9 MPa and approximately 13 MPa at the age of 2 days and between approximately 24 MPa and approximately 49 MPa at the age of 28 days. The highest levels of compressive strength were reached with the kaolinite clays (European Cement Research Academy, 2014). Therefore another objective of the study is, through experimental laboratory research and development, to better explain the suitability of the calcined clay for use in cement making process.

Pulverized fuel ash (PFA) is also used in the study. The manufacturing of Portland cement composite concrete uses PFA as a supplementary cementitious material (SCM) (Kırgız, 2015a). The use of SCM overcomes various negative chemical problems and contributes to the physical and mechanical features of the hardened cement-based material through enhancement of its hydraulic and pozzolanic activity. PFA is defined as an SCM and is classified differently in regard to various institutions such as the American Standard Testing and Material (ASTM) and the CSA in various countries. The specification of the ASTM depends on the chemical composition of the PFA. The standard stipulates that the sum of SiO<sub>2</sub> + Al<sub>2</sub>O<sub>3</sub> + Fe<sub>2</sub>O<sub>3</sub> has to be more than 70%. Anthracite or bituminous coal fuel ash is referred to as Class F fuel ash. If its SiO<sub>2</sub> + Al<sub>2</sub>O<sub>3</sub> + Fe<sub>2</sub>O<sub>3</sub> sum is less than 50% in composition, the lignite or sub-bituminous coal fuel ash is referred to as Class C fuel ash. While the ASTM evaluates PFA as two classes, the CSA lays down PFA as three classes. According to classification of PFA by the CSA, F type fuel ash contains a calcium (CaO) oxide content lower than 8%. The second type, called CI fuel ash, includes a CaO content between 8% and 20%. The last type is CH fuel ash and comprises a

CaO content of more than 20%. PFA has notable benefits on cement-based composite materials (CBCMs). The following paragraphs summarize its benefits on CBCM systems (Kirgiz, 2015b, 2018). PFA reduces the water demand of CBCM, and thus accordingly the use of good quality fuel ash along with the high fineness and low CaO content may allow the composite concrete to be mixed at a lower water quantity when compared to the Portland cement composite concrete manufactured at the same workability. High-dosage level fuel ash by mass of total cement binder along with a low water content may eliminate the bleeding and segregation because of pozzolanic activity of PFA. The substitution level of the low-CaO Class F fuel ash for the Portland cement increases the early-age compressive strength gain decreasing in the CBCM, but it shows a positive effect on the compressive strength gain in the long term (Kirgiz, 2015b, 2018). The benefit list of PFA is long. Coal burning results not only in PFA but also in bottom ash that is generated by various industries that require high temperatures in their manufacturing. The bottom ash's mechanical properties are thoroughly studied in several countries. There is a regular need to consider the quality of the bottom ash in order to enhance its use as a suitable substitution material for fine aggregate and course aggregate in CBCM as well as a subground material for infrastructure. Because of mineralogical and geochemical changes, bottom ash's pH varies between 8 and 11. For all possible types of utilization of bottom ash, it is very beneficial for the mechanical properties to consider a heavy metallic content prior to utilization. Removing all metals creates a homogeneous and mechanically strong material. Furthermore, other uses are being investigated. An example of other uses is low-tensile strength composite concrete, such as outdoor tiles. The use of bottom ash for composite concrete is quite substantial in modern society; hence large markets for bottom ash utilization exist (Kirgiz, 2015b, 2018).

The need for new building materials due to growth in population must be addressed with the use and discovery of new building materials that are capable of being alternatives to current building materials. Cement is the newest alternative for Portland cement, according to the experimental research that has been made utilizing various forms of recycling and utilization of waste. The aim of the new cement is to use ingredients such as HW, PFA, bottom ash, Mediterranean soil, and calcined clay. The lack of research on the making of new cement with coal waste such as PFA and bottom ash inspires the researchers all over the world to conduct new experimental studies that showcase how the waste can be utilized for human interest in construction and development of structures and infrastructure. PFA and bottom ash are the examples of waste that can be utilized in cement production. It is, however, necessary to pay attention to the properties and content of cement used in composite concrete. Research suggests that the use of fly ash that is extensive in cement clinkerization and its partial replacement for cement will lead to reduction of heat of hydration. Therefore it slows down the chemical reactions in the hydration of cement, and it accelerates the setting time of cement as well (Sebayang et al., 2012).

The combination of the PFA as an additional material and the SCM is often referred to as composite cement in the Portland cement industry. The use of PFA is a wise step in the cement manufacturing because it has an amorphous silica content

and its reuse provides limitless recycling opportunities for both composite cement and energy. With a high silica content, PFA meets the characteristics of cement and pozzolanic latent material (Tumingan et al., 2016). The use of saturated PFA is one of the ways to reduce high exposure in the hydration process against the density of cement in composite concrete (Victor, 2012). The setting time of cement is the starting process of a chemical compound reaction that occurs in cement just after the cement reacts with water so that the composite cement can become hard and withstand pressure. The use of PFA leads to a reduction in air pollution that impacts the economy negatively. It has been observed that 0.9 tons of CO<sub>2</sub> are produced per ton of cement production. In addition the cement composition is 10% by weight in cubic units of composite concrete. Thus the use of PFA, bottom ash, HW, Mediterranean soil, and the calcined clay makes new composite cement possible to help reduce atmospheric CO<sub>2</sub> emissions as a form of ecofriendly engineering and design (Chirag & Jain, 2014). The effect of adding a certain quantity of the waste will increase the strength of cement-based composites (Marthinus et al., 2015).

## 6.2 Research methodology

In testing and evaluating of new clinker concentrates a comparative study is used to analyze chemical compounds of the Mediterranean pozzolanic soil, the HW, the calcined clay, the PFA, the bottom ash, and new cement clinkers manufactured from the waste and measure the physical properties of new cement to examine the level of similarity and difference between Portland cement and new cement. In every new cement study the testing of chemical properties must be done on each raw material that has been processed to concentrate and form cement. After that, physical testing on new cement concentrate was carried out. To obtain optimum results the methods used are based on the reference to ASTM in testing and evaluating the chemical properties of the Mediterranean pozzolanic soil, the HW, the calcined clay, the PFA, the bottom ash, and the new cement clinker manufactured from the wastes and such physical properties of the new cement as density and fineness as well as the setting time of new cement composite paste.

### 6.2.1 Tools and materials used

New cement concentrate is formed by utilizing the management of waste recycling, such as utilization of HW by substitution of Portland cement using Mediterranean soil, clay, fly ash, and bottom ash. Fig. 6.2 illustrates the clinkerization from the waste concentrate used in the study.

The combustion of raw material is conducted in a box fire machine that can withstand heat up to 1800°C. The temperature control of combustion was carried out using a TI-1500 infrared sanfix thermometer tool. Fig. 6.3 shows the cement raw material before the combustion process to become the cement concentrate.



**Figure 6.2** The clinkerization from the waste concentrate used in the study.

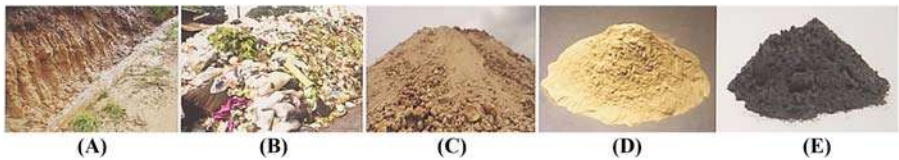


**Figure 6.3** The cement raw material before the combustion process to become the cement concentrate: (A) the Mediterranean soil; (B) the household waste; (C) the calcined clay; (D) the pulverized fuel ash; and (E) the bottom ash.

To analyze the setting time of new cement composite paste the Vicat tool was used. To analyze the fineness of new cement the Blaine tool was used. The examination of chemical compounds of the wastes and new cement was conducted at a chemistry laboratory, while the physical properties of new cement were established in a construction material laboratory in Indonesia.

### 6.2.2 Research procedures

In order to form a new cement concentrate, all the main waste ingredients were heated to a temperature of 1375°C. After all ingredients are burnt for 4 hours, cooling and refinement were performed. The concentrate-shaped cement material was then subjected to test for examining its chemical structure. In order to assess the compatibility of new cement



the ability to achieve the chemical structure, the fineness, the density, the initial and final setting times, and the normal consistency were measured. The empirical Eq. (6.2) of the concentrate-forming of new cement can be derived as follows:

The empirical Eq. (6.2) of the concentrate-forming of cement can be derived as follows:

$$\sum R_{ff} = \frac{\sum S + \sum I \sum N \sum A \sum R}{100} \quad (6.2)$$

where  $\sum R_{ff}$  = Cement concentrate (kg),  $\sum S$  = Mediterranean soil concentrate (%),  $\sum I$  = Soil concentrate (%),  $\sum N$  = Household waste concentrate (%),  $\sum A$  = Fly ash concentrate (%),  $\sum R$  = Bottom ash concentrate (%).

### 6.2.2.1 Chemical analysis of the wastes and new cement

Before mixing of the wastes together to make a new cement concentrate a recent study established the chemical composition of the Mediterranean pozzolanic soil, the HW, the calcined clay, the fuel ash, and the bottom ash in accordance with the ASTM C114-07 standard wet chemical analysis method (ASTM C114-07, 2007). The chemical composition of the new cement composition was determined using the energy-dispersive X-ray fluorescence (XRF) method suggested by Wheeler in 1983 (Wheeler, 1983).

### 6.2.2.2 X-ray powder diffraction analysis of new cement manufactured

Using ASTM C1365-18, numerous comprehensive studies were carried out on the mineralogy of cement (ASTM C1365-18, 2018). Fig. 6.4 illustrates the mineral graph of the XRD equipment, which was used to identify the major part and definition of the diffraction angle  $2\theta$  in the study.

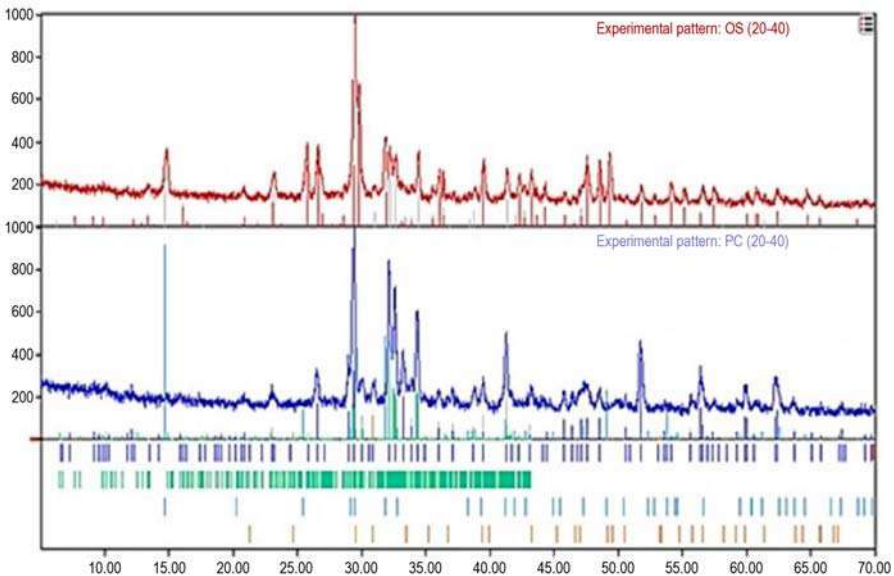


**Figure 6.4** The mineral graph of the XRD equipment, which was used to identify the major part and definition of the diffraction angle  $2\theta$  in the study.

Theoretical equations of Bogue calculation and such Bogue chemical compounds as  $C_3S$ ,  $C_2S$ ,  $C_3A$ , and  $C_4AF$  have created some debate regarding on the strength mechanism of Bogue chemical compounds. In the light of the debate the studies evaluate the mineralogy of new cement using XRD in accordance with ASTM C1365-18 standard method (ASTM C1365-18, 2018). Diffraction deals with constructive interference of X-ray scattering from a sample and follows Bragg's law through Eq. (6.3).

$$\theta = \arcsin\left(\frac{n\lambda}{2d}\right) \quad (6.3)$$

where  $\theta$  is the diffraction angle indicated in the study,  $n$  is a constant,  $\lambda$  is the wavelength of the X-ray scattered from new cement, and  $d$  is the distance between two adjacent parallel lattice planes in the inner crystal structure (ASTM C1365-18, 2018).

### 6.2.2.3 Fineness of new cement

In order to determine the quantity of cement particles lower than  $200\ \mu\text{m}$  in size the fineness test of new cement was carried out using the sieve of  $200\ \mu\text{m}$  mesh. The fineness of the new cement was determined in accordance with ASTM C 204-18e1 standard method (ASTM C204-18e1, 2018). The study applied the following summary steps: (1) A representative sample of new cement is obtained; (2) the new cement is rubbed between the hands to break up the lumps; (3) 100 g sample of new cement is weighed and recorded as  $W_1$ ; (4) 100 g of new cement is poured onto the sieve of  $200\ \mu\text{m}$  mesh, and the lid is placed; (5) the sieve is shaken for 15 minutes, with planetary and linear movements; (6) the residue retained on the sieve of  $200\ \mu\text{m}$  mesh is weighed and recorded as  $W_2$ ; (7) the percentage of weight of cement retained on the sieve ( $W_f$ ) is calculated as in Eq. (6.4) (ASTM C204-18e1, 2018). The study repeated the above steps of fineness experiment with three different samples of new cement and recorded the fineness results to calculate the average value.

$$W_f = \frac{W_2}{W_1} \times 100 \quad (6.4)$$

### 6.2.2.4 Density of new cement

In order to establish the density of new cements and the Portland cement the study used the rules of the standard method specified in ASTM C 188-95 (ASTM C 188-C195, 1995). For that aim the following steps were engaged in the test: (1) A clean and dry Le Chatelier flask ( $W_1$ ) is weighed; (2) the new cement sample is filled up to half of the flask (about 50 mg); (3) the Le Chatelier flask is weighed along with the sample ( $W_2$ ); (4) kerosene is put in the flask until the flask is about half full; (5) the contents are mixed thoroughly with a glass rod to remove the entrapped air; (6) the mixing is continued, and more kerosene is added until the flask is flushed up to the graduated mark; (7) the outside is dried, and the mixture is weighed again ( $W_3$ ); (8) the flask is removed and dried and filled with

kerosene up to the graduated mark; (9) the flask outside is dried, and the weight is taken ( $W_4$ ) (ASTM C 188-C195, 1995). Eq. (6.5) calculates the density as it is:

$$\gamma = \frac{(W_2 - W_1)}{[(W_2 - W_1) - (W_3 - W_4) \times 0.79]} \quad (6.5)$$

In Eq. (6.5) the symbol of  $\gamma$  stands for the density of cement as  $\text{g/cm}^3$ , and the number of 0.79 stands for the density of the kerosene used.

#### 6.2.2.5 Consistency of new cement paste

The consistency of cement paste test is performed to determine the water demand that is to be added in cement to attain normal consistency of cement paste composite. The study used the ASTM C 187-04 standard method (ASTM C187-04, 2004) to assess the consistency of new cement composite paste. Its steps may be summarized as follows: (1) 400 g of new cement is obtained and placed in a bowl to prevent humidity; (2) the standard consistency of water is assumed to be 28%, and the same quantity of water is added in cement and mixed; (3) the cement composite paste is mixed thoroughly between 3 and 5 minutes; (4) the cement composite paste is filled in the Vicat mold correctly; (5) then the Vicat mold is placed on the glass plate; (6) it should be checked that the plunger should touch the surface of Vicat mold gently; (7) the plunger is released and allowed it to sink into the test mold; (8) the penetration of the plunger is recorded from the bottom of the mold indicated on the scale; (9) the same experiment is repeated by adding different percentages of water until the penetration of the plunger is in between 5 and 7 mm on the Vicat apparatus scale (ASTM C187-04, 2004). The study repeated the above steps of consistency experiment using three different samples of cement composite paste and recorded the consistency results to calculate the average value accurately. The importance of the consistency test stems from the fact that when water is mixed with cement, its hydration process starts. Surplus addition of water in cement leads up to an increase in water-to-cement ratio, and the increased water reduces the strength of cement paste after it hardens. If less water is added than required, the cement paste composite is not properly hydrated, and the insufficient water content leads up to the loss on strength, especially compressive strength.

#### 6.2.2.6 Setting time of new cement paste

When cement is mixed with water, it makes cement paste that results in hydration products. The paste can be molded into any desired shape due to its workability. Within its setting time the cement composite paste proceeds with reaction; further mixing the water, slowly the cement composite paste starts losing its workability to set and harden. This whole cycle is called the setting time of cement composite

paste. There are two periods known as initial and final setting times. The study used the ASTM C 191-19 standard method (ASTM C191-19, 2019) to measure the setting time of cement composite paste as summarized as follows: (1) 400 g of new cement is weighed and placed in a bowl to prevent humidity; (2) water is added by three fifths ( $3/5$ ) milliliter of weight of cement in the bowl; (3) the water and cement sample are mixed in the bowl; (4) the Vicat mold is filled with the mix; (5) then the Vicat mold is placed on the special glass plate; (6) it should be checked that the plunger of Vicat equipment should touch the surface of Vicat mold gently; (7) the plunger is released and allowed to sink into the test mold; (8) the penetration of the plunger is recorded from the bottom of the mold indicated on the scale; (9) the same penetration is repeated at different positions on the mold until the plunger stops penetrating  $5 \pm 2$  mm from the bottom of the mold. At  $5 \pm 2$  mm penetration, this time is recorded as the initial time of setting of the cement composite paste (ASTM C191-19, 2019). After starting setting time of cement composite paste the plunger is replaced with one with an annular attachment. The time period between the moment water is added to the cement and the time at which the needle makes an impression on the surface of the cement composite paste, while the attachment fails to do so, is recorded as the final setting time of cement composite paste (ASTM C191-19, 2019).

## 6.3 Results and discussion

The new research that has been conducted includes XRF and XRD analyses on new cement concentrates as well as some physical properties such as granular fineness, specific surface, bulk density, consistency, and setting-time of new cement.

### 6.3.1 Chemical composition of the wastes

Wet chemistry, also known as the brench method and wet analysis, is the current and certain method to determine chemical compositions of bulk materials such as waste, cement, lime, and gypsum. It conventionally uses such reagents and tools as acids, beakers, and flasks to decompose the solid and/or bulk sample in a liquid and identifies and quantifies the elements in the sample through various calculation techniques and instrumentation. If it is necessary, the technique of separation and isolation is applied to the sample. Stoichiometric methods, such as the gravimetric method and the volumetric method, are used in wet chemical analysis, enabling the chemical analysis of the sample quantitatively. There are two wet chemical analysis types; qualitative analysis identifies which elements exist in the sample, and quantitative analysis determines the quantity of elements in the sample. The chemical analysis results of various wastes used in the manufacturing of cement concentrate is shown in Table 6.1.

**Table 6.1** The chemical analysis results of various wastes used in the manufacturing of cement concentrate.

Chemical compound (%)	Mediterranean soil	Household waste	Calcined clay	Fly ash	Bottom ash
SiO <sub>2</sub>	60.93	46.65	30.63	22.14	15.2
Al <sub>2</sub> O <sub>3</sub>	0.44	2.28	3.41	3.84	2.99
Fe <sub>2</sub> O <sub>3</sub>	0.15	0.18	0.2	0.2	0.2
CaO	19.35	11.09	0.51	6.87	1.41
SO <sub>3</sub>	1.66	1.01	0.36	0.89	0.15
Na <sub>2</sub> O	0.01	2.24	0.01	0.37	1.03
K <sub>2</sub> O	0.09	11.98	0.23	0.58	0.17
MgO	0.018	0.02	0.02	0.03	0.02
P <sub>2</sub> O <sub>5</sub>	N/A	0.47	N/A	N/A	N/A
LOI	N/A	N/A	N/A	N/A	N/A

LOI, loss on ignition; N/A, not available.

Almalkawi et al. in 2019 reported a very significant study on the industrial waste for using new geopolymer binders as green construction materials. The authors needed to identify the chemical composition of the new geopolymer binder as the chemical composition of the waste plays a significant role in the properties and development of new hydraulic geopolymer binders. Results of the study show the science community that a ternary blend of combustion ashes could be used to manufacture hydraulic geopolymer binders of targeted strength and the upcycling of wastes safely (Almalkawi et al., 2019). A similar study has been performed on waste packing glass bottles and reported by Ibrahim and Meawad in 2018 (Ibrahim & Meawad, 2018). Researchers in the current study needed to determine the chemical composition of waste, and they applied wet chemistry to the waste. The study contributes to a better understanding of the powder of uncolored, green, and brown soda-lime glass types that are available to be used as SCMs, and the ions responsible for their color do not have an effect on their performance.

ASTM C 618 defines that fly ash pozzolana utilized should contain silicon oxide (SiO<sub>2</sub>) + aluminum oxide (Al<sub>2</sub>O<sub>3</sub>) + iron oxide (Fe<sub>2</sub>O<sub>3</sub>) ≥ 70 wt.% (ASTM C618-19, 2019). In the current study the contents of SiO<sub>2</sub>, Al<sub>2</sub>O<sub>3</sub>, Fe<sub>2</sub>O<sub>3</sub>, and calcium oxide (CaO) suggest valuable chemical compositions and potential for latently hydraulic materials and will enable slow strength development for clinkers, cement, and cement-based materials. Other studies stand for the necessity of the chemical composition identification for new cement and conventional cement. One of them is a current study published by Ruiz-Sánchez et al. in 2019, entitled Waste marble dust: An interesting residue to produce cement (Ruiz-Sánchez et al., 2019). This study makes six clinker types with waste marble dust. To understand their chemistry the study performs wet chemical analysis on them. Its results reveal that the

mineralogical composition of waste marble dust is based on the presence of CaO, and its physicochemical analysis confirmed its feasibility as a pure and clean byproduct. Moreover, one of the authors (Kırgız, 2015b) in the article published an interesting and valuable article entitled “Use of ultrafine marble and brick particles as raw materials in cement manufacturing.” These two studies and the current study are in agreement with each other because all studies support the manufacturing of new hydraulic cements from human-based wastes.

### 6.3.2 Chemical composition of new cement

The chemical analysis results of cement concentrate and Portland cement and their comparison are shown in Table 6.2

**Table 6.2** Comparison of the chemical analysis results of the new cement concentrate and that of Portland cement.

Chemical compounds (%)	New cement	Portland cement
C <sub>3</sub> S	69	65
C <sub>2</sub> S	7.3	15
C <sub>3</sub> A	10.3	8
C <sub>4</sub> AF	3.1	12
Silicon oxide (SiO <sub>2</sub> )	21.2	20.6
Aluminum oxide (Al <sub>2</sub> O <sub>3</sub> )	7.8	5
Iron oxide (Fe <sub>2</sub> O <sub>3</sub> )	4.4	2.9
Calcium oxide (CaO)	68.4	63.9
Sulfur oxide (SO <sub>3</sub> )	3.2	2.5
Sodium + Potassium oxide Na <sub>2</sub> O + K <sub>2</sub> O	1.5	0.8
Magnesium oxide (MgO)	4.8	1.5
Loss on Ignition (LOI)	Not available	1.5

Analyses using XRF are performed based on identification and enumeration of X-ray radiation occurring from the photoelectric effect event. The photoelectric effect occurs because the electrons in target atoms (samples) are hit by high-energy collisions (gamma radiation, X-rays). The guideline used in this test is ASTM C 114-07 standard method (ASTM C114-07, 2007), where the references are normative references which are considered highly relevant in the process of testing chemical compounds of cement. Table 6.2 shows the chemical content of Portland cement according to ASTM C 114-07 standard rules (ASTM C114-07, 2007). The main forming ingredients of the new cement are, as shown by the testing result of concentrate chemical elements in Table 6.2, CaO and SiO<sub>2</sub>, greater than 89.7% in total. Because of the abundance of C<sub>3</sub>S, new hydraulic cement could be classified as alite type cement along with the belite, the tricalcium aluminate, and the brownmillerite.

### 6.3.3 X-ray powder diffraction analysis of new cement

Brownmiller and Bogue made the first application of XRD on Portland cement particles in 1930 (Brownmiller & Bogue, 1930), only discovering the X-rays 35 years later. At the time of 1930, Portland cement clinker was considered to be composed mainly of either a complex single compound made of lime, alumina, and silica or separate silicate compounds including various amounts of lime. In their breakthrough study, Brownmiller and Bogue compared X-ray diffraction patterns obtained from a commercial Portland cement clinker to those obtained from individually synthesized phases (Brownmiller & Bogue, 1930). The comparison demonstrated the presence of tricalcium silicate (alite) as the primary clinker phase, as suggested previously by Le Châtelier (1882, 1905) and analyzed by Törnebohm (1897). Furthermore the concentrate is tested using XRD. The X-ray diffraction test results are then analyzed by search and matching. From the results of the analysis, it has been observed that the chemical composition of cement indicates such similar compounds as those existing in the Portland cement of the same quantity. Of all the chemical elements present in the Portland cement, the most important chemical elements are  $\text{Ca}_3\text{SiO}_5$  (alite/ $\text{C}_3\text{S}$  = tricalcium silicate),  $\text{Ca}_2\text{SiO}_5$  (belite/ $\text{C}_2\text{S}$  = dicalcium silicate),  $\text{Ca}_3\text{Al}_2\text{O}_6$  (aluminat/ $\text{C}_3\text{A}$  = tricalcium aluminate), and  $\text{Ca}_3\text{Al}_2\text{FeO}_{10}$  (ferrite/ $\text{C}_4\text{AF}$  = tetra calcium alumino ferrite). In new cement, these four chemical elements have been obtained after combustion at high and controlled temperatures between 1375°C and 1400°C.

### 6.3.4 Physical properties

#### 6.3.4.1 Fineness of new cement—sieve passing method and specific surface method

It is the total surface area of cement that makes the material available for hydration because the hydration of the cement-based material starts at the surface of the cement particle. Therefore hydration depends on the fineness of the cement particle, and for a rapid development of strength, such high fineness as in the current study is necessary. However, the cost of grinding and the effect of fineness on other properties, such as workability issues of fresh cement-based materials, long-term strength, and gypsum demand, must be considered. Fineness is a significant property of cement and is necessary to measure through the specific surface method ( $\text{m}^2/\text{kg}$ ) in regard to BS and ASTM standards. The specific surface of cement could be determined by the air permeability method, which measures the pressure drop when dry air flows at a constant velocity through a bed of cement of known porosity and thickness. Nath and Kumar (2020) reported in their current study that the finer particles provided better properties and microstructures for cement-based materials in 2020 (Nath & Kumar, 2020). Kan et al. (2019) published a scientific study that mentioned the fineness activity property for cement-based bulk materials (Kan et al., 2019). Table 6.3 gives the fineness of new cement and the Portland cement measured in the experimental study.

**Table 6.3** The fineness of new cement and the Portland cement measured in the experimental study.

Type of fineness measure	Type of material	
	New cement	Portland cement
200 $\mu\text{m}$ sieve passing (%)	56	52
Specific surface ( $\text{kg}/\text{m}^3$ )	1200	1250

The fineness value for the new cement in the current study passes through the 200 mesh sieve by 56% with a solid weight of  $1200 \text{ kg}/\text{m}^3$ , while for the equivalent quantity for Portland cement, it is 52% with a solid weight  $1250 \text{ kg}/\text{m}^3$ . The smoother the cement, the greater will be the surface of the granules so that the hydration with water will be faster and will have a large demand for water. Fig. 6.5 shows a process of measuring the fineness and the density of new cement (A) and the Portland cement (B).

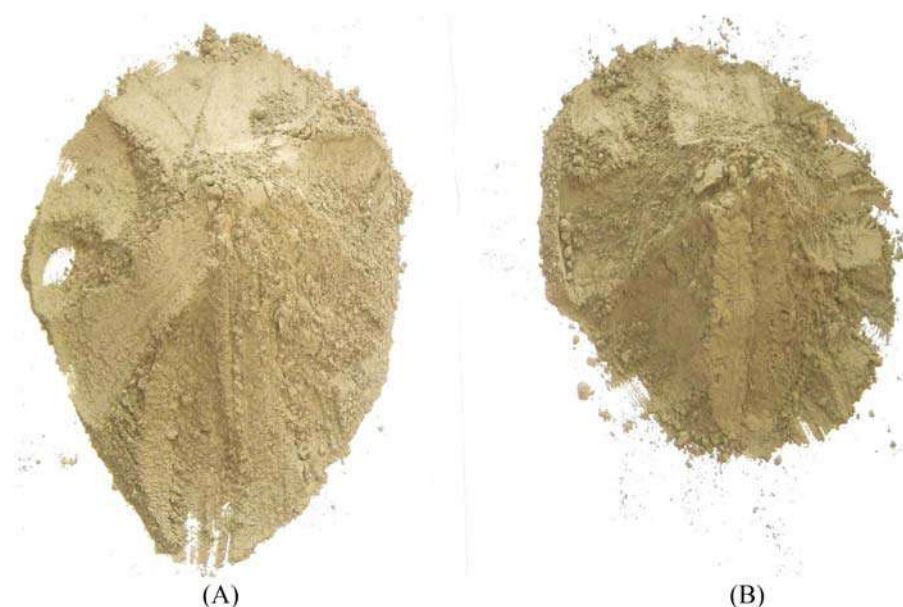


**Figure 6.5** A process of measuring the fineness and the density of cement: (A) new cement and (B) the Portland cement that is used as a comparator in testing the physical properties.

In a cement-based mixture the ratio of water to cement is defined as (water weight)/(cement weight) and often abbreviated as w/c. The w/c ratio has a strong influence on the strength of the concrete. For certain mixtures, increasing the ratio w/c will decrease strength at all ages, and a lower w/c ratio will increase the strength of the concrete (Nicholas, 2014). Ghasemi et al. (2019) presented a current study that examined a relationship between the specific surface of mortar constituent and the flow of mortar in



2019 (Ghasemi et al., 2019). This significant study reveals that the water demand of mortar depended on the surface area of the mixture ingredients; estimation of the specific surface area was improved by accounting for angularity, while water content and paste film thicknesses were vital for predicting the flowability (Ghasemi et al., 2019).

#### 6.3.4.2 Density of new cement

The adjustment of the bulk density in conjunction with compression and a water reducer could ease workability of concrete as suspension (Servais et al., 2002). Many studies which consider optimization of the final properties of concrete and cement-based materials have been carried out on the bulk density, and a number of theoretical models are developed to predict the bulk density of granular materials (Alexander & Mindess, 2010; Chateau, 2011; Fennis & Walraven, 2012; Larrard, 1999). The density of Portland cement is 3.15 g/mL, while the density of the new cement is 3.05 g/mL, as determined in the current experimental research. In this case the density test refers to the ASTM C 188-95 formulation (ASTM C 188-C195, 1995). The result of physical characteristic test of the new cement in the form of density of fresh concrete unit is 2081 kg/m<sup>3</sup> with its dry weight of 2032 kg/m<sup>3</sup>, which is lower than the fresh weight of concrete using Portland cement, which is 2525 kg/m<sup>3</sup>. Moreover, these models are related to the curve optimization of bulk density, compression of bulk density, and the quantity calculation. First, selection of the concrete and cement-based material has to be started with the selection of side edge space of formwork for construction elements so that the rust ratio could be placed in the space. This selection needs the bulk density of concrete mixture used. Last the bulk density model depends on the theoretical density of the concrete and cement-based material mixture. This theoretical density could be calculated mathematically by measuring the bulk density of different mean sizes of the particles in the cement (Fennis & Walraven, 2012; Kirgiz, 2019).

#### 6.3.4.3 Consistency and setting time of new cement

The cement setting time is the starting process of a chemical compound reaction that occurs in cement just after the cement reacts with water so that the cement can become hard and withstand pressure. Table 6.4 presents the consistency of new cement and Portland cement and the penetration depth and the water demand.

**Table 6.4** Consistency properties of the new cement and of Portland cement and the penetration depth and the water demand.

Types of cement	Consistency (%)	Penetration depth (mm)	Water demand (mL)
New cement	37	25	185
Portland cement	25	24	130

In this experimental research, the measured setting time of the new cement and the Portland cement is as shown in Fig. 6.6. The cement that has been mixed with water or

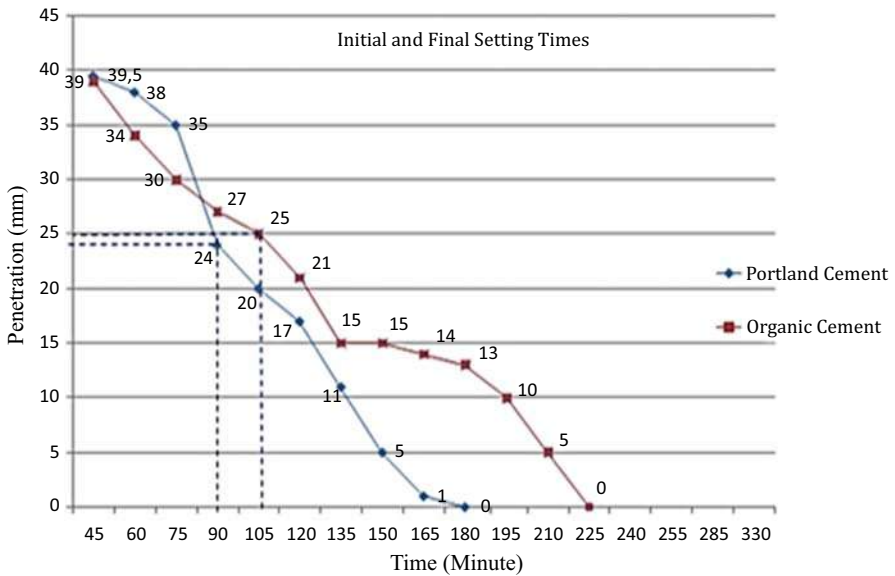


**Figure 6.6** Initial and final setting time.

the cement at a humid temperature causes a chemical reaction in the form of setting of cement particles. The time required by the cement during the setting process shortly after a chemical reaction with water or a humid temperature causes the cement to harden; the reference used in this test is the ASTM C 191-19 standard method (ASTM C191-19, 2019). The initial and final setting times of the new cement and Portland cement were tested using a 1 mm diameter Vicat needle method for the Portland cement that penetrated the cement paste as deep as 24 mm in the 90th minute after the needle was removed. The water content used for the setting test of the Portland cement was 25% water content with normal consistency. The standard used for normal consistency is ASTM C 187-04 standard method (ASTM C187-04, 2004). The initial setting time of new cement penetrating for the cement paste was 25 mm deep after 105 minutes. The water content used for this initial setting test was the 37% water content with normal consistency. By ASTM C 191-19 standard (ASTM C191-19, 2019) the initial setting time should not be less than 45 minutes. The final setting time of Portland cement is at 180 minutes, while for new cement, it is at 225 minutes. The obtained time of setting results for both the new cement and the Portland cement comply with ASTM C 191-19.

## 6.4 Conclusions

From the results of examination of fineness, density, and chemical properties of the new cement, there is resemblance with Portland cement chemical compounds. This can be seen from the XRF and XRD test results. The test results of physical properties of cement based on empirical studies approach the normative references on ASTM. Based

on the results of the cement feasibility test, it can be assumed that the cement investigated can be used for structural and nonstructural work as well as for the installation of brick walls and stucco walls. This is demonstrated by the ability of the new cement to undergo chemical setting and binding of fine aggregate as a support material in a construction work process. However, in order to obtain a more optimal approach to cement as an alternative cement, it is deemed necessary to undertake advanced experimental studies to ensure that the quality of cement can be as expected based on the reference of ASTM. So in the end the problem of waste and the effort of saving the environment from the accumulation of waste can be thought of handling wisely through the approach of experimental study as an alternative building material, which in this case is as an alternative cement other than Portland cement.

## References

- Alexander, M., & Mindess, S. (2010). *Aggregates in concrete*. CRC Press.
- Almalkawi, A. T., Balchandra, A., & Soroushian, P. (2019). Potential of using industrial wastes for production of geopolymer binder as green construction materials. *Construction and Building Materials*, 220, 516–524. Available from <https://doi.org/10.1016/j.conbuildmat.2019.06.054>.
- ASTM C 188-C195. (1995). *Standard test method for density of hydraulic cement*. ASTM International. Available from <http://www.astm.org>.
- ASTM C114-07. (2007). *Standard test methods for chemical analysis of hydraulic-cement*. ASTM International. Available from <http://www.astm.org>.
- ASTM C1365-18. (1365). *Standard test method for determination of the proportion of phases in portland cement and portland-cement clinker using x-ray powder diffraction analysis*. ASTM International. Available from <http://www.astm.org>.
- ASTM C187-04. (2004). *Standard test normal consistency of hydraulic cement*. ASTM International. Available from <http://www.astm.org>.
- ASTM C191-19. (2019). *Standard test methods for time of setting of hydraulic cement by vicat needle*. ASTM International. Available from <http://www.astm.org>.
- ASTM C204-18e1. (2018). *Standard test methods for fineness of hydraulic cement by air-permeability apparatus*. ASTM International. Available from <http://www.astm.org>.
- ASTM C618-19. (2019). *Standard specification for coal fly ash and raw or calcined natural pozzolan for use in concrete*. ASTM International. Available from <http://www.astm.org>.
- Brownmiller, L. T., & Bogue, R. H. (1930). X-ray method applied to a study of the constitution of Portland cement. *Bureau of Standards Journal Research; A Journal of Science and its Applications*, 5, 813–830. Available from <https://doi.org/10.6028/jres.005.051>.
- Chateau, X. (2011). In N. Roussel (Ed.), *Particle packing and the rheology of concrete*. Woodhead Publishing Limited, Elsevier, <https://doi.org/10.1016/B978-0-85709-028-7.50006-6>.
- Chirag, G., & Jain, A. (2014). Green concrete efficient and eco-friendly construction materials. *IMPACT: International Journal of Research in Engineering & Technology*, 2(2), 259–264.
- European Cement Research Academy (2014). The use of natural calcined clays as a main constituent in cement. [https://ecra-online.org/fileadmin/ecra/newsletter/ECRA\\_Newsletter\\_3-2014.pdf](https://ecra-online.org/fileadmin/ecra/newsletter/ECRA_Newsletter_3-2014.pdf).
- Fennis, S. A. A. M., & Walraven, J. C. (2012). Using particle packing technology for sustainable concrete mixture design. *Heron*, 57(2), 73–101. Available from <http://heronjournal.nl/57-2/1.pdf>.

- Ghasemi, Y., Emborg, M., & Cwirzen, A. (2019). Exploring the relation between the flow of mortar and specific surface area of its constituents. *Construction and Building Materials*, 211, 492–501. Available from <https://doi.org/10.1016/j.conbuildmat.2019.03.260>.
- Ibrahim, S., & Meawad, A. (2018). Assessment of waste packaging glass bottles as supplementary cementitious materials. *Construction and Building Materials*, 182, 451–458. Available from <https://doi.org/10.1016/j.conbuildmat.2018.06.119>.
- Joseph, A. M., Snellings, R., Van den Heede, P., Matthys, S., & De Belie, N. (2018). The use of municipal solidwaste incineration ash in various building materials: A Belgian point of view. *Materials*, 11(1). Available from <https://doi.org/10.3390/ma11010141>.
- Kan, L. L., Shi, R. X., & Zhu, J. (2019). Effect of fineness and calcium content of fly ash on the mechanical properties of Engineered Cementitious Composites (ECC). *Construction and Building Materials*, 209, 476–484. Available from <https://doi.org/10.1016/j.conbuildmat.2019.03.129>.
- Kikuchi, R. (2001). Recycling of municipal solid waste for cement production: Pilot-scale test for transforming incineration ash of solid waste into cement clinker. *Resources, Conservation and Recycling*, 31(2), 137–147. Available from [https://doi.org/10.1016/S0921-3449\(00\)00077-X](https://doi.org/10.1016/S0921-3449(00)00077-X).
- Kırğız, M. (2019). Smart nanoconcretes and cement-based materials: Section 3—Nano size particle packing for nanoconcretes and cement based materials: Mathematical models, theory, and technology.
- Kırğız, M. (2015a). Use of ultrafine marble and brick particles as raw materials in cement manufacturing. *Materials and Structures*, 48(9), 2929–2941.
- Kırğız, M. S. (2015b). Advance treatment by nanographite for Portland pulverised fly ash cement (the class F) systems. *Composites Part B: Engineering*, 82, 59–71. Available from <https://doi.org/10.1016/j.compositesb.2015.08.003>.
- Kırğız, M. S. (2018). Green cement composite concept reinforced by graphite nano-engineered particle suspension for infrastructure renewal material. *Composites Part B: Engineering*, 154, 423–429. Available from <https://doi.org/10.1016/j.compositesb.2018.09.012>.
- Larrard. (1999). *Concrete mixture proportioning: A scientific approach*. CRC Press.
- Le Châtelier, H. (1882). Recherches Expérimentales sur la Constitution des Ciments et la Théorie de Leur Prise. *C.R. Acad. Sci. Paris*, 94, 867–869.
- Le Châtelier, H. (1905). *Experimental researches on the constitution of hydraulic mortars*. McGraw-Hill.
- Marthinus, A. P., Sumajouw, M. D. J., & Windah, R. S. (2015). Pengaruh Penambahan Abu Terbang (Fly Ah) Terhadap Kuat Tarik Belah Beton. *Jurnal Sipil Statik*, 3(11), 729–736. Available from <https://ejournal.unsrat.ac.id/index.php/jss/article/view/10662>.
- Nath, S. K., & Kumar, S. (2020). Role of particle fineness on engineering properties and microstructure of fly ash derived geopolymer. *Construction and Building Materials*, 233. Available from <https://doi.org/10.1016/j.conbuildmat.2019.117294>.
- Nicholas, W. B. (2014). *Understanding cement, low concrete strenght, ten potential cement-related causes*. London: WHD Microanalysis Consultan Ltd..
- Oktavianus, O. (2015). Pengelolaan Sampah di Kota Makassar Dengan Bank Sampah. <http://artikel-opiniku.blogspot.co.id/2015/08/pengelolaansampahdikotamakassar.html>.
- Ruiz-Sánchez, A., Sánchez-Polo, M., & Rozalen, M. (2019). Waste marble dust: An interesting residue to produce cement. *Construction and Building Materials*, 224, 99–108. Available from <https://doi.org/10.1016/j.conbuildmat.2019.07.031>.
- Sebayang, S., Widyawati, R., & Habibie, B. M. (2012). Pengaruh Abu Terbang Terhadap Sifat-sifat Mekanik Beton Alir Ringan Alwa. *Jurnal Teknik Sipil UBL*, 3(1), 247–256. Available from <http://jurnal.ubl.ac.id/index.php/JTS/article/view/274>.

- Servais, C., Jones, R., & Roberts, I. (2002). The influence of particle size distribution on the processing of food. *Journal of Food Engineering*, 51(3), 201–208. Available from [https://doi.org/10.1016/S0260-8774\(01\)00056-5](https://doi.org/10.1016/S0260-8774(01)00056-5).
- Siddique, R. (2010). Use of municipal solid waste ash in concrete. *Resources, Conservation and Recycling*, 55(2), 83–91. Available from <https://doi.org/10.1016/j.resconrec.2010.10.003>.
- Törnebohm, A. E. (1897). Die Petrographie des Portland-Cements. *Thonind.-Ztg*, 21(110), 1148–1151.
- Tumingan, T., Tjaronge, M. W., Sampebulu, V., & Djamaluddin, R. (2016). Penyerapan dan Porositas Pada Beton Menggunakan Bahan Pond Ash Sebagai Pengganti Pasir. *Jurnal Politeknologi*, 15(1), 456–465. Available from <https://doi.org/10.32722/pt.v15i1.776>.
- Verheye, & Rosa (2005). Mediterranean soils, in land use and land cover. Encyclopedia of Life Support Systems (EOLSS).
- Victor, S. (2012). Influence of high temperature on the workability of fresh ready-mixed concrete. *ITB Engineering*, 44(1), 21–32.
- Wheeler, B. (1983). Chemical analysis of portland cement by energy dispersive x-ray fluorescence. *Cement, Concrete and Aggregates*, 5(2), 123–127. Available from <https://doi.org/10.1520/CCA10262J>.
- Yustikarini, R. (2017). Proceeding Biology Education Conference- Evaluasi dan Kajian Penanganan Sampah dalam Mengurangi Beban Tempat Pemrosesan Akhir Sampah di TPA Milangasri, 14(1) Magetan Regency.

# Alkali-activated hydraulic binder geopolymer with ground granulated blast furnace slag

7

Mehmet Serkan Kırgız<sup>1</sup> and Hasan Biricik<sup>2</sup>

<sup>1</sup>Northwestern University, Chicago, IL, United States, <sup>2</sup>Department of Civil Engineering, Construction Materials Laboratory, Yıldız Teknik University, Bakırköy, İstanbul, Turkey

## 7.1 Introduction

Conventional Portland cement increases significantly the global CO<sub>2</sub> release: Between 2022–2030 years the calculated quantity will be  $1.54 \pm 0.2$  Gt CO<sub>2</sub>, that is, approximately 7% of the total anthropogenic CO<sub>2</sub> emission (Kırgız et al., 2021). Although the cement industry could develop energy efficiency importantly, increasing cement demand has resulted in failure of much of the positive influence (Schneider et al., 2011). Additionally the CO<sub>2</sub> release, which is from the calcination of farina at 1400°C–1450°C, is approximately 55%–60%. This calcination process could not be influenced by improving energy efficiency in the production of Portland cement (Damtoft et al., 2008). Consequently, research and development of alternative ecology-friendly binders should be reorganized as a great opportunity to reduce CO<sub>2</sub> release (Flatt et al., 2012; Gartner & Hirao, 2015). Geopolymers, which are sometimes taken into account as a subgroup of materials activated by alkali, are promising materials in this case (Provis, 2014). While undoubtedly conventional cement can be completely replaced, it may serve as an ecology-friendly binder related to the local raw materials suitably (Provis, 2018). Geopolymer-based materials can be mixed to have tailored properties when compared to cement-based materials, namely, better durability against effects naturally and artificially (Aiken et al., 2017; Albitar et al., 2017; Bakharev, 2005), better heat insulation (Kong & Sanjayan, 2010; Sarker et al., 2014; Sarker & McBeath, 2015), lower creep and drying shrinkage (Sagoe-Crentsil et al., 2013), and higher strength for forces (Al Bakri et al., 2013). Nevertheless, the formation of efflorescence can be considered as a potential problem if it is not properly controlled by, for example, mix design (Zhang et al., 2014). In terms of reactions of dangerous alkali aggregate, geopolymer-based materials have often demonstrated better performance than cement-based materials (García-Lodeiro et al., 2007). Nevertheless, attention should be canalized for the proper selection of the type and dose of alkali activator, the

type of binder, and the type of aggregate stack in the geopolymer-based material production (Shi et al., 2015). Technology in alkali-activated materials also permits waste disposal for a number of industrial byproducts (Mehta & Siddique, 2016), such as slag, fly ash (Kirgiz, 2018), marble powder (Kirgiz, 2016), calcined clay waste, and so on (Awoyera et al., 2020; Biricik et al., 2021).

In addition, since plenty of comprehensive works are performed on the conventional cement-based material use, the geopolymer-based material does not come to the fore (Douglas Hooton, 2015). Nevertheless, in such countries as Ukraine (DSTU B V.2.7-181, 2009) the use of alkaline cement is already accepted in the mainstream. However, blending the byproduct and its ratio and chemical admixtures for geopolymer-based materials and the testing process are still inadequate (Biricik et al., 2021). In the light of information mentioned, it is expected that the book chapter could fill the gap between geopolymer-based materials and industrial byproducts. For that aim, manufacturing of geopolymer-based materials with ground granulated blast furnace slag (GGBFS) and physicomechanical testing of the geopolymer-based material and their current data were discussed in the current comprehensive chapter.

## 7.2 Materials and methods

### 7.2.1 Materials

Constituent materials of high-performance geopolymers (HPGs) are in the GGBFS as supplementary binder materials, a combination of NaOH and NaS as an alkali activator, standard mortar sand, and water in this chapter. The chemical composition of the GGBFS is shown in Table 7.1.

**Table 7.1** Chemical composition of the GGBFS.

Chemical composition (%)	Types of ground granulated blast furnace slag 4000 Blaine (cm <sup>2</sup> /g)	6000 Blaine (cm <sup>2</sup> /g)
Silicon oxide (SiO <sub>2</sub> )	38.4	37.7
Aluminum oxide (Al <sub>2</sub> O <sub>3</sub> )	10.2	10
Iron oxide (Fe <sub>2</sub> O <sub>3</sub> )	1.5	1.5
Calcium oxide (CaO)	37.7	37.5
Magnesium oxide (MgO)	7.8	8
Sulfur oxide (SO <sub>3</sub> )	0.6	0.65
Clor (Cl <sup>-</sup> )	0.038	0.25
Sodium oxide (Na <sub>2</sub> O)	0.3	0.3
Potassium oxide (K <sub>2</sub> O)	0.8	0.8
Loss on Ignition (LOI)	2	2.6

## 7.2.2 Mixing, handling, placing, and molding of high-performance geopolymers

The HPG was prepared with a blending of NaO and NaS, sand, water, and GGBFS to evaluate mechanical properties—compressive and flexural strengths—and physical properties—change in weight and capillary water absorption. To initiate activation between the GGBFS and water and alkalis, compounds of the geopolymer specimen were prepared with 1 (NaO + NaS): 4.16 (GGBFS 400 m<sup>2</sup>/kg): 2.08 (water): 12.5 (sand) or 1 (NaO + NaS): 4.17 (GGBFS 600 m<sup>2</sup>/kg): 1.96 (water): 12.5 (sand). Table 7.2 summarizes preparation of the HPG with constituent materials and their portions.

**Table 7.2** Preparation of HPGs with constituent materials and their portions.

Types of geopolymer	Constituent materials and their portions for one cubic meter				
	GGBFS (kg)	Water (L)	Sand (kg)	NaO (kg)	NaS (kg)
HPG-400	462	231	1386	32.3	78.5
HPG-600	463	218	1390	32	79

## 7.2.3 Methods

The test of capillary water absorption was performed on the 28th- and 56th-day with prism samples of 40 × 40 × 50 mm with the standard rules of ASTM C 1585-13. To establish the capillarity coefficient as  $K$  a regression analysis among  $Q/F$  and  $t$  was performed. With the correlation equation (Eq. (7.1)),  $K$  was determined as the capillarity coefficient (cm<sup>2</sup>/seconds).

$$K = \frac{Q^2}{F^2 \times t} \quad (7.1)$$

where  $K$  stands for the capillarity coefficient (cm<sup>2</sup>/seconds),  $Q$  indicates the water quantity (cm<sup>3</sup>) absorbed by the specimen,  $F$  stands for the cross-section surface of specimen absorbed capillary water (cm<sup>2</sup>), and  $t$  indicates the water absorption time of specimen (seconds) through capillarity.

Tests of change of mass were performed on prism samples with dimensions of 40 × 40 × 160 mm according to the rules of ASTM C1792-14 standard.

$$W = \left( \frac{W_{sh} - W_k}{W_k} \right) \times 100 \quad (7.2)$$

where  $W$  is the mass change ratio (%),  $W_{sh}$  is the sample mass (gr) at ( $t$ ) time, and  $W_k$  is the initial sample mass (gr).



Test of flexure was carried out on prism specimens, which were molded in size of  $40 \times 40 \times 160$  mm according to the rules of BS EN 196-1:2016 standard. To the rules of BS EN 196-1:2016 standard, test of compression was conducted on specimens, fractured in the test of flexure, with the size of  $40 \times 40 \times 50$  mm. For each type of mortar the test of flexure and compression was performed at the 3rd, 7th, 28th, and 56th day of water curing.

## 7.3 Results and discussion

### 7.3.1 Capillary water absorption

The results of capillary water absorption of HPG are given in Table 7.3. The minimum quantity of water absorption is determined in the HPG-4000 containing the GGBFS and the combination of NaOH/NaS, and its capillary water absorption reaches 0.002428 g on the 56th day at the 56th minute.

**Table 7.3** The results of capillary water absorption of HPG.

Property	Duration		High-performance geopolymer	
	Day	Minute	HPG-400	HPG-600
Capillary water absorption	28	0	0.0024	0.0025
		1	0.002405	0.002503
		4	0.002414	0.002510
		9	0.002429	0.002520
		16	0.002446	0.002538
		25	0.002468	0.002561
		36	0.002495	0.002591
		49	0.002525	0.002625
		64	0.002560	0.002662
		56	0	0.00239
	1		0.002397	0.00251
	4		0.002397	0.002520
	9		0.002397	0.002530
	16		0.002397	0.002548
	25		0.002397	0.002571
	36		0.002428	0.00260
	49		0.002428	0.00263
	64		0.002428	0.002672

The maximum quantity of water absorption is determined in the HPG-6000 containing the GGBFS and the combination of NaOH/NaS, and its water absorption reaches 0.002672 g on the 56th day at the 56th minute. There are current results published, which recommended that the capillarity of water in porous media is untypical,

such as HPG. This certainly means that the capillarity of water in porous media is not related to the time square root. This is inconsistent with laboratory results. This relationship between the time square root and capillarity of water is not with regard to each other, as would be expected. In other words, it is independent of the capillarity mechanism which we tried to understand by capillarity of water or diffusion of water: There could be correlation via a mathematical model in which the fluidity of wet is proportional to the water saturated. This proportion is known as the capillarity coefficient. For capillarity of water the capillarity coefficient is the hydraulic diffusivity. Its unit is  $(\text{length})^2$  multiplied by  $(\text{time})^{-1}$  and depends on the square of the absorption of water (Hall & Hoff, 2009). From the practical point of view the result reveals that the difference in Blaine fineness and days of test leads to reducing the absorption of capillary water in the HPG (Table 7.3).

### 7.3.2 Coefficient of capillarity

Table 7.4 shows the coefficient of capillarity of HPG at the age 28 and 56 days. There were plenty of comprehensive works on coefficient of capillarity reported by numerous researchers. The works recommended that coefficient of capillarity and pore were linked with each other on different scales and sizes.

The pore size distribution could be on the pores among the hydrates of geopolymers that are on the nanosize, 0.5–100 nm. Gajewicz-Jaromin et al. recommended that the pore structure of the material is extensively linked to the smaller void of interlayer between the hydrates (Gajewicz et al., 2016; Maruyama et al., 2014, 2019). Moreover, in 2019, Hall reported a current suggestion for the coefficient of capillarity in the material changing phase with time via a powerful relationship between capillarity coefficient and coefficient of diffusivity (Hall, 2019). Previously the first suggestion on the coefficient of capillarity was given by Lockington and Parlange (Lockington & Parlange, 2003). A huge difference between them is that the suggestion of Lockington and Parlange has a diffusivity of coefficient varying with time, while Hall's one does not include the time dependence; it observes at the duration of moving of the water in the material. The result of coefficient of capillarity is much closer in the line of Hall's suggestion in the chapter. Hall suggests that in the test of ingress of water the moment rises by a healing of the porosity (Hall, 2019). As can be seen and understood in Table 7.4 the difference in coefficient of capillarity relates to the days of test and the Blaine fineness. In other words, it is clearly proved that the higher coefficient of capillarity is due to the lower Blaine fineness of GGBFS used in the HPG.

**Table 7.4** The coefficient of capillarity of HPG at the age 28 and 56 days.

Types of test	Duration	HPG-400	HPG-600
Coefficient of capillarity	28 days	1.1	1.25
	56 days	1.02	1.25

### 7.3.3 Flexural capacity

Table 7.5 shows the results of flexural capacity of HPG at the age of 3, 7, 28, and 56 days. At a constant NaOH-to-NaS ratio of 1:2.12 and a Blaine fineness of 600 m<sup>2</sup>/kg, HPG-600 demonstrated the greatest flexural capacity as 7 MPa at 56 days. The flexural capacity of HPG-600 at the age of 56 days is, respectively, over 22%, 19%, and 1% greater than that of both HPG-400 and HPG-600 at the age of 3, 7, and 28 days, Table 7.5.

**Table 7.5** The results of flexural capacity of HPG at the age of 3, 7, 28, and 56 days.

Type of test	Duration (day)	HPG-400	HPG-600
Flexural capacity	3	2.8	5.7
	7	4.3	5.8
	28	5.8	6.8
	56	6.5	7

A few comprehensive studies were published to better understand the link among geopolymerization and flexural capacity in much respected outlets. For example the mechanism of geopolymerization starts with the next four initial stages in the mixing of geopolymer materials: (1) giving and taking of ions, (2) electrolyzing, (3) overcoming the barrier of matrix web, and (4) release of elements of Si and Al (Mataalkah et al., 2017). After the initial stages the formation of a geopolymer most probably follows the next main stages: union, gelling, regrouping, and geopolymerization (Duxson et al., 2007). Li et al. and Hajimohammadi et al. have discussed on geopolymerization since 2010 (Hajimohammadi et al., 2011; Li et al., 2010). A significant dissimilarity between the geopolymerization of silicate (Si) and aluminate (Al) is related with the releasing ratio and reaction capacity of the Si and the Al with hydrates in the geopolymer material. Especially the solid-based silica particle reacts slower than the colloid silicate microbubble in the polymerization stage in the mixing. Hajimohammadi et al. have studied on a novel trend for activators of silicon through blending a solid silicon particle from geothermal resources and a sodium silicon microbubble, including solid sodium–aluminum as a resource of aluminate. They have unveiled some significant results; for example a solid silicon particle from geothermal resources resulted in the formation of an insoluble high-silicon-ratio crystalline matrix known as analcime (NaAlSi<sub>2</sub>O<sub>6</sub> · H<sub>2</sub>O); most of its bulk happened near the silicon particles reacted with nothing; they specified that the microstructure of geopolymer was much more heterogeneous than that of the control sample (Hajimohammadi et al., 2011).

### 7.3.4 Uniaxial compression strength

Table 7.6 shows the results of uniaxial compression strength at the age of 3, 7, 28, and 56 days. At a constant NaOH-to-NaS ratio of 1:2.1 and a Blaine fineness of 600 m<sup>2</sup>/kg, HPG-600 obtained the greatest uniaxial compression strength as 63.6 MPa at 56 days.

**Table 7.6** The results of uniaxial compression strength at the age 3, 7, 28, and 56 days.

Type of test	Duration (day)	HPG-400	HPG-600
Uniaxial compression strength	3	12.2	27.5
	7	21.1	47.7
	28	38	60.3
	56	58.5	63.6

The uniaxial compression strength of HPG-600 at the age of 56 days is, respectively, over 231%, 133%, and 5.4% greater than that of HPG-600 at the age of 3, 7, and 28 days. At a constant Blaine fineness of 400 m<sup>2</sup>/kg, HPG-400 obtained the second greatest uniaxial compression strength as 58.5 MPa at 56 days. The uniaxial compression strength of HPG-400 at the age of 56 days is, respectively, over 479%, 311%, and 172% greater than that of HPG-400 at the age of 3, 7, and 28 days. A similar trend of the uniaxial compression strength feature of the geopolymer material was published by various researchers. For example, Purdon recommended that the most useful solid is alumina–silicate polymer in the geopolymerization stage for the fuel ash from coal combustion, either alone or in combination with GGBFS (Purdon, 1940). Heitzmann et al. utilized the GGBFS as a calcium-rich alumina–silicate byproduct in the geopolymer material activated by a combination of NaOH–NaS alkali (Heitzmann et al., 1987). The GGBFS, which is the byproduct of manufacturing of pig iron in a high-temperature furnace, includes oxides of silicon, aluminum, and minor impurities with regard to the source of iron ore and coke. In previous and current works the masonry units used the alkali-activated system to get the durability purpose grow as well (Ahmari & Zhang, 2015). According to Li et al., use of calcium-rich alumina–silicate or calcium hydroxide led to rapid setting and high strength at early ages (Li et al., 2013). Nevertheless, the replacement of GGBFS with calcium hydroxide resulted in a retardation of both strength and workability in the inner system of the geopolymer (Nematollahi et al., 2015).

## 7.4 Conclusions

In this chapter the effect of two different Blaine fines of GGBFS on the physical and mechanical properties of HPG activated by a combination of NaOH/NaS alkali content is evaluated. A combination of GGBFS and alkali and water is mixed to make cost-effective and sustainable HPG systems develop. The summarized results are as below:

Capillary water absorption is retarded approximately 50% since the temperature of water curing increases from ambient to 22°C. Capillary water absorption growth is between 3% and 3.5% as HPG is cured at the same temperature range under laboratory conditions. Therefore the water curing saturated lime at 22 ± 2°C is favorable if the lower capillary water absorption is required in HPG system. In regard to the Blaine fineness the coefficient of capillarity would be reduced from 28 to 56

days in HPG-400. There is no difference in the coefficient capillarity of HPG-400 with the coefficient capillarity of HPG-600 at both 28 and 56 days. The GGBFS and alkali-based HPG system demonstrated an increase in the flexural capacity continuously. This increase was carried out in a broad range of 2.8–7 MPa between the ages of 3 and 56 days. The GGBFS and alkali-based HPG system obtained an increase in the uniaxial compression strength continuously. This increase was carried out in a broad range of 12.2 and 63.8 MPa between the ages of 3 and 56 days. This increase supported the conclusion in the test of flexural capacity. This development unveiled that wet curing is a must for HPG systems made of the GGBFS and the combination of NaOH/NaS alkali in the chapter.

## References

- Ahmari, S., & Zhang, L. (2015). *The properties and durability of alkali-activated masonry units. Handbook of alkali-activated cements, mortars and concretes* (pp. 643–660). Elsevier Inc. Available from <https://doi.org/10.1533/9781782422884.4.643>.
- Aiken, T. A., Sha, W., Kwasny, J., & Soutsos, M. N. (2017). Resistance of geopolymer and Portland cement based systems to silage effluent attack. *Cement and Concrete Research*, 92, 56–65. Available from <https://doi.org/10.1016/j.cemconres.2016.11.015>.
- Al Bakri, A. M. M., Kamarudin, H., Binhussain, M., Nizar, I. K., Rafiza, A. R., & Zarina, Y. (2013). Comparison of geopolymer fly ash and ordinary portland cement to the strength of concrete. *Advanced Science Letters*, 19(12), 3592–3595. Available from <https://doi.org/10.1166/asl.2013.5187>.
- Albitar, M., Mohamed Ali, M. S., Visintin, P., & Drechsler, M. (2017). Durability evaluation of geopolymer and conventional concretes. *Construction and Building Materials*, 136, 374–385. Available from <https://doi.org/10.1016/j.conbuildmat.2017.01.056>.
- Awoyera, P. O., Kirgiz, M. S., Vilorio, A., & Ovallos-Gazabon, D. (2020). Estimating strength properties of geopolymer self-compacting concrete using machine learning techniques. *Journal of Materials Research and Technology*, 9(4), 9016–9028. Available from <https://doi.org/10.1016/j.jmrt.2020.06.008>.
- Bakharev, T. (2005). Resistance of geopolymer materials to acid attack. *Cement and Concrete Research*, 35(4), 658–670. Available from <https://doi.org/10.1016/j.cemconres.2004.06.005>.
- Biricik, H., Kirgiz, M. S., Galdino, A. G. d. S., Kenai, S., Mirza, J., Kinuthia, J., Ashteyat, A., Khatab, A., & Khatib, J. (2021). Activation of slag through a combination of NaOH/NaS alkali for transforming it into geopolymer slag binder mortar—assessment the effects of two different Blaine fines and three different curing conditions. *Journal of Materials Research and Technology*, 14, 1569–1584. Available from <https://doi.org/10.1016/j.jmrt.2021.07.014>.
- Damtoft, J. S., Lukasik, J., Herfort, D., Sorrentino, D., & Gartner, E. M. (2008). Sustainable development and climate change initiatives. *Cement and Concrete Research*, 38(2), 115–127. Available from <https://doi.org/10.1016/j.cemconres.2007.09.008>.
- Douglas Hooton, R. (2015). Current developments and future needs in standards for cementitious materials. *Cement and Concrete Research*, 78, 165–177. Available from <https://doi.org/10.1016/j.cemconres.2015.05.022>.
- DSTU B V.2.7-181. (2009). *Alkaline cements specifications*. National Standard of Ukraine.

- Duxson, P., Fernández-Jiménez, A., Provis, J. L., Lukey, G. C., Palomo, A., & Van Deventer, J. S. J. (2007). Geopolymer technology: The current state of the art. *Journal of Materials Science*, 42(9), 2917–2933. Available from <https://doi.org/10.1007/s10853-006-0637-z>.
- Flatt, R. J., Roussel, N., & Cheeseman, C. R. (2012). Concrete: An eco material that needs to be improved. *Journal of the European Ceramic Society*, 32(11), 2787–2798. Available from <https://doi.org/10.1016/j.jeurceramsoc.2011.11.012>.
- Gajewicz, A. M., Gartner, E., Kang, K., McDonald, P. J., & Yermakou, V. (2016). A <sup>1</sup>H NMR relaxometry investigation of gel-pore drying shrinkage in cement pastes. *Cement and Concrete Research*, 86, 12–19. Available from <https://doi.org/10.1016/j.cemconres.2016.04.013>.
- García-Lodeiro, I., Palomo, A., & Fernández-Jiménez, A. (2007). Alkali-aggregate reaction in activated fly ash systems. *Cement and Concrete Research*, 37(2), 175–183. Available from <https://doi.org/10.1016/j.cemconres.2006.11.002>.
- Gartner, E., & Hirao, H. (2015). A review of alternative approaches to the reduction of CO<sub>2</sub> emissions associated with the manufacture of the binder phase in concrete. *Cement and Concrete Research*, 78, 126–142. Available from <https://doi.org/10.1016/j.cemconres.2015.04.012>.
- Hajimohammadi, A., Provis, J. L., & Van Deventer, J. S. J. (2011). The effect of silica availability on the mechanism of geopolymerisation. *Cement and Concrete Research*, 41(3), 210–216. Available from <https://doi.org/10.1016/j.cemconres.2011.02.001>.
- Hall, C. (2019). Capillary imbibition in cement-based materials with time-dependent permeability. *Cement and Concrete Research*, 124, 105835. Available from <https://doi.org/10.1016/j.cemconres.2019.105835>.
- Heitzmann, R. F., Fitzgerald, M., & Sawyer, J. L. (1987). Mineral binder and compositions employing the same, Mineral binder and compositions employing the same. US Patent, 4.
- Hall, C., & Hoff, W. D. Water Transport in Brick, Stone and Concrete, 2nd, CRC Press, 2009.
- Kirgiz, M. S. (2016). Advancements in mechanical and physical properties for marble powder-cement composites strengthened by nanostructured graphite particles. *Mechanics of Materials*, 92, 223–234. Available from <https://doi.org/10.1016/j.mechmat.2015.09.013>.
- Kirgiz, M. S. (2018). Green cement composite concept reinforced by graphite nano-engineered particle suspension for infrastructure renewal material. *Composites Part B: Engineering*, 154, 423–429. Available from <https://doi.org/10.1016/j.compositesb.2018.09.012>.
- Kirgiz, M. S., Galdino, A. G. d. S., Kinuthia, J., Khitab, A., Ul Hassan, M. I., Khatib, J., El Naggari, H., Thomas, C., Mirza, J., Kenai, S., Nguyen, T. A., Nehdi, M., Syarif, M., Ashteyat, A., Gobinath, R., Soliman, A., Tagbor, T. A., Kumbhalkar, M. A., Bheel, N., & Tiwary, C. S. (2021). Synthesis, physico-mechanical properties, material processing, and math models of novel superior materials doped flake of carbon and colloid flake of carbon. *Journal of Materials Research and Technology*, 15, 4993–5009. Available from <https://doi.org/10.1016/j.jmrt.2021.10.089>.
- Kong, D. L. Y., & Sanjayan, J. G. (2010). Effect of elevated temperatures on geopolymer paste, mortar and concrete. *Cement and Concrete Research*, 40(2), 334–339. Available from <https://doi.org/10.1016/j.cemconres.2009.10.017>.
- Li, C., Sun, H., & Li, L. (2010). A review: The comparison between alkali-activated slag (Si + Ca) and metakaolin (Si + Al) cements. *Cement and Concrete Research*, 40(9), 1341–1349. Available from <https://doi.org/10.1016/j.cemconres.2010.03.020>.

- Li, X., Wang, Z., & Jiao, Z. (2013). Influence of curing on the strength development of calcium-containing geopolymer mortar. *Materials*, 6(11), 5069–5076. Available from <https://doi.org/10.3390/ma6115069>.
- Lockington, D. A., & Parlange, J. Y. (2003). Anomalous water absorption in porous materials. *Journal of Physics D: Applied Physics*, 36(6), 760–767. Available from <https://doi.org/10.1088/0022-3727/36/6/320>.
- Maruyama, I., Nishioka, Y., Igarashi, G., & Matsui, K. (2014). Microstructural and bulk property changes in hardened cement paste during the first drying process. *Cement and Concrete Research*, 58, 20–34. Available from <https://doi.org/10.1016/j.cemconres.2014.01.007>.
- Maruyama, I., Ohkubo, T., Haji, T., & Kurihara, R. (2019). Dynamic microstructural evolution of hardened cement paste during first drying monitored by 1H NMR relaxometry. *Cement and Concrete Research*, 122, 107–117. Available from <https://doi.org/10.1016/j.cemconres.2019.04.017>.
- Matalkah, F., Xu, L., Wu, W., & Soroushian, P. (2017). Mechanochemical synthesis of one-part alkali aluminosilicate hydraulic cement. *Materials and Structures*, 50, 97.
- Mehta, A., & Siddique, R. (2016). An overview of geopolymers derived from industrial by-products. *Construction and Building Materials*, 127, 183–198. Available from <https://doi.org/10.1016/j.conbuildmat.2016.09.136>.
- Nematollahi, B., Sanjayan, J., & Shaikh, F. U. A. (2015). Synthesis of heat and ambient cured one-part geopolymer mixes with different grades of sodium silicate. *Ceramics International*, 41(4), 5696–5704. Available from <https://doi.org/10.1016/j.ceramint.2014.12.154>.
- Provis, J. L. (2014). Introduction and scope. In J. L. Provis & J. S. J. Van Deventer (Eds.), *RILEM TC 224-AAM: Alkali activated materials, state-of-the-art report*. RILEM.
- Provis, J. L. (2018). Alkali-activated materials. *Cement and Concrete Research*, 114, 40–48. Available from <https://doi.org/10.1016/j.cemconres.2017.02.009>.
- Purdon, A. (1940). The action of alkalis on blast-furnace slag. *Journal of the Society of Chemical Industry*, 59, 191–202.
- Sagoe-Crentsil, K., Brown, T., & Taylor, A. (2013). Drying shrinkage and creep performance of geopolymer concrete. *Journal of Sustainable Cement-Based Materials*, 2(1), 35–42. Available from <https://doi.org/10.1080/21650373.2013.764963>.
- Sarker, P. K., Kelly, S., & Yao, Z. (2014). Effect of fire exposure on cracking, spalling and residual strength of fly ash geopolymer concrete. *Materials and Design*, 63, 584–592. Available from <https://doi.org/10.1016/j.matdes.2014.06.059>.
- Sarker, P. K., & McBeath, S. (2015). Fire endurance of steel reinforced fly ash geopolymer concrete elements. *Construction and Building Materials*, 90, 91–98. Available from <https://doi.org/10.1016/j.conbuildmat.2015.04.054>.
- Schneider, M., Romer, M., Tschudin, M., & Bolio, H. (2011). Sustainable cement production-present and future. *Cement and Concrete Research*, 41(7), 642–650. Available from <https://doi.org/10.1016/j.cemconres.2011.03.019>.
- Shi, C., Shi, Z., Hu, X., Zhao, R., & Chong, L. (2015). A review on alkali-aggregate reactions in alkali-activated mortars/concretes made with alkali-reactive aggregates. *Materials and Structures/Materiaux et Constructions*, 48(3), 621–628. Available from <https://doi.org/10.1617/s11527-014-0505-2>.
- Zhang, Z., Provis, J. L., Reid, A., & Wang, H. (2014). Fly ash-based geopolymers: The relationship between composition, pore structure and efflorescence. *Cement and Concrete Research*, 64, 30–41. Available from <https://doi.org/10.1016/j.cemconres.2014.06.004>.

# Natural rubber latex-substituted-bitumen binder and bitumen binder-based materials used in highway

8

*Theresah Osei<sup>1</sup>, Trinity Ama Tagbor<sup>2</sup>, Johannes A.M. Awudza<sup>3</sup> and Mehmet Serkan Kirgiz<sup>4</sup>*

<sup>1</sup>Council for Scientific and Industrial Research, Building and Road Research Institute, Kumasi, Ghana, <sup>2</sup>Council for Scientific and Industrial Research, Institute of Industrial Research, Accra, Ghana, <sup>3</sup>Department of Chemistry, Kwame Nkrumah University of Science and Technology, Kumasi, Ghana, <sup>4</sup>Northwestern University, Chicago, IL, United States

## 8.1 Introduction

Bitumen is used mainly as a binder in asphalt pavements for road construction in many developing countries. In recent times, more roads are being constructed for the speedy delivery of goods and services in in the world. There has also been a general increase in vehicle ownership, resulting in increased pressures from vehicle tires. These pressures have led to a high level of stresses exerted on asphalt surfaces, which are exhibited as deformation, surface cracking, fatigue, and reflective cracking, which can result in dangerous road traffic conditions. Ghana depends on imported bitumen, which costs averagely \$250 km<sup>-1</sup> in constructing bituminous roads. Since 2020 the country has been importing averagely 6000 metric tons of bitumen for road construction yearly (UN Statistics Division, 2021).

Bitumen in asphalt pavement generally softens easily, and this situation may become worse due to the relatively high temperatures experienced in some months during the year in a typical tropical country like Ghana. Thus vehicle tires could easily penetrate the softened asphalt pavement and cause damages such as road cracks and severe road potholes of bituminous roads (Khodary & Abd El-Sadek HSE-S, 2014). Therefore there is a need to modify bitumen so as to increase the softening point temperature as well as decrease the penetration point for better performance and more durable asphalt roads.



Polymer modification of bitumen is generating a great deal of research interest worldwide due to the fact that polymers contribute viscoelastic characteristics to the rheological properties of bitumen. It has been reported that the application of polymer materials improves the quality of bitumen by reducing cracks caused by traffic loads, weakness in cohesion of binders caused by exposure to moisture and temperature effects, and so on (Ali et al., 2013). Polymers normally used as modifiers are styrene butadiene rubber, styrene butadiene styrene (SBS), polychloroprene, natural rubber, and ethylene vinyl acetate (Zhu et al., 2014). However, natural rubber has a major advantage compared to other polymers in an emulsion formulation because it can be used in liquid form (Forbes et al., 2001).

Addition of rubber to bitumen provides an elastic property to the bitumen, which increases the viscosity and softening point temperature as well as decrease the penetration value (Nuha et al., 2011). The rubber particles swell in the bitumen to form a gel which causes an increase in viscosity. At high temperature a rubber-modified asphalt pavement under load stretches without ripping and returns to its original position when the applied load is released. This prevents deformation as well as stripping of asphalt pavement (Swetha, 2014). Rubber also introduces a self-healing property onto the asphalt pavement by forming a three-dimensional network around asphalt binder under load when cracks develop. The binder then softens and cracks fuse back as the temperature increases. Rubber in asphalt road improves skid resistance of vehicles. Incorporation of natural rubber into bitumen would increase the softening point and viscosity, thereby making it less susceptible to temperature (Nuha et al., 2011).

Though Ghana has large plantations of rubber trees which are used in the production of rubber, the use of rubber to modify bitumen is relatively uncommon; meanwhile, it is common to find bituminous roads in deplorable state due to early deterioration. This report forms part of results from preliminary studies conducted on locally available natural rubber and AC 10 bitumen to generate scientific data which may contribute to promoting its use in the construction of bituminous road.

### **8.1.1 Objective**

The objectives of the study were to prepare a natural rubber–bitumen binder-based composite with different percentages of natural rubber latex and to study the effect of various percentages of natural rubber latex on the rheological properties of the bitumen-based binder. The change in functional properties of the natural rubber–bitumen-based binder composite was measured by using Fourier-transform infrared (FTIR) spectroscopy.

## 8.2 Materials and method

### 8.2.1 Bitumen-based binder

The bitumen-based binder used for this study is AC 10 grade bitumen obtained from a local road contractor in Kumasi, Ghana.

#### 8.2.1.1 Natural rubber latex

Natural rubber latex, manufactured locally, was obtained from Ghana Rubber Estate Limited, Eastern Region, Ghana. The rubber was stored in 5% liquid ammonia to prevent coagulation of the latex.

#### 8.2.1.2 Sample preparation

The blends were prepared using the melt blend techniques. The bitumen was weighed into a stainless steel bucket and heated to a temperature of 160°C on a Sybron Thermolyne HP-A1915B hot plate. Under fluid conditions the latex was slowly added at percentages of 1, 2, 3, 4, 5, and 10, while the speed of the mixer was maintained at 120 rpm and the temperature was kept at 160°C. Mixing continued for 1 hour to produce homogeneous mixtures. The blends were then transferred to 500 g tin containers labeled and stored for rheological testing. No samples were prepared for 6%–9% due to inadequate funding and also because earlier studies reported optimum performance between 4%–5% (Abdulrahman et al., 2019; Krishnapriya, 2015). However, 10% replacement was prepared, and studied results of these will inform future studies.

#### 8.2.1.3 Laboratory analysis

The following analyses were carried out on the prepared composite of bitumen binder.

##### Penetration point

Penetration is used to measure the hardness or softness of a binder. This test was done in accordance with ASTM D5-97 (ASTM D5-97, 1997).

##### Softening point temperature

The ring and ball apparatus is used to determine the temperature at which a bitumen sample can no longer support the weight of a 3.5 g steel ball. The test was done according to method described in ASTM D36/D36M-142020 (2020).

##### Kinematic viscosity

Viscosity is a measure of fluid deformation due to shear stress or tensile stress. Measurements were made at 135°C according to the test method stated in ASTM D2170/D2170M-10 (ASTM D2170/D2170M-10, 2010).

### Specific gravity

The specific gravity of the bituminous mixture was measured according to the test protocol described in ASTM D 70-97 (ASTM D70-97, 1997). This is the ratio of mass of a given volume of bitumen to the mass of an equal volume of water at 27°C, and this is done by preparation of a cube sample in the semisolid or solid state.

### Short-term aging test

Short-term aging determines the effects of heat and atmospheric oxygen during mixing, storage, and laying of asphalt binder. This test was done using the rotating cylinder aging test according to the procedure stated in ASTM D1754/D1754M-20 (ASTM D1754/D1754M-20, 2020).

### Flash point

The flash point test is useful in determining that an asphalt binder has been prepared with solvents that meet the desired range of flammability. The flash point test was done according to the test procedure described in ASTM D3143/D3143M-19 (ASTM D3143/D3143M-19, 2019).

### Fourier-transform infrared spectroscopy test

FTIR analysis was conducted on the crude bitumen, natural rubber latex, and the blends. FTIR spectra were measured using an Interspec 200-X. All spectra were obtained at wavenumbers ranging from 4000 to 400 cm<sup>-1</sup>.

### Penetration index and temperature susceptibility

Penetration index and temperature susceptibility were calculated using the equation below:

$$PI = \frac{1952 - (500 \times \log(\text{Pen } 25) - 20 \times SP)}{50 \times \log(\text{Pen } 25) - SP - 120}$$

$$A = \frac{(\log \text{PEN}@25^\circ\text{C} - \log 800)}{(25 - \text{ASTM softening point})}$$

where *PI* is the penetration index, Pen25 is penetration at 25°C in tenth of millimeters, *SP* is the softening point temperature in °C, and *A* is temperature susceptibility. Table 8.1 gives further information on the tests conducted on the various samples with their respective codes.

**Table 8.1** Tests, specimen number, size of specimens, identification of specimen, code tests, specimen number, size of specimens, identification of specimen, and codes.

Test/reference	Justification	No. of specimens tested	Size of specimen	Sample ID	Codes
Penetration test (ASTM D5-97)	The test determines the softness or hardness of bitumen	Three each	500 g of each specimen was prepared for all the tests	PBL	(PBL01, PBL02, PBL03), (PBL11, PBL12, PBL13), (PBL21, PBL22, PBL23), (PBL31, PBL32, PBL33), (PBL41, PBL42, PBL43), (PBL51, PBL52, PBL53) and (PBL101, PBL102, PBL103)
Softening point temperature (ASTM D 36–70)	The temperature at which a bitumen sample can no longer support the weight of a 3.5 g steel ball	Three each		SPBL	(SPBL <sub>01</sub> , SPBL <sub>02</sub> , SPBL <sub>03</sub> ), (SPBL <sub>11</sub> , SPBL <sub>12</sub> , SPBL <sub>13</sub> ), (SPBL <sub>21</sub> , SPBL <sub>22</sub> , SPBL <sub>23</sub> ), (SPBL <sub>31</sub> , SPBL <sub>32</sub> , SPBL <sub>33</sub> ), (SPBL <sub>41</sub> , SPBL <sub>42</sub> , SPBL <sub>43</sub> ), (SPBL <sub>51</sub> , SPBL <sub>52</sub> , SPBL <sub>53</sub> ), and (SPBL <sub>101</sub> , SPBL <sub>102</sub> , SPBL <sub>103</sub> )
Kinematic viscosity (ASTM D-2170–10)	Measures the deformation of fluid due to shear stress or tensile stress and is a basic parameter used to investigate the rheological properties of bitumen	Three each		KVBL	(KVBL <sub>01</sub> , KVBL <sub>02</sub> , KVBL <sub>03</sub> ), (KVBL <sub>12</sub> , KVBL <sub>12</sub> ), (KVBL <sub>13</sub> ), (KVBL <sub>21</sub> , KVBL <sub>22</sub> , KVBL <sub>23</sub> ), (KVBL <sub>31</sub> , KVBL <sub>32</sub> , KVBL <sub>33</sub> ), (KVBL <sub>41</sub> , KVBL <sub>42</sub> , KVBL <sub>43</sub> ), (KVBL <sub>51</sub> , KVBL <sub>52</sub> , KVBL <sub>53</sub> ) and (KVBL <sub>101</sub> , KVBL <sub>102</sub> , KVBL <sub>103</sub> )

(Continued)

**Table 8.1** (Continued)

Test/reference	Justification	No. of specimens tested	Size of specimen	Sample ID	Codes
Specific gravity (ASTM D 70-76)	The ratio of mass of a given volume of bitumen to the mass of equal volume of water at 27°C	Three each		SGBL	(SGBL <sub>01</sub> , SGBL <sub>02</sub> , SGBL <sub>03</sub> ), (SGBL <sub>11</sub> , SGBL <sub>12</sub> , SGBL <sub>13</sub> ), (SGBL <sub>21</sub> , SGBL <sub>22</sub> , SGBL <sub>23</sub> ), (SGBL <sub>31</sub> , SGBL <sub>32</sub> , SGBL <sub>33</sub> ), SGBL <sub>41</sub> ), (SGBL <sub>42</sub> , SGBL <sub>43</sub> ), (SGBL <sub>51</sub> , SGBL <sub>52</sub> , SGBL <sub>53</sub> ), and (SGBL <sub>101</sub> , SGBL <sub>102</sub> , SGBL <sub>103</sub> )
Flash point (ASTM D3143)	Determines if asphalt binder has been prepared with solvents that meet the desired range of flammability and that the product has not been contaminated with lower-flash point solvents	Three each		FPBL	(FPBL <sub>51</sub> , FPBL <sub>52</sub> , FPBL <sub>53</sub> ) and (FPBL <sub>101</sub> , FPBL <sub>102</sub> , FPBL <sub>103</sub> )
Short-term aging (ASTM D 1754)	Determines the loss of volatile or oily components which result in change in mass. It can also result from incorporation of oxygen into the asphalt binder	Three each		SABL	(SABL <sub>51</sub> , SABL <sub>52</sub> , SABL <sub>53</sub> ) and (SABL <sub>101</sub> , SABL <sub>102</sub> , SABL <sub>103</sub> )
FTIR (Interspec 200-X Fourier-transform infrared spectrometer)	Determines the change in functional group of the blends	Three each		FTIR	(FB <sub>1</sub> , FB <sub>2</sub> , FB <sub>3</sub> ), (FL <sub>1</sub> , FL <sub>2</sub> , FL <sub>3</sub> ), and (FBL <sub>51</sub> , FBL <sub>52</sub> , FBL <sub>53</sub> )

## 8.3 Results and discussion

The results of the various tests as well as spectroscopy test are presented in [Table 8.2](#).

**Table 8.2** Specification and physical analysis of unmodified bitumen binder. Specification and physical analysis of unmodified bitumen binder.

Property of bitumen binder	Standard specification for bitumen binder by GHA	Result analysis of AC 10
Softening point temperature(°C)	48–59	53
Viscosity at 135°C (Cs)	300	356
Penetration	–	140
Specific gravity (g/cm <sup>3</sup> )	1.01–1.06	1.01
Loss in mass after aging (%)	–	–

Ghana Highway Authority has outlined specification for bitumen binder used for road construction in Ghana, which is represented in [Table 8.2](#). Also included in the table are results of tests conducted on the conventional bitumen binder used in this study.

### 8.3.1 Penetration point

[Fig. 8.1](#) is a representation of results obtained for the penetration test, penetration quantity, and latex percentage in modified bitumen binder.

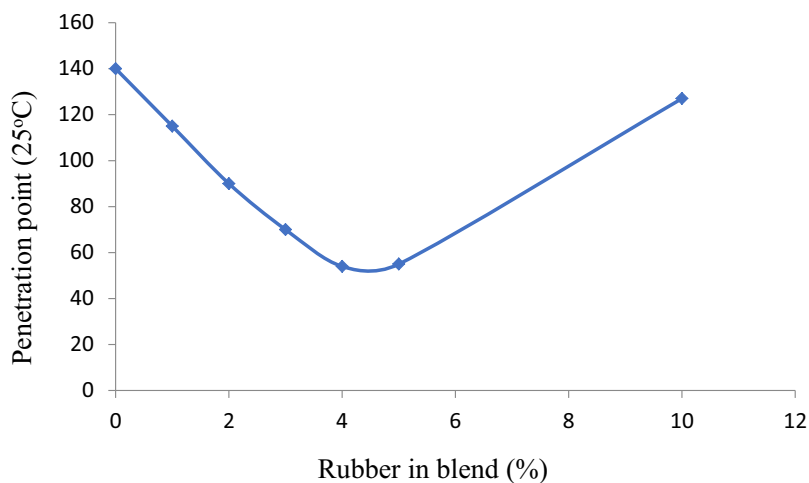


**Figure 8.1** The penetration test results—penetration quantity and latex percentage in modified bitumen binder.

Penetration depends on the stiffness of the binder. From Fig. 8.1, addition of 1% natural rubber latex to the bitumen binder caused a decrease in the penetration values. This suggests that the penetration value of the modified bitumen binder is highly dependent on the natural rubber concentrations. Addition of 1%, 2%, 3%, 4%, and 5% natural rubber latex to the bitumen binder decreases the penetration value by 25, 48, 70, 84, and 85 dmm, respectively, as compared to the crude bitumen binder. A decrease in penetration value as latex concentration increases results from the interaction and swellings of the rubber particles which impart elastic properties onto the blend, therefore increasing the viscosity. This trend in penetration values was observed by Cai et al. (2010) when assessing the performance of SBS latex at different concentrations in bitumen binder emulsion. Nuha, Asim, Mohamed, and Mahrez (2011) also observed a similar trend when analyzing the effect of crumb rubber on the physical and rheological properties of bitumen binder. The rubber-modified bitumen binder shows the least penetration value between 4% and 5% rubber concentrations, which then increases as rubber concentration increases. The increase might have resulted from the coagulation of rubber particles, which then decreases the elastic effect of the blends. Ten (10%) of latex loading increased the penetration value to 127 dmm, representing an overall change of 13 dmm as compared to the unmodified bitumen binder. This indicates that a further increase of rubber may cause an increase in the penetration, in which case the blends would be highly susceptible to temperature and would cause deterioration when applied on the road.

### 8.3.2 Softening point temperature ( $^{\circ}\text{C}$ )

The results from the softening point temperature test are represented in Fig. 8.2. The softening point temperatures of the blends occur in a reverse direction of the penetration point as the rubber content increases after 1%. From the results the softening point temperature decreased to  $46^{\circ}\text{C}$  at 1% latex loading from  $53^{\circ}\text{C}$  and increased with concentration of latex and peaked between 4% and 5% latex concentrations.

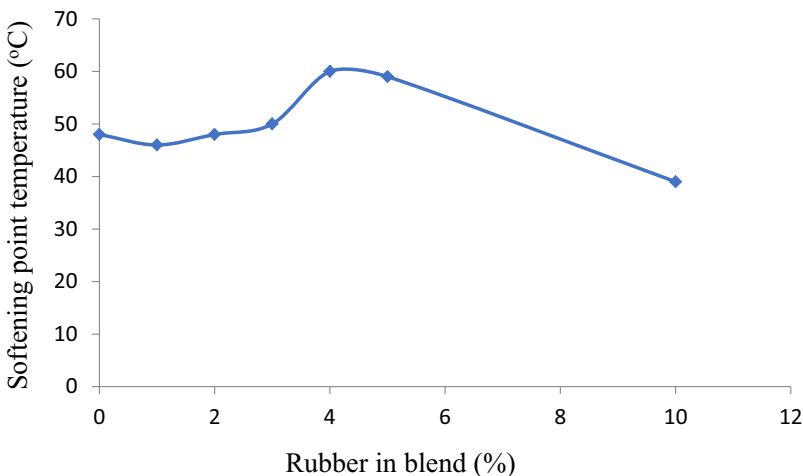


**Figure 8.2** Softening temperature point ( $^{\circ}\text{C}$ ) and latex (%) in modified bitumen binder. Softening temperature point ( $^{\circ}\text{C}$ ) and latex (%) in modified bitumen binder.

The increase in softening point temperature as the rubber level increases is similar to the results obtained by Swetha (2014) in their research into the effect of natural rubber on bitumen binder properties. From Fig. 8.2 a steep decrease after 5% latex concentration is observed with a change in temperature of 20°C. The increase is as a result of the introduction of elastic properties of the rubber causing the blends to be highly viscous, therefore increasing the temperature at which the material becomes soft. The decrease in softening point temperature between 5% and 10% latex levels may have resulted in increased latex particles, leading to coagulation instead of blending and hence a decrease in elasticity of the blend.

### 8.3.3 Viscosity analysis

The results of the viscosity test are presented in Fig. 8.3. Fig. 8.3 shows the trend of viscosity of the modified bitumen binder blends as the percentage of rubber increases. Addition of 1% latex to bitumen binder decreases the viscosity to about 30% as compared to the unmodified bitumen binder, which then increases as latex concentration increases.

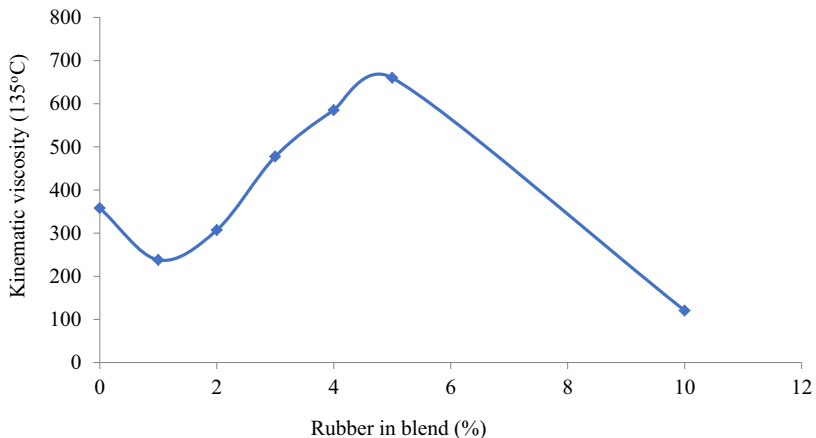


**Figure 8.3** Viscosity at 135°C and latex (%) in modified bitumen binder. Viscosity at 135°C and latex (%) in modified bitumen binder.

This could be ascribed to the fact that the elastic effect at 1% rubber loading was limited and as rubber concentration increases, elasticity also increases, hence resulting in a highly viscous blend. Zhang et al. (2009) observed a trend similar to the above when rubber concentration to the bitumen binder increases. This may have resulted from the dissolution and dispersion of natural rubber in the bitumen binder matrix, leading to an enhanced viscosity. The decrease in viscosity after 5% rubber levels could be due to an increase rubber particles resulting in coagulation instead of swelling, thereby limiting the elastic effect on the blend.



### 8.3.4 Specific gravity test

Fig. 8.4 represents results obtained for the specific gravity test on the blends. The density and specific gravity of bituminous materials are affected by the chemical composition, temperature, and the presence of impurities. Fig. 8.4 shows an increase in the specific gravity of the blend as the latex concentration increases. The specific gravity increases to 2% latex, remains constant, and peaks at 5% latex concentration.

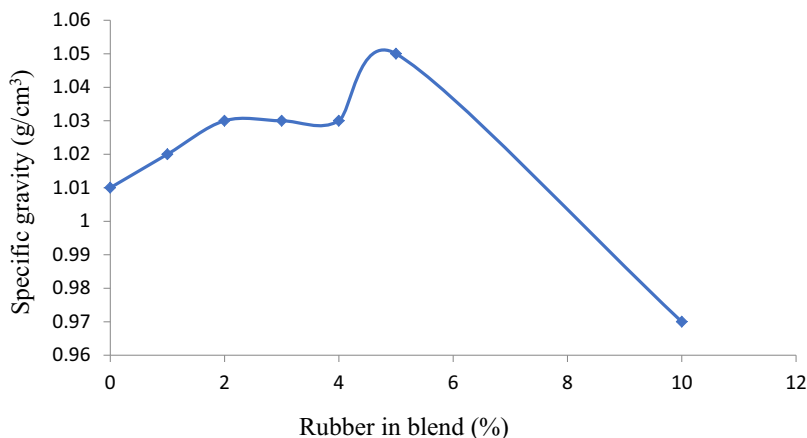


**Figure 8.4** Specific gravity and latex (%) in modified bitumen binder. Specific gravity and latex (%) in modified bitumen binder.

The increase in specific gravity may have resulted from a decrease in pore size of the bitumen binder as rubber was introduced hence reduced void. The reduction in void would decrease permeability of moisture and air. Also the bitumen binder content in the blends reduces as rubber is increased, resulting in an overall increase in specific gravity (Blazejowski et al., 2014). This signifies that the rubber has a significant effect on the bitumen binder. Therefore their use in construction may contribute to a decrease penetration to moisture and air and therefore a reduction in aging.

### 8.3.5 Temperature susceptibility and penetration index

Table 8.3 represents the calculated temperature susceptibility and penetration index of the latex bitumen binder blends and the conventional bitumen binder. The table depicts an increase in temperature susceptibility as rubber levels increase, which was within the range of 0.027–0.042. The penetration index of modified bitumen binder was within the ranges of  $-0.2$  and  $+2.4$ , which are lower than that of the unmodified bitumen binder, that is,  $+2.7$ .

**Table 8.3** Temperature susceptibility and penetration index.

Blend	Penetration value	Softening point	Temperature susceptibility	Penetration index
0	140	53	0.027034	2.756633
1	115	46	0.030085	1.979531
2	90	48	0.033887	1.134326
3	70	50	0.037785	0.383241
4	54	60	0.041811	-0.29292
5	55	59	0.041526	-0.24802
10	127	39	0.028546	2.359427

The penetration index should be within the range of  $-1$  and  $+1$  to make it suitable for pavement construction (Abir, 2015). This indicates that the blends containing 3%, 4%, and 5% natural rubber could be suitable for pavement construction. Blends containing 1%, 2%, and 10% of natural rubber did not meet the standard required stated in (BS EN 12591:2009, 2009) and therefore may not be suitable for pavement construction.

### 8.3.6 Flash point, aging, and viscosity of selected blends

The results obtained for aging, flash point, and viscosity after aging for 5% and 10% natural rubber bitumen binder blends are presented in Table 8.4. Table 8.4 shows the viscosity after aging, flash point, and change in mass after aging. It is observed that the viscosity of the 10% binary blend before aging was 120 Cst as compared to 1705 Cst, giving an aging index of 14.208.

**Table 8.4** Flash point, aging, and viscosity of selected blends.

Blends	Flash point (°C)	Viscosity before aging (Cst)	Viscosity after aging (Cst)	Change in mass after aging (%)	Aging index
5% latex	356	660	760	0.112	1.152
10% latex	377	120.5	1705	0.135	14.208

This suggests that modification of bitumen binder using 10% natural rubber latex may be highly susceptible to cracks under loading. Also a higher flash point of the blend containing 10% natural rubber suggests an increase of powdered components in the blend. A viscosity increase of 15% after aging with loss in mass of 0.112% for the blend with 5% natural rubber indicates that the blend would have high storage stability than the blend containing 10% natural rubber.

### 8.3.7 Fourier-transform infrared analysis

From Fig. 8.5 it was observed that the peak display at  $1639\text{ cm}^{-1}$  corresponding to  $\text{sp}^2\text{ C}=\text{C}$  or  $\text{C}=\text{O}$  stretching vibration, which is found on the rubber spectrum, could not be seen on the spectrum of the modified bitumen binder. The strongest peak at  $3369\text{ cm}^{-1}$ , which is a stretching vibration of N-H from ammonia, also disappeared after blending.

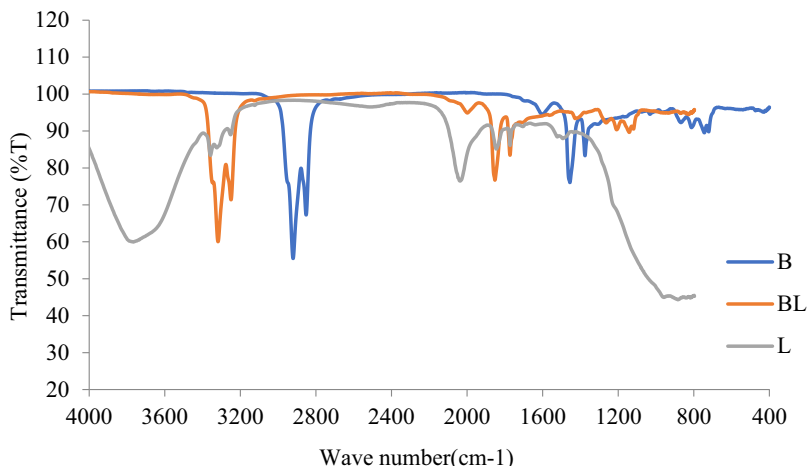


**Figure 8.5** FTIR spectroscopy analysis of conventional bitumen binder (B), latex (L), and blend (BL); B—spectrum for crude bitumen binder, L—spectrum for natural rubber latex, BL—spectrum for 5% rubber–bitumen binder blend. *FTIR*, Fourier-transform infrared.

This indicates that addition of rubber has no influence on the functional structure of the blend. However, there was a shift to a higher wavenumber of the blend as compared to the conventional bitumen binder. This resulted from inhibition of hydrogen bonding due to evaporation of water molecules during blending. There was also no change in peak intensity of the spectrum of the blend (BL) as compared to the spectrum of the crude bitumen binder (B), indicating that blending proceeded physically.

## 8.4 Conclusions

The study analyzed the change in rheological properties when natural rubber latex was added to bitumen binder at percentage concentrations of 1, 2, 3, 4, 5, and 10. The properties tested are penetration point, viscosity, softening point, specific gravity, and change in mass after aging. The FTIR spectroscopy test was used to determine change in functional groups of the blends. The results of this study show a

general decrease in rheological properties of bitumen binder upon addition of 1% rubber, which increases as the percentage rubber increases for all the properties tested except penetration point. No change in functional group was observed for the blend tested when compared with the spectrum of the unmodified bitumen binder, but there was a shift of IR spectrum to a higher wavenumber. Short-term aging test results indicate that addition of 5% natural rubber latex to bitumen binder showed significant improvement on the rheological properties tested. The calculated penetration index had shown a significant change in temperature susceptibility of the blends. The study has revealed that addition of 4%–5% natural rubber latex to bitumen binder could serve as an alternative binder for asphalt pavement.

## References

- Abdulrahman, S., Hainin, M. R., Idham, M. K., Hassan, N. A., Warid, M. N. M., Yaacob, H., Azman, M., & Puan, O. C. (2019). Physical properties of warm cup lump modified bitumen. *IOP Conference Series: Materials Science and Engineering*, 527(1), 012048. Available from <https://doi.org/10.1088/1757-899x/527/1/012048>.
- Abir, R. (2015). Waste Rubber Bitumen Modifier. *International Journal of Engineering Research and General Science*, 3(5), 109–119.
- Ali, S., Yusof, I., Hermadi, M., Alfergani, M., & Sinusi, A. A. (2013). Pavement performance with carbon black and natural rubber (latex). *International Journal of Engineering and Technology*, 2(3), 124.
- ASTM D5-97. (1997). *Standard Test Method for Penetration of Bituminous Materials*. ASTM International.
- ASTM D36/D36M-14 (2020). (2020). *Standard Test Method for Softening Point of Bitumen*. ASTM International.
- ASTM D70-97. (1997). *Standard Test Method for Specific Gravity and Density of Semi-Solid Bituminous Materials*. ASTM International.
- ASTM D1754/D1754M-20. (1754). *Standard Test Method for Effects of Heat and Air on Asphaltic Materials (Thin-Film Oven Test)*. ASTM International.
- ASTM D2170/D2170M-10. (2170). *Standard Test Method for Kinematic Viscosity of Asphalts*. ASTM International.
- ASTM D3143/D3143M-19. (3143). *Standard Test Method for Flash Point of Cutback Asphalt With Tag Open-cup Apparatus*. ASTM International.
- Blazejowski, K., Olszacki, J., & Peciakowski, H. (2014). *Bitumen Handbook*. Płock, Poland: Orlen Asphalt.
- BS EN 12591:2009. (2009). *Bitumen and Bituminous Binders. Specifications for Paving Grade Bitumens*. British Standard Institute (BSI).
- Cai, H. M., Wang, T., Zhang, J. Y., & Zhang, Y. Z. (2010). Preparation of an SBS latex-modified bitumen emulsion and performance assessment. *Petroleum Science and Technology*, 28(10), 987–996. Available from <https://doi.org/10.1080/10916460902939436>.
- Forbes, A., Haverkamp, R. G., Robertson, T., Bryant, J., & Bearsley, S. (2001). Studies of the microstructure of polymer-modified bitumen emulsions using confocal laser scanning microscopy. *Journal of Microscopy*, 204(3), 252–257. Available from <https://doi.org/10.1046/j.1365-2818.2001.00955.x>.

- Khodary, F., & Abd El-Sadek HSE-S, M. S. (2014). Mechanical properties of modified asphalt concrete mixtures using Ca(OH)<sub>2</sub> nanoparticles. *International Journal of Civil Engineering and Technology*, 5, 61.
- Krishnapriya, M. G. (2015). Performance evaluation of natural rubber modified bitumen mixes. *Journal of Civil, Environmental, Water Resources and Infrastructure Engineering*, 5(1), 1–12.
- Nuha, S. M., Asim, H. A., Mohamed, R. K., & Mahrez, A. (2011). Effect of crumb rubber concentration on the physical and rheological properties of rubberised bitumen binders. *International Journal of the Physical Sciences*, 6(4), 684–690.
- Swetha, D. V. (2014). Effect of natural rubber on the properties of bitumen and bituminous mixes. *International Journal of Civil Engineering and Technology*, 5(10), 9–21.
- UN Statistics Division. (2021). *Energy Statistics Database*. United Nations.
- Zhang, J., Wang, J., Wu, Y., Sun, W., & Wang, Y. (2009). Thermal behaviour and improved properties of SBR and SBR/Natural bitumen modified bitumens. *Iranian Polymer Journal (English Edition)*, 18(6), 465–478. Available from <http://journal.ipi.ac.ir/manuscripts/IPJ-2009-06-4416.pdf>.
- Zhu, J., Birgisson, B., & Kringos, N. (2014). Polymer modification of bitumen: Advances and challenges. *European Polymer Journal*, 54(1), 18–38. Available from <https://doi.org/10.1016/j.eurpolymj.2014.02.005>.

# Marble powder as hydraulic binder substitution

9

S. Kenai<sup>1</sup>, B. Benabed<sup>2</sup> and H. Soualhi<sup>2</sup>

<sup>1</sup>Civil Engineering Department, University Blida 1, Blida, Algeria, <sup>2</sup>Civil Engineering Department, University of Laghouat, Laghouat, Algeria

## 9.1 Introduction

Waste recycling is an important part of sustainable development because reusing waste materials can reduce environmental impact and save natural resources, energy, and total cost. Because of its large consumption capacity, the construction industry is one of the best targets for solid waste reutilization. Among the solid waste materials, marble waste generated during the cutting process should not be overlooked due to its large quantity and the serious environmental problems encountered (Rana et al., 2015; Li et al., 2019). Marble powder (MP) has a negative impact on people's social and industrial activities. When it dries, it becomes airborne and contributes to severe air pollution. It causes occupational health issues and has an impact on machines and instruments installed in industrial zones. It also reduces land productivity by reducing porosity, water absorption, and percolation and affects water quality during the rainy season, reducing storage capacity and harming aquatic life.

Marble is a metamorphic stone formed by the transformation of limestone, which is composed solely of calcite ( $\text{CaCO}_3$ ). It is distinguished by its beauty, great variety, and smooth and shiny appearance, making it one of the most noble rocks that can exist. According to previous research, 30%–40% of processed marble in factories corresponds to production waste (Tugrul Tunc, 2019). Utilizing the aforementioned potential in the industry yields significant returns in terms of economic and environmental performance (Uygunoglu et al., 2014). Reutilization of such a large quantity of marble waste is not an easy task. Usually, marble waste is reused as a cement replacement or aggregate replacement in the production of concrete. When used as a cement replacement, MP is added to replace a portion of the cement or cementitious materials, and this addition of MP as a cement replacement has been found to have significant effects on the fresh, hardened, and durability properties of concrete.

## 9.2 Advantages of marble powder

MP can be used as a filler in concrete and paving materials and helps to reduce total void content in concrete. It can be used as an admixture in concrete so that mechanical strength and durability of concrete can be improved. The use of MP for the

production of other products can reduce the environmental pollution. MP could be mixed with concrete, cement, or synthetic resins to make building stones. It can also be used as a paint filler or for the manufacture of white cement.

### 9.3 Applications of marble powder

Marble production involves several stages, including extraction, sawing, shaping, and polishing, all of which generate waste, including MP. The MP can be used in many applications such as coating, decorative plaster, paint, ceramic industry, glass industry, and manufacture of paper and plastic materials.

## 9.4 Properties of marble powder

### 9.4.1 Particle size

One of the most significant factors for the purpose of use of MP is particle size. The particle size of MP varies greatly depending on the marble source and the MP's intended use in concrete or mortar. MP can be used to substitute fine aggregate or a portion of the cement. Typical particle sizes of MP and cement are given in Fig. 9.1. Cement and MP have more or less the same granular distribution (Dada et al., 2021).

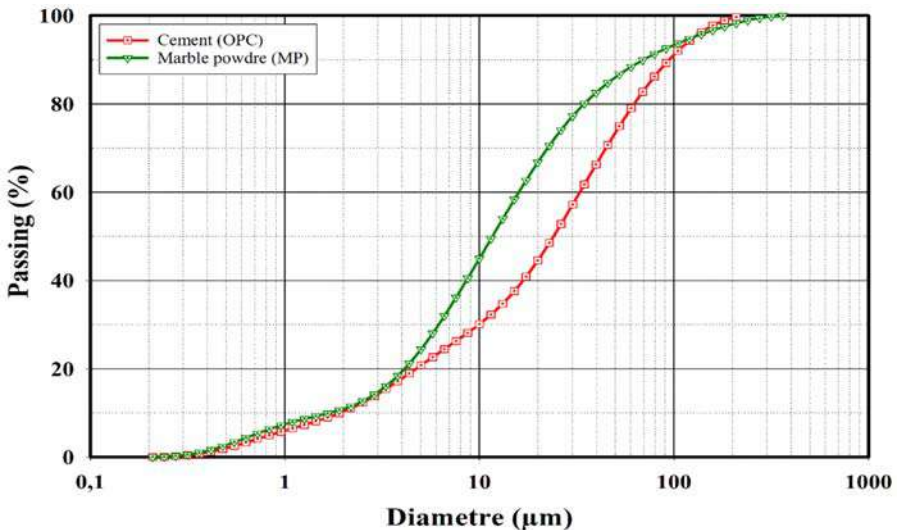


**Figure 9.1** Particle size distributions of marble powder and cement (Dada et al., 2021).

The morphology, particle size, and shape of materials studied using scanning electron microscopy (SEM) are given in Fig. 9.2. It can be seen that the MP has granular uniformity (Dada et al., 2021).

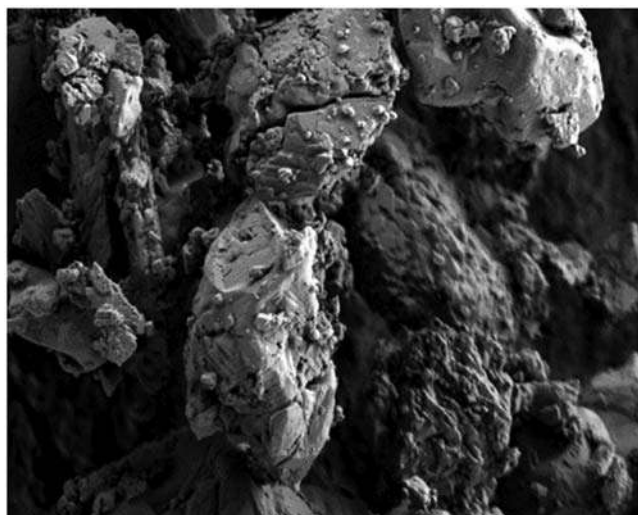


**Figure 9.2** SEM analysis of marble powder (Dada et al., 2021). SEM, Scanning electron microscopy.

#### 9.4.2 Physical properties

Specific gravity and fineness are the most widely measured physical characteristics of MP. The physical parameters of the marble wastes studied in the literature are summarized in Table 9.1.

The MP specific gravity and fineness range from 2.19 to 2.87 and from 215 to 928 m<sup>2</sup>/kg, respectively (Uysal & Yilmaz, 2011; Ergün, 2011; Gesoğlu et al., 2012; Belaidi et al., 2012; Vijayalakshmi et al., 2013; Aliabdo et al., 2014; Rana et al., 2015; Rodrigues et al., 2015; Tennich et al., 2015; Boukhelkhal et al., 2016; Choudhary et al., 2016; Alyamac et al., 2017; Djebri et al., 2017; Toubal Seghir et al., 2018; Singh et al., 2019; Alyousef et al., 2019; Kumar, Singla, et al., 2020; Benjeddou et al., 2020; Safiddine et al., 2021; Dada et al., 2021).

**Table 9.1** Physical properties of marble powder.

References	Specific gravity	Fineness (m <sup>2</sup> /kg)	References	Specific gravity	Fineness (m <sup>2</sup> /kg)
Ergün (2011)	2.68	596	Boukhelkhal et al. (2016)	2.7	360
Uysal and Yilmaz (2011)	2.71	888	Djebri et al. (2017)	2.68	550
Gesoğlu et al. (2012)	2.71	519	Alyamac et al. (2017)	2.71	392
Belaidi et al. (2012)	2.7	350	Toubal Seghir et al. (2018)	2.74	387

(Continued)



**Table 9.1** (Continued)

References	Specific gravity	Fineness (m <sup>2</sup> /kg)	References	Specific gravity	Fineness (m <sup>2</sup> /kg)
Vijayalakshmi et al. (2013)	2.38	351	Singh et al. (2019)	2.67	350
Aliabdo et al. (2014)	2.5	399	Alyousef et al. (2019)	2.69	946
Tennich et al. (2015)	2.42	653	Kumar (2020)	3.73	381
Rodrigues et al. (2015)	2.71	215	Benjeddou et al. (2020)	2.7	386–928
Rana et al. (2015)	2.87	736	Dada et al. (2021)	2.69	240
Choudhary et al. (2016)	2.87	238	Safiddine et al. (2021)	2190	393

### 9.4.3 Chemical properties

The chemical composition of the MP differs according to the origin and the deposit of the bedrock. X-ray diffraction is commonly used to perform chemical analysis and quantitative mineralogical characterizations of the MP.

The chemical compositions of different MPs used in many studies are reported in Table 9.2. It can be noticed that the highest present element in the MP is calcium oxide (CaO), which varies between 28.63% and 83.22% (Uysal & Yilmaz, 2011; Ergün, 2011; Gesoğlu et al., 2012; Belaidi et al., 2012; Aliabdo et al., 2014; Rana et al., 2015; Rodrigues et al., 2015; Tennich et al., 2015; Boukhelkhal et al., 2016; Choudhary et al., 2016; Alyamac et al., 2017; Djebri et al., 2017; Toubal Seghir et al., 2018; Singh et al., 2019; Alyousef et al., 2019; Kumar, et al., 2020; Benjeddou et al., 2020; Dada et al., 2021).

**Table 9.2** Chemical properties of marble powder.

References	SiO <sub>2</sub>	CaO	MgO	Al <sub>2</sub> O <sub>3</sub>	Fe <sub>2</sub> O <sub>3</sub>	SO <sub>3</sub>	K <sub>2</sub> O	TiO <sub>2</sub>	Na <sub>2</sub> O	LOI
Ergün (2011)	0.18	51.70	0.4	0.67	0.44	–	0.21	–	–	46.04
Uysal and Yilmaz (2011)	0.70	55.49	0.23	0.29	0.12	–	1.80	–	2.44	42.83
Gesoğlu et al. (2012)	1.29	52.45	0.54	0.39	0.78	–	0.11	–	–	43.90
Belaidi et al. (2012)	1.00	52.6	2.1	0.2	0.2	0.07	0.04	0.01	0.06	43.63
Aliabdo et al. (2014)	1.12	83.22	0.52	0.73	0.05	0.56	0.09	–	1.12	2.50
Tennich et al. (2015)	1.69	49.07	4.47	1.04	0.21	–	–	–	–	43.46
Rodrigues et al. (2015)	1.39	54.20	0.64	0.32	0.14	–	–	–	0.04	42.60

(Continued)

**Table 9.2** (Continued)

References	SiO <sub>2</sub>	CaO	MgO	Al <sub>2</sub> O <sub>3</sub>	Fe <sub>2</sub> O <sub>3</sub>	SO <sub>3</sub>	K <sub>2</sub> O	TiO <sub>2</sub>	Na <sub>2</sub> O	LOI
Rana et al. (2015)	44.1	42.13	3.72	2.2	2.98	—	—	—	0.08	3.50
Choudhary et al. (2016)	0.61	30.41	21.67	0.28	0.58	—	0.03	—	0.08	44.26
Boukhelkhal et al. (2016)	0.42	56.01	0.12	0.13	0.06	0.01	0.01	0.01	0.43	42.78
Djebri et al. (2017)	0.48	54.91	0.72	0.10	0.12	0.46	0.05	—	0.08	43.55
Alyamac et al. (2017)	28.35	40.45	16.25	0.17	9.7	0.02	0.01	—	0.05	4.84
Toubal Seghir et al. (2018)	0.05	56.94	0.92	0.05	0.02	0.32	0.01	—	—	41.63
Singh et al. (2019)	3.86	28.63	16.9	4.62	0.78	—	—	—	—	43.30
Alyousef et al. (2019)	3.00	52.28	0.50	0.14	0.39	—	—	—	—	42.60
Kumar et al. (2020)	5.96	38.56	15.27	0.53	0.82	0.07	0.03	—	0.05	—
Benjeddou et al. (2020)	3.00	52.28	0.50	0.14	0.39	—	—	—	—	42.60
Dada et al. (2021)	0.42	56.01	0.12	0.13	0.06	0.01	0.01	0.01	0.06	43.43

## 9.5 Effect of marble powder on fresh properties of cement/mortar/concrete

### 9.5.1 Workability

Workability can be defined as the suitability of the material or how easy it is to set up. It can be determined by slump test, spreading test, flow time with an LCPC workabilimeter (mortar), and V-funnel flow time tests (mortar and concrete).

Dada et al. (2021) investigated the effect of MP substitution on the fresh properties of concrete equivalent mortar. They noted that introducing 5%–30% MP increases slump and decreases flow time. On the other hand the substitution of 40% of cement by PM has a reverse effect (Cf, Fig. 9.3). The MP has a filling power as well as a diluting effect, making the cement grains more mobile. Furthermore, its inert action releases a portion of the mixing water at an early stage of hydration, lubricating the grains and improving the workability of the combination (Belaidi et al., 2012; Dada et al., 2021).

Boukhelkhal et al. (2016) studied the effect of replacing cement with MP in self-compacting concrete fresh properties, where they replaced the cement with 5%, 10%, 15%, and 20% of MP. They found that all the mixtures had good filling ability, with slump flow values ranging from 70 to 74 cm, and when cement is replaced with MP the slump flow values increases and the V-funnel flow time decreases (Boukhelkhal et al., 2016).

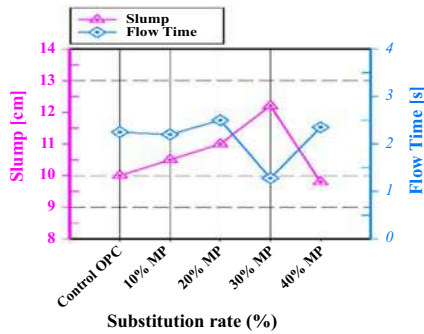


**Figure 9.3** Effect of MP on workability of mortar (Dada et al., 2021).

Kirgiz (2016) used MP as a replacement for fine aggregates in concrete, while Rashwan et al. (2020) used it as a replacement for cement in concrete. The results are summarized in Table 9.3. They found that increasing the percentage of MP decreases concrete slump when MP is used as fine aggregate replacement (Kirgiz, 2016). On the other hand, when it is used as cement replacement, it has a reversed effect (Rashwan et al., 2020).

**Table 9.3** Effect of marble powder in slump of concrete.

References	MP (%)	Slump (mm)	Applications
Kirgiz (2016)	0	65	MP replacement as fine aggregate in concrete
	10	60	
	15	40	
	20	30	
Rashwan et al. (2020)	0	175	MP replacement as cement in concrete
	10	180	
	20	185	
	30	230	
	40	245	

MP, Marble powder.

Most other researchers have reported that the use of MP increases workability (Belaidi et al., 2012; Bostanci, 2020; Chahour & Safi, 2020; Prokopski et al., 2020; Safiddine et al., 2021). On the other hand a reduction in slump was also obtained by other authors (Vijayalakshmi et al., 2013; Rana et al., 2015; Talah et al., 2015; Vardhan et al., 2019a).

### 9.5.2 Setting time

The use of MP delays the setting time. Initial and final setting times increase with the increase in MP amount (Singh et al., 2017a; Ashish, 2019). On the other hand the normal consistency decreased with the increase of MP.

Rashwan et al. observed an acceleration in the initial and final setting times at a lower amount of MP up to 20%. The use of MP up to 40% delayed the initial setting times and accelerated the final setting times. On the other hand the normal consistency increased with increasing MP (Rashwan et al., 2020). Standard consistency and initial and final setting times of the investigated studies are reported in Table 9.4.

**Table 9.4** Consistency and setting time.

References	MP (%)	Consistency (%)	Initial setting time (s)	Final setting time (s)
Singh et al. (2017b)	0	32.5	107	224
	10	31.5	120	235
	15	30.25	125	249
	20	30	132	270
	25	29.75	140	285
Ashish (2019)	0	28.5	120	240
	10	28	164	268
	15	28	198	297
Rashwan et al. (2020)	0	24.5	175	260
	10	25.5	160	220
	20	26.5	165	230
	30	27.5	185	250
	40	28.5	185	250

MP, Marble powder.

### 9.5.3 Rheological behavior

The rheological parameters (plastic viscosity and the yield stress) are very important to control the placement of mortar and concrete and also to ensure the quality of the filling of the formwork. Many researchers found that the inclusion of MP as a substitution of cement decreases both the yield stress and the plastic viscosity of mortar and concrete (cf. Fig. 9.4). This is due to the MP particles being less angular and coarse as well as the lesser requirement for superplasticizers and also the increase in the volume of paste caused by the difference in the density of the cement and that of the MP (Belaidi et al., 2012, 2016; Boukhelkhal et al., 2016; Dada et al., 2021; Safiddine et al., 2021).

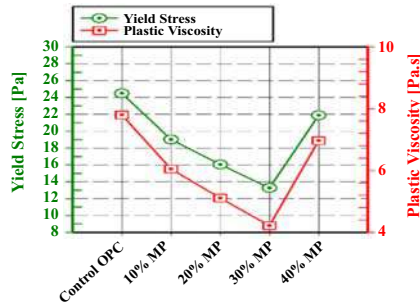


**Figure 9.4** Effect of marble powder on the rheological behavior of mortar. *Source:* Dada, H., Belaidi, A. S. E., Soualhi, H. et al. (2021) Influence of temperature on the rheological behaviour of eco-mortar with binary and ternary cementitious blends of natural pozzolana and marble powder. *Powder Technology*, 384, 223–235. <https://doi.org/10.1016/j.powtec.2021.02.019>.

### 9.5.4 Hydration heat

The hydration heat of concrete is primarily related to the amounts of  $C_3S$ ,  $C_3A$ , and  $C_4AF$  in Portland cement (PC). The presence of these components in cement increases hydration heat, but the blended pozzolanic additives delay cement hydration. Prošek et al. (2020) investigated the hydration of PC pastes with MP ranging from 5% to 50% as a replacement for cement. Hydration heat flow was measured using an eight-chamber TAM Air isothermal calorimeter; each mixture occupied two chambers, and hydration heat flux was measured for 7 days at a constant temperature of 20°C. Each container was inserted into a chamber containing a sample weighing between 25 and 38 g after compaction. The cumulative hydration heat was calculated by integrating the heat flow over the measurement time. Calorimetry results revealed that the more MP in a mixture, the more cumulative heat was released during the first 7 days of hardening. Péra et al. (1999) found similar results when studying the effects of  $CaCO_3$  on  $C_3S$  hydration. In this study, PC with a high  $C_3S$  content (74.6 wt.%) was used with MP, which is mostly  $CaCO_3$  (95 wt.%). The presence of MP influenced not only cumulative heat but also heat flow development. The absolute heat/heat flux values plotted in Fig. 9.5 show that the presence of MP inhibits rapid hydration of  $C_3S$ . Heat flux, on the other hand, was slightly accelerated by the presence of MP for the 20–40 hours period.

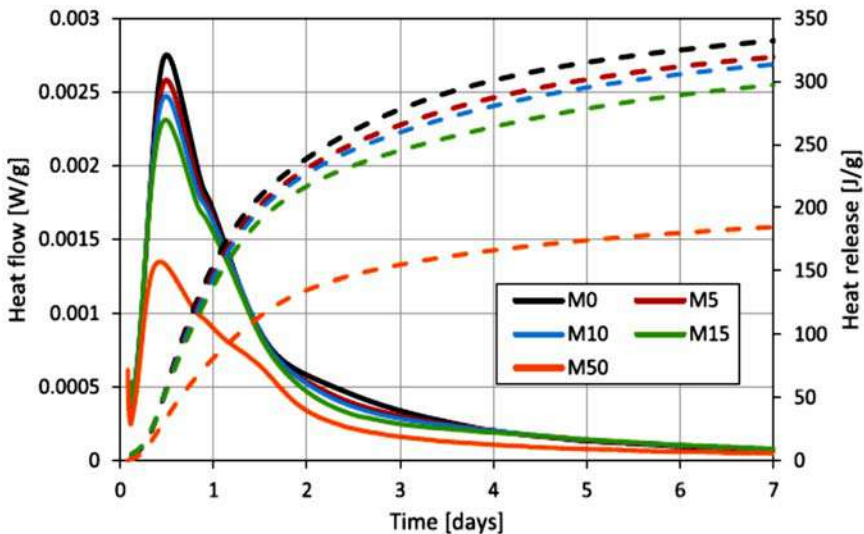


**Figure 9.5** Hydration heat flow (solid lines) and cumulative heat (dashed lines) (Prošek et al., 2020).

## 9.6 Effect of marble powder on the hardened properties

### 9.6.1 Strength activity index of mixtures incorporating marble powder

Abbas et al. (2020) determined the strength activity index (SAI) for mixtures incorporating various proportions of MP ranging from 0% to 50% at ages of 7, 14, 28, and 56 days. ASTM C311 (ASTM 2018) (*Standard Test Methods for Sampling and Testing Fly Ash or Natural Pozzolans for Use in Portland-Cement Concrete*) was used to calculate SAI values. SAI results for MP mixtures incorporating various proportions of MP. At 28 days, mixtures containing 5%, 10%, and 15% MP had SAI values of 91%, 83%, and 77%, respectively. However, for mixtures with higher MP dosages (> 20% by cement weight) the SAI was less than 75%. SAI was found to be higher at later ages for tested mixtures containing MP. For example the mixture incorporating 5% of MP achieved SAI of 91% and 94% at 28 and 56 days, respectively.

### 9.6.2 Thermal analysis of mixtures incorporating marble powder

Abbas et al. (2020) used thermogravimetric analysis (TGA) and differential thermal analysis (DTA) to investigate the hydration kinetics in mortar mixtures containing MP. Changes in mineralogical composition and mass loss were investigated for mixtures containing 15% MP and control mixtures without MP. Small fragments were extracted from specimens and ground into powder. A crucible containing approximately 10 mg of powder samples was placed in a furnace. Thermal analysis was carried out at a rate of 20°C

per minute. The testing was terminated at 1200°C. For the control specimen the DTA curve exhibited an endothermic peak at approximately 79°C. This is most likely due to the elimination of absorbed water. Another peak was observed at 575°C due to decomposition of calcium hydroxide (CaOH<sub>2</sub>). An endothermic peak was also observed at around 835°C due to decomposition of calcium carbonate (CaCO<sub>3</sub>). (Abbas et al., 2017; Almeida & Sichiari, 2006; Moropoulou et al., 2004).

According to the TGA graph the mass loss in the control specimen without WMP was approximately 30% and most of it occurred between 600°C and 850°C, primarily related to the decomposition of CaOH<sub>2</sub> and CaCO<sub>3</sub> (Moropoulou et al., 2004).

The DTA curve for the mixture containing 15% MP presented an endothermic peak at approximately 70°C due to the removal of absorbed water. At 330°C an exothermic peak occurred, which is related to CSH (Almeida & Sichiari, 2006). An endothermic peak was observed at approximately 560°C due to CaOH<sub>2</sub> decomposition. Another endothermic peak was observed at 847°C, primarily due to calcium carbonate decomposition. The TGA curve up to 1100°C showed a mass loss of approximately 33% for the mixture containing 15% MP. A significant portion of this mass loss occurred between 650°C and 900°C.

### 9.6.3 Compressive strength

Compressive strength is the most required mechanical property in concrete and mortar. Compressive strength decreases with increasing MP as a replacement for cement in all ages of 3, 7, 28, and 65 days (Toubal Seghir et al., 2018). Table 9.5 summarises the results of Rodrigues et al. (2015), Yamanel et al. (2019), and Rashwan et al. (2020).

The majority of the previous researchers have observed a decrease of compressive strength with substitution of MP as cement. This reduction is attributed to the phenomenon of dilution of pozzolanic reactions (Heikal & Morsy, 2000; Ergün, 2011; Belaidi et al., 2012, 2016; Aliabdo et al., 2014; Rana et al., 2015; Yamanel, 2015; Mashaly et al., 2016; Yamanel et al., 2019; Belouadah et al., 2021; Dada et al., 2021).

### 9.6.4 Flexural tensile strength

Ergün (2011) found a loss of flexural tensile strength of concrete which becomes greater with higher replacement rates (Ergün, 2011; Rodrigues et al., 2015). The majority of studies have shown that the flexural strength decreases with the increase in the rate of substitution of cement by MP (Yamanel, 2015; Mashaly et al., 2016; Yamanel et al., 2019; Rashwan et al., 2020). Table 9.5 gives the results of the effect of MP on flexural tensile strength of concrete from Rodrigues et al. (2015), Yamanel et al. (2019), and Rashwan et al. (2020).

### 9.6.5 Splitting tensile strength

Splitting tensile strength of concrete decreases with increasing rate of replacement of cement by MP. Rodrigues et al. (2015) obtained maximum reduction of 30% in concrete splitting tensile strength. Aliabdo et al. (2014) found that for higher

substitution ratios of MP, they obtained lower splitting tensile strength values than those of the reference mix without MP. Ergün (2011) obtained results comparable to those of other researchers, with lower values at higher replacement rates. Table 9.5 gives the results of mechanical properties from Rodrigues et al. (2015) and Rashwan et al. (2020).

**Table 9.5** Effect of marble powder on mechanical properties of concrete.

References	MP (%)	Compressive strength at 28 days (MPa)	Flexural strength at 28 days (MPa)	Tensile splitting strength at 28 days (MPa)
Rodrigues et al. (2015)	0	47.1	—	3.1
	10	43.7	—	2.5
	20	43.2	—	2.4
	30	34.4	—	2.3
Yamanel et al. (2019)	0	52.7	8.6	—
	5	52.1	8.6	—
	10	48.7	8.0	—
	15	46.3	7.7	—
	20	42.8	7.2	—
Rashwan et al. (2020)	0	55.41	5.70	5.3
	10	52.56	5.60	4.8
	20	47.76	5.30	4.5
	30	37.46	4.12	3.5
	40	35.70	4.00	3.1

MP, Marble powder.

### 9.6.6 Modulus of elasticity

Rodrigues et al. (2015) studied the influence of the rate of substitution of cement by MP in concrete on the modulus of elasticity with percentages ranging from 5% to 20% with steps of 5% (cf. Fig. 9.6). Their results show that the modulus of elasticity decreases as the replacement rate increases, with a maximum loss of 10.3% with a rate of 20% of MP. However, the addition of superplasticizers increased the values of the modulus of elasticity. This can be explained by the increase in the compactness of the granular mixture (Rodrigues et al., 2015). Other researchers have obtained comparable results for static and dynamic moduli of elasticity (Uysal & Yilmaz, 2011; Tennich et al., 2015).



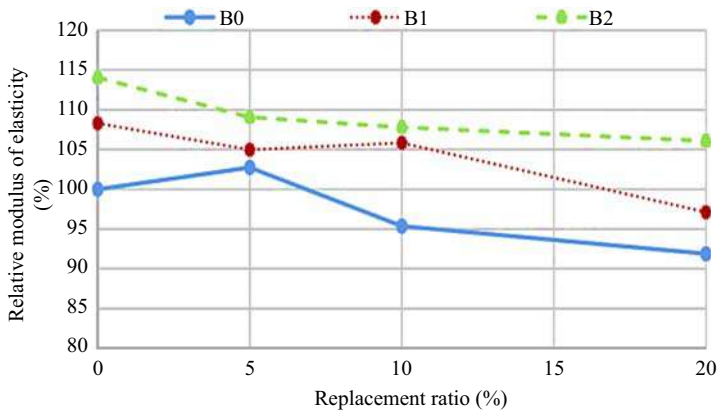


**Figure 9.6** Effect of marble powder on relative modulus of elasticity of concrete (Rodrigues et al., 2015).

## 9.7 Microstructure

SEM images in Fig. 9.7 illustrate the microstructure characteristics of some MP-modified cement pastes. It is shown that MP-blended cement specimens are denser and less porous than control specimens. The microstructure of pastes is composed of amorphous particles of calcium silicate hydrate (CSH) and calcium hydroxide (CH) crystals that appear in massive layers. Ettringite (E) needles are located in pores; then the paste is totally hydrated, and all voids are completely filled (Aliabdo et al., 2014; Alyousef et al., 2018).

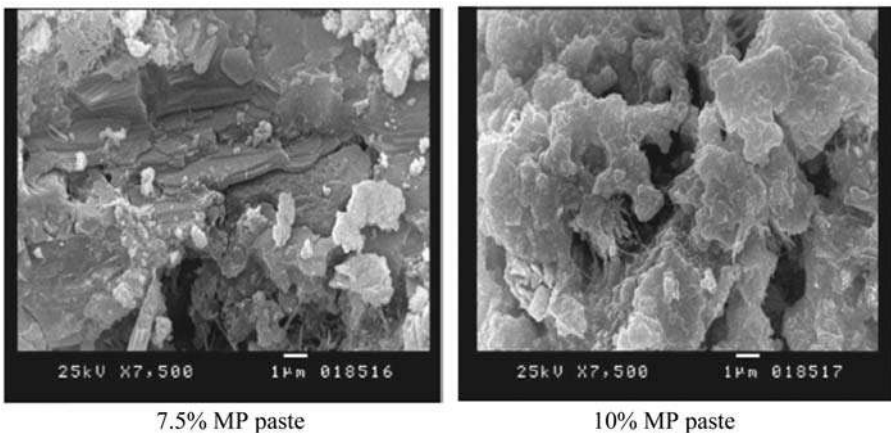


**Figure 9.7** SEM analysis for paste samples containing marble powder (Aliabdo et al., 2014). SEM, Scanning electron microscopy.

SEM analysis of specimens with and without MP performed by (Kumar, et al., 2020) indicated that the morphology is distinct in terms of pore structure (cf. Fig. 9.8). The matrix of control mix is heterogeneous with the presence of cracks and large pores (Demirel, 2010). In addition, there are large crystals of calcium hydroxide (CH) distributed irregularly in the matrix. In comparison, with substitution of cement by 5.0% of MP the matrix seems to be comparatively more homogeneous with a lesser number of pores and negligible cracks. This is due to the filling effect of MP particles in the concrete (Rodrigues et al., 2015; Wu et al., 2020). Thus the porosity of hardened concrete is minimized due to the presence of MP. In addition, smaller and well-distributed crystals of calcium hydroxide are observed in the matrix of specimens containing MP. This is due to the occupation of pores by MP particles leaving almost no space for growth of calcium hydroxide crystals (Kırgız, 2016). Other researchers also reported densification of matrixes by introducing MP particles (Rana et al., 2015). The presence of ettringite needles in the pores, which minimize pores' size and cracks, has been reported (Aliabdo et al., 2014). MP particles are also supposed to control the reaction between alkali and silica in the matrix and hence minimize the expansion (Munir et al., 2017). Thus optimal use of MP leads to strength enhancement with improved microstructures.

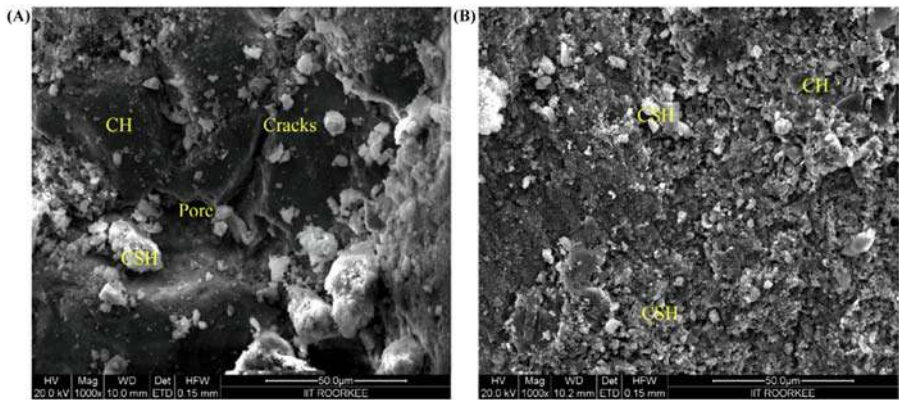


**Figure 9.8** Micrographs of (A) control mix and (B) specimen in the presence of 5.0% MP (Kumar, et al., 2020). *MP*, Marble powder.

SEM analysis performed by Vardhan et al. (2015) as shown in Fig. 9.9 revealed that hardened paste of control mortar is fully matured and voids are filled up. In cement mortar containing 10% MP, equant grain type morphologies of CSH gel and needles of ettringite are observed. However, SEM images of cement paste containing 30%, 40%, and 50% MP as a cement replacement reveal the presence of a large number of voids. SEM images of mortar containing 40% and 50% MP show long and slender needles of ettringite and fibrous crystals of CSH. CSH fibrous crystals started to fill the voids. This type of morphology of CSH gel is formed at the early age of cement paste hydration. In other words the presence of fibrous crystals of CSH gel in SEM images of cement paste containing 40% and 50% MP

as replacement of cement indicates delay in hydration process. SEM images of cement mortar containing 20%, 40%, and 50% MP show the presence of crystals of calcium hydroxide (CH). The results of compressive strength test of cement mortar mixtures also confirm the formation of less dense microstructures when MP is used in cement mortar. Formation of an imprecise CSH gel and a higher percentage of voids in mortar mixtures might have affected their compressive strength (Rana et al., 2015).

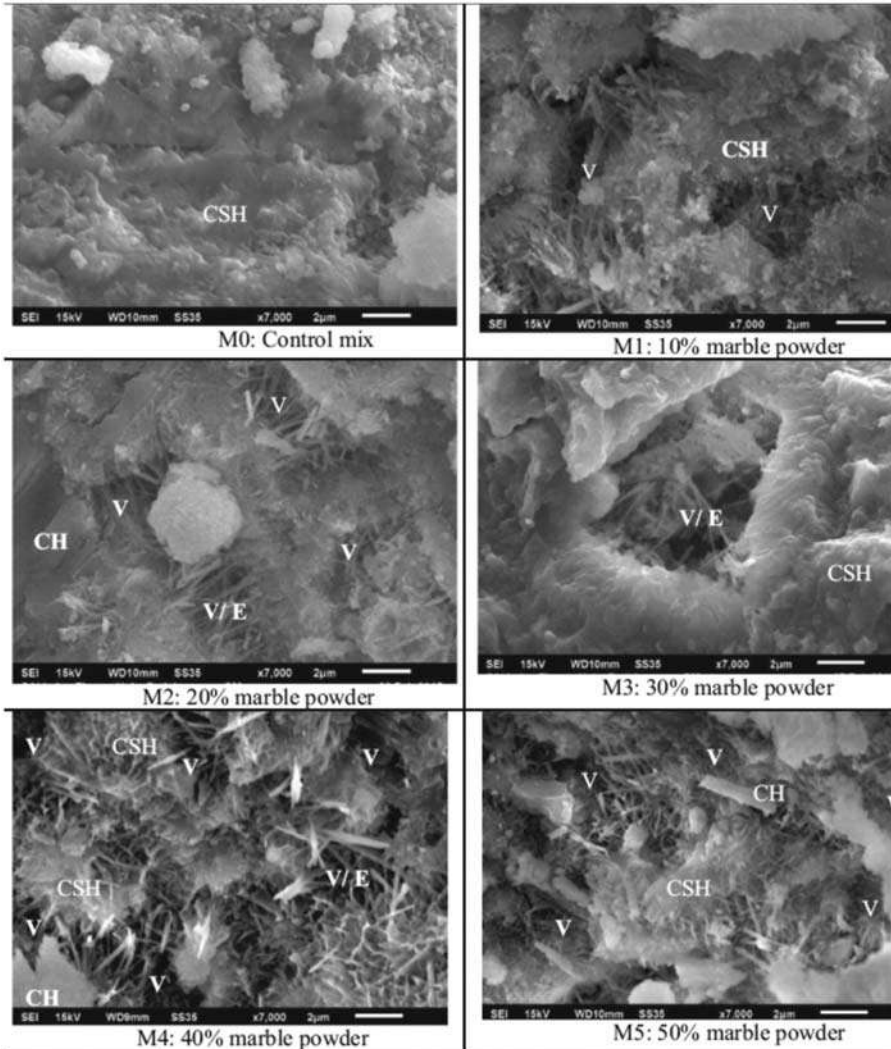


**Figure 9.9** SEM morphology of mortar containing MP as replacement of cement (Vardhan et al., 2015). CH, Calcium hydroxide; CSH, calcium silicate hydrate; E, ettringites; MP, marble powder; SEM, scanning electron microscopy; V, voids.

## 9.8 Durability properties of concrete made with marble powder

Durability refers to the ability of concrete to withstand weathering, chemical attack, and abrasion without losing its engineering properties. The lower the volume of pores in concrete, the more durable it is because it reduces the intrusion of air, water, or chemicals into the aggregate bonding.

### 9.8.1 Permeability

Permeability is essential for the durability of concrete in harsh environments such as frost damage, acid attack, sulfate attack, corrosion, and alkali–aggregate reaction. Concrete permeability is critical in determining the rates of mass transport relevant to destructive chemical action. Concrete permeability is primarily determined by the size, distribution, and continuity of the pores in the hydrated paste of the concrete. The degree of hydration and water–cement ratio are important factors that influence the pore structure of the paste. Because MP is finer, it affects the capillary pores of the concrete matrix by obstructing voids and gaps. The reduced permeability of these concrete mixes is due to the reduction in pore continuum and volume.

According to the results of [Khaliq et al., 2016](#), increasing the proportion of MP from 0% to 10% reduces the permeability of concrete; this is because MP acts as a filler, filling up all the gaps inside the concrete during the hardening process. However, beyond the 10% limit, all of the cavities are filled with MP, and this latter no longer acts as a filler but rather as an overburdening additive. When the 10% limit is exceeded and 15% is reached the water flow through the concrete mass increases dramatically. This is due to the reduction of cement amount that reduces the CHS (calcium hydro silicate) component, which is responsible for reducing gel pores. Furthermore, beyond the 15% limit the permeability was negatively affected, and increasing the percentage further would not affect the permeability but would have an effect on the compressive and split tensile strengths and consistency of the concrete ([Talah et al., 2015](#)).

[Singh et al. \(2019\)](#) reported that mixes containing 10%–15% MP replacement showed better permeability results than the control mix, but further addition of MP resulted in increasing permeability. [Rana et al. \(2015\)](#) also concluded that the addition of MP up to 15% enhanced resistance to water penetration and reduced the penetration depth considerably. The volume of permeable voids was found to reduce due to refinement in pore filling trend of concrete. However, beyond 15% of MP replacement an increase in volume of permeable voids was observed. A further increase in MP increased the depth of penetration due to reduction in porosity and an increase of fines in blended mixes ([Demirel, 2010](#); [Arel, 2016](#)). According to the rating given by [Cather et al. \(1984\)](#) the concrete mixtures with MP are rated under the “good” category. The improvement in resistance to air permeability is attributed to the filler effect of MP as it reduces the permeable pores in concrete. The reason for this could be improper bonding of aggregates due to a lesser amount of cement available for the hydration process ([Singh et al., 2017b](#)).

Binici et al. (2007) and Binici and Aksogan (2018) also concluded that the addition of MP up to 15% reduces the water penetration depth significantly. The permeability of concrete depends upon the pore size, pore distribution, and their interconnectivity. MP being finer than cement might have filled the capillary pores of concrete matrix and blocked their connectivity. The reduction in pore continuity and volume might have resulted in reduced permeability of these concrete mixes. Comparable results were found by Singh et al. (2017b). However, concrete containing 20% and 25% MP displayed poor resistance to permeation. At high replacement levels the filler effect could not compensate for poor microstructures of concrete due to reduced cement content.

### 9.8.2 Water absorption

The performance of concrete exposed to harsh environments is determined by how permeable the pore system is. Surface absorption in concrete is determined by a number of factors, including mix proportions, the presence of admixtures, voids, the degree of hydration, the type of placement, and the chemical properties of the cementitious material. Water is the main cause of the degradation of building materials. It penetrates into porous media, transports harmful substances, and freezes inside. When a homogeneous porous material has a constant hydraulic potential at its wet surface, liquid can reach significant heights due to the capillary absorption (Hanžič & Ilić, 2003). It has been shown that MP as substitution to cement reduces concrete water absorption values at lower W/C ratios (Sardinha et al., 2016; Khodabakhshian et al., 2018; Li et al., 2018; Selim et al., 2020; Zhang et al., 2020).

Li et al. (2018) studied the effectiveness of using MP as a paste replacement in reducing water absorption. As a result, adding MP as a paste replacement always reduced the water absorption rates at any given W/C ratio. For example, at a W/C ratio of 0.55, increasing the MP volume from 0% to 20% reduced water absorption rates by 72.7% and 78.7%, respectively, whereas at a W/C ratio of 0.40, increasing the MP volume from 0% to 20% reduced water absorption rates by 45.5% and 32.4%, respectively. As a result, using MP as a paste replacement has been shown to be an effective way to improve mortars' water resistance.

Boukhelkhal et al. (2017) found that that the increase in the amount of substituted MP leads to an increase in the water absorption. The incorporation of MP at substitution levels of 5%, 10%, 15%, and 20% increases the water absorption rate by 9.26%, 9.47%, 9.9%, and 10.9%, respectively. It was noted that all tested self-compacting concrete have low water absorption (less than 10%), except for mixes that include 20% of MP. On the other hand the obtained water absorption values of MP mixtures are superior to those found in mortar mixtures incorporating fly ash, silica fume, and metakaolin (1.8%–4.2%). This may be attributed to the use of inert materials that have a low filling effect because both cement and MP have approximately similar finenesses (Tasdemir, 2003; Siddique, 2013).

Binici et al. (2007) reported that with 15% MP the concrete was considerably more resistant to water ingress than concrete with limestone powder. Gameiro et al. (2014) and Topçu et al. (2009) also showed that the incorporation of MP is beneficial by reducing concrete water absorption.

### 9.8.3 Porosity

One of the most important parameters for both strength and durability in concrete is porosity. Less voids in concrete provide a more compact structure as well as the desired strength and durability values. The use of mineral or chemical additives, as well as low w/c ratios, is among the most important factors in reducing porosity in concrete.

Aliabdo et al. (2014) studied the effect of MP as cement replacement on the porosity of concrete. The replacement ratios, which have been studied, were 0%, 5%, 7.5%, 10%, and 15% by weight (Fig. 9.10). It can be seen that concrete porosity improves with the increase of MP and is comparable to control specimens. This improvement in porosity could be explained by the filler effect of marble dust (Aliabdo et al., 2014; Rana et al., 2015; Ulubeyli et al., 2016; Aydin & Arel, 2019b; Atyeh & Aydin, 2020; Prošek et al., 2020; Varadharajan, 2020).

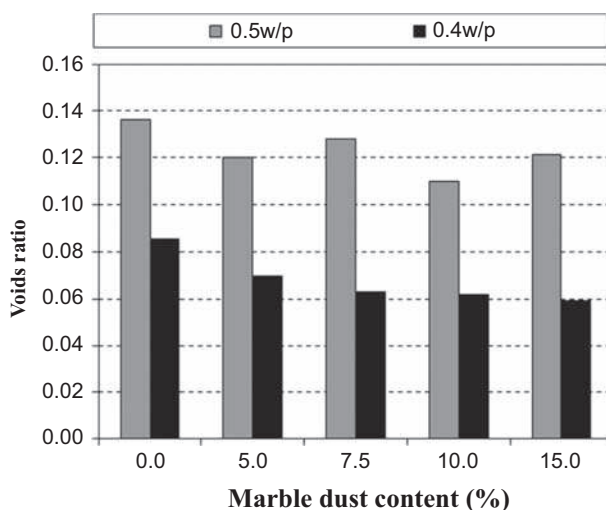


**Figure 9.10** Porosity values of concrete made with MP as a partial replacement of cement (Aliabdo et al., 2014). MP, Marble powder.

According to Prošek et al. (2020), lowering porosity by adding MP is vital for cementitious composites to achieve high compressive strength. This effect can be achieved through a microfilling effect with low amounts of added MP (5–15 wt.%). Total porosity increased by 5% for the 50 wt.% addition due to higher pore volume peaks. These findings are consistent with those of other studies (Aliabdo et al., 2014; Hebhoub et al., 2011; Uygunoglu et al., 2012). Several authors have

studied the impact of coarser fractions and concluded that regardless of the amount incorporated, they are incapable of reducing the porosity of cementitious matrices, supporting the assumption of microfilling effects (Rana et al., 2015; Talah et al., 2015; Seghir et al., 2019).

### 9.8.4 Shrinkage

MP is an inert material, and shrinkage is known to be a function of cement hydration. When shrinkage is restricted, it causes internal tensile stress, which results in shrinkage cracks; thus the drying shrinkage reduction property of MP is found to be significant and advantageous. The drying shrinkage is affected by various factors affecting the pore structure in concrete (w/c ratio, cement amount, mineral additions, etc.). Because of the improved pore structure of the concrete, there will be no evaporation of water from the capillary pores, resulting in less drying shrinkage and no deterioration of concrete. Low w/c ratios and the substitution of mineral additives for cement at certain ratios reduce drying shrinkage. Yamanel et al. (2019) studied the effect of MP as cement replacement on the shrinkage of mortars. The results given in Fig. 9.11 show that the shrinkage of all mortars increased with increasing time because shrinkage is a function of cement hydration. However, replacing MP with cement resulted in a partial reduction in shrinkage values when compared to the control cement mortar. This reduction in shrinkage increases with the increase of the level of substitution of cement with MP. This is due to a decrease in cement content caused by the partial replacement of MP with cement. Vardhan et al. (2019b), Li et al. (2018), Valdez et al. (2011), and Hlubocký and Prošek (2017) found similar results of reduced drying shrinkage for conventional and self-compacting concrete-based MP.

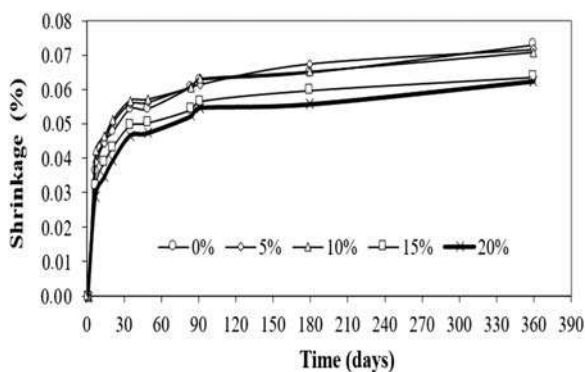


**Figure 9.11** Shrinkage results of concrete mixtures containing MP as cement replacement (Yamanel et al., 2019). MP, Marble powder.

### 9.8.5 Sulfate resistance

Sulfate solutions can deteriorate concrete by attacking the hardened cement paste. The precise chemical reaction depends on the type of sulfate present and the type of cement used. Ground water in some clay soils is a source of magnesium and calcium sulfates. These salts react in concrete with  $\text{Ca}(\text{OH})_2$  and calcium aluminate hydrate to form gypsum and calcium sulfoaluminate. These products have a much higher volume than the compounds they replace, causing the concrete to expand and crack. The rate and extent of sulfate attack are determined by the ease with which sulfate ions penetrate the concrete as well as the chemical resistance of the cement paste. [Boukhelkhal et al. \(2017\)](#) examined the  $\text{MgSO}_4$  sulfate resistance of MP mortars. For mixes containing MP the strength gain increases until 180 days. The strength gain of 5, 10, 15, and 20 MP mixes is about 13%, 26%, 28%, and 21% for immersion periods of 28, 56, 90, and 180 days, respectively. This demonstrates that the inclusion of 10% of MP by partial replacement of cement is considered the optimum substitution rate. The strength gain might be attributed to the continuous hydration of anhydrated cement products and the reaction of  $\text{MgSO}_4$  with  $\text{Ca}(\text{OH})_2$  to form two elements (gypsum and ettringite) which fill in the micropores, leading to a denser structure. The reduction in strength gain is due to the expansion effect of the sulfate attack, which leads to the formation of microcracks and softening of the cement matrix ([Tian & Cohen, 2000](#); [Ghrici et al., 2006](#); [Uysal & Yilmaz, 2011](#)).

[Aydin and Arel \(2019a\)](#) investigated the sodium sulfate resistance of concrete with different amounts of MP. The mass loss tended to increase with increasing amount of MP in the mixture. The highest mass loss was obtained for the pure marble mixture. The mass loss increased by 23.84% when comparing pure cement with pure marble mixtures at 90 days. This increase was 22.89% at 7 days, showing the effects of hydration on the matrix composites. [Binici et al. \(2007\)](#) reported that with the increase of percentage MP an increase in sulfate resistance of concrete is observed. Sulfate resistance of concrete increased significantly with the increase in the MP content for a period up to 12 months of exposure ([Hameed et al., 2012](#)). Sodium sulfate resistance of concrete is found to improve for around 15% cement replacement with MP ([Boukhelkhal et al., 2019](#)). According to the sodium sulfate durability test the marble cement paste composites were classified as medium-to-high-sulfate-resistant [the mass loss due to sulfate should be between 6% and 16% (ASTM C88)].

Durability properties of composites are directly related to their porosity ([Aydin & Doven, 2006](#); [Aydin, 2016](#); [Aydin & Arel, 2019b, 2019a](#)): The lower the porosity, the higher the durability that can be achieved. With continuous hydration and reactions of the marble cement pastes the bonding between the marble particles and marble cement interface improves. This can decrease the porosity of the matrix and provide a tightly packed structure, thereby increasing the strength of the composite ([Douglas Hooton, 2015](#); [Hewlett & Liska, 2019](#); [Lothenbach et al., 2011](#)).



### 9.8.6 Acid resistance

Concrete durability is primarily affected by aggressive chemical environments. The most harmful acid solutions to concrete are sulfuric, nitric, and hydrochloric. Even at low concentrations, their negative effects on building structures are faster and more obvious than sulfate attack. The calcium hydroxide component is known to be the most vulnerable to acid attacks (Makhloufi et al., 2012). Adding additional cementitious materials appears to be appropriate because they consume calcium hydroxide and densify the cement matrix and increase resistance to external sulfate and acid attacks (Bertron et al., 2005; Oueslati & Duchesne, 2012; Senhadji et al., 2014; Tennich et al., 2020).

Boukhelkhal et al. (2019) examined the variation of strength loss of mortars stored in HCl acid solution and in H<sub>2</sub>SO<sub>4</sub>. The result shows that adding MP led to lower strength loss and better resistance to HCl and H<sub>2</sub>SO<sub>4</sub> attack. The positive effect of MP may be due to the higher fineness of MP compared to cement, which leads to a denser structure and consequently higher resistance to hydrochloric acid attack. Furthermore the reduction in the cement amount decreases the calcium hydroxide content, which is the most vulnerable component in the case of acid attack. Another reason that can explain the best performance of MP is the presence of high content of calcium carbonate (CaCO<sub>3</sub>) in MP mixtures, which increases the ability of MP mixtures to consume more aggressive acid (Senhadji et al., 2014). Comparable results were found by Raghunath et al. (2019). The chemical attack by sulfuric acid is more deleterious than sulfate attack, where the former involves the sulfate ions for attack besides the hydrogen ions for dissolution (Bassuoni & Nehdi, 2007).

### 9.8.7 Alkali–silica reaction

Alkali–silica reaction (ASR) is a chemical reaction that occurs between alkalis in PC and certain types of silica in aggregates. It causes the formation of expansive gels, which causes the concrete to crack. The cycle is repeated until the concrete is no longer usable. The presence of ASR will initially cause a measurable expansion of concrete.

Munir et al. (2017) studied the efficiency of waste MP in controlling ASR of concrete. ASR expansion test was performed on concrete specimens incorporating MP in various dosages. As per ASTM C1260 the aggregate source can be considered as ASR if expansion reaches more than 0.1% and 0.2% after 14 and 28 days, respectively. Based on observed results, a reduction in mortar bar expansion after replacing cement with MP was obtained. For instance, 28% and 50% reduction in expansion was observed for mortar bars with 10% and 40% MP as substitution to cement, respectively. The highest reduction in expansion was observed for mortar bars incorporating 40% MP. After 28 days, all the mortar bar specimens incorporating MP showed expansion less than 0.2%. Previous studies reported that the formation of CSH is effective in reducing ASR expansion (Beglarigale & Yazici, 2014; Abbas et al., 2017; Kazmi et al., 2017).

Mortar with 10% MP as substitution to cement showed reduction in expansion due to formation of CSH as shown by mineralogical analysis (Munir et al., 2017). Furthermore, the amount of alkalis was also reduced after replacing cement with MP. For instance the amount of alkalis observed in cement and MP was 0.84% and 0.48%, respectively. Therefore the reduction in the amount of alkalis played a key role in reducing expansion after replacing cement with MP. Thomas (2011) reported that ASR expansion can be controlled by reducing the amount of alkalis. In the examined study, specimens incorporating 10% MP in replacement of cement showed 28% reduction in expansion.

Water demand of mortar mixtures increased with increasing replacement ratio of MP to achieve the constant flow. Therefore in order to examine the effect of increased water demand on the performance of ASR distress, mortar bars with an increased water–cement ratio (corresponding to a constant flow of 110 mm) were also examined. Reduction in expansion was observed after replacing cement with MP. For instance, specimens incorporating 10% MP and 40% MP in replacement of cement showed expansion of 0.164% and 0.111%, respectively. Mortar bars incorporating 40% MP showed the highest reduction in expansion. Mortar bars with varying water–cement ratios showed more expansion than mortar bars with a constant water–cement ratio. For example, mortar bars incorporating 20% MP showed an expansion of 0.123% for constant water–cement ratios and 0.154% for varying water–cement ratios. However, all the mortar bars incorporating MP in replacement of cement showed an expansion less than the ASTM C1260 specified limit for reactivity. Mortar with a constant W/C ratio showed decreased expansion as result of shrinkage due to high water demand. In previous studies, ASR expansion was also controlled using other waste materials (Shafaatian et al., 2013; Kandasamy & Shehata, 2014; Afshinnia & Rangaraju, 2015; Munir et al., 2017).

Abbas et al. (2020) also explored the potential of using MP as partial replacement for cement for controlling the ASR expansion and cracking. Mortar bars tests were performed incorporating various proportions of MP for a constant w/c ratio. The results revealed a progressive decrease in ASR expansion with the incorporation of MP. A high MP dosage appears to be effective in controlling ASR and limiting the associated expansion. MP was added as partial cement replacement and because MP has a lower alkali content (0.13%) in comparison with that of the cement (0.58%); significant dilution effect of alkalis in the pore solution occurs with higher MP dosage, which can lead to mitigating ASR damage (Thomas, 2011). Furthermore, due to its low silica content, MP is not pozzolanic. As a result the cement dilution effect may result in increased porosity. This additional porosity may temporarily relieve pressure from the ASR gel, contributing to the observed decrease in ASR expansion and cracking. The formation of carboaluminates may also help to reduce ASR.

### 9.8.8 Carbonation

Carbonation occurs in concrete when the calcium-containing phases are attacked by carbon dioxide from the air and converted to calcium carbonate. Cement paste

contains 25–50 wt.% calcium hydroxide ( $\text{Ca}(\text{OH})_2$ ), implying that the fresh cement paste has a pH of at least 12.5. A fully carbonated paste has a pH of around 7. When  $\text{Ca}(\text{OH})_2$  is removed from the paste, hydrated CSH releases CaO, which carbonates. The rate of carbonation is affected by the concrete's porosity and moisture content.

Rana et al. (2015) reported that increasing MP content in mixes yielded rising carbonation depths. Permeability and other durability properties of mixes prepared with MP were found to improve up to 10% MP content. However, resistance to carbonation of these mixes was observed to be reducing. The bicarbonate alkalinity of MP (89 mg/L) was found to be low, compared to that of cement (113 mg/L). This could be the reason for high carbonation depths for these mixes (Singh et al., 2017b).

Li et al. (2018) investigated the effectiveness of adding MP as paste replacement in reducing the carbonation depth. The result revealed that adding up to 20% MP as paste replacement always reduced the carbonation depth. Moreover, at a lower W/C ratio the percentage reduction in carbonation depth was larger. For instance, at a W/C ratio of 0.55, increasing the MP volume from 0% to 20% decreased the carbonation depth by 31.3%, whereas at a W/C ratio of 0.40, increasing the MP volume from 0% to 20% decreased the carbonation depth by 42.9%. Therefore the addition of MP as paste replacement is proven to be an effective way to improve the carbonation resistance of mortar.

Singh et al. (2017b) found that mixes with MP showed less resistance to carbonation as compared to the control mix. Mixtures with 25% MP content showed the highest carbonation depth of around 19 mm as compared to the control mix. The concrete carbonation depth depends on its porosity; higher MP content in mortar already caused higher porosity, which causes higher ingress of  $\text{CO}_2$  into the sample, which forms carbonation by reacting with portlandite. Yamanel et al. (2019) and Gameiro et al. (2014) reported similar results on the behavior of concrete subjected to carbonation effect (Topçu et al., 2009; Demirel, 2010; Yang et al., 2015).

### 9.8.9 Chloride permeability

The rapid chloride permeability test, as described in ASTM C 1202, is a well-known test for determining concrete resistance to chloride ion penetration. This test determines the charge passed (in Coulombs) through a concrete specimen, providing an indirect measurement of the concrete permeability to chloride. Sharobim et al. (2017) studied the effect of MP on rating chloride permeability of SCC mixes. Results are given in Fig. 9.12, which shows that the charge decreased at 10% MP compared with the control one, but above 10% of MP the charge increased compared to mix containing 10% MP. Permeability of concrete depends on the porosity of concrete. Porosity of concrete decreases as MP percentages increase because MP fills the voids between particles. However, increasing MP over 10% reduces cement content, which makes the bond between particles weak, and hence the loss in thickness increases.

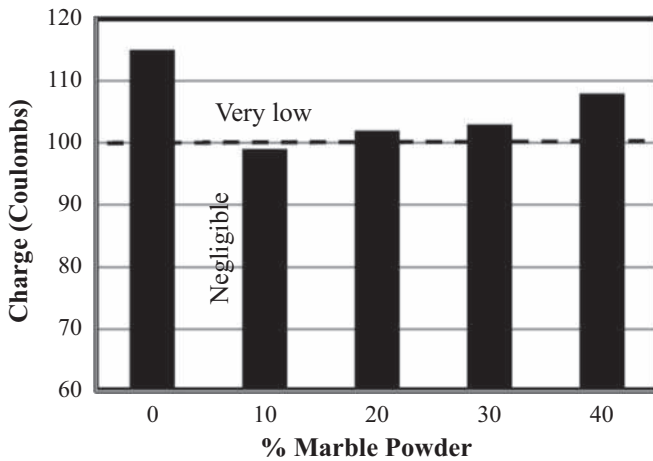


**Figure 9.12** Effect of MP on rating of chloride permeability of concrete (Sharobim et al., 2017). MP, Marble powder.

Rana et al. (2015) investigated chloride penetration for concrete with different MP contents. They found that for all the mixes, very low diffusion coefficients were observed. The chloride diffusion coefficients were found to decrease up to 10% of cement replacement by MP, but higher MP content resulted in increased diffusion coefficients. The substitution of 5%–10% cement by MP might have resulted in reduction of these capillary passages and led to reduced chloride ion migration. However, replacement of more than 10% MP might have impaired the bonding of concrete constituents due to the smaller available quantity of cement. The poor bonding of concrete might have resulted in an increased number of capillary passages and increased chloride migration (Binici et al., 2007; Ergün, 2011; Talah et al., 2015; Yang et al., 2015; Sharobim et al., 2017; Singh et al., 2017b; Raghunath et al., 2019; Sancheti et al., 2020).

### 9.8.10 Corrosion

Corrosion is the degradation of a material as a result of a reaction with its environment. Degradation implies deterioration of the material's physical properties. This can be a material weakening due to a loss of cross-sectional area, or it can be a metal shattering due to hydrogen embrittlement. Corrosion of steel reinforcement causes concrete cracking and, eventually, spalling. Concrete deteriorates less in adverse environmental conditions when it is of high quality. Steel in concrete initially and in most cases remains in a passive state for sustained long periods of time due to the high alkalinity of the concrete pore fluid. Corrosion begins as a result of either a decrease in alkalinity caused by carbonation or the breakdown of the passive layer caused by chloride ion attack. The time it takes for corrosion to begin is

largely determined by the thickness and quality of the concrete cover as well as the permeability of the concrete.

Rana et al. (2015) carried out corrosion tests on concrete with different contents of MP ranging from 0% to 25%. The results showed that less corrosion was observed in the mixes with 5% and 10% of MP in contrast to other mixes. The minimum corrosion and maximum corrosion were observed for mixes with 5% and 25%, respectively. After 6 cycles, each specimen was broken and all three rebars were taken out. No corrosion was observed in rebars of mixes with 5%, whereas a little corrosion was observed in one rebar of the control mix. Corrosion was witnessed in two rebars for mixes with 25%. It is clear from the results that substitution of 5%–10% cement by MP enhances the corrosive resistance of concrete. However, 15%–25% MP content in concrete damaged the corrosive resistance of concrete (Hameed & Sekar, 2009).

### 9.8.11 Fire resistance (high temperature resistance)

Yamanel et al. (2019) investigated the fire performance of mortar containing MP as cement substitution. Prismatic samples measuring  $40 \times 40 \times 160$  mm were subjected to elevated temperature tests. Temperatures of 300°C, 600°C, and 900°C were applied to specimens. After being exposed to high temperatures the specimens were cooled in the furnace to room temperature. Specimens were subjected to compressive and flexural tests following a cooling period. The results for the compressive strength tests given in Table 9.6 show that all mortars gained strength after being exposed to 300°C. The increase in strength ranged between 3% and 9%. At 300°C, MP mortars performed as good as or better than cement mortar. When the amount of MP in the mortar was increased, the performance of the mortar improved at 300°C exposures due to thermal drying and thermal dehydration of cement paste. All mortars lost their strength when the temperature was raised to 600°C and 900°C. At 600°C exposure, the reduction rate was in the order of 40%. At 900°C exposure, it was in the range of 65%. When control cement mortar and MP mortar were compared, the MP mortar performed similarly or better than the control cement mortar.

**Table 9.6** Compressive strength test results after high temperature (MPa) (%) (Yamanel et al., 2019).

Mix no	20°C	300°C/20°C	600°C/20°C	900°C/20°C
M-0	52.7	54.6(1.04)	31.9(0.61)	18.1(0.34)
M-5	52.1	53.7(1.04)	29.9(0.57)	18.6(0.36)
M-10	48.7	51.4(1.04)	27.8(0.57)	15.8(0.32)
M-15	46.3	49.1(1.04)	28.8(0.62)	16.4(0.35)
M-20	42.8	46.7(1.04)	27.2(0.64)	15.5(0.36)

### 9.8.12 Resistance to freeze and thaw cycling

Freezing–thawing resistance of concrete depends on the adequacy of air void system, the soundness of aggregate, degree of hydration and strength of binding paste, and maturity and moisture content of concrete. Freeze thaw durability is evaluated using the test procedure given by ASTM C666. The resistance to freeze and thaw of concrete incorporating marble dust was investigated by [Ince et al. \(2020\)](#). It is noteworthy that the concrete specimens were water cured for 28 days before they were placed into the freeze and thaw chamber. The results demonstrate that concrete control specimens subjected to freeze and thaw cycles yielded a greater strength loss compared to the concrete specimens with marble dust. The use of marble dust enhanced the freeze and thaw resistance of concrete significantly. These results are in good agreement with the compressive strength loss of concrete. As the number of freeze and thaw cycles increases, the subsequent hydraulic pressure in the matrix system increases, which results in a progressive development of microcracks and hence leads to a mass loss of the concrete specimen. The formation of cracks and hence the mass loss of the concrete specimens obviously lead to a greater loss of strength in those samples. The significant decrease in the compressive strength loss demonstrated the substantial contribution of marble dust on the increased resistance to freezing and thawing of concrete ([Binici & Aksogan, 2018](#); [Bakis, 2019](#)).

### 9.8.13 Abrasion resistance

Abrasion of concrete occurs as a result of object scraping, rubbing, skidding, or sliding across its surface. Concrete abrasion resistance is influenced by several factors, including compressive strength, surface finish, aggregate properties, hardener types, and curing. Concrete abrasion resistance is primarily determined by its compressive strength. As a result, air entrainment, water–cement ratio, and aggregate types and properties, which influence compressive strength of concrete, should also influence abrasion resistance of concrete. Hardened paste has a low abrasion resistance in general. The use of hard aggregates and a low water-to-cement ratio has been found to be very effective in increasing concrete abrasion/erosion resistance ([Singh et al., 2019](#)).

Available literature studies show that the replacement of cement with MP reduced abrasion resistance, meaning an increased abrasion value of sample in comparison to control cement mortar. A higher replacement ratio results in a higher abrasion value ([Yamanel et al., 2019](#)). This is found to be comparable to the results of [Koçyiğit & Çay \(2018\)](#), [Singh et al. \(2019\)](#). A higher abrasion value of marble containing mortar versus control cement mortar can be explained by the nature of marble itself. It is known that hardness of marble is lower than that of siliceous materials. Replacing cement particles with somewhat softer materials might result in higher abrasion.

[Sharobim et al. \(2017\)](#) found that the loss in abrasion resistance increases as MP percentages increase, except at 10% MP, where a loss in abrasion resistance was observed. The decrease of loss in abrasion resistance at 10% MP may be explained

by possible binding activity caused by MP, which fills the voids and confers an abrasion resistance. Increasing MP over 10% reduces cement content, which makes the bond between particles weak, so loss in abrasion resistance increases. [Binici et al. \(2007\)](#) reported that the abrasion results were better for the replacement of sand with MP as compared to limestone dust. Even with limestone dust, no significant decrease was observed for up to 15% inclusion. [Rodrigues et al. \(2015\)](#) and [Singh et al. \(2019\)](#) also found a decrease in abrasion resistance with an increase in MP content. The incorporation of superplasticizers resulted in an increase in the abrasion resistance, which is mainly due to the water reduction power of these plasticizers, which leads to an increase in the compactness of concrete ([Singh et al., 2017a](#)).

## 9.9 Economic aspect

Many authors have studied the cost efficiency analysis of MP-based concrete. MP is a waste material and therefore is freely available, except for the transportation costs. Results obtained by [Ince et al. \(2020\)](#) showed that incorporating MP resulted in a slight decrease in the cost efficiency factor of concrete incorporating MP. The slight decrease observed in the cost efficiency factor of concrete is mainly due to the decrease in compressive strength of concrete incorporating MP. Incorporating MP in concrete led to a substantial increase in the calcium oxide (CaO) content ([Arel, 2016](#)).

[Singh et al. \(2017a\)](#) analyzed the costs for 1 m<sup>3</sup> concrete with 15% cement replacement by MP and with 25% sand replacement by MP. The first case (MP as cement replacement) indicates a benefit of 9.08%, while the second case (MP as sand replacement) incurs a loss of 3.4%. However, it must be noted that the environmental impacts of sand replacement by MP are huge. Moreover the availability of sand in future for construction activities will be very difficult, and its cost will be very high. Replacement of cement reduces the cost of concrete production, reduces the consumption of cement, and also provides better strength and durability.

Most studies concluded that replacing cement with MP at ratios of 5%–10% enhances the mechanical properties of concrete with no negative impacts. According to [Ergün \(2011\)](#), MP replacement of 5% increases the compressive and flexural strengths of concrete by 12% and 5%, respectively. A compressive strength increase of 12% reduces the cost by US\$4 m<sup>-3</sup>. [Rodrigues et al. \(2015\)](#) reported that the compressive strength is retained up to an MP substitution ratio of 10%. They stated that 10% substitution decreases the cost by 7 US\$ per cubic meter with no remarkable change in compressive strength. [Uysal and Yilmaz \(2011\)](#) similarly reported that replacing cement with MP at 10% preserves the compressive strength.

In contrast, MP at 20% replacement ratio reduces the cost by 12 US\$ per cubic meter because it decreases the compressive strength by 10%–20%. [Gesoglu et al. \(2012\)](#) found that 20% replacement of cement with MP reduces the compressive strength by 13.46%. [Topçu et al. \(2009\)](#) determined that 40% MP substitution reduces the compressive strength by 42%. [Arel \(2016\)](#), [Khodabakhshian et al.](#)

(2018), [Aydin and Arel \(2019b\)](#) reported that the incorporation of MP as substitution for high amounts of cement may significantly improve the material cost effectiveness of concrete. As waste materials the costs of MP are not prohibitively high. From this viewpoint, MP brings no additional cost to producers and can be effectively employed in concrete applications ([Uysal & Sumer, 2011](#)).

## 9.10 Environmental performance

Replacing cement with alternative materials would minimize its negative environmental effects. The recycling of MP in mortar/concrete production has two major ecofriendly advantages, namely, environmental sustainability. First, using MP in mortar/concrete, a widely used construction material, would significantly reduce the amount of MP disposed of in landfills. The dumping of MP into landfills has resulted in a rapid depletion of the limited landfill capacity, particularly in densely populated areas where new landfill sites are difficult to find. Due to the rapid depletion of landfill capacity, stonework factories are required to pay high fees for dumping MP into landfills. MP recycling would help to alleviate the environmental impact of waste disposal.

Second, adding MP to mortar/concrete reduces the required amount of cement production. The main contributor to the carbon footprint of mortar/concrete production is the cement content ([Purnell & Black, 2012](#); [Yang et al., 2015](#)). The cement content accounts for more than 90% of the carbon footprint of mortar/concrete (the manufacture of 1.0 ton of cement generates about 0.9 ton of CO<sub>2</sub>). Because of the addition of MP, the reduction in cement content would significantly reduce the carbon footprint and thus improve the environmental sustainability ([Li et al., 2019](#)).

According to [Ergün \(2011\)](#), [Uysal and Yilmaz \(2011\)](#), [Gesoglu et al. \(2012\)](#), [Rodrigues et al. \(2015\)](#), [Arel \(2016\)](#), replacing 10% of the cement with MP would reduce the cement production from 65.52 to 62.73 million tons and the CO<sub>2</sub> release from 69.7 to 58.96 million tons. Worldwide the cement production would fall from its 2014 levels (4.2 billion tons) to 3.78 billion tons; correspondingly the CO<sub>2</sub> release would fall from 3.95 to 3.55 billion tons ([Çankaya & Pekey, 2018](#)). A similar analysis of the CO<sub>2</sub> emissions can be found in other studies ([Ergün, 2011](#); [Uysal & Yilmaz, 2011](#); [Gesoglu et al., 2012](#); [Arel, 2016](#); [Maddalena et al., 2018](#); [Aydin & Arel, 2019b](#)).

According to [Arel \(2016\)](#), using MP in concrete production reduces environmental pollution and benefits the economy. The author reported that replacing cement with 5%–10% MP improves the mechanical properties of concrete and reduces the costs of concrete production and the CO<sub>2</sub> emissions of cement production by about 17% and 12%, respectively ([Khodabakhshian et al., 2018](#)).

[Li et al. \(2019\)](#) reported that up to 20% MP by volume of mortar may be added as paste replacement to the mortar to reduce the cement content by 33.3%. In practice, therefore, it may be better to limit the MP volume at 15%, in which case the cement content would be reduced by 25.1%. On the other hand, with MP added as



cement replacement, up to 10% MP by volume of the original cement content may be added to the mortar to reduce the cement content by 10.0%. Hence, in terms of both waste utilization and carbon footprint reduction, the paste replacement method is more effective than the cement replacement method.

## 9.11 Conclusion

One of the primary goals of sustainability is to profitably utilize waste materials while reducing the use of natural resources as much as possible. The technical significance of using wastes and byproducts in concrete production is expressed by concrete performance improvement. When industrial wastes are recycled, not only are CO<sub>2</sub> emissions reduced but also residual products from other industries are reused, resulting in less material being dumped as landfill and more natural resources being saved. Because the cement industry emits a large amount of CO<sub>2</sub> as a result of clinker calcinations, the use of waste MP as an additive material in cement production can help to reduce CO<sub>2</sub> emissions as well the cost of cement production.

Workability of concrete with MP was reduced due to the large surface area of waste MP. The mechanical and durability properties can be achieved using MP as cement replacement. The high levels of replacement lead to delayed hydration of the mix and porous microstructures, as is visible from the microstructure studies on the materials.

Moreover, reduction of cement decreases the cost as cement is an expensive component and replacement of cement can lead to development of economical as well as sustainable concrete. The use of MP could lead to better economic and environmental performance and hence to more sustainable concrete industry and more sustainable development. The effect of chemical properties of MP and the combination of MP with recycled aggregates and/or pozzolanic materials on the properties of concrete mixtures need further investigations. Numerical studies for the prediction of properties of concrete mixtures with MP and life cycle assessment of MP-based products compared to other systems need also to be studied.

## References

- Abbas, S., Ahmed, A., Nehdi, M. L., et al. (2020). Eco-friendly mitigation of alkali-silica reaction in concrete using waste-marble powder. *Journal of Materials in Civil Engineering*, 32, 04020270. Available from [https://doi.org/10.1061/\(asce\)mt.1943-5533.0003312](https://doi.org/10.1061/(asce)mt.1943-5533.0003312).
- Abbas, S., Kazmi, S. M. S., & Munir, M. J. (2017). Potential of rice husk ash for mitigating the alkali-silica reaction in mortar bars incorporating reactive aggregates. *Construction and Building Materials*, 132, 61–70. Available from <https://doi.org/10.1016/j.conbuildmat.2016.11.126>.
- Afshinnia, K., & Rangaraju, P. R. (2015). Influence of fineness of ground recycled glass on mitigation of alkali-silica reaction in mortars. *Construction and Building Materials*, 81, 257–267. Available from <https://doi.org/10.1016/j.conbuildmat.2015.02.041>.

- Aliabdo, A. A., Abd Elmoaty, A. E. M., & Auda, E. M. (2014). Re-use of waste marble dust in the production of cement and concrete. *Construction and Building Materials*, 50, 28–41. Available from <https://doi.org/10.1016/j.conbuildmat.2013.09.005>.
- Almeida, A. E. F. de S., & Sichieri, E. P. (2006). Thermogravimetric analyses and mineralogical study of polymer modified mortar with silica fume. *Materials Research*, 9, 321–326. Available from <https://doi.org/10.1590/S1516-14392006000300012>.
- Alyamac, K. E., Ghafari, E., & Ince, R. (2017). Development of eco-efficient self-compacting concrete with waste marble powder using the response surface method. *Journal of Cleaner Production*, 144, 192–202. Available from <https://doi.org/10.1016/j.jclepro.2016.12.156>.
- Alyousef, R., Benjeddou, O., Khadimallah, M. A., et al. (2018). Study of the effects of marble powder amount on the self-compacting concretes properties by microstructure analysis on cement-marble powder pastes. *Advances in Civil Engineering*, 2018, 17–20. Available from <https://doi.org/10.1155/2018/6018613>.
- Alyousef, R., Benjeddou, O., Soussi, C., et al. (2019). Effects of incorporation of marble powder obtained by recycling waste sludge and limestone powder on rheology, compressive strength, and durability of self-compacting concrete. *Advances in Materials Science and Engineering*, 2019. Available from <https://doi.org/10.1155/2019/4609353>.
- Arel, H. S. (2016). Recyclability of waste marble in concrete production. *Journal of Cleaner Production*, 131, 179–188. Available from <https://doi.org/10.1016/j.jclepro.2016.05.052>.
- Ashish, D. K. (2019). Concrete made with waste marble powder and supplementary cementitious material for sustainable development. *Journal of Cleaner Production*, 211, 716–729. Available from <https://doi.org/10.1016/j.jclepro.2018.11.245>.
- Atiyeh, M., & Aydin, E. (2020). Data for bottom ash and marble powder utilization as an alternative binder for sustainable concrete construction. *Data Brief*, 29, 105160. Available from <https://doi.org/10.1016/j.dib.2020.105160>.
- Aydin, E. (2016). Novel coal bottom ash waste composites for sustainable construction. *Construction and Building Materials*, 124, 582–588. Available from <https://doi.org/10.1016/j.conbuildmat.2016.07.142>.
- Aydin, E., & Arel, H. Ş. (2019a). High-volume marble substitution in cement-paste: Towards a better sustainability. *Journal of Cleaner Production*, 237. Available from <https://doi.org/10.1016/j.jclepro.2019.117801>.
- Aydin, E., & Arel, H. Ş. (2019b). Data for the marble-cement paste composites for sustainable construction. *Data Brief*, 26. Available from <https://doi.org/10.1016/j.dib.2019.104528>.
- Aydin, E., & Doven, A. G. (2006). Influence of water content on ultrasonic pulse-echo measurements through high volume fly ash cement paste—Physicomechanical characterization. *Research in Nondestructive Evaluation*, 17, 177–189. Available from <https://doi.org/10.1080/09349840600788004>.
- Bakis, A. (2019). Increasing the durability and freeze-thaw strength of concrete paving stones produced from Ahlat stone powder and marble powder by special curing method. *Advances in Materials Science and Engineering*, 2019. Available from <https://doi.org/10.1155/2019/3593710>.
- Bassuoni, M. T., & Nehdi, M. L. (2007). Resistance of self-consolidating concrete to sulfuric acid attack with consecutive pH reduction. *Cement and Concrete Research*, 37, 1070–1084. Available from <https://doi.org/10.1016/j.cemconres.2007.04.014>.
- Beglarigale, A., & Yazici, H. (2014). Mitigation of detrimental effects of alkali-silica reaction in cement-based composites by combination of steel microfibers and ground-granulated blast-furnace slag. *Journal of Materials in Civil Engineering*, 26, 04014091. Available from [https://doi.org/10.1061/\(asce\)mt.1943-5533.0001005](https://doi.org/10.1061/(asce)mt.1943-5533.0001005).

- Belaidi, A. S. E., Azzouz, L., Kadri, E., & Kenai, S. (2012). Effect of natural pozzolana and marble powder on the properties of self-compacting concrete. *Construction and Building Materials*, 31, 251–257. Available from <https://doi.org/10.1016/j.conbuildmat.2011.12.109>.
- Belaidi, A. S. E., Kenai, S., Kadri, E.-H., et al. (2016). Effects of experimental ternary cements on fresh and hardened properties of self-compacting concretes. *Journal of Adhesion Science and Technology*, 30. Available from <https://doi.org/10.1080/01694243.2015.1099864>.
- Belouadah, M., Rahmouni, Z. E., Tebbal, N., & El Hassen Hicham, M. (2021). Evaluation of concretes made with marble waste using destructive and non-destructive testing. *Annales de Chimie Science des Matériaux*, 45, 361–368. Available from <https://doi.org/10.18280/acsm.450501>.
- Benjeddou, O., Alyousef, R., Mohammadhosseini, H., et al. (2020). Utilisation of waste marble powder as low-cost cementing materials in the production of mortar. *Journal of Building Engineering*, 32, 101642. Available from <https://doi.org/10.1016/j.jobbe.2020.101642>.
- Bertron, A., Duchesne, J., & Escadeillas, G. (2005). Accelerated tests of hardened cement pastes alteration by organic acids: Analysis of the pH effect. *Cement and Concrete Research*, 35, 155–166. Available from <https://doi.org/10.1016/j.cemconres.2004.09.009>.
- Binici, H., & Aksogan, O. (2018). Durability of concrete made with natural granular granite, silica sand and powders of waste marble and basalt as fine aggregate. *Journal of Building Engineering*, 19, 109–121. Available from <https://doi.org/10.1016/j.jobbe.2018.04.022>.
- Binici, H., Kaplan, H., & Yilmaz, S. (2007). Influence of marble and limestone dusts as additives on some mechanical properties of concrete. *Scientific Research and Essays*, 2, 372–379. Available from <https://doi.org/10.5897/SRE.9000594>.
- Bostanci, S. C. (2020). Use of waste marble dust and recycled glass for sustainable concrete production. *Journal of Cleaner Production*, 251, 119785. Available from <https://doi.org/10.1016/j.jclepro.2019.119785>.
- Boukhelkhal, A., Azzouz, L., Belaïdi, A. S. E., & Benabed, B. (2016). Effects of marble powder as a partial replacement of cement on some engineering properties of self-compacting concrete. *Journal of Adhesion Science and Technology*, 30, 2405–2419. Available from <https://doi.org/10.1080/01694243.2016.1184402>.
- Boukhelkhal, A., Azzouz, L., Benabed, B., & Belaïdi, A. (2017). Strength and durability of low-impact environmental self-compacting concrete incorporating waste marble powder. *Building Materials and Structures*, 4, 31–41.
- Boukhelkhal, A., Azzouz, L., Kenai, S., et al. (2019). Combined effects of mineral additions and curing conditions on strength and durability of self-compacting mortars exposed to aggressive solutions in the natural hot-dry climate in North African desert region. *Construction and Building Materials*, 197, 307–318. Available from <https://doi.org/10.1016/j.conbuildmat.2018.11.233>.
- Çankaya, S., & Pekey, B. (2018). Comparative life cycle assessment of clinker production with conventional and alternative fuels usage in Turkey. *International Journal of Environmental Science and Development*, 9, 213–217. Available from <https://doi.org/10.18178/ijesd.2018.9.8.1103>.
- Cather, R., Figg, J. W., Marsden, A. F., & O'Brien, T. P. (1984). Improvements to the figg method for determining the air permeability of concrete. *Magazine of Concrete Research*, 36, 241–245. Available from <https://doi.org/10.1680/mac.1984.36.129.241>.

- Chahour, K., & Safi, B. (2020). Mechanical behavior and chemical durability of marble-based mortar: Application to panels subjected to punching. *Construction and Building Materials*, 232, 117245. Available from <https://doi.org/10.1016/j.conbuildmat.2019.117245>.
- Choudhary, A., Shah, V., & Bishnoi, S. (2016). Effect of low cost fillers on cement hydration. *Construction and Building Materials*, 124, 533–543. Available from <https://doi.org/10.1016/j.conbuildmat.2016.07.088>.
- Dada, H., Belaidi, A. S. E., Soualhi, H., et al. (2021). Influence of temperature on the rheological behaviour of eco-mortar with binary and ternary cementitious blends of natural pozzolana and marble powder. *Powder Technology*, 384, 223–235. Available from <https://doi.org/10.1016/j.powtec.2021.02.019>.
- Demirel, B. (2010). The effect of the using waste marble dust as fine sand on the mechanical properties of the concrete. *International Journal of Physical Sciences*, 5, 1372–1380.
- Djebri, N., Rahmouni, Z. E., & Belagraa, L. (2017). Experimental investigation on the effect of marble powder on the performance of self-compacting concrete (SCC). *Mining Science*, 24, 183–194. Available from <https://doi.org/10.5277/msc172411>.
- Douglas Hooton, R. (2015). Current developments and future needs in standards for cementitious materials. *Cement and Concrete Research*, 78, 165–177. Available from <https://doi.org/10.1016/j.cemconres.2015.05.022>.
- Ergün, A. (2011). Effects of the usage of diatomite and waste marble powder as partial replacement of cement on the mechanical properties of concrete. *Construction and Building Materials*, 25, 806–812. Available from <https://doi.org/10.1016/j.conbuildmat.2010.07.002>.
- Gameiro, F., De Brito, J., & Correia da Silva, D. (2014). Durability performance of structural concrete containing fine aggregates from waste generated by marble quarrying industry. *Engineering Structures*, 59, 654–662. Available from <https://doi.org/10.1016/j.engstruct.2013.11.026>.
- Gesoglu, M., Güneyisi, E., Kocabağ, M. E., et al. (2012). Fresh and hardened characteristics of self compacting concretes made with combined use of marble powder, limestone filler, and fly ash. *Construction and Building Materials*, 37, 160–170. Available from <https://doi.org/10.1016/j.conbuildmat.2012.07.092>.
- Ghrici, M., Kenai, S., & Meziane, E. (2006). Mechanical and durability properties of cement mortar with Algerian natural pozzolana. *Journal of Materials Science*, 41, 6965–6972. Available from <https://doi.org/10.1007/s10853-006-0227-0>.
- Hameed, M. S., & Sekar, A. S. S. (2009). Properties of green concrete containing quarry rock dust and marble sludge powder as fine aggregate. *Journal of Engineering and Applied Science*, 4, 83–89.
- Hameed, M. S., Sekar, A. S. S., Balamurugan, L., & Saraswathy, V. (2012). Self-compacting concrete using marble sludge powder and crushed rock dust. *KSCCE Journal of Civil Engineering*, 16, 980–988. Available from <https://doi.org/10.1007/s12205-012-1171-y>.
- Hanžič, L., & Ilič, R. (2003). Relationship between liquid sorptivity and capillarity in concrete. *Cement and Concrete Research*, 33, 1385–1388. Available from [https://doi.org/10.1016/S0008-8846\(03\)00070-X](https://doi.org/10.1016/S0008-8846(03)00070-X).
- Hebhoub, H., Aoun, H., Belachia, M., et al. (2011). Use of waste marble aggregates in concrete. *Construction and Building Materials*, 25, 1167–1171. Available from <https://doi.org/10.1016/j.conbuildmat.2010.09.037>.
- Heikal, M., & Morsy, M. S. (2000). Limestone-filled pozzolanic cement. *Cement and Concrete Research*, 30, 1827–1834.
- Hewlett, P.C., & Liska M. (2019). *Lea's chemistry of cement and concrete, Fifth Edition*. ISBN: 9780081007952. Available from <https://doi.org/10.1016/C2013-0-19325-7>. Butterworth-Heinemann.

- Hlubocký, L., & Prošek, Z. (2017). Shrinkage of cement composite with material based on waste marble and limestone. *Key Engineering Materials*, 731, 80–85. Available from <https://doi.org/10.4028/http://www.scientific.net/KEM.731.80>, KEM.
- Ince, C., Hamza, A., Derogar, S., & Ball, R. J. (2020). Utilisation of waste marble dust for improved durability and cost efficiency of pozzolanic concrete. *Journal of Cleaner Production*, 270, 122213. Available from <https://doi.org/10.1016/j.jclepro.2020.122213>.
- Kandasamy, S., & Shehata, M. H. (2014). The capacity of ternary blends containing slag and high-calcium fly ash to mitigate alkali silica reaction. *Cement and Concrete Composites*, 49, 92–99. Available from <https://doi.org/10.1016/j.cemconcomp.2013.12.008>.
- Kazmi, S. M. S., Munir, M. J., Patnaikuni, I., & Wu, Y. F. (2017). Pozzolanic reaction of sugarcane bagasse ash and its role in controlling alkali silica reaction. *Construction and Building Materials*, 148, 231–240. Available from <https://doi.org/10.1016/j.conbuildmat.2017.05.025>.
- Khaliq, S. U., Shahzada, K., Alam, B., et al. (2016). Marble powder's effect on permeability and mechanical properties of concrete. *International Journal of Civil and Environmental Engineering*, 10, 537–542.
- Khodabakhshian, A., de Brito, J., Ghalehnovi, M., & Asadi Shamsabadi, E. (2018). Mechanical, environmental and economic performance of structural concrete containing silica fume and marble industry waste powder. *Construction and Building Materials*, 169, 237–251. Available from <https://doi.org/10.1016/j.conbuildmat.2018.02.192>.
- Koçyiğit, Ş., & Çay, V. V. (2018). Mechanical properties of the composite material produced by the mixture of expanded perlite, waste marble dust and Tragacanth. *European Journal of Technology*, 8, 124–133. Available from <https://doi.org/10.36222/ejt.481221>.
- Kumar, R. (2020). Modified mix design and statistical modelling of lightweight concrete with high volume micro fines waste additive via the box-Behnken design approach. *Cement and Concrete Composites*, 113, 103706. Available from <https://doi.org/10.1016/j.cemconcomp.2020.103706>.
- Kumar, V., Singla, S., & Garg, R. (2020). Strength and microstructure correlation of binary cement blends in presence of waste marble powder. *Materials Today: Proceedings*, 43, 857–862. Available from <https://doi.org/10.1016/j.matpr.2020.07.073>.
- Kırgız, M. S. (2016). Fresh and hardened properties of green binder concrete containing marble powder and brick powder. *European Journal of Environmental and Civil Engineering*, 20, s64–s101. Available from <https://doi.org/10.1080/19648189.2016.1246692>.
- Li, L. G., Huang, Z. H., Tan, Y. P., et al. (2018). Use of marble dust as paste replacement for recycling waste and improving durability and dimensional stability of mortar. *Construction and Building Materials*, 166, 423–432. Available from <https://doi.org/10.1016/j.conbuildmat.2018.01.154>.
- Li, L. G., Huang, Z. H., Tan, Y. P., et al. (2019). Recycling of marble dust as paste replacement for improving strength, microstructure and eco-friendliness of mortar. *Journal of Cleaner Production*, 210, 55–65. Available from <https://doi.org/10.1016/j.jclepro.2018.10.332>.
- Lothenbach, B., Scrivener, K., & Hooton, R. D. (2011). Supplementary cementitious materials. *Cement and Concrete Research*, 41, 1244–1256. Available from <https://doi.org/10.1016/j.cemconres.2010.12.001>.
- Maddalena, R., Roberts, J. J., & Hamilton, A. (2018). Can Portland cement be replaced by low-carbon alternative materials? A study on the thermal properties and carbon emissions of innovative cements. *Journal of Cleaner Production*, 186, 933–942. Available from <https://doi.org/10.1016/j.jclepro.2018.02.138>.

- Makhloufi, Z., Kadri, E. H., Bouhicha, M., & Benaissa, A. (2012). Resistance of limestone mortars with quaternary binders to sulfuric acid solution. *Construction and Building Materials*, 26, 497–504. Available from <https://doi.org/10.1016/j.conbuildmat.2011.06.050>.
- Mashaly, A. O., El-kaliouby, B. A., Shalaby, B. N., et al. (2016). Effects of marble sludge incorporation on the properties of cement composites and concrete paving blocks. *Journal of Cleaner Production*, 112, 731–741. Available from <https://doi.org/10.1016/j.jclepro.2015.07.023>.
- Moropoulou, A., Bakolas, A., & Aggelakopoulou, E. (2004). Evaluation of pozzolanic activity of natural and artificial pozzolans by thermal analysis. *Thermochim Acta*, 420, 135–140. Available from <https://doi.org/10.1016/j.tca.2003.11.059>.
- Munir, M. J., Kazmi, S. M. S., & Wu, Y. F. (2017). Efficiency of waste marble powder in controlling alkali–silica reaction of concrete: A sustainable approach. *Construction and Building Materials*, 154, 590–599. Available from <https://doi.org/10.1016/j.conbuildmat.2017.08.002>.
- Oueslati, O., & Duchesne, J. (2012). The effect of SCMs and curing time on resistance of mortars subjected to organic acids. *Cement and Concrete Research*, 42, 205–214. Available from <https://doi.org/10.1016/j.cemconres.2011.09.017>.
- Prokopski, G., Marchuk, V., & Huts, A. (2020). The effect of using granite dust as a component of concrete mixture. *Case Studies in Construction Materials*, 13. Available from <https://doi.org/10.1016/j.cscm.2020.e00349>.
- Prošek, Z., Nežerka, V., & Tesárek, P. (2020). Enhancing cementitious pastes with waste marble sludge. *Construction and Building Materials*, 255. Available from <https://doi.org/10.1016/j.conbuildmat.2020.119372>.
- Purnell, P., & Black, L. (2012). Embodied carbon dioxide in concrete: Variation with common mix design parameters. *Cement and Concrete Research*, 42, 874–877. Available from <https://doi.org/10.1016/j.cemconres.2012.02.005>.
- Péra, J., Husson, S., & Guilhot, B. (1999). Influence of finely ground limestone on cement hydration. *Cement and Concrete Composites*, 21, 99–105. Available from [https://doi.org/10.1016/S0958-9465\(98\)00020-1](https://doi.org/10.1016/S0958-9465(98)00020-1).
- Raghunath, P. N., Suguna, K., Karthick, J., & Sarathkumar, B. (2019). Mechanical and durability characteristics of marble-powder-based high-strength concrete. *Scientia Iranica A*, 26, 3159–3164. Available from <https://doi.org/10.24200/sci.2018.4953.1005>.
- Rana, A., Kalla, P., & Csetenyi, L. J. (2015). Sustainable use of marble slurry in concrete. *Journal of Cleaner Production*, 94, 304–311. Available from <https://doi.org/10.1016/j.jclepro.2015.01.053>.
- Rashwan, M. A., Al - Basiony, T. M., Mashaly, A. O., & Khalil, M. M. (2020). Behaviour of fresh and hardened concrete incorporating marble and granite sludge as cement replacement. *Journal of Building Engineering*, 32, 101697. Available from <https://doi.org/10.1016/j.jobbe.2020.101697>.
- Rodrigues, R., De Brito, J., & Sardinha, M. (2015). Mechanical properties of structural concrete containing very fine aggregates from marble cutting sludge. *Construction and Building Materials*, 77, 349–356. Available from <https://doi.org/10.1016/j.conbuildmat.2014.12.104>.
- Safiddine, S., Soualhi, H., Benabed, B., et al. (2021). Effect of different supplementary cementitious materials and superplasticizers on rheological behavior of eco-friendly mortars. *EPA—Journal of Silicate Based and Composite Materials*, 73, 119–129. Available from <https://doi.org/10.14382/epitoanyag-jsbcm.2021.18>.
- Sancheti, G., Jain, K. L., & Bhargava, S. (2020). Mechanical and durability performance of concrete made with waste marble and fly ash. *Jordan Journal of Civil Engineering*, 14, 305–318.

- Sardinha, M., de Brito, J., & Rodrigues, R. (2016). Durability properties of structural concrete containing very fine aggregates of marble sludge. *Construction and Building Materials*, *119*, 45–52. Available from <https://doi.org/10.1016/j.conbuildmat.2016.05.071>.
- Seghir, N. T., Mellas, M., Sadowski, Ł., et al. (2019). The utilization of waste marble dust as a cement replacement in air-cured mortar. *Sustainability*, *11*, 1–14. Available from <https://doi.org/10.3390/su11082215>.
- Selim, F. A., Hashem, F. S., & Amin, M. S. (2020). Mechanical, microstructural and acid resistance aspects of improved hardened Portland cement pastes incorporating marble dust and fine kaolinite sand. *Construction and Building Materials*, *251*, 118992. Available from <https://doi.org/10.1016/j.conbuildmat.2020.118992>.
- Senhadji, Y., Escadeillas, G., Mouli, M., et al. (2014). Influence of natural pozzolan, silica fume and limestone fine on strength, acid resistance and microstructure of mortar. *Powder Technology*, *254*, 314–323. Available from <https://doi.org/10.1016/j.powtec.2014.01.046>.
- Shafaatian, S. M. H., Akhavan, A., Maraghechi, H., & Rajabipour, F. (2013). How does fly ash mitigate alkali-silica reaction (ASR) in accelerated mortar bar test (ASTM C1567)? *Cement and Concrete Composites*, *37*, 143–153. Available from <https://doi.org/10.1016/j.cemconcomp.2012.11.004>.
- Sharobim, K., Hassan, H., & Ragheb, S. (2017). Durability improvement of self compacting recycled aggregate concrete using marble powder. *Port-Said Engineering Research Journal*, *21*, 68–77. Available from <https://doi.org/10.21608/pserj.2017.33292>.
- Siddique, R. (2013). Compressive strength, water absorption, sorptivity, abrasion resistance and permeability of self-compacting concrete containing coal bottom ash. *Construction and Building Materials*, *47*, 1444–1450. Available from <https://doi.org/10.1016/j.conbuildmat.2013.06.081>.
- Singh, M., Choudhary, K., Srivastava, A., et al. (2017a). A study on environmental and economic impacts of using waste marble powder in concrete. *Journal of Building Engineering*, *13*, 87–95. Available from <https://doi.org/10.1016/j.jobe.2017.07.009>.
- Singh, M., Srivastava, A., & Bhunia, D. (2017b). An investigation on effect of partial replacement of cement by waste marble slurry. *Construction and Building Materials*, *134*, 471–488. Available from <https://doi.org/10.1016/j.conbuildmat.2016.12.155>.
- Singh, M., Srivastava, A., & Bhunia, D. (2019). Long term strength and durability parameters of hardened concrete on partially replacing cement by dried waste marble powder slurry. *Construction and Building Materials*, *198*, 553–569. Available from <https://doi.org/10.1016/j.conbuildmat.2018.12.005>.
- Talah, A., Kharchi, F., & Chaid, R. (2015). Influence of marble powder on high performance concrete behavior. *Procedia Engineering*, *114*, 685–690. Available from <https://doi.org/10.1016/j.proeng.2015.08.010>.
- Tasdemir, C. (2003). Combined effects of mineral admixtures and curing conditions on the sorptivity coefficient of concrete. *Cement and Concrete Research*, *33*, 1637–1642. Available from [https://doi.org/10.1016/S0008-8846\(03\)00112-1](https://doi.org/10.1016/S0008-8846(03)00112-1).
- Tennich, M., Kallel, A., & Ben Ouedzou, M. (2015). Incorporation of fillers from marble and tile wastes in the composition of self-compacting concretes. *Construction and Building Materials*, *91*, 65–70. Available from <https://doi.org/10.1016/j.conbuildmat.2015.04.052>.
- Tennich, M., Ouedzou, M. B., & Kallel, A. (2020). Durabilité des bétons autoplaçants à base des déchets de marbre et de carrelage exposés à l'attaque du sulfate. *Journées Nationales Du Béton (JNB)*, 5–7.

- Thomas, M. (2011). The effect of supplementary cementing materials on alkali-silica reaction: A review. *Cement and Concrete Research*, *41*, 1224–1231. Available from <https://doi.org/10.1016/j.cemconres.2010.11.003>.
- Tian, B., & Cohen, M. D. (2000). Does gypsum formation during sulfate attack on concrete lead to expansion? *Cement and Concrete Research*, *30*, 117–123. Available from [https://doi.org/10.1016/S0008-8846\(99\)00211-2](https://doi.org/10.1016/S0008-8846(99)00211-2).
- Topçu, I. B., Bilir, T., & Uygunoğlu, T. (2009). Effect of waste marble dust content as filler on properties of self-compacting concrete. *Construction and Building Materials*, *23*, 1947–1953. Available from <https://doi.org/10.1016/j.conbuildmat.2008.09.007>.
- Toubal Seghir, N., Mellas, M., Sadowski, L., & Žak, A. (2018). Effects of marble powder on the properties of the air-cured blended cement paste. *Journal of Cleaner Production*, *183*, 858–868. Available from <https://doi.org/10.1016/j.jclepro.2018.01.267>.
- Tugrul Tunc, E. (2019). Recycling of marble waste: A review based on strength of concrete containing marble waste. *Journal of Environmental Management*, *231*, 86–97. Available from <https://doi.org/10.1016/j.jenvman.2018.10.034>.
- Ulubeyli, G. C., Bilir, T., & Artir, R. (2016). Durability properties of concrete produced by marble waste as aggregate or mineral additives. *Procedia Engineering*, *161*, 543–548. Available from <https://doi.org/10.1016/j.proeng.2016.08.689>.
- Uygunoglu, T., Topçu, I. B., & Çelik, A. G. (2014). Use of waste marble and recycled aggregates in self-compacting concrete for environmental sustainability. *Journal of Cleaner Production*, *84*, 691–700. Available from <https://doi.org/10.1016/j.jclepro.2014.06.019>.
- Uygunoglu, T., Topcu, I. B., Gencel, O., & Brostow, W. (2012). The effect of fly ash content and types of aggregates on the properties of pre-fabricated concrete interlocking blocks (PCIBs). *Construction and Building Materials*, *30*, 180–187. Available from <https://doi.org/10.1016/j.conbuildmat.2011.12.020>.
- Uysal, M., & Sumer, M. (2011). Performance of self-compacting concrete containing different mineral admixtures. *Construction and Building Materials*, *25*, 4112–4120. Available from <https://doi.org/10.1016/j.conbuildmat.2011.04.032>.
- Uysal, M., & Yilmaz, K. (2011). Effect of mineral admixtures on properties of self-compacting concrete. *Cement and Concrete Composites*, *33*, 771–776. Available from <https://doi.org/10.1016/j.cemconcomp.2011.04.005>.
- Valdez, P., Barragán, B., Girbes, I., et al. (2011). Uso de residuos de la industria del mármol como filler para la producción de hormigones autocompactantes. *Construction Materials*, *61*, 61–76. Available from <https://doi.org/10.3989/mc.2010.55109>.
- Varadharajan, S. (2020). Determination of mechanical properties and environmental impact due to inclusion of flyash and marble waste powder in concrete. *Structures*, *25*, 613–630. Available from <https://doi.org/10.1016/j.istruc.2020.03.040>.
- Vardhan, K., Goyal, S., Siddique, R., & Singh, M. (2015). Mechanical properties and micro-structural analysis of cement mortar incorporating marble powder as partial replacement of cement. *Construction and Building Materials*, *96*, 615–621. Available from <https://doi.org/10.1016/j.conbuildmat.2015.08.071>.
- Vardhan, K., Siddique, R., & Goyal, S. (2019a). Strength, permeation and micro-structural characteristics of concrete incorporating waste marble. *Construction and Building Materials*, *203*, 45–55. Available from <https://doi.org/10.1016/j.conbuildmat.2019.01.079>.
- Vardhan, K., Siddique, R., & Goyal, S. (2019b). Influence of marble waste as partial replacement of fine aggregates on strength and drying shrinkage of concrete. *Construction and Building Materials*, *228*, 116730. Available from <https://doi.org/10.1016/j.conbuildmat.2019.116730>.



- Vijayalakshmi, M., Sekar, A. S. S., & Ganesh Prabhu, G. (2013). Strength and durability properties of concrete made with granite industry waste. *Construction and Building Materials*, 46, 1–7. Available from <https://doi.org/10.1016/j.conbuildmat.2013.04.018>.
- Wu, Y. F., Kazmi, S. M. S., Munir, M. J., et al. (2020). Effect of compression casting method on the compressive strength, elastic modulus and microstructure of rubber concrete. *Journal of Cleaner Production*, 264, 121746. Available from <https://doi.org/10.1016/j.jclepro.2020.121746>.
- Yamanel, K. (2015). *Investigation of Kayseri area properties of waste marble powder mortar*. Graduate School of Natural and Applied Sciences. Erciyes University.
- Yamanel, K., Durak, U., İlkentapa, S., Atabey, I. I., Karahan, O., & Duran, C. (2019). Influence of waste marble powder as a replacement of cement on the properties of mortar. *Revista De La Construcción. Journal of Construction*, 18, 290–300. Available from <https://doi.org/10.7764/rdlc.18.2.290>.
- Yang, K. H., Jung, Y. B., Cho, M. S., & Tae, S. H. (2015). Effect of supplementary cementitious materials on reduction of CO2 emissions from concrete. *Journal of Cleaner Production*, 103, 774–783. Available from <https://doi.org/10.1016/j.jclepro.2014.03.018>.
- Zhang, S., Cao, K., Wang, C., et al. (2020). Effect of silica fume and waste marble powder on the mechanical and durability properties of cellular concrete. *Construction and Building Materials*, 241, 117980. Available from <https://doi.org/10.1016/j.conbuildmat.2019.117980>.

# Gray cement, white cement, gypsum, and lime modified with graphite nanoparticles

10

*Mehmet Serkan Kirgiz*

Northwestern University, Chicago, IL, United States

## 10.1 Introduction

Currently, various industries would like to transform materials into construction materials with the help of nanotechnology (Raki et al., 2010). To make nanomaterial-reinforced cement-based composites with tailored mechanical properties the blending of different sorts of nanomaterials into Portland cement (PC) is a major success provided by nanotechnology for material science. Especially carbon-based nanomaterials, for example, carbon black, carbon nanofibers (De Jong & Geus, 2000; Zhou et al., 2009), graphite nanoparticles (GNPs) (Kirgiz, 2015, 2018; Kirgiz, 2018), graphene (Compton & Nguyen, 2010; Geim & Novoselov, 2007; Gómez-Navarro et al., 2010; Zhu et al., 2010), graphene nanoplates (Geim & Novoselov, 2007), graphene oxide (Geim & Novoselov, 2007; Marcano et al., 2010; Zhu et al., 2010), and reduced graphene oxide (Compton & Nguyen, 2010; Gómez-Navarro et al., 2010), have attracted enormous amounts of research effort (Kirgiz 2015a, 2015c, 2015b; Kirgiz, 2014, 2016) because of improvement effect of the carbon-based nanomaterials on physico-mechanico-chemical properties of PC. Carbon nanomaterial mainly consists of metallic carbon atoms which have powerful interfrictions between each other as well as a low density, a high Blaine specific surface area, and chemical properties which activate physicomachanical properties of cement-based materials (Kirgiz, 2018). However, carbon nanomaterials, especially GNPs, provide unique properties, for example, interfacing thermally/electrically (Bandaru et al., 2017; Compton & Nguyen, 2010; Zhu et al., 2010), self-cleaning (Compton & Nguyen, 2010; Wan et al., 2016; Zhu et al., 2010), self-sensing (Compton & Nguyen, 2010; Power et al., 2018; Zhu et al., 2010), and shielding electromagnetically (Compton & Nguyen, 2010; Zhu et al., 2010) for cement-based construction materials.

To make cement-based construction materials develop in terms of mechanical properties (Chen et al., 2011) and durability (Shamsaei et al., 2018), carbon-based nanopowders and fibers could be blended to cement parcel and mixing design of cement-based construction materials. This blending will provide novel properties,

for example, noticing of strength (Du et al., 2013) and monitoring of temperature changing (Han et al., 2015; Xu et al., 2018). The aim of this chapter is to transform PC, white cement, gypsum, and lime-based conventional mortars into high-technology mortars modified through GNPs.

## 10.2 Materials and methods

The materials used are PC, white cement, gypsum, lime, mortar sand, drinkable water, and GNPs. Table 10.1 gives details related to the materials.

**Table 10.1** Details related to the materials used; chemical components of the materials.

Chemical component (%)	Materials				
	Portland cement	White cement	Gypsum	Lime	Graphite nanoparticles
C	–	–	–	–	99.9
CaSO <sub>4</sub>	0–5	–	> 94	–	–
CaO	60–66	65–67	< 1 for free lime	< 56	–
CO <sub>2</sub>	–	–	–	< 44	–
SiO <sub>2</sub>	18–25	20–22	< 1	–	–
Al <sub>2</sub> O <sub>3</sub>	4–6	4–4.5	–	–	–
Fe <sub>2</sub> O <sub>3</sub>	1–3	0.2–0.3	–	–	–
MgO	0.5–1	1.5–2.5	–	–	–
SO <sub>3</sub>	1–2	2–2.5	–	–	–
Na <sub>2</sub> O	0.5–1.5	0.1–0.4	–	–	–
K <sub>2</sub> O	0.3–1	–	–	–	–
Cl <sup>-1</sup>	< 0.0001	–	< 0.01	–	–
Loss on ignition	< 0.5	< 0.1	< 0.3	< 1	0.1

### 10.2.1 Transforming of conventional binder into binder and mortar including graphite nanoparticles

Table 10.2 explains transforming of conventional binder into binder and mortar including GNPs. With the addition of GNPs, four mortar mixes were prepared. Also, four more mortar mixes were prepared without addition of GNPs. This means that the mortar without the addition of GNPs is the control specimen for the mortar made of the addition of GNPs.

**Table 10.2** Transforming Conventional Binder into Binder and Mortar Including Graphite Nanoparticles.

Types of binder		Portland cement (%)	White cement (%)	Gypsum (%)	Lime (%)	Graphite nanoparticles (%)
Conventional binders	Portland cement	100	0	0	0	0
	White cement	0	100	0	0	0
	Gypsum	0	0	100	0	0
	Lime	0	0	0	100	0
High-technology binders	Portland cement modified through graphite nanoparticles	100	0	0	0	0.22
	White cement modified through graphite nanoparticles	0	100	0	0	0.22
	Gypsum modified through graphite nanoparticles	0	0	100	0	0.22
	Lime modified through graphite nanoparticles	0	0	0	100	0.22

The mix proportions were 1 (binder): 3 (sand): 2 (water). Therefore the water to binder ratio was 0.5. The binder was PC, white cement, gypsum, or lime in the mortars. The quantity of GNPs used was  $1.3 \text{ kg/m}^3$  in the mixes (Table 10.2).

### 10.3 Casting, mixing, and specimen preparation

Target assets were chosen. The bending moment should not be less than 0.1 MPa on the 28th day and 0.3 MPa on the 180th day, and the compressive strength should not be less than 3 MPa on the 28th day and 3.5 MPa on the 180th day in both traditional binder mortar and binder mortar including GNPs. The size of the specimen was kept constant as prism  $50 \times 100 \times 200 \text{ mm}$ . Before putting the specimen in the mold the binder and sand or the binder and sand and GNPs in Table 10.2 were first mixed for 30 seconds in a steel bowl with a mixer at low speed. After that dry mixing, water was added into the bowl while the mixer was working to produce the mortar specimen. The mixer was mixed with the fresh mortar specimen at low speed for another 30 seconds and at high speed for a third 30 seconds. Then the mixer was stopped for 15 seconds to scrape down the mortar specimen from the inner side of the bowl. At the last stage of mixing the mixer was operated at high speed for 60 seconds. Later, with the mixing of the specimen the prism mold was filled with fresh mortar specimen (BS EN 197-1:2011, 2019). Subsequently the hardening process of the specimen occurred in the humidity cabinet for 24 hours; all mortar specimens were demolded and cured in a curing cabinet of water until characterization.

## 10.4 Characterization

The mechanical properties, which are the bending moment strength, the compressive strength, and the splitting tensile strength, were analyzed on the 28th day and 180th day in the temperature-controlled laboratory, where there are two computer-controlled-strength sets for the measurement of compressive strength, bending moment strength, and splitting tensile strength. The process in BS EN 197-1 and ASTM C1006/C1006M-20a for determination of the compressive strength, bending moment strength, and splitting tensile strength was followed (ASTM C1006/C1006M-20a, 2020; BS EN 197-1:2011, 2019). For each mixture at each age, five mortar specimens were tested and the average was taken to be the representative strength. To evaluate relationships between the properties of mortar and present math equations, regression analysis was used.

## 10.5 Results and discussion

### 10.5.1 Compressive strength

As shown in Fig. 10.1, mortars including up to 0.22% GNP have greater compressive strength than the mortar with 0% GNP for a curing period of 28 days. As the water-to-binder ratio of 0.50 is constant for all mortars and is sufficient for the quantity of mixture constituents, the mortar with 0.22% GNP showed higher 28th-day compressive strength results than the mortar without the GNP (Fig. 10.1)

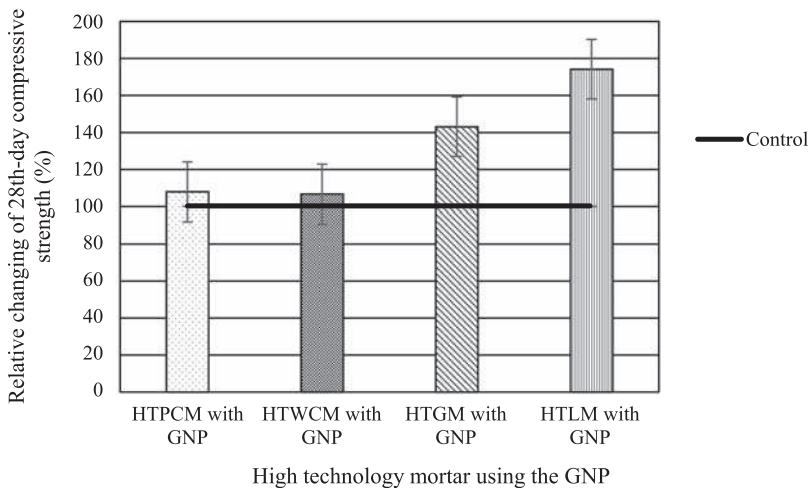


**Figure 10.1** The 28th-day relative compressive strength of mortar, the GNP content, and control mortar.

This means that there is a significant increase in the compressive strength because of the 0.22% GNP supplement. This could also be attributed to the GNPs' powerful effect on calcium hydroxide (CH) to make the CH transform into calcium carbon hydroxide. Fig. 10.2 shows the 180th-day relative compressive strength of mortar, the GNP content, and control mortar. The same strength gain trend at the 28th-day continued at the 180th-day compressive strength. The mortar including the GNPs has greater compressive strength than the mortar specimen which includes CEM type I 32.5N cement, the white cement, the gypsum binder, and the lime binder without the GNP at 180 days.

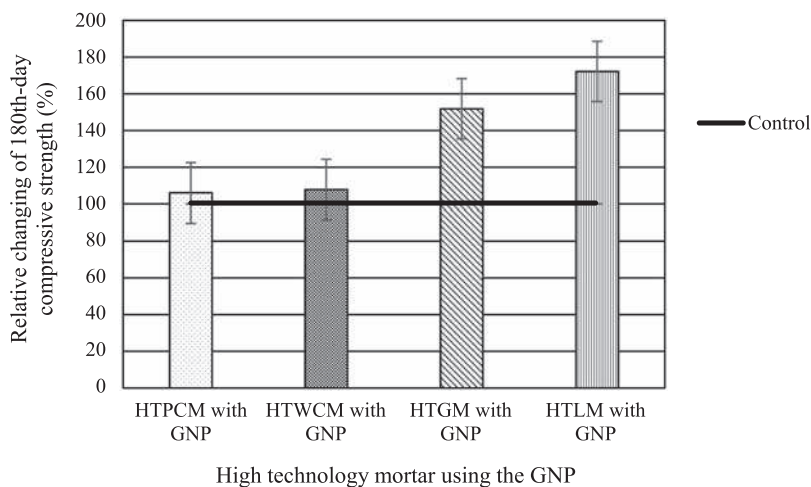


**Figure 10.2** The 180th-day relative compressive strength of mortar, the GNP content, and control mortar.

Moreover, based on the compressive strength results the 0.22% GNP supplement produced a maximum compressive strength of 35.1 and 40 MPa for the CEM type I 32.5N mortar at 28 and 180 days, respectively. Therefore from the practical and economical point of view, it can be concluded that the 0.22% GNP is a significant activator for both the PC binder and the gypsum binder and the lime binder. The compressive strength in the mortar containing the GNPs is referred to both the continued hydration of PC and the activation reaction between the GNP and the CH component of the binder, regardless of binder type. The above results support the findings of Khayat and Meng, who reported that ultra-high-strength concrete containing the GNP supplement yields ultrapowerful compressive strength. The data indicate that the unit weight decreases with an increase in ash content. This is because of the low specific gravity of the incinerator ash compared to the sand replaced. However, the decrease beyond 20% incinerator ash is insignificant (Meng & Khayat, 2016).

## 10.6 Mathematical model for estimation of compressive strength

In a current paper, Popovics et al. recommended a clear experimental evidence that compressive strength is dependent on the composition of cement-based materials. Various materials need various calibration curves, and additional regression results addressed the complex properties of mortar, such as compact ability and dispersion ability of the composition (Popovics et al., 1990). The conclusion of Popovics's research on regressions between the properties of cement-based materials is that some additional properties have to be measured, for example, compressive strength, bending moment, and splitting tensile strength. Recently, several studies on relationships between compressive strength and bending moment of cement and concrete materials have been published (ACI Committee, 1997; Ahmed et al., 2008; Geron & Paultre, 2000; Mindess et al., 2003). In those studies, compressive strength is estimated from bending moment, whose mathematical models are of either power law or exponential function. It is pointed out that the suggested regression should be just used for similar compositions of cement-based materials. In the presence of the literature overview on strength estimation, it is pointed out that there exist some limitations regarding the possibility of establishing a general relation between compressive strength and bending moment for cement, lime, and gypsum-based materials in terms of change in mixture constituents, different curing conditions, different binder types, and different SCMs added. Therefore the chapter could fill the gap in strength estimation of various conventional binders as well as conventional binders including the GNPs. Fig. 10.3 shows the regression relationship between compressive strength and bending moment at 28 days, estimation of the math equation of compressive strength from bending moment, and r square for math models of binder mortars including the GNPs.

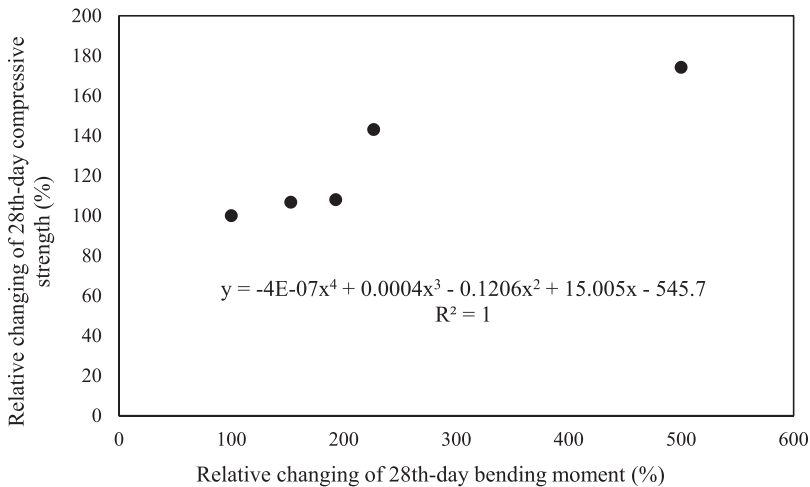


**Figure 10.3** Regression relationship between compressive strength and bending moment at 28 days, estimation of the math equation of compressive strength from bending moment, and r square for math models of binder mortars including the GNPs.

Fig. 10.4 shows the regression relationship between compressive strength and bending moment at 180 days, estimation of the math equation of compressive strength from bending moment, and  $r$  square for math models of binder mortars including the GNPs. Furthermore, it is possible to use the equations in Figs. 10.3 and 10.4 to validate future works in relation to the strength estimation. Figs. 10.3 and 10.4 also solve the need for standard correlation between the compressive strength and bending moment of binder-based mortar with the GNPs.

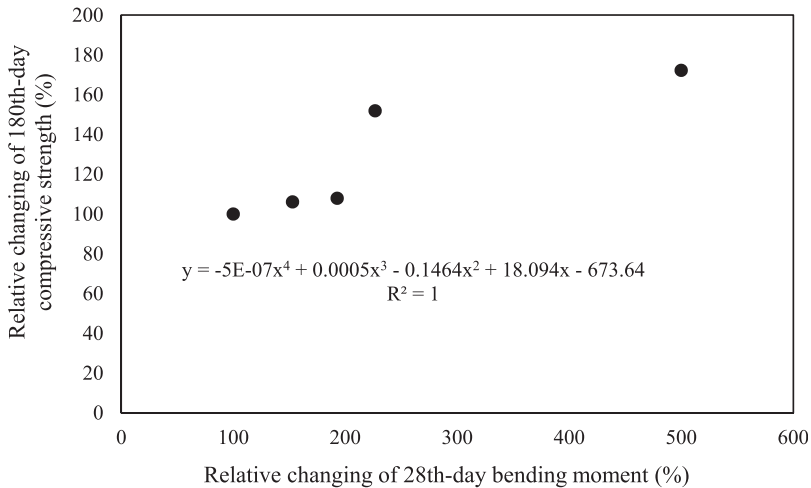


**Figure 10.4** Regression relationship between compressive strength and bending moment at 180 days, estimation of the math equation of compressive strength from bending moment, and  $r$  square for math models of binder mortars including the GNPs.

Here,  $x$  is the relative bending moment of mortar and  $y$  stands for the 28th-day/180th-day relative compressive strength. Maximum  $r^2$  is 1 at the age of both 28 and 180 days. The degree of regression is a forceful indicator for the presence of a reliable relationship and the degree of relationship. As could be understood from equations the fourth-degree mathematical equations depend on the compressive strength results of mortar obtained at 28 and 180 days.

## 10.7 Bending moment

Mortar is a highly complex heterogeneous material whose answer to moment related to not only the answer of the individual constituents but also the friction between those constituents. The microstructure of mortar in the presence of a broad



dispersion of aggregate pieces can differ from bulk pieces to binders and supplementary particles, which turns out to be the interfacial transition zone (ITZ). The ITZ is a key feature for hardness, bending moment, and capillarity of binder-based mortar including fine mortar sand due to its generally lower density and decreased strength when compared to that of provided bulk binder cement matrix (Kırgız, 2020). Fig. 10.5 shows the relative bending moment of mortar made of the addition of GNPs and the relative bending moment of control mortar with no addition of GNPs at 28 days and the content of the GNP.

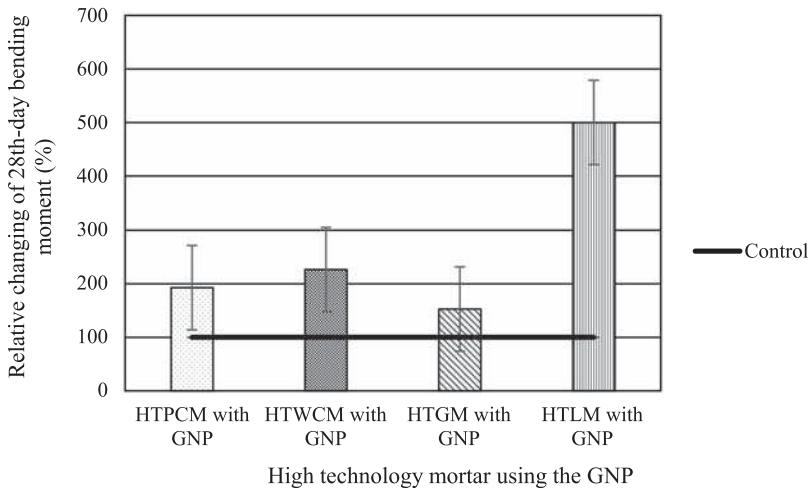


**Figure 10.5** Relative bending moment of mortar made of the addition of the GNPs and relative bending moment of control mortar with no addition of the GNPs at 28 days and the content of the GNPs.

Supplementing of 0.22% GNP increases the 28th-day bending moment from 1.4, 1.5, 1.7, and 0.1 MPa to 2.7, 3.4, 2.6, and 0.5 MPa for the PC mortar, the white cement mortar, the gypsum mortar, and the lime mortar, respectively (Fig. 10.5). At 28 days, adding 0.22% GNP for mortars made of 100% CEM I 32.5N cement leads to 92% increase in the bending moment, and beyond this increase a remarkable hardness is observed. The bending moment of mortar containing white cement gets increased up to 266.67% with the addition of 0.22% GNP. The comparative increments in bending moment of 100% gypsum and 100% lime mortars with 0.22% GNP are recorded as 52.9% and 500%, respectively. Fig. 10.6 shows the relative bending moment of the mortar with the addition of the GNPs and the relative bending moment of control mortar with no addition of the GNPs at 180 days and the content of the GNPs.

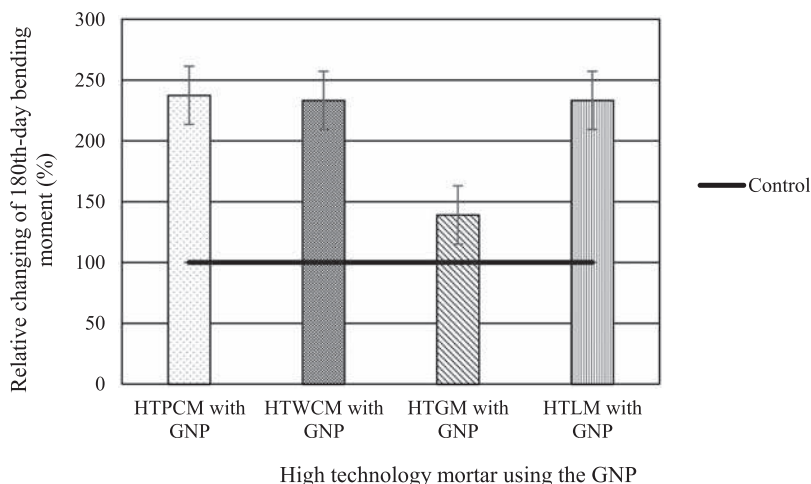


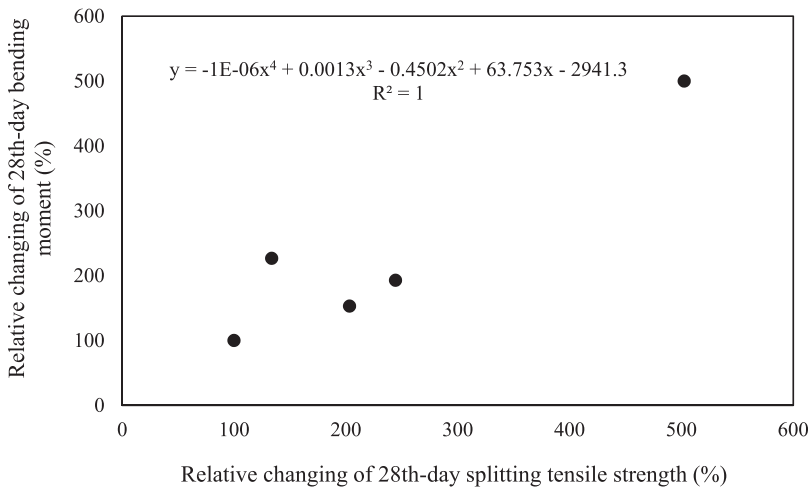
**Figure 10.6** Relative bending moment of mortar made of the addition of the GNPs and relative bending moment of control mortar with no addition of the GNPs at 180 days and the content of the GNPs.

Additionally, similar growth of the 28th-day bending moment is provided by the GNP supplement for the 180th-day bending moment of mortar. The 0.22% GNP also increases the 180th-day bending moment strength from 1.6, 1.8, 2.3, and 0.3 MPa to 3.8, 4.2, 3.2, and 0.7 MPa for the PC mortar, the white cement mortar, the gypsum mortar, and the lime mortar, respectively (Fig. 10.6). At 180 days, adding 0.22% GNP for mortars made of 100% CEM I 32.5N cement leads to 237.5% increase in the bending moment, and similar to this increase a remarkable growth is observed. The bending moment of mortar containing white cement gets increased up to 233.3% with the addition of 0.22% GNP. The comparative increments in bending moment strength of 100% gypsum and 100% lime mortars with 0.22% GNP are recorded as 39.1% and 233.3%, respectively. For better understanding the effect of 0.22% GNP on the bending moment strength of mortar the work presented a comparison between the results of 28th-day bending moment and 180th-day bending moment in Figs. 10.5 and 10.6. The effect of addition 0.22% GNP on bending moment from 28 to 180 days in water curing is measured as 40.7% increment for 100% CEM I 32.5N mortar, 23.5% increment for 100% white cement mortar, 23% increase for 100% gypsum mortar, and 40% growth for 100% lime mortar. This increment argument is in line with other research studies where the GNPs led to a higher bending moment than zirconium-based (Phrompet et al., 2019; Fattahi et al., 2020) and titanium-based (Nayebi et al., 2020; Shahedi Asl et al., 2020) high-performance ceramics due to the metallic structure of GNPs (Istgaldi et al., 2020; Pourmohammadie Vafa et al., 2020; Shahedi Asl et al., 2019). Additionally the observed highest bending moment strength of mortar composite with 0.22% GNP addition is also in line with other existing results, demonstrating better bending

moment properties through the GNP addition for high-performance ceramic composites. The authors evaluated the properties of Al-Mg-Si alloy-based composites modified with steel, steel–graphite hybrid mixing, and SiC powder (Alaneme et al., 2019). Their results revealed that the stiffness of the composite rose by about 11% along with a rise in steel powder from 4% to 8% and the stress in the composite with 8% steel powder and compressive, bending, and splitting tensile strengths was greater than that of the composite modified with 8% SiC powder. The results are attributed to the fact that SiC is tailored by steel powder, which also contains carbon element and could enhance grain refinement and interface bonding and the inherent ductility of solid. The last study carried out by Kurian et al. is on the need of multifunctional flexible and stretchable graphite–silicone rubber composites (Kurian et al., 2020). They have studied mechanical properties of graphite (GRP) flakes and an elastomer–silicone rubber to manufacture conductive flexible films electrically. They have found the fact that the GRP develops not only mechanical properties of flexible films but also electrical conductivity and thermal conductivity positively.

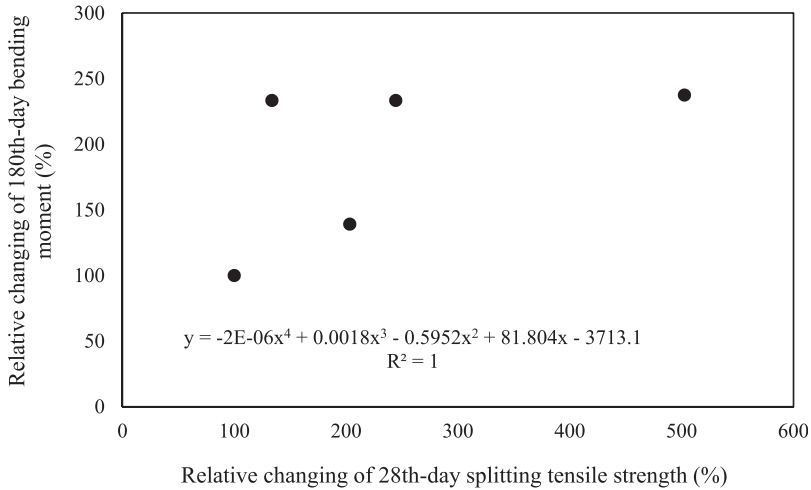
## 10.8 Mathematical model for prediction of bending moment

Fig. 10.7 shows correlation between the 28th-day bending moment and the splitting tensile strength measured. The suggested math model for prediction of 28th-day bending moment from splitting tensile strength is demonstrated in Fig. 10.7.



**Figure 10.7** Regression relationship between bending moment and splitting tensile strength at 28 days, estimation of the math equation of bending moment from splitting tensile strength, and r square for math models of binder mortars including the GNPs.

Maximum  $r^2$  is 1 at the age of 28 days. The degree of regression as  $r^2$  is a forceful indicator for the presence of relationship and the degree of relationship. As could be understood from the equation in Fig. 10.7 the fourth-degree mathematical equation depends on the bending moment results of mortar obtained. Fig. 10.8 shows correlation between the 180th-day bending moment and the splitting tensile strength measured. The suggested math model for prediction of 180th-day bending moment from splitting tensile strength is demonstrated in the equation in Fig. 10.8.



**Figure 10.8** Regression relationship between bending moment and splitting tensile strength at 180 days, estimation of the math equation of bending moment from splitting tensile strength, and  $r$  square for math models of binder mortars including the GNPs.

Maximum  $r^2$  is 1 at the age of 180 days. The degree of regression as  $r^2$  is a forceful indicator for the presence of relationship and the degree of relationship. As could be understood from the equation in Fig. 10.8 the fourth-degree mathematical equation depends on the bending moment results of mortar obtained at 180 days. Considering the activation effect of the GNPs on the conventional binder and mortar the GNP is developed for the aggregate interlock, thereby increasing the early and overall bending moment. The bending moment of the mortar including the GNPs was found over the range of those of the conventional mortar made of PC, white cement, gypsum, and lime. This pointed out that the aggregate interlock, along with the compressive strength, helps in improving the bending moment in mortar structures. The polynomial-type equations were found to be suitable in predicting the bending moment of the mortar. A significant development was observed in the estimation of bending moment when a number of curing days were considered. Further study on the effect of other factors such as strength levels, aggregate properties and mineralogy, admixture types, specimen moisture content, compaction

and curing conditions, and specimen geometry on the bending moment of the mortar should be conducted to better understand their effects and achieve more accurate estimating equations.

## 10.9 Splitting tensile strength

As shown in Fig. 10.9, mortars including up to 0.22% GNP have greater splitting tensile strength than the mortar with no the addition of the GNPs for a curing period of 28 days. As the water-to-binder ratio of 0.50 is constant for all mortars and is sufficient for the quantity of mixture constituents, the mortar with 0.22% GNP showed higher 28th-day splitting tensile strength results than the mortar without the GNPs (Fig. 10.9).

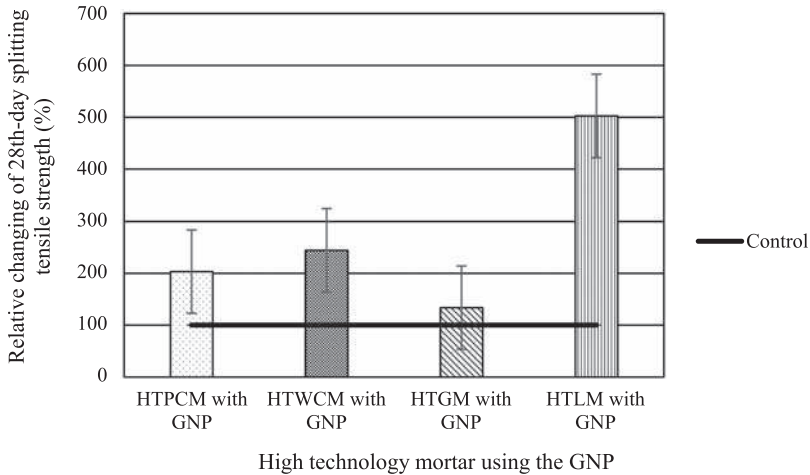


**Figure 10.9** Relative splitting tensile strength of mortar made of the addition of the GNPs and relative bending moment of control mortar with no addition of the GNPs at 28 days and the content of the GNP.

At 28 days, adding 0.22% GNP for mortar made of 100% CEM I 32.5N cement leads to 103.2% increase in the splitting tensile strength, and beyond this increase a remarkable hardness is observed. The splitting tensile strength of mortar containing white cement gets increased up to 144.4% with the addition of 0.22% GNP. The comparative increments in splitting tensile strength of 100% gypsum and 100% lime mortars with 0.22% GNP are recorded as 33.2% and 500%, respectively. This means that there is a significant increase in the splitting tensile strength because of the 0.22% GNP supplement. This could also be attributed to the GNPs' powerful effect on calcium hydroxide (CH) to make the CH transform into calcium carbon

hydroxide. Fig. 10.10 shows the 180th-day splitting tensile strength of mortar, the GNP content, and control mortar. The same strength gain trend at the 28th day continued at the 180th-day splitting tensile strength. The mortar including the GNPs has greater splitting tensile strength than the mortar specimen which includes CEM type I 32.5N cement, the white cement, the gypsum binder, and the lime binder without the GNPs at 180 days.

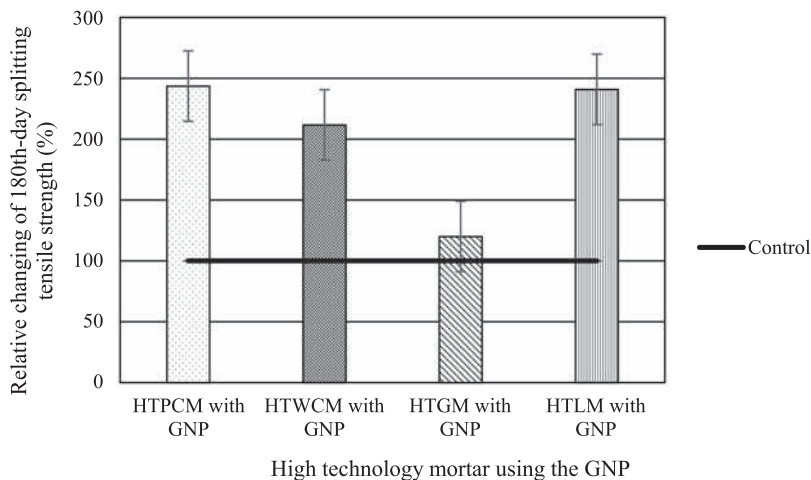


**Figure 10.10** Relative splitting tensile strength of mortar made of the addition of the GNPs and relative bending moment of control mortar with no addition of the GNPs at 180 days and the content of the GNPs.

Additionally, similar growth of the 28th-days splitting tensile strength is provided by the GNP supplement for the 180th-day splitting tensile strength of mortar. At 180 days, adding 0.22% GNP for mortar made of 100% CEM I 32.5N cement leads to 143.6% increase in the splitting tensile strength, and similar to this increase a remarkable growth is observed. The splitting tensile strength of mortar containing white cement gets increased up to 111.7% with the addition of 0.22% GNP. The comparative increments in splitting tensile strength of 100% gypsum and 100% lime mortars with 0.22% GNP are recorded as 20% and 140.9%, respectively. For better understanding the effect of 0.22% GNP on the splitting tensile strength of mortar the work presented a comparison between the results of 28th-days splitting tensile strength and 180th-days splitting tensile strength in Figs. 10.9 and 10.10. The effect of adding 0.22% GNP on splitting tensile strength from 28 days to 180 days in water curing is measured as 22.7% increment for 100% CEM I 32.5N mortar, 15.6% increment for 100% white cement mortar, 10.8% increase for 100% gypsum mortar, and 40% growth for 100% lime mortar.

## 10.10 Mathematical model for estimation of splitting tensile strength

Fig. 10.11 shows regression relationship between splitting tensile strength and compressive strength at 180 days, estimation of the math equation of splitting tensile strength from compressive strength, and  $r$  square for math models of binder mortars including the GNPs. In the current paper, plenty of studies on the relationship between splitting tensile strength and compressive strength of cement-based materials are summarized (ACI Committee 318, 1999; Carino & Lew, 1982; Carneiro & Barcellos, 1953; Comite European du Beton, 1990; Gardner et al., 1988; Oluokun et al., 1991; Raphael, 1984). In those studies, splitting tensile strength is estimated from compressive strength, whose mathematical models are of either power law or exponential function. It is pointed out that the suggested regression should be just used for similar compositions of cement-based materials. In the presence of the literature overview on strength estimation, it is pointed out that there exist some limitations regarding the possibility of establishing a general relation between splitting tensile strength and compressive strength for cement, lime, and gypsum-based materials in terms of change in mixture constituents, different curing conditions, different binder types, and different SCMs added. Therefore the chapter could fill the gap in splitting tensile strength estimation of various conventional binders as well as conventional binders including the GNPs.

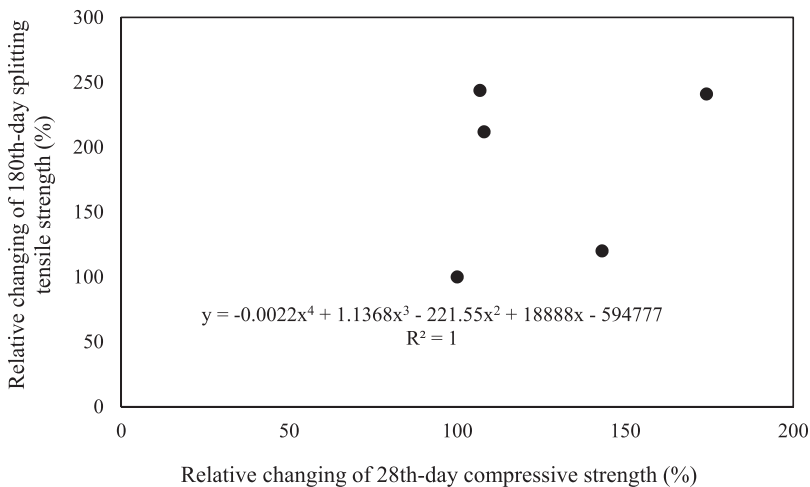


**Figure 10.11** Regression relationship between splitting tensile strength and compressive strength at 180 days, estimation of the math equation of splitting tensile strength from compressive strength, and  $r$  square for math models of binder mortars including the GNPs.

Maximum  $r^2$  is 1 at the age of 180 days. The degree of regression as  $r^2$  is a forceful indicator for the presence of relationship and the degree of relationship. As could be understood from the equation in Fig. 10.11 the fourth-degree mathematical equation depends on the compressive strength results of mortar obtained at 180 days. Considering the activation effect of the GNPs on the conventional binder and mortar the GNPs are transformed from CH to CCH, thereby increasing the early and overall splitting tensile strength. The splitting tensile strength of the mortar including the GNPs was found over the range of conventional mortars made of PC, white cement, gypsum, and lime. This pointed out that the type of binder, along with the compressive strength, helps in improving the splitting tensile strength in mortar structures. The polynomial-type equations were found to be suitable in predicting the splitting tensile strength of the mortar. A significant development was observed in the estimation of splitting tensile strength when a number of curing days were considered.

## 10.11 Conclusion

In this work, various mortar mixtures were employed, which helped obtain compressive strength, bending moment, and splitting tensile strength relatively as well as a general trend in the relationship between compressive strength and bending moment and splitting tensile strength of the cement-based materials in the literature and the relationships between the compressive strength and bending moment and splitting tensile strength of mortars with and without the addition of the GNPs.

The effect of activation of the GNPs on the binder and mortar is significant as the ITZ can be improved, thereby increasing the early and overall strengths. The compressive strength, bending moment, and splitting tensile strength of the mortar with the GNPs were found over the range of those of the conventional mortar without addition of the GNPs. This pointed out that the transforming effect of the GNPs from CH to CCH helps in developing the strengths in the structure of mortar. The polynomial-type equation was found to be suitable in estimating the compressive strength, bending moment, and splitting tensile strength of the mortar. Considering the estimation of the equation of the strengths the curing day was found to be necessary. The most significant development was observed in the compressive strength since the GNPs increased the compressive strength from 32.5 MPa to 40 MPa in the PC mortar from the curing day of 28–180. This means that CEM I 32.5N cement can be used instead of CEM I 42.5N cement.

## References

- ACI Committee. (1997). *State-of-the-art report on highstrength concrete*. ACI 363R-92. American Concrete Institute, Farmington Hills.
- ACI Committee 318. (1999). *Building code requirements for structural concrete*. American Concrete Institute.



- Ahmed, M., Dad Khan, M. K., & Wamiq, M. (2008). Effect of concrete cracking on the lateral response of RCC buildings. *Asian Journal of Civil Engineering Building and Housing*, 9(1), 25–34.
- Alaneme, K. K., Fajemisin, A. V., & Maledi, N. B. (2019). Development of aluminium-based composites reinforced with steel and graphite particles: Structural, mechanical and wear characterization. *Journal of Materials Research and Technology*, 8(1), 670–682. Available from <https://doi.org/10.1016/j.jmrt.2018.04.019>.
- ASTM C1006/C1006M-20a. (2020). *Standard test method for splitting tensile strength of masonry units*. ASTM International.
- Bandaru, P. R., Yamada, H., Narayanan, R., & Hoefler, M. (2017). The role of defects and dimensionality in influencing the charge, capacitance, and energy storage of graphene and 2D materials. *Nanotechnology Reviews*, 6(5), 421–433. Available from <https://doi.org/10.1515/ntrev-2016-0099>.
- BS EN 197-1:2011. (2019). *Cement composition, specifications and conformity criteria for common cements*. British Standards Institution.
- Carino, N. J., & Lew, H. S. (1982). Re-examination of the relation between splitting tensile and compressive strength of normal weight concrete. *ACI Journal Proceedings*, 79(3).
- Carneiro, F.L. L., & Barcellos, A. (1953). Tensile strength of concrete. RILEM Bulletin No. 13. *Union of testing and research laboratories for materials and structures*.
- Chen, S. J., Collins, F. G., Macleod, A. J. N., Pan, Z., Duan, W. H., & Wang, C. M. (2011). Carbon nanotube-cement composites: A retrospect. *IES Journal Part A: Civil and Structural Engineering*, 4(4), 254–265. Available from <https://doi.org/10.1080/19373260.2011.615474>.
- Comite European du Beton. (1990). CEB-FIP model code for concrete structures: Evaluation of the time dependent behaviour of concrete. *Bulletin d'Information*.
- Compton, O. C., & Nguyen, S. T. (2010). Graphene oxide, highly reduced graphene oxide, and graphene: Versatile building blocks for carbon-based materials. *Small (Weinheim an der Bergstrasse, Germany)*, 6(6), 711–723. Available from <https://doi.org/10.1002/sml.200901934>.
- De Jong, K. P., & Geus, J. W. (2000). Carbon nanofibers: Catalytic synthesis and applications. *Catalysis Reviews—Science and Engineering*, 42(4), 481–510. Available from <https://doi.org/10.1081/CR-100101954>.
- Du, H., Quek, S.T., & Pang, S.D. (2013). Smart multifunctional cement mortar containing graphite nanoplatelet. In *Proceedings of SPIE—The international society for optical engineering* (Vol. 8692). <https://doi.org/10.1117/12.2009005>.
- Fattahi, M., Babapoor, A., Delbari, S. A., Ahmadi, Z., Sabahi Namini, A., & Shahedi Asl, M. (2020). Strengthening of TiC ceramics sintered by spark plasma via nano-graphite addition. *Ceramics International*, 46(8), 12400–12408. Available from <https://doi.org/10.1016/j.ceramint.2020.01.291>.
- Gardner, N. J., Sau, P. L., & Cheung, M. S. (1988). Strength development and durability of concretes cast and cured at 0 C. *ACI Materials Journal*, 85(6), 529–536.
- Geim, A. K., & Novoselov, K. S. (2007). The rise of graphene. *Nature Materials*, 6(3), 183–191. Available from <https://doi.org/10.1038/nmat1849>.
- Geron, F. D. R. L., & Paultre, P. (2000). Prediction of modulus of rupture of concrete. *ACI Structural Journal*, 97(2), 193–200.
- Gómez-Navarro, C., Meyer, J. C., Sundaram, R. S., Chuvilin, A., Kurasch, S., Burghard, M., Kern, K., & Kaiser, U. (2010). Atomic structure of reduced graphene oxide. *Nano Letters*, 10(4), 1144–1148. Available from <https://doi.org/10.1021/nl9031617>.
- Han, B., Sun, S., Ding, S., Zhang, L., Yu, X., & Ou, J. (2015). Review of nanocarbon-engineered multifunctional cementitious composites. *Composites Part A: Applied Science*

- and Manufacturing*, 70, 69–81. Available from <https://doi.org/10.1016/j.compositesa.2014.12.002>.
- Istgaldi, H., Shahedi Asl, M., Shahi, P., Nayebi, B., & Ahmadi, Z. (2020). Solid solution formation during spark plasma sintering of ZrB<sub>2</sub>–TiC–graphite composites. *Ceramics International*, 46(3), 2923–2930. Available from <https://doi.org/10.1016/j.ceramint.2019.09.287>.
- Kirgiz, M. S. (2015). Advance treatment by nanographite for Portland pulverised fly ash cement (the class F) systems. *Composites Part B: Engineering*, 82, 59–71. Available from <https://doi.org/10.1016/j.compositesb.2015.08.003>.
- Kirgiz, M. S. (2016). Advancements in mechanical and physical properties for marble powder-cement composites strengthened by nanostructured graphite particles. *Mechanics of Materials*, 92, 223–234. Available from <https://doi.org/10.1016/j.mechmat.2015.09.013>.
- Kirgiz, M. S. (2014). Advances in physical properties of C class fly ash cement systems blended nanographite - Part 1. *ZKG International*, 67(12), 42–48. Available from <http://www.zkg-online.info/en/index.html>.
- Kirgiz, M. S. (2018). Pulverized fuel ash cement activated by nanographite. *ACI Materials Journal*, 115(6), 803–812. Available from <https://doi.org/10.14359/51689101>.
- Kirgiz, M. S. (2020). *Nano size particle packing for nanoconcretes and cement based materials: Mathematical models, theory, and technology. Smart nanoconcretes and cement-based materials*. Elsevier. Available from <https://doi.org/10.1016/B978-0-12-817854-6.00003-9>.
- Kirgiz, M. S. (2015a). Advances in physical properties of C class fly ash–cement systems blended nanographite- Part 2. *ZKG International*, 60–67.
- Kirgiz, M. S. (2018). Green cement composite concept reinforced by graphite nano-engineered particle suspension for infrastructure renewal material. *Composites Part B: Engineering*, 154, 423–429. Available from <https://doi.org/10.1016/j.compositesb.2018.09.012>.
- Kirgiz, M. S. (2015b). Supernatant nanographite solution for advance treatment of C class fly ash–cement systems—Part 1. *ZKG International*, 56–65.
- Kirgiz, M. S. (2015c). Supernatant nanographite solution for advance treatment of C class fly ash–cement systems—Part 2. *ZKG International*, 42–47.
- Kurian, A. S., Mohan, V. B., Souri, H., Leng, J., & Bhattacharyya, D. (2020). Multifunctional flexible and stretchable graphite-silicone rubber composites. *Journal of Materials Research and Technology*, 9(6), 15621–15630. Available from <https://doi.org/10.1016/j.jmrt.2020.11.021>.
- Marcano, D. C., Kosynkin, D. V., Berlin, J. M., Sinitiskii, A., Sun, Z., Slesarev, A., Alemany, L. B., Lu, W., & Tour, J. M. (2010). Improved synthesis of graphene oxide. *ACS Nano*, 4(8), 4806–4814. Available from <https://doi.org/10.1021/nn1006368>.
- Meng, W., & Khayat, K. H. (2016). Mechanical properties of ultra-high-performance concrete enhanced with graphite nanoplatelets and carbon nanofibers. *Composites Part B: Engineering*, 107, 113–122. Available from <https://doi.org/10.1016/j.compositesb.2016.09.069>.
- Mindess, S., Young, J., & Darwin, D. (2003). *Concrete* (2nd ed., pp. 1–644). Prentice Hall.
- Nayebi, B., Parvin, N., Aghazadeh Mohandesi, J., & Shahedi Asl, M. (2020). Densification and toughening mechanisms in spark plasma sintered ZrB<sub>2</sub>-based composites with zirconium and graphite additives. *Ceramics International*, 46(9), 13685–13694. Available from <https://doi.org/10.1016/j.ceramint.2020.02.156>.
- Oluokun, F. A., Burdette, E. G., & Deatherage, J. H. (1991). Splitting tensile strength and compressive strength relationship at early ages. *ACI Materials Journal*, 88(2), 115–121.
- Phrompet, C., Sriwong, Ruttanapun, & Mechanical, & Dielectric.. (2019). Thermal and anti-bacterial properties of reduced graphene oxide (rGO)-nanosized C3AH<sub>6</sub> cement nanocomposites for smart cement-based materials. *Composites Part B: Engineering*, 175.

- Popovics, S., Rose, J. L., & Popovics, J. S. (1990). The behaviour of ultrasonic pulses in concrete. *Cement and Concrete Research*, 20(2), 259–270. Available from [https://doi.org/10.1016/0008-8846\(90\)90079-D](https://doi.org/10.1016/0008-8846(90)90079-D).
- Pourmohammadie Vafa, N., Ghassemi Kakroudi, M., & Shahedi Asl, M. (2020). Advantages and disadvantages of graphite addition on the characteristics of hot-pressed ZrB<sub>2</sub>–SiC composites. *Ceramics International*, 46(7), 8561–8566. Available from <https://doi.org/10.1016/j.ceramint.2019.12.086>.
- Power, A. C., Gorey, B., Chandra, S., & Chapman, J. (2018). Carbon nanomaterials and their application to electrochemical sensors: A review. *Nanotechnology Reviews*, 7(1), 19–41. Available from <https://doi.org/10.1515/ntrev-2017-0160>.
- Raki, L., Beaudoin, J., Alizadeh, R., Makar, J., & Sato, T. (2010). Cement and concrete nanoscience and nanotechnology. *Materials*, 3(2), 918–942. Available from <https://doi.org/10.3390/ma3020918>.
- Raphael, J. M. (1984). Tensile strength of concrete. *Journal of the American Concrete Institute*, 81(2), 158–165.
- Shahedi Asl, M., Nayeibi, B., Motallebzadeh, A., & Shokouhimehr, M. (2019). Nanoindentation and nanostructural characterization of ZrB<sub>2</sub>–SiC composite doped with graphite nano-flakes. *Composites Part B: Engineering*, 175. Available from <https://doi.org/10.1016/j.compositesb.2019.107153>.
- Shahedi Asl, M., Pazhouhanfar, Y., Sabahi Namini, A., Shaddel, S., Fattahi, M., & Mohammadi, M. (2020). Role of graphite nano-flakes on the characteristics of ZrB<sub>2</sub>-based composites reinforced with SiC whiskers. *Diamond and Related Materials*, 105. Available from <https://doi.org/10.1016/j.diamond.2020.107786>.
- Shamsaei, E., de Souza, F. B., Yao, X., Benhelal, E., Akbari, A., & Duan, W. (2018). Graphene-based nanosheets for stronger and more durable concrete: A review. *Construction and Building Materials*, 183, 642–660. Available from <https://doi.org/10.1016/j.conbuildmat.2018.06.201>.
- Wan, S., Bi, H., & Sun, L. (2016). Graphene and carbon-based nanomaterials as highly efficient adsorbents for oils and organic solvents. *Nanotechnology Reviews*, 5(1), 3–22. Available from <https://doi.org/10.1515/ntrev-2015-0062>.
- Xu, Y., Zeng, J., Chen, W., Jin, R., Li, B., & Pan, Z. (2018). A holistic review of cement composites reinforced with graphene oxide. *Construction and Building Materials*, 171, 291–302. Available from <https://doi.org/10.1016/j.conbuildmat.2018.03.147>.
- Zhou, Z., Lai, C., Zhang, L., Qian, Y., Hou, H., Reneker, D. H., & Fong, H. (2009). Development of carbon nanofibers from aligned electrospun polyacrylonitrile nanofiber bundles and characterization of their microstructural, electrical, and mechanical properties. *Polymer*, 50(13), 2999–3006. Available from <https://doi.org/10.1016/j.polymer.2009.04.058>.
- Zhu, Y., Murali, S., Cai, W., Li, X., Suk, J. W., Potts, J. R., & Ruoff, R. S. (2010). Graphene and graphene oxide: Synthesis, properties, and applications. *Advanced Materials*, 22(35), 3906–3924. Available from <https://doi.org/10.1002/adma.201001068>.

# Calcined clay as hydraulic binder substitution



S. Kenai<sup>1</sup>, J. Khatib<sup>2</sup> and M. Ghrici<sup>3</sup>

<sup>1</sup>Civil Engineering Department, University Blida 1, Blida, Algeria, <sup>2</sup>Faculty of Engineering, Department of Civil and Environmental Engineering, Beirut Arab University, Beirut, Lebanon, <sup>3</sup>Civil Engineering Department, University of Chlef, Algeria

## 11.1 Introduction

Concrete has been widely used in the construction industry due to its simple production process, low price, and generally good performance. However, the cement industry consumes high energy and emits a high amount of CO<sub>2</sub> into the atmosphere, which is estimated at about 7% of carbon dioxide production worldwide. The partial replacement of cement by mineral admixtures such as fly ash, silica fume, blast furnace slag, or natural pozzolana in cementing materials (mortar or concrete) would help to overcome these problems and lead to improvement in the workability, strength, and durability of cementing materials.

Calcined clays are more promising than other mineral additions such as slag, fly ash, and natural pozzolana as their global suppliers are limited compared to cement production worldwide (Avet et al., 2016). Clay is widely available and if calcined it could be used as a cement substitution. When heated to about 600°C–800°C, kaolinite clay produces a reactive amorphous phase (Fernandez et al., 2011). Calcined clay could be obtained from different types of clay, such as kaolinitic clay, but also could be obtained from waste calcined brick and can be used in concrete as cement or fine aggregate replacement (Khatib, 2005).

In Europe, according to the European Union report presented in 2011 the amount of construction and demolition waste generated annually in Europe is approximately 1 billion tons, including waste calcined clay brick (Manfredi et al., 2011). Pacheco-Torgal and Jalali (2010) also found that the amount of waste generated by the European ceramic industry was typically 3%–7% by weight of red clay brick total production, suggesting that millions of clay brick wastes were generated every year.

Therefore the ground calcined bricks has the potential to be used as eco-type cementitious materials, which could benefit the environment by increasing construction waste consumption and reducing CO<sub>2</sub> emission by cement industries (Zhao et al., 2020). It is widely reported that sintered clay brick can be used as a pozzolanic material, which is rich in pozzolanic ingredients. Recently, Olofinnade et al. (2018) found that various research efforts have examined the possibility of reusing comminuted clay brick waste generated by ceramic and brick industries and

from construction waste as pozzolanic material to partially replace cement in mortar and concrete.

This chapter describes the research carried out by several researchers to evaluate the effects of calcined clay either from kaolinite clays or from brick powder on the properties of fresh and hardened pastes, mortars, and concrete.

## 11.2 Materials

Clay is a widely spread material in the world, cheap, and easily accessible (Hewlett & Liska, 2019). At the same time, it is a material with a great diversity in terms of mineralogical composition; hence numerous literature items are devoted to the analysis of the possibility of using clays from specific deposits for the production of cement, bricks, and tiles.

Clay bricks are produced by the drying and firing of clay or shale raw material, forming a sintered porous structure. Clays are mixtures of clay minerals that are hydrated aluminosilicates from the chemical point of view. Kaolinite, illite, chlorite, halloysite, and montmorillonite are the most important clay minerals as far as ceramic technology is concerned (Navrátilová & Rovnaníková, 2016). High-grade kaolinitic clays, that is, clays with a composition to be useful in the ceramic (white-ware and refractory) industry and the paper industry, are expensive, and their availability is limited. Therefore more recent research on the use of clays in brick making has investigated low-grade kaolinitic clays (i.e., kaolinitic clays that are not in demand from the ceramic industry, often because of too high concentrations of minor elements and/or an insufficient kaolinite content) as well as clays with illite or smectite as the dominating clay mineral (Msinjili et al., 2021).

Alujas et al. (2015) indicated that most of the studies on calcined clays focused on the relationship between specific clay minerals (mainly kaolinite, montmorillonite, and illite), calcination temperatures, and pozzolanic reactivity. These studies have shown that kaolinite has the highest pozzolanic activity and a lower activation temperature, followed by montmorillonite, whereas illite, mixed layer illite/smectite, and sepiolites exhibit only moderate to low pozzolanic reactivity, even at high calcination temperatures.

The maximum firing temperature reached by most brick manufacturers is 1100°C, and depending on demand the bricks usually require between 36 and 48 hours in the kiln. In addition, Baronio and Bindat (1997) found that the temperature and duration of the treatment must be chosen very carefully as a function of the minerals contained in the clay. The heating during the brick production resulted in the altering of the primary composition of the raw clay by breaking down the crystalline structure and forming of silica and alumina in amorphous state.

The new trend to recycle clay brick waste is grinding it into clay brick powder (CBP). Previous research results have demonstrated the feasibility to use CBP as an eco-type supplementary material for its potential. CBP is generated by grinding and sieving crushed waste brick as shown in Fig. 11.1.



**Figure 11.1** Various cases of calcined clay brick (CCB). (A) The original CCB; (B) the crushed CCB; (C) the powder CCB.

After grinding the amorphous Al phase and Si phase in CBP can react with alkalis from cement hydration to form calcium silicate hydrate (CSH) and calcium aluminosilicate hydrate (Shao et al., 2019). In addition, Zhao et al. (2020) concluded that the reactivity of CBP was enhanced with the decrease of particle cement replacement size, and the finer CBP could accelerate the early-age hydration of cement.

The American Concrete Institute in its report ACI 232.1R-12, 2012 defines pozzolanic material as “siliceous and aluminous material, which in itself possesses little or no cementitious value but will, in finely divided form and in the presence of moisture, chemically react with calcium hydroxide at ordinary temperatures to form compounds possessing cementitious properties.” In order for the CBP material to be considered a pozzolanic material, it must meet the chemical and physical requirements of pozzolanic materials required by various countries (Table 11.1).

**Table 11.1** Chemical and physical requirements of pozzolanic materials.

Chemical and physical properties	ASTM C618 (2018)	CSA A3001-08 (2010)	JG/T 315 (2011)
SiO <sub>2</sub> + Al <sub>2</sub> O <sub>3</sub> + Fe <sub>2</sub> O <sub>3</sub> (min, %)	70.0	/	70.0
SO <sub>3</sub> (max, %)	4.0	3.0	3.5
Chloride content (max, %)	/	/	0.06
Moisture content (%) (max, %)	3.0	/	1.0
Loss on ignition (max, %)	10.0	10.0	8.0
Fineness: amount retained when wet-sieved on 45 μm sieve (max, %)	34.0	34.0	20.0
Strength activity index: with Portland cement, at 7 days (% of control) (min, %)	75.0	/	/
Strength activity index: with Portland cement, at 28 days (% of control) (min, %)	75.0	/	60.0
Water requirement: percent of control (max, %)	115.0	/	/
Soundness: autoclave expansion or contraction (max, %)	0.8	0.8	0.8

A study was performed on different types of clay brick samples obtained from various parts of European countries and pulverized into powder and used to replace the cement. Results from the chemical tests for pozzolanic activity found that all the tested clay brick samples exhibited good pozzolanic activity (Olofinnade et al., 2018). Moreover, several authors (O'Farrell, 1999; Bektas et al., 2008; Olofinnade & Ogara, 2021) reported on the suitability of using finely brick powder as partial cement replacement in both concrete and mortar for sustainable construction.

## 11.3 Fresh concrete properties

### 11.3.1 Consistency

The influence of adding CBP in cement paste on the normal consistency has been studied by many researchers (Bektas et al., 2008; Ma et al., 2021; Pitarch et al., 2021; Nasr et al., 2020), and the results indicate that water requirement increases with the increase in CBP contents, which can be attributed to the irregular shapes and rough surfaces of CBPs. On the other hand the CBP particle size also has a great influence on the water requirement of cementitious composites. The fineness of CBP affects the water demand of the mixture when CBP replacements are the same. Zhao et al. (2020) analyzed the effect of CBP with four different particle sizes (Table 11.2) on the water requirement for a normal consistency when replacing 30% of the cement.

**Table 11.2** Physical properties of binder materials (Zhao et al., 2020).

Type	Cement	CBP1	CBP2	CBP3	CBP4
D10 ( $\mu\text{m}$ )	3.1	5.0	1.6	1.0	0.6
D50 ( $\mu\text{m}$ )	13.1	27.1	15.8	10.5	3.4
D90 ( $\mu\text{m}$ )	45.8	91.1	55.3	33.3	24.1
Density ( $\text{g}/\text{cm}^3$ )	3.15	2.73	2.72	2.71	2.68
Specific surface area ( $\text{m}^2/\text{kg}$ )	384.1	253.3	367.2	554.4	795.4

As shown in Fig. 11.2 the incorporation of CBP could increase the water requirement of normal consistency depending upon the particle size of CBP. Compared with M0 the water requirement of normal consistency for M1 increases by 15.4%, while that for M4 increases by only 4.6%. This is due to the initial pores in CBP being destroyed after increased grinding, and some irregular edges of the CBP particle can be further polished; in this case the microstructure of the CBP is improved, which can provide an obvious lubricating effect and offset the increase in the amount of required water caused by an increase in the specific surface area (Ma et al., 2021).

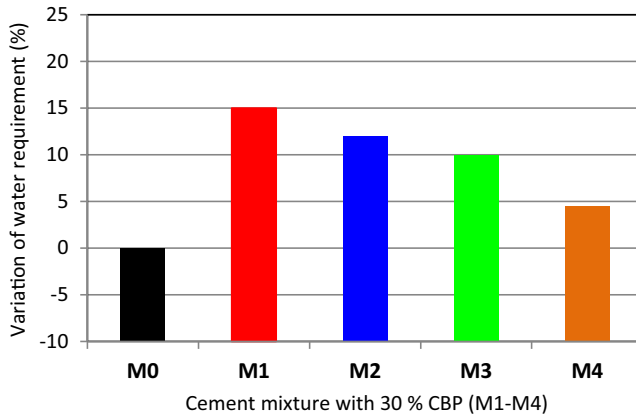


**Figure 11.2** Water requirement of cement mixture with and without RBP (Zhao et al., 2020).

### 11.3.2 Setting time

The proportion of CBP replacement has a significant effect on the values of initial and final setting times of cementitious composites. Several researchers (Bektas et al., 2008; Kirgiz, 2016; Olofinnade et al., 2018; Nasr et al., 2020; Pitarch et al., 2021; Wu et al., 2021) found that when the dosage of CBP increases the initial and final setting times of cementitious composites were prolonged. On the other hand, Zhao et al. (2020) indicated that replacing part of cement with CBP has a double-sided effect on the setting of paste (Fig. 11.3). On one hand the replacement of cement produces the dilution effect and reduces the cement hydration products, which delays the setting time. On the other hand the CBP particles will act as nucleation centers which accelerate the formation of hydration products. When the nucleation effect of RBP is dominant the setting time of cementitious composites is decreased.

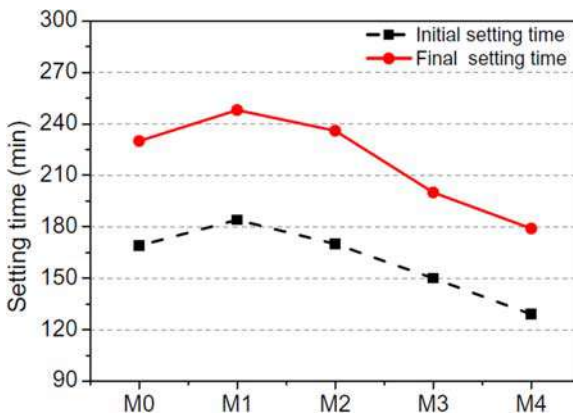


**Figure 11.3** Setting time of cement pastes with and without CBP (Zhao et al., 2020).



### 11.3.3 Workability

Ge et al. (2015) studied the influence of substitution level (0%–30%) and particle size of CBP on the workability of fresh concrete. Three groups of concrete mixtures were designed: Type A, Type B, and Type C with varied particle size distribution of the clay brick particles. Type A CBP had a smaller particle size and higher absorption. Type C CBP had a larger particle size and lower absorption. Type B CBP is in the middle. They concluded that the slump of the mixture decreases with increasing CBP content, and the reduction in the mixture slump is more significant with high-volume CBP incorporation. However, the increased CBP fineness leads to an increase in the slump when the CBP replacement ratios are the same. Moreover, this result was also reported in the studies of Ma et al. (2021), as shown in Fig. 11.4.

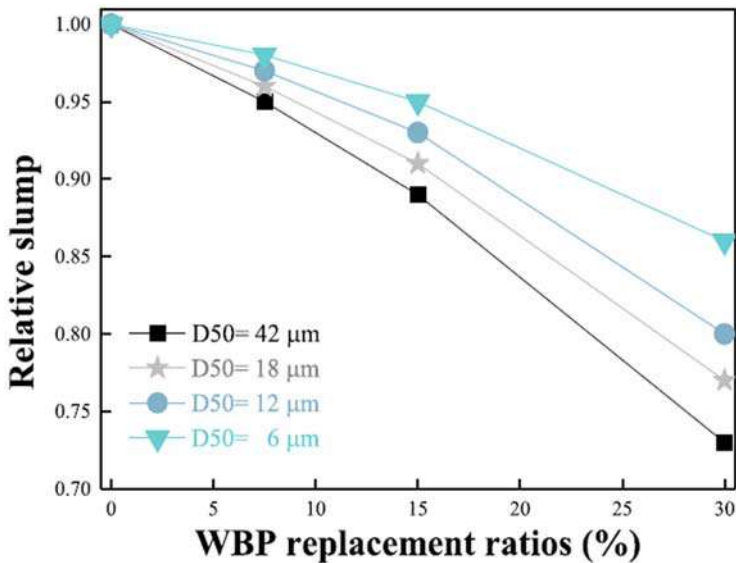


Figure 11.4 Effect of waste brick powder (WBP) on slump (Ge et al., 2015).

In addition, several researchers (Heidari & Hasanpour, 2013; Kırgız, 2016; Olofinnade et al., 2018; Castillo et al., 2020; Nasr et al., 2020; Wu et al., 2021; Msinjili et al., 2021) have found that the fluidity of cementitious materials decreases with the increased substitution rates of CBP. The reduction in flow rate can be attributed to the ability of the CBP to absorb water, the roughness of its surface, and the angularity, which led to the loss of a part of the mixing water and thus reduced the flow rate (Nasr et al., 2020).

## 11.4 Mechanical properties

### 11.4.1 Effect of type and content of clay minerals

The type of clay minerals has a large effect on the performance of cement with calcined clay. Kaolinite is the most reactive material. [Fernandez et al. \(2011\)](#) stated that kaolinite has more enhanced pozzolanic activity compared to illite and montmorillonite as it has a different decomposition process, resulting in more important loss of crystallinity. The pozzolanic activity of the calcined kaolinite resulted in higher compressive strength than ordinary cement paste.

[Hollanders et al. \(2016\)](#) tested eight clay types with four kaolinitic, three smectitic, and one illitic clay and calcined them in temperatures ranging from 500°C to 900°C and studied the pozzolanic reactivity at 3–90 days. They found that the kaolinitic clays are the most reactive compared to smectitic and illite clays, which show poor pozzolanic activity. [Avet et al. \(2016\)](#) studied the pozzolanic activity of calcined clay of different kaolinite contents ranging from 0% to 95%. Comparable compressive strength of mortar was obtained after 3 days for a very high kaolinite content of 95% and after 7 days for 40% kaolinite content.

[Poussardin et al. \(2020\)](#) studied the effect of calcined natural argillaceous-carbonate containing palygorskite, smectite, and dolomite as partial substitution of cement and proved its potential as a cement replacement material.

### 11.4.2 Compressive strength

Replacement of cement with 5%–10% of calcined kaolinite [metakaolin (MK)] has been shown to improve the mechanical properties of mortar and concrete at the early stage and long term as well as the durability because of its pozzolanic reactivity ([Khatib & Wild, 1996](#); [Singh & Garg, 2006](#); [Siddique & Klaus, 2009](#); [Khatib, 2008](#); [Khatib, 2009](#)). Other researchers reported that up to 15% of substitution of OPC with MK improves the mechanical properties of mortar and concrete, but beyond 15% replacement level the strength decreases ([Parande et al. \(2008\)](#)). Similar results were also reported by [Said-Mansour et al. \(2011\)](#) with an increase in the compressive strength of mortar up to 20% substitution level, but a decrease in strength at 30% of MK was observed. The optimum compressive strength was observed at 10% substitution level.

[Barkat et al. \(2019\)](#) combined MK and limestone to produce self-compacting mortar with improved rheological properties and improved mechanical and durability performance. At 25% of MK substitution level the increase in compressive strength as compared to reference mortar was 21% and 23% at 90 and 180 days, respectively.

Waste fired ground brick is widely available in construction sites and brick factories. It has been used as cement replacement and found to give comparable performance to OPC mortar and concrete. [Si-Ahmed et al. \(2018\)](#) stated that at substitution rates of 5% and 10%, long-term-comparable strength of waste ground brick-based mortar is obtained as compared to reference mortars.

### 11.4.2.1 Effect of combination of limestone and calcined clay

A combination of MK and limestone was attempted and found to lead to a better performance as a synergetic effect of both limestone and calcined clay is obtained. Compressive strength for this binder seems to be comparable to that for ordinary cement concrete beyond 7 days of age. The highest compressive strength at early ages up to 7 days was for 10% MK and 10% limestone, but at 28 days the highest strength was obtained at higher metakaolin (15%) and low limestone (5%) contents (Said-Mansour et al., 2011).

Diaz et al. (2017) combined a clinker, calcined clay, and limestone with a replacement level of clinker of up to 50%. They found that the cost production is reduced by 15%–25% and that the ecological impact of cement production is reduced as greenhouse gas emissions are reduced by 20%–23% as compared to conventional solutions. The combination of both calcined clay and limestone allows higher substitution (up to 50%) and hence reduces cost without affecting the mechanical properties and with improvement in some aspects of durability (Scrivener et al., 2018).

Reddy et al. (2021) compared the limestone calcined clay cement (LC3)-based concrete to ordinary and pozzolana cement M40 grade concrete. They concluded that LC3 concrete with 50% replacement level is beneficial in terms of both strength and durability with an average increase in strength of 5%. The 7 and 28 days compressive strengths for LC3 concrete were better than those of OPC and pozzolana-based concretes. The early strength up to 7 days was higher for LC3 mixes as compared to pozzolana mixes.

Although the quality of kaolinite affects the performance of LC3 concrete, it has been shown that the use of low or intermediate kaolinite content could produce acceptable concrete performance. It should be noted that high-grade kaolinite clays are expensive, whereas medium- and low-grade kaolinite clays are low cost and more available and could be used in most parts of the world. Alujas et al. (2015) showed that good performance could be obtained with low-grade clays.

Maraghechi et al. (2018) studied the performance of LC3 cement and mortar using five different clays with different kaolinite contents of 17%–95%. LC3 mixes were with 50% cement replacement level, and the calcined clay to limestone ratio was 2:1. At 1 day of curing the strength of LC3 mixes was lower than that of ordinary cement, but at 3 days of curing the strength of LC3 mixes of clay with 95% kaolinite was comparable. At 7 days, LC3 mortars showed comparable or higher compressive strength for mixes with more than 40% kaolinite content, and at 28 and 90 days of curing, all the mixes showed higher compressive strength, except those with a very low kaolinite content of 17%. The increase in 28 days compressive strength was 9%–34%.

Akindahunsi et al. (2020) performed an experimental investigation on some calcined clays from Nigeria at 800°C for 1 hour and chose two of them with more than 30% kaolinite content as partial substitution of cement. The level of substitution was either 35% or 50% with a ratio of calcined clay to limestone of 1:1 and a water/binder ratio of 0.5. They concluded that the calcined clay with 50% kaolinite

content performed better than that of 35% clay content, though the later could still be used in cementitious blends. The strength of LC3 concrete was lower than that of reference at 2 days of curing, but remarkable improvement in strength was observed at 7 days and beyond with comparable or superior strength for mixes with 50% kaolinite content. The mixes with 32% kaolinite content led to a compressive strength higher than 25 MPa at 28 days, showing the potential of using low kaolinite content clays in concrete production.

Antoni et al. (2012) showed that LC3 cement with 5% limestone and 10% MK has higher compressive strength than the reference mix at all ages. 30% (10% limestone and 20% MK) and 45% (30% MK and 15% limestone) of clinker substitution led to better compressive strength at 7 and 28 days than plain clinker cement. The 60% substitution (20% limestone and 40% MK) presented 93% of the ordinary cement 28 days compressive strength. The study showed that gypsum addition should be carefully balanced as it has a considerable effect on early age strength and the reaction of the aluminates.

Tironi et al. (2012) studied mortar with 30% substitution of cement with two different calcined clays from different deposits in Argentina which have different kaolinite contents (48% and 76%) and proved the better performance in terms of compressive strength of the clay with a higher kaolinite content of 76%. The compressive strength for the high-kaolinite mix was comparable to that of 100% ordinary Portland cement at 7 days and higher at 28 days (49 MPa as compared to 31 MPa). The increase in strength is due to the pozzolanic reaction and lower pore size distribution.

Dixit et al. (2021b) studied the feasibility of low-grade kaolinite marine clays with 20%–40% of kaolinite content from five sources of waste from excavation works. The clays were calcined at 700°C and used as 30% by weight of cement substitution with a ratio of calcined clay to limestone of 2:1. The reduction in compressive strength was in the range of 10%–20%.

Dhandapani et al. (2018) reported that limestone calcined clay cement was found to have a better durability than ordinary Portland and fly ash-based blended cement. The strength development was better than fly ash mix and comparable with the control (i.e., 100% cement). For a similar water/binder ratio and similar mixture proportions the strength of LC3 mixes was higher than that of OPC and fly ash mixes at all ages. The superior performance was explained by the more compact and dense microstructure of the LC3 binder due to the pozzolanic reactivity of the calcined clay and the complementary reaction between calcined clay and limestone (Antoni et al., 2012).

Rodriguez and Tobon (2020) reported a lower compressive strength at an early age (less than 7 days) and similar compressive strength beyond 28 days of curing, compared with the control, when using low-grade calcined kaolinite clay as partial cement replacement. The sulfate content ( $\text{SO}_3$ ) has only a marginal effect on the early age compressive strength. The type of calcined clay and its reactivity affect the mechanical performance of LC3 concrete. Tironi et al. (2017) reported similar 28 days compressive strength for LC3 mortar at 20% replacement level for flash calcined clay, but 40% replacement level for low-grade calcined clay led to a lower compressive strength even at 90 days of age.

Nguyen et al. (2020) studied the performance of limestone calcined clay cement concrete using two types of calcined clay of different chemical and mineralogical compositions and from different calcination processes. They found that the early age compressive strength of LC3 concrete was comparable to that of concrete with ordinary Portland cement. The best performance for 28 days compressive strength was at 20% by weight of cement replacement for the flash calcined clay with an amorphous content of 50.9% by weight and at 44% of cement replacement for rotary kiln calcined clay with an amorphous content of 78.8%.

Du and Dai Pang (2020) studied the high-performance concrete properties incorporating 30% and 45% calcined kaolinite clay and limestone cement replacement and confirmed the synergetic effect of both on the performance of concrete. Calcined clay was obtained by calcining local clay at 800°C. Compressive strength was found to be lower than that of OPC mixes at an early age but improves substantially and becomes comparable from 7 days onward, particularly for 30% cement replacement level. The low early strength compared to OPC mix is due to the cement dilution effect. The improvement in compressive strength at a later age was explained by the pozzolanic reaction of calcined clay, which produces C-A-S-H gels and carboaluminate phases. This shows the possibility of using LC3 binder in particular applications that require high-strength concrete such as highway bridges, high-rise buildings, and prestressed concrete. The substitution level of 30% was found to be superior to that of 45%.

#### 11.4.2.2 *Combination of calcined clay with other additions*

Calcined clay has been combined with other mineral additions to improve successfully some aspects of mortar and concrete at the fresh and hardened states. Calcined clay was combined with other pozzolanic materials such as 20% of clay-palm kernel shells, and improvement in strength was reported as additional CSH were formed (Bediako et al., 2017).

Dixit et al. (2021a) combined limestone with calcined clay and fly ash and replaced 40% and 60% of cement with 3:1 ratio of clay:limestone and 2:1:1 ratio of clay:fly ash:limestone. The mixes with fly ash achieved better workability and comparable strength from 28 days up to 1000 days for 40% cement replacement and 30% lower strength for 60% replacement level as compared to binary mixes with calcined clay and limestone.

Syarif et al. (2021) studied a quinary cement by combining calcined clay waste with fly ash, bottom ash, mediterranean soil, and household waste ash and concluded that the new binder has comparable mechanical properties to OPC-based mixes and could be used for structural and nonstructural applications.

#### 11.4.3 *Splitting tensile and flexural strengths*

Little data are available on splitting tensile and flexural strengths, but the tendency is similar to that of compressive strength. LC3 mixes showed comparable splitting tensile strength to OPC mixes and higher splitting tensile strength than the

pozzolana mixes (Reddy et al., 2021). The flexural strength was also found to improve with LC3 mixes as compared to OPC and pozzolana mixes for M40 grade concrete with an average increase of 7% due to the dense compact morphology (Reddy et al., 2021). Khatib and Hibbert (2005) found that there is an improvement in the flexural strength of slag concrete in the presence of MK, especially at high slag content. Using 60% slag and 20% MK as partial cement replacement increased the flexural strength well above that of the control.

#### 11.4.4 Elastic and dynamic moduli

The effect of LC3 on elastic modulus is less significant than that of compressive strength. The elastic modulus was comparable for LC3 mixes as compared to other conventional mixes and higher for 50% replacement level (Dhandapani et al., 2018). The effect of kaolinite content seems to be less on the elastic modulus than the compressive strength. Akindahunsi et al. (2020) found comparable elastic moduli for mixes with 35% and 50% levels of substitution with calcined clay and limestone as compared to reference concrete for both calcined clays with 32% and 50% of kaolinite content.

The elastic modulus of LC3 concrete was 10.9% and 31.8% higher than that of ordinary cement concrete for flash calcined clay and low-grade calcined clay, respectively (Tironi et al. (2017)). Other researchers using the same flash calcined clay reported an increase in the elastic modulus for LC3 concrete (Nguyen et al., 2018). Du and Dai Pang (2020) also reported improvement in the elastic modulus for LC3 high-performance concrete at long term because of the reduced pore connectivity and the capillary porosity refinement due to the reaction among Portlandite, limestone, and calcined clay, leading to a comparable or slightly superior elastic modulus to OPC mix.

Khatib and Hibbert (2005) conducted an experimental study on the effect of MK on the properties of concrete containing slag. The dynamic modulus of elasticity was found to increase with the increase in MK content up to 20% as partial cement replacement. Replacing 10% and 20% cement with MK yielded similar dynamic moduli. The presence of MK in slag concrete mixes has led to an increase in dynamic modulus.

## 11.5 Shrinkage

MK has been reported to lower the early age autogenous shrinkage and drying shrinkage and increase the long-term autogenous shrinkage when the MK content is increased from 5% to 15% (Brooks & Johari, 2001). This is in agreement with results reported elsewhere on mortar (Khatib et al., 2009). The presence of fly ash and MK in cement mortar has led to further reduction in drying shrinkage (Khatib et al., 2009).

Du and Dai Pang (2020) noted a higher autogenous shrinkage for high-performance concrete with LC3 binder and a low water/binder ratio of 0.3 due to the pozzolanic reaction of calcined clay and the C-A-S-H gels produced. However, drying shrinkage is reduced because the reaction of calcined clay and limestone will reduce the amount of water available to escape from concrete and also due to the refined pore structures in LC3 mixes, which hinders the movement of moisture onward. The drying shrinkage for mixes with 30% and 45% cement replacement was 240 microstrains at 182 days as compared to 365 microstrains for reference concrete.

Dhandapani et al. (2018) reported a marginal increase or comparable shrinkage for LC3 mixes when compared with other OPC and fly ash mixes, probably because of the higher water/binder ratio of 0.42 for LC3 mixes, but the shrinkage was comparable for mixes with the same water/binder ratio.

## 11.6 Durability properties

### 11.6.1 General

Sabir et al. (2001) indicated that using MK and calcined clay in cementitious systems can lead to an improvement in some durability properties. These include the refinement in pore structure, reduction of water transport, and ingress of aggressive species such as chloride and sulfate ions. Also they indicated that the high cost of MK may be prohibitive for construction professionals to use, but if the demand increases, the cost is bound to reduce. Sharma et al. (2021) conducted a review on using limestone calcined clay cement in construction. They reported on the durability properties of concrete containing limestone calcined clay cement and concluded that there are economic and environmental benefits in using the materials in cementitious systems. Also they recommended further areas of research on the use of calcined clay in concrete, including rapid tests to assess the quality of calcined clay, the effect of impurities and calcining temperature, the most suitable admixtures to be used when calcined clay is present, creep and shrinkage in traditional and pre-stressed concrete, effects of carbonation on pore structure, fire resistance, and the effect of harsh environmental conditions.

### 11.6.2 Absorption, porosity, and pore structure

Khatib and Wild (1996) conducted an experimental study on the pore size distribution of cement paste containing up to 15% MK as partial cement replacement. They found that although the total pore volume of the paste increases, there was a systematic increase in the pore refinement when MK is included in the paste. This refinement is demonstrated by the decrease in the threshold diameter and the increase in the percentage of small pores. Tironi et al. (2012) used 30% clay, calcined at 700°C, as partial cement replacement in the production of mortar. The water to binder ratio and the proportion of binder to sand were 0.5 and 1:3,

respectively. The specimens were subjected to water curing after 24 hours in the molds. Also, they found that there is reduction in the total pore volume in the presence of calcined clay. Also the percentage of small pores was found to increase when calcined clay is included in the mortar. This was attributed to the pozzolanic reaction which caused a refinement in the pore structure.

[Khatib and Clay \(2004\)](#) reported the results on an experimental investigation on the water absorption by total immersion and capillary rise for concrete containing between 0% and 20% MK as partial cement replacement for up to 90 days of curing. The water absorption by capillary action decreases with the increase in MK content. However, there was a slight increase in absorption by total immersion when the content of MK increases. For all MK mixtures, there was a slight increase in absorption by total immersion and capillary rise between 14 and 28 days of curing. The water absorption by total immersion and capillary rise follow the same trend for total pore volume and the refinement in pore structure of MK paste reported in a previous investigation ([Khatib & Wild, 1996](#)), in that the water absorption by total immersion is related to the total pore volume and the capillary water uptake is affected by the size of pores. Similarly, [Musbau et al. \(2021\)](#) reported that using high-content limestone calcined clay in concrete leads to both a higher initial surface water absorption and total water absorption. However, with the increase in curing age the difference in absorption is much reduced and at 90 days of curing the absorption of calcined clay concrete is somewhat similar to the control. A reduction in water absorption by capillary action (i.e., sorptivity) was observed by [Dhandapani et al. \(2018\)](#) for concretes containing calcined clay at all ages of curing. Moreover, [Meddah et al. \(2020\)](#) conducted a study on the use of calcined clay sourced locally on the properties of cement hydrated lime mortar. They replaced the cement with up to 80% calcined clay. All mortar mixes containing calcined clay had more porosity and water absorption. The interesting finding about the research was that at 50% and 80% calcined clay the porosity was noticeably lower than those at 10% and 25%. Also the water absorption at 50% calcined clay was much lower than those at 10% and 25% replacement. This was attributed to the filling effect of calcined clay particles at higher dosages. [Du and Dai Pang \(2020\)](#) carried out an experimental study on the liquid transport of high-performance concrete incorporating calcined clay. The cement was replaced with 30% and 45% calcined clay and limestone fines. The clay was calcined at 800°C. The calcium hydroxide production is substantially less in pastes containing calcined clay, which in turn may have a positive effect on certain durability properties. There was a sharp reduction, more than 100%, in concrete sorptivity when calcined clay is present. The sorptivity at 30% and 45% replacement of cement with calcined clay and limestone was nearly the same. This reduction in liquid transport in the presence of calcined clay was explained by the refinement in pore structure and the more tortuous pathways.

[Zhang et al. \(2020\)](#) produced engineering-based composites (i.e., mortar) based on fly ash, cement, calcined clay (i.e., MK), and limestone fines. PVA fiber was added to all mixes. They determined the porosity and pore size distribution for the composites as well as the mortar and paste portions. The presence of calcined clay



seems to have resulted in an increase in porosity, critical diameter, and average pore diameter in the presence of calcined clay. This is in agreement with the results reported by [Khatib and Wild \(1996\)](#), where a noticeable improvement in the pore refinement was observed, indicated by the reduced critical pore diameter and the higher percentage of small pores.

[Dixit et al. \(2021a\)](#) conducted an experimental study on the effect of calcined clay on the properties of concrete. Limestone and fly ash were included in some of the mixtures. The proportion of calcined clay to limestone and the calcined clay to fly ash to limestone were 3:1 and 2:1:1, respectively. These materials replaced 40% and 60% of the cement. Although the porosity may increase in the presence of calcined clay, there is a noticeable decrease in the threshold diameter and an increase in the percentage of small pores when calcined clay is included in the system, indicating a refined pore structure. The water absorption data were similar to those of the total pore volume.

[Sun et al. \(2021\)](#) reported the results of an experimental investigation on chloride penetration of ultra-high-performance concrete containing calcined clay tailing. Other cementitious materials were used in mixes including limestone powder, silica fume, and gypsum. The total pore volume was found to increase in the presence of calcined clay. However, there is a higher proportion of small pores for mixes containing calcined clay than the control mix. Also from the scanning electron microscopy observation, it was concluded that the interfacial transition zone was denser when calcined clay is included in the mix. This confirmed the results obtained by [Khatib and Clay \(2004\)](#) on absorption by capillary action.

[Olofinnade and Ogara \(2021\)](#) examined the microstructure of concrete containing 10% calcined clay as partial replacement of cement and up to 50% crushed clay brick as replacement of sand with a low water to binder ratio of 0.25. Generally the presence of calcined clay and 10% crushed clay brick led to the formation of more CSH gel and a dense aggregate paste matrix. This caused an increase in strength and would lead to a better durability performance due to the refinement of pore structure. However, at 50% crushed clay brick, replacement caused a more porous interfacial zone, which would lead to reduced durability.

[Reddy et al. \(2021\)](#) compared the effect of using calcined clay on the performance of concrete grade M40. The control mix had a proportion of 1 (cement): 1.65 (sand): 2.95 (coarse aggregate): 0.4 (water/cement). In the calcined clay mix the cement was partially replaced with 30% calcined clay and 15% limestone. The rest of the ingredients remained constant. The presence of calcined clay resulted in a substantial reduction in chloride ion penetration in that the charge passed in coulombs was 2553 and 412 for the control mix and the calcined clay mix, respectively. The total and the rate of water absorption were lower in the concrete containing calcined clay.

### **11.6.3 Permeability, chloride ingress, and carbonation**

[Dhandapani et al. \(2018\)](#) conducted a comprehensive experimental study on the effect of including calcined clay on the durability properties of concrete. Concrete

mixes were cured for 28, 56, and 90 days. It was concluded that the presence of calcined clay resulted in a denser microstructure of concrete, which led to a reduction in chloride penetration and higher resistivity and oxygen permeability index.

Du and Dai Pang (2020) conducted an experimental investigation on the liquid transport of high-performance concrete up to 30% calcined clay as partial cement replacement. There was a substantial reduction in chloride ion diffusion into concrete in the presence of calcined clay. The chloride resistance varied from nearly  $6 \times 10^{-12} \text{ m}^2/\text{s}$  for the control to about 1.8 and  $2 \times 10^{-12} \text{ m}^2/\text{s}$  for mixes with 20% and 30% calcined clay replacement. The refinement in pore structure is likely to have been the reason for the reduced chloride penetration in the presence of calcined clay.

Dixit et al. (2021a) reported that the chloride resistance of concrete increases in the presence of calcined clay. This was attributed to the refined pore structure and the formation of discontinuous pores in the presence of calcined clay. This refinement will continue as long as there is calcium hydroxide in the pore for the densification of the matrix. Sun et al. (2021) reported the results of an experimental investigation on pore structure and chloride penetration of ultra-high-performance concrete containing calcined clay tailing. Other cementitious materials were used in mixes, including limestone powder, silica fume, and gypsum. Results similar to those by Dixit et al. (2021a) were obtained.

Rathnarajan et al. (2021) examined the extent of carbonation of concrete containing limestone calcined clay and found that the long-term carbonation depth can be similar to that of the control concrete if an appropriate design method is adopted.

#### 11.6.4 Sulfate resistance

Khatib and Wild (1998) examined the sulfate resistance of mortar containing up to 25% of MK as partial cement replacement. The binder to cement ratio and the water to binder ratio for all mixes were 1:2.5 and 0.55, respectively. Two types of cement were employed, containing different  $C_3A$  contents of 7.5% and 11.7%. Sulfate resistance was assessed by the length and the weight change of mortars immersed in 5% sodium sulfate solution for 520 days. Also visual assessment of specimens was used to complement the length and weight changes. Replacing cement with more than 10% MK increased the sulfate resistance. At 20 and 25% MK, there is hardly any damage to the specimens after 520 days of exposure. Using high- $C_3A$  cement led to a noticeable sulfate attack compared to that of lower  $C_3A$  cement. The increased sulfate resistance was mainly attributed to the consumption of calcium hydroxide and the refinement of pore structure in the presence of MK (Wild et al., 1996; Khatib & Wild, 1998).

A similar study was conducted by Wild et al. (1997) on the sulfate resistance of cement mortar containing ground clay brick calcined (GCBC) at temperatures ranging from 600°C to 1100°C. The cement was partially replaced with 10 and 20% GCBC. The water to binder ratio and the binder to sand content were similar to those reported by the authors in a different investigation (Khatib & Wild, 1998). At

10% cement replacement the sulfate resistance was higher for mortar containing 10% ground brick calcined at temperatures above 800°C, whereas at 20% replacement, there is an improvement in sulfate resistance at temperatures above 700°C. The reduced sulfate resistance below 800°C was attributed to the activated clay and the high sulfate level in the clay calcined at these temperatures. However, the increased sulfate resistance beyond 800°C calcining temperature was attributed to the lower sulfate content of the clay and the presence of active glass phase.

### **11.6.5 Abrasion and skid resistance**

Awolusi et al. (2021) examined the effect of including calcined clay on the abrasion and skid resistance of concrete for pavement and flooring applications. Cement was replaced with 0 to 5% calcined clay. There was a slight increase in water absorption of concrete with the increase in calcined clay content. At 5% cement replacement with calcined clay the skid resistance was higher than that of the control, whereas a slight reduction is obtained at 2.5% replacement. However, the abrasion resistance is slightly lower in the presence of calcined clay. They concluded that the optimum calcined clay replacement for skid and abrasion resistance was found to be 5%.

### **11.6.6 Fire resistance**

Gunjal and Kondraivendhan (2021) compared the fire resistance of traditional concrete with that containing calcined clay. The binder of the calcined clay concrete consisted of 30% calcined clay, 15% limestone, 5% gypsum, and 50% clinkers. The concretes were exposed to a temperature up to 800°C. There was a decrease in compressive strength at 200°C. The decrease was substantial beyond a temperature of 400°C, where tiny cracks appeared on the surface of specimens for traditional concrete and concrete containing calcined clay.

## **11.7 Economic and environmental aspects**

Producing calcined clay requires nearly half the calcining temperature compared to that for Portland cement. Therefore partial replacement of cement with calcined clay should have economic and environmental benefits. Compared to cement, the reduction in calcining temperature should reduce the carbon dioxide emission into the atmosphere and the associated cost. MK (i.e., calcined clay) is still expensive to produce depending upon the purity of the calcined clay and the processing involved in the preparation before calcining. With more large-scale utilization of calcined clay the cost of production should reduce. The durability of cementitious systems containing calcined clay is improved, and consideration should be made when considering life cycle analysis. Using calcined clay in construction should play a role in sustainable development and addressing the challenges discussed at the recent COP26 conference which was held in Glasgow-UK, in November 2021 in terms of

reducing harmful gases into the atmosphere (COP21, 2021). Generally, clay is available locally, so the transportation cost will be reduced and this will cause further reduction in carbon dioxide emission. The local economy and society would be supported through the creation of local employment, thus improving the livelihood of inhabitants.

## 11.8 Conclusions

The combined effect of calcined clay and limestone improves the mechanical properties of concrete and mortar beyond 7 days of age because of the refinement of the pore structure due to pozzolanic reaction and filling effect. Comparable mechanical properties to ordinary cement concrete could be achieved with the appropriate replacement rate. Generally, using calcined clay as partial replacement of cement in cementitious systems leads to a lower permeability, a lower rate of water absorption by capillary action and more pore structure refinement. This in turn will improve the durability performance in that less chloride ion penetration, higher sulfate resistance would be obtained. More research on the effect of calcined clay in concrete on alkali-aggregate reaction, depth of carbonation, abrasion, and fire resistance would be useful.

Further studies are needed for calcined clay limestone and limestone/calcined clay cement concrete for long-term durability tests under aggressive environments such as sulfate attack, chloride attack, acid attack, freeze/thaw resistance, and performance under hot climate conditions. Calcined clay is obtained from local materials. Therefore it is expected to be more environmentally friendly through the reduction in transportation cost and the less energy required compared to cement. Local employment would be enhanced, thus contributing to the local economy and the welfare of the society.

## References

- ACI 232.1R-12 (2012). *Report on the use of raw or processed natural pozzolans in concrete. standard by American Concrete Institute.*
- Akindahunsi, A. A., Avet, F., & Scrivener, K. (2020). The Influence of some calcined clays from Nigeria as clinker substitute in cementitious systems. *Case Studies in Construction Materials*, 13, e00443. Available from <https://doi.org/10.1016/j.cscm.2020.e00443>.
- Alujas, A., Fernández, R., Quintana, R., Scrivener, K. L., & Martirena, F. (2015). Pozzolanic reactivity of low-grade kaolinitic clays: Influence of calcination temperature and impact of calcination products on OPC hydration. *Applied Clay Science*, 108, 94–101.
- Antoni, M., Rossen, J., Martirena, F., & Scrivener, K. (2012). Cement substitution by a combination of metakaolin and limestone, cement and concrete research. *Cement and Concrete Research*, 42, 1579–1589.
- Awolusi, T. F., Sojobi, A. O., Oguntayo, D. O., Akinkulore, O. O., & Orogbade, B. O. (2021). Effects of calcined clay, sawdust ash and chemical admixtures on strength and

- properties of concrete for pavement and flooring applications using Taguchi approach. *Case Studies in Construction Materials*, 15, e00568. Available from <https://doi.org/10.1016/j.cscm.2021.e00568>.
- ASTM C618. (2018). *Standard specification for coal fly ash and raw or calcined natural pozzolan for use in concrete*.
- Avet, F., Snellings, R., Diaz, A. A., Ben-Haha, M., & Scrivener, K. (2016). Development of a new rapid, relevant and reliable test method (R3) to evaluate the pozzolanic reactivity of calcined Kaolinitic clays. *Cement and Concrete Research*, 85, 1–11.
- Barkat, A., Kenai, S., Menadi, B., Kadri, E., & Soualhi, H. (2019). Effect of local metakaolin addition on rheological and mechanical performance of self-compacting limestone cement concrete. *Journal of Adhesion Science and Technology*, 33(9), 963–985.
- Baronio, G., & Bindat, L. (1997). Study of the pozzolanicity of some bricks and clays. *Construction and Building Materials*, 11(1), 41–46.
- Bektas, F., Kejin, W., & Ceylan, H. (2008). Use of ground clay bricks as a pozzolanic materials in concrete. *Journal of ASTM International*, 5(10).
- Bediako, M., Tristan KeVERN, J., & Dodoo-Arhin, D. (2017). Co-fired Ghanaian clay-palm kernel shells pozzolan: Thermogravimetric  $^{29}\text{Si}$  and  $^{27}\text{Al}$  MA NMR characteristics. *Construction and Building Materials*, 153, 430–435.
- Brooks, J. J., & Johari, M. A. (2001). Effect of metakaolin on creep and shrinkage of concrete. *Cement and Concrete Composites*, 23, 495–502.
- Castillo, M., Hernández, K., Rodríguez, J., & Eyzaguirre, C. (2020). Low permeability concrete for buildings located in marine atmosphere zone using clay brick powder. *IOP Conf. series: Materials science and engineering*, 758.
- COP21. (2021). <https://ukcop26.org/> Accessed 10.01.22.
- CSA A3001-08. (2010). *Cementitious materials for use in concrete*, Canada.
- Dhandapani, Y., Sakthivel, T., Santhanam, M., Gettu, R., & Pillai, R. G. (2018). Mechanical properties and durability performance of concretes with limestone calcined clay cement (LC3). *Cement and Concrete Research*, 107, 136–151. Available from <https://doi.org/10.1016/j.cemconres.2018.02.005>.
- Diaz, Y. C., et al. (2017). Limestone calcined clay cement as a low-carbon solution to meet expanding cement demand in emerging economies. *Development Engineering*, 2, 82–91.
- Dixit, A., Du, H., Dang, J., & Dai Pang, S. (2021a). Quaternary blended limestone-calcined clay cement concrete incorporating fly ash. *Cement and Concrete Composites*, 123, 104174. Available from <https://doi.org/10.1016/j.cemconcomp.2021.104174>.
- Dixit, A., Du, H., & Pang, S. D. (2021b). Performance of mortar incorporating calcined clays with varying kaolin content. *Journal of Cleaner Production*, 282, 124513. Available from <https://doi.org/10.1016/j.jclepro.2020.124513>.
- Du, H., & Dai Pang, S. (2020). High-performance concrete incorporating calcined kaolin clay and limestone as cement substitute. *Construction and Building Materials*, 264, 120152. Available from <https://doi.org/10.1016/j.conbuildmat.2020.120152>.
- Fernandez, R., Martinrena, F., & Scrivener, K. (2011). The origin of the pozzolanic activity of calcined clay minerals: A comparative between kaolinite, illite and montmorillonite. *Cement and Concrete Research*, 41, 113–122.
- Ge, Z., Wang, Y., Sun, R., Wu, X., & Guan, Y. (2015). Influence of ground waste clay brick on properties of fresh and hardened concrete. *Construction and Building Materials*, 98, 128–136.
- Gunjaj, S. M., & Kondraivendhan, B. (2021). High temperature impact on calcined clay-limestone cement concrete (LC3). *Materials Today: Proceedings*. Available from <https://doi.org/10.1016/j.matpr.2021.10.300>.

- Heidari, A., & Hasanpour, B. (2013). Effects of waste bricks powder of gachsaran company as a pozzolanic material in concrete. *Asian Journal of Civil Engineering (BHRC)*, 14(5), 755–763.
- Hewlett, P., & Liska, M. (2019). *Lea's chemistry of cement and concrete* (5th ed.). Elsevier Science & Technology Books.
- Hollanders, S., Adriaens, R., Skibsted, J., Cizer, O., & Elsen, J. (2016). Pozzolanic reactivity of pure calcined clays. *Applied Clay Science*, 132–133, 552–560.
- JG/T 315. (2011). *Natural pozzolanic materials used for cement mortar and concrete*, China.
- Khatib, J. M. (2005). Properties of concrete containing fine recycled aggregates. *Cement and Concrete Research Journal*, 35(4), 763–769. Available from <https://doi.org/10.1016/j.cemconres.2004.06.017>, April 2005.
- Khatib, J. M. (2008). Metakaolin concrete at a low water to binder ratio. *Construction and Building Materials Journal*, 22(8), 1691–1700. Available from <https://doi.org/10.1016/j.conbuildmat.2007.06.003>, August 2008.
- Khatib, J.M. (2009). Low curing temperature of metakaolin concrete. *American Society of Civil Engineers (ASCE)—Materials in Civil Engineering Journal*, 21(8), 362–367, ISSN 0899-1561/2009/8-362-367 DOI: 10.1061/(ASCE)0899-1561(2009)21:8(362).
- Khatib, J. M., & Clay, R. M. (2004). Absorption characteristics of metakaolin concrete. *Cement and Concrete Research*, 34(1), 19–29. Available from [https://doi.org/10.1016/S0008-8846\(03\)00188-1](https://doi.org/10.1016/S0008-8846(03)00188-1).
- Khatib, J. M., & Hibbert, J. J. (2005). Selected engineering properties of concrete incorporating slag and metakaolin. *Construction and Building Materials Journal*, 19(6), 460–472. Available from <https://doi.org/10.1016/j.conbuildmat.2004.07>, July 2005.
- Khatib, J. M., Kayali, O., & Siddique, R. (2009). Dimensional stability and strength of cement-fly ash-metakaolin mortar. *American Society of Civil Engineers (ASCE)—Materials in Civil Engineering Journal*, 21(9), 523–528. Available from [https://doi.org/10.1061/\(ASCE\)0899-1561\(2009\)21:9\(523\)](https://doi.org/10.1061/(ASCE)0899-1561(2009)21:9(523)), September.
- Khatib, J. M., & Wild, S. (1996). Pore size distribution of metakaolin paste. *Cement and Concrete Research*, 26(10), 1545–1553.
- Khatib, J. M., & Wild, S. (1998). Sulphate resistance of metakaolin mortar. *Cement and Concrete Research*, 28(1), 83–92.
- Kırgız, M. S. (2016). Fresh and hardened properties of green binder concrete containing marble powder and brick powder. *European Journal of Environmental and Civil Engineering*.
- Ma, Z., Tang, Q., Wu, H., Xu, J., & Liang, C. (2021). Mechanical properties and water absorption of cement composites with various fineness and contents of waste brick powder from C&D waste. *Cement and Concrete Composites*, 114, 103758.
- Manfredi, S., Pant, R., Pennington, D. W., & Versmann, A. (2011). Supporting environmentally sound decisions for waste management with LCT and LCA. *International Journal of Life Cycle Assessment*, 16(9), 937–939.
- Maraghechi, H., Avet, F., Wong, H., Kamyab, H., & Scivener, K. (2018). Performance of limestone calcined clay cement (LC3) with various kaolinite contents with respect to chloride transport. *Materials and Structures*, 51–125.
- Meddah, M. S., Benkari, N., Al-Saadi, S. N., & Al Maktoumi, Y. (2020). Sarooj mortar: From a traditional building material to an engineered pozzolan-mechanical and thermal properties study. *Journal of Building Engineering*, 32, 101754. Available from <https://doi.org/10.1016/j.jobbe.2020.101754>.
- Musbau, K. D., Kolawole, J. T., Babafemi, A. J., & Olalusi, O. B. (2021). Comparative performance of limestone calcined clay and limestone calcined laterite blended cement

- concrete. *Cleaner Engineering and Technology*, 4, 100264. Available from <https://doi.org/10.1016/j.clet.2021.100264>.
- Msinjili, N. S., Vogler, N., Sturm, P., Neubert, M., Schröder, H.-J., Kühne, H.-C., Hüniger, K.-J., & Gluth, G. J. G. (2021). Calcined brick clays and mixed clays as supplementary cementitious materials: Effects on the performance of blended cement mortars. *Construction and Building Materials*, 266, 120990.
- Nasr, M. S., Shubbar, A. B., Abed, Z. A. R., & Ibrahim, M. S. (2020). Properties of eco-friendly cement mortar contained recycled materials from different sources. *Journal of Building Engineering*, 31, 101444.
- Navrátílová, E., & Rovnaníková, P. (2016). Pozzolanic properties of brick powders and their effect on the properties of modified lime mortars. *Construction and Building Materials*, 120, 530–539.
- Nguyen, Q. D., Khan, M. S. H., & Castel, A. (2018). Engineering properties of limestone calcined clay concrete. *Journal of Advanced Concrete Technology*, 16, 345–357.
- Nguyen, Q. D., Afroz, S., & Castel, A. (2020). Influence of calcined clay reactivity on the mechanical properties and chloride diffusion resistance of limestone calcine clay cement (LC3) concrete. *Journal of Marine Science and Engineering*, 8, 301.
- Olofinnade, O., & Ogara, J. (2021). Workability, strength, and microstructure of high strength sustainable concrete incorporating recycled clay brick aggregate and calcined clay. *Cleaner Engineering and Technology*, 3, 100123. Available from <https://doi.org/10.1016/j.clet.2021.100123>.
- O'Farrell, M. (1999). *The durability of mortar with ground clay brick as partial cement replacement*. PhD Thesis, University of Glamorgan, UK.
- Olofinnade, O. M., Ede, A. N., & Booth, C. A. (2018). *Sustainability of waste glass powder and clay brick powder as cement substitute in green concrete. Handbook of environmental materials management*. Springer.
- Pacheco-Torgal, F., & Jalali, S. (2010). Reusing ceramic wastes in concrete. *Construction and Building Materials*, 24, 832–838.
- Parande, A. K., Babu, B. R., Karthik, M. A., Kumaar, D. K. K., & Planiswamy. (2008). Study on strength and corrosion performance of steel embedded in metakaolin concrete/mortar. *Construction and Building Materials*, 22, 127–134.
- Pitarch, A. M., Reig, L., Gallardo, A., Soriano, L., Borrachero, M. V., & Rochina, S. (2021). Reutilization of hazardous spent fluorescent lamps glass waste as supplementary cementitious material. *Construction and Building Materials*, 292(4), 123424.
- Poussardin, V., Paris, M., Tagnit-Hamou, A., & Deneele, D. (2020). Potential for calcination of palygorskite-bearing argillaceous carbonate. *Applied Clay Science*, 198, 105846.
- Rathnarajan, S., Dhanya, B. S., Pillai, R. G., Gettu, R., & Santhanam, M. (2021). Carbonation model for concretes with fly ash, slag, and limestone calcined clay-using accelerated and five-year natural exposure data. *Cement and Concrete Composites*, 104329. Available from <https://doi.org/10.1016/j.cemconcomp.2021.104329>.
- Reddy, K. P., Rao, B. C. M., Yadav, M. J., & Giri, P. S. N. R. (2021). Comparative studies on LC3 based concrete with OPC & PPC based concretes. *Materials Today: Proceedings*, 43, 2368–2372. Available from <https://doi.org/10.1016/j.matpr.2021.01.833>.
- Rodriguez, C., & Tobon, J. I. (2020). Influence of calcined clay/limestone, sulfate and clinker proportions on cement performance. *Construction and Building Materials*, 251, 119050.
- Sabir, B. B., Wild, S., & Bai, J. (2001). Metakaolin and calcined clays as pozzolans for concrete: A review. *Cement and Concrete Composites*, 23(6), 441–454. Available from [https://doi.org/10.1016/S0958-9465\(00\)00092-5](https://doi.org/10.1016/S0958-9465(00)00092-5).

- Said-Mansour, M., Kadri, E., Kenai, S., Ghrici, M., & Bennaceur, R. (2011). Influence of calcined clay on mortar properties. *Construction and Building Materials*, 25, 2275–2282.
- Scrivener, K., et al. (2018). Calcined clay limestone cements (LC3). *Cement and Concrete Research*, 114, 49–56.
- Shao, J., Gao, J., Zhao, Y., & Chen, X. (2019). Study on the pozzolanic reaction of clay brick powder in blended cement Pastes. *Construction and Building Materials*, 213, 209–215.
- Sharma, M., Bishnoi, S., Martirena, F., & Scrivener, K. (2021). Limestone calcined clay cement and concrete: A state-of-the-art review. *Cement and Concrete Research*, 149, 106564. Available from <https://doi.org/10.1016/j.cemconres.2021.106564>.
- Si-Ahmed, M., Kenai, S., & Ghorbel, E. (2018). Performance of cement mortar with waste ground clay brick. *MRS Advances*. Available from <https://doi.org/10.1557/adv.2018.291>.
- Siddique, R., & Klaus, J. (2009). Influence of metakaolin on the properties of mortar and concrete: A review. *Applied Clay Science*, 43(3–4), 392–400.
- Singh, M., & Garg, M. (2006). Reactive pozzolana from Indian clays-Their use in cement mortars. *Cement and Concrete Research*, 36(2006), 1903.
- Sun, Y., Yu, R., Wang, S., Zhou, Y., Zeng, M., Hu, F., Shui, Z., Rao, B., Yuan, S., Luo, Z., & Ma, S. (2021). Development of a novel eco-efficient LC2 conceptual cement based ultra-high performance concrete (UHPC) incorporating limestone powder and calcined clay tailings: Design and performances. *Journal of Cleaner Production*, 315, 128236. Available from <https://doi.org/10.1016/j.jclepro.2021.128236>.
- Syarif, M., Kirgiz, M. S., Galdin, A. G. D., El-Neggar, A. M. H., Mirza, J., Khatib, J., Kenai, S., et al. (2021). Development and assessment of cement and concrete made of the burning of quinary by-product. *Journal of Materials Research and Technology*, 15(2021), 3708–3721.
- Tironi, A., Scian, A. N., & Irassar, E. F. (2017). Blended cements with limestone filler and kaolinite calcined clay: Filler and pozzolanic effects. *Journal of Materials in Civil Engineering*, 29(9), 04017116.
- Tironi, A., Trezza, M. A., Scian, A. N., & Irassar, E. F. (2012). Incorporation of calcined clays in mortars: Porous structure and compressive strength. *Procedia Materials Science*, 1, 366–373. Available from <https://doi.org/10.1016/j.mspro.2012.06.049>.
- Wild, S., Khatib, J. M., & Jones, A. (1996). Relative strength, pozzolanic activity and cement hydration in superplasticised metakaolin concrete. *Cement and Concrete Research Journal*, 16(10), 1537–1544, 1996.
- Wild, S., Khatib, J. M., & O'Farrell, M. (1997). Sulphate resistance of mortar, containing ground brick clay calcined at different temperatures. *Cement and Concrete Research*, 27(5), 697–709.
- Wu, H., Xiao, J., Liang, C., & Ma, Z. (2021). Properties of cementitious materials with recycled aggregate and powder both from clay brick waste. *Buildings*, 11, 119.
- Zhang, D., Jaworska, B., Zhu, H., Dahlquist, K., & Li, V. C. (2020). Engineered Cementitious Composites (ECC) with limestone calcined clay cement (LC3). *Cement and Concrete Composites*, 114, 103766. Available from <https://doi.org/10.1016/j.cemconcomp.2020.103766>.
- Zhao, Y., Gao, J., Liu, C., Chen, X., & Xu, Z. (2020). The particle-size effect of waste clay brick powder on its pozzolanic activity and properties of blended cement. *Journal of Cleaner Production*, 242, 118521.



This page intentionally left blank

# Properties of concrete containing coal bottom ash as hydraulic binder substitution

12

Khairunisa Muthusamy<sup>1</sup>, Wang Hui Wong<sup>1</sup>, Nabilla Mohamad<sup>1</sup>, Jose Rajan<sup>2</sup>, Ahmed Mokhtar Albshir Budiea<sup>3</sup>, Anwar P.P. Abdul Majeed<sup>4</sup> and Mehmet Serkan Kirgiz<sup>5</sup>

<sup>1</sup>Faculty of Civil Engineering Technology, University Malaysia Pahang, Pahang, Malaysia,

<sup>2</sup>Faculty of Industrial Science and Technology, University Malaysia Pahang, Pahang, Malaysia, <sup>3</sup>Faculty of Industrial Management, University Malaysia Pahang, Pahang, Malaysia, <sup>4</sup>Faculty of Manufacturing and Mechatronics Engineering Technology,

University Malaysia Pahang, Pahang, Malaysia, <sup>5</sup>Northwestern University, Chicago, IL, United States

*The use of coal bottom ash (CBA) as a partial cement substitute on the effect of concrete workability is studied.*

## 12.1 Introduction

Concrete is a flexible substance that is produced using natural resources with cement as a binding agent. The use of natural resources rises every year owing to urban and rural growth. Cement manufacturing requires the use of large amounts of raw materials, energy, and heat. [World Business Council for Sustainable Development International Energy Agency Technology Roadmap: Low-Carbon Technology for the Indian Cement Industry \(2013\)](#) projected in 2050 the demand for cement in the range of 780–1361 million tons. [Argiz et al. \(2018\)](#) observed that when 1 ton of Portland cement is manufactured, it releases approximately 0.8 tons of carbon dioxide. The calcination process and combustion for energy generation during cement production are the processes with the greatest effect to the environment ([Durastanti & Morretti, 2020](#)). Alternative sustainable materials are needed to enhance the performance of concrete to minimize the use of natural resources ([Jayakumar et al., 2021](#)). Utilizing the freely available locally generated waste to replace the harvesting of natural resources for cement production would also contribute to preservation of natural nonrenewable resources and reduce degradation of the environment and wildlife.

At the same time the expanding population with their growing needs and flourishing industries causes an increase in energy demand in many parts of the world. Coal became one of the materials to generate energy in thermal power production

(Park et al., 2020). It is one of the biggest energy sources in the world, fueling nearly 40% of the world's electricity. In Malaysia, since 1988, seven of its power plants utilize coal as their raw material for electricity production (Marto & Tan, 2016). Coal combustion products have increased significantly throughout the years when gas plants have been replaced by a coal-fired electricity plant in Malaysia (Foo, 2015). The total capacity of coal-fired power plants in Malaysia is estimated at approximately 15,000 MW by 2020, with an estimated 0.657 million tons of coal-fueled ash per year (Tobias, 2020). According to Ramakrishna et al. (2018), coal ash generated from the combustion was estimated about 1 billion tons yearly globally. Yao et al. (2015) stated that the majority of the nonrecycled coal ash would be disposed at landfill sites and thus increase the amount of waste material and raise the treatment cost. Furthermore, PSR (2015) stated that the GCBA includes heavy metals, and if eaten, drank, or breathed, they may cause cancer and nervous system effects such as cognitive impairments, developmental delays, and behavioral issues. Generally the option of throwing this byproduct at the landfill poses threat to the living things and pollutes the environment. Besides that, continuous discarding of this industrial byproduct would consume larger spaces of land which can be used for community development purposes.

The approach of inventing concrete products by utilizing waste materials such as ground CBA as a mix component would decrease manufacturing cost, environmental protection, and landfill (Muthusamy et al., 2020). In view of sustainable environment, many researchers (Balapour et al., 2020; Roberto et al., 2021; Singh & Siddique, 2016; Singh et al., 2019; Siddique, 2013) have investigated the potential use of CBA as aggregate replacement in concrete. Realizing the pressing environmental issues due to harvesting of limestone and processes of cement production the option of channeling the CBA for cement production would be rewarding to the environment. Thus the present research investigates the effect of CBA as partial cement replacement on fresh and mechanical properties of concrete.

## 12.2 Methodology

### 12.2.1 Preparation of raw materials

Concrete was made in this study using ordinary Portland cement, tap water, sand, coarse aggregate, and CBA. As fine aggregate, local river sand was utilized. The modulus of fineness and the absorption of water are 2.87 and 6.22, respectively. We utilized crushed granite aggregate from a nearby source. Tap water was utilized to mix and cure the concrete. CBA was collected from a coal-fired power station on Malaysia's west coast. As shown in Fig. 12.1 the collected CBA was coarse and inappropriate for use as a partial cement substitute. It was processed using a Los Angeles abrasion machine to produce a fine powder that met the (ASTM C618, 2019) fineness standard. The outcome of a wet sieve test indicates that the majority of finely ground CBA particles flow through a 45  $\mu\text{m}$  sieve with just 13.9% remaining on the sieve fulfilling the requirement stated in ASTM C618-19 (2019). The ground CBA is shown in Fig. 12.2. Table 12.1 shows the chemical composition of the CBA used.



**Figure 12.1** Raw CBA. *CBA*, Coal bottom ash.



**Figure 12.2** Ground CBA. *CBA*, Coal bottom ash.

**Table 12.1** Chemical composition of coal bottom ash.

Chemical composition	Percentage
$\text{Al}_2\text{O}_3$	19.30
$\text{SiO}_2$	60.14
$\text{P}_2\text{O}_5$	0.24
$\text{SO}_3$	0.42
$\text{K}_2\text{O}$	1.19
$\text{CaO}$	3.56
$\text{TiO}_2$	1.26
$\text{MnO}$	0.21
$\text{Fe}_2\text{O}_3$	13.59

### 12.2.2 Preparation of concrete and testing

A total of five concrete mixtures have been prepared with different CBA percentages as shown in Table 12.2. The control specimen is of 100% Ordinary Grade 30 Portland cement. Other mixes were produced by integrating 10%, 20%, 30%, 40%, and 50% of ground CBA as a partial cement substitute. All specimens were cured by immersing it in water until the testing date. The workability of concrete mixture was measured through slump test conducted in accordance with BSEN 12350–2 (2019). The compressive strength test and splitting tensile strength test were conducted following the procedure stated in BS EN 12390-3 (2009) and BS EN 12390-6 (2009), respectively. The hardened concrete testing was conducted at 7, 28, and 56 days.

**Table 12.2** Concrete mixture proportion.

Replacement level (%)	Mix proportion (kg/m <sup>3</sup> )				
	Cement	CBA	Aggregates		Water
			Fine	Coarse	
0	400	0	751	996	260
10	360	40	751	996	260
20	320	80	751	996	260
30	280	120	751	996	260
40	240	160	751	996	260
50	200	200	751	996	260

## 12.3 Result and discussion

### 12.3.1 Workability

The use of CBA as a partial cement substitute affects concrete workability on the basis of Fig. 12.3. The concrete mixtures exhibit slump values between 135 and 190 mm. The use of CBA at 20% and above increases the workability of concrete mixture. The difference in the fineness of cement and CBA is one of the factors that affect the mix workability. The wet sieve test result shows that about 13.9% CBA is retained on the sieve as compared only 1.2% of cement. This result indicated that the larger-sized CBA possesses a lower surface area, which reduces the water requirement to coat it as compared to finer-size cement. The same trend shows that workability is increased when coal ground ash is used as a cement substitute for mortar (Kim, 2015).

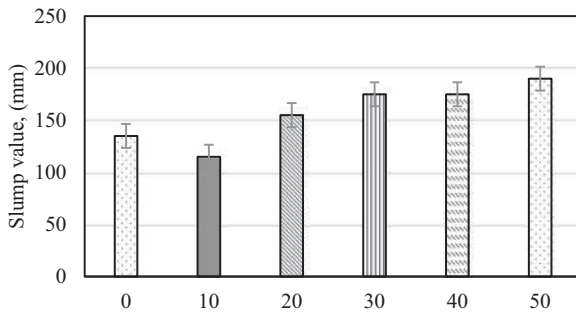


**Figure 12.3** Effect of ground coal bottom ash content on concrete workability.

### 12.3.2 Compressive strength

The compressive strength result of concrete with various contents of CBA is illustrated in Fig. 12.4. All concrete specimens exhibit a continuous concrete strength increment throughout the curing age. The use of continuous water treatment allows for an enhanced hydration process that contributes to densification of internal structures, resulting in enhancement of concrete bearing capacity. The inclusion of CBA disturbs the concrete strength. Concrete with 10% CBA experiences 15% strength declination as compared to the reference specimen. Concrete exhibits a continuous drop in strength as a larger content of CBA is used. Concrete produced using 50% CBA demonstrates the lowest compressive strength. A similar trend in terms of drop of concrete strength upon incorporation of CBA has also been reported by researchers elsewhere, [Kim, 2015](#) and [Argiz et al., 2017](#).

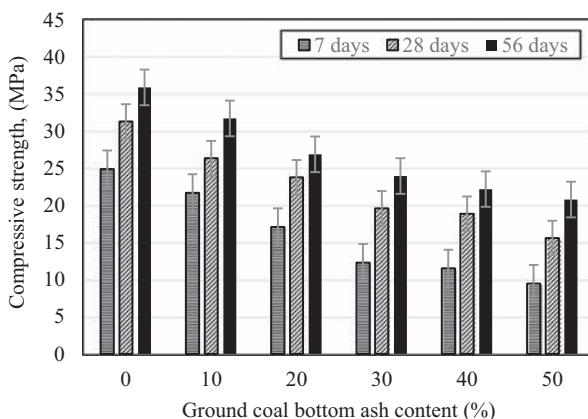


**Figure 12.4** Compressive strength result.

### 12.3.3 Splitting tensile strength

From Fig. 12.5, it has been noticed that the impact of the crushed CBA as cement substitution in concrete has led to a reduction of concrete splitting tensile strength. The plain specimen shows the greatest splitting tensile strength. The strength of concrete with 10% of CBA substitution level is 5.83% lower compared to control mix. Similar to the compressive strength result the splitting tensile strength value of concrete continues to drop gradually as a larger amount of ash is integrated in the mix. Concrete is made with 50% ground CBA. Rougher ground CBA is hard for activation of the pozzolanic reaction when replaced with cement. Last a similar tendency has been observed by [Mangi et al. \(2018\)](#), who reported the decrease of concrete strength with the growing quantity of CBA used as a cement substitute in concrete mixture.

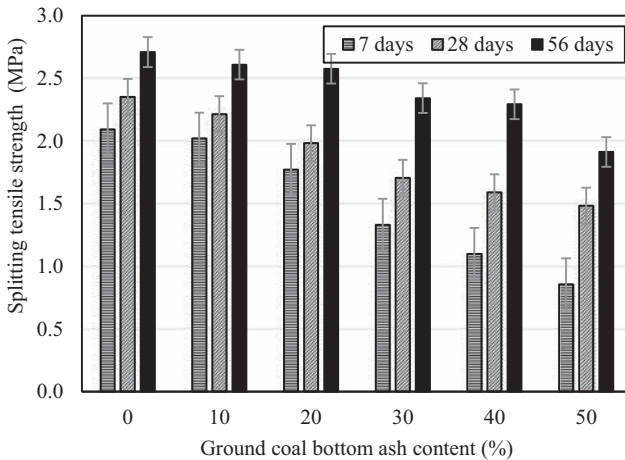


**Figure 12.5** Splitting tensile strength result.

## 12.4 Conclusion

Several conclusions could be drawn from the experimental test results. The conclusions are as follows:

1. The use of ground CBA which is less fine than cement affects the workability and compressive strength concrete.
2. Excessive use of ground CBA reduces compressive strength and splitting tensile strength significantly.
3. The use of a coarser size of CBA disturbs the pozzolanic reaction that could have contributed to concrete strength enhancement.
4. The strength performance of concrete containing CBA after it is ground to nanosize is recommended for future research.

## References

- Argiz, C., Moragues, A., & Menendez, E. (2018). Use of ground coal bottom ash as cement constituent in concretes exposed to chloride environments. *Journal of Cleaner Production*, *170*, 25–33.
- Argiz, C., Sanjuán, M. Á., & Menéndez, E. (2017). Coal bottom ash for Portland cement production. *Advances in Materials Science and Engineering*, 2017. Available from <https://doi.org/10.1155/2017/6068286>.
- ASTM C618. (2019). *Standard specification for fly ash and raw material or calcined natural pozzolan for use as a mineral admixture in Portland cement concrete*. Part 5. West Conshohocken, PA.
- ASTM C618-19. (2019). *Standard specification for coal fly ash and raw or calcined natural pozzolan for use in concrete*. West Conshohocken, PA: ASTM International.
- Balapour, M., Zhao, W., Garboczi, E. J., Nay, Y. O., Spatari, S., Hsuan, Y. G., Billen, P., & Farnam, Y. (2020). Potential use of lightweight aggregate (LWA) produced from bottom coal ash for internal curing of concrete systems. *Cement and Concrete Composites*, *105*, 103428. Available from <https://doi.org/10.1016/j.cemconcomp.2019.103428>.
- BS EN 12390-3 (2009). *Testing hardened concrete, Compressive strength of test specimens*. London: BS EN 12390-3.
- BS EN 12390-6 (2009). *Testing hardened concrete. Tensile splitting strength of test specimens*.
- Durastanti, C., & Morretti, L. (2020). Environmental impacts of cement production: A statistical analysis. *Applied Sciences*, *10*, 8212. Available from <https://doi.org/10.3390/app10228212>.
- Foo, K. Y. (2015). A vision on the opportunities, policies and coping strategies for the energy security and green energy development in Malaysia. *Renewable and Sustainable Energy Reviews*, *51*, 1477–1498.
- Jayakumar, G., Mathews, M. E., Kiran, T., Yadav, B. S. K., Kanagaraj, B., & Anand, N. (2021). Development and strength assessment of sustainable high strength fiber reinforced concrete. *Materials Today: Proceedings*. Available from <https://doi.org/10.1016/j.matpr.2021.06.132>.
- Kim, H. K. (2015). Utilization of sieved and ground coal bottom ash powders as a coarse binder in high-strength mortar to improve workability. *Construction Building Materials*, *91*, 57–64. Available from <https://doi.org/10.1016/j.conbuildmat.2015.05.017>.
- Mangi, S. A., Ibrahim, M. H. W., Jamaluddin, N., Shahidan, S., Arshad, M. F., Memon, S. A., & Jaya, R. P. (2018). Influence of ground coal bottom ash on the properties of concrete. *International Journal of Sustainable Construction Engineering and Technology*, *9*, 26–34.
- Marto, A., & Tan, C. S. (2016). Properties of coal bottom ash from power plants in Malaysia and its suitability as geotechnical engineering material. *Jurnal Teknologi*, *78*(8-5), 1–10.
- Muthusamy, K., Rasid, M. H., Jokhio, G. A., Budiea, A. M. A., Hussin, M. W., & Mirza, J. (2020). Coal bottom ash as sand replacement in concrete: A review. *Construction and Building Materials*, *236*, 117507. Available from <https://doi.org/10.1016/j.conbuildmat.2019.117507>.
- Park, S., Kim, M., Lim, Y., Yu, J., Chen, S., Woo, S. W., & Kim, H. S. (2020). Characterization of rare earth elements present in coal ash by sequential extraction. *Journal of Hazardous Materials*, *123760*. Available from <https://doi.org/10.1016/j.jhazmat.2020.123760>.



- PSR. (2015). *Coal ash: Hazardous to human health*. <<http://www.psr.org/assets/pdfs/coal-ash-hazardous-to-human-health.pdf>>
- Ramakrishna, C., Thenepalli, T., Nam, S. Y., Kim, C., & Ahn, J. W. (2018). The brief review on coal origin and distribution of rare earth elements in various coal ash samples. *Journal of Energy Engineering*, 27, 61–69.
- Roberto, R. A., Belén, G. F., Sindy, S. P., & Emilio, J. B. (2021). Masonry mortars, precast concrete and masonry units using coal bottom ash as a partial replacement for conventional aggregates. *Construction and Building Materials*, 283, 122737.
- Siddique, R. (2013). Compressive strength, water absorption, sorptivity, abrasion resistance and permeability of self-compacting concrete containing coal bottom ash. *Construction and Building Materials*, 47, 1444–1450.
- Singh, N., Mithulraj, M., & Arya, S. (2019). Utilization of coal bottom ash in recycled concrete aggregates based self compacting concrete blended with metakaolin. *Resources, Conservation and Recycling*, 144, 240–251.
- Singh, M., & Siddique, R. (2016). Effect of coal bottom ash as partial replacement of sand on workability and strength properties of concrete. *Journal of Cleaner Production*, 112, 620–630. Available from <https://doi.org/10.1016/j.jclepro.2015.08.001>.
- Rohnstock, T. (2020). *Bottom ash utilisation study in Malaysia*. RWE Technology International GmbH. <<https://www.group.rwe/en/our-portfolio/worldwide-project-references/bottom-ash-utilisation-study-in-malaysia>>
- World Business Council for Sustainable Development. (2013). *International Energy Agency Technology Roadmap: Low-carbon technology for the Indian cement industry*.
- Yao, Z. T., Ji, X. S., Sarker, P. K., Tang, J. H., Ge, L. Q., Xia, M. S., & Xi, Y. Q. (2015). A comprehensive review on the applications of coal fly ash. *Earth-Science*, 141, 105–121.

# Upcycling of recycled asphalt pavement aggregate and recycled concrete aggregate and silica fume in roller-compacted concrete

13

Ahmed M. Ashteyat<sup>1</sup>, Ala' Taleb Obaidat<sup>2</sup>, Baenah Al Tawalbeh<sup>1</sup> and Mehmet Serkan Kirgiz<sup>3</sup>

<sup>1</sup>Department of Civil Engineering, University of Jordan, Amman, Jordan, <sup>2</sup>Civil Engineering Department, Philadelphia University, Amman, Jordan, <sup>3</sup>Northwestern University, Chicago, IL, United States

## 13.1 Introduction

Construction demolition waste (CDW) enabled a considerable economic growth for both the developed countries and underdeveloped countries in the world. In recent decades, CDW was gathered from the roads and the highways being out of service and the reinforced concrete buildings collapsed, which contained an excess quantity of solid waste, such as recycled asphalt aggregate and recycled concrete aggregate (RCA), because the CDW was the largest waste stream in the world. According to the 2008/98/EC EU directive an average European resident generates more than 160 tons of CDW in a lifetime, and it reported that this waste would not get reduced through time (EU Directive 2008/98/EC, 2008). The international experience on CDW shows that 10% RCA has been used within concrete mixing in UK (de Vries, 1996; Collins, 1996); the concrete has mixed with 154,000 tons of RCA in Holland, and 40% of recycling of CDW has been used by Germany in various applications in construction since the beginning of 1991 (Acker, 1996). However, much of its quantity is still put on earth with the aim of the landfilling, so this landfilling process causes a higher cost in the construction technology (Azevedo Azevedo et al., 2020). On the other hand the concrete composite needs an excess aggregate source, cement, and water to build high-quality roads and highways, dams, buildings, and other types of construction based on cement and concrete, for example, roller-compacted concrete (RCC). It is a special dry and slumpless concrete, made of aggregate stack, water, and a low quantity of cement content and laid down through roller compaction method in roads and highways, like being in a foundation of a building. The RCC that was mostly used in the construction systems

had massive structures and large horizontal surfaces such as dams (Abdel-Halim et al., 1999), airport runways (ACI, 2001), and highways (ACI, 2001; Debieb et al., 2010) because of its easy workability, rapid setting time, and high compressive strength gain with a low content of cement and water. The difference between RCC and conventional concrete depended on the grading of aggregate stack, the types of mineralogical admixture, and the consistency. It is essential that the RCC has to be dry enough to be compacted by vibration rollers but wet enough to prepare and achieve the homogeneity between ingredients of concrete in the mixing and compaction (ACI, 2001). The workability of RCC is affected by relative volume, quantity of the cement paste, and the grading of aggregate stack combined.

Usually, construction activities consume several materials such as concrete, steel, stone, and other waste materials. However, the cost of these materials is very high in addition to the environmental impact. Many of the structures get damaged in the Middle East region due to the effect of sunlight and high temperature. The buildings may experience severe damages and hence need to be demolished. As such the recycled or waste materials from damaged structures can be used to replace coarse and fine aggregate, such as recycled asphalt pavement aggregate (RAPA) (Courard et al., 2010), RCA (Debieb et al., 2009), crumb rubber (Fakhri & Amoosoltani, 2017), silica fume (SF) (Fakhri & Saberi, 2016; Adamn et al., 2018), fly ash, glass powder, and tire rubber (Ahmed et al., 2017; Ferrebee et al., 2014). Aghabaglou and Ramyar (Aghabaglou & Ramyar, 2013) used high-volume fly ash (HVFA) to evaluate the properties of RCC mixtures in 2013. It was concluded that the use of fly ash increased the optimum water content and decreased the solid compactness in the RCC mixtures. As the replacement of fly ash with cement increased, the strength was decreased. However, the replacement of fly ash with aggregate stack increased the strength in the RCC system. Adamn et al. (2018) studied the mechanical properties and performance of the RCC made of the replacement of fine aggregate by crumb rubber and the substitution of HVFA and nanosilica by cement in 2018. The results showed that the fresh density of RCC increased with the increase of nanosilica; however, it decreased with increasing crumb rubber in the RCC mixture. On the other hand the replacing of fine aggregate with the HVFA decreased the compressive strength, the splitting tensile strength, the flexural strength, the modulus of elasticity, and abrasion resistance in the RCC mixture containing high-content crumb rubber. Finally the result showed that with the increase of substitution ratio between nanosilica and HVFA the mechanical properties improved. The impact of resistance increased in the HVFA included in RCC made of 10% crumb rubber and nanosilica as well.

Courard et al. (2010) evaluated the mechanical performance and durability of RCC mixtures with concrete road recycled aggregates (RCA) in 2010. The results showed that the RCC made of RCA exhibited very good performance. However, the RCA led to reduce approximately 60% in the compressive strength in the RCA. Debieb et al. (2010) studied the effect of using RCA polluted in chloride and sulfate solution on the mechanical properties and durability of RCC mixtures in 2010

years. The results showed that the mechanical properties of RCC containing 100% coarse and fine recycled aggregates reduced about 30% when compared to the RCC with 100% of natural aggregate (NA) stack. On the other hand the oxides of chloride and sulfate in the RCA did not affect the properties of RCC containing 100% of coarse and fine recycled aggregate stack; nevertheless, the RCC polluted in sea water (RRCC-Sw) presented losses of mass of approximately 100% when compared to the RCC that was not polluted in sea water. Instead of mass loss the swelling was high, more than 200%, because of the delayed ettringite formation in the RCC. In 2015, Chafika et al. evaluated the effect of mechanical properties and durability on three series of RCC mixtures with RAPA (Chafika et al., 2015). These series include 100% of coarse and fine aggregate stack, 50% fine and 50% coarse RAPA combination, and 100% of coarse RAPA. The results showed that the replacing of NA aggregate with RAPA reduced the compressive strength between 32% and 55%, the splitting tensile strength approximately 56%, and the modulus of elasticity approximately 30%. Lam et al. reported the feasibility of the use of electric arc furnace (EAF) slag as aggregate in RCC mix in 2018 years. They concluded that the compressive strength, the splitting tensile strength, and the modulus of elasticity decreased with the increasing of EAF slag aggregate. However, they noted that 20% replacement of EAF slag aggregate with fly ash in RCC pavement (RCCP) mixture improved the mechanical properties in the long term (Lam et al., 2018). In another study in 2017 years, Lam et al. examined the effect of EAF slag aggregate and fly ash on the mechanical properties and durability of RCC. The EAF was used instead of the NA with three substitution ratios (0%, 50%, and 100%), and the cement was replaced by fly ash at three ratios (0%, 20%, and 40%) (Lam et al., 2017). The results showed that the compressive strength and the sulfate resistance of the RCCP mixture was slightly affected by EAF, although the water absorption and abrasion resistance of RCCP increased with EAF slag aggregate. The addition of 20% of fly ash improved the compressive strength and durability in the mixtures. However, the compressive strength of RCCP mixtures continued to decrease even if the fly ash was increased more than 20%. The expansion of the interfacial zone of RCCP was greater than that of the control specimen because of the different hydration process between calcium oxide (CaO), water, cement, and the EAF slag aggregate used (Lam et al., 2017).

In 2017 years, Fakhri and Amoosoltani studied the mechanical properties of RCC designed with reclaimed asphalt pavement and crumb rubber at different percentages, that is, between 25% and 100% for RAPA and between 5% and 25% for crumb rubber (Fakhri & Amoosoltani, 2017). The experimental program included preparation of three beam specimens (70 mm × 70 mm × 240 mm), which were fabricated for each mix combination of RCC. The results showed that the workability and compaction effort of the RCC mixture increased with a decrease in optimum moisture content and dry density because of the lower water absorption ratio of

RAPA and addition of crumb rubber. Use of RAPA in the mix design of RCC decreased the compressive strength of RCC, especially once RAPA was used more than 50%, because of the lower adhesion between cement and aggregate in the mixture. However, the use of 5% crumb rubber increased the compressive strength in the RCC mix. Incorporating of RAPA and crumb rubber also increased the energy absorbency of RCC, nevertheless; this combination of aggregate stack was not proficient to heighten the stiffness and the modulus of elasticity in a level wanted by the scientists (Fakhri & Amoosoltani, 2017). Modarres and Hosseini studied the mechanical properties of RCC designed with NA, RAPA, and rice husk ash (RHA) at different percentages, which were between 3% and 5% in 2014 (Modarres & Hosseini, 2014). The results showed that RHA affected the energy absorbency and resiliency of the RCC which carried out the reduction in the modulus of rupture. On the other hand, RCC mixes containing RAPA as aggregate had a lower fatigue life than conventional RCC. There was a meaningful relationship between the energy absorbency and fatigue response of the RCC. The higher stress ratios indicated that the mix showed higher energy absorbency and better behavior under repeated loadings. There was a reverse relationship between fatigue life and material porosity. As the RCC with RAPA contained 3% RHA, the porosity decreased, and the fatigue increased. However, as it included 5% RHA, the RHA ratio resulted in higher porosity and lower fatigue in the RCC with RAPA.

Ashteyat et al. evaluated the effect of using white cement bypass dust (WCBPD) and polypropylene fiber (PPF) on the mechanical properties and durability of RCC. Fifteen RCC mixes were prepared with the replacement of cement by 10%, 20%, 30%, and 40% of the WCBPD and addition of PPF in two percentages of 0.25% and 0.5% (Ashteyat et al., 2019). It was concluded that the compressive strength for the mixes exceeded 27.6 MPa, except for the mix prepared with 40% replacement of cement by WCBPD. The modulus of elasticity for the mixes decreased significantly as the WCBPD replacement ratio increased, when compared to the control specimen. The water absorption for the mixes was between 3% and 5%, and the increase of the WCBPD for mixes increased the water absorption. The dynamic modulus of elasticity decreased with the addition of WCBPD, but the use of the PPF improved the dynamic modulus of elasticity. After freezing and thawing the weight loss for the RCC mixes increased with use WCBPD, and the use of PPF decreased the loss of weight significantly.

Arabiyat et al. studied the influence of RAPA and RCA on shear features of concrete beam in 2021. They unveiled that for the RAPA beams, experimental shear capacity increased as the RAPA replacement levels decreased; for RAPA–RCA beams, experimental shear capacity decreased when the RCA replacement levels increased, and for RCA beams, experimental shear capacity increased as RCA replacement levels decreased. However, they concluded that the capacity of theoretical shear strength was more conservative than that of the experimental results. Therefore the theoretical shear equations can be applicable to the beams constructed with recycled aggregates. Recently the use of RAPA and RCA in roller-compacted beams could be taken into account as an efficient method (Arabiyat et al., 2021). Shatarat et al., in 2019, presented a significant study related to the influence of

RAPA and RCA on axial compressive strength of reinforced concrete columns. The use of RAPA and RCA in reinforced concrete columns resulted in a retardation in the ability of compression force carrying. They concluded that experimental results are greater than the theoretical strength calculated (Shatarat et al., 2019). In 2018, Shatarat et al. evaluated the effect of using RAPA and RCA on the properties of old concrete. They prepared samples made of replacement of NA with RAPA and RCA wholly. Their results displayed that using RCA, RAPA, and RAPA–RCA combination developed both the physical properties of old concrete and the mechanical properties of old concrete significantly (Shatarat et al., 2018). In 2017, Katkhuda et al. reported the effect of SF on mechanical properties of concrete containing RAPA. Their results demonstrated that the mechanical properties decrease since the content of RAPA increases; the greatest decrease in the compressive strength is in the fine RAPA mixture, while the decrease in the splitting tensile and flexural strengths is almost the same in both fine RAPA mixture and coarse RAPA mixture (Katkhuda et al., 2017). From these previous studies, it can be concluded that the replacing of cement mass with the SF was not evaluated in the RCC with the aggregate stack combination of RCA and RAPA. Therefore the aim of this innovative study is evaluating the effect of substitution of SF with common cement on the properties of RCC with RCA and RAPA. This research also examines the efficiency of using RCA, RAPA, and SF in manufacturing of RCC. To achieve this aim, 27 RCC mixes were cast, in which NA stacks were totally replaced by the combination of RCA and RAPA stacks at 90%, 80%, 70%, 60%, 50%, 40%, 30%, 20%, and 10%, and common cement was partially replaced by SF at three percentages of 0%, 2.5%, and 5%. The most important innovation presented by the study is that the RCC was prepared without NA. Therefore the study also copes with the surplus consumption of natural resources and the surplus emission of carbon dioxide.

## 13.2 Experimental work

This section provides a summary of the experimental program implemented. It provides information on the types and the source of the materials used, mix design, test setup, laboratory tests, and the characteristics of the casted specimens. Many tests were carried out on fresh and hardened properties of RCC, including the compressive strength, the splitting tensile strength, the static modulus of elasticity, the flexural strength, the density, and the water absorption.

### 13.2.1 Materials

Portland pozzolanic cement CEM II/B-P 42.5N, which complies with the European and Jordanian standard specifications JS 30-1 and European standard specifications EN 197-1:2011, was used along with three types of coarse and fine aggregate in all

mixtures (BS EN 197-1:2011, 2011). Of all these aggregate types the RCA obtained from crushed cubes and specimens has been used as a base for heavy machinery for 10 years, with the RAPA obtained from a highway project for Greater Amman Municipality. The aggregates were supplied in two size groups of 4.75–19 mm and 75  $\mu\text{m}$ –4.75 mm. The well-graded combined aggregate stack was produced by combining 45% coarse aggregate stack and 52% fine aggregate stack. Sieve analysis was done for all types of aggregate starting with a sieve size of 25 mm and ending with 75  $\mu\text{m}$ . Both RCA and RAPA stacks also have angular, circular, cubic, and rectangular shape grains and have no grain amorphous. Because of crushing process applied for RCA and RAPA, the aggregate stack has a rough surface with the previous binder. The fineness modulus of RCA is similar to the fineness modulus of RAPA, 4.09. Additionally the maximum grain size of both RCA and RAPA was 19 mm. Daracem SP6RR (AA) was used as a chemical admixture during mixing of fresh RCC in the dosage of 1%–2.5% by weight of cement in order to increase the workability of RCC. Daracem SP6RR (AA) was used as a chemical admixture during mixing of fresh RCC in the dosage of 1%–2.5% by weight of cement to increase the workability of RCC. SF, which is formed from the condensed gas escaping from EAFs from the production of elemental silicon or alloys containing silicon, was used as a replacement material for common cement in the mixtures of RCC. The grain size of SF used varies from 0.1 to 0.2  $\mu\text{m}$ . The blaine surface area of SF is approximately 20,000  $\text{m}^2/\text{kg}$ , and the bulk density of SF is 250  $\text{kg}/\text{m}^3$ . The chemical composition of SF consists of 87%  $\text{SiO}_2$ , 1.17%  $\text{Al}_2\text{O}_3$ , 0.63%  $\text{Fe}_2\text{O}_3$ , 0.9%  $\text{CaO}$ , 4.4%  $\text{MgO}$ , 1.2%  $\text{K}_2\text{O}$ , 1.3  $\text{Na}_2\text{O}$ , 1%  $\text{SO}_3$ , and 5.4% LOI.

### 13.2.1.1 Mix design

The mixture content and proportions were calculated according to soil compaction method based on establishing a relationship between the dry density and the moisture content of the RCC (ACI Committee 211, 2002). Regularly the cementitious content varies between 10% and 17% in the RCC pavement. With the varying cementitious content the RCC samples include 210 and 360 kg cement per cubic meter. However, three different cement contents (10%, 11%, and 12%) for the low cement content of the RCC and four moisture contents for each cement content (4.5%, 5%, 5.5%, and 6%) were used in this research. According to the results of compressive strength, it was found that the highest compressive strength of RCC was achieved with the cement content of 250  $\text{kg}/\text{m}^3$  and the optimum water content of 5.2% at 7 days. Therefore this cement content and optimum water content will be used in the mixes of the RCC. Table 13.1 shows the groups, the title and mixture proportion, the optimum water content, and the maximum dry density for each mix. The RCC used in Bullmoose Coal Mine was used as the control mix because it consisted of RCA, RAPA, and SF and is a very good example of industrial application of RCC.

**Table 13.1** The groups, title and mixture proportion, the optimum water content, and the maximum dry density for each mix.

Group	Mixture	Optimum water content (%)	Maximum dry density (kg/m <sup>3</sup> )	
A	90%RCA +10% RAPA	5.8	2042	
	80% RCA + 20% RAPA	5.8	2225	
	70% RCA +30% RAPA	5	2228	
	60% RCA + 40% RAPA	5.4	2204	
	50% RCA + 50% RAPA	6	2038	
	40% RCA +60% RAPA	5.8	2086	
	30% RCA +70% RAPA	5.3	2079	
	20% RCA + 80% RAPA	5.5	2044	
	10% RCA + 90% RAPA	5.5	2028	
B	90%RCA +10% RAPA + 2.5%SF	5.4	2018	
	80% RCA + 20% RAPA + 2.5%SF	5.3	2137	
	70% RCA +30% RAPA + 2.5%SF	5	2075	
	60% RCA + 40% RAPA + 2.5%SF	5.4	2096	
	50% RCA + 50% RAPA + 2.5%SF	4.6	1964	
	40% RCA +60% RAPA + 2.5%SF	5.5	2028	
	30% RCA +70% RAPA + 2.5%SF	5	2068	
	20% RCA + 80% RAPA + 2.5%SF	5.4	2028	
	10% RCA + 90% RAPA + 2.5%SF	5.5	2042	
	C	90%RCA +10% RAPA + 5%SF	5.5	1964
		80% RCA + 20% RAPA + 5%SF	5	1936
		70% RCA +30% RAPA + 5%SF	5	1920
		60% RCA + 40% RAPA + 5%SF	5.5	1836
		50% RCA + 50% RAPA + 5%SF	4.5	1952
		40% RCA +60% RAPA + 5%SF	5.4	1932
30% RCA +70% RAPA + 5%SF		5.1	2068	
20% RCA + 80% RAPA + 5%SF		5.4	2000	
10% RCA + 90% RAPA + 5%SF		5.4	2060	



### 13.2.1.2 Concrete mixing, casting, and curing

A tilting drum mixer of  $0.18 \text{ m}^3$  was used for mixing the ingredients. The following steps summarize the mixing, the casting, and the curing of the RCC specimens. First, coarse aggregate was added with a part of water. Second, cementitious materials (cement and SF) and fine aggregate were added gradually. Finally the remaining amount of water was added. The RCC specimens were prepared using cylindrical molds with dimensions of  $150 \text{ mm} \times 300 \text{ mm}$  and prism molds with dimensions of  $100 \text{ mm} \times 100 \text{ mm} \times 500 \text{ mm}$ , as shown in Fig. 13.1. Before casting the molds were cleaned and oiled to avoid concrete sticking to the internal faces of the molds. After mixing, concrete was poured into three layers in the cylinders and prisms and then compacted according to ASTM C 1435 by a vibrating compaction hammer (ASTM C1435/C1435M-20, 2020). The hammer had a minimum mass (without a tamping plate) of  $10 \pm 0.2 \text{ kg}$ . It also had a minimum power input of  $900 \text{ W}$  and could provide at least 2000 impacts per minute. This vibrating hammer was attached to a circular steel plate attached to a metal shaft, which inserts into the vibrating hammer chuck (see Fig. 13.2). The diameter was  $140 \pm 3 \text{ mm}$  and has a mass of  $3 \pm 0.1 \text{ kg}$  according to ASTM C 1435. The vibrating hammer was placed on the concrete, and then it was started and the concrete was allowed to consolidate under the plate. The vibrating hammer was stopped after a maximum of 20 seconds vibration period for each layer according to ASTM C 1435 (Ashteyat et al., 2019; ASTM C1435/C1435M-20, 2020).



**Figure 13.1** Prism mold with the specimen of the RCC. RCC, Roller-compacted concrete.



**Figure 13.2** Cylindrical molds with the specimens of the RCC. RCC, Roller-compacted concrete.

The casted specimens were left in molds for 24 hours, covered with a wet burlap. After that the molds were removed, and specimens were placed in a water tank to cure for 28 days. For each mix, 15 cylindrical specimens and three prisms were cast for testing of the physical properties, the mechanical properties, and durability.

## **13.2.2 Testing procedure**

### **13.2.2.1 Compressive strength**

Ninety cylinders with 150 mm diameter and 300 mm height were cast and tested to measure the 28 days compressive strength. The test was performed according to ASTM C 39 (Ashteyat et al., 2019; ASTM C39/C39M-21, 2021) after the curing period ended. The results of these cylinders were used to evaluate the effect of using RCA, RAPA, and SF on the compressive strength of RCC mixture.

### **13.2.2.2 Splitting tensile strength**

The splitting tensile strength is an indirect method to determine the tensile strength of concrete by placing a concrete cylinder at the horizontal axis between plates of a testing. Ninety cylindrical specimens sized 150 mm × 300 mm were tested to evaluate the splitting tensile strength according to ASTM C496 (Ashteyat et al., 2019; ASTM C496/C496M-17, 2017) using an MFL Prüf-systeme Universal Testing Machine for cylindrical specimens with different percentages of RCA, RAPA, and SF, as shown in Fig. 13.3.



**Figure 13.3** Failure of the cylinder after the splitting load was applied.

### 13.2.2.3 Flexural strength

In order to study the effect of RCA, RAPA, and SF on the flexural strength of the RCC, 90 prism specimens sized 500 mm in length, 100 mm in height, and 100 mm in width were cast and tested after curing of 28 days. The test was carried out according to ASTM C293 (Ashteyat et al., 2019; ASTM C293/C293M-16, 2016) using a simple beam with center loading (uniaxial load) for a prism, as shown in Fig. 13.4. The length of the prism is equal to 500 mm, and the distance between the centers of the support equals to 300 mm for the prism.



**Figure 13.4** Flexural strength test with one-point loading method.

### 13.2.2.4 Static modulus of elasticity

The static modulus of elasticity of RCC mixture was measured by using cylindrical specimens sized 150 mm  $\times$  300 mm. The modulus of elasticity of RCC was evaluated after 28 days of curing according to ASTM C469 (Ashteyat et al., 2019; ASTM C469/C469M-14e1, 2014). A linear variable differential transformer (LVDT) is connected to

the concrete specimens to determine deformation, as shown in Fig. 13.5. The readings of the stress and strain were recorded to establish a new relationship between stress and strain. Then the modulus of elasticity was calculated by the ratio between stress and strain in the elastic part before the yield point. For brittle materials, like concrete, the elastic area can be taken from zero stress to 0.45 f<sub>c</sub>.



**Figure 13.5** Modulus of elasticity test for cylindrical specimens and the reading of stress and strain with the LVDT. *LVDT*, Linear variable differential transformer

### 13.2.2.5 Density

The wet and dry densities are very important factors for RCC to achieve high compressive strength with low cement and water content. The maximum density is found for RCC at optimum water content by soil compaction method for all mixes. The wet density determined according to ASTM C 138/C138 (ASTM C138/C138M-17a, 2017).

### 13.2.2.6 Water absorption

The concrete water absorption is a fast durability evaluation test that can give us information to estimate the pore structure in a concrete element. In this test the percentage of water absorption from aggregate and fill with pores is evaluated by putting the specimens in the oven at  $110^{\circ}\text{C} \pm 5^{\circ}\text{C}$  for not less than 24 hours; then they are submerged in water for 48 hours. The equation used to calculate the absorption percentage includes  $W_1$  (representing the oven-dry specimens) and  $W_2$  (representing the saturated mass after immersion in water) according to ASTM 642-13 (ASTM C642-13, 2013) to calculate the water absorption percentage according to Eq. (13.1).

$$\text{Absorption percent \%} = \frac{W2 - W1}{W1} \quad (13.1)$$

### 13.3 Results and discussion

#### 13.3.1 Compressive strength

Fig. 13.6 and Table 13.2 present the compressive strength of RCC mixes at different RCA and RAPA aggregate percentages and replacement of common cement through the SF at two percentages of 2.5% and 5%.

**Table 13.2** Compressive strength test results for the RCC mixes containing RCA, RAPA, and SF.

Group	Types of specimen	Compressive strength (MPa)
		28 days
A	Control	15.2
	90%RCA + 10%RAPA	11.80
	80%RCA + 20%RAPA	11.35
	70%RCA + 30%RAPA	11.32
	60%RCA + 40%RAPA	10.63
	50%RCA + 50%RAPA	15.25
	40%RCA + 60%RAPA	14.22
	30%RCA + 70%RAPA	14.68
	20%RCA + 80%RAPA	13.07
	10%RCA + 90%RAPA	12.97
B	90%RCA + 10%RAPA + 2.5%SF	10.06
	80%RCA + 20%RAPA + 2.5%SF	10.13
	70%RCA + 30%RAPA + 2.5%SF	10.30
	60%RCA + 40%RAPA + 2.5%SF	14.33
	50%RCA + 50%RAPA + 2.5%SF	12.99
	40%RCA + 60%RAPA + 2.5%SF	15.53
	30%RCA + 70%RAP + 2.5%SF	10.42
	20%RCA + 80%RAPA + 2.5%SF	12.06
	10%RCA + 90%RAPA + 2.5%SF	10.99
	C	90%RCA + 10%RAPA + 5%SF
80%RCA + 20%RAPA + 5%SF		9.11
70%RCA + 30%RAPA + 5%SF		9.69
60%RCA + 40%RAPA + 5%SF		9.40
50%RCA + 50%RAPA + 5%SF		13.55
40%RCA + 60%RAPA + 5%SF		11.75
30%RCA + 70%RAPA + 5%SF		16.44
20%RCA + 80%RAPA + 5%SF		10.98
10%RCA + 90%RAPA + 5%SF		9.00

NA, Not available.

As seen in Fig. 13.6 the compressive strength of the RCC with RCA, RAPA, and SC is comparable to that of control RCC used in the Bullmoose Coal Mine. Use of RCA and RAPA in the RCC mixes significantly reduced the compressive strength for the mixes, except for 50%RCA + 50%RAPA, 40% RCA + 60%RAPA + 2.5%SF, and 30% RCA + 70% RAPA + 5%SF (Table 13.2). It can be seen from Table 13.2 that the reduction in the compressive strength is between 3.4% and 40% when compared with the compressive strength of the RCC. In contrast to previous negative growth, 50%RCA + 50%RAPA, 40% RCA + 60%RAPA + 2.5%SF, and 30% RCA + 70%RAPA + 5%SF increased the compressive strength between 0.32% and 8.15%.

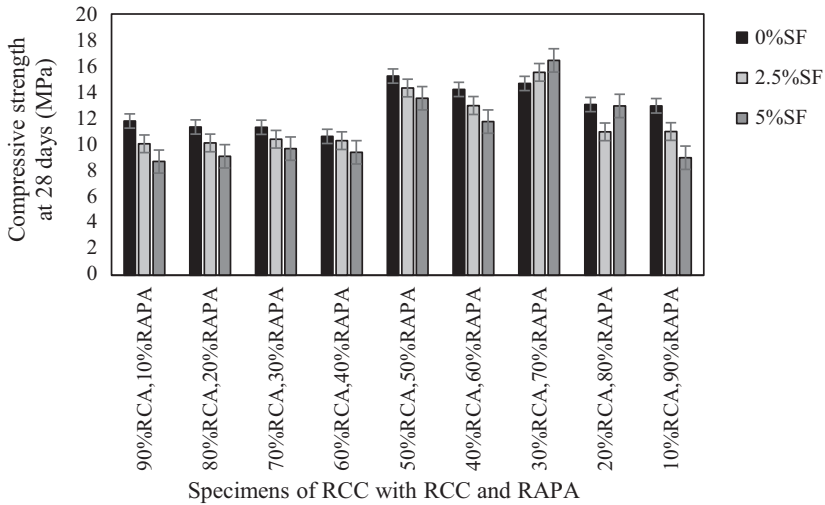


**Figure 13.6** Average compressive strength and standard errors for the RCC with RCA and RAPA and for the RCC with and without SF after 28 days of curing. RCC, Roller-compacted concrete; RCA, recycled concrete aggregate; RAPA, recycled asphalt pavement aggregate.

Considering the effect of SF content on the compressive strength of the RCC the replacement of 2.5%SF with common cement reduced the compressive strength from 62.7% to 76%, except for 40%RCA + 60%RAPA + 2.5%SF. The reduction of compressive strength as a result of the replacement of 5%SF with common cement was from 63.5% to 80.7% in the RCC, except for 30%RCA + 70%RAPA + 5%SF. Although RCA and RAPA were used in the RCC, the replacement of 2.5%SF with cement increased the compressive strength, more than 1.5%. The growth of compressive strength was 8.15% in 30%RCA + 70%RAPA + 5%SF because of the replacement of 5%SF with cement.



**Figure 13.7** Failure shape for RCC specimens under the load of compression. *RCC*, Roller-compacted concrete.

It could be noted that the increase of SF in these mixtures would lead to an important decrease in compressive strength because of the low water-to-cement ratio and the manufacturing process of common RCC. Nevertheless, 40% RCA + 60%RAPA + 2.5%SF and 30%RCA + 70%RAPA + 5%SF showed the most promising result for future studies and applications of RCC. The reduction in the compressive strength may be due to the amount of bitumen and cement attached to the RAPA and RCA particles. Hence use of the coarse and fine aggregate combination of RAP and RCA had adverse effects on the compressive strength in the RCC. Settari et al. noticed a similar trend, where since RAPA was used in the production of RCC, its aggregate stack reduced the compressive strength of the RCC (Settari et al., 2015). Modarres and Hosseini reported an increase in compressive strength of RCC made of rubber and the replacement of 7% SF with common cement (Modarres & Hosseini, 2014). Fig. 13.7 shows the failure shape for RCC specimens under the load of compression.

### 13.3.2 Splitting tensile strength

Table 13.3 presents the splitting tensile strength of RCC mixes at different RCA and RAPA aggregate percentages and replacement of common cement through SF at two percentages of 2.5% and 5%. The splitting tensile strength of RCC mixture made of the aggregate combination of RCA and RAPA and the replacement of cement with SF was tested at the curing age of 28 days.

**Table 13.3** Splitting tensile strength test results for the RCC mixes containing RCA, RAPA, and SF.

Group	Types of specimen	Splitting tensile strength (MPa)
		28 days
A	Control	NA
	90%RCA + 10%RAPA	1.95
	80%RCA + 20%RAPA	1.85
	70%RCA + 30%RAPA	1.44
	60%RCA + 40%RAPA	1.61
	50%RCA + 50%RAPA	1.74
	40%RCA + 60%RAPA	1.58
	30%RCA + 70%RAPA	1.87
	20%RCA + 80%RAPA	1.40
B	10%RCA + 90%RAPA	1.33
	90%RCA + 10%RAPA + 2.5%SF	1.87
	80%RCA + 20%RAPA + 2.5%SF	1.66
	70%RCA + 30%RAPA + 2.5%SF	1.46
	60%RCA + 40%RAPA + 2.5%SF	1.40
	50%RCA + 50%RAPA + 2.5%SF	1.60
	40%RCA + 60%RAPA + 2.5%SF	1.42
	30%RCA + 70%RAP + 2.5%SF	1.94
	20%RCA + 80%RAPA + 2.5%SF	1.33
C	10%RCA + 90% RAPA + 2.5%SF	1.30
	90%RCA + 10%RAPA + 5%SF	1.82
	80%RCA + 20%RAPA + 5%SF	1.54
	70%RCA + 30% RAPA + 5%SF	1.64
	60%RCA + 40%RAPA + 5%SF	1.23
	50%RCA + 50%RAPA + 5%SF	1.56
	40%RCA + 60%RAPA + 5%SF	1.31
	30%RCA + 70%RAPA + 5%SF	2.05
	20%RCA + 80% RAPA + 5%SF	1.37
10%RCA + 90%RAPA + 5%SF	1.22	

NA, not available.

In reference to [Table 13.3](#) and [Fig. 13.8](#), it was noted that the splitting strength of RCC reduced, although it was prepared with the replacement of 2.5% and 5% SF with common cement, except for the mixture of 30%RCA + 70%RAPA + 5%SF. The replacement of %5SF with common cement increased the splitting tensile strength in the mixture of 30%RCA + 70%RAPA + 5%SF. Therefore the highest splitting tensile strength was obtained from the mixture of 30%RCA + 70% RAPA + 5%SF. This means that the replacement of 5%SF with cement led to the growth between 25% and 32%.



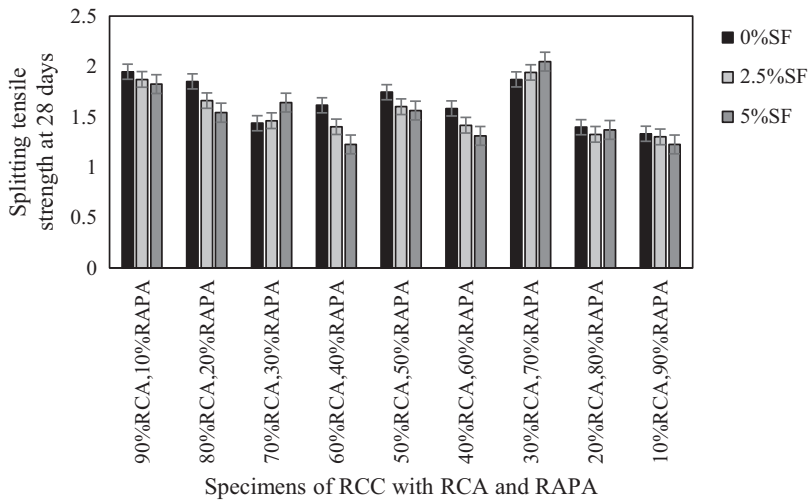


**Figure 13.8** Average and error bar of the splitting tensile strength for RCC made of the combination of RCA and the RAPA aggregate, and the replacement of SF with cement after 28 days of curing. *RCC*, Roller-compacted concrete; *RCA*, recycled concrete aggregate; *RAPA*, recycled asphalt pavement aggregate.

The splitting tensile strength of other mixtures with RCA and RAPA was lower than that of 30%RCA + 70%RAPA + 5%SF. According to the literature results the splitting tensile strength for RCC with RCA and RAPA did not exceed 2 MPa at 28 days. According to the results of Ferrebee et al. and Saadi the splitting tensile strength evaluated did not exceed 2.5 MPa at 28 days (Ferrebee et al., 2014; Saadi, 2010). Debieb et al. reported that the decrease in the splitting tensile strength was approximately 56% (Debieb et al., 2010). According to the results of Shafigh et al. (2012) the ratio of the splitting tensile strength to compressive strength was between 8% and 14% for normal concrete; most of the mixes satisfied the criteria.

### 13.3.3 Flexural strength

Fig. 13.9 and Table 13.4 show the effect of the replacement of SF with cement on the flexural strength of RCC with the combination of RCA and the RAPA aggregate.

**Table 13.4** Flexural strength test results for the RCC mixes containing RCA, RAPA, and SF.

Group	Types of specimen	Flexural strength (MPa)
		28 days
A	Control	NA
	90%RCA + 10%RAPA	4.58
	80%RCA + 20%RAPA	4.65
	70%RCA + 30%RAPA	4.75
	60%RCA + 40%RAPA	7.65
	50%RCA + 50%RAPA	4.86
	40%RCA + 60%RAPA	5.22
	30%RCA + 70%RAPA	8.11
	20%RCA + 80%RAPA	7.01
	10%RCA + 90%RAPA	6.89
B	90%RCA + 10%RAPA + 2.5%SF	4.65
	80%RCA + 20%RAPA + 2.5%SF	4.79
	70%RCA + 30%RAPA + 2.5%SF	6.13
	60%RCA + 40%RAPA + 2.5%SF	6.22
	50%RCA + 50%RAPA + 2.5%SF	5.51
	40%RCA + 60%RAPA + 2.5%SF	5.01
	30%RCA + 70%RAPA + 2.5%SF	6.49
	20%RCA + 80%RAPA + 2.5%SF	6.25
	10%RCA + 90%RAPA + 2.5%SF	6.10
	C	90%RCA + 10%RAPA + 5%SF
80%RCA + 20%RAPA + 5%SF		4.94
70%RCA + 30%RAPA + 5%SF		7.3
60%RCA + 40%RAPA + 5%SF		5.32
50%RCA + 50%RAPA + 5%SF		6.24
40%RCA + 60%RAPA + 5%SF		4.52
30%RCA + 70%RAPA + 5%SF		5.55
20%RCA + 80%RAPA + 5%SF		5.13
10%RCA + 90%RAPA + 5%SF		5.03

NA, not available; RCC, Roller-compacted concrete; RCA, recycled concrete aggregate; RAPA, recycled asphalt pavement aggregate.

The flexural strength of RCC with the aggregate stack of RCA and RAPA was greater than that of the RCC with SF at 28 days. The greatest flexural strength was in the 30%RCA + 70%RAPA specimens. As noted the flexural strength decreased significantly since the RCA and RAPA content increased (Table 13.4 and Fig. 13.9). The greatest quantity of modulus of rupture in modified RCC reached 8.11 MPa at 30%RCA + 70%RAPA, 0%SF. However, when the replacement ratio of SF in mixtures is more the modulus of rupture quantity increases slightly.

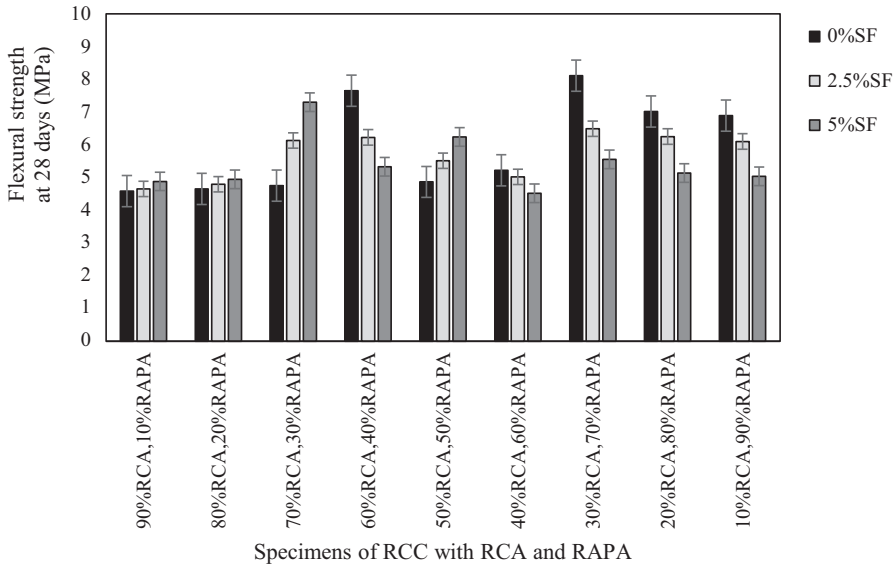


**Figure 13.9** Average and error bar of the flexural strength for RCC made of the combination of RCA and the RAPA aggregate, and the replacement of SF with cement after 28 days of curing. *RCC*, Roller-compacted concrete; *RCA*, recycled concrete aggregate; *RAPA*, recycled asphalt pavement aggregate.

As noted the modulus of rupture of 70%RAC + 30%RAPA mix increased to 7.30 MPa at 5%SF, similar to the quantity of 7.46 MPa for N.A,0%SF (Table 13.4). The modulus of rupture of modified RCC with NA replacement by using 60%RAC + 40% AP and 30%RAC + 70%RAPA at 0%SF had a higher modulus of rupture compared to conventional RCC concrete. Therefore using RCA and RAPA in RCC mixtures slightly has improved the modulus of rupture with 2.5% at 60%RAC + 40%RAPA and 8.7% at 30%RAC + 70%RAPA compared to the modulus of rupture of control mixtures. According to the results of the study carried out by Hamad et al. the replacement of NA with different percentages of RCA did not adversely affect the flexural strength of RCC (Hamad et al., 2018). Refaie et al. reported that the flexural strength of RCC with RCA was greater, over 4%, than that of RCC with NA (Refaie et al., 2010).

According to the results of the study carried out by Hamad et al. the replacement of NA with different percentages of RCA did not adversely affect the flexural strength of RCC (Hamad et al., 2018). Refaie et al. reported that the concrete flexural strength of RCC with RCA was higher by approximately 4% compared to that of RCC with NA (Refaie et al., 2010).

### 13.3.4 Modulus of elasticity

The modulus of elasticity of RCC varies in the same way as the compressive strength, and the results are shown in Fig. 13.10 and Table 13.5.

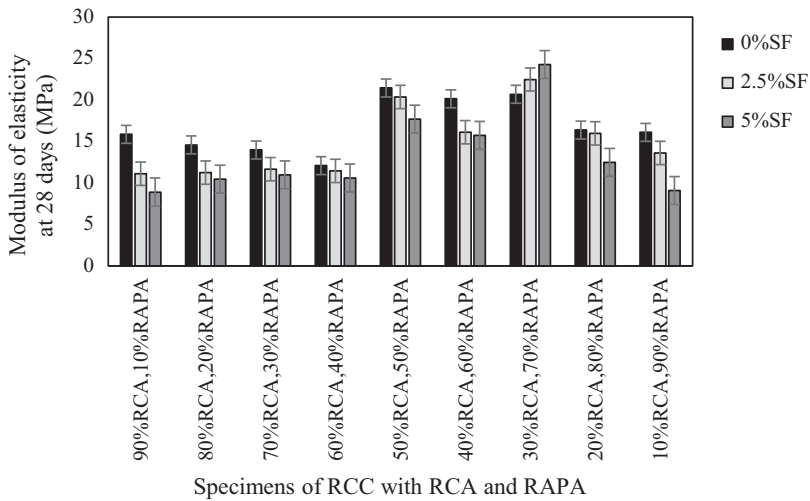


**Figure 13.10** Average and error bar of the modulus of elasticity for RCC made of the combination of RCA and the RAPA aggregate, and the replacement of SF with cement after 28 days of curing.

**Table 13.5** Modulus of elasticity results for the RCC mixes containing RCA, RAPA, and SF.

Group	Types of specimen	Modulus of elasticity (GPa)
		28 days
A	Control	NA
	90%RCA + 10%RAPA	15.86
	80%RCA + 20%RAPA	14.58
	70%RCA + 30%RAPA	13.98
	60%RCA + 40%RAPA	12.10
	50%RCA + 50%RAPA	21.45
	40%RCA + 60%RAPA	20.15
	30%RCA + 70%RAPA	20.68
	20%RCA + 80%RAPA	16.37
B	10%RCA + 90%RAPA	16.10
	90%RCA + 10%RAPA + 2.5%SF	11.11
	80%RCA + 20%RAPA + 2.5%SF	11.25
	70%RCA + 30%RAPA + 2.5%SF	11.67
	60%RCA + 40%RAPA + 2.5%SF	11.45
	50%RCA + 50%RAPA + 2.5%SF	20.37
	40%RCA + 60%RAPA + 2.5%SF	16.13
	30%RCA + 70%RAP + 2.5%SF	22.47
	20%RCA + 80%RAPA + 2.5%SF	15.97
10%RCA + 90%RAPA + 2.5%SF	13.61	

(Continued)

**Table 13.5** (Continued)

Group	Types of specimen	Modulus of elasticity (GPa)
		28 days
C	90%RCA + 10%RAPA + 5%SF	8.90
	80%RCA + 20%RAPA + 5%SF	10.45
	70%RCA + 30%RAPA + 5%SF	10.97
	60%RCA + 40% RAPA + 5%SF	10.61
	50%RCA + 50%RAPA + 5%SF	17.68
	40%RCA + 60%RAPA + 5%SF	15.75
	30%RCA + 70%RAPA + 5%SF	24.26
	20%RCA + 80%RAPA + 5%SF	12.47
	10%RCA + 90%RAPA + 5%SF	9.10

NA, not available; RCC, Roller-compacted concrete; RCA, recycled concrete aggregate; RAPA, recycled asphalt pavement aggregate.

As noted the modulus of elasticity increased significantly as the SF replacement ratio increased in conventional RCC. However, the replacement of SF with cement retarded the compressive strength in the RCC mixtures with the aggregate stack of RCA and RAPA. As a result the modulus of elasticity decreased, except for the mixture of 30% RCA + 70%RAPA. The modulus of elasticity increased with the increase of the SF replacement ratio in mixes of RCC with RCA and RAPA. The highest modulus of elasticity was obtained from the specimens of the 30%RAC + 70%RAP, over 24 MPa (Table 13.5). At 2.5% SF the reduction of modulus of elasticity was in the range of 53.22%–76.86%. While there was replacement of 5%SF with cement in the RCC mixtures, the reduction was between 54.48% and 85% in the RCC with the RCA and the RAPA aggregate stack. Fig. 13.10 shows the average results and error bars of the modulus of elasticity test of cylindrical specimens at 28 days. The retardation of modulus of elasticity is related to a decrease in the compressive strength due to the bitumen and the cement paste attached with aggregate stack. This is probably due to poor adhesion between the new cement paste with the new aggregate stack in the RCC. According to the results of the study carried out by Settari et al. the reduction of modulus of elasticity reached 53% in the RCC because of the use of RAPA as aggregate stack (Settari et al., 2015). This decrease in modulus of elasticity is confirmed by other research studies, which means that the reduction of modulus of elasticity was acceptable at 50% RCA + 50%RAPA,0%SF, 40%RCA + 60%RAPA,0%SF, 30%RCA + 70%RAP,0%SF, 30%RCA + 70%RAP,2.5%SF, and 30% RCA + 70%RAPA,5%SF.

### 13.3.5 Water absorption

Fig. 13.11 shows the water absorption of all RCC prepared. The concrete water absorption is a fast durability evaluation test that can provide information including the pore structure and durability for readers, even under freeze–thaw conditions, and eliminate seepage in the pavement through the RCC mixtures.

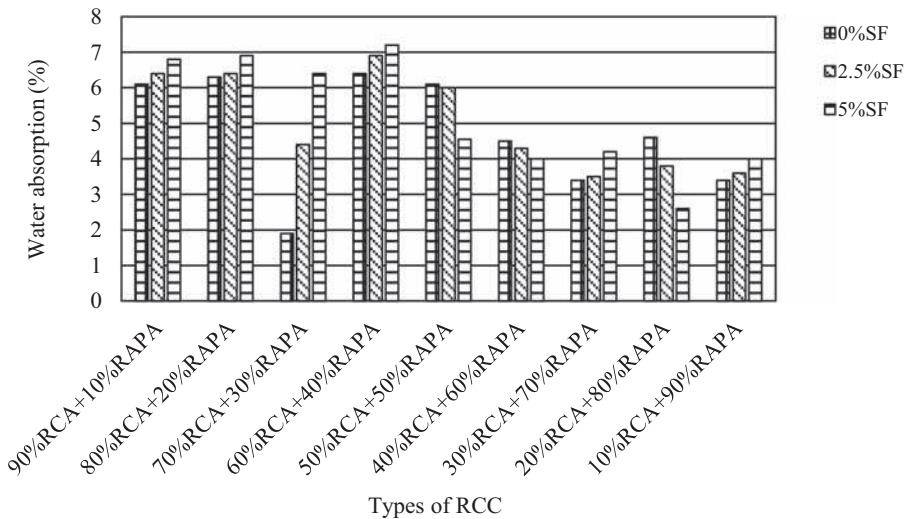


**Figure 13.11** Average water absorption for RCA and RAPA mixtures with and without SF after 28 days of curing. *RCA*, recycled concrete aggregate; *RAPA*, recycled asphalt pavement aggregate

The type, rate of absorption of aggregate, and use of pozzolanic materials may have an influence on the water absorption of RCC specimens with RAPA, RCA, and SF. It can be noted from Fig. 13.11 that the water absorption of specimens was retarded with increasing SF content because the fineness modulus of SF is greater than that of cement. This meant that the SF fills the gap between cement matrix and aggregate stack very well. The highest water absorption ratio that was reached is 7.22% in the RCC consisting of 60%RCA + 40%RAPA and 5%SF. As would be noted the water absorption of RCC mixes with a higher replacement ratio of RCA is higher than that of the RCC with RAPA because the old cement matrix upper surface of RCA absorbs much more water than that of RAPA covered with bitumen. Also the research unveiled that the most water absorption of RCC is between 3% and 5%. The average water absorption ratio is similar in accordance with literature findings (CEB-FIP, 1989; Olorunsogo & Padayachee, 2016) in the study. Therefore mixtures have satisfied the criteria of minimum water absorption, except for the water absorption of 90%RCA + 10%RAPA,0%SF, 80%RCA + 20%RAPA,0%SF, 90%RCA + 10%RAPA,2.5%SF, 80%RCA + 20%RAPA,2.5%SF, 60%RCA + 40%RAPA,2.5%SF, 50%RCA + 50%RAPA,2.5%SF, 90%RCA + 10%RAPA,5%SF, 80%RCA + 20%RAPA,5%SF, 70%RCA + 30%RAPA,5%SF, and 60%RCA + 40%RAPA,5%SF, which have exceeded the extreme limit. On the other hand, there are mixtures that showed a water absorption ratio lower than the minimum water absorption ratio—70%RCA + 30%RAPA,0%SF, 30%RCA + 70%RAPA,2.5%SF, and 20%RCA + 80%RAPA,5%SF. According to Settari et al. (Settari et al., 2015), water absorption increased by about 20%–60% in comparison with the reference RCC. In

this research, when the water absorption of RCC is compared to that of research of Settari et al. it was concluded that SF retarded the water absorption of RCC including both RCA and RAPA. Olorunsogo and Padayachee (Olorunsogo & Padayachee, 2016) have found a 29% increase in water absorption of the concrete with 100% RCA because it has contained no SF in the RCC.

### 13.3.6 Density

Fig. 13.12 shows the density of RCC with different replacement percentages of RCA, RAPA, and SF. The wet density of RCC expresses the ratio of the fresh concrete mass to the volume of the mold. However, another important factor is the optimum water content because it influences the dry density of RCC. This means that there is a powerful relationship between the optimum water content and the dry density of RCC. As would be noted from Fig. 13.12 the dry density of conventional and modified RCC has decreased significantly since the SF replacement ratio increased. Because of the specific gravity difference between the SF and the cement, the unit weight in volume of RCC with the SF decreased when compared to the unit weight in volume of RCC with cement only. Also, RCA and RAPA are materials that are different from each other due to the bitumen and cement attached with aggregate.

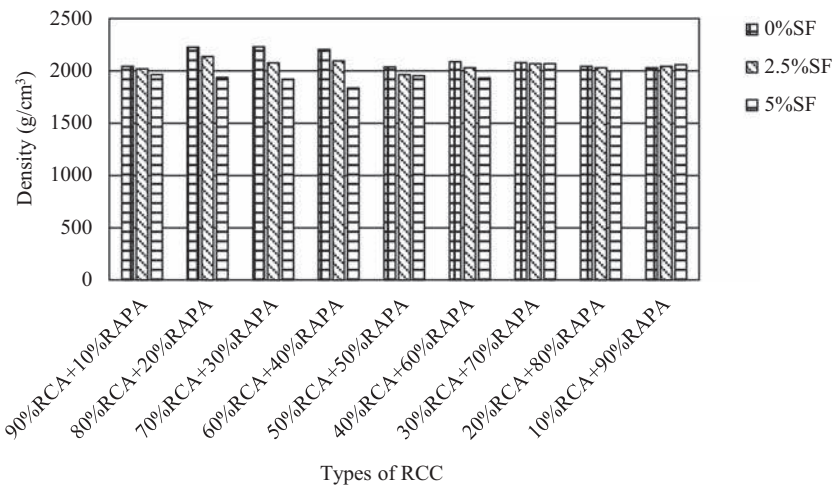


**Figure 13.12** Average density of RCC with different replacement percentages of RCA, RAPA, and SF. RCC, Roller-compacted concrete; RCA, recycled concrete aggregate; RAPA, recycled asphalt pavement aggregate.

This different binder resulted in inducing a lower density and greater capacity of water absorption in the RCC with RCA and RAPA. Therefore using RCA and RAPA as replacement of NA in mixtures was not a heavy impact for the

compactness and dry density of the RCC. The decrease in density of RCC prepared was between 12% and 14% approximately. The greatest dry density is in the RCC made of 80%RCA&20%RAPA,0%SF. With the average density measured in the study the RCC made with RAPA, RCA, and SF is in the class of middle-density construction materials. According to [Settari et al. \(2015\)](#) and Courard et al. ([Debieb et al., 2010](#)) the dry density of RCC with RAPA and RCA depends on the compacting ability of RCC strongly. In other words the replacement percentage of RAPA and RCA influences both the compactness and the dry density.

### 13.4 Conclusions

An experimental program was conducted to evaluate the effect of the replacement of SF with cement on the mechanical properties and modulus of elasticity of the RCC containing RCA and RAPA. The following conclusions could be drawn from the study:

1. The use of RCA and the RAPA as aggregate stack in the preparation of the RCC decreases the mechanical properties of the RCC.
2. The decrease in the mechanical properties of RCC was compensated with the replacement of 2.5% SF with cement at 28 days. The decrease in the mechanical properties of the RCC is due to the bitumen and cement paste attached on the surface of RCA and RAPA, which would affect the interlocking bond between the new cement paste and the recycled aggregate stack.
3. Based on the results of the mechanical properties and the modulus of elasticity of the RCC the combination of RCA and the RAPA aggregate stack with different percentages can be used as a subbase for road pavements or some projects such as low traffic pavements, rural roads, and the large areas of pedestrian. Also the use of RCA and RAPA would considerably reduce the cost of RCC and would reduce the potential risk regarding the effects of RCA and RAPA on the environment.
4. The most innovative result also depends upon the receipt of 30%RCA + 70%RAPA + 5% SF mixture because its mechanical properties are the greatest in the study. Moreover, since the RCC with 30%RCA + 70%RAPA + 5%SF is eco-friendly and a sustainable highway material, its receipt could be used by construction industry in both road manufacturing and highway manufacturing.

### References

- Abdel-Halim, M., Al-Omari, M. A., & Iskender, M. M. (1999). Rehabilitation of the spillway of Sama EI-Serhandam in Jordan, using roller compacted concrete. *Engineering Structures*, 21 (6), 497–506. Available from [https://doi.org/10.1016/S0141-0296\(97\)00224-1](https://doi.org/10.1016/S0141-0296(97)00224-1).
- ACI (2001). *State of the—art report on roller compacted concrete pavement*, American Concrete Institute Report, ACI.325.10-95.
- ACI Committee 211. (2002). 3R-02, *Roller guide for selecting proportions for no-slump concrete*, January 11.
- Acker, A. v. (1996). Recycling of concrete at a precast concrete plant. *Betonwerk + Fertigteil-Tech*, 6, 91–101.



- Adamn, M., Mohammed, B. S., & Mohd, S. L. (2018). Mechanical properties and performance of high volume fly ash roller compacted concrete containing crumb rubber and nano silica. *Construction and Building Materials*, 171, 521–538. Available from <https://doi.org/10.1016/j.conbuildmat.2018.03.138>.
- Aghabaglou, A., & Ramyar, K. (2013). Mechanical properties of high-volume fly ash roller compacted concrete designed by maximum density method. *Construction and Building Materials*, 38, 356–364. Available from <https://doi.org/10.1016/j.conbuildmat.2012.07.109>.
- Ahmed, O., Harbec, D., Tagnit-Hamou, A., & Gagne, R. (2017). Production of roller compacted concrete using glass powder: Field study. *Construction and Building Materials*, 133, 533–541. Available from <https://doi.org/10.1016/j.conbuildmat.2016.12.099>.
- Arabiyat, S., Abdel Jaber, M., Katkhuda, H., & Shatarat, N. (2021). Influence of using two types of recycled aggregates on shear behavior of concrete beams. *Journal of Construction and Building Materials*, 279, 122475, Elsevier, volume.
- Ashteyat, A. M., Rjoub, Y. S. A., Murad, Y., & Asaad, S. (2019). Mechanical and durability behavior of roller—compacted concrete containing white cement by pass dust and polypropylene fiber. *European Journal of Environmental and Civil Engineering*, 2116–7214. Available from <https://doi.org/10.1080/19648189.2019.1652694>.
- ASTM C138/C138M-17a. (2017). *Standard test method for density (unit weight), yield, and air content (gravimetric) of concrete*. West Conshohocken, PA: ASTM International. Available from <http://www.astm.org>.
- ASTM C1435/C1435M-20. (2020). *Standard practice for molding roller-compacted concrete in cylinder molds using a vibrating hammer*. West Conshohocken, PA: ASTM International, <http://www.astm.org>.
- ASTM C293/C293M-16. (2016). *Standard test method for flexural strength of concrete (using simple beam with center-point loading)*. West Conshohocken, PA: ASTM International. Available from <http://www.astm.org>.
- ASTM C39/C39M-21. (2021). *Standard test method for compressive strength of cylindrical concrete specimens*. West Conshohocken, PA: ASTM International. Available from <http://www.astm.org>.
- ASTM C469/C469M-14e1. (2014). *Standard test method for static modulus of elasticity and poisson's ratio of concrete in compression*. West Conshohocken, PA: ASTM International. Available from <http://www.astm.org>.
- ASTM C496/C496M-17. (2017). *Standard test method for splitting tensile strength of cylindrical concrete specimens*. West Conshohocken, PA: ASTM International. Available from <http://www.astm.org>.
- ASTM C642-13. (2013). *Standard test method for density, absorption, and voids in hardened concrete*. West Conshohocken, PA: ASTM International. Available from <http://www.astm.org>.
- Azevedo Azevedo, A. R. G., Cecchin, D., Carmoa, D. F., Silva, F. C., Campos, C. M. O., Shtrucka, T. G., Marvila, M. T., & Monteiro, S. N. (2020). Analysis of the compactness and properties of the hardened state of mortars with recycling of construction and demolition waste (CDW). *Journal of Materials Research & Technology*, 9(3), 5942–5952.
- BS EN 197-1:2011. (2011). *Cement. Composition, specifications and conformity criteria for common cements*. British Standard Institute.
- CEB-FIP. (1989). Diagnosis and assessment of concrete structures state of art report. *CEB Bulletin*, 192, 83–85.
- Chafika, S., Debieb, F., Kadri, E., & Boukendakdji, O. (2015). Assessing the effect of recycled asphalt pavement materials on the performance of roller compacted concrete. *Construction and Building Materials*, 101, 617–621.

- Collins, R. J. (1996). Increasing the use of recycled aggregates in construction. In *Proc. of international conference: Concrete in the service of mankind. I. Concrete for environment enhancement and protection* (pp. 130–139). Dundee, Scotland.
- Courard, L., Michel, F., & Delhez, P. (2010). Use of concrete road recycled aggregate for roller compacted concrete. *Construction and Building Materials*, 24, 390–395. Available from <https://doi.org/10.1016/j.conbuildmat.2009.080.040>.
- de Vries, P. (1996). Concrete recycled: Crushed concrete aggregate. In *Proc. of international conference: Concrete in the service of mankind. I. Concrete for environment enhancement and protection* (pp. 121–130). Dundee, Scotland.
- Debieb, F., Courard, L., Kenai, S., & Degeimbre, R. (2009). Roller compacted concrete with contaminated recycled aggregates. *Construction and Building Materials*, 23, 3382–3387. Available from <https://doi.org/10.1016/j.conbuildmat.2009.060.031>.
- Debieb, F., Courard, L., Kenai, S., & Degeimbre, R. (2010). Mechanical and durability properties of concrete using contaminated recycled aggregates. *Cement and Concrete Composites*, 32(6), 421–426. Available from <https://doi.org/10.1016/j.cemconcomp.2010.03.004>.
- EU Directive 2008/98/EC. (2008). *Waste and repealing certain directives*. The European Parliament and of Council, BE. <https://eur-lex.europa.eu/legal-content/EN/TXT/HTML/?uri=CELEX:02008L0098-20180705&from=EN>.
- Fakhri, M., & Amoosoltani, E. (2017). The effect of reclaimed asphalt pavement and crumb rubber on mechanical properties of roller compacted concrete pavement. *Construction and Building Materials*, 137, 470–484. Available from <https://doi.org/10.1016/j.conbuildmat.2017.010.136>.
- Fakhri, M., & Saberi, K. F. (2016). The effect of waste rubber particles and silica fume on the mechanical properties of roller compacted concrete pavement. *Journal of Cleaner Production*, 521–530. Available from <https://doi.org/10.1016/j.jclepro.2016.040.017>.
- Ferrebee, E. C., Brand, A. S., Kachwalla, A. S., Roesler, J. R., Gancarz, D. J., & Pforr, J. E. (2014). Fracture properties of roller compacted concrete with virgin and recycled aggregates. *Transportation Research Record: Journal of the Transportation Research Board*, 244(1), 128–134.
- Hamad, B., Dawi, A., Daou, A., & Chehab, G. (2018). Studies of the effect of recycled aggregates on flexural, shear, and bond splitting beam structural behavior. *Case Studies in Construction Materials*. Available from <https://doi.org/10.1016/j.cscm.2018.e00186>.
- Katkhuda, H., Shatarat, N., & Hyari, K. (2017). Effect of silica fume on mechanical properties of concrete containing recycled asphalt pavement. *Structural Engineering and Mechanics: An International Journal*, 62(3), 357–364.
- Lam, M. N., Duc-Hien, L., & Jaritngam, S. (2018). Compressive strength and durability properties of roller compacted concrete pavement containing electric arc furnace slag aggregate and fly ash. *Construction and Building Materials*, 19(2018), 912–922. Available from <https://doi.org/10.1016/j.conbuildmat.2018.10.080>.
- Lam, M. N., Jaritngam, S., & Duc-Hien, L. (2017). Roller compacted concrete pavement made of electric arc furnace slag aggregate: Mix design and mechanical properties. *Construction and Building Materials*, 154, 485–495. Available from <https://doi.org/10.1016/j.conbuildmat.2017.07.240>.
- Modarres, A., & Hosseini, Z. (2014). Mechanical properties of roller compacted concrete containing rice husk ash with original and recycled asphalt pavement material. *Materials and Design*, 64, 227–236. Available from <https://doi.org/10.1016/j.matdes.2014.070.072>.
- Olorunso, F. T., & Padayachee, N. (2016). Performance of recycled concrete monitored by durability index. *Cement and Concrete Research*, 32(2), 179–185.

- Refaie, A. F., Elminilmy, T. M., & Bahaa, T. (2010). Flexural strength of concrete beams with recycled concrete aggregates. *Journal of Engineering and Applied Science*, 57(5), 355–375.
- Saadi, K. (2010). Formulation et étude d'un béton de route à base de Matériaux locaux. Civil Engineering Department, Université of Blida, Master Thesis, Blida, Algeria.
- Settari, C., Debieb, F., Kadri, E. I. H., & Boukendakdji, O. (2015). Assessing the effects of recycled asphalt pavement materials on the performance of roller compacted concrete. *Construction and Building Materials*, 101, 617–621. Available from <https://doi.org/10.1016/j.conbuildmat.2015.10.039>.
- Shafigh, P., Jumaat, M. Z., Bin Mahmud, H. M., & Hamid, N. A. A. (2012). Lightweight concrete made from crushed oil palm shell: Tensile strength and effect of initial curing on compressive strength. *Construction and Building Materials*, 27(1), 252–258. Available from <https://doi.org/10.1016/j.conbuildmat.2011.07.051>.
- Shatarat, N., Abde Alhaq, A., Katkhuda, H., & Abdel Jaber, M. (2019). Investigation of axial compressive behavior of reinforced concrete columns using recycled coarse aggregate and recycled asphalt pavement aggregate. *Journal of Construction and Building Materials*, 217, 384–393.
- Shatarat, N., Katkhuda, H., Hyari, K., & Asi, I. (2018). Effect of using recycled coarse aggregate and recycled asphalt pavement on the properties of pervious concrete. *Structural Engineering and Mechanics: An International Journal*, 67(3), 283–290.

# Clay and natural latex as admixture in binary and ternary bitumen binder system for transportation and geotechnical applications

14

Theresah Osei<sup>1</sup>, Trinity Ama Tagbor<sup>2</sup>, Johannes A.M. Awudza<sup>3</sup> and Mehmet Serkan Kirgiz<sup>4</sup>

<sup>1</sup>Council for Scientific and Industrial Research, Building and Road Research Institute, Kumasi, Ghana, <sup>2</sup>Council for Scientific and Industrial Research, Institute of Industrial Research, Accra, Ghana, <sup>3</sup>Department of Chemistry, Kwame Nkrumah University of Science and Technology, Kumasi, Ghana, <sup>4</sup>Northwestern University, Chicago, IL, United States

## 14.1 Introduction

Road pavement is one of the major infrastructure, which plays a vital role in economy, study, security, hospitalization, and many other purposes of a country. Recently, various issues such as increased traffic load and growth-permissible vehicle pressure have increased tension in the pavement layers, therefore; it is needed for reducing the useful life of asphalt pavements (Airey, 2004). The performance of pavements is generally influenced by the loading magnitude, configuration, and load repetitions by heavy vehicles. Road pavements must show satisfactory resistance against fatigue cracking, rutting, creep, and slippage (Amini et al., 2021; Mousavinezhad et al., 2019). Bitumen is a thermoplastic material of hydrocarbons including paraffins, saturates, aromatics, resins, and graphitic bitumenenes. It is extensively used as a very effective binder for mineral aggregates to form an effective mixture of pavement construction materials. At high temperature, it acts like a viscous liquid, and at low temperature, it acts like an elastic solid. Bitumen can play a significant role as one of the key materials used in asphalt mixtures, and adjusting the properties of bitumen can impressively delay these failures and minimize them in some cases (Mirsepahi et al., 2020). Though polymer-modified bitumen is known to have improved adhesion, impermeability, oxidation, aging resistance, temperature sensitivity, durability, rutting, and fatigue resistance (Bulatović et al., 2014), various methods and research studies and a wide range of additives have been investigated to further improve the properties and performance

of bitumen in asphalt mixtures. These materials include rubber, gilsonite, styrene–butadiene–styrene, ethylene–vinyl acetate, and nanomaterials. Natural rubber, a sustainable resource (Bindu et al., 2020), aids in dissipating developed stresses, grips asphalt altogether, resists the asphalt flow, and enhances the shear resistance (Wen et al., 2017). Its innate elastomer properties result in resistance to rutting, fatigue cracking (Krishnapriya, 2015), stripping, and long-term pavement performance of pavements (Shaffie et al., 2015). The discrete feature of natural rubber is its high stability, excellent tear strength, fatigue resistance, and aptitude to extend durability of asphalt pavements (Transportation Research Board, 2017). In addition, natural rubber has excellent dynamic properties with a low hysteresis loss and good low-temperature properties (Vasavi & Durga, 2014).

Additionally, nanomaterials are used as additives in polymer-modified bitumen and used alone for modification. Clays are mostly used as nanomaterial additives. Nanoclays are naturally occurring minerals that mainly include kaolinite clay, vermiculite, and montmorillonite (Százdi, 2006). The reasons for preference of nanoclays are easy attainability from natural sources and being economic. Due to the small size and the high surface area of clays (Yao et al., 2013), their addition solves separation, storing, and transportation problems, while reducing the density difference between bitumen and polymer mix (Golestani et al., 2012). Nanoclay advances the rheological performance and physical properties of binders and mixtures by dispersion between polymer chains and the formation of nanocomposite polymer–clay (Abdelrahman et al., 2014). The chapter evaluates the effects of clay from two different sources on the properties of natural rubber–bitumen composite.

## 14.2 Materials and method

### 14.2.1 Bitumen

Bitumen used for this study is AC-10 grade base bitumen obtained from a local road contractor in Kumasi, Ghana.

### 14.2.2 Natural rubber latex

Natural rubber latex, manufactured locally, was obtained from Ghana Rubber Estate Limited, Western Region, Ghana. The rubber was stored in 5% liquid ammonia to prevent coagulation of the latex.

### 14.2.3 Clay samples

Clay samples were mined from Anfoega clay site in the Volta Region and Adankwame in the Ashanti Region of Ghana.

#### **14.2.4 Sample preparation**

The clay samples from both sites were ground with a mortar and pestle, sieved with 500  $\mu$  sieve, and stored in plastic containers. The following test was conducted on the clay samples.

#### **14.2.5 Absorption test**

Absorption of clay body is the quantity of water that can seep through fired clay irrespective of glaze or coating. This test was done according to [ASTM C140-01 \(2001\)](#).

### **14.3 Particle size distribution**

Particle size distribution is stated as a fraction passing a particular sieve size. This test was done according to test method stated in [ASTM D7928-21e1 \(2021\)](#).

#### **14.3.1 Compaction**

Compaction is the application of energy mechanically to solid samples in order to rearrange the particles and also reduce the void ratio. Compaction test was conducted with ASTM D698-12 standard method ([ASTM D698-12, 2012](#)).

#### **14.3.2 Atterberg limit (plastic and liquid limit)**

Plasticity is a property of materials that accrue nonrecoverable deformation when a load is applied. The liquid limit and plastic limit were determined using the test method stated in with BS 1377 ([BS 1377-2:1990, 1990](#)).

### **14.4 Hydrogen ion concentration (pH)**

This is the negative log of hydrogen ion concentration in water-based solutions. The pH of the clay samples was determined in accordance with BS 1377 ([BS 1377-3:2018 + A1:2021, 2021](#)).

### **14.5 Preparation of blends**

The blends were prepared by adding natural rubber latex at percentages of 1, 3, and 5 at 1% and 3% clay by weight to the base bitumen. The bitumen was weighed into a stainless steel bucket and heated to a temperature of 160°C on a Sybron Thermolyne HP-A1915B Hot plate. Under fluid conditions the latex was slowly added, while the speed of the mixer was maintained at 120 rpm and the temperature was kept 160°C. Mixing continued for 1 hour to produce homogeneous mixtures.

The blends were then transferred to 500 g tin containers labeled and stored for rheological testing. The ternary blends were prepared at latex percentages of 0, 1, 3, and 5. Depending on the percentages the bitumen was heated to fluid conditions and the clay added. To the homogeneous mixture the latex was added and blended for 1 hour. This is stored in a stainless steel container for further analysis.

#### **14.5.1 Laboratory analysis**

The following analyses were carried out on the prepared composite.

#### **14.5.2 Penetration point**

Penetration is used to measure the hardness or softness of a binder. This test was done in accordance with [ASTM D5-97 \(1997\)](#).

#### **14.5.3 Softening point temperature**

The ring and ball apparatus is used to determine the temperature at which a bitumen sample can no longer support the weight of a 3.5 g steel ball. The test was done according to the method described in [ASTM D36/D36M-12 \(2012\)](#).

#### **14.5.4 Kinematic viscosity**

Viscosity is a measure of fluid deformation due to shear stress or tensile stress. Measurements were made at 135°C according to test method stated in [ASTM D2170/D2170M-10 \(2010\)](#).

#### **14.5.5 Specific gravity**

The specific gravity of the bituminous mixture was measured according to the test protocol described in [ASTM D70-03 \(2003\)](#). This is the ratio of the mass of a given volume of bitumen to the mass of an equal volume of water at 27°C, and this is done by preparation of a cube sample in the semisolid or solid state.

#### **14.5.6 Short-term aging test**

Short-term aging determines the effects of heat and atmospheric oxygen during mixing, storage, and laying of asphalt binder. This test was done using the rotating cylinder aging test according to the procedure stated in [ASTM D1754/D1754M-09 \(2009\)](#).

#### **14.5.7 Flash point**

The flash point test is useful in determining that an asphalt binder has been prepared with solvents that meet the desired range of flammability. The flash point test was done according to the test procedure described in [ASTM D3143/D3143M-19 \(2019\)](#).

## 14.6 Results

Results obtained from the analysis of clay and blends are presented below.

### 14.6.1 Atterberg limit and pH

Results of atterberg limit and particle size distribution and pH of the clay are presented in Table 14.1. The table depicts Anfoega (ANC) to be acidic, whereas Adankwame (ADC) is alkaline. ANC has a higher plasticity index as compared to that of ADC.

**Table 14.1** Results of atterberg limit and pH.

Type of sample	Atterberg limit			pH
	LL	PL	PI	
ADC	39	25.1	13.8	9.06
ANC	54.3	26.9	27.4	4.67

The pH value of a clay sample plays an important role in its properties. A high pH value coagulates the particle of the binder, whereas a low pH value dissolves the particle size of the binder (Allan & Qiong, 2012). From Table 14.1, ANC is found to be acidic, whereas ADC is basic. Wet clay retains water and expands in volume. This expansion is related to the ability of the clay to take up water. The plasticity index of ANC and ADC samples differs significantly and suggests that ANC sample can absorb water and shrink more as compared to ADC. From Table 14.1, ANC sample is expected to have smaller particle sizes, well compacted, and increase the ability to absorb physical water. This was confirmed in Tables 14.2 and 14.3 as ANC had the least maximum dry density (MDD) value with high optimum moisture content (OMC) and a high clay percentage when compared with ADC. The ability of bitumen to flow at a reduced temperature is a favorable property during storage. Addition of high plastic clay reduces the viscosity by reducing the particle size as well as the elastic effect, therefore enhancing flow of bitumen during storage (Widyatmoko, n.d.). The concentration of hydrogen ion (pH) also affects the binding properties for construction. A high pH value coagulates the particle of the binder, whereas a low pH value dissolves the particle size of the binder. The particle size of bitumen determines the viscosity; that is, a reduced particle size increases the flow, whereas an increased particle size decreases flow of the binder. From the results of the physical analysis, it can be concluded that ANC has the ability to improve the storage stability of the modified bitumen as compared to the ADC.



### 14.6.2 Compaction, moisture content, and specific gravity

Table 14.2 shows the results of compaction test moisture content and specific gravity

Table 14.2 illustrates clay from Anfoega having a higher OMC and the least MDD when compared with ADC.

**Table 14.2** Results of compaction, moisture content (MC), and specific gravity (Gs) of clay.

Type of sample	Compaction		Moisture content (%)	Specific gravity (g/cm <sup>3</sup> )
	MDD	OMC		
ADC	1.71	16.5	1.24	2.77
ANC	1.63	18.5	2.4	2.78

MDD, Maximum dry density; OMC, optimum moisture content.

### 14.6.3 Particle size distribution

Fig. 14.1 is the result obtained for determination of individual particles. The results show clay from ADC having a clay content less than 15% as against 65% of ANC. None of the clays have gravel content.

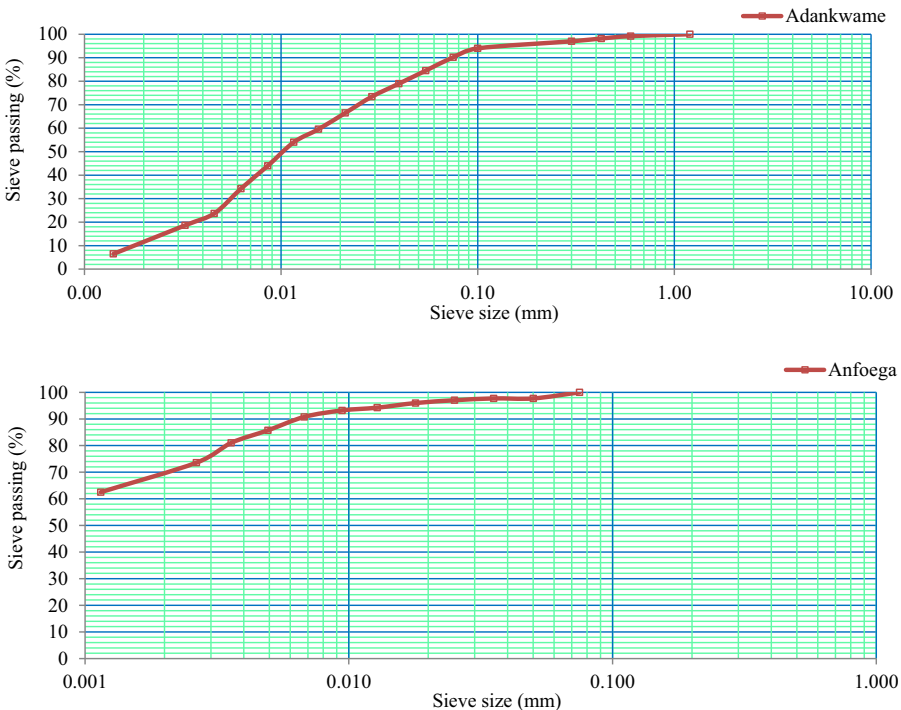


**Figure 14.1** Particle size distribution of the clay samples.

### 14.6.4 Penetration point

The result for the penetration point of the blending of clay is presented in Fig. 14.2. The below figure depicts a slight increase in penetration point between 1% and 3% of rubber with blends containing 3% clay from Anfoega, whereas that of 1% decreases with increasing rubber concentration. However, blends containing ADC revealed an increase in penetration point after addition of 3% rubber at both percentages.

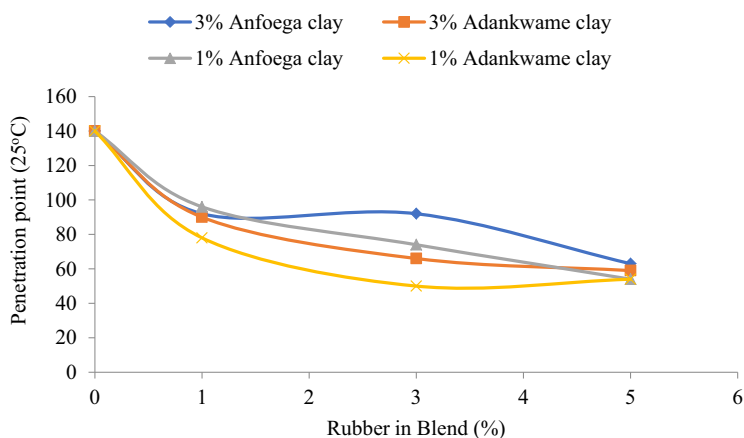


**Figure 14.2** Penetration point for blends at different percentages of clay when rubber concentration increases.

Fig. 14.2 depicts a decrease in penetration values for all the blends tested when compared with the unmodified bitumen. However, blends with ADC have the highest decrease as compared with ANC blends. There was a continuous decrease in penetration as the percentage of latex increases when 1% ADC was added and started increasing gradually after addition of 5% latex. This indicates that clay content in these blends has no/less significant effect on the elastic property of the rubber (Widyatmoko, n.d.). However, there could be sand particle interference due to an increased penetration value of the blends containing 3% ADC. ANC blends behave different from the graph obtained for ADC. A constant penetration value for 3% ANC between 1% and 3% rubber indicates a balanced plastic–elastic effect on the blends. Increasing the elastic effect beyond 3% rubber shows an increase in viscosity and subsequently a decrease in penetration value. The plastic effect of 1% ANC was insignificant as compared to 3% ANC; hence there was a decrease in penetration values as the rubber concentration increases.

### 14.6.5 Softening point

The result for the softening point of the blending of clay is presented in Fig. 14.3. The figure exhibits a decrease in softening point for all the blends at 1% rubber concentration, which then increases as the rubber percentage increases.

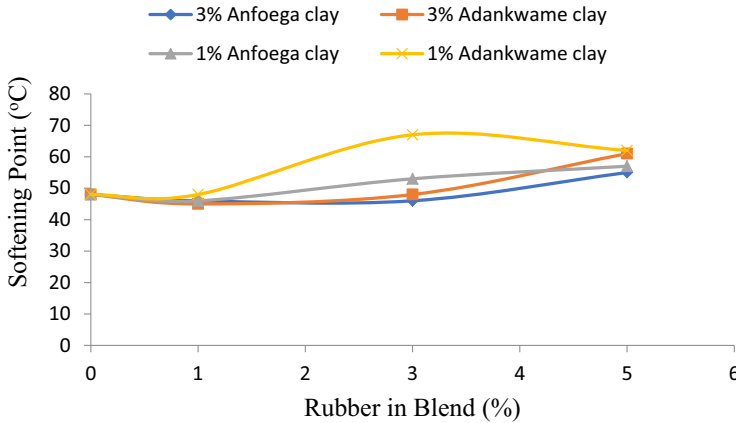


**Figure 14.3** Softening point for blends at different percentages of clay when the rubber concentration increases.

Observation from Fig. 14.3 indicates that the effect of clay content on the softening point was not linear. The variation of blends with ANC at both percentages was very small as compared to that of the Adankwame. However, both clays have a higher softening point at a lower clay concentration. This could be due to the fact that at lower clay loading the particles were separated from one another and this allows the bitumen-latex blend to flow as it would do without the clay. Also the plastic effect at a low clay concentration was insignificant making the blend highly elastic, leading to an increased temperature at which it softens. At 3% clay content, plasticity and pH become enormous, which then decrease the elasticity as well as viscosity, resulting in a reduced softening point.

## 14.7 Kinematic viscosity

The result for the softening point of the blending of clay is shown in Fig. 14.4. There is an increase in viscosity of blends with ANC as the rubber concentration increases. Blends containing 3% clay from ADC also increase lineally as the concentration of rubber increases. However, blends with 1% clay from ADC increase to 3% and decrease as the percentage of rubber increases.

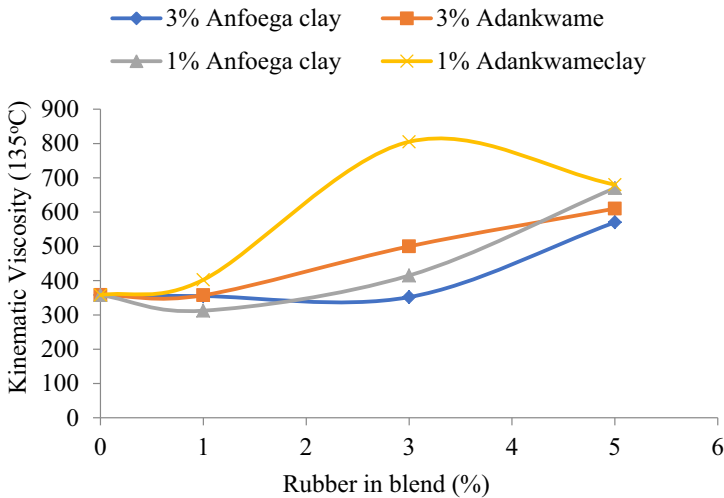


**Figure 14.4** Kinematic viscosity at 135°C for blends at different percentages of clay when the rubber concentration increases.

The purpose for the addition of clay was to decrease the elastic effect of the added rubber, which would decrease the viscosities; thereby, pumping of the blends becomes less easy and hence there is high storage stability. The lower viscosities at a higher clay concentration (3%) indicate a decrease elastic effect of the rubber as well as particle size of the bitumen compared to a lower clay concentration (1%). ANC has lower viscosity than ADC because of its ability to decrease the particle size of the rubber–bitumen blends and therefore increasing flow. 1% ADC had the minimal effect on rubber bitumen, leading to high viscosity. However, from the graph, ANC recorded the least viscosity at increased rubber content. This suggests that acidic clay was able to decrease the elastic effect of the rubber on the bitumen blend, as suggested by [Widyatmoko \(n.d.\)](#).

## 14.8 Specific gravity

The result for the softening point of the blending of clay is shown in [Fig. 14.5](#). The figure depicts an increase in specific gravity for all the blends along with an increase in concentration of rubber.

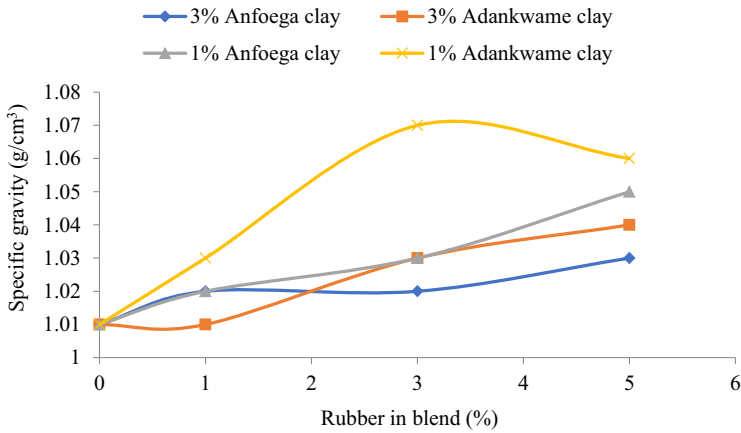


**Figure 14.5** Specific gravity for blends at different percentages of clay when the rubber concentration increases.

From Fig. 14.5, it could be observed that addition of 1% clay samples gave a higher specific gravity than 3% clay samples. This is as a result of high bitumen content in the blend containing 1% clay compared to 3% clay. 3% ANC had the least specific gravity values. This indicates that the clay was able to dissolve the particle size of the bitumen, which resulted in a decrease in volume of the blend, leading to an increase in density. The 3% ADC was supposed to have a high specific gravity resulting from coagulation of bitumen particles, leading to a decrease in volume. However, high content of sand and silt acted as impurities, which then increased the density, and hence there is a decrease in specific gravity. Rubber promotes age hardening of bitumen as rubber bitumen road stretches under load without ripping. As it stretches, it increases the pore size of the bitumen, which encourages incorporation of water and oxygen which cause hardening (Widyatmoko, n.d.).

### 14.8.1 Aging and flash point

Table 14.3 shows the results of flash point and aging test of the selected blends. It shows that blends with clay from Adankwame have lower change in mass after aging as compared to blends with clay from Anfoega. The flash point test indicated that all the selected blends have a flash point above the minimum for modified bitumen.

**Table 14.3** Results obtained for aging test and flash point analysis.

Type of composite	Flash point	Viscosity	Change in mass after aging (%)	Aging index
3% latex with 3% AD	363	808	0.121	1.004
5% latex with 1% AD	317	683	0.111	1.004
5% latex with 1% AN	335	675	0.132	1.007
5% latex with 3% AN	347.2	750	0.124	1.316

Clay is expected to encapsulate the volatile component of the bitumen more effectively and consequently lower loss in mass after aging (Widyatmoko, n.d.). Clay from Anfoega is acidic and highly plastic; therefore it is expected to decrease the pore size and elasticity of the blend as compared to clay from Adankwame. This will then decrease incorporation of oxygen efficiently as the clay concentration increases. Therefore it is expected that the aging index for ANC samples is lower than that for ADC samples. However, from the table, it could be observed that 1% ADC has a lower aging index value as compared to 1% ANC. This could be ascribed to the fact that the lower clay concentration (1%) had no or little significant effect on the elasticity during aging. Therefore incorporation of oxygen and moisture was equal for both samples.

## 14.9 Conclusions

This chapter focuses on the effect of clay as an additive in natural rubber bitumen modification. Clays from ANC in the Volta region and ADC in the Ashanti region were used in the study. Laboratory tests such as Atterberg limit, particle size distribution, water absorption, pH, and compaction were carried out on the clay. Blends were prepared at natural rubber latex percentages of 0, 1, 3, and 5 and with clay concentrations of 1% and 3%. Physical properties such as viscosity, specific gravity, softening point, penetration point, flash point, and short-term aging were performed on the modified bitumen. The pH values for ANC and ADC were 4.67 and 9.06, respectively. ANC was found to contain high clay content, a smaller particle size, and a higher plasticity index as compared ADC. For the analysis of the blends, ADC performed better at a latex concentration of 3%, whereas ANC performed better at a latex concentration of 5%. The loss in mass after the aging test for the selected blends indicated that blends with ANC have a higher aging index as compared to blends with ADC. The flash points for the blends were within the maximum limit for modified bitumen. From the result, it can be concluded that the two clay samples have different positive effects on the rubber-modified bitumen.

## References

- Abdelrahman, M., Katti, D. R., Ghavibazoo, A., Upadhyay, H. B., & Katti, K. S. (2014). Engineering physical properties of asphalt binders through nanoclay-asphalt interactions. *Journal of Materials in Civil Engineering*, 26(12). Available from [https://doi.org/10.1061/\(ASCE\)MT.1943-5533.0001017](https://doi.org/10.1061/(ASCE)MT.1943-5533.0001017).
- Airey, G. D. (2004). Styrene butadiene styrene polymer modification of road bitumens. *Journal of Materials Science*, 39(3), 951–959. Available from <https://doi.org/10.1023/B:JMSC.0000012927.00747.83>.
- Allan, J., & Qiong, Z. (2012). *Modified bitumens derived from particle stabilization emulsion* (5th ed.). Istanbul, Turkey: Euorasphalt and Eurobitumen Congress.

- Amini, A., Ziari, H., Saadatjoo, S. A., Hashemifar, N. S., & Goli, A. (2021). Rutting resistance, fatigue properties and temperature susceptibility of nano clay modified asphalt rubber binder. *Construction and Building Materials*, 267. Available from <https://doi.org/10.1016/j.conbuildmat.2020.120946>.
- ASTM C140-01. (2001). *Standard test methods for sampling and testing concrete masonry units and related units*. ASTM International. <https://doi.org/10.1520/C0140-01>
- ASTM D5-97. (1997). *Standard test method for penetration of bituminous materials*. ASTM International.
- ASTM D36/D36M-12. (2012). *Standard test method for softening point of bitumen*. ASTM International.
- ASTM D70-03. (2003). *Standard test method for specific gravity and density of semi-solid bituminous materials*. ASTM International.
- ASTM D698-12. (2012). *Standard test methods for laboratory compaction characteristics of soil using standard effort (12 400 ft-lbf/ft<sup>3</sup> (600 kN-m/m<sup>3</sup>))*. ASTM International.
- ASTM D1754/D1754M-09. (1754). *Standard test method for effect of heat and air on asphaltic materials (thin-film oven test)*. ASTM International.
- ASTM D2170/D2170M-10. (2170). *Standard test method for kinematic viscosity of asphalts*. ASTM International.
- ASTM D3143/D3143M-19. (3143). *Standard test method for flash point of cutback asphalt with tag open-cup apparatus*. ASTM International.
- ASTM D7928-21e1. (7928). *Standard test method for particle-size distribution (gradation) of fine-grained soils using the sedimentation (hydrometer) analysis*. ASTM International.
- Bindu, C. S., Joseph, M. S., Sibinesh, P. S., George, S., & Sivan, S. (2020). Performance evaluation of warm mix asphalt using natural rubber modified bitumen and cashew nut shell liquid. *International Journal of Pavement Research and Technology*, 13(4), 442–453. Available from <https://doi.org/10.1007/s42947-020-0241-7>.
- BS 1377–2:1990. (1990). *Methods of test for soils for civil engineering purposes classification tests*. British Standard Institute.
- BS 1377–3:2018 + A1:2021. (2021). *Methods of test for soils for civil engineering purposes—chemical and electro-chemical testing*. British Standard Institute.
- Bulatović, V. O., Rek, V., & Marković, K. J. (2014). Effect of polymer modifiers on the properties of bitumen. *Journal of Elastomers and Plastics*, 46(5), 448–469. Available from <https://doi.org/10.1177/0095244312469964>.
- Golestani, B., Moghadas Nejad, F., & Sadeghpour Galooyak, S. (2012). Performance evaluation of linear and nonlinear nanocomposite modified asphalts. *Construction and Building Materials*, 35, 197–203. Available from <https://doi.org/10.1016/j.conbuildmat.2012.03.010>.
- Krishnapriya, M. G. (2015). Performance evaluation of natural rubber modified bituminous mixes. *Journal of Civil, Structural, Environmental, Water Resources and Infrastructure Engineering Research (JCSEWIER)*, 5(1), 1–12.
- Mirsepahi, M., Tanzadeh, J., & Ghanoon, S. A. (2020). Laboratory evaluation of dynamic performance and viscosity improvement in modified bitumen by combining nanomaterials and polymer. *Construction and Building Materials*, 233. Available from <https://doi.org/10.1016/j.conbuildmat.2019.117183>.
- Mousavinezhad, S. H., Shafabakhsh, G. H., & Jafari Ani, O. (2019). Nano-clay and styrene-butadiene-styrene modified bitumen for improvement of rutting performance in asphalt mixtures containing steel slag aggregates. *Construction and Building Materials*, 226, 793–801. Available from <https://doi.org/10.1016/j.conbuildmat.2019.07.252>.
- Shaffie, E., Ahmad, J., Arshad, A.K., Kamarun, D., & Kamaruddin, F. (2015). Stripping performance and volumetric properties evaluation of hot mix asphalt (HMA) mix design

- using natural rubber latex polymer modified binder (NRMB). In R. Hassan, M. Yusoff, A. Alisibramulisi, N. M. Amin, & Z. Ismail (Eds.), *Proceedings of the international civil and infrastructure engineering conference 2014*. Springer.
- Százdi, L. T. (2006). *Structure–property relationships in polymer/layered silicate nanocomposites*. Budapest University of Technology and Economics.
- Transportation Research Board. (2017). *NCHRP practice-ready solutions for warm mix asphalt*. [https://onlinepubs.trb.org/onlinepubs/nchrp/nchrp\\_researchtopichighlights\\_01.pdf](https://onlinepubs.trb.org/onlinepubs/nchrp/nchrp_researchtopichighlights_01.pdf)
- Vasavi, S. D., & Durga, R. K. (2014). Effect of natural rubber on the properties of bitumen and bituminous mixes. *International Journal of Civil Engineering and Technology*, 5(10), 9–21.
- Wen, Y., Wang, Y., Zhao, K., & Sumalee, A. (2017). The use of natural rubber latex as a renewable and sustainable modifier of asphalt binder. *International Journal of Pavement Engineering*, 18(6), 547–559. Available from <https://doi.org/10.1080/10298436.2015.1095913>.
- Widyatmoko, I. (n.d.). Sustainability of bituminous materials. In *Sustainability of construction materials* (2nd ed., pp. 343–370). Woodhead Publishing Series in Civil and Structural Engineering. <https://doi.org/10.1016/B978-0-08-100370-1.00014-7>
- Yao, H., You, Z., Li, L., Goh, S. W., Lee, C. H., Yap, Y. K., & Shi, X. (2013). Rheological properties and chemical analysis of nanoclay and carbon microfiber modified asphalt with Fourier transform infrared spectroscopy. *Construction and Building Materials*, 38, 327–337. Available from <https://doi.org/10.1016/j.conbuildmat.2012.08.004>.



This page intentionally left blank

# A clean approach through recycling of brick kiln dust and crumb waste rubber tires in the manufacturing of clayey bricks and cementitious composites

15

*Abdul Qadir Bhatti<sup>1</sup> and Anwar Khitab<sup>2</sup>*

<sup>1</sup>Department of Civil Engineering, Faculty of Engineering, Islamic University of Madinah, Madinah, Saudi Arabia, <sup>2</sup>Civil Engineering, Mirpur University of Science and Technology, Mirpur, AJ&K, Pakistan

## 15.1 Introduction

The history of construction is characterized by a number of trends. The most important are the durability and strength of the material used in the construction. In ancient times, construction materials were perishable, such as wood, grasses, and animal fibers. However, with the evolution of time, materials that provide more strength and durability were identified and developed, such as lime, gypsum, mud, and gravel. Later, attempts were made to manufacture more strong and durable binding materials such as cement. Cement gained popularity due to the rapid development of its strength (of the order of a month) as compared to other competitive binding materials like lime and clay, which take several months to even years for full strength development. This makes cement a perfect material for situations where more strength and/or early development of strength are required. Finally a versatile and synthetic material, that is, concrete, is invented with higher strength and long-term reliability (Anwar & Anwar, 2016). Concrete technology has now become a gigantic field with many innovations during the past few decades. During the course of time, several new types of concrete have been developed (Khitab et al., 2015). Concrete is considered to be the first extraterrestrial construction material (Khitab et al., 2016). While concrete is a useful versatile material, it has also brought with it many hazards for the environment. It has also contributed to global warming. For this reason, concrete researchers are in continuous efforts to bring down its hazards and to make it greener and environment-friendly and no-to-slight compromise over its strength and durability. One of the methods to make concrete environment-friendly is the replacement of its ingredients like cement and aggregates by green materials, which have a low environmental impact. In the last few decades, many researchers have tried to find out ways to incorporate industrial

wastes in concrete to make it more economical and pollution-free (Lee et al., 2014). Recent advances also include the use of many alternatives (other than cement) in cementitious composites with the aim that stronger and durable products are manufactured with lesser dependence on cement (Biricik et al., 2021; Kirgiz et al., 2021; Syarif et al., 2021).

Clayey bricks present another important building material owing to their ease of manufacturing, handling, and transportation (United States Bureau of Standards, 2011). As a matter of fact, billions of clayey bricks are manufactured each year, which are consuming a huge amount of fertile clay. This clay needs to be preserved for protecting the ecosystem. Like concrete, many research groups are also occupied exploring novel ways for replacing the clay in clayey bricks. The successful recycling of waste materials as partial replacement of clay is reported by many researchers worldwide. Wastes like coal ash, fly ash, sludge, spent grains, glass grit, tea waste, kraft pulp, and many others have been reported by Kadir et al. in their review work (Kadir & Sarani, 2012).

This chapter reiterates the importance of manufacturing greener cementitious and clayey materials. The focus is on the recycling of two industrial wastes in these materials, namely, waste brick powder (WBP) and waste crumb rubber. The WBP is presented as a partial replacement of cement and clay in cementitious and clayey materials, respectively. Waste rubber (particle form) is described as a partial replacement of fine aggregates in cementitious composites.

## 15.2 Concrete

### 15.2.1 *Ingredients*

Concrete is one of the most widely used materials in the construction industry due to its easiness, low expenditure, good performance, and versatile applications. Over the past few years, more and more research has been done to produce concrete with the desired characteristics. However, concrete features have changed so far with the emergence of user needs (Anwar et al., 2014).

Conventional concrete is a mixture of cement, natural aggregates (fine and coarse), and water. Besides these three principle constituents, there are some other materials that are used to achieve or improve the quality of concrete or to provide additional desired properties like the achievement of an earlier set time, retardation of the setting time, workability with lower water content, and air entrainment (Neville, 2012). These admixtures may be natural substances or mineral admixtures like finely crushed glasses, silts, volcanic ash, silica ash, fly ash, and so on. Another type of admixture may consist entirely of special chemical compounds, which are further classified on the basis of their function; they are required to perform in the concrete mix. Chemical admixtures include accelerators, retarders, plasticizers, and air-entertaining agents (Dodson, 2013). For instance, calcium chloride can be used in mass concrete during winter to accelerate strength development.

### **15.2.2 Environmental hazards**

Carbon dioxide (CO<sub>2</sub>) emission is a challenging factor for our healthy environment. Worldwide, cement production results in more than  $1.6 \times 10^9$  tons of emissions from all social activities (Shimoda, 2016). The cement industry is largely dependent on coal, which leads to very high emission levels of nitrous oxide and sulfur. These gases produce global warming, which is a major threat to the environment.

The increasing demand for construction throughout the world has increased the demand for more production of concrete ingredients from natural resources such as limestone, rocks, and other mines. Calcite and silica are the main components of cement that are obtained from rocks, sand, and clay (Babor et al., 2009). These natural resources should be preserved and managed properly. Similarly, sand deposits are also an asset and need proper management so that they are available to the coming generations.

### **15.2.3 Greenization**

Green concrete is defined as concrete which uses waste materials as constituents or its manufacturing process leads to minimal environmental damage (Suhendro, 2014). It is expected to have a high performance and a sustainable life cycle. Waste materials such as WBP, blast furnace slag, fly ash, silica fume, recycled glass, coal bottom ash, wood ash, and many others are used as an alternative for cement in the production of green concrete. Recycled concrete materials, waste plastic, demolition waste, recycled glass aggregate, foundry sand, and stone crusher waste are used as alternatives for aggregate in the production of green concrete. Therefore there can be two types of replacements in cementitious materials: One is that of reactive materials like cement, and the other is that of inert materials like aggregates.

### **15.2.4 Replacement of natural aggregates**

Natural aggregate resources are diminishing universally due to their continuous use in concrete. The unfavorable effect of nonstop fine and coarse aggregate withdrawal from rivers is also a major concern. Finding new substituting materials for viable growth so as to significantly decrease the depletion of natural resources is the need of the day. It has now become imperative to protect the rights of the future generation. High depletion of natural resources directed to environmental degradation. To incorporate this vision, waste material usage becomes a primary goal for the worldwide construction industry. Some of the significant works in this regard are highlighted in the following paragraphs.

#### **15.2.4.1 Copper slag**

Copper slag is a byproduct of copper quarrying and as such is a waste material. During manufacturing, impurities become slag which floats on the molten metal. Slag that is soaked in water produces scraps, as shown in Fig. 15.1. According to

Al-Jabri et al., 40% of copper slag can be used as a replacement for sand in order to manufacture high-performance concrete with enhanced characteristics (Al-Jabri et al., 2009).



**Figure 15.1** Copper slag as a replacement for sand to manufacture high-performance concrete. Waste copper slag.

#### 15.2.4.2 Iron powder

Waste iron powder is a residue of iron, a powder-like material, produced during laser cutting of iron and steel. The waste iron slag in solid and powder form is shown in Fig. 15.2 (Jalil et al., 2019). This waste material is a burden on society and its environment. According to Ismail et al. the compressive strength and fresh and dry densities increase, but slump values of the iron concrete decrease with an increase of waste iron powder (Ismail & Al-Hashmi, 2008).

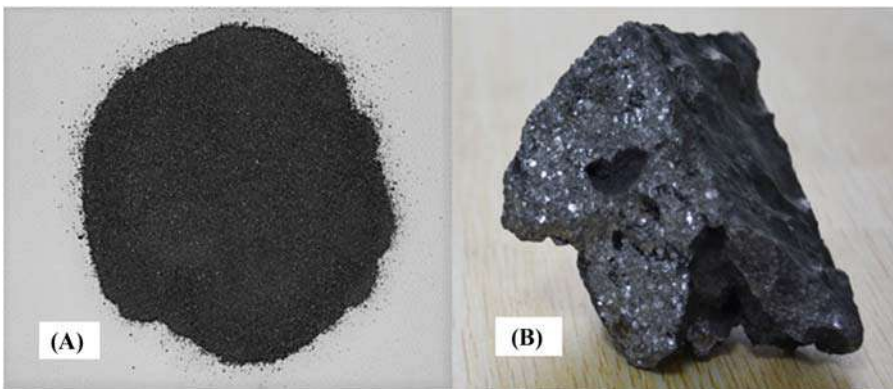


**Figure 15.2** The waste iron slag in solid and powder forms. Waste iron slag: (A) powder form and (B) solid form.

Source: From Jalil, A., Khitab, A., Ishtiaq, H., Bukhari, S. H., Arshad, M. T., & Anwar, W. (2019). Evaluation of steel industrial slag as partial replacement of cement in concrete. *Civil Engineering Journal*, 5(1), 181–190. <https://doi.org/10.28991/cej-2019-03091236>.

### 15.2.4.3 Corn cub ash

Corn cub ash is a residue obtained from the open burning of corncobs. The raw and powder forms are shown in Fig. 15.3. This waste material proves hazardous for environmental health. Being an air pollutant, it stimulates global warming. By incorporating this material as sand, green concrete can be produced. According to Memon et al. the density, ultrasonic pulse velocity (UPV), and slump increase by increasing waste corn cub ash. However, this lightweight concrete presents a slight compromise on compressive strength (Memon et al., 2019).



**Figure 15.3** The raw form of corn cub and the powder form of corn cub ash. (A) Corn cub before burning and (B) ash.

## 15.3 Waste rubber tires

The rapid development of the vehicle industry has rendered a huge growth in discarded waste tires, and this has created a critical problem, which has been called “black pollution.” There are more than 1 billion waste tires generated annually (Liu et al., 2016). Waste tires are nonbiodegradable solids wastes; when disposed into landfills, they can affect soil fertility and vegetation (Batayneh et al., 2008). The combustion of tires can pollute the environment very badly, creating air pollution (Wakili et al., 2018).

### 15.3.1 Crumb rubber

Crumb rubber is produced by ambient grinding of the waste vehicular tires. The waste rubber tires and ground waste are shown in Fig. 15.4. Several researchers have documented the use of crumb rubber as a partial of natural aggregates (Anwar & Khan, 2020; Batayneh et al., 2008). According to Matsimbe, the compressive strength increases by

replacing sand up to 5% WCR with a decrease in fresh and hardened density (Matsimbe et al., 2020). This shows that lightweight concrete can be manufactured by using waste crumb rubber without compromising the strength at lower dosages.



**Figure 15.4** The waste rubber tires and the ground waste rubber tire. Waster rubber: (A) tires (B) powder.

## 15.4 Rubberized concrete

Ordinary cementitious composites consist of two types of materials: reactive materials such as cement and inert materials like aggregates. Waste rubber is an inert material. As such, it can be used as a partial replacement for sand. Some researchers have tried rubber particles as partial replacement of coarse aggregates, but owing to the very low crushing strength of rubber, the resulting concrete was observed to possess very low strength (Khitab et al., 2017). Atef et al. replaced cement (Type 42.5N) with crumb rubber (0%–25% in 5% increment) in cement paste (Atef et al., 2021). They have reported a drastic reduction in compressive strength. The strength of the cement (a water to binder ratio of 0.3 with 5% replacement) was equivalent to that of the control specimen using Type 32.5N cement. However, the partial replacement of fine aggregates by waste rubber particles has gained some success over the past few decades, and some important work has been documented in this regard. Two types of studies are available at large in the literature. One corresponds to the use of untreated rubber particles, and the second one deals with that of the rubber particles pretreated with water and different chemical solutions.

### 15.4.1 Untreated rubber particles as replacement of fine aggregates

Khan et al. used different proportions of crumb rubber as a partial replacement of sand in concrete (Khan & Khitab, 2020). They have reported that the partial replacement of sand via crumb rubber decreases the workability of concrete, primarily due to a

decrease in viscosity of the concrete mix. Nevertheless, every time a true slump was observed. The main features observed are mentioned as follows:

1. Reduction of slump
2. Reduction of weight
3. Enhancement in porosity
4. Enhancement of water absorption
5. Lowering of thermal conduction
6. Lowering of strength

The slump is reduced owing to the fact that rubber particles being shock absorbers hinder the compacting effort during the test. Compaction is vital for expelling air bubbles out of the mix. Poor compaction also leads to more voids. On one hand, rubber particles have a low density in comparison to the natural aggregates, and on the other hand, they do not allow full compaction. The porous nature of the crumb rubber is shown in Fig. 15.5. The voids present in the particles are highlighted with red circles. Both these factors lead to a lower weight, higher porosity, and higher insulation. It was also observed that the interstitial transition zone between the rubber particles and the surrounding cementitious matrix was of poor quality having cracks and voids. This led to the lower mechanical strength of the finished products. Telmat et al. studied the effect of rubber particles as partial replacement of fine aggregates on the strength and ductility of the concrete (Telmat et al., 2021). They have reported that while the strength decreases, the ductility increases as a function of rubber content (0%–25% as partial replacement of fine aggregates). Bandarage et al. investigated the effect of rubber particles (passing through ASTM sieve # 4) on the mechanical properties (compressive strength and modulus of elasticity) of the concrete (Bandarage & Sadeghian, 2020). They have reported a decrease in both the parameters with an increase in rubber content.

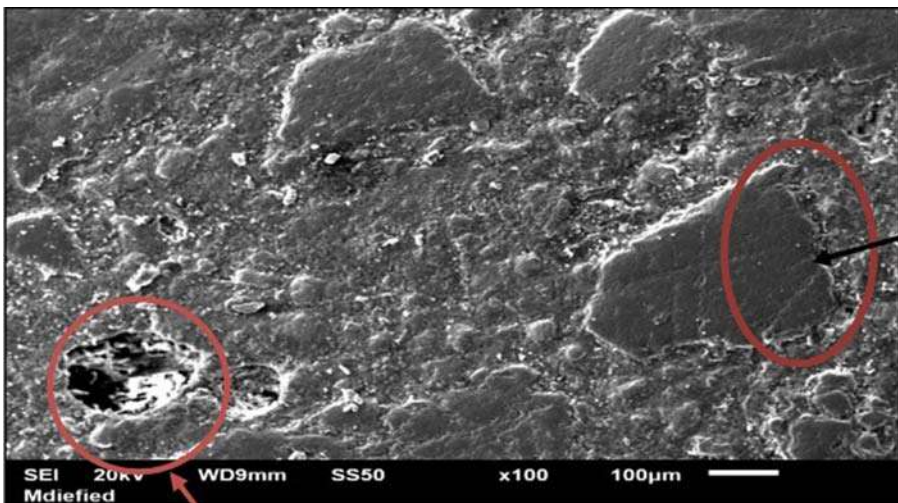


**Figure 15.5** The porous nature of the crumb rubber and optical microscopy image of crumb rubber particles.



### **15.4.2 Treated rubber particles as replacement of fine aggregates**

Si et al. studied the durability properties of cementitious composites (mortars and concrete) using rubber particles treated with NaOH solution as partial replacement of fine aggregates (Si et al., 2017). They have reported enhanced durability properties for concrete with 15% partial replacement and for mortar with 25% partial replacement of fine aggregates by NaOH-treated rubber particles. Feng et al. also utilized NaOH + KH570 (methacryloxypropyltrimethoxy)-treated rubber particles as partial replacement of fine aggregates (10%, 15%, and 20%) for examining the effect on abrasion resistance of concrete (Feng et al., 2021). They have reported an enhanced abrasion resistance accompanied by a lower compressive strength. They have further elaborated that the abrasion resistance increases with an increase in replacement as well as the size of the rubber particles. Khern et al. studied the effect of different pretreatment solutions (tap water, NaOH, and calcium hypochlorite ( $\text{Ca}(\text{ClO})_2$ )) and the duration of pretreatment on the strength and thermal conductivity of the concrete (Khern et al., 2020). They have reported that the pretreatment enhances the strength and the thermal conductivity owing to the stronger bond of the treated rubber particles with the surrounding cement matrix. They have further emphasized that the bond is stronger if the particles are treated for a longer duration. Xue et al. studied the properties of the cement mortar containing rubber particles treated with 1% polyvinyl alcohol solution (Zhang et al., 2017). Their findings reveal the enhancement of impact resistance with an increase in the replacement level from 0%–30% of fine aggregates by treated rubber particles. Nevertheless, the compressive and flexural strengths decrease with an increase in rubber content.

### **15.4.3 Rubber powder as an admixture**

Apart from the partial replacement of fine aggregates by waste rubber particles, some researchers also emphasized the use of finely ground powder of waste rubber as an admixture for concrete. Chylík et al. used fine crumb rubber as an admixture to enhance the durability of the concrete in the European environment (Chylík et al., 2017). Their study reveals that the admixture enhances the void content and reduces the workability and mechanical strength. They have reported that the admixture increases the resistance of the concrete against the deicing chemicals. Segre et al. added untreated and NaOH-treated rubber particles (max. size 35  $\mu\text{m}$  particles with 10% by mass of the cement) to cement pastes (Segre & Joekes, 2000). They have reported enhancement of mechanical strength with treated rubber particles. They have attributed this increase of strength to more adhesion associated with the surface treatment.

## 15.5 Waste brick powder

WBP is an appropriate material to partially replace cement in concrete due to its pozzolanic nature (Arif et al., 2021). The manufacturing of clay bricks involves exposure to higher temperatures, ranging from 600°C to 1000°C, which change the structure of the silicates (in clay) from a crystalline phase to an amorphous phase (Letelier et al., 2018).

Brick dust emitted from bricks kilns as well as demolished brick masonry creates respiratory diseases and pollutes the environment. Tons of brick waste as shown in Fig. 15.6 are generated each year, which needs to be handled properly. According to Amakye et al., brick powder reacts with portlandite ( $\text{Ca}(\text{OH})_2$ ) in hydrated cement and converts it into calcium silicate hydrate gel (C-S-H) (Amakye et al., 2021).



**Figure 15.6** Brick waste and waste brick powder. Waste brick: (A) kilns, (B) demolition sites, and (C) powder.

### 15.5.1 Use in concrete

Brick units can be collected from demolished and dumping sites. Grinding this brick powder into fine powder produces WBP. For use as a replacement for cement the ground powder must pass through a 75  $\mu$  sieve to get a particle size distribution which is nearly equal to that of cement. WBP contains 30%–40%, 20%–30% silica ( $\text{SiO}_2$ ), 20%–25% alumina ( $\text{Al}_2\text{O}_3$ ), 10%–20% iron oxide ( $\text{Fe}_2\text{O}_3$ ), and a minor quantity (0%–5%) of calcium oxide ( $\text{CaO}$ ). This composition highlights that WBP is an aluminosilicate supplementary cementitious material (SCM) (Pacawska & Wilińska, 2020). As the cumulative percentage of alumina, silica, and iron in WBP is more than 75%, it can be a pozzolana of high potential that can be used as a partial replacement of cement in concrete. Before using WBP as SCM in concrete, it is recommended to conduct a strength activity index test, for example, ASTM C11/C311M (Bentz et al., 2011).

### 15.5.1.1 Workability

Many researchers have reported an increase in workability when cement is partially replaced by WBP. Ayaz et al. partially replaced cement by 0%, 5%, 10%, 15%, and 20% (by mass) of WBP. They concluded that when the concrete is prepared by replacing the cement with WBP the workability of the prepared matrix is increased. Their results showed that the slump was increased up to the replacement level of 15%. The increase in workability was attributed to the ball-bearing effect of WBP particles (Arif et al., 2021). Also, pozzolanas take part in hydration at a later stage (secondary hydration); as such, more water is present at the time of casting, which increases the workability (Khitab et al., 2022). The effect of WBP on workability is shown in Fig. 15.7. It can be seen that the addition results in a fluid concrete with a true slump.



**Figure 15.7** The effect of WBP on workability of concrete. WBP, waste brick powder.

### 15.5.1.2 Fresh and hardened densities

WBP is lighter than cement. Its specific gravity is  $1250 \text{ kg/m}^3$ , which is 40% that of the cement (Arif et al., 2021). As such the partial replacement of cement by WBP should result in lighter fresh and hardened cementitious composites. Arif et al. have reported a 2% decrease in density when 10% cement was replaced by WBP.

### 15.5.1.3 Compressive strength

The compressive strength of concrete is a measure of the durability of concrete. It highlights the serviceability of the structure under different loading actions. This test can be performed for 3, 7, 14, and 28 days (to examine the strength development) according to ASTM C-39 (Standard Test Method for Compressive Strength of Cylindrical Concrete Specimens, 2021).

Several works are on hand, which describe the enhancement of the compressive strength of concrete if its cement is partially replaced by WBP. Wong et al.

performed an investigation on a few samples prepared by replacing cement with WBP in different percentages (0%, 5%, 10%, 15%, 20%, and 50%) (Wong et al., 2018). They reported that up to 20% of cement replacement the compressive strength and some durability properties were enhanced due to potential pozzolanic activity of brick dust particles with cement and other constituents of concrete.

#### 15.5.1.4 Ultrasonic pulse velocity test

UPV test is an important nondestructive test for examining the quality of cementitious composites. In this test an ultrasonic wave is passed through the given sample, as shown in Fig. 15.8.



**Figure 15.8** An ultrasonic wave velocity setup and sample. Ultrasonic pulse velocity testing of concrete.

UPV is a measure of the quality of cementitious composites. A higher value indicates a good-quality material in accordance with Table 15.1.

**Table 15.1** Quality of concrete on the basis of ultrasonic pulse velocity (UPV).

Ultrasonic pulse velocity ( $\times 10^3$ km/s)	Concrete quality
Above 4.5	Excellent
3.5–4.5	Good
3.0–3.5	Moderate
2.5–3.0	Poor
2.0–2.5	Very poor

The quality of concrete is affected by the presence of voids in the prepared sample (Caputo et al., 2017). Lower values of velocities are encountered when the quality of concrete is not good or is compromising. A higher velocity is achieved when the quality is good in terms of homogeneity, density, and uniformity of the prepared concrete sample. Arif et al. have reported that the inclusion of WBP in concrete promotes the formation of ettringites in pores, which enhance the particle to particle contact within the material, and UPV increases (Arif et al., 2021).

### 15.5.2 Use in clayey bricks

Clay is a natural material and is the principal ingredient of clayey bricks. The increase in construction activities is demanding a huge quantity of clayey bricks that in return are directly depleting the natural reserves of clay. Therefore the process of recycling waste in brick manufacturing is required to preserve the natural deposits of clay.

WBP is found in bulk near the brick manufacturing kilns as well as the demolition sites, as shown in Fig. 15.6. Such waste finds its suitable application for the manufacturing of bricks. Many researchers have addressed this issue and proposed different waste materials like rice husk ash, sugarcane bagasse, marble, ceramic wastes, and so on. (Kazmi, Abbas, Munir et al., 2016; Kazmi, Abbas, Saleem et al., 2016; Munir et al., 2018; Riaz et al., 2020).

This chapter focuses on the recycling of the WBP in manufacturing clayey bricks by partially replacing the clay. The motivation arises from the fact that WBP is a high-temperature transformed phase of the natural clay. The oxide compositions of the two materials are presented in Table 15.2 (Khitab et al., 2021).

**Table 15.2** Oxide composition of clay and WBP.

Oxides	Clay	Waste brick powder	Recommended for brick manufacturing
SiO <sub>2</sub>	59.2	46.4	50–60
Al <sub>2</sub> O <sub>3</sub>	16.6	29.7	20–30
Fe <sub>2</sub> O <sub>3</sub>	6.9	7.8	5–6
SO <sub>3</sub>	–	5.2	–
CaO	13.1	4.9	1–5
TiO <sub>2</sub>	0.9	3.9	–
K <sub>2</sub> O	2.9	1.8	–

Source: From Khitab, A., Riaz, M. S., Jalil, A., Khan, R. B., Anwar, W., Khan, R. A., Arshad, M. T., Kirgiz, M. S., Tariq, Z., & Tayyab, S. (2021). Manufacturing of clayey bricks by synergistic use of waste brick and ceramic powders as partial replacement of clay. *Sustainability*, 13(18). <https://doi.org/10.3390/su131810214>.

The oxide composition dictates that with a few minor variations, WBP may be adapted as a partial replacement of clay in manufacturing the clayey bricks. Riaz et al. have pointed out that WBP has a lower density than fresh clay owing to a

porous and thin structure (Riaz et al., 2019). They partially replaced the clay from 0%–25% by mass in 5% increments. They have reported that the replacement decreases the crushing strength, unit weight, and thermal conductivity while increasing the resistance to efflorescence, water absorption, and porosity. They have recommended a partial replacement of 10% as optimum because the higher replacement levels drastically reduce the bricks' strength.

## 15.6 Conclusion

Based on the work related to the use of waste rubber particles in cementitious materials, it can be concluded that it is more imperative to use them as partial replacement of fine aggregates. There are certain limitations, which should be looked at before their incorporation. For example the pretreatment with some compatible solutions like NaOH, calcium hypochlorite ( $\text{Ca}(\text{ClO})_2$ ), or polyvinyl alcohol imparts additional adhesion with the surrounding cement matrix. The compaction of rubberized concrete is another problem the researchers should look forward to resolving. Rubber particles are light and have shock-absorbing characteristics, which hinder proper compacting efforts. As such, it becomes difficult to expel air with conventional compaction methods. This also reduces the mechanical strength. However, rubberized concrete to date is declared suitable vis-a-vis durability properties and at the same time provides an efficient and green solution, where a lightweight, thermal insulation, and low strength are required.

WBP increases the compressive strength of cementitious composites at lower partial replacements (up to 20% by mass of cement). This is attributed to the pozzolanic nature of WBP, which promotes more calcium-silicate-hydrate (C-S-H) gel. WBP also decreases the density of the cementitious composites due to the lower density of WBP as compared to cement. WBP also enhances the workability of the cement mixes due to its ball-bearing effect and its pozzolanic nature, which provides more water for the lubrication of the mix.

WBP can also be used in manufacturing clayey bricks as a partial replacement for fresh clay owing to the fact that the chemical composition of both materials complies with each other to a large extent. WBP particles have porous and skinny structures, which result in lighter bricks with lower strength but higher void content, which provides more sustainability.

## References

- Al-Jabri, K. S., Hisada, M., Al-Oraimi, S. K., & Al-Saidy, A. H. (2009). Copper slag as sand replacement for high performance concrete. *Cement and Concrete Composites*, 31(7), 483–488. Available from <https://doi.org/10.1016/j.cemconcomp.2009.04.007>.
- Amakye, S. Y., Abbey, S. J., & Olubanwo, A. O. (2021). Consistency and mechanical properties of sustainable concrete blended with brick dust waste cementitious materials. *SN Applied Sciences*, 3(4), 420. Available from <https://doi.org/10.1007/s42452-021-04430-w>.

- American Society for Testing and Materials (ASTM). (2021). Standard Test Method for Compressive Strength of Cylindrical Concrete Specimens. In *ASTM C39/C39M-21, book of standards volume: 04.02*. Available from [https://doi.org/10.1520/C0039\\_C0039M-21](https://doi.org/10.1520/C0039_C0039M-21)
- Anwar, K., & Anwar, W. (2016). *Classical building materials. Advanced research on nano-technology for civil engineering applications* (1st ed., pp. 1–27). IGI Global. Available from [10.4018/978-1-5225-0344-6.ch001](https://doi.org/10.4018/978-1-5225-0344-6.ch001).
- Anwar, K., & Khan, R. B. N. (2020). Enhancing physical, mechanical and thermal properties of rubberized concrete. *Engineering and Technology Quarterly Reviews*, 3(1), 33–45. Available from [https://papers.ssrn.com/sol3/papers.cfm?abstract\\_id=3610526](https://papers.ssrn.com/sol3/papers.cfm?abstract_id=3610526).
- Anwar, K., Alam, M., Riaz, H., & Rauf, S. (2014). Smart concretes: Review. *International Journal of Advances in Life Science and Technology*, 1(2), 47–53. Available from <https://doi.org/10.18488/journal.72/2014.1.2/72.2.47.53>.
- Arif, R., Khitab, A., Kirgiz, M. S., Khan, R. B. N., Tayyab, S., Khan, R. A., Anwar, W., & Arshad, M. T. (2021). Experimental analysis on partial replacement of cement with brick powder in concrete. *Case Studies in Construction Materials*, 15, e00749. Available from <https://doi.org/10.1016/j.cscm.2021.e00749>.
- Atef, M., Bassioni, G., Azab, N., & Abdellatif, M. H. (2021). Assessment of cement replacement with fine recycled rubber particles in sustainable cementitious composites. *Journal of the Mechanical Behavior of Materials*, 30(1), 59–65. Available from <https://doi.org/10.1515/jmbm-2021-0007>.
- Babor, D., Plian, D., & Judele, L. (2009). Environmental impact of concrete. *The Bulletin of the Polytechnic Institute of Jassy*, 66(70), 27–36. Available from <http://www.bipcons.ce.tuiasi.ro/Content/ArticleInformation.php?ArticleID=161>.
- Bandarage, K., & Sadeghian, P. (2020). Effects of long shredded rubber particles recycled from waste tires on mechanical properties of concrete. *Null*, 9(1), 50–59. Available from <https://doi.org/10.1080/21650373.2019.1676839>.
- Batayneh, M. K., Iqbal, M., & Ibrahim, A. (2008). Promoting the use of crumb rubber concrete in developing countries. *Waste Management*, 28(2008), 2171–2176. Available from <https://doi.org/10.1016/j.wasman.2007.09.035>.
- Bentz, D. P., Durán-Herrera, A., & Galvez-Moreno, D. (2011). Comparison of ASTM C311 strength activity index testing vs. testing based on constant volumetric proportions. *Journal of ASTM International*, 9(1), 2011. Available from [https://www.researchgate.net/publication/234154842\\_Comparison\\_of\\_ASTM\\_C311\\_Strength\\_Activity\\_Index\\_Testing\\_vs\\_Testing\\_Based\\_on\\_Constant\\_Volumetric\\_Proportions](https://www.researchgate.net/publication/234154842_Comparison_of_ASTM_C311_Strength_Activity_Index_Testing_vs_Testing_Based_on_Constant_Volumetric_Proportions).
- Biricik, H., Kirgiz, M. S., Galdino, A. G., de, S., Kenai, S., Mirza, J., Kinuthia, J., Ashteyat, A., Khitab, A., & Khatib, J. (2021). Activation of slag through a combination of NaOH/NaS alkali for transforming it into geopolymer slag binder mortar—assessment of the effects of two different Blaine fines and three different curing conditions. *Journal of Materials Research and Technology*, 14, 1569–1584. Available from <https://doi.org/10.1016/j.jmrt.2021.07.014>.
- Caputo, F., Xu, L., & Huang, Y. (2017). Effects of voids on concrete tensile fracturing: A mesoscale study. *Advances in Materials Science and Engineering*, 2017, 7989346. Available from <https://doi.org/10.1155/2017/7989346>.
- Chylík, R., Trtík, T., Fládr, J., & Bílý, P. (2017). Mechanical properties and durability of crumb rubber concrete. *IOP Conference Series: Materials Science and Engineering*, 236. Available from <https://doi.org/10.1088/1757-899X/236/1/012093>.
- Dodson, V. H. (2013). *Concrete admixtures. VNR structural engineering series*. Springer Science & Business Media.

- Feng, L.-Y., Chen, A.-J., & Liu, H.-D. (2021). Effect of waste tire rubber particles on concrete abrasion resistance under high-speed water flow. *International Journal of Concrete Structures and Materials*, 15(1), 37. Available from <https://doi.org/10.1186/s40069-021-00475-8>.
- Ismail, Z. Z., & Al-Hashmi, E. A. (2008). Reuse of waste iron as a partial replacement of sand in concrete. *Waste Management (New York, N.Y.)*, 28(11), 2048–2053.
- Jalil, A., Khitab, A., Ishtiaq, H., Bukhari, S. H., Arshad, M. T., & Anwar, W. (2019). Evaluation of steel industrial slag as partial replacement of cement in concrete. *Civil Engineering Journal*, 5(1), 181–190. Available from <https://doi.org/10.28991/cej-2019-03091236>.
- Kadir, A. A., & Sarani, N. A. (2012). An overview of wastes recycling in fired clay bricks. *International Journal of Integrated Engineering*, 4(2), 53–69. Available from <https://core.ac.uk/download/pdf/268562803.pdf>.
- Kazmi, S. M. S., Abbas, S., Munir, M. J., & Khitab, A. (2016). Exploratory study on the effect of waste rice husk and sugarcane bagasse ashes in burnt clay bricks. *Journal of Building Engineering*, 7, 372–378. Available from <https://doi.org/10.1016/j.jobe.2016.08.001>.
- Kazmi, S. M. S., Abbas, S., Saleem, M. A., Munir, M. J., & Khitab, A. (2016). Manufacturing of sustainable clay bricks: Utilization of waste sugarcane bagasse and rice husk ashes. *Construction and Building Materials*, 120, 29–41. Available from <https://doi.org/10.1016/j.conbuildmat.2016.05.084>.
- Khan, R. B. N., & Khitab, A. (2020). Enhancing physical, mechanical and thermal properties of rubberized concrete. *Engineering and Technology Quarterly Reviews*, 3(1), 33–45. Available from [https://papers.ssrn.com/sol3/papers.cfm?abstract\\_id=3610526](https://papers.ssrn.com/sol3/papers.cfm?abstract_id=3610526).
- Khern, Y. C., Paul, S. C., Kong, S. Y., Babafemi, A. J., Angraini, V., Miah, M. J., & Šavija, B. (2020). Impact of chemically treated waste rubber tire aggregates on mechanical, durability and thermal properties of concrete. *Frontiers in Materials*, 7, 90. Available from <https://www.frontiersin.org/article/10.3389/fmats.2020.00090>.
- Khitab, A., Anwar, W., Mansouri, I., Tariq, M. K., & Mehmood, I. (2015). Future of civil engineering materials: A review from recent developments. *Reviews on Advanced Materials Science*, 42(2015), 20–27. Available from <https://citeseerx.ist.psu.edu/viewdoc/download?doi=10.1.1.1080.6447&rep=rep1&type=pdf>.
- Khitab, A., Anwar, W., Mehmood, I., Kazmi, S. M. S., & Munir, M. J. (2016). Lunar concrete: Prospects and challenges. *Astronomy Reports*, 60(2), 306–312. Available from <https://doi.org/10.1134/S1063772916020050>.
- Khitab, A., Arif, I., Awan, F. A., Anwar, A., & Mughal, A. (2017). Use of waste rubber tyre in concrete: Mini review. *International Journal for Innovative Research in Multidisciplinary Field*, 3(12), 21–23. Available from <https://www.ijrmf.com/wp-content/uploads/201712004.pdf>.
- Khitab, A., Khan, R. A., Riaz, M. S., Bashir, K., Tayyab, S., & Khan, R. B. N. (2022). *Utilization of waste brick powder for manufacturing green bricks and cementitious materials* (pp. 361–370). Springer International Publishing. Available from [https://doi.org/10.1007/978-3-030-76073-1\\_18](https://doi.org/10.1007/978-3-030-76073-1_18).
- Khitab, A., Riaz, M. S., Jalil, A., Khan, R. B., Anwar, W., Khan, R. A., Arshad, M. T., Kirgiz, M. S., Tariq, Z., & Tayyab, S. (2021). Manufacturing of clayey bricks by synergistic use of waste brick and ceramic powders as partial replacement of clay. *Sustainability*, 13(18). Available from <https://doi.org/10.3390/su131810214>.
- Kirgiz, M. S., Galdino, A. G., de, S., Kinuthia, J., Khitab, A., Ul Hassan, M. I., Khatib, J., El Naggari, H., Thomas, C., Mirza, J., Kenai, S., Nguyen, T. A., Nehdi, M., Syarif, M.,



- Ashteyat, A., Gobinath, R., Soliman, A., Tagbor, T. A., Kumbhalkar, M. A., ... Tiwary, C. S. (2021). Synthesis, physico-mechanical properties, material processing, and math models of novel superior materials doped flake of carbon and colloid flake of carbon. *Journal of Materials Research and Technology*, 15, 4993–5009. Available from <https://doi.org/10.1016/j.jmrt.2021.10.089>.
- Lee, Y.-L., Koh, H.-B., Sam, T.-H., Yeoh, D. E. C., bin Mustapa, S., Pang, C.-F., & Hung, Y.-T. (2014). *Use of solid wastes as construction materials*, . (1st ed., pp. 685–736). *Handbook of environment and waste management*, (Vol. 2, pp. 685–736). World Scientific Publishing Co Pte Ltd. Available from [https://doi.org/10.1142/9789814449175\\_0011](https://doi.org/10.1142/9789814449175_0011).
- Letelier, V., Ortega, J. M., Muñoz, P., Tarela, E., & Moriconi, G. (2018). Influence of waste brick powder in the mechanical properties of recycled aggregate concrete. *Sustainability*, 10(4). Available from <https://doi.org/10.3390/su10041037>.
- Liu, H., Wang, X., Jiao, Y., & Sha, T. (2016). Experimental investigation of the mechanical and durability properties of crumb rubber concrete. *Materials (Basel, Switzerland)*, 9(3). Available from <https://doi.org/10.3390/ma9030172>.
- Matsimbe, J., Ghambi, S., & Samson, A. (2020). Application of the BowTie method in accident analysis: Case of Kaziwiziwi coal mine. *Engineering and Technology Quarterly Reviews*, 3(2), 127–136. Available from [https://www.researchgate.net/publication/348115519\\_Application\\_of\\_the\\_BowTie\\_Method\\_in\\_Accident\\_Analysis\\_Case\\_of\\_Kaziwiziwi\\_Coal\\_Mine](https://www.researchgate.net/publication/348115519_Application_of_the_BowTie_Method_in_Accident_Analysis_Case_of_Kaziwiziwi_Coal_Mine).
- Memon, S. A., Javed, U., & Khushnood, R. A. (2019). Eco-friendly utilization of corncob ash as partial replacement of sand in concrete. *Construction and Building Materials*, 195, 165–177. Available from <https://doi.org/10.1016/j.conbuildmat.2018.11.063>.
- Munir, M. J., Abbas, S., Nehdi, M. L., Kazmi, S. M. S., & Khitab, A. (2018). Development of eco-friendly fired clay bricks incorporating recycled marble powder. *Journal of Materials in Civil Engineering*, 30(5). Available from <https://ascelibrary.org/doi/abs/10.1061/%28ASCE%29MT.1943-5533.0002259>.
- Neville, A. M. (2012). *Properties of concrete* (5th ed.). Pearson.
- Pacewska, B., & Wilińska, I. (2020). Usage of supplementary cementitious materials: Advantages and limitations. *Journal of Thermal Analysis and Calorimetry*, 142(1), 371–393. Available from <https://doi.org/10.1007/s10973-020-09907-1>.
- Riaz, M. H., Khitab, A., Ahmad, S., Anwar, W., & Arshad, M. T. (2020). Use of ceramic waste powder for manufacturing durable and eco-friendly bricks. *Asian Journal of Civil Engineering*, 21(2), 243–252. Available from <https://doi.org/10.1007/s42107-019-00205-2>.
- Riaz, M. H., Khitab, A., & Ahmed, S. (2019). Evaluation of sustainable clay bricks incorporating Brick Kilm dust. *Journal of Building Engineering*, 24, 100725. Available from <https://doi.org/10.1016/j.jobe.2019.02.017>.
- Segre, N., & Joekes, I. (2000). Use of tire rubber particles as addition to cement paste. *Cement and Concrete Research*, 30, 1421–1425, 2000.
- Shimoda, T. (2016). *History of cement manufacturing technology*. History of Cement Manufacturing Technology; Survey Report of Systematization of Technology. [http://sts.kahaku.go.jp/diversity/document/system/pdf/093\\_e.pdf](http://sts.kahaku.go.jp/diversity/document/system/pdf/093_e.pdf)
- Si, R., Guo, S., & Dai, Q. (2017). Durability performance of rubberized mortar and concrete with NaOH-Solution treated rubber particles. *Construction and Building Materials*, 153, 496–505. Available from <https://doi.org/10.1016/j.conbuildmat.2017.07.085>.
- Suhendro, B. (2014). Toward green concrete for better sustainable environment. *Procedia Engineering*, 95, 305–320. Available from <https://doi.org/10.1016/j.proeng.2014.12.190>.

- Syarif, M., Kirgiz, M. S., Galdino, A. G., de, S., Naggar, M. H. E., Mirza, J., Khatib, J., Kenai, S., Nehdi, M., Kinuthia, J., Khatab, A., Thomas, C., Gobinath, R., Hassan, M. I. U., Wu, Y. K., Ashteyat, A., Soliman, A., Muthusamy, K., Janardhanan, T., . . . Tiwary, C. S. (2021). Development and assessment of cement and concrete made of the burning of quinary by-product. *Journal of Materials Research and Technology*, 15, 3708–3721. Available from <https://doi.org/10.1016/j.jmrt.2021.09.140>.
- Telmat, D. E., Benazzouk, A., Hadjab, H., & Beji, H. (2021). A comparative study of the influence of rubber particle size on the ductility of cement concrete based on energy's dissipation method. *International Journal of Sustainable Building Technology and Urban Development*, 61–78. Available from <https://doi.org/10.22712/susb.20210006>.
- United States. Bureau of Standards. (2011). *Fire-clay brick: Their manufacture, properties, uses and specifications. National Bureau of Standards circular* (Vol. 282, p. 1926). U.S. Government Printing Office. Available from [https://books.google.com.pk/books/about/Fire\\_clay\\_Brick.html?id=Hwc3J8XYt-kC&redir\\_esc=y](https://books.google.com.pk/books/about/Fire_clay_Brick.html?id=Hwc3J8XYt-kC&redir_esc=y).
- Wakili, B. A., Garba., Engr, A., Yerima, A. B., Wakil, Z. A., & Yakubu, K. (2018). Appraisal of concrete using modified waste tyre rubber chips as partial replacement of coarse aggregate. *International Journal of Civil Engineering, Construction and Estate Management*, 6(2), 25–45. Available from <https://www.eajournals.org/wp-content/uploads/Appraisal-of-Concrete-Using-Modified-Waste-Tyre-Rubber-Chips-as-Partial-Replacement-of-Coarse-Aggregate.pdf>.
- Wong, C. L., Mo, K. H., Yap, S. P., Alengaram, U. J., & Ling, T.-C. (2018). Potential use of brick waste as alternate concrete-making materials: A review. *Journal of Cleaner Production*, 195, 226–239. Available from <https://doi.org/10.1016/j.jclepro.2018.05.193>.
- Zhang, P., Xue, G., & Cao, M. (2017). Effect of modified rubber particles mixing amount on properties of cement mortar. *Advances in Civil Engineering*, 8643839. Available from <https://doi.org/10.1155/2017/8643839>, 2017.

This page intentionally left blank

# Self-compacting concrete blended with fly ash and ground granulated blast furnace slag

16

*Naraindas Bheel<sup>1</sup>, Paul Awoyera<sup>2</sup>, Irfan Ali Shar<sup>3</sup> and Mehmet Serkan Kirgiz<sup>4</sup>*

<sup>1</sup>Department of Civil and Environmental Engineering, Universiti Teknologi Petronas, Bandar Seri Iskandar, Tronoh, Perak, Malaysia, <sup>2</sup>Department of Civil Engineering, Covenant University, Ota, Nigeria, <sup>3</sup>Department of Civil Engineering, ISRA University Hyderabad, Sindh, Pakistan, <sup>4</sup>Northwestern University, Chicago, IL, United States

## 16.1 Introduction

Concrete is an artificial composite of binding material, aggregates (fine and coarse aggregates), and water. Concrete plays a major role in the construction field, especially in framed structures. Concrete has some limitations; for example, it needs compaction accompanied with more open space for compaction as concrete cannot maintain strength at congested areas. Due to these limitations, researchers are trying to develop concrete that can be self-compacted with the utilization of mineral admixtures (Manjula & Felixkala, 2018). A special type of concrete with excellent deformability and high resistance against segregation developed in Japan around the 19th century is known as self-compacting concrete (SCC). SCC is high-performance concrete that does not require any compaction/vibration during placing of concrete. However, it can easily flow through congested areas where heavy reinforcement is encountered (Okamura, 1997). The behavior of SCC to flow under gravity is due to air bubbles present in the mixture. Hence SCC does not need any type of compaction and settles down quickly under its self-weight (Anjali et al., 2015). Bleeding water from concrete mix and other common problems occurring during mixing process are barred in the case of SCC. At the same time the mix covers the entire area uniformly (Jawahar et al., 2012). With the high flowability of SCC the mixture can be pumped with high slump at a long distance (Iures & Bob, 2010). Moreover the use of this concrete will dramatically reduce concreting time and noise pollution and on the other hand reduces vibration costs (Grdic et al., 2008). Due to high flowability/liquidity properties of SCC, bleeding and segregation problems arise during mixing, transporting, and placing processes (Anjali et al., 2015). To mitigate such problems the possible solution is enhancing the viscosity of the mixture with use of additives (Correa-Yepes et al., 2018; Manjula & Felixkala, 2018). Compared with traditional vibrated concrete, SCC has obvious

advantages in terms of reducing construction costs and improving the construction environment, which are significant forward steps in the direction of sustainably developed concrete. However, compared to the vibrated concrete, unit SCC often requires higher volume binder levels (cement and cementitious materials) in the present technology. This will not only increase the cost of SCC but also significantly elevate its environmental burden. Therefore some researchers have recently focused on the development of an ecofriendly version of SCC (Fantilli & Chiaia, 2013; Long et al., 2015; Proske et al., 2013; Şahmaran et al., 2011). Therefore the use of Portland cement (PC) is reduced in the mixture of SCC to make an ecofriendly version. PC occupies a major portion and is an integral constituent of concrete but not an ecofriendly material. There are serious environmental concerns regarding the manufacturing process of PC as manufacturing processes discharge a large amount of greenhouse gases including carbon dioxide CO<sub>2</sub>. According to a previous report, it was estimated that 1 ton PC production requires 1.6 tons of raw materials (Ahmed et al., 2011) and about 6.5 million BTUs of energy. At the same time, approximately 1 ton of carbon dioxide is discharged into the atmosphere (Naik & Kraus, 1999; Shafiqh et al., 2013). It has been reported that cement industry alone contributes annually about 1.65 billion tons and nearly 7% of total greenhouse gases into the atmosphere (Hardjito et al., 2004; Hardjito et al., 2009; Malhotra, 2002; McCaffrey, 2002). In order to negate the impacts of cement manufacturing processes on the ecosystem, there is a need to discover new possibilities and strategies to bring improvement in concrete materials for sustainable environmental conditions by substituting PC with other alternative materials (Kong & Sanjayan, 2008; Naik & Kraus, 1999). However, several experimental investigations are being carried out around the globe to form an ecofriendly atmosphere with reduction in usage of PC and incorporating byproducts such as rice husk ash, wheat straw ash, coal fly ash, and ground granulated blast furnace slag (GGBFS) and other pozzolanic materials as alternatives to PC (Ariffin et al., 2013). The use of industrial and agricultural waste byproducts possessing pozzolanic properties aids in reducing utility of PC in concrete; thereby there is a decline in trend of greenhouse gas emissions (Mehta, 2002; Naik & Kraus, 1999).

With awareness in the field of research, consumption of fly ash and GGBFS industrial byproducts in concrete has acquired an extensive attractiveness around the world as an effort to embrace sustainability in PC and concrete industry and as a positive footstep toward creating cement industry environment-friendly (Park et al., 2016). Rapid growth in population and industrialization has triggered power requirements manifold. Similarly, power generation plants are causing a huge amount of byproducts as fly ash (FA) because of increased consumption of pulverized coal (Ramachandran, 1996). As FA stands at number 5 with respect to the world's largest source of raw material (Mukherjee et al., 2008). With industrial developments, about 800 million tons of FA will be produced (Fernández-Jiménez & Palomo, 2005). However, use of FA is just 20%–30% of total estimated quantity, where the rest of the quantity is disposed off in landfills (Duxson et al., 2007; Palomo et al., 1999; Roy, 1999). If this trend of waste deposition goes on, then it has an ability to deteriorate human environment elements such as air, food, land,

shelter, and water (Ahmaruzzaman, 2010; Mukherjee et al., 2008; Ramachandran, 1996; Shafiqh et al., 2013). Investigations are being carried out to restore the eco-friendly environment by utilizing FA in other avenues of life. Besides the FA particles, being very fine, possess pozzolanic and cementitious properties; hence they have the ability to be admired and utilized as a mineral admixture in mortar and concrete (Mukherjee et al., 2008). Favorable results revealed when researchers utilized FA in concrete to examine its pozzolanic property in fresh and hardened phases (Ahmaruzzaman, 2010; Mukherjee et al., 2008; Shafiqh et al., 2013).

On the other hand, this trend of consumption of FA in concrete has environmental and cost benefits as this reduces emission of greenhouse gases in the atmosphere, savings in energy consumption, and natural resources (Ahmaruzzaman, 2010; Mukherjee et al., 2008). Furthermore, GGBFS is a waste of the metallurgical industry. The mixture of iron ore, limestone, and coke enters the kiln at temperatures between 15,000°C and 16,000°C. The resulting slag is weighed in the pig iron. The slag comprises 35%–45% silicon dioxide ( $\text{SiO}_2$ ) and about 45% calcium oxide. The oxide composition is nearly similar to that of PC. After the removal of molten iron the slag comprising the silicon–aluminum slag is quickly immersed in the liquid with the formation of glassy particles (Elchalakani et al., 2014; Kumar Karri et al., 2015; Kuo et al., 2014; Parande et al., 2008; Wang, 2008). Glass-like particles are dewatered and then pressed to the required size (Shariq et al., 2010; Shoubi et al., 2013). This crushed slag is called granulated blast furnace slag. Ground granulated blast is an ecofriendly building material. By replacing cement with crushed blast furnace slag, it is possible to control carbon dioxide emissions to a certain extent (Siddique & Kaur, 2012; Suresh & Nagaraju, 2015).

Moreover, GGBFS develops the impermeability, corrosion resistance, and sulfate resistance of SCC mixture. Owing to these characteristics of GGBFS SCC mixture, the service life of the assembly is amplified and maintenance costs are minimized. The huge percentage of GGBFS by the weight of PC in the mixture of SCC not only utilizes waste material but also protects the consumption of natural resources and energy (Elchalakani et al., 2014; Hossain et al., 2018; Qiu, 2020). Therefore, different researchers carried out the studies for utilization of FA as substitution of cement and GGBFS as substitution of PC individually, but the combined usage of FA and GGBFS as substitution of PC in the mixture of SCC is very limited. Hence to improve the different properties of fresh and hardened states of SCC mixture, to reduce the consumption of PC, and consequently to reduce the cost and  $\text{CO}_2$  release and encourage proper utilization of waste material of coal-fired power plants, in this study, effects of FA and GGBFS as substitution cement on the selected properties of SCC mixture are investigated individually and combined.

## 16.2 Materials and methodology

### 16.2.1 Materials

FA and GGBFS were used as binding materials in SCC mixture. However, FA was collected from Lakhra Power Plant Jamshoro with prior permission. After collecting

FA, it was dried under the sun for a certain time and then it was sieved through 75  $\mu\text{m}$  to remove unwanted particles. The sieved ash served as a cementitious ingredient in SCC mixture. Besides the GGBFS was collected from Steel Mill Karachi with prior permission. After collecting GGBFS, it was sieved through 75  $\mu\text{m}$  to eliminate large particles and then it was utilized as replacement for cement in the SCC mixture. Moreover the PC was used as a binding constituent in SCC mixture, and PC was obtained from local market Jamshoro, Sindh, Pakistan. The chemical composition of FA, GGBFS, and PC is given in Table 16.1. Furthermore the hill sand was utilized as fine aggregates (F.A) which passed from #4 sieve, and crushed stone served as coarse aggregates (C.A) which passed from 12 mm and were retained from #4 sieve. These aggregates were obtained from the local market in the region of Jamshoro, Sindh, Pakistan. The physical properties of aggregates are shown in Table 16.2. In addition, drinking water served in mixing and curing for SCC mixture and a superplasticizer was used as an chemical admixture for this experimental work.

**Table 16.1** Chemical composition of GGBFS, FA, and PC.

Compound	GGBFS	Fly ash	PC
SiO <sub>2</sub>	37.22	60.50	20.78
Al <sub>2</sub> O <sub>3</sub>	10.37	24.25	5.11
Fe <sub>2</sub> O <sub>3</sub>	1.23	4.82	3.17
CaO	35.66	1.75	60.22
Na <sub>2</sub> O	0.23	0.24	0.18
SO <sub>3</sub> specific gravity	0.34 2.25	1.48 2.22	2.86 3.15

**Table 16.2** Physical properties of aggregates.

Property	F.A	C.A
Fineness modulus	2.32	—
Specific gravity	2.63	2.66
Absorption (%)	1.30	0.65
Bulk density (kg/m <sup>3</sup> )	1890	1760

## 16.3 Mix proportion

This research work was performed on the SCC mixtures for determining fresh and hardened properties of SCC mixture blended with FA and GGBFS together. However, five mixtures of SCC were prepared with a water/binder ratio of 0.40, in which one mixture of SCC was made with plain concrete which possesses cement

only; four mixtures of SCC were prepared with inclusion of 5%, 10%, 15%, and 20% of FA; four mixtures of SCC were made blended with 5%, 10%, 15%, and 20% of GGBFS as cementitious materials; and the remaining other mixtures were prepared with the combined use of FA and GGBFS, such as 5% (2.5% FA and 2.5% GGBFS), 10% (5% FA and 5% GGBFS), 15% (7.50% FA and 7.50% GGBFS), and 20% (10% FA and 10% GGBFS) by the cement's weight. Moreover, various trial mixes with and without inclusion of the chemical admixture were performed to develop SCC mixture. Furthermore the hardened properties of SCC mixture were analyzed after the attainment of early fresh properties of SSC mixture, and it was dispensed into the molds. In addition the concrete specimens were removed from mold after 24 hours of casting and then these specimens were kept in a curing water tank till the testing day. The details of mix proportions are exhibited in [Table 16.3](#).

**Table 16.3** Details of mix proportions ( $\text{kg}/\text{m}^3$ ).

Mix proportion	Cement	FA	GGBFS	Water	F.A	C.A	SP (%)
C	500	0	0	200	880	640	2
FA5	475	25	0	200	880	640	2
FA10	450	50	0	200	880	640	2
FA15	425	75	0	200	880	640	3
FA20	400	100	0	200	880	640	3
GGBFS5	475	0	25	200	880	640	2
GGBFS10	450	0	50	200	880	640	2
GGBFS15	425	0	75	200	880	640	3
GGBFS20	400	0	100	200	880	640	3
FA2.5GGBFS2.5	475	12.50	12.50	200	880	640	2
FA5GGBFS5	450	25	25	200	880	640	2
FA7.50GGBFS7.50	425	37.50	37.50	200	880	640	3
FA10GGBFS10	400	50	50	200	880	640	3

## 16.4 Testing methods

### 16.4.1 Fresh properties of self-compacting concrete mixture

The fresh properties of SCC mixture with inclusion of FA and GGBFS in terms of filling ability (slump flow, V-funnel, and T50 flow), passing ability (J-ring and L-box), and sieve segregation test were analyzed. However, slump flow was measured. The workability of SCC mixture with inclusion of FA and GGBFS as replacement for cement by consuming ([ASTM C1611/C1611M-18](#), [Standard](#)



Test Method for Slump Flow of Self-Consolidating Concrete, 2018) the code procedure and V-funnel was analyzed on SCC mixture with accumulation of FA and GGBFS as cementitious constituents by obeying EN 12350-9: (2010). Similarly, T50 flow was determined. The workability of SCC mixture including FA and GGBFS as cement substitute components was determined by following EFNARC (2005) the code procedure. Besides, J-ring test was performed on fresh properties of SCC mixture with addition of FA and GGBFS as cement replacement constituents under EN 12350-12: (2010), and L-box was investigated on the fresh properties of SCC mixture blended with FA and GGBFS as cementitious components by detection under EN 12350-10: (2010). Moreover, sieve segregation was performed with fresh properties of SCC mixture including FA and GGBFS as replacement for cement by obeying EN 12350-11:(2010) code procedure.

#### **16.4.2 Hardened properties of self-compacting concrete mixture**

The hardened properties of SCC mixture with accumulation of FA and GGBFS as replacement for cement in terms of compressive, split tensile, and flexural strengths of SCC mixture and water penetration depth of SCC mixture at 28 and 90 days consistently were analyzed. However, five concrete cubes (100 mm × 100 mm × 100 mm) were cast for exploring the compressive strength of SCC mixture blended with FA and GGBFS as cementitious components by using B. EN, 2009a, and five cylindrical specimens (200 mm × 100 mm) were prepared for splitting tensile strength of SCC mixture with inclusion of FA and GGBFS as replacement for cement as per B. EN, 2009b. Similarly, five prisms (500 mm × 100 mm × 100 mm) were tested for flexural strength of SCC mixture with addition of FA and GGBFS as cementitious materials by applying B. S. EN, 2009. All these concrete specimens were tested on 28 and 90 days, respectively. Moreover the water penetration depth of SCC mixture blended with FA and GGBFS as cementitious constituents was analyzed by using the code procedure (“Testing Hardened Concrete: Part 8: Depth of Penetration of Water under Pressure,” 2009) at 28 and 180 days.

## **16.5 Results and discussion**

### **16.5.1 Fresh concrete results**

The results of fresh properties of SCC mixture with inclusion of various proportions of FA and GGBFS as cement replacement ingredients individually and in combination in the mixture are tabulated in Table 16.4.

**Table 16.4** Fresh properties of SCC.

Concrete mix	Filling ability properties			Passing ability properties		Segregation resistance property	SP (%)
	Slump flow (mm)	V-funnel (Scec)	T50 flow (Scec)	L-box (ratio)	J-ring (mm)	Sieve segregation (%)	
C	685	11.50	4.82	0.84	2.5	8.45	2
FA5	720	10.15	4.45	0.88	4.45	5.20	2
FA10	750	9.88	3.96	0.92	7.30	4.75	2
FA15	786	9.40	3.78	0.86	8.50	7.25	3
FA20	810	8.50	3.40	0.89	6.92	7.45	3
GGBFS5	670	9.89	4.70	0.94	5.60	8.88	2
GGBFS10	655	11.20	4.55	0.96	7.50	9.35	2
GGBFS15	638	9.22	4.20	0.84	5.80	9.78	3
GGBFS20	625	10.12	3.95	0.95	8.20	10.15	3
FA2.5GGBFS2.5	710	9.95	4.60	0.86	4.50	8.60	2
FA5GGBFS5	725	11	4.12	0.90	7.35	8.76	2
FA7.5GGBFS7.50	740	10.50	3.70	0.85	6.70	9.30	3
FA10GGBFS10	765	9.15	3.33	0.90	7.10	9.50	3

### 16.5.1.1 Slump flow

This test was performed on the fresh properties of SCC mixture, including different percentages of FA and GGBFS individually and in combination in the mixture as shown in [Table 16.4](#). However, the suitable value for slump flow of SCC mixture is suggested by 650–850 mm ([EFNARC, 2005](#)). Besides the slump flow of SCC mixture without addition of a superplasticizer and inclusion 1% of superplasticizer is less than recommended values. Therefore the use of the superplasticizer is increased from 2% to 3% in the control mixture of SCC to achieve slump flow within the suggested range. The slump flow recorded with 5.11%, 9.48%, 14.75%, and 18.25% while using 5%, 10%, 15%, and 20% of FA is greater than that of SCC mixture without addition of FA by the mass of PC. It was revealed that the slump flow was increased as the extent of FA rises in the mixture of SCC. This increment in slump flow is due to the spherical shape particles of FA, which increases the slump flow. A similar trend was observed by [Dhiyaneshwaran et al. \(2013\)](#). Moreover the slump flow acquired by 2.20%, 4.37%, 6.86%, and 8.76% at 5%, 10%, 15%, and 20% of GGBFS is lower than that of the control mixture of SCC. It was noted that the slump flow is reduced while utilizing GGBFA and rises in the mixture of SCC. The reduction in slump flow is due to GGBFS's more specific surface area as compared to PC. This statement is associated to [Güneyisi & Gesoğlu \(2008\)](#). Furthermore the combined use of FA and GGBFS in the mixture of SCC is inclined in the slump flow of SCC mixture with addition of a superplasticizer.

However, the use of a superplasticizer in the SCC mixture improves the flowability by plummeting plastic viscosity and yielding stress. In addition the optimum slump flow can be obtained by dissolving action of the superplasticizer in the mixture, which results in a decrease in the water demand with entrapment among flocculated particles.

### 16.5.1.2 V-funnel

This test was performed on the fresh properties of SCC mixture, including different percentages of FA and GGBFS individually and in combination in the mixture, as shown in [Table 16.4](#). However, the suitable value for V-funnel of SCC mixture is proposed by 6–12 seconds ([EFNARC, 2005](#)). Besides the V-funnel of SCC mixture without addition of a superplasticizer and inclusion 1% of superplasticizer is less than recommended values. Therefore the use of a superplasticizer is increased from 2% to 3% in the control mixture of SCC to achieve a V-funnel within the recommended range. It was revealed that the V-funnel time was decreased as the extent of FA rises in the mixture of SCC. The outcomes of this study directed that all mixtures of SCC meet the needs of an acceptable flow time and had good filling ability and segregation resistance. It was noted that 20% of FA by the weight of PC displays superior performance as compared to other proportions of SCC mixture. This statement was linked with that of [Mushtaq & Nasier \(2018\)](#), that is, the V-funnel time of SCC mixture was reduced as the extent of FA rises in the mixture of SCC. A similar trend was observed by [Dhiyaneshwaran et al. \(2013\)](#). Moreover the V-funnel recorded with 14%, 2.61%, 19.82%, and 12% at 5%, 10%, 15%, and 20% of GGBFS is less than that of the control mixture of SCC with addition of GGBFS by the mass of PC. It was worth noting that the V-funnel is reduced while utilizing GGBFA and rises in the mixture of SCC. This finding is related to other research investigations ([Güneyisi & Gesoğlu, 2008](#); [Hassan et al., 2010](#)). Furthermore the optimum V-funnel time was noted by 11.50 seconds at control mix of SCC, and the minimum flow time was measured by 9.15 seconds at 10% of FA combined with 10% of GGBFS as a cementitious material in the mixture of SCC. It was detected that the V-funnel time was reduced while using GGBFS and FA in the mixture of SCC. The outcomes of this study directed that all mixtures of SCC meet the needs of an acceptable flow time and have good filling ability and segregation resistance. It was noted that 10% of FA combined with 10% of GGBFS by the weight of PC displays superior performance as compared to other proportions of SCC mixture.

### 16.5.1.3 T50 flow

This test was performed on the fresh properties of SCC mixture, including different percentages of FA and GGBFS individually and in combination in the mixture as shown in [Table 16.4](#). However, a suitable value for T50 of SCC mixture is proposed by 2–5 seconds ([EFNARC, 2005](#)). [Table 16.4](#) indicates that the T50 flow

time was estimated in the range of 4.82–3.40 seconds. The maximum outcomes of T50 flow were recorded by 4.82 seconds while consuming 0% of FA, and the smallest T50 flow time was measured by 3.40 seconds at 20% of FA by the weight of PC in the mixture of SCC. It was observed that the dosages of FA increase in the mixture of SCC, which results in reducing the T50 flow time. From the outcome, it was clear that the T50 flow time of SCC displays the best performance while using 20% of FA in the SCC mixture. This observation was associated with [Dhiyaneshwaran et al. \(2013\)](#), where the T50 flow time was decreased with augmentation in the level of FA in the mixture of SCC. Moreover the ultimate outcomes of T50 flow were recorded by 4.82 seconds while consuming 0% of GGBFS, and the smallest T50 flow time was measured by 3.95 seconds at 20% of GGBFS by the weight of PC in the mixture of SCC. It was observed that the dosages of GGBFS increase in the mixture of SCC, which results in a reduction of the T50 flow time. From the outcome, it was clear that the T50 flow time of SCC displays the best performance while using 20% of GGBFS in the SCC mixture. This observation was associated with [Güneyisi et al., 2009](#), where the T50 flow time was decreased with augmentation in the level of metakaolin in the mixture of SCC. Furthermore the optimum T50 flow time was noted by 4.82 seconds at control mix of SCC, and the minimum T50 flow time was measured by 3.33 seconds at 10% of FA combined with 10% of GGBFS as a cementitious material in the mixture of SCC. It was detected that the T50 flow time was reduced while using GGBFS and FA in the mixture of SCC. In addition, from the outcome, it was clear that the T50 flow time of SCC displays the best performance while using 10% of FA along with 10% of GGBFS in the SCC mixture.

#### 16.5.1.4 Blocking ratio (L-box test)

This test was performed on the fresh properties of SCC mixture, including different percentages of FA and GGBFS individually and in combination in the mixture, as shown in [Table 16.4](#). However, L-box test is utilized to evaluate the flow of SCC concrete and the level by which it is subject to blocking by reinforcement. Besides, it is suggested that suitable values for blocking ratio of SCC mixture are in the range of 0.80 to 1.0 ([EFNARC, 2005](#)). Moreover the blocking ratio of SCC mixture without addition of a superplasticizer and inclusion 1% of superplasticizer is less than recommended values. Therefore the use of a superplasticizer is increased from 2% to 3% in the control mixture of SCC to achieve a blocking ratio within the suggested range. The outcomes of this study revealed that the blocking ratio of SCC mixture is reduced while consuming the FA in the mixture. It was noted that the L-box ratio for all mixtures of SCC is greater than 0.80 as per EFNARC standard. Hence it was concluded that the passing ability of SCC mixture is enhanced with improvement in the dosages of FA as a cementitious material. This aspect was linked with that of [Mushtaq and Nasier \(2018\)](#), that is, the blocking ratio of SCC mixture is inclined as the extent of FA rises in the mixture of SCC. A similar trend was observed by [Dhiyaneshwaran et al. \(2013\)](#). Moreover the outcomes of this study revealed that the blocking

ratio of SCC mixture is reduced while consuming the GGBFS in the mixture. This reduction in L-box ratio is due to GGBFS's more specific surface area than PC. This observation is correlated to [Güneyisi & Gesoğlu \(2008\)](#). It was seen from obtained results in [Table 16.4](#) that the L-box ratio for all mixtures of SCC blended with various proportions of GGBFS as a cement replacement material in the mixture of SCC is more than 0.80, which is suggested by EFNARC standard. Furthermore the results of SCC mixture blended with GGBFS and FA together show that the L-box ratio is reduced while utilizing GGBFS and FA together in the mixture of SCC. It was revealed that the blocking ratio for all mixtures of SCC with various percentages of FA and GGBFS by the weight of PC is greater than 0.80 as per EFNARC standard. Hence it was concluded that the passing ability of SCC mixture is enhanced with improvement in the dosages of FA and GGBFS as a cementitious material.

#### 16.5.1.5 *J-ring*

This test was performed on the fresh properties of SCC mixture, including different percentages of FA and GGBFS individually and in combination in the mixture, as shown in [Table 16.4](#). However, J-ring test is utilized to evaluate the flow of SCC mixture, and the range of 0–10 mm is suggested ([EFNARC, 2005](#)). Moreover the value from J-ring test of SCC mixture without addition of a superplasticizer and inclusion 1% of superplasticizer is less than recommended values. Therefore the use of a superplasticizer is increased from 2% to 3% in the control mixture of SCC to achieve the J-ring of SCC mixture within the recommended range. The outcomes of this study revealed that the J-ring test of SCC mixture is dropped while consuming the FA in the mixture as compared to the control mixture of SCC. This reduction in J-ring is owing to reduction in cohesiveness and the lack in paste volume of FA as compared to PC. A similar investigation was observed by other researchers ([Aswathy & Paul, 2015](#)). Moreover the outcomes of this study revealed that the J-ring test of SCC mixture is plummeted while consuming the GGBFS in the mixture as compared to the control mixture of SCC. This reduction in J-ring is owing to GGBFS's more specific surface area than PC. This study is related to a similar study by [Güneyisi & Gesoğlu, 2008](#). Furthermore the J-ring of SCC mixture is reduced while using GGBFS and FA as a cementitious material in the mixture. It was observed that the J-ring of SCC mixture blended with FA along with GGBFS in the mixture with inclusion of 2% to 3% of superplasticizer has been observed within the required range ([EFNARC, 2005](#)).

#### 16.5.1.6 *Sieve segregation*

This test was performed on the fresh properties of SCC mixture, including different percentages of FA and GGBFS individually and in combination in the mixture, as shown in [Table 16.4](#). However, sieve segregation is utilized to evaluate the flow of SCC concrete, and suitable values for sieve segregation of

SCC mixture are suggested to be in the range of 0% to 12% (EFNARC, 2005). Moreover the sieve segregation of SCC mixture with addition 2% to 3% of superplasticizer in the control mixture of SCC is performed to achieve sieve segregation of SCC mixture within the proposed range. The outcomes of this study revealed that the sieve segregation of SCC mixture is reduced while consuming the FA in the mixture. This reduction in sieve segregation of SCC mixture is reduced due to porosity of FA as a cementitious material. This trend has been observed by other researchers (Aswathy & Paul, 2015). Moreover the sieve segregation of SCC mixture is increased while using GGBFS in the mixture. This improvement in sieve segregation of SCC mixture is due to GGBFS's more specific surface area as compared to PC. A similar study was observed by Güneysi and Gesoğlu (2008), where the sieve segregation of SCC mixture is enhanced but increases to the extent of metakaolin in the mixture. Furthermore the sieve segregation of SCC mixture is improved with the growth in the dosages of GGBFS along with FA as a cementitious material. The conclusion of this study was that the sieve segregation of SCC mixture blended with 10% of GGBFS along with 10% of FA displays a satisfactory performance of fresh properties of SCC mixture associated to more segregation resistance, deformability, passing, and filling capabilities by using 2% and 3% of superplasticizer in the mixture.

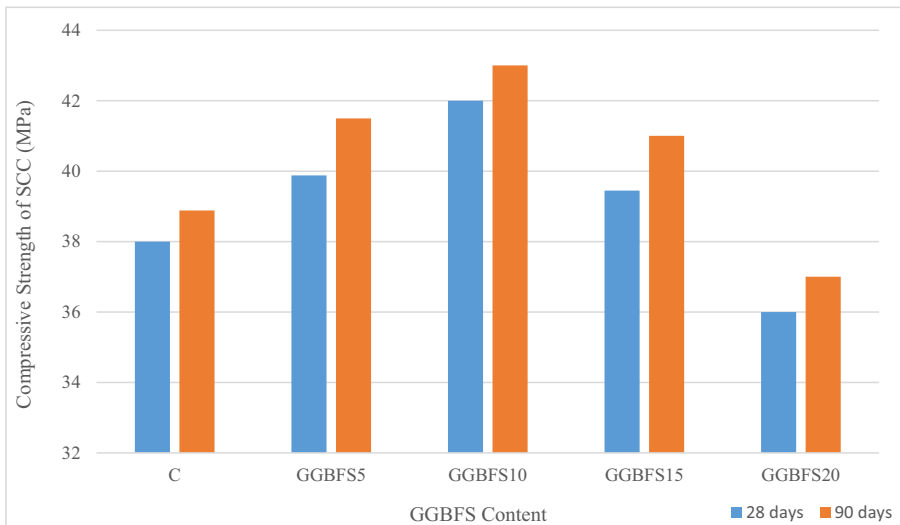
## 16.6 Hardened concrete results

The hardened properties of SCC mixture in terms of compressive, tensile, and flexural strengths and water penetration depth were performed on hardened concrete for all SCC mixes.

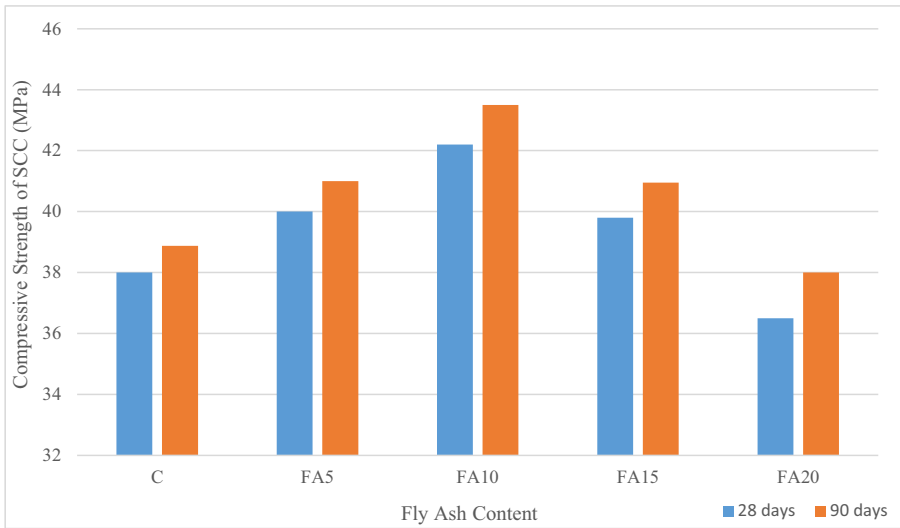
### 16.6.1 Compressive strength of self-compacting concrete mixture

Fig. 16.1 indicates compressive strength of SCC mixture blended with GGBFS by the weight of PC in the mixture after 28 and 90 days. The ultimate compressive strength of SCC mixture was observed to be 42 and 43 MPa at 10% of GGBFS, and the lowest strength was noted to be 36 and 37 MPa at 20% of GGBFS by the weight of PC in the mixture at 28 and 90 days, respectively. The results of this work indicated that the compressive strength of SCC mixture is improved while using GGBFS up to 15% and then it gets reduced. The increase in compressive strength is due to the filling influence, dilution effect, and pozzolanic response of GGBFS with CH (Khatib & Hibbert, 2005; Said-Mansour et al., 2011; Wild et al., 1996). This study is similar to Parande et al., 2008, where the compressive strength of SCC was found to be minimum while utilizing MK more than 15% in the mixture. Similarly, Fig. 16.2 indicates the compressive strength of SCC mixture blended with FA by the weight of PC in the

mixture at 28 and 90 days, respectively. The results of maximum compressive strength of SCC mixture blended with 10% of FA as a cementitious material are recorded as 42.20 and 43.50 MPa, and the minimum strength of SCC mixture with addition of 20% FA as replacement for PC is noted as 36.50 and 38 MPa at 28 and 90 days, respectively. It was perceived that the use of FA in the mixture of SCC is increased up to 15%, which provides maximum compressive strength of SCC mixture, and with further inclusion of FA in the mixture, it starts reducing. This growth in the compressive strength of SCC mixture may be due to the influence of the active pozzolanic reaction of FA, and the silica content in FA particles enhances the development of C-S-H, which is accountable for improving the strength (Guru Jawahar et al., 2013; Wild et al., 1996). This aspect was correlated to different researchers (Mermerdaş et al., 2012; Poon et al., 2006). Moreover, Fig. 16.3 indicates compressive strength of SCC mixture blended with GGBFS and FA by the weight of PC together in the mixture after 28 and 90 days. The supreme amount of compressive strength of SCC mixture with addition of 10% (5% FA and 5% GGBFS) FA and GGBFS by the mass of PC is noted as 43.35 and 44.65 MPa, and the lowest amount of compressive strength of SCC mixture blended with 20% (10% of FA and 10% of GGBFS) of FA and GGBFS in the mixture is estimated as 40 and 41 MPa at 28 and 90 days, respectively. The outcome of this work showed that the combined use of FA and GGBFS as replacement for PC up to 15% (7.50% of FA and 7.50% of GGBFS) of FA and GGBFS in the mixture achieved the highest compressive strength of SCC mixture, and with further addition of GGBFS and FA the compressive strength gets reduced.



**Figure 16.1** Compressive strength of SCC mixture blended with GGBFS.



**Figure 16.2** Compressive strength of SCC mixture blended with fly ash.

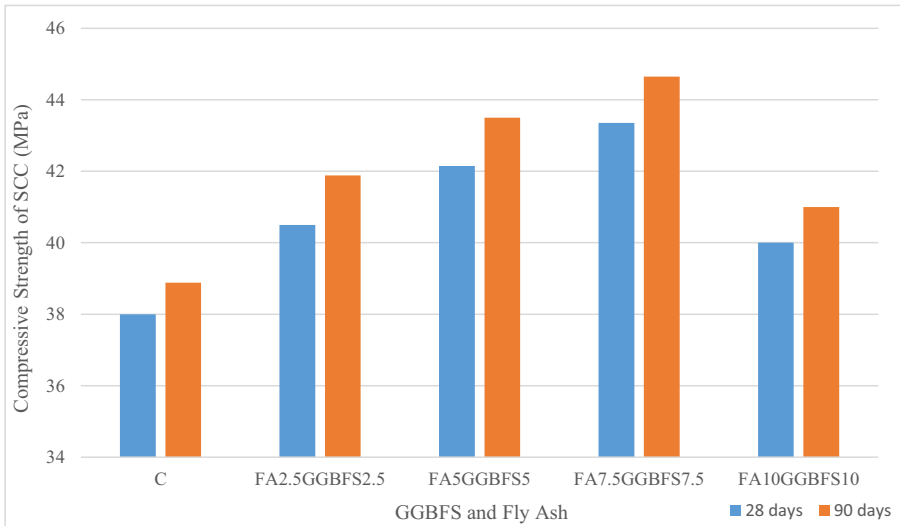


**Figure 16.3** Compressive strength of SCC mixture blended with GGBFS and fly ash.

### 16.6.2 Splitting tensile strength of self-compacting concrete mixture

Fig. 16.4 indicates split tensile strength of SCC mixture blended with GGBFS by the weight of PC in the mixture after 28 and 90 days. The ultimate split tensile strength of SCC mixture was observed as 4 and 4.20 MPa at 10% of GGBFS, and the lowest



strength was noted as 3.36 and 3.55 MPa at 20% of GGBFS by the weight of PC in the mixture at 28 and 90 days, respectively. The results of this work indicated that the split tensile strength of SCC mixture is improved while using GGBFS up to 15% and then it gets reduced. This observation is related to [Madandoust and Mousavi \(2012\)](#). Similarly, [Fig. 16.5](#) indicates the split tensile strength of SCC mixture blended with FA by the weight of PC in the mixture at 28 and 90 days, respectively. The results of maximum split tensile strength of SCC mixture blended with 10% of FA as a cementitious material are recorded as 4.05 and 4.25 MPa, and the minimum strength of SCC mixture with addition of 20% FA as replacement for PC is noted as 3.45 and 3.60 MPa at 28 and 90 days, respectively. It was perceived that the use of FA in the mixture of SCC is increased up to 15%, which provides maximum split tensile strength of SCC mixture, and with further inclusion of FA in the mixture, it starts reducing. This aspect was correlated to that of [Billong et al. \(2011\)](#). Moreover, [Fig. 16.6](#) indicates split tensile strength of SCC mixture blended with GGBFS and FA by the weight of PC together in the mixture after 28 and 90 days. The supreme amount of split tensile strength of SCC mixture with addition of 10% (5% FA and 5% GGBFS) FA and GGBFS by the mass of PC is noted as 4.04 and 4.22 MPa, and the lowest amount of split tensile strength of SCC mixture blended with 20% (10% of FA and 10% of GGBFS) of FA and GGBFS in the mixture is estimated as 3.40 and 3.58 MPa at 28 and 90 days, respectively. The outcome of this work showed that the combined use of FA and GGBFS as replacement for PC up to 15% (7.50% of FA and 7.50% of GGBFS) of FA and GGBFS in the mixture achieved the highest split tensile strength of SCC mixture, and with further addition of GGBFS and FA the compressive strength gets reduced. This increase in the split tensile strength of SCC mixture is due to the fact that the specific surface area of FA and GGBFS is more than that of PC.

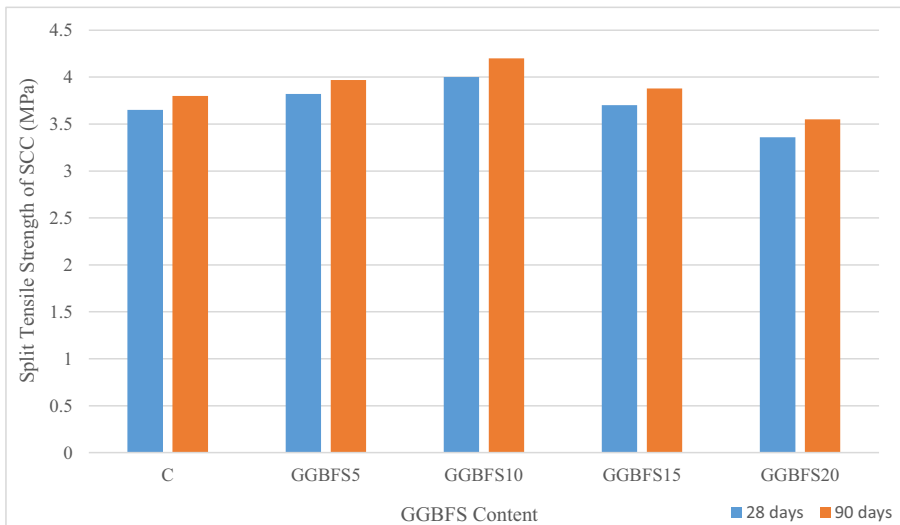


**Figure 16.4** Split tensile strength of SCC mixture blended with GGBFS.

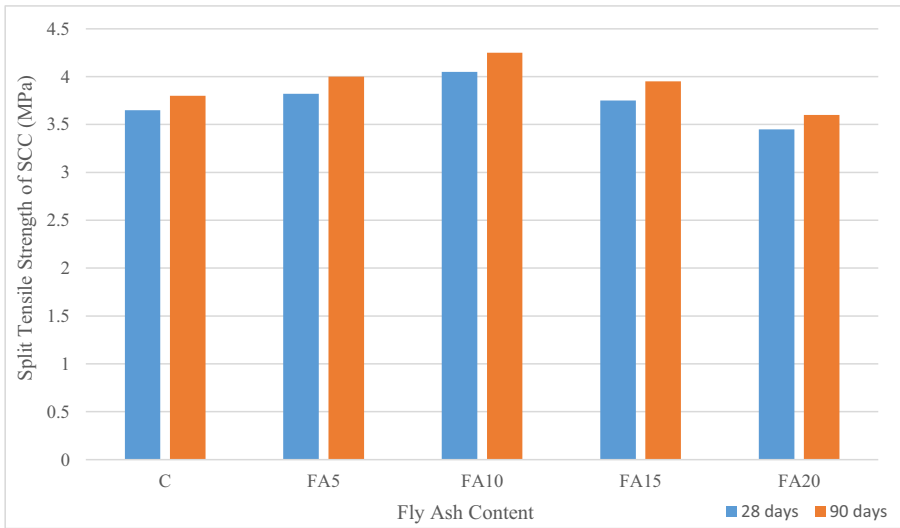


**Figure 16.5** Split tensile strength of SCC mixture blended with fly ash.

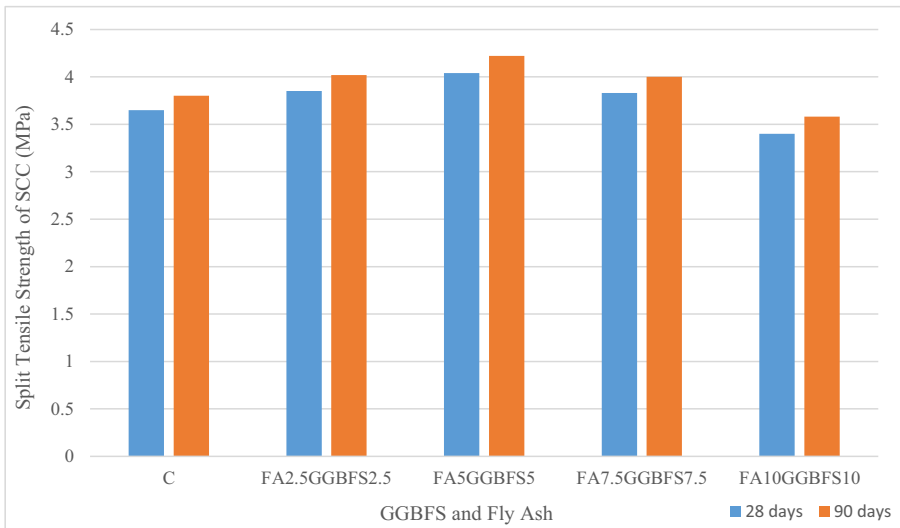


**Figure 16.6** Split tensile strength of SCC mixture blended with GGBFS and fly ash.

### 16.6.3 Flexural strength of self-compacting concrete mixture

Fig. 16.7 indicates flexural strength of SCC mixture blended with GGBFS by the weight of PC in the mixture after 28 and 90 days. The ultimate flexural strength of SCC mixture was observed as 6.22 and 6.32 MPa at 10% of GGBFS, and the lowest strength was noted as 5.40 and 5.62 MPa at 20% of GGBFS by the weight of PC in the mixture at 28 and 90 days, respectively. The results of this work indicated that the flexural strength of SCC mixture is improved while using GGBFS up to 15% and then it gets reduced. This observation is related to Bheel et al. (2020). Similarly, Fig. 16.8 indicates the flexural strength of SCC mixture blended with FA by the weight of PC in the mixture at 28 and 90 days, respectively. The results of maximum flexural strength of SCC mixture blended with 10% of FA as a cementitious material are recorded as 6.25 and 6.36 MPa, and the minimum strength of SCC mixture with addition of 20% FA as replacement for PC is noted as 5.50 and 5.70 MPa at 28 and 90 days, respectively. It was perceived that the use of FA in the mixture of SCC is increased up to 15%, which provides maximum flexural strength of SCC mixture, and with further inclusion of FA in the mixture, it starts reducing. Moreover, Fig. 16.9 indicates flexural strength of SCC mixture blended with GGBFS and FA by the weight of PC together in the mixture after 28 and 90 days. The supreme amount of flexural strength of SCC mixture with addition of 10% (5% FA and 5% GGBFS) FA and GGBFS by the mass of PC is noted as 6.30 and 6.40 MPa, and the lowest amount of flexural strength of SCC mixture blended with 20% (10% of FA and 10% of GGBFS) of FA and GGBFS in the mixture is estimated as 5.42 and 5.66 MPa at 28 and 90 days, respectively. The outcome of this work showed that the combined use of FA and GGBFS as replacement for PC up to 15% (7.50% of FA and 7.50% of GGBFS) of FA and GGBFS in the mixture achieved the highest flexural strength of SCC mixture, and with further addition of GGBFS and FA the flexural strength gets reduced.

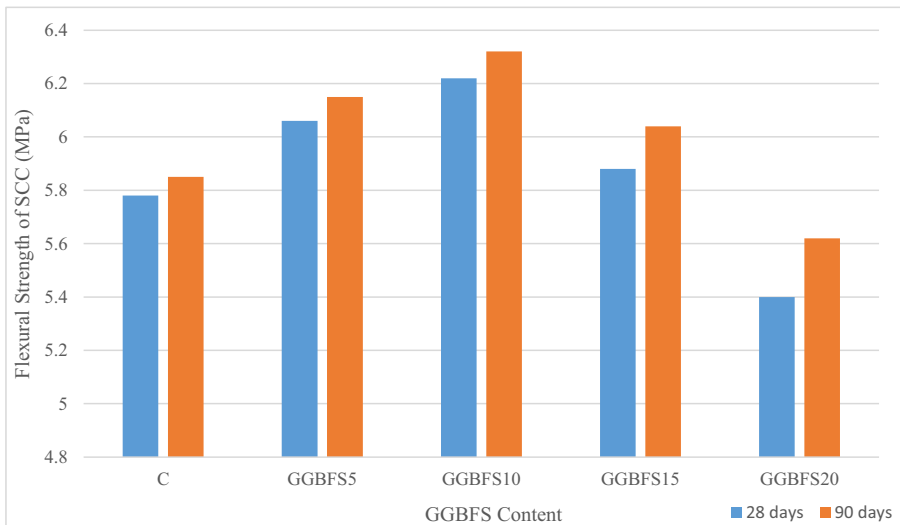


**Figure 16.7** Flexural strength of SCC mixture blended with GGBFS.

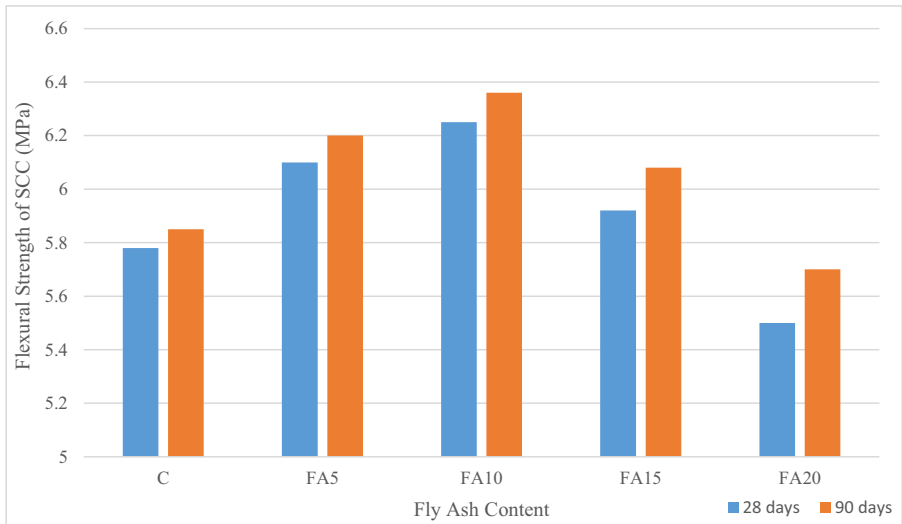


**Figure 16.8** Flexural strength of SCC mixture blended fly ash.

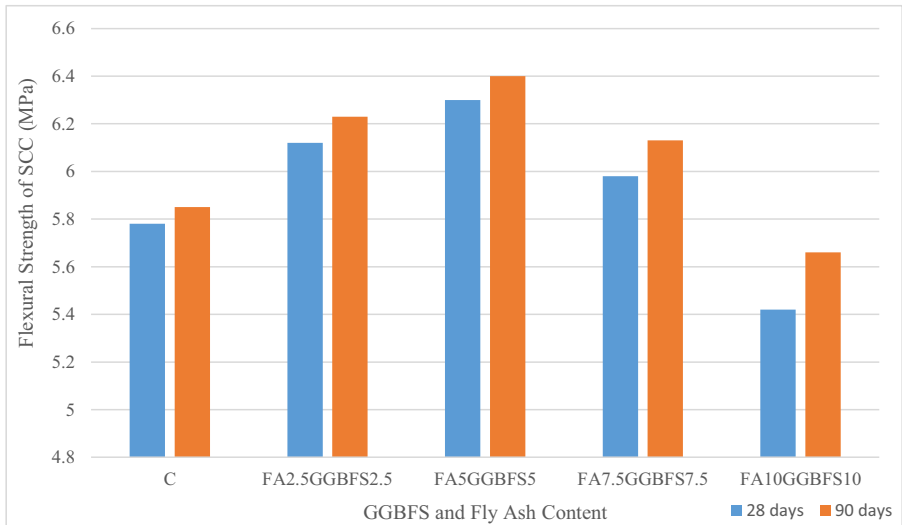
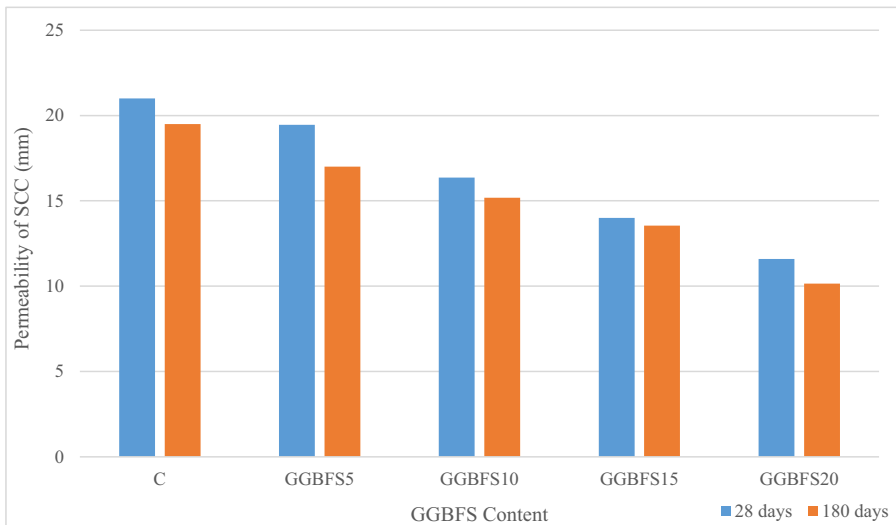


**Figure 16.9** Flexural strength of SCC mixture blended with GGBFS and FA.

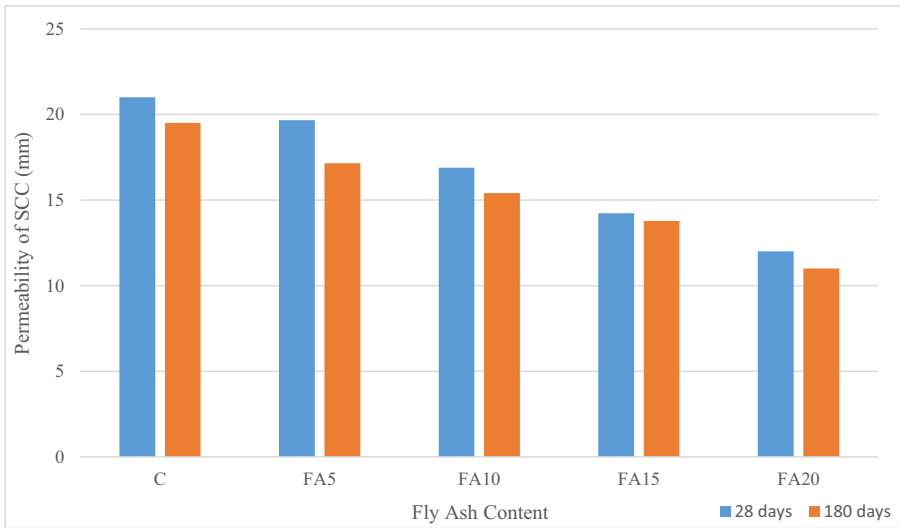
#### 16.6.4 Water penetration depth of self-compacting concrete mixture

Fig. 16.10 indicates the water penetration depth of SCC mixture blended with GGBFS by the weight of PC in the mixture after 28 and 180 days. The ultimate permeability of SCC mixture was observed by 21 and 19.50 mm at 0% of GGBFS, and the lowest permeability of SCC mixture was noted as 11.60 and 10.15 mm at 20% of GGBFS by the

weight of PC in the mixture at 28 and 180 days, respectively. The results of this work indicated that the permeability of SCC mixture is reduced while growing the GGBFS content in the mixture. This observation is related to [Marto et al. \(2011\)](#). Similarly, [Fig. 16.11](#) indicates the permeability of SCC mixture blended with FA by the weight of PC in the mixture at 28 and 180 days, respectively. The results of maximum permeability of SCC mixture blended with 0% of FA as a cementitious material are recorded as 21 and 19.50 mm, and the minimum permeability of SCC mixture with addition of 20% FA as replacement for PC is noted as 12 and 11 mm at 28 and 180 days, respectively. It was perceived that the use of FA in the mixture of SCC is increased, which results in reducing the permeability of SCC mixture. Almost the same behavior in terms of water penetration has been reported by different researchers ([Kasemchaisiri & Tangtermsirikul, 2008](#); [Khatri et al., 1997](#)). This aspect was correlated by [Güneyisi et al. \(2009\)](#), where the permeability was reduced by 29% at 15% of MK as a cementitious constituent as compared to plain concrete. Moreover, [Fig. 16.12](#) indicates the permeability of SCC mixture blended with GGBFS and FA by the weight of PC together in the mixture after 28 and 180 days. The supreme amount of water penetration depth of SCC mixture with addition of 0% (0% FA and 0% GGBFS) FA and GGBFS by the mass of PC is noted as 21 and 19.50 mm, and the lowest amount of permeability of SCC mixture blended with 20% (10% of FA and 10% of GGBFS) of FA and GGBFS in the mixture is estimated as 10.55 and 10 mm at 28 and 180 days, respectively. The outcome of this work showed that the combined use of FA and GGBFS as replacement for PC increased to provide reduction in the permeability of SCC mixture. The permeability is an essential parameter of concrete durability. It was shown that less permeability of SCC mixture displays high resistance against chemical attacks and also improves the durability of concrete mixture ([Ramezaniapur et al., 2011](#); [Wesche et al., 1989](#)).



**Figure 16.10** Permeability of SCC mixture blended with GGBFS.



**Figure 16.11** Permeability of SCC mixture blended with fly ash.

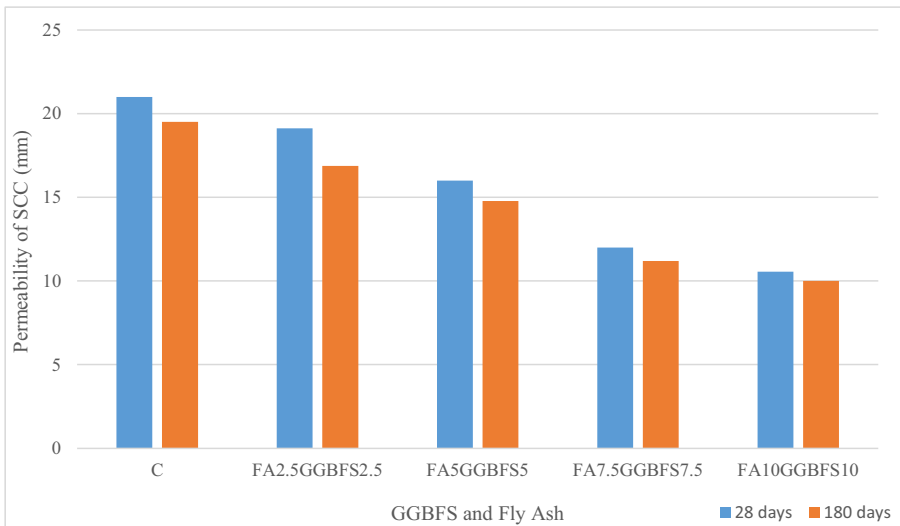


**Figure 16.12** Permeability of SCC mixture blended with GGBFS and fly ash.

## 16.7 Conclusion

It was concluded from the conducted research that

- The slump flow recorded as 5.11%, 9.48%, 14.75%, and 18.25% while using 5%, 10%, 15%, and 20% of FA is greater than that of SCC mixture without addition of FA by the mass of PC. Similarly the slump flow acquired by 2.20%, 4.37%, 6.86%, and 8.76% at

5%, 10%, 15%, and 20% of GGBFS is lower than that of the control mixture of SCC. Moreover the combined use of FA and GGBFS in the mixture of SCC is inclined in the slump flow of SCC mixture with addition of a superplasticizer. However, the use of a superplasticizer in the SCC mixture improves the flowability by plummeting plastic viscosity and yielding stress.

- The V-funnel time was decreased as the extent of FA rises in the mixture of SCC. Similarly the V-funnel recorded as 14%, 2.61%, 19.82%, and 12% at 5%, 10%, 15%, and 20% of GGBFS is less than that of the control mixture of SCC with addition of GGBFS by the mass of PC. Moreover the optimum V-funnel time was noted as 11.50 seconds at the control mix of SCC, and the minimum flow time was measured as 9.15 seconds at 10% of FA combined with 10% of GGBFS as a cementitious material in the mixture of SCC. It was detected that the V-funnel time was reduced while using GGBFS and FA in the mixture of SCC. It was noted that 10% of FA combined with 10% of GGBFS by the weight of PC displays superior performance as compared to other proportions of SCC mixture.
- The maximum outcomes of T50 flow were recorded by 4.82 seconds while consuming 0% of FA, and the smallest T50 flow time was measured by 3.40 seconds at 20% of FA by the weight of PC in the mixture of SCC. Similarly the ultimate outcomes of T50 flow were recorded by 4.82 seconds while consuming 0% of GGBFS, and the smallest T50 flow time was measured by 3.95 seconds at 20% of GGBFS by the weight of PC in the mixture of SCC. Moreover the optimum T50 flow time was noted by 4.82 seconds at the control mix of SCC, and the minimum T50 flow time was measured by 3.33 seconds at 10% of FA combined with 10% of GGBFS as a cementitious material in the mixture of SCC. It was detected that the T50 flow time was reduced while using GGBFS and FA in the mixture of SCC. In addition, from the outcome, it was clear that the T50 flow time of SCC acquired the best performance while using 10% of FA along with 10% of GGBFS in the SCC mixture.
- The outcome of this study revealed that the blocking ratio of SCC mixture is reduced while consuming the FA in the mixture. Similarly the outcome of this study revealed that the blocking ratio of SCC mixture is reduced while consuming the GGBFS in the mixture. This reduction in L-box ratio is due to GGBFS's more specific surface area than PC. Moreover the results of SCC mixture blended with GGBFS and FA together showed that the L-box ratio is reduced while utilizing GGBFS and FA together in the mixture of SCC. It was revealed that the blocking ratio for all mixtures of SCC with various percentages of FA and GGBFS by the weight of PC is greater than 0.80 as per EFNARC standard.
- The outcome of this study revealed that the J-ring test of SCC mixture is dropped while consuming the FA in the mixture as compared to the control mixture of SCC. This reduction in J-ring owing to reduction in cohesiveness and the lack in paste volume of FA as compared to PC. Similarly the outcome of this study revealed that the J-ring test of SCC mixture is plummeted while consuming the GGBFS in the mixture as compared to the control mixture of SCC. Moreover the J-ring of SCC mixture is reduced while using GGBFS and FA as a cementitious material in the mixture. It was observed that the J-ring of SCC mixture blended with FA along with GGBFS in the mixture with inclusion of 2% to 3% of superplasticizer has been observed within the required range of EFNARC.
- The outcome of this study revealed that the sieve segregation of SCC mixture is reduced while consuming the FA in the mixture. Similarly the sieve segregation of SCC mixture is increased while using GGBFS in the mixture. Moreover the sieve segregation of SCC mixture is improved with the growth in the dosages of GGBFS along with FA as a cementitious material. The conclusion of this study is that the sieve segregation of SCC mixture blended with

10% of GGBFS along with 10% of FA provides a satisfactory performance of fresh properties of SCC mixture associated to more segregation resistance, deformability, passing, and filling capabilities by using 2% and 3% of superplasticizer in the mixture.

- The ultimate compressive strength of SCC mixture was observed as 42 and 43 MPa at 10% of GGBFS and the lowest strength was noted as 36 and 37 MPa at 20% of GGBFS by the weight of PC in the mixture at 28 and 90 days, respectively. Similarly the results of maximum compressive strength of SCC mixture blended with 10% of FA as a cementitious material are recorded as 42.20 and 43.50 MPa, and the minimum strength of SCC mixture with addition of 20% FA as replacement for PC is noted as 36.50 and 38 MPa at 28 and 90 days, respectively. Moreover the supreme amount of compressive strength of SCC mixture with addition of 10% (5% FA and 5% GGBFS) FA and GGBFS by the mass of PC is noted as 43.35 and 44.65 MPa and the lowest amount of compressive strength of SCC mixture blended with 20% (10% of FA and 10% of GGBFS) of FA and GGBFS in the mixture is estimated as 40 and 41 MPa at 28 and 90 days, respectively.
- The ultimate split tensile strength of SCC mixture was observed as 4 and 4.20 MPa at 10% of GGBFS and the lowest strength was noted as 3.36 and 3.55 MPa at 20% of GGBFS by the weight of PC in the mixture at 28 and 90 days, respectively. Similarly the results of maximum split tensile strength of SCC mixture blended with 10% of FA as a cementitious material are recorded as 4.05 and 4.25 MPa and the minimum strength of SCC mixture with addition of 20% FA as replacement for PC is noted as 3.45 and 3.60 MPa at 28 and 90 days, respectively. Moreover the supreme amount of split tensile strength of SCC mixture with addition of 10% (5% FA and 5% GGBFS) FA and GGBFS by the mass of PC is noted as 4.04 and 4.22 MPa, and the lowest amount of split tensile strength of SCC mixture blended with 20% (10% of FA and 10% of GGBFS) of FA and GGBFS in the mixture is estimated by 3.40 and 3.58 MPa at 28 and 90 days, respectively.
- The ultimate flexural strength of SCC mixture was observed as 6.22 and 6.32 MPa at 10% of GGBFS and the lowest strength was noted as 5.40 and 5.62 MPa at 20% of GGBFS by the weight of PC in the mixture at 28 and 90 days, respectively. Similarly the results of maximum flexural strength of SCC mixture blended with 10% of FA as a cementitious material are recorded as 6.25 and 6.36 MPa and the minimum strength of SCC mixture with addition of 20% FA as replacement for PC is noted as 5.50 and 5.70 MPa at 28 and 90 days, respectively. Moreover the supreme amount of flexural strength of SCC mixture with addition of 10% (5% FA and 5% GGBFS) FA and GGBFS by the mass of PC is noted as 6.30 and 6.40 MPa, and the lowest amount of flexural strength of SCC mixture blended with 20% (10% of FA and 10% of GGBFS) of FA and GGBFS in the mixture is estimated as 5.42 and 5.66 MPa at 28 and 90 days, respectively.
- The ultimate permeability of SCC mixture was observed as 21 and 19.50 mm at 0% of GGBFS and the lowest permeability of SCC mixture was noted as 11.60 and 10.15 mm at 20% of GGBFS by the weight of PC in the mixture at 28 and 180 days, respectively. Similarly the results of maximum permeability of SCC mixture blended with 0% of FA as a cementitious material are recorded as 21 and 19.50 mm and the minimum permeability of SCC mixture with addition of 20% FA as replacement for PC is noted as 12 and 11 mm at 28 and 180 days, respectively. Moreover the supreme amount of water penetration depth of SCC mixture with addition of 0% (0% FA and 0% GGBFS) FA and GGBFS by the mass of PC is noted as 21 and 19.50 mm and the lowest amount of permeability of SCC mixture blended with 20% (10% of FA and 10% of GGBFS) of FA and GGBFS in the mixture is estimated as 10.55 and 10 mm at 28 and 180 days, respectively.
- Based on these conducted research studies the combined use of FA and GGBFS up to 10% is optimum for structural applications.



## References

- Ahmaruzzaman, M. (2010). A review on the utilization of fly ash. *Progress in Energy and Combustion Science*, 36(3), 327–363. Available from <https://doi.org/10.1016/j.pecs.2009.11.003>.
- Ahmed, M. F., Nuruddin, M. F., & Shafiq, N. (2011). Compressive strength and workability characteristics of low-calcium fly ash-based self-compacting geopolymer concrete. *International Journal of Civil and Environmental Engineering*, 5(2), 64–70.
- Anjali, D., Vivek, S. S., & Dhinakaran, G. (2015). Compressive strength of metakaolin based self-compacting concrete. *International Journal of ChemTech Research*, 8(2), 622–625. Available from [http://sphinxesai.com/2015/ch\\_vol8\\_no2/3/\(622-625\)V8N2.pdf](http://sphinxesai.com/2015/ch_vol8_no2/3/(622-625)V8N2.pdf).
- Ariffin, M. A. M., Bhutta, M. A. R., Hussin, M. W., Mohd Tahir, M., & Aziah, N. (2013). Sulfuric acid resistance of blended ash geopolymer concrete. *Construction and Building Materials*, 43, 80–86. Available from <https://doi.org/10.1016/j.conbuildmat.2013.01.018>.
- ASTM C1611/C1611M-18 (2018). Standard test method for slump flow of self-consolidating concrete.
- Aswathy, P. U., & Paul, M. M. (2015). Behaviour of self compacting concrete by partial replacement of fine aggregate with coal bottom ash. *Behaviour*, 2(10), 45–52.
- Bheel, N., Abbasi, S. A., Awoyera, P., Olalusi, O. B., Sohu, S., Rondon, C., & Echeverría, A. M. (2020). Fresh and hardened properties of concrete incorporating binary blend of metakaolin and ground granulated blast furnace slag as supplementary cementitious material. *Advances in Civil Engineering*, 2020, 1–8. Available from <https://doi.org/10.1155/2020/8851030>.
- Billong, N., Melo, U. C., Kamseu, E., Kinuthia, J. M., & Njopwouo, D. (2011). Improving hydraulic properties of lime-rice husk ash (RHA) binders with metakaolin (MK). *Construction and Building Materials*, 25(4), 2157–2161. Available from <https://doi.org/10.1016/j.conbuildmat.2010.11.013>.
- Correa-Yepes, J. A., Rojas-Reyes, N. R., & Tobón, J. I. (2018). Effect of fly ash and silica fume on rheology, compressive strength and self-compacting in cement mixtures. *DYNA*, 85(206), 59–68. Available from <https://doi.org/10.15446/dyna.v85n206.68960>.
- Dhiyaneshwaran, S., Ramanathan, P., Baskar, I., & Venkatasubramani, R. (2013). Study on durability characteristics of self-compacting concrete with fly ash. *Jordan Journal of Civil Engineering*, 7(3), 342–353. Available from <http://elearning.just.edu.jo/jjce/issues/paper.php?p=2536.pdf>.
- Duxson, P., Provis, J. L., Lukey, G. C., & van Deventer, J. S. J. (2007). The role of inorganic polymer technology in the development of “green concrete. *Cement and Concrete Research*, 37(12), 1590–1597. Available from <https://doi.org/10.1016/j.cemconres.2007.08.018>.
- EFNARC. (2005). *The European guidelines for self-compacting concrete. In Specification production and use.* EFNARC.
- Elchalakani, M., Aly, T., & Abu-Aisheh, E. (2014). Sustainable concrete with high volume GGBFS to build Masdar City in the UAE. *Case Studies in Construction Materials*, 1, 10–24. Available from <https://doi.org/10.1016/j.cscm.2013.11.001>.
- EN, B. (2009a). Testing hardened concrete. *Compressive strength of test specimens* (pp. 12390–12393).
- EN, B. (2009b). Testing hardened concrete. *Tensile splitting strength of test specimens* (pp. 12390–12396).

- EN, B.S. (2009). *Testing hardened concrete—Part 5: Flexural strength of test specimens* (pp. 12390–12395). British Standards Institution-BSI and CEN European Committee for Standardization.
- EN 12350-9: (2010). Testing fresh concrete Part 9: Self-compacting concrete: V-funnel test.
- EN 12350-10: (2010). Testing fresh concrete Part 10: Self-compacting concrete: L box test.
- EN 12350-11:(2010). Testing fresh concrete Part 11: Self compacting concrete: Sieve segregation test. BSI Standards.
- EN 12350-12: (2010). Testing fresh concrete Part 12: Self-compacting concrete: J-ring test.
- Fantilli, A. P., & Chiaia, B. (2013). Eco-mechanical performances of cement-based materials: An application to self-consolidating concrete. *Construction and Building Materials*, 40, 189–196. Available from <https://doi.org/10.1016/j.conbuildmat.2012.09.075>.
- Fernández-Jiménez, A., & Palomo, A. (2005). Composition and microstructure of alkali activated fly ash binder: Effect of the activator. *Cement and Concrete Research*, 35(10), 1984–1992. Available from <https://doi.org/10.1016/j.cemconres.2005.03.003>.
- Grdic, Z., Despotovic, I., & Toplicic-Curcic, G. (2008). Properties of self-compacting concrete with different types of additives. *Facta Universitatis—Series: Architecture and Civil Engineering*, 173–177. Available from <https://doi.org/10.2298/FUACE0802173G>.
- Güneyisi, E., & Gesoğlu, M. (2008). Properties of self-compacting mortars with binary and ternary cementitious blends of fly ash and metakaolin. *Materials and Structures*, 41(9), 1519–1531. Available from <https://doi.org/10.1617/s11527-007-9345-7>.
- Güneyisi, E., Gesoglu, M., & Özbay, E. (2009). Evaluating and forecasting the initial and final setting times of self-compacting concretes containing mineral admixtures by neural network. *Materials and Structures*, 42(4), 469–484. Available from <https://doi.org/10.1617/s11527-008-9395-5>.
- Guru Jawahar, J., Sashidhar, C., Ramana Reddy, I. V. ., & Annie Peter, J. (2013). Micro and macrolevel properties of fly ash blended self compacting concrete. *Materials and Design*, 46, 696–705. Available from <https://doi.org/10.1016/j.matdes.2012.11.027>.
- Hardjito, D., Wallah, S. E., Sumajouw, D. M., & Rangan, B. V. (2004). Factors influencing the compressive strength of fly ash-based geopolymer concrete. *Civil Engineering Dimension*, 6(2), 88–93.
- Hardjito, Djwantoro, Cheak, C. C., & Lee Ing, C. H. (2009). Strength and setting times of low calcium fly ash-based geopolymer mortar. *Modern Applied Science*. Available from <https://doi.org/10.5539/mas.v2n4p3>.
- Hassan, A. A. A., Lachemi, M., & Hossain, K. M. A. (2010). Effect of metakaolin on the rheology of self-consolidating concrete. *RILEM Bookseries*, 1, 103–112. Available from [https://doi.org/10.1007/978-90-481-9664-7\\_9](https://doi.org/10.1007/978-90-481-9664-7_9).
- Hossain, M. U., Poon, C. S., Dong, Y. H., & Xuan, D. (2018). Evaluation of environmental impact distribution methods for supplementary cementitious materials. *Renewable and Sustainable Energy Reviews*, 82, 597–608. Available from <https://doi.org/10.1016/j.rser.2017.09.048>.
- Iures, L., & Bob, C. (2010). The future concrete: Self-compacting concrete. *buletinul institutului politehnic din lasi. Sectia Constructii*, 56(2).
- Jawahar, J. G., Sashidhar, C., Reddy, I. R., & Peter, J. A. (2012). A simple tool for self compacting concrete mix design. *International Journal of Advances in Engineering & Technology*, 3(2).
- Kasemchaisiri, R., & Tangtermsirikul, S. (2008). Properties of self-compacting concrete incorporating bottom ash as a partial replacement of fine aggregate. *ScienceAsia*, 34(1), 87–95. Available from <https://doi.org/10.2306/scienceasia1513-1874.2008.34.087>.

- Khatib, J. M., & Hibbert, J. J. (2005). Selected engineering properties of concrete incorporating slag and metakaolin. *Construction and Building Materials*, 19(6), 460–472. Available from <https://doi.org/10.1016/j.conbuildmat.2004.07.017>.
- Khatri, R. P., Sirivivatnanon, V., & Yang, J. L. (1997). Role of permeability in sulphate attack. *Cement and Concrete Research*, 27(8), 1179–1189. Available from [https://doi.org/10.1016/S0008-8846\(97\)00119-1](https://doi.org/10.1016/S0008-8846(97)00119-1).
- Kong, D. L. Y., & Sanjayan, J. G. (2008). Damage behavior of geopolymer composites exposed to elevated temperatures. *Cement and Concrete Composites*, 30(10), 986–991. Available from <https://doi.org/10.1016/j.cemconcomp.2008.08.001>.
- Kumar Karri, S., Rao, G. V. R., & Raju, P. M. (2015). Strength and durability studies on GGBS concrete. *International Journal of Civil Engineering*, 34–41. Available from <https://doi.org/10.14445/23488352/ijce-v2i10p106>.
- Kuo, W. T., Wang, H. Y., & Shu, C. Y. (2014). Engineering properties of cementless concrete produced from GGBFS and recycled desulfurization slag. *Construction and Building Materials*, 63, 189–196. Available from <https://doi.org/10.1016/j.conbuildmat.2014.04.017>.
- Long, G., Gao, Y., & Xie, Y. (2015). Designing more sustainable and greener self-compacting concrete. *Construction and Building Materials*, 84, 301–306. Available from <https://doi.org/10.1016/j.conbuildmat.2015.02.072>.
- Madandoust, R., & Mousavi, S. Y. (2012). Fresh and hardened properties of self-compacting concrete containing metakaolin. *Construction and Building Materials*, 35, 752–760. Available from <https://doi.org/10.1016/j.conbuildmat.2012.04.109>.
- Malhotra, V. M. (2002). Introduction: Sustainable development and concrete technology. *Concrete International*, 24(7).
- Manjula, V., & Felixkala, T. (2018). Development of slag based lower strength self compacting concrete and experimental assessment on its strength and elastic properties. *International Journal of Civil Engineering and Technology*, 9(2), 56–62. Available from <http://www.iaeme.com/ijciet/index.asp>.
- Marto, A., Awang, A.R., & Makhtar, A.M. (2011). Compaction characteristics and permeability of tanjung bin coal ash mixtures. In *IPCBEE in Proc. of the International Conference on Environment Science and Engineering: Selected papers* (Vol. 8, pp. 134–137).
- McCaffrey, R. (2002). Climate change and the cement industry. *Global cement and lime magazine*. Environmental special issue, 15.
- Mehta, P. K. (2002). Greening of the concrete industry for sustainable development. *Concrete International*, 24(7), 23–28.
- Mermerdaş, K., Gesoğlu, M., Güneyisi, E., & Özturan, T. (2012). Strength development of concretes incorporated with metakaolin and different types of calcined kaolins. *Construction and Building Materials*, 37, 766–774. Available from <https://doi.org/10.1016/j.conbuildmat.2012.07.077>.
- Mukherjee, A. B., Zevenhoven, R., Bhattacharya, P., Sajwan, K. S., & Kikuchi, R. (2008). Mercury flow via coal and coal utilization by-products: A global perspective. *Resources, Conservation and Recycling*, 52(4), 571–591. Available from <https://doi.org/10.1016/j.resconrec.2007.09.002>.
- Mushtaq, I., & Nasier, S. (2018). Self compacting concrete design and performance using fly ash. *International Journal of Civil Engineering and Technology*, 9(4), 436–445. Available from [http://www.iaeme.com/MasterAdmin/UploadFolder/IJCIET\\_09\\_04\\_048/IJCIET\\_09\\_04\\_048.pdf](http://www.iaeme.com/MasterAdmin/UploadFolder/IJCIET_09_04_048/IJCIET_09_04_048.pdf).

- Naik, T. R., & Kraus, R. N. (1999). The role of flowable slurry in sustainable developments in civil engineering. *Materials and construction: Exploring the connection*, 826–834.
- Okamura, H. (1997). Self-compacting high-performance concrete. *Concrete International*, 19(7), 50–54.
- Palomo, A., Grutzeck, M. W., & Blanco, M. T. (1999). Alkali-activated fly ashes: A cement for the future. *Cement and Concrete Research*, 29(8), 1323–1329. Available from [https://doi.org/10.1016/S0008-8846\(98\)00243-9](https://doi.org/10.1016/S0008-8846(98)00243-9).
- Parande, A. K., Ramesh Babu, B., Aswin Karthik, M., Deepak Kumar, K. K., & Palaniswamy, N. (2008). Study on strength and corrosion performance for steel embedded in metakaolin blended concrete/mortar. *Construction and Building Materials*, 22(3), 127–134. Available from <https://doi.org/10.1016/j.conbuildmat.2006.10.003>.
- Park, Y., Abolmaali, A., Kim, Y. H., & Ghahremannejad, M. (2016). Compressive strength of fly ash-based geopolymer concrete with crumb rubber partially replacing sand. *Construction and Building Materials*, 118, 43–51. Available from <https://doi.org/10.1016/j.conbuildmat.2016.05.001>.
- Poon, C. S., Kou, S. C., & Lam, L. (2006). Compressive strength, chloride diffusivity and pore structure of high performance metakaolin and silica fume concrete. *Construction and Building Materials*, 20(10), 858–865. Available from <https://doi.org/10.1016/j.conbuildmat.2005.07.001>.
- Proske, T., Hainer, S., Rezvani, M., & Graubner, C. A. (2013). Eco-friendly concretes with reduced water and cement contents - Mix design principles and laboratory tests. *Cement and Concrete Research*, 51, 38–46. Available from <https://doi.org/10.1016/j.cemconres.2013.04.011>.
- Qiu, Q. (2020). A state-of-the-art review on the carbonation process in cementitious materials: Fundamentals and characterization techniques. *Construction and Building Materials*, 247. Available from <https://doi.org/10.1016/j.conbuildmat.2020.118503>.
- Ramachandran, V. S. (1996). Concrete admixtures handbook: *Properties, science and technology* (pp. 657–680). Elsevier.
- Ramezani-pour, A. A., Pilvar, A., Mahdikhani, M., & Moodi, F. (2011). Practical evaluation of relationship between concrete resistivity, water penetration, rapid chloride penetration and compressive strength. *Construction and Building Materials*, 25(5), 2472–2479. Available from <https://doi.org/10.1016/j.conbuildmat.2010.11.069>.
- Roy, D. M. (1999). Alkali-activated cements: Opportunities and challenges. *Cement and Concrete Research*, 29(2), 249–254. Available from [https://doi.org/10.1016/S0008-8846\(98\)00093-3](https://doi.org/10.1016/S0008-8846(98)00093-3).
- Şahmaran, M., Lachemi, M., Erdem, T. K., & Yücel, H. E. (2011). Use of spent foundry sand and fly ash for the development of green self-consolidating concrete. *Materials and Structures*, 44(7), 1193–1204. Available from <https://doi.org/10.1617/s11527-010-9692-7>.
- Said-Mansour, M., Kadri, E. H., Kenai, S., Ghrici, M., & Bennaceur, R. (2011). Influence of calcined kaolin on mortar properties. *Construction and Building Materials*, 25(5), 2275–2282. Available from <https://doi.org/10.1016/j.conbuildmat.2010.11.017>.
- Shafiq, P., Jumaat, M. Z., Mahmud, H. B., & Alengaram, U. J. (2013). Oil palm shell lightweight concrete containing high volume ground granulated blast furnace slag. *Construction and Building Materials*, 40, 231–238. Available from <https://doi.org/10.1016/j.conbuildmat.2012.10.007>.
- Shariq, M., Prasad, J., & Masood, A. (2010). Effect of GGBFS on time dependent compressive strength of concrete. *Construction and Building Materials*, 24(8), 1469–1478. Available from <https://doi.org/10.1016/j.conbuildmat.2010.01.007>.

- Shoubi, M. V., Barough, A. S., & Amirsoleimani, O. (2013). Assessment of the roles of various cement replacements in achieving the sustainable and high performance concrete. *International Journal of Advances in Engineering & Technology*, 6(1).
- Siddique, R., & Kaur, D. (2012). Properties of concrete containing ground granulated blast furnace slag (GGBFS) at elevated temperatures. *Journal of Advanced Research*, 3(1), 45–51. Available from <https://doi.org/10.1016/j.jare.2011.03.004>.
- Suresh, D., & Nagaraju, K. (2015). Ground granulated blast slag (GGBS) in concrete—A review. *IOSR Journal of Mechanical and Civil Engineering*, 12(4), 76–82.
- Testing hardened concrete: Part 8: Depth of penetration of water under pressure (2009). British Standard Institution, 12390–12398.
- Wang, H. Y. (2008). The effects of elevated temperature on cement paste containing GGBFS. *Cement and Concrete Composites*, 30(10), 992–999. Available from <https://doi.org/10.1016/j.cemconcomp.2007.12.003>.
- Wesche, K., Alonso, I. L., Bijen, I., Schubert, P., Berg, W. V., & Rankers, R. (1989). Test methods for determining the properties of fly ash and of fly ash for use in building materials. *Materials and Structures*, 22(4), 299–308. Available from <https://doi.org/10.1007/BF02472563>.
- Wild, S., Khatib, J. M., & Jones, A. (1996). Relative strength, pozzolanic activity and cement hydration in superplasticised metakaolin concrete. *Cement and Concrete Research*, 26(10), 1537–1544. Available from [https://doi.org/10.1016/0008-8846\(96\)00148-2](https://doi.org/10.1016/0008-8846(96)00148-2).

# Use of alternative recycled fillers in bituminous mixtures: a review

17

R. Joumblat<sup>1</sup>, H. Kassem<sup>1</sup>, A. Elkordi<sup>1,2</sup> and J. Khatib<sup>1,3</sup>

<sup>1</sup>Faculty of Engineering, Department of Civil and Environmental Engineering, Beirut Arab University, Beirut, Lebanon, <sup>2</sup>Faculty of Engineering, Department of Civil Engineering, Alexandria University, Alexandria, Egypt, <sup>3</sup>Faculty of Science and Engineering, University of Wolverhampton, Wolverhampton, United Kingdom

## 17.1 Introduction

The rapid growth of the population has pushed the road paving industry toward the utilization of sustainable construction materials. These include industrial wastes such as bottom ashes and recycled materials. The incorporation of such materials as a replacement of raw materials has grown in recent years, especially in asphalt concrete mixtures, when the conventional resources began to get scarce (Tuncan et al., 2003). In fact, producing natural aggregates has been causing intensive consumption and exploitation of natural resources, leading to permanent changes in the natural environment, such as depletion of virgin materials and disturbance of the ecosystem (Akbulut & Güreç, 2007; Kono et al., 2018). Moreover the increase of waste production is what forces nations to look for new sustainable ways to recycle and incorporate these waste products into road construction industry (Ali et al., 1996; Paranaivithana & Mohajerani, 2006). According to the existing state of the art, different waste products have been incorporated and used as construction materials in hot mix asphalt (HMA) mixtures and in concrete and cement applications. Municipal solid waste (MSW) in road construction (Xue et al., 2009) has been used lately in different applications (Kamon et al., 2000; Aubert et al., 2004b) and has been attracting attention globally as this type of waste can be incorporated as virgin material. Various researchers have been investigating in this direction. Perpetual research studies continue the study for better investigation of these materials (Abukhattala, 2016). Additionally, since 1980 the generation of MSW in the United States is increased by 65% to reach at present about 250 million tons yearly with 11.7% incinerated with energy recovery, 34.7% recycled and composted, and 53.6% landfilled (U S Environmental Protection, 2010). As the waste production's volume remains to increase, emerging technologies are evolving to decrease the volume and the weight of waste by 60% to 90%; one of these technologies is incineration of MSW (An et al., 2014).

Different combustion technologies are employed to burn MSW (Defra, 2013); however, these technologies are all separated to three major sections: incineration, energy recovery, and air pollution control (APC) (Khalid, 2019; Singh et al., 2011).

The residual products produced after combustion are referred to as municipal solid waste incineration (MSWI) ash. By definition, MSWI ash is the byproduct produced during the combustion of MSW in incinerators (Xue et al., 2009). Mass burn (MB), refuse-derived fuel (RDF), and fluidized bed combustion (FBD) are technologies used to combust MSW (Keppert et al., 2012; Haukohl et al., 1999). Mass burning is the incineration of heterogeneous, “as received” MSW. This technique requires minimal or no pretreatment along the lines of shredding, fine sorting, or reduction of size (Yin et al., 2018a). The majority of MSW facilities are MB plants with movable grate (Khalid, 2019; Haukohl et al., 1999). RDF technology requires pretreatment of MSW in order to remove noncombustible and noncarbonaceous materials. FBD technology is applied for homogenized and preheated MSW. This technology is for particular types of wastes, notably industrial waste (Haukohl et al., 1999).

The residual ash products collected from MSWI are bottom ash (BA), fly ash (FA), and APC residues. BA is a noncombustible material of the waste feed rich in metal scraps and poor in heavy metals. It is released from the furnace grate and can be assembled in two discharge systems: wet BA and dry BA discharge (Kahle et al., 2015). Wet BA discharge is frequently used; BA is collected in a water quenching bath and allowed to cool down in order to make handling easier and reduce dust issues (Kahle et al., 2015). The water in the discharge system is found out to be an alkaline water medium. BA consists of 25% of the total amount of MSW and 80% of total combusted ash (Tang et al., 2018).

Dust particles (FA) and other pollutants (APC residues) can be removed by electrostatic precipitators and scrubbers. These particles are classified as hazardous and harmful waste as they are rich in heavy metals, toxic organic compounds, and chloride content.

The main concern related to the incineration of MSW is air pollution as the incineration produces high volumes of flue gases. Residues, dust, heavy metals, and organic and inorganic compounds in addition to other pollutants such as HCl, HF, and SO<sub>2</sub>, generated from insufficient combustion, are carried by flue gases. The literature has shown that implementing APC devices reduces the emission of flue gases (An et al., 2014; Haukohl et al., 1999; Millrath et al., 2004; Santagata et al., 2014), shifting the air pollution concern to another concern associated with leaching from the disposal of MSWI ashes in landfills.

Different researchers have been studying the engineering and environmental effects of incorporating MSWI ashes (BA or FA) in bituminous applications. Ferreira et al. (Brunner & Rechberger, 2015; Zhang et al., 2020) investigated the different concentrations of metals in MSWI-FA. The results showed that different heavy metals are present in high concentrations in MSWI-FA along the lines of zinc, lead, iron, magnesium, manganese, chromium, and cadmium. The presence of heavy metals in MSWI-FA may affect the sustainability in addition to environmental aspects. Lynn et al. (2017) assessed the sustainable use of MSWI-BA in the road construction industry by analyzing and evaluating its characteristics and performance in pavement applications. The results demonstrated that MSWI-BA can be used in subbase and road base layers to a considerable percentage depending on the binder content and performance requirement. An et al. (2015) studied the effect of

using MSWI-BA as a partial replacement of fine aggregates in bituminous mixtures at different percentages. They concluded that the highest Marshall stability, the highest tensile strength ratio, and the highest moisture stability were developed at 20% replacement, whereas the flow increases as MSWI-BA replacement increases. [Romeo et al. \(2018\)](#) evaluated the effect of using MSWI-FA as a filler in HMA mixtures. Different mixtures were prepared and tested at different asphalt binder contents and different filler types. Results showed that MSWI-FA can be used as a filler in HMA mixtures if the MSWI-FA underwent the water leaching process. The mechanical properties of samples with MSWI-FA as a filler are in agreement with the ones of the conventional HMA mix. [Mirković et al. \(2019\)](#) studied the effect of using FA as partial or total replacement of fillers in HMA mixtures. Satisfactory results were achieved with the addition of FA; the stability and flow of mixes were in agreement with the results of the control mix prepared with 100% of the traditional filler.

The work presented here aims at providing a comprehensive review on the available literature and potential applications on the incorporation of bottom and fly ashes from municipal waste incineration as replacement of fillers in bituminous mixtures. The literature review presented covers the findings of research studies and practical experience covering methods to be followed and optimal incorporation scenarios in different areas: (1) management practices of MSWI, (2) application of MSWI ashes in road paving industry, and (3) environmental influence regarding the use of MSWI ashes.

## 17.2 Management practices of municipal solid waste incineration ashes

Management of MSW engages all the procedures and the measures needed to control MSW from its initial phase to its last phase ([Branch](#)); this could include waste assembling, waste transportation, waste treatment and disposal, and monitoring and controlling of the waste management process ([de S. Pereira & Fernandez, 2019](#)). Various technologies have been employed regarding management of MSW disposal. The predominant used technology in developing countries is landfilling ([Kamaruddin et al., 2017](#)). However, environmental pollution and soil contamination resulting from landfilling leachate are marked as growing environmental concerns in the Middle East region ([Zafar, 2018](#)). It is important to note that most landfills in this region consist of nonsanitary landfills known as waste dumps. Soil and water contamination, ecosystem damage, harmful gas emission, and landfilling leachate are some of the characteristics of nonsanitary landfills. Landfilling leachate is defined as the liquid released from solid waste, in general, with the presence of water. This liquid is extremely rich in inorganic salts and toxicity, very high pH with chemical oxygen demand, and biochemical oxygen demand, carrying dissolved or suspended materials from different materials and biodecomposition procedures ([Kamaruddin et al., 2017](#)). The composition of this liquid, leachate, changes over



the time depending on several factors such as the composition of the solid waste, the climatic conditions, the chemical and physical conditions, and age of the landfill (Kamaruddin et al., 2017).

As a matter of fact, efficient landfill design can limit the contamination, consequently limiting the environmental and health hazards by separating solid waste from the enclosing environment (Jovanov et al., 2018; Vehlow, 2012). New MSW techniques are emerging particularly for the management of uninsulated organic waste, namely, mechanical-biological treatment (MBT), composting, and waste to energy (WTE) (Hadidi et al., 2020). MBT consists of physical and biological isolation of various types of waste found in MSW by biological stabilization of organic matter (Fei et al., 2018). MSWs are first mechanically and biologically pretreated, followed by an aerobic treatment to ensure the biological stabilization of degradable elements (Scaglia et al., 2013). This technology has been broadly endorsed, in particular in Europe (Fei et al., 2018). As a matter of fact, around 180 MBT plants were established in Europe between 1990 and 2010. Composting is another safe emerging technology of waste management. It is an aerobic method where degradable components are degraded and converted into organic and inorganic byproducts under the influence of microorganisms (Tay & Goh, 1991). These byproducts can be used as biofertilizers in addition to soil quality improvement (Ayilara et al., 2020). Additionally, they act as a barrier protecting the underground water from being polluted by MSW landfilling as microbes and other chemical and harmful pollutants are decreased during the composting process (Ayilara et al., 2020). WTE technology, often named MSW to energy, is considered as the most efficient emerged technology as it inhibits the production of around 50 million tons of CO<sub>2</sub> emitted due to fuel burning (Abdullah et al., 2019). However, this technology is not supported globally as there is a consideration that energy generated from waste depresses waste recycling (Abdullah et al., 2019; Malinauskaite et al., 2017). Six strategies are present in WTE technology: MB, gasification, plasma arc gasification, anaerobic digestion, RDF, and solid recovered fuel (Hadidi et al., 2020). In general, MB is the most widespread WTE method as it consumes large amounts of MSW, compared to MBT and composting technologies, in order to convert them into beneficial energy types as generation of electricity and reduction of environmental damage (Chandler et al., 1997). All solid and organic waste types can be treated in MB. WTE technology is able to decrease waste by 80%. Developing countries, such as the Middle East, rely on MSW landfilling as a disposal method as they require effective MSW management practices (Brunner & Rechberger, 2015). Furthermore, Asian and European countries consider separating the products of MSWI ashes: BA, FA, and APC residues; on the contrary, in the United States, these products are not detached, named combined ash, and are disposed in landfills (Kim et al., 2016). Despite the fact that the United States is considered as the greatest waste production country, the rate of MSW recycling is found out to be significantly low with no MSW recycling practices (Kim et al., 2016). In Middle-Eastern countries, Saudi Arabia is an example; up to 15% of MSW is recycled and generally is disposed unsegregated to landfills, keeping this management method the most dominant as a result of the vast availability of land and a low cost of resources

up to 15% of MSW (Hadidi et al., 2020). The reutilization of MSWI ashes is widely promoted; in fact, BA and FA are reused in applications related to civil engineering notably in road construction and roadway paving industry.

## 17.3 Municipal solid waste incineration ashes as road construction material

### 17.3.1 Municipal solid waste incineration bottom ash

#### 17.3.1.1 Properties of bottom ash

MSWI-BA is the main byproduct residue of the incineration procedure operated at high temperatures between 850°C and 1000°C. It is considered as a porous, coarse, and angular material, having a rough surface that might pass or remain on the burning grate; therefore grate ash can be found in MSWI-BA. This synthetically developed porous and heterogeneous product is characterized by dark gray to black color, including some unburnt materials, glass, minerals, ceramics, and organic carbon in addition to ferrous and nonferrous elements (Santagata et al., 2014; Wiles & Shepherd, 1999). BA represents 85% to 95% by weight of total whole amount of produced residue and has considerably highly reactive properties (Cho et al., 2020). Some BA phases are totally or partially dissolved when this product is soaked in water, such as salts and sulfates (full dissolution) or glass phases (partial dissolution), leading to the creation of new phases and new reactions with the surrounding carbon dioxide (Speiser et al., 2001). Moreover, BA can be classified as fine, medium, and coarse particles, which are persistent with the fact that it is a heterogeneous material (Chang & Wey, 2006).

Scanning electron microscopy with energy-dispersive X-ray analysis (SEM-EDX) and spectroscopic analysis ensure accurate information about the composition and morphology of MSWI-BA. Calcium (Ca), sulfur (S), chlorine (Cl), potassium (K), and sodium (Na) are mostly detected (Chang & Wey, 2006), in addition to other elements such as silicon (Si), iron (Fe), barium (Ba), and aluminum (Al) (Cho et al., 2020). Additionally, dangerous elements are mapped in reduced quantities along the lines of zinc (Zn), copper (Cu), lead (Pb), chromium (Cr), nickel (Ni), cadmium (Cd), and arsenic (As) (Hartmann et al., 2015). The concentration of heavy metals present in BA decreases with the increase of mean particle size, except for particle sizes of 1–1.4 mm (Chimenos et al., 1999; Yu et al., 2013). This can be explained by the fact that greater volatilization is linked to coarser particles as their retention time is longer than that of fine particles, which have a shorter retention time in addition to their ability to catch more volatile species as their surface area is considerably high (Song et al., 2004). A high concentration of calcium is found out in MSWI-BA; in contrast the distribution of sulfur is observed to be dispersed, which indicates the presence of calcium carbonate and calcium sulfate,  $\text{CaCO}_3$ , and  $\text{CaSO}_4$  (Chang & Wey, 2006). The distribution of sodium and chlorine was observed to be similar to the one of calcium and sulfur, leading to the formation of sodium chloride ( $\text{NaCl}$ )

compound; however, the distribution of potassium was displayed to be different, forming potassium oxide ( $K_2O$ ) in minor concentration. By combining the chemical maps of calcium and chlorine, calcium chloride ( $CaCl_2$ ) can also be detected in MSWI-BA. Other major compounds can be detected in high concentrations, such as silicon dioxide ( $SiO_2$ ), iron oxide ( $FeO_3$ ), and aluminum oxide ( $Al_2O_3$ ). Sodium oxide ( $Na_2O$ ), magnesium oxide ( $MgO$ ), and titanium oxide ( $TiO_2$ ) are detected in minor concentrations (Cho et al., 2020). Oxides are the primary compounds in MSWI-BA, and silicon dioxide is the predominant one (Lynn et al., 2017).

In order to determine the connecting system of the BA elements, X-ray powder diffraction (XRD) should be conducted. MSWI byproduct toxicity is defined as the degree to which an element, product, or residue can cause damage and harmful effects over a long period of time. It depends not only on the concentration of the residue but also on the speciation of this residue (Li et al., 2004). Quartz, calcite, anhydrite, albite, anorthite, and  $K_2O$  consist of the main crystalline phases in MSWI-BA. It should be noted that no detection of  $K_2O$  was observed when MSWI-BA is soaked in water (Yin et al., 2018a; Yu et al., 2013).

The production of hydroxides from calcium oxides will result in a high MSWI-BA pH in the range of 10.5–12.2 (Chandler et al., 1997). A study in Belgium indicated that the specific gravity of MSWI-BA ranges from 1.1 to 2.7 and that the dry density ranges from 0.95 to 1.75  $g/cm^3$ , whereas moisture content of MSWI-BA is greatly dependent on postincineration treatments and storage methods (Joseph et al., 2018). Lynn et al. (2017) stated an average specific gravity of MSWI-BA of 2.3 based on 32 samples, with a range between 1.2 and 2.8. Furthermore, they indicated absorption values ranging from 2.9% to 14.2% for coarse fractions and from 1.0% to 17.1% for fine fractions.

## **17.3.2 Application of bottom ash in bituminous mixtures**

### **17.3.2.1 Replacement of fine aggregates**

Several researchers investigated the use of MSWI ashes in HMA mixes. Ongoing studies continue the examination for optimal use of MSWI ashes, and the suitability of using MSWI-BA as fine aggregate substitutes in asphalt mixtures has been assessed as this byproduct is, to some degree, similar to the traditional natural aggregates. Incineration bottom ash (IBA) was examined as a fine aggregate substitute in asphalt concrete pavement in an experimental study in 2019 by conducting different physical tests. The results indicated that the substitution of fine aggregates by IBA enhanced the adhesion between the aggregates and the binder–aggregate adhesion (Luo et al., 2017). Improvement of engineering properties was also indicated, such as stability and indirect tensile strength. Up to 80% of fine aggregate replacement by MSWI-BA can be used to achieve good engineering properties and performance enhancement (Luo et al., 2017; Ni et al., 2017).

Luo et al. (2017) examined the engineering and environmental properties of using MSWI-BA as partial replacement for conventional aggregate in HMA mixtures. Various MSWI-BA contents were mixed (10%, 20%, 30%, and 40% by total weight

of the mix) with a conventional asphalt binder in order to achieve the objectives of the experimental study. The results of the investigation on the potential of using MSWI-BA in HMA asphalt showed that as the MSWI-BA substitution percentage increases the tensile strength ratio decreases. The authors recommended a replacement of up to 10% for surface course and up to 20% for base course as MSWI-BA developed low rutting resistance. The concentrations of heavy metals in MSWI-BA were below the regulatory limits. This can be explained by the fact that the coating of the particles of MSWI-BA by asphalt binder decreases the concentrations of heavy metals in leachates (Ni et al., 2017; Hassan & Al-Shamsi, 2010). Consequently, investigation research studies were carried out to determine the relationship between the design techniques and the beneficial use of MSWI-BA (Ni et al., 2017; Show et al., 2000). Different studies reported that MSWI-BA has substantial potential to be used in HMA mixtures. On the other hand, MSWI-BA tends to substitute fine aggregates instead of coarse aggregates. In an experimental study, mechanical properties and performance of HMA containing MSWI-BA as aggregate at different percentages (30%, 60%, and 80%) were analyzed in addition to moisture sensitivity, stiffness, and creep. The use of MSWI-BA in HMA mixes proved to enhance the stiffness of the mixes excluding the mix at high percentage replacement (80%) and to enhance the rutting resistance of HMA mixes (Hassan & Khalid, 2010a). A study in 2010 evaluated the use of MSWI-BA as fine aggregate replacement by up to 40% by weight using Marshall mix design method. The dynamic modulus results showed that as the percentage of replacement increases, lower mix stiffness is developed; as a consequence a maximum value of 20% of replacement of MSWI-BA was recommended (Hassan & Al-Shamsi, 2010). Dynamic creep, moisture sensibility, and low-temperature bending were conducted in an experimental study in order to assess the engineering properties of HMA mixtures containing MSWI-BA as an aggregate substitute (Liu et al., 2014). The results indicated that the use of MSWI-BA enhanced the rutting resistance of mixtures in addition to moisture susceptibility and anticrack performance. It is recommended to limit the use of MSWI-BA replacement to 30% by mass of the aggregate (Liu et al., 2014). The creep and viscous behavior of asphaltic mixtures were strongly affected by the use of MSWI-BA (Hassan & Khalid, 2010b). The highest increase in the tensile strength was indicated at 60% replacement of MSWI-BA without causing brittleness concern (Hassan & Khalid, 2008). However, another study stated that MSWI-BA enhanced the tensile strength of the HMA mix combined with a high flow rate, low voids in mineral aggregate, and satisfactory stability values (Huang et al., 2006).

### 17.3.2.2 Use of bottom ash as a mineral filler

Using MSWI-BA caused an enhancement in the tensile strength when used as a replacement for natural filler material in addition, improving the resilient modulus and the fracture behaviors of HMA mixes (Santagata et al., 2014). A study in 2020 reviewed different waste materials that could be used as fillers in asphaltic mixtures, including MSWI-BA (Choudhary et al., 2020). The authors of this research study indicated that MSWI ashes have the potential to be used as filler replacement as they

developed excellent performance, such as dynamic and Marshall stability, in addition to fatigue life when compared to performance of mixes with conventional fillers (Xue et al., 2009; Choudhary et al., 2020). However, higher moisture susceptibility was developed with the mixes containing MSW ashes, which is directly linked to the decrease in the aggregate–binder adhesion caused by low calcium oxide and high silicon dioxide content (Choudhary et al., 2020). Numerous laboratory experimental tests were conducted to assess the potential of MSWI-BA as a mineral filler in HMA mixtures. The results of the investigation suggested that the use of MSWI-BA as mineral filler replacement enhanced the moisture sensitivity, resilient modulus, skid resistance, and structural stability of mixes with no impact on Marshall stability or on rutting resistance (Ali et al., 1996; Huang et al., 2006; Asi & Assa'ad, 2005; Churchill & Amirkhani, 1999; Garrick & Chan, 1993; Ksaibati & Plancher, 2005; Lentz et al., 1994; Shimaoka et al., 2001; Shuler, 1976; Tapkin, 2008; Zeng & Ksaibati, 2003). Some authors evaluated the impact of using 9% BA as mineral filler replacement and conducted dynamic modulus test (Goh & You, 2008). The results showed that the value of the dynamic modulus had decreased with the substitution of BA, which may lead to a decrease in the rutting resistance and in the rut depth when this value is used in the mechanistic empirical pavement design guide (MEPDG). However, it is important to note that MEPDG was not designed for mixes with BA. It is recommended to use lime with BA mixes in order to enhance its rutting resistance (Goh & You, 2008). An experimental investigation was conducted in 2014 to study the performance characteristics of HMA mixes with vitrified municipal solid waste bottom ash (VMSW-BA) as a mineral filler substitute (Santos et al., 2013). Vitrification is when subjecting MSW-BA to a high-temperature procedure. This process yields a homogeneous and inert material that has minimal to no pollution risk. The experimental results showed that the use of VMSWI-BA as mineral filler replacement results in considerably satisfactory pavement performance (Santos et al., 2013). The heterogeneous nature of MSWI-BA greatly affects the damage behavior of HMA as the thickness and the strength of the interfacial transition zone are not similar for each aggregate–binder pair (Yuan et al., 2017). Based on this fact, some authors evaluated the effect of the interfacial zone on the tensile damage behavior of HMA mixes with MSWI-BA. The interfacial transition zone is defined as the zone of asphalt mastic around the aggregate; its properties are greatly linked to those of the aggregate and should be considered when evaluating the damage mechanism of HMA mixes (Yuan et al., 2017). The numerical results showed that the damage begins initially along the interfacial transition zones and circulates progressively along these areas due to the difference in stiffness between the aggregate particle and the mastic. Similarly the interfacial transition zone thickness has a considerable impact on the tensile strength of mixes.

### **17.3.3 Municipal solid waste incineration fly ash**

#### **17.3.3.1 Properties of fly ash**

MSWI-FA represents around 3% to 5% of the total amount of byproducts produced by the incineration of MSW (Xue et al., 2009; Chandler et al., 1997; Mohammed

Alhassan & Tanko, 2012) depending on the conditions of the MSWI, the different types of MSW, and the treatment techniques of flue gas (Xue et al., 2009). MSWI-FA is generally gray or dark gray and classified as fine particle along with dusty appearance (Chandler et al., 1997; Mohammed Alhassan & Tanko, 2012).

The two samples FA<sub>1</sub> and FA<sub>2</sub> of MSWI-FA differ only by the temperature of separation, which is higher than 700°C for FA<sub>1</sub> and between 500°C and 700°C for FA<sub>2</sub> (Keppert et al., 2012). As seen, these nonuniform and irregular particles have rough surfaces and are full of pores, which lead to higher surface areas, allowing the accumulation of volatile metals on the particle surfaces. The principal factor that determines the general composition of ashes is incineration of MSW. In addition, there are other factors, such as the incineration plant technology (separation efficiency of filters, APC devices), the temperature of ash separation point, and redox conditions (Keppert et al., 2012; Belevi & Langmeier, 2000; Belevi & Moench, 2000). Most MSWI-FA elements showed consistent change in their contents depending on the temperature of flue gas (Keppert et al., 2012). The physical properties of MSWI-FA have been recorded (Cho et al., 2020). The density usually ranges between 1.7 and 2.4 kg/m<sup>3</sup>, which is relatively lower than other densities of materials used in the pavement industry (Tay & Goh, 1991; Goh & Tay, 1993). A study carried out in 2016 found out that the diameters of most particles of MSWI-FA (over 80% of MSWI-FA particles) are between 0.105 and 0.154 mm; additionally only 5% of MSWI-FA particles are smaller than 0.063 mm and greater than 0.154 mm (Xinghua et al., 2016).

It is worth noting that the mass fraction decreases as the MSWI-FA particles are smaller than 0.09 mm. However, the mass fraction decreases as the MSWI-FA particles are larger than 0.105 mm. The low ratio of MSWI-FA particles results from the collision, heterogeneous condensation, and homogeneous nucleation of small particles into larger ones (Chang et al., 2000). Unburned particles represent the coarse particles of MSWI-FA as these particles had been discharged by air drafts into dust catchers; however, they are present in a low ratio (Xinghua et al., 2016). Research has shown that the pH of MSWI-FA is considerably in the range of 10–12 and sometimes can be even higher (An et al., 2015; Chang & Wey, 2006). This is primarily caused by the presence of a high amount of calcium oxide (CaO); the high alkalinity causes the MSWI-FA to have high resistance to changes in environmental pH (Xinghua et al., 2016; Chang et al., 2000; Hansen et al., 2001).

The chemical composition, mineralogical composition, and morphology of MSWI-FA are developed by X-ray fluorescence, XRD, and scanning electron microscopy (SEM), respectively. Many researchers have investigated the chemical composition of MSWI-FA (Xinghua et al., 2016; Diliberto et al., 2020; Du et al., 2018; Kalogirou & Themelis, 1937; Rémond et al., 2002). Silicon dioxide, calcium oxide, and aluminum oxide are the principal components of MSWI-FA. It can be noted that MSWI-FA is not chemically inert; however, it is rich in heavy metals and volatile elements such as lead, zinc, cadmium, and arsenic, making it a toxic and hazardous waste (Cho et al., 2020; Xinghua et al., 2016; Bie et al., 2016; Lu et al., 2020). The presence of heavy metals, high aluminum content in addition to the high chlorine content in MSWI-FA, mainly originated from the plastics and

kitchen waste in MSW, is one of the most important obstacles of using MSWI-FA as a construction material as it increases the exposure of corrosion of reinforced concrete structures when MSWI-FA and cement are mixed (Chandler et al., 1997; Wiles & Shepherd, 1999; Xinghua et al., 2016; Astrup et al., 2008; Aubert et al., 2007, 2004a; Lam et al., 2010). The results of the mineralogical composition of washed and unwashed samples of MSWI-FA of the study conducted by Lu et al., 2020 show that the mineralogical composition of MSWI-FA sample is totally different before and after FA washing. Several researchers evaluated different methods to reduce the negative effects of MSWI-FA. The main treatment methods are (1) extraction and separation using water; (2) chemical stabilization by carbon dioxide, phosphoric acid, ferrous sulfate, sodium sulfide, and orthophosphate; (3) addition of lime, cement, asphalt, and gypsum, which is the most common in the industry, but this method may not be effective as some elements such as zinc, molybdenum, chromium, and cadmium may not be adequately covered to meet the regulatory leaching standards; and (4) thermal treatments such as vitrification or pyrolysis (Vehlow, 2012; Chandler et al., 1997; Astrup et al., 2008). Researchers have investigated the potential of converting MSWI-FA into a nontoxic material (Kalogirou & Themelis, 1937). A combination of thermal and chemical techniques has been suggested to reduce the chlorinated organic pollutant to zero in addition to recover heavy metals from MSWI-FA.

### 17.3.3.2 Application of fly ash in bituminous mixtures

#### Use of fly ash as a mineral filler

Several researchers have addressed the potential of using MSWI-FA as traditional mineral filler replacement in bituminous mixtures. An experimental research conducted in 2019 evaluated the pavement performance on bituminous mixtures containing MSWI-FA as filler substitution (Yan et al., 2019). The MSWI-FA proved to improve significantly the bituminous mortar characteristics by reducing the phase angle, penetration, and creep rate; however, it increased the softening point, complex shear modulus, rutting factor, and creep stiffness (Yan et al., 2019). MSWI-FA had an insignificant negative effect on the low-temperature properties and a substantial positive effect on the high-temperature properties compared to the conventional mineral filler (Yan et al., 2019; Musselman et al., 1994). Romeo et al. (2018) conducted a laboratory experimental study to investigate the use of MSWI-FA as a filler replacement in HMA mixtures. For this objective, several HMA mixtures with the same gradation were tested using two different types of MSWI-FA. Results showed that the tensile strength is considerably affected when adding MSWI-FA as a filler (Romeo et al., 2018). Mechanical properties have been evaluated with the addition of FA to replace the traditional mineral filler (Tapkin, 2008; Melaku et al., 2022). The results showed that the addition of MSWI-FA as a filler in samples increased Marshall stability and decreased the flow. Additionally the alteration in the mechanical properties is essential as they influence the behavior of asphalt pavement under applied loads. Based on the results, it is recommended to use MSWI-FA in particular for wearing courses to substitute the mineral filler (Tapkin,

2008; Ogunro et al., 2004). FA has demonstrated to enhance the performance of asphalt pavement and decreases the cost and environmental impacts, which makes FA an appropriate material for use in HMA mixtures (Garrick & Chan, 1993; Ogunro et al., 2004; Sobolev et al., 2014). Additionally the investigation at micro-scale showed that FA particles induced crack-arresting within binder matrix (Sobolev et al., 2014). Xue et al. (2009) evaluated the possibility of using MSWI-FA as partial replacement of mineral fillers in stone mastic asphalt mixtures. MSWI-FA displayed considerably superior performance concerning mechanical evaluation testing, such as dynamic stability, water susceptibility, fatigue life, and rutting. Despite that, MSWI-FA samples showed higher moisture susceptibility than the conventional samples; as a consequence the adhesion between asphalt binder and aggregates is reduced (Xue et al., 2009). Another possible application for the use of MSWI-FA in asphalt concrete mixtures is its use as fine aggregate replacement. This type of application is considered, in some way, a new concept, as insufficient studies are found. The authors of this study had evaluated the use of MSWI-FA as substitution of both fine and filler replacement in bituminous mixtures. The results indicated that when using MSWI-FA as fine aggregate replacement, the difference between the average dynamic modulus for different mixes was not statistically significant within the zone of low reduced frequencies, indicating no effect of MSWI-FA within this zone and thus suggesting no change in the rutting resistance of the asphalt mixture. Whereas, the difference between the average dynamic modulus for different mixes was statistically significant within zones of moderate and high reduced frequencies, indicating that as the percentage replacement increases, the stiffness decreases, and thus suggesting that the mixture becomes more resistant to fatigue and thermal cracking. For mineral filler replacement, statistical analysis showed no evidence that the dynamic modulus is different for different replacement percentage along the entire domain of the mastercurve, suggesting that there is no effect of MSWI-FA. (Joumbat et al., 2022a,b,c).

## **17.4 Environmental effect of municipal solid waste incineration ashes as a road construction material**

### **17.4.1 Leaching characteristics of municipal solid waste incineration ashes**

The leaching characteristics of MSWI ashes are considered as crucial parameters preventing these residues to be used without contaminating the environment due to the presence of heavy metals, salts, and organic micropollutants (Santos et al., 2013; Penque, 2007; Sabbas et al., 2003; Shi & Kan, 2009). Several countries have put into practice their own procedures regarding leaching tests and fixed toxic value limits in order to assess the leaching potential of heavy metals, organic micropollutants, and soluble salts when MSWI residues are disposed to landfill or exposed to soil and water (Astrup et al., 2008; Wiles, 1996). Research has proved that



MSWI-FA has considerably higher amounts of soluble salts (potassium, sodium, calcium, and chlorine), toxic elements (lead, zinc, chromium, nickel, and copper), and organic contaminants (chlorinated aromatic compounds such as chlorobenzenes and polychlorinated biphenyls in addition to polycyclic aromatic hydrocarbons) than MSWI-BA as a consequence of vaporization of metals during MSW incineration, accompanied by adhesion of vaporized metals on the surface MSWI-FA particles (Penque, 2007; Sabbas et al., 2003; Huang et al., 2003a, 2003b). Some researchers have investigated the MSWI-BA and MSWI-FA from 25 different plants from 1998 to 2010 and indicated that MSWI-FA surpasses the leaching limit values for chlorine, zinc, lead, molybdenum, mercury, chromium, cadmium, and sulfate; however, MSWI-BA surpasses the leaching limit values for chlorine, sulfate, molybdenum, copper, antimony, and selenium (Hjelmar, 2012).

It has been reported that the leaching of metals is multidimensional as it is highly dependent on several factors: (1) the type of leachate; (2) pH: the leaching of organic and inorganic constituents from solid to liquid phase is under the control of pH (Cornelis et al., 2012); (3) liquid/solid ratio, defined as liquid volume that is in contact with dry mass of solid material, which is a crucial factor as leaching of heavy metals is governed by solubility (Hyks, 2008), in that a higher liquid to solid ratio helps in the dissolution of minerals, speeding the formation of heavy metals up (Mizutani et al., 1996; Yao et al., 2014); (4) the chemical compounds and particle morphology of MSWI residues resulting from the high combustion temperature, which renders the MSWI residues thermodynamically unstable and affected by the weathering and aging techniques, thus influencing the chemical and morphological characteristics and causing a drop in pH value by carbonation (Arickx et al., 2010; Meima & Comans, 1997; Yao et al., 2010); (5) properties of the MSWI ash such as bulk content, particle size distribution, and chemical speciation (Tapkin, 2008) as pollutants are concentrated in smaller particles (Yao et al., 2014; Chen et al., 2008; Xia et al., 2017); (6) influence of time; (7) kinetics; and (8) chemical speciation (Hyks, 2008; Luo et al., 2019).

The leaching potential of MSWI residues can be explored experimentally by different methods such as batch leaching tests, column leaching tests, and pH-static leaching tests to assess the release of toxic elements from the leachate (Yin et al., 2018a). However, batch leaching tests and column leaching tests are the most frequent test procedures used. Batch leaching tests are considered as static, simple, and fast leaching methods, where the leaching test conditions are fixed, such as contact duration, pH, and liquid/solid ratio; however, information regarding kinetics is not provided in this method (Speiser et al., 2001; Kalbe et al., 2008). On the other hand, column leaching tests are considered as nonstatic as the conditions are similar to the conditions developed in the field and simulate the flow of percolating water (groundwater) through a porous layer of ash; hence the environmental effects of the MSWI ash can be evaluated (Yin et al., 2018b). The results provided from column leaching tests may be more reliable than those of batch leaching tests; however, the column leaching tests consume more time, are higher in testing cost, and necessitate more equipment (Pecorini et al., 2017).

### **17.4.2 Municipal solid waste incineration ash leaching reduction and treatments**

The leaching potential of MSWI ashes can be substantially decreased by several methods. These techniques are grouped into three categories: (1) chemical and physical separation, (2) stabilization and solidification, and (3) thermal treatment. Stabilization/solidification and thermal treatment are the most used techniques at present (Mangialardi, 2003). The separation process consists of washing and electrochemical techniques (Lam et al., 2010). The purpose of washing techniques is to reduce most of the content of leachable salts, heavy metals, soluble chlorides, and alkali in MSWI residues by either water or acids (Toledo et al., 2018). The electrochemical technique is a new separation method to reduce the toxic leaching elements in MSWI ashes by applying an electric field. As a consequence the reduction and oxidation reactions are triggered on the surface of two electrodes connected to an external voltage source that assists in the migration of pollutants (Acar & Alshawabkeh, 1993). The stabilization and solidification techniques can be divided into acceleration carbonation, hydrothermal solidification, and chemical stabilization (Dou et al., 2017; Jing et al., 2007; Zhang et al., 2016). Accelerated carbonation method is an effective technique to reduce leaching of toxic elements of MSWI ashes derived from natural weathering and aging. In this process the mineralogical properties are altered by carbonation reaction between carbon dioxide and alkali (Ni et al., 2017; Rendek et al., 2006). Hydrothermal solidification solidifies the MSWI ashes at low temperatures and treats the ash on a large scale, causing a significant reduction in the concentration of heavy metals in the MSWI ashes (Jing et al., 2007; Shi et al., 2017). It is considered relatively as an effective treatment technique and a sustainable recycling technique by means of converting MSW into valuable products (Hu et al., 2015; Luo et al., 2018). Chemical stabilization is considered as one of the major treatment methods for leaching reduction by immobilizing heavy metals in MSWI ashes. Both organic and inorganic additives are added, so soluble metallic minerals are converted into less soluble forms (Wang et al., 2015). On the other side the purpose of thermal treatment is to decrease the leachability of toxic residues, to remove toxic compounds, to reduce the volume of the residue, and to generate useful material (Luo et al., 2019). The main methods are vitrification, melting and fusion, and sintering (Liu et al., 2014). However, vaporization is able to vaporize toxic trace elements from MSWI residues. Vitrification consists of melting the residue by means of additives to form a homogeneous liquid phase, followed by a cooling phase to create a vitreous, inert, and chemically stable glassy material (Stabile et al., 2019). Melting and fusion techniques form a heterogeneous slag mixture consisting of glassy material and crystalline phases with no additives used (Luo et al., 2019). Sintering process is heat-induced coalescence and densification of porous solid particles, operated below the melting points of their main components producing a product with low porosity, high strength, and a high density compared to the original ash (Luo et al., 2019).

## 17.5 Conclusions and recommendations

The existing management practices for MSWI ashes are examined along with their advantages to be used as road construction materials. The results demonstrated that MSWI ashes can be used in the pavement industry. The extensive review targeted the following areas: (1) the management practices for MSWI ashes currently employed with a deep comparison between several countries; (2) the physical, chemical, morphological, mineralogical, and leaching properties of MSWI-BA and MSWI-FA; (3) the engineering characteristics and performance of bituminous mixes including MSWI-BA as a fine aggregate and a filler as a replacement of natural aggregates; (4) the engineering characteristics and performance of bituminous mixes including MSWI-FA as a filler as a substitution of traditional mineral filler in HMA mixes; (5) the environmental effects of MSWI ashes as road construction materials; and (6) the current treatment techniques and methods to reduce leachate from MSWI ashes. In accordance with the comprehensive review of the characterization of MSWI-BA and MSWI-FA in addition to the assessment of their performance the following conclusions and recommendations can be drawn (Levaggi et al., 2020).

- Incineration is employed in many countries for the reason that it is an effective method to reduce the MSW weight and volume to be disposed in landfills.
- Different treatment methods have been promoted, tested, and proved to be a sustainable alternative technique for leachate reduction.
- The utilization of MSWI ashes in the pavement industry yielded satisfactory and acceptable engineering performance; however, leachates discharged from the contact with water raise environmental concerns.
- SEM results displayed that MSWI-FA is heterogeneous and consists of irregular particles owing to the high concentration of heavy metals, organic microcontaminants, salts, and the condensation of volatile compounds. This morphological property is associated with the leaching behavior of heavy metals and is behind the reason why MSWI-FA is considered to be more toxic than MSWI-BA.
- The optimal use of MSWI ashes as sustainable replacement of mineral fillers has demonstrated to be advantageous and a feasible alternative for the performance of bituminous mixtures and asphalt pavements in addition to the environment after suitable leaching reduction treatments.
- MSWI-BA has substantial potential to partially replace traditional fine aggregates and mineral fillers in HMA mixes and commonly has yielded satisfactory performance.
- Few field execution and long-term performance studies are reported regarding the replacement potential and techniques of MSWI ashes in HMA mixtures with MSWI-BA and MSWI-FA.
- Quality-control procedures, extensive ingredient analysis, and blending guides for MSWI ashes from various sources are to be developed to promote their safe and efficient application in the road construction sector.

## References

- Abdullah, M. H., Rashid, A. S. A., Anuar, U. H. M., Marto, A., & Abuelgasim, R. (2019). Bottom ash utilization: A review on engineering applications and environmental aspects. *IOP Conference Series: Materials Science and Engineering*, 527(1), 012006. Available from <https://doi.org/10.1088/1757-899X/527/1/012006>.

- Abukhettala, M. (2016). Use of recycled materials in road construction. *International Conference on Civil, Structural and Transportation Engineering (ICCSTE'16)*, 138, 1–8.
- Acar, Y. B., & Alshawabkeh, A. N. (1993). Principles of electrokinetic remediation. *Environmental Science and Technology*, 27(13), 2638–2647. Available from <https://doi.org/10.1021/es00049a002>.
- Akbulut, H., & Güreç, C. (2007). Use of aggregates produced from marble quarry waste in asphalt pavements. *Building and Environment*, 42(5), 1921–1930. Available from <https://doi.org/10.1016/j.buildenv.2006.03.012>.
- Ali, N., Chan, J. S., Simms, S., Bushman, R., & Bergan, A. T. (1996). Mechanistic evaluation of fly ash asphalt concrete mixtures. *Journal of Materials in Civil Engineering*, 8(1). Available from [https://doi.org/10.1061/\(ASCE\)0899-1561\(1996\)8:1\(19\)](https://doi.org/10.1061/(ASCE)0899-1561(1996)8:1(19)).
- An, J., Golestani, B., Nam, B.H., & Lee, J.L. (2015). Sustainable utilization of MSWI bottom ash as road construction materials, part I: Physical and mechanical evaluation. In *Airfield and highway pavements 2015: Innovative and cost-effective pavements for a sustainable future—proceedings of the 2015 international airfield and highway pavements conference*. pp. 225–235.
- An, J., Kim, J., Golestani, B., Tasneem, K.M., Muhit, B.A., Nam, B.H., & Behzadan, A.H. (2014). Evaluating the use of waste-to-energy bottom ash as road construction materials. Report Contract No. BDK78-977-20. State of Florida Department of Transportation: Tallahassee, FL.
- Arickx, S., De Borger, V., Van Gerven, T., & Vandecasteele, C. (2010). Effect of carbonation on the leaching of organic carbon and of copper from MSWI bottom ash. *Waste Management*, 30(7), 1296–1302.
- Asi, I., & Assa'ad, A. (2005). Effect of Jordanian oil shale fly ash on asphalt mixes. *Journal of Materials in Civil Engineering*, 17(5), 553–559.
- Astrup, T., Crillesen, K., Bojsen, K., Ornebjerg, H., Robert, M., Brua, Jean-Francois, Friege, H., & Bader, C. (2008). Management of APC residues from WTE Plants: An overview of management options and treatment methods. *International Solid Waste Association*.
- Aubert, J. E., Husson, B., & Sarramone, N. (2007). Utilization of municipal solid waste incineration (MSWI) fly ash in blended cement. Part 2. Mechanical strength of mortars and environmental impact. *Journal of Hazardous Materials*, 146(1–2), 12–19.
- Aubert, J. E., Husson, B., & Vaquier, A. (2004a). Metallic aluminum in MSWI fly ash: Quantification and influence on the properties of cement-based products. *Waste Management*, 24(6), 589–596.
- Aubert, J. E., Husson, B., & Vaquier, A. (2004b). Use of municipal solid waste incineration fly ash in concrete. *Cement and Concrete Research*, 34(6), 957–963.
- Ayilara, M.S., Olanrewaju, O.S., Babalola, O.O., & Odeyemi, O. (2020). Waste management through composting: Challenges and potentials. In *Sustainability (Switzerland)*, 12(4456), 1–23.
- Belevi, H., & Langmeier, M. (2000). Factors determining the element behavior in municipal solid waste incinerators. 2. Laboratory experiments. *Environmental Science and Technology*, 34(12), 2507–2512.
- Belevi, H., & Moench, H. (2000). Factors determining the element behavior in municipal solid waste incinerators. 1. Field studies. *Environmental Science and Technology*, 34(12), 2501–2506.
- Bie, R., Chen, P., Song, X., & Ji, X. (2016). Characteristics of municipal solid waste incineration fly ash with cement solidification treatment. *Journal of the Energy Institute*, 89, 704–712.
- Branch, S. United Nations Statistics Division.
- Brunner, P. H., & Rechberger, H. (2015). Waste to energy—Key element for sustainable waste management. *Waste Management*, 37, 3–12.

- Chandler, A. J., Eighmy, T. T., Hartlén, J., Helmar, O., Kosson, D. S., Sawell, S. E., van Der Sloot, H. A., & Vehlou, J. (1997). *Municipal solid waste incinerator residues*. Amsterdam, the Netherlands: Elsevier.
- Chang, F. Y., & Wey, M. Y. (2006). Comparison of the characteristics of bottom and fly ashes generated from various incineration processes. *Journal of Hazardous Materials*, *138*(3), 594–603.
- Chang, M. B., Huang, C. K., Wu, H. T., Lin, J. J., & Chang, S. H. (2000). Characteristics of heavy metals on particles with different sizes from municipal solid waste incineration. *Journal of Hazardous Materials*, *79*(3), 229–239.
- Chen, J. S., Chu, P. Y., Chang, J. E., Lu, H. C., Wu, Z. H., & Lin, K. Y. (2008). Engineering and environmental characterization of municipal solid waste bottom ash as an aggregate substitute utilized for asphalt concrete. *Journal of Materials in Civil Engineering*, *20*(6).
- Chimenos, J. M., Segarra, M., Fernández, M. A., & Espiell, F. (1999). Characterization of the bottom ash in municipal solid waste incinerator. *Journal of Hazardous Materials*, *64*(3), 211–222.
- Cho, B. H., Nam, B. H., An, J., & Youn, H. (2020). Municipal solid waste incineration (MSWI) ashes as construction materials—a review. *Materials*, *13*(14), 1–30.
- Choudhary, J., Kumar, B., & Gupta, A. (2020). Utilization of solid waste materials as alternative fillers in asphalt mixes: A review. *Construction and Building Materials*, *234*, 117271.
- Churchill, E. V., & Amirkhanian, S. N. (1999). Coal ash utilization in asphalt concrete mixtures. *Journal of Materials in Civil Engineering*, *11*(4).
- Cornelis, G., Gerven, T., Van., & Vandecasteele, C. (2012). Antimony leaching from MSWI bottom ash: Modelling of the effect of pH and carbonation. *Waste Management*, *137*(3), 1284–1292.
- Defra. (2013). Incineration of municipal solid waste. [https://assets.publishing.service.gov.uk/government/uploads/system/uploads/attachment\\_data/file/221036/pb13889-incineration-municipal-waste.pdf](https://assets.publishing.service.gov.uk/government/uploads/system/uploads/attachment_data/file/221036/pb13889-incineration-municipal-waste.pdf).
- de S. Pereira, T., & Fernandino, G. (2019). Evaluation of solid waste management sustainability of a coastal municipality from northeastern Brazil. *Ocean and Coastal Management*, *179*, 104839. Available from <https://doi.org/10.1016/j.ocecoaman.2019.104839>.
- Diliberto, C., Meux, E., Diliberto, S., Garoux, L., Marcadier, E., Rizet, L., & Lecomte, A. (2020). A zero-waste process for the management of MSWI fly ashes: Production of ordinary Portland cement. *Environmental Technology (United Kingdom)*, *41*(9).
- Dou, X., Ren, F., Nguyen, M. Q., Ahamed, A., Yin, K., Chan, W. P., & Chang, V. W. C. (2017). Review of MSWI bottom ash utilization from perspectives of collective characterization, treatment and existing application. *Renewable and Sustainable Energy Reviews*, *79*, 24–38.
- Du, B., Li, J., Fang, W., Liu, Y., Yu, S., Li, Y., & Liu, J. (2018). Characterization of naturally aged cement-solidified MSWI fly ash. *Waste Management*, *80*, 101–111.
- Fei, F., Wen, Z., Huang, S., & De Clercq, D. (2018). Mechanical biological treatment of municipal solid waste: Energy efficiency, environmental impact and economic feasibility analysis. *Journal of Cleaner Production*, *178*, 731–739.
- Garrick, N. W., & Chan, K. L. (1993). Evaluation of domestic incinerator ash for use as aggregate in asphalt concrete. *Transportation Research Record*, *1418*, 30–34.
- Goh, A. T. C., & Tay, J. H. (1993). Municipal solid-waste incinerator fly ash for geotechnical applications. *Journal of Geotechnical Engineering*, *119*(5).
- Goh, S. W., & You, Z. (2008). A preliminary study of the mechanical properties of asphalt mixture containing bottom ash. *Canadian Journal of Civil Engineering*, *35*(10), 1114–1119.

- Hadidi, L. A., Ghaithan, A., Mohammed, A., & Al-Ofi, K. (2020). Deploying municipal solid waste management 3R-WTE framework in Saudi Arabia: Challenges and future. *Sustainability (Switzerland)*, 12(5711), 1–18. Available from <https://doi.org/10.3390/su12145711>.
- Hansen, H. K., Pedersen, A. J., Ottosen, L. M., & Villumsen, A. (2001). Speciation and mobility of cadmium in straw and wood combustion fly ash. *Chemosphere*, 45(1), 123–128.
- Hartmann, S., Koval, L., Škrobánková, H., Matýsek, D., Winter, F., & Purgar, A. (2015). Possibilities of municipal solid waste incinerator fly ash utilisation. *Waste Management and Research*, 33(8), 740–747. Available from <https://doi.org/10.1177/0734242X15587545>.
- Hassan, H. F., & Al-Shamsi, K. (2010). Characterisation of asphalt mixes containing MSW ash using the dynamic modulus  $IE^*$  test. *International Journal of Pavement Engineering*, 11(6), 575–582. Available from <https://doi.org/10.1080/10298436.2010.501865>.
- Hassan, M. M., & Khalid, H. (2008). Mix design and rutting resistance of bituminous mixtures containing incinerator bottom ash aggregates. In *Efficient transportation and pavement systems: Characterization, mechanisms, simulation, and modeling—proceedings of the 4th international gulf conference on roads*.
- Hassan, Mohamed Mostafa, & Khalid, H. (2010a). Mechanical and environmental characteristics of bituminous mixtures with incinerator bottom ash aggregates. *International Journal of Pavement Engineering*, 11, 83–94. Available from <https://doi.org/10.1080/10298430802524800>.
- Hassan, Mohamed Mostafa, & Khalid, H. A. (2010b). Compressive deformation behaviour of asphalt mixtures containing incinerator bottom ash aggregate. *Road Materials and Pavement Design*, 11(2), 633–652. Available from <https://doi.org/10.1080/14680629.2010.9690297>.
- Haukoht, J., Rand, T., & Marxen, U. (1999). Decision makers' guide to municipal solid waste incineration. *The World Bank*.
- Hjelmar, O. (2012). *How can ashes be expected to perform in relation to end-of waste criteria for waste-derived aggregates? Proceedings of the ash utilization, ashes in a sustainable society*. Sweden: Stockholm, January 25–27.
- Hu, Y., Zhang, P., Li, J., & Chen, D. (2015). Stabilization and separation of heavy metals in incineration fly ash during the hydrothermal treatment process. *Journal of Hazardous Materials*, 299, 149–157.
- Huang, C. M., Chiu, C., Te, Li, K. C., & Yang, W. F. (2006). Physical and environmental properties of asphalt mixtures containing incinerator bottom ash. *Journal of Hazardous Materials*, 137(3), 1742–1749.
- Huang, Y., Takaoka, M., & Takeda, N. (2003a). Chlorobenzenes removal from municipal solid waste incineration fly ash by surfactant-assisted column flotation. *Chemosphere*, 52(4), 735–743.
- Huang, Y., Takaoka, M., Takeda, N., & Oshita, K. (2003b). Polychlorinated biphenyls removal from weathered municipal solid waste incineration fly ash by collector-assisted column flotation. *Journal of Hazardous Materials*, 100(1–3), 259–270.
- Hyks, J. (2008). *Leaching from municipal solid waste incineration residues*. Technical. University of Denmark.
- Jing, Z., Matsuoka, N., Jin, F., Hashida, T., & Yamasaki, N. (2007). Municipal incineration bottom ash treatment using hydrothermal solidification. *Waste Management*, 27(2), 287–293.
- Joseph, A. M., Snellings, R., VandenHeede, P., Matthys, S., & DeBelie, N. (2018). The use of municipal solid waste incineration ash in various building materials: A Belgian point of view. *Materials*, 11(1), 1–30. 141. Available from <https://doi.org/10.3390/ma11010141>.
- Jovanov, D., Vujić, B., & Vujić, G. (2018). Optimization of the monitoring of landfill gas and leachate in closed methanogenic landfills. *Journal of Environmental Management*, 216, 32–40.

- Joumbat, R., Al Basiouni Al Masri, Z., Absi, J., & Elkordi, A. (2022a). Investigation of using Municipal solid waste incineration fly ash as alternative aggregates replacement in hot mix asphalt. *Road Materials and Pavement Design*, 24(5), 1290–1309. Available from <https://doi.org/10.1080/14680629.2022.2071756>.
- Joumbat, R., Al Basiouni Al Masri, Z., & Elkordi, A. (2022b). Dynamic modulus and phase angle of municipal solid waste incinerated fly ash used as filler substitution in asphalt concrete mixtures. *International Journal of Pavement Research and Technology*, 2022 (3), 1–21. Available from <https://doi.org/10.1007/s42947-022-00190-x>.
- Joumbat, R., Elkordi, A., Khatib, J., Al Basiouni Al Masri, Z., & Absi, J. (2022c). Characterisation of asphalt concrete mixes with municipal solid waste incineration fly ash used as fine aggregates substitution. *International Journal of Pavement Engineering*. Available from <https://doi.org/10.1080/10298436.2022.2099855>.
- Kahle, K., Kamuk, B., Kallesøe, J., Fleck, E., Lamers, F., Jacobsson, L., & Sahlén, J. (2015). Bottom ash from waste plants metal recovery and utilization. *ISWA (International Solid Waste Association)*.
- Kalbe, U., Berger, W., Eckardt, J., & Simon, F. G. (2008). Evaluation of leaching and extraction procedures for soil and waste. *Waste Management*, 28(6), 1027–1038.
- Kalogirou, E., & Themelis, N. (1937). Fly ash characteristics from waste-to-energy facilities and processes for ash stabilization. *Iswa.Org*.
- Kamaruddin, M. A., Yusoff, M. S., Rui, L. M., Isa, A. M., Zawawi, M. H., & Alrozi, R. (2017). An overview of municipal solid waste management and landfill leachate treatment: Malaysia and Asian perspectives. *Environmental Science and Pollution Research*, 24, 26988–27020.
- Kamon, M., Katsumi, T., & Sano, Y. (2000). MSW fly ash stabilized with coal ash for geotechnical application. *Journal of Hazardous Materials*, 76(2–3), 265–283.
- Keppert, M., Pavlík, Z., Tydlitát, V., Volfová, P., Švarcová, S., Šyc, M., & Černý, R. (2012). Properties of municipal solid waste incineration ashes with respect to their separation temperature. *Waste Management and Research*, 30(10), 1041–1048.
- Khalid, M. (2019). *An investigation into the treatment and modeling of municipal solid waste incineration (MSWI) air pollution APC residues*. London: University of East London.
- Kim, J., An, J., Nam, B. H., & Tasneem, K. M. (2016). Investigation on the side effects of municipal solid waste incineration ashes when used as mineral addition in cement-based material. *Road Materials and Pavement Design*, 17(2), 345–364.
- Kono, J., Ostermeyer, Y., & Wallbaum, H. (2018). Investigation of regional conditions and sustainability indicators for sustainable product development of building materials. *Journal of Cleaner Production*, 196, 1356–1364.
- Ksaibati, K., & Plancher, H. (2005). *Moisture resistance of bottom ash*. Laramie: University of Wyoming.
- Lam, C. H. K., Ip, A. W. M., Barford, J. P., & McKay, G. (2010). Use of incineration MSW ash: A review. *Sustainability*, 2, 1943–1968. Available from <https://doi.org/10.1016/10.3390/su2071943>.
- Lentz, D., Demars, K.R., Long, R.P., & Garrick, N.W. (1994). Performance and analysis of incinerator bottom ash as structural fill. University of Connecticut, JHR 94-232.
- Levaggi, L., Levaggi, R., Marchiori, C., & Trecroci, C. (2020). Waste-to-energy in the EU: The effects of plant ownership, waste mobility, and decentralization on environmental outcomes and welfare. *Sustainability (Switzerland)*, 12(14): 5743, 1–12.
- Li, M., Xiang, J., Hu, S., Sun, L. S., Su, S., Li, P. S., & Sun, X. X. (2004). Characterization of solid residues from municipal solid waste incinerator. *Fuel*, 83(10), 1397–1405.

- Liu, D., Li, L., & Cui, H. (2014). Utilization of municipal solid waste Incinerator Bottom Ash Aggregate in asphalt mixture. In *Asphalt pavements—proceedings of the international conference on asphalt pavements, ISAP 2014*.
- Lu, Y., Tian, A., Zhang, J., Tang, Y., Shi, P., Tang, Q., & Huang, Y. (2020). Physical and chemical properties, pretreatment, and recycling of municipal solid waste incineration fly ash and bottom ash for highway engineering: A literature review. *Advances in Civil Engineering*, 2020, 1–17. Available from <https://doi.org/10.1155/2020/8886134>.
- Luo, H., Cheng, Y., He, D., & Yang, E. H. (2019). Review of leaching behavior of municipal solid waste incineration (MSWI) ash. *Science of the Total Environment*, 668, 90–103.
- Luo, H., Law, W. W., Wu, Y., Zhu, W., & Yang, E. H. (2018). Hydrothermal synthesis of needle-like nanocrystalline zeolites from metakaolin and their applications for efficient removal of organic pollutants and heavy metals. *Microporous and Mesoporous Materials*, 272, 8–15.
- Luo, H. L., Chen, S. H., Lin, D. F., & Cai, X. R. (2017). Use of incinerator bottom ash in open-graded asphalt concrete. *Construction and Building Materials*, 149, 497–506.
- Lynn, C. J., Ghataora, G. S., & Dhir OBE, R. K. (2017). Municipal incinerated bottom ash (MIBA) characteristics and potential for use in road pavements. *International Journal of Pavement Research and Technology*, 10(2), 185–201.
- Malinauskaitė, J., Jouhara, H., Czajczyńska, D., Stanchev, P., Katsou, E., Rostkowski, P., Thorne, R. J., Colón, J., Ponsá, S., Al-Mansour, F., Anguilano, L., Krzyżyńska, R., López, I. C., Vlasopoulos, A., & Spencer, N. (2017). Municipal solid waste management and waste-to-energy in the context of a circular economy and energy recycling in Europe. *Energy*, 141, 2013–2044.
- Mangialardi, T. (2003). Disposal of MSWI fly ash through a combined washing-immobilisation process. *Journal of Hazardous Materials*, 98(1–3), 225–240.
- Meima, J. A., & Comans, R. N. J. (1997). Geochemical modeling of weathering reactions in municipal solid waste incinerator bottom ash. *Environmental Science and Technology* (19), 31(5), 1269–1276.
- Melaku, R., Ness, S., Gedafa, B., & Suleiman, N. (2022). Investigating the use of fly ash for sustainable asphalt binders. Eleventh International Conference on the Bearing Capacity of Roads, Railways and Airfields, Volume 3 – Hoff, Mork & Saba (eds). 436–444.
- Millrath, K., Roethel, F. J., & Kargbo, D. M. (2004). Waste-to-energy residues—The search for beneficial uses. *Proceedings of 12TH Annual North American Waste to Energy Conference, NAWTEC12*.
- Mirković, K., Tošić, N., & Mladenović, G. (2019). Effect of different types of fly ash on properties of asphalt mixtures. *Advances in Civil Engineering*, 2019, 1–11. Available from <https://doi.org/10.1155/2019/8107264>.
- Mizutani, S., Yoshida, T., Sakai, S. I., & Takatsuki, H. (1996). Release of metals from MSW I fly ash and availability in alkali condition. *Waste Management*, 16(5–6), 537–544.
- Mohammed Alhassan, H., & Tanko, A. M. (2012). Characterization of solid waste incinerator bottom ash and the potential for its use. *International Journal of Engineering Research and Applications (IJERA)*, 2(4), 516–522.
- Musselman, C. N., Killeen, M. P., Crimi, D., Hasan, S., Zhang, X., Gress, D. L., & Eighmy, T. T. (1994). The Laconia, New Hampshire bottom ash paving project. *Studies in Environmental Science*.
- Ni, P., Xiong, Z., Tian, C., Li, H., Zhao, Y., Zhang, J., & Zheng, C. (2017). Influence of carbonation under oxy-fuel combustion flue gas on the leachability of heavy metals in MSWI fly ash. *Waste Management*, 67, 171–180.



- Ogunro, V. O., Inyang, H. I., Hooper, F., Young, D., & Oturkar, A. (2004). Gradation control of bottom ash aggregate in superpave bituminous mixes. *Journal of Materials in Civil Engineering*, 16(6), 604–613.
- Paranavithana, S., & Mohajerani, A. (2006). Effects of recycled concrete aggregates on properties of asphalt concrete. *Resources, Conservation and Recycling*, 48(1), 1–12.
- Pecorini, I., Baldi, F., Bacchi, D., Camevale, E. A., & Corti, A. (2017). Leaching behaviour of hazardous waste under the impact of different ambient conditions. *Waste Management*, 63, 96–106.
- Penque, A. (2007). *Examination of chlorides in municipal solid waste to energy combustion residue: Origins, fate and potential for treatment*. New York: Columbia University.
- Rendek, E., Ducom, G., & Germain, P. (2006). Carbon dioxide sequestration in municipal solid waste incinerator (MSWI) bottom ash. *Journal of Hazardous Materials*, 128(1), 73–79.
- Romeo, E., Mantovani, L., Tribaudino, M., & Montepara, A. (2018). Reuse of stabilized municipal solid waste incinerator fly ash in asphalt mixtures. *Journal of Materials in Civil Engineering*, 30(8).
- Rémond, S., Pimienta, P., & Bentz, D. P. (2002). Effects of the incorporation of municipal solid waste incineration fly ash in cement pastes and mortars: I. Experimental study. *Cement and Concrete Research*, 32(2), 303–311.
- Sabbas, T., Poletini, A., Pomi, R., Astrup, T., Hjelmar, O., Mostbauer, P., Cappai, G., Magel, G., Salhofer, S., Speiser, C., Heuss-Assbichler, S., Klein, R., & Lechner, P. (2003). Management of municipal solid waste incineration residues. *Waste Management*, 23(1), 61–88.
- Santagata, E., Bassani, M., & Baglieri, O. (2014). Use of vitrified municipal solid waste bottom ash as a filler substitute in asphalt mixtures. In *Sustainability, eco-efficiency and conservation in transportation infrastructure asset management—Proceedings of the 3rd international conference on transportation infrastructure, ICTI 2014*.
- Santos, R. M., Mertens, G., Salman, M., Cizer, Ö., & Van Gerven, T. (2013). Comparative study of ageing, heat treatment and accelerated carbonation for stabilization of municipal solid waste incineration bottom ash in view of reducing regulated heavy metal/metalloid leaching. *Journal of Environmental Management*, 128, 807–821.
- Scaglia, B., Salati, S., Di Gregorio, A., Carrera, A., Tambone, F., & Adani, F. (2013). Short mechanical biological treatment of municipal solid waste allows landfill impact reduction saving waste energy content. *Bioresource Technology*, 143, 131–138.
- Shi, D., Hu, C., Zhang, J., Li, P., Zhang, C., Wang, X., & Ma, H. (2017). Silicon-aluminum additives assisted hydrothermal process for stabilization of heavy metals in fly ash from MSW incineration. *Fuel Processing Technology*, 165, 44–53.
- Shi, H. S., & Kan, L. L. (2009). Leaching behavior of heavy metals from municipal solid wastes incineration (MSWI) fly ash used in concrete. *Journal of Hazardous Materials*, 164(2–3), 750–754.
- Shimaoka, T., Miyawaki, K., Hanashima, M., & Hirao, T. (2001). Application of bottom ash as road construction material. *Beneficial use of recycled materials in transportation applications*, 759–769. Arlington, Virginia. Available from <http://worldcat.org/isbn/0923204490>.
- Show, K.-Y., Tay, J.-H., & Cheong, H.-K. (2000). *Reuse of incinerator ash—current and future trends. Sustainable construction: Use of incinerator ash*. London: Thomas Telford Publishing.
- Shuler, T.S. (1976). *The effects of bottom ash upon bituminous sand mixtures*. Publication FHWA/IN/JHRP-76/11. Joint Highway Research Project, Indiana Department of Transportation and Purdue University, West Lafayette, IN.

- Singh, R. P., Tyagi, V. V., Allen, T., Ibrahim, M. H., & Kothari, R. (2011). An overview for exploring the possibilities of energy generation from municipal solid waste (MSW) in Indian scenario. *Renewable and Sustainable Energy Reviews*, *15*(9), 4797–4808.
- Sobolev, K., Flores Vivian, I., Saha, R., Wasiuddin, N. M., & Saltibus, N. E. (2014). The effect of fly ash on the rheological properties of bituminous materials. *Fuel*, *116*, 471–477.
- Song, G. J., Kim, K. H., Seo, Y. C., & Kim, S. C. (2004). Characteristics of ashes from different locations at the MSW incinerator equipped with various air pollution control devices. *Waste Management*, *24*(1), 99–106.
- Speiser, C., Baumann, T., & Niessner, R. (2001). Characterization of municipal solid waste incineration (MSWI) bottom ash by scanning electron microscopy and quantitative energy dispersive x-ray microanalysis (SEM/EDX). *Fresenius' Journal of Analytical Chemistry*, *370*, 752–759. Available from <https://doi.org/10.1007/s002160000659>.
- Stabile, P., Bello, M., Petrelli, M., Paris, E., & Carroll, M. R. (2019). Vitrification treatment of municipal solid waste bottom ash. *Waste Management*, *95*, 250–258.
- Tang, Q., Gu, F., Chen, H., Lu, C., & Zhang, Y. (2018). Mechanical evaluation of bottom ash from municipal solid waste incineration used in roadbase. *Advances in Civil Engineering*, *2018*, 1–8. Available from <https://doi.org/10.1155/2018/5694908>.
- Tapkin, S. (2008). Mechanical evaluation of asphalt-aggregate mixtures prepared with fly ash as a filler replacement. *Canadian Journal of Civil Engineering*, *35*(1), 27–40.
- Tay, J., & Goh, A. T. C. (1991). Engineering properties of incinerator residue. *Journal of Environmental Engineering*, *117*(2), 210–224.
- Toledo, M., Siles, J. A., Gutiérrez, M. C., & Martín, M. A. (2018). Monitoring of the composting process of different agroindustrial waste: Influence of the operational variables on the odor impact. *Waste Management*, *76*, 266–274.
- Tuncan, M., Tuncan, A., & Cetin, A. (2003). The use of waste materials in asphalt concrete mixtures. *Waste Management and Research*, *21*(2), 83–92.
- U S Environmental Protection. (2010). *Municipal solid waste generation, recycling, and disposal in the united states: Facts and figures for 2010*. AMBRA GmbH.
- Vehlow, J. (2012). Waste-to-energy ash management in Europe. In R. A. Meyers (Ed.), *Encyclopedia of sustainability science and technology*. New York: Springer.
- Wang, F. H., Zhang, F., Chen, Y. J., Gao, J., & Zhao, B. (2015). A comparative study on the heavy metal solidification/stabilization performance of four chemical solidifying agents in municipal solid waste incineration fly ash. *Journal of Hazardous Materials*, *300*, 451–458.
- Wiles, C., & Shepherd, P. (1999). *Beneficial use and recycling of municipal waste combustion residues—A comprehensive resource document*. National Renewable Energy Laboratory (NREL), Boulder, CO.
- Wiles, C. C. (1996). Municipal solid waste combustion ash: State-of-the-knowledge. *Journal of Hazardous Materials*, *47*(1–3), 325–344.
- Xia, Y., He, P., Shao, L., & Zhang, H. (2017). Metal distribution characteristic of MSWI bottom ash in view of metal recovery. *Journal of Environmental Sciences (China)*, *52*, 178–189.
- Xinghua, H., Shujing, Z., & Hwang, J. Y. (2016). Physical and chemical properties of MSWI fly ash. *Characterization of Minerals, Metals, and Materials*, *2016*, 451–459. Available from [https://doi.org/10.1007/978-3-319-48210-1\\_56](https://doi.org/10.1007/978-3-319-48210-1_56).
- Xue, Y., Hou, H., Zhu, S., & Zha, J. (2009). Utilization of municipal solid waste incineration ash in stone mastic asphalt mixture: Pavement performance and environmental impact. *Construction and Building Materials*, *23*(2), 989–996.

- Yan, K., Li, L., Zheng, kaigao, & Ge, D. (2019). Research on properties of bitumen mortar containing municipal solid waste incineration fly ash. *Construction and Building Materials*, *218*, 657–666.
- Yao, J., Li, W. B., Tang, M., Fang, C. R., Feng, H. J., & Shen, D. S. (2010). Effect of weathering treatment on the fractionation and leaching behavior of copper in municipal solid waste incinerator bottom ash. *Chemosphere*, *81*(5), 571–576. Available from <https://doi.org/10.1016/j.chemosphere.2010.08.038>.
- Yao, Q., Samad, N. B., Keller, B., Seah, X. S., Huang, L., & Lau, R. (2014). Mobility of heavy metals and rare earth elements in incineration bottom ash through particle size reduction. *Chemical Engineering Science*, *118*, 214–220.
- Yin, K., Dou, X., Ren, F., Chan, W. P., & Chang, V. W. C. (2018a). Statistical comparison of leaching behavior of incineration bottom ash using seawater and deionized water: Significant findings based on several leaching methods. *Journal of Hazardous Materials*, *344*, 635–648. Available from <https://doi.org/10.1016/j.jhazmat.2017.11.004>.
- Yin, K., Chan, W. P., Dou, X., Ren, F., & Wei-Chung Chang, V. (2018b). Cr, Cu, Hg and Ni release from incineration bottom ash during utilization in land reclamation—Based on lab-scale batch and column leaching experiments and a modeling study. *Chemosphere*, *197*, 741–748.
- Yu, J., Sun, L., Xiang, J., Jin, L., Hu, S., Su, S., & Qiu, J. (2013). Physical and chemical characterization of ashes from a municipal solid waste incinerator in China. *Waste Management and Research*, *31*(7), 663–673. Available from <https://doi.org/10.1177/0734242X13485793>.
- Yuan, Y., Zhu, X., Li, L., & Wang, H. (2017). Effect of the interfacial zone on the tensile-damage behavior of an asphalt mixture containing MSWI bottom ash aggregates. *Journal of Materials in Civil Engineering*, *29*(4).
- Zafar, S. (2018). Waste management outlook for the middle east. In: Brinkmann, R., Garren, S. (eds) *The Palgrave Handbook of Sustainability*. Palgrave Macmillan, Cham. Available from [https://doi.org/10.1007/978-3-319-71389-2\\_9](https://doi.org/10.1007/978-3-319-71389-2_9).
- Zeng, M., & Ksaibati, K. (2003). Evaluation of moisture susceptibility of asphalt mixtures containing bottom ash. *Transportation Research Record*, *1832*(1), 25–33.
- Zhang, J., Zhang, S., & Liu, B. (2020). Degradation technologies and mechanisms of dioxins in municipal solid waste incineration fly ash: A review. *Journal of Cleaner Production*, *250*, 119507. Available from <https://doi.org/10.1016/j.jclepro.2019.119507>.
- Zhang, Y., Cetin, B., Likos, W. J., & Edil, T. B. (2016). Impacts of pH on leaching potential of elements from MSW incineration fly ash. *Fuel*, *184*, 815–825.

# Ecology-based green clay–hemp brick material made with ground granulated blast-furnace slag

18

*Jonathan Oti<sup>1</sup>, John Kinuthia<sup>1</sup> and Mehmet Serkan Kirgiz<sup>2</sup>*

<sup>1</sup>School of Engineering, Faculty of Computing, Engineering and Science, University of South Wales, Pontypridd, United Kingdom, <sup>2</sup>Northwestern University, Chicago, IL, United States

## 18.1 Introduction

Research has shown that about 30% of the global CO<sub>2</sub> emissions arise due to high energy usage in activities associated with the production of construction and building materials (Oti, Kinuthia, et al., 2010; Oti, 2010; Biswas, 2014; UNEP, 2009). Much of the energy used in building materials takes place in the manufacture of a few extensively used materials, which involve high-temperature kiln processes, notably iron and steel, cement, clay bricks plus tiles, and glass. Therefore, energy-saving strategy concentrating on low carbon building material development intended at achieving a zero-to-negative carbon profile in building, using industrial by-product materials and low-energy additives, is a development that will benefit both the present and future generations and is a step toward more sustainable building construction (Oti et al., 2010; Oti, 2010).

At the present time, energy price trends are high because of the scarcity of energy sources, while energy consumption is increasing continuously worldwide. Researchers have been working hard to reduce the energy usage and CO<sub>2</sub> emission in clay building masonry units. For example, the study by Webb (1994) on mechanical pressed stabilized soil products was able to achieve a saving of at least 40% of the energy usage in a building by using stabilized soil blockwork walling, when compared to concrete blockwork. Venkatarama Reddy and Jagadish (2003) studied the embodied energy of common and alternative building materials. A comparison of the energy content of steam-cured soil blocks and burnt bricks was made. Their finding showed that steam-cured soil blocks are 35% more energy efficient than burnt clay bricks. Esmeray and Atis (2019) reported on the potential of utilizing sewage sludge, oven slag, and fly ash for clay brick production. Sutcu et al. (2019) reported on the use of recycled bottom ash and fly ash wastes for eco-friendly clay brick production. Other workers (Kariyawasam & Jayasinghe, 2016; Khadka & Shakya, 2016; Dao et al., 2018) used chemical stabilizers such as cement or lime to soil to improve mechanical characteristics. Unfortunately, the addition of chemical stabilizers reduces the moisture buffering capacity and hygrothermal inertia of the

material (McGregor et al., 2014; Arrigoni et al., 2017) while largely increasing the carbon footprint (Worrell et al., 2001). Labat et al. (2016) produced straw-clay materials with a density of 241–531 kg/m<sup>3</sup> and thermal conductivity of 0.071–0.12 W/(m K). Al Rim et al. (1999) produced clay–cement–wood composites with a density of 370–1170 kg/m<sup>3</sup> and thermal conductivity from 0.08 to 0.24 W/(m K). Mazhoud et al. (2017) reported on the mechanical properties of hemp–clay and hemp stabilized clay composites. Renouard et al. (2014) reported on the characterization of ultrasonic impact on coir, flax, and hemp fibers.

The key sustainability issue this book chapter intends to address is the current lack of significant engagement regarding the utilization of waste from various industrial processes in the building industry. It should be noted that the use of activated slag such as ground granulated blast-furnace slag (GGBS) with clay waste and natural fiber in building components (outside use in normal concrete applications) is rare in the UK. This paper and any viable building products emerging from it are therefore quite innovative.

## 18.2 Methodology

### 18.2.1 Materials

The Lower Oxford Clay (LOC) used in this study was supplied by Hanson Brick Company Ltd., from their Stewartby brick plant in Bedfordshire, UK. The chemical and physical properties of the LOC are listed in Table 18.1. Two types of lime were used in this study. L1 is quicklime (CaO) while L2 is hydraulic lime. Both L1 and L2 were supplied by Tŷ-Mawr Lime Ltd., Llangasty, Brecon, UK. The use of lime for clay soil stabilization has been extensively applied in civil engineering practices such as foundations, roadbeds, embankments, and piles (Boardman et al., 2001). In practice, between 1 and 3 wt.% lime is needed for modifying soil properties and between 2 and 8 dry wt.% lime for stabilization. Previous research work by the current research team used 6 wt.% lime (Oti & Kinuthia, 2012a) for the stabilization of kaolinite clay for road construction. In the current work, a maximum dosage of 4 wt.% lime was chosen after several laboratory trials. GGBS used in this work was in compliance with BS EN 15167-1:2006 (BS EN 15167-1, 2006), and it is a by-product material generated from the iron-making industry. The Portland cement (PC) was manufactured in accordance with BS EN 197-1:2011 (BS EN 197-1, 2011). The chemical and physical properties of the GGBS and PC are listed in Table 18.1. The industrial hemp used in this research work was supplied by Lime Technology UK; it is a specially processed hemp for the construction application that provides optimum characteristics from vapor permeability and thermal and acoustic insulation. It is produced in commercial quantities by Lhoist UK, Buxton, Derbyshire. Industrial hemp is a natural material that has the potential to reduce not only the CO<sub>2</sub> emissions but also serve as a renewable building resource. It is the wood (fibrous) part of the hemp called hemp shiv that is used as a composite with the binder. The engineering properties of the industrial hemp used for this current

**Table 18.1** Chemical and physical properties of Lower Oxford Clay, quicklime, hydraulic lime GGBS, and PC.

Oxides	LOC	L1	L2	GGBS	PC
CaO	6.15	89.2	66.6	41.99	63.00
SiO <sub>2</sub>	46.73	3.25	4.77	35.35	20.00
Al <sub>2</sub> O <sub>3</sub>	18.51	0.19	1.49	11.59	6.00
MgO	1.13	0.45	0.56	8.04	4.21
Fe <sub>2</sub> O <sub>3</sub>	6.21	0.16	0.71	0.35	3.00
MnO	0.07	0.05	0.08	0.45	0.03–1.11
S <sup>2-</sup>	–	< 0.01	< 0.01	1.18	–
SO <sub>3</sub>	–	2.05	< 0.01	0.23	2.30
SO <sub>4</sub>	–	2.46	< 0.01	–	–
CaCO <sub>3</sub>	–	–	–	–	–
TiO <sub>2</sub>	1.13	–	–	–	–
K <sub>2</sub> O	4.06	0.01	0.25	–	–
N <sub>2</sub> O	–	0.02	0.04	–	–
FeO	0.8	–	–	–	–
P <sub>2</sub> O <sub>5</sub>	0.17	–	–	–	–
Na <sub>2</sub> O	0.52	–	–	–	–
CO <sub>3</sub>	–	4.00	3.00	–	–
Soluble silica	–	1.10	4.77	–	–
<b>Physical properties</b>					
Insoluble residue	–	4.1	2	0.3	0.5
Bulk density (kg/m <sup>3</sup> )	(1100–1250)	(1150–1300)	490	1200	1400
Relative density	2.63	2.8	2.4	2.9	3.1
Blaine fineness (m <sup>2</sup> /kg)	–	430–1450	300–1400	450	365
pH	–	13.9	12.9	–	–
Liquid limit (LL) (%)	67	–	–	–	–
Plastic limit (PL) (%)	35	–	–	–	–
Plasticity index (%)	32	–	–	–	–
Color	Gray	Off-white	White	Off-white	Gray
Glass content	–	–	–	≈ 90	–
<b>Notation</b>					
LOC	Lower Oxford Clay				
L1	Quicklime				
L2	Hydraulic lime				
GGBS	Ground granulated blast-furnace slag				
PC	Portland cement				

**Table 18.2** Engineering properties of the industrial hemp.

Properties	Composition
Flux content (%)	35
Hiv content (%)	65
Length of hiv (mm)	8.1–15
Width of hiv (mm)	0.6–1.5
Thickness of hiv (mm)	2–6.5
Bulk density (kg/m <sup>3</sup> )	82
Rate of water absorption (%)	117

work are listed in Table 18.2. The orientation of the mineral planes of the natural hemp in the X-ray diffractometer is shown in Fig. 18.1. Analysis of the results shows four very strong peaks for Ca, SiO<sub>2</sub>, MAD-10 Feldspar, and Wollastonite. The quantification of the element by weight % showed that the hemp consists mainly of 44.67% C K, 52.89% O K, 0.09% Mg K, 0.06% AL K, 0.27% Si K, 0.14% S K, 1.20% K K, 0.69% Ca K, and 0.19% Cu K.

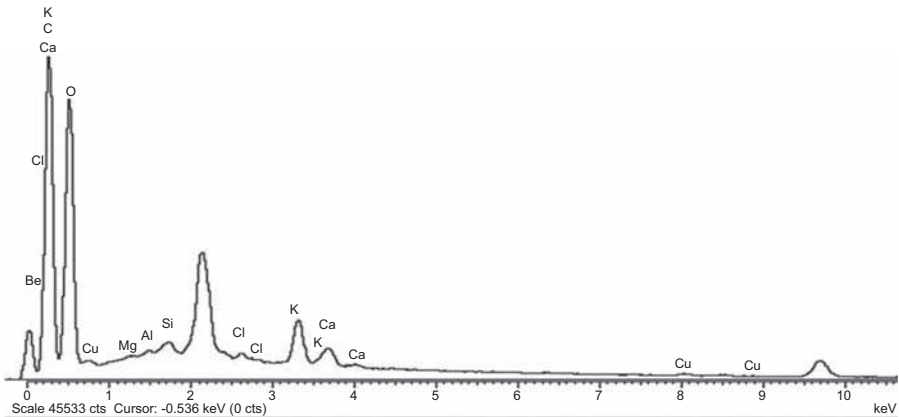


**Figure 18.1** X-ray diffraction of the hemp fiber (C = Ca, O = SiO<sub>2</sub>, Mg = MgO, Al = Al<sub>2</sub>O<sub>3</sub>, Si = SiO<sub>2</sub>, Cl = KCl, K = MAD-10 Feldspar, Ca = Wollastonite).

### 18.2.2 Mix composition, sample preparation, and testing

Table 18.5 reports the details of the mix compositions of the stabilized cylinder specimens made using varying proportions of the two types of lime (L1 and L2) or PC blended with GGBS to stabilize the LOC and industrial hemp at 20% maximum stabilizer content. The clay content in the mix design was replaced by 2% industrial hemp shiv to improve the carbon profile of the stabilized mixture.

A series of trials for blend optimization was conducted by the authors in their previous studies (Oti et al., 2009, 2010; Oti, 2010; Oti & Kinuthia, 2012b; Kinuthia & Oti, 2012). At the end of the trials, optimal blending ratios (4%L: 16%GGBS and 4%PC: 16%GGBS) were adopted, based on the experience gathered by the authors in their previous research work (Oti et al., 2008a, 2008b, 2010; Oti, 2010). For sample preparation, it was found necessary to establish target dry density and moisture content values. Therefore, Proctor Compaction tests were carried out in accordance with BS 1924-2: 1990 (BS 1924-2, 1990); for details, see previous studies (Oti et al., 2010; Oti, 2010) (Table 18.3).

**Table 18.3** Mix composition of the blended hemp–LOC mixture (material for one cylindrical test specimen).

Stabilizers	Mix code	Moisture	Lime	Lime	PC	GGBS	LOC	Hemp	Water
		Content	L1	L2					
L1–GGBS	4%L1:16%GGBS	27%	10.5		0	42	257.25	5.25	85
L2–GGBS	4%L2:16%GGBS	27%	0	10.5	0	42	257.25	5.25	85
PC–GGBS	4%PC:16%GGBS	27%	0	0	10.5	42	257.25	5.25	85
L1–GGBS	4%L1:16%GGBS	30%	10.5		0	41	251.86	5.14	92
L2–GGBS	4%L2:16%GGBS	30%	0	10.5	0	41	251.86	5.14	92
PC–GGBS	4%PC:16%GGBS	30%	0	0	10.5	41	251.86	5.14	92
L1–GGBS	4%L1:16%GGBS	33%	10.5	0	0	40.1	245.6	5	99.3
L2–GGBS	4%L2:16%GGBS	33%	0	10.5	0	40.1	245.6	5	99.3
PC–GGBS	4%PC:16%GGBS	33%	0	0	10.5	40.1	245.6	5	99.3

In the current research work, a much higher stabilizer dosage of 20% was used to ensure that the manufactured product is capable of carrying loads for medium-higher application, as required by most building standards and not merely for low-cost category; for detail, see previous works (Oti et al., 2010; Oti, 2010).

Dry materials capable of producing three compacted cylindrical test specimens, each of dimensions 50 mm in diameter and 100 mm in length, were thoroughly mixed in a variable-speed Kenwood Chef Major KM250 mixer; for detail, see previous works (Oti et al., 2010; Oti, 2010). Immediately after mixing, the materials were compressed into cylinders, to the prescribed dry density and moisture content. A steel mold fitted with a collar was used to accommodate all the material required for one sample, and specimen compaction was carried out using a hydraulic jack. After compaction, the cylinder specimens were extruded (see Fig. 18.2), using a steel plunger. They were then weighed, wrapped in cling film, and labeled before being placed in sealed plastic containers at room temperature of about  $20^{\circ}\text{C} \pm 2^{\circ}\text{C}$ . The samples were then moist cured for 3, 7, 14, and 28 days.



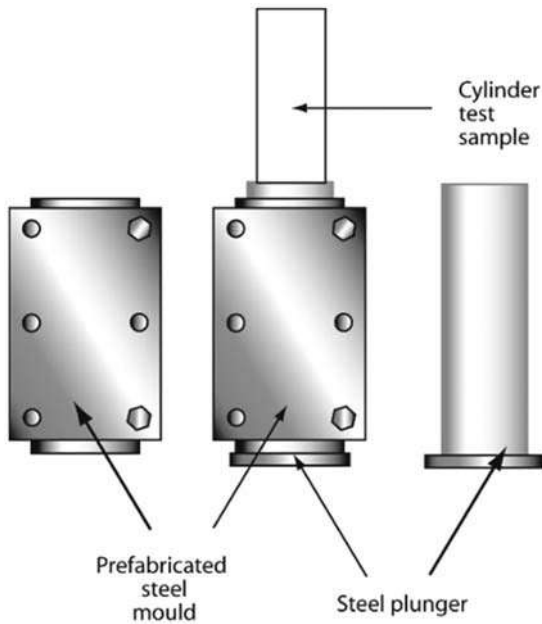


**Figure 18.2** Steel mold (extension collar not shown) and the extruded cylindrical test specimen.

Two cylindrical test specimens representing each of the various mix compositions were prepared for durability testing (resistance to linear expansion upon partial soaking in water). To affect partial soaking, the cling film wrapping the test specimens was carefully cut and removed at about the bottom 10 mm, using a sharp razor. The samples were then placed on a platform in a plastic tank, with the exposed surface in contact with the platform. The specimens were then allowed to moist cure in the tank, by ensuring that water was always present below the platform upon which the test specimens were placed. To minimize evaporation and drying out of the test specimens, the plastic container was fitted with a lid that was always used to cover the container. The lid was also fitted with a digital gauge to monitor linear expansion (see [Fig. 18.3](#)).

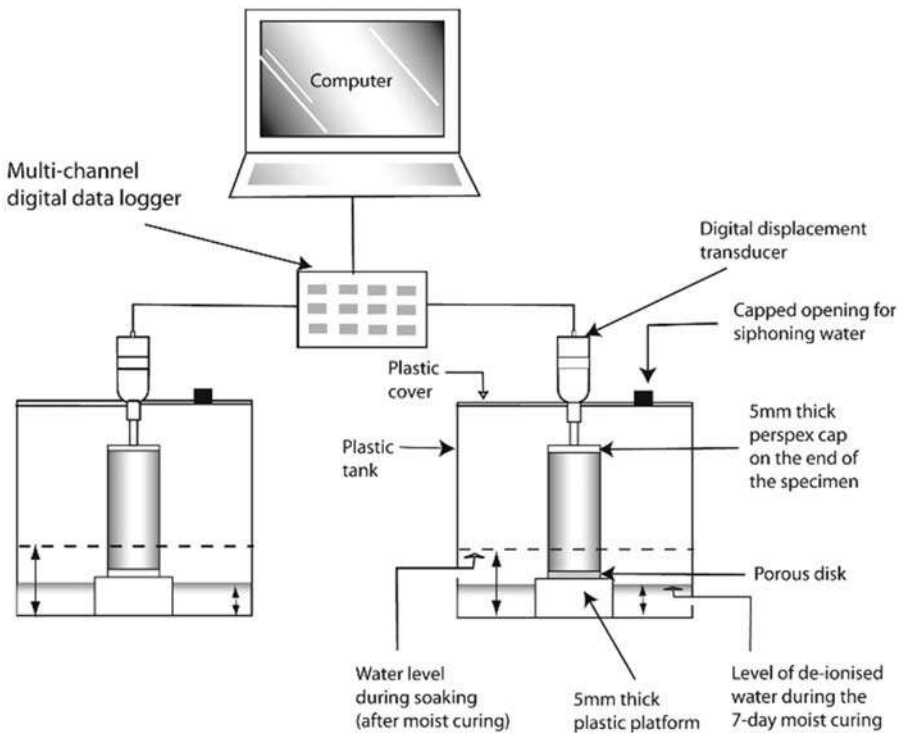


**Figure 18.3** A 64-channel data logger (MX2000 VJ Tech) for recording linear expansion measurements.

This process of moist curing was allowed to take place for the initial 7 days of specimen preparation. Thereafter, the specimens were partially immersed in water to a depth of 10 mm above their base by carefully increasing the water level in the tank with a siphon, thus ensuring minimal disturbance of the specimens. This process of curing after raising the water level is referred to as soaking. Linear expansion measurements were recorded during moist curing and subsequent soaking. This was done automatically, and the readings were recorded by a computer digital device every 12 hours.

The monitoring of the linear expansion measurements was completed on a daily basis until no further significant expansion was observed. Both the moist-curing and soaking environments were within sealed systems in order to reduce the availability of carbon dioxide that would otherwise cause carbonation of the lime in the hydrating system, which may reduce the amount of lime available for pozzolanic reaction. For soaking, deionized water was used to avoid specimen contamination from metallic or other ion species in the water.

A total of 126 test cylinder specimens were prepared, 108 for strength testing and 18 for linear expansion tests. At the end of the curing period, three samples per

mix proportion were tested for compressive strength at the age of 3, 7, 14, and 28 days in accordance with BS 1924-2: 1990 (BS 1924-2, 1990), using a Hounsfield testing machine at a compression loading rate of 1 mm/min. Two samples per mix proportion at the moisture content of 27%, 30%, and 33% were used to determine the linear expansion behavior of the compacted cylinders during moist curing and during subsequent soaking in deionized water.

## 18.3 Result and discussion

### 18.3.1 Strength development of the lime–GGBS and PC–GGBS stabilized systems

The compressive strength results of L1–GGBS, L2–GGBS, and PC–GGBS cylinder specimens compacted at 27%, 30%, and 33% moisture content and cured at room temperature of about  $20^{\circ}\text{C} \pm 2^{\circ}\text{C}$  for up to 28 days are shown in Fig. 18.4A–D. It was observed that at the early curing ages (3 days), the L2–GGBS and PC–GGBS blends exhibited lower strength values than that of L1–GGBS.

The highest strength value obtained at the end of the 3-day moist curing was  $857 \text{ kN/m}^2$  at 27% compaction moisture content. Similar trends were observed at 7 and 14 days of curing age (the L1–GGBS blend stabilized cylinder specimens tended to have higher strength value at all compaction moisture content).

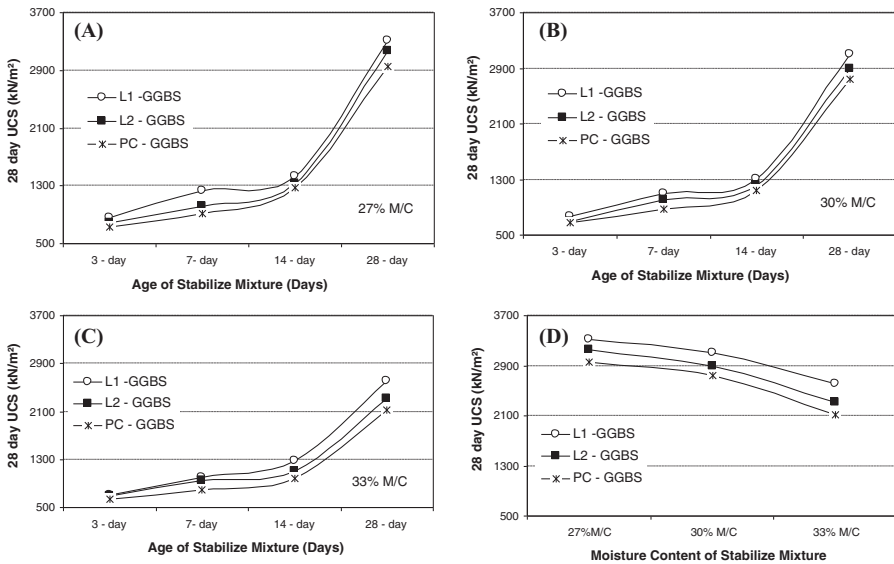


Figure 18.4 (A–D) Strength development of various stabilized systems.

At the end of the 28-day moist curing period, there was a significant improvement in the strength values of all compacted cylinder specimens at 27%, 30%, and 33% compaction moisture contents. As observed previously (3, 7, and 14 days), the highest strength value this time was 3316 kN/m<sup>2</sup>, again this value was for the L1–GGBS mixture. It is interesting to note that previous work (Kinuthia & Oti, 2012) with mixes without hemp indicates that there is significant strength gain with age up to 28 days for the mixtures stabilized with lime and GGBS (L1–GGBS and L2–GGBS), and the highest strength of 3200 kN/m<sup>2</sup> was observed for mix L1–GGBS at 27%. The gain in unconfined compressive strength with age was lower for the mixture with PC and GGBS (PC–GGBS) at all compaction moisture contents. The lime-activated GGBS stabilizer has significantly higher influence on strength than the equivalent PC-based system as observed from the results and the addition of hemp has a higher influence on strength development at the end of the 28-day moist curing period.

The overall performance of the two different limes and PC, each blended with GGBS, shows that when the compaction moisture content was increased from 27% up to 33%, the strength values of the cylinder specimen for all blended stabilized mixtures were significantly reduced.

The mechanism for the hydration cycle may be complex and can be difficult to explain in detail. But in general, one major activity that takes place is the modification of the soil as a result of ion exchange. The other activity that takes place during the hydration process is the solidification of the clay soil as a result of pozzolanic reaction. The difference in the hydration reactions between lime and GGBS may lead to a difference in the microstructure of the stabilized system. The reactions that take place may be very complex, for example, the calcium oxide (CaO) from lime or GGBS may react with the clay soil particles to form calcium hydroxide Ca(OH)<sub>2</sub>. The system may have high concentrations of calcium ions (Ca<sup>2+</sup>) and hydroxide ions (OH<sup>-</sup>). Then, an exchange of cation may occur in the whole system, and during this process, sodium ion (Na<sup>+</sup>) and potassium ion (K<sup>+</sup>) are displaced (Oti et al., 2010; Oti, 2010).

The replacement of monovalent sodium and potassium ions by divalent calcium ions during the ion exchange process may induce changes in the soil properties within the first hour of the hydration process. The concentration of divalent calcium ions induces the flocculation of the clay colloids which then transform the plastic soil particles to a granular state, while the monovalent sodium and potassium ions enhance dispersion. The sodium ion (Na<sup>+</sup>) and potassium ion (K<sup>+</sup>) in the lime and GGBS potentially increase the exchangeable cation in the entire blended system (Oti et al., 2010; Oti, 2010). This may be another reason for the variation in strength values in the stabilized mixtures. The increase in compaction moisture content of the compacted cylinder specimens from 27% to 33% produced a significant reduction in strength values, observed with all the stabilizer blends, at all mix proportions at the optimal blending ratio of 4%:16% L/PC:GGBS.

### 18.3.2 Linear expansion

Fig. 18.5A–F illustrates the expansion behavior during moist curing and subsequent soaking of the various samples (L1–GGBS, L2–GGBS, and PC–GGBS) at 27%,

30%, and 33% compaction moisture content. The linear expansions during the 7-day moist curing observed so far suggest very low expansion for all the stabilizer blends, within the range of 0%–0.7%. No noticeable shrinkage was noted.

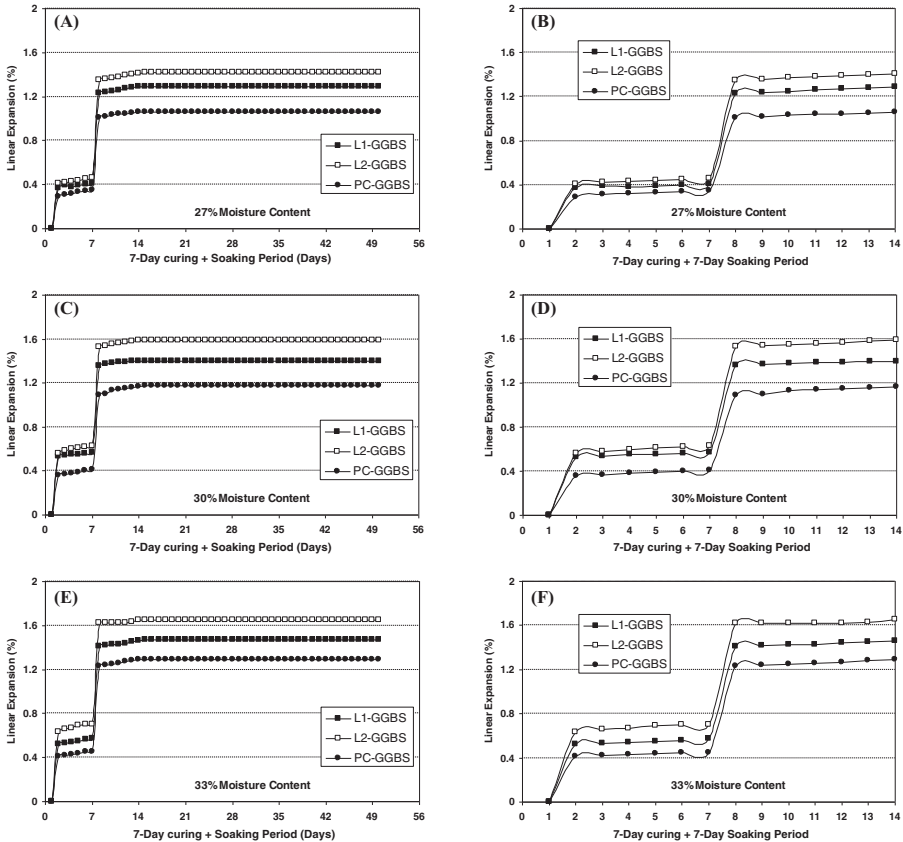


**Figure 18.5** (A–F) Linear expansion measurements during moist curing (7 days) and subsequent soaking of the stabilized cylinder specimens, made at 27%–33% compaction moisture content.

The linear expansion during soaking of the blended cylinder specimens suggests relatively more rapid expansion upon soaking, with the highest recorded expansion being about 1.65%, recorded for the L2–GGBS blend at 33% compaction moisture content. The least linear expansion was 1.06%, observed from the specimens made using the PC–GGBS blend at 27% compaction moisture content. Interestingly, this stabilizer blend recorded the least strength development.

The total overall expansion rate of the samples (0%–1.65%) at the compaction moisture content of 27%, 30%, and 33% is within the acceptable limit for the durability of stabilized clay masonry units. The total maximum 50-day linear

expansion is summarized in Fig. 18.6. It is interesting to note that in previous work (Oti et al., 2009, 2010; Oti, 2010; Oti & Kinuthia, 2012b; Kinuthia & Oti, 2012) with mixes without hemp, the blend made with quicklime (L1–GGBS) showed the highest expansive behavior, with the highest recorded expansion magnitude of about 1.6% at 33% compaction moisture content. The lowest linear expansion of 0.9% was observed from the blended optimized cylinder specimens made using the PC–GGBS blend. The addition of hemp has no significant influence on the rate of expansion.

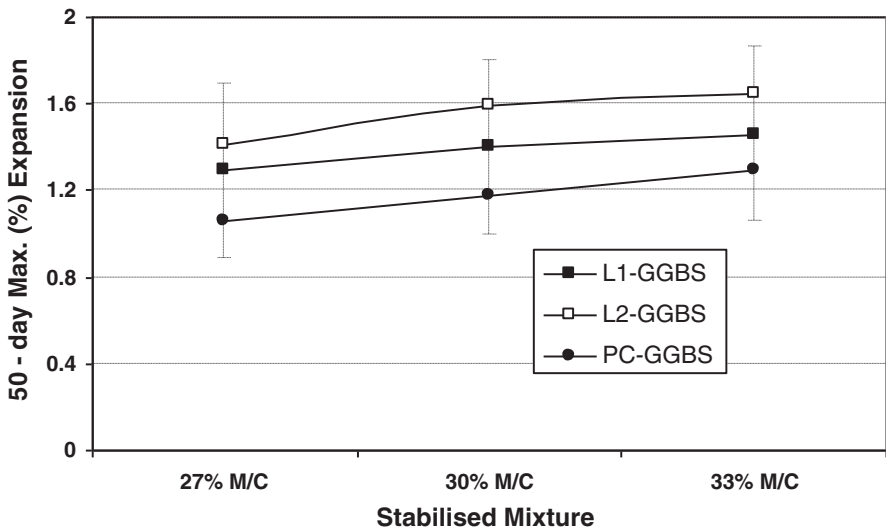


**Figure 18.6** Total (maximum) 50-day linear expansion measurements for moist curing (7 days) and subsequent soaking of the stabilized cylinder specimens, made at 27%–33% compaction moisture content.

Swelling and linear expansion of stabilized clay soil is common and is known to be associated with the formation of a colloidal product (gel intermixed with ettringite), which forms on the surface of the clay particles during curing. When in a saturated condition, ettringite grows and develops from this colloidal product (Oti et al., 2010; Oti, 2010). It has the capability of imbibing large amounts of water and dramatically increases the swelling potential of the stabilized soil, especially if lime is used as a stabilizer (Oti et al., 2010; Oti, 2010). However, the introduction of a cementing agent, such as PC or GGBS, modifies the chemical interaction of the clay–lime system, thereby altering the types of reactions and thus potentially altering any disruptions that the reaction by-product may cause. It is therefore not surprising that the test specimens made using PC–GGBS expanded much less relative to those stabilized using a lime–GGBS blended binder (Oti et al., 2010; Oti, 2010).

Over the 50-day linear expansion observation period, all the samples either attained terminal linear expansion or continued to expand at a negligible rate. The linear expansion started during the 7-day curing period and increased when the specimens were soaked in water after the 7-day moist-curing period. This expansion was more stable for the rest of the 36 days of soaking. The PC–GGBS blended LOC samples recorded significantly lower expansion values compared with the lime–GGBS stabilized LOC. The overall reduction in linear expansion is likely to be due to the formation of cementitious products (Oti et al., 2010; Oti, 2010). The cementitious gels cement the soil particles together and enable them to resist the considerable swelling pressures, which can be generated when ettringite forms in the presence of water (Oti et al., 2010; Oti, 2010). The hydration of the PC–GGBS stabilizer blend is much more rapid compared with the pozzolanic reaction of lime–GGBS with clay. This hydration reaction is known to consume lime (Oti et al., 2010; Oti, 2010).

One possible explanation why the lime–GGBS stabilized test specimens expanded relatively more compared with the PC–GGBS specimens is perhaps because of relatively more ettringite formation during the hydration process in the lime–GGBS blended matrix, with the ettringite subsequently imbibing large quantities of water, leading to expansion. Other hydration products may also fill the void space of the stabilized system, thus enhancing both strength and volume stability upon subsequent soaking (Oti et al., 2009, 2008c, 2010; Oti, 2010; Oti & Kinuthia, 2012b; Kinuthia & Oti, 2012).

The fact that higher strength magnitudes in the lime–GGBS system were observed and it is the same system that expanded the most suggests that volume stability is a sensitive balance between void space and cementation. GGBS may also play the role of diluting the stabilized system, thus reducing the amount of expansive products in the pore space and also increasing the effective water-to-stabilizer ratio. This would enable a greater degree of CaO hydration (Oti et al., 2010; Oti, 2010). This minimizes any possible disruption to the hardened product and the overall expansion may be reduced. In addition to the above hypotheses, GGBS may also mitigate the expansion by providing a surface upon which lime can be adsorbed and subsequently interact by activating the hydration process with the enhanced pH environment (Oti et al., 2008c, 2010; Oti, 2010).

### **18.3.3 Laboratory stabilized clay–hemp brick manufacture**

In order to establish the viability of the transition from the laboratory cylinder specimens produced elsewhere to actual brick production, a full-scale steel mold was fabricated with a view to producing full-sized bricks for further testing, rather than using cylinder test specimens. This enabled laboratory-scale production of full-sized building bricks of dimensional configuration of  $215 \times 102.5 \times 65$  mm using the L1–GGBS, L2–GGBS, and PC–GGBS mixtures at 27% moisture content. The results were an immediate success, as demonstrated in Fig. 18.7 (full-sized clay bricks made at laboratory scale).



**Figure 18.7** Freshly prepared clay–hemp bricks using L1–GGBS, L2–GGBS, and PC–GGBS mixtures.

### 18.3.4 Cost analysis hemp–clay brick

The identification of a potential market for all the stabilized hemp–clay brick types (L1–GGBS, L2–GGBS, and PC–GGBS) manufactured at 27% moisture content, could be an influential factor for a successful unfired clay masonry brick development program. A cost–benefit analysis was conducted for all the stabilized hemp–clay brick types to provide a protocol for measuring the efficient allocation of resources. The overall aim is to provide the researchers/planner with a set of values that are useful to determine the feasibility of the stabilized hemp–clay brick project from an economic standpoint. To calculate the payback period for all the hemp–clay brick types, the energy cost was determined. Since the thermal load is cumulative, the energy used ( $E$ ) is calculated by the following equation (Al-Hadhrami & Ahmad, 2009):

$$E = \frac{0.024 \times D}{R \times C} \text{ kWh/m}^2$$

where  $D$  is the degree-days of the location ( $D = 2185$ ),  $R$  is the thermal resistance of the brick sample, and  $C$  is the coefficient of thermal performance of the system ( $C = 2.16$ ). The total discounted cost or a net present value (NPV) per square meter of brick surface area is calculated using the following equation:

$$NPV = E \times PWF \times EC + BC \quad (\text{£/m}^2)$$

where  $E$  is the annual energy consumption,  $EC$  is the energy cost (8 pence/kWh),  $PWF$  is the present worth factor, and  $BC$  is the cost stabilized hemp–clay brick. The present worth factor,  $PWF$ , is calculated using the following equations:

$$PWF = \frac{1}{i - e} \left\langle 1 - \left( \frac{1 - e}{1 - i} \right)^n \right\rangle \text{ for } e \neq i$$

$$PWF = n \cdot (i + e) \text{ for } e = i$$

where  $e$  is the energy inflation rate (3.5%),  $i$  is the discount rate (6%), and  $n$  is the lifetime of the stabilized hemp–clay brick (30 years). The inflation rate, the



discounted rate, and the present worth factor are presented in Table 18.4 and it can be seen that the values are the same for all brick types.

**Table 18.4** The inflation and discount values of the stabilized hemp–clay bricks.

Brick type	$e$ (%)	$i$ (%)	$n$ (years)	PWF	EC (pence/kWh)
L1–GGBS	3.5	6.0	30	0.0962	8.0
L2–GGBS	3.5	6.0	30	0.0962	8.0
PC–GGBS	3.5	6.0	30	0.0962	8.0

$e$ , inflation rate;  $i$ , discount rate;  $n$ , lifetime of the unfired bricks.

The cost analysis along with the energy use and the net present value for all the stabilized hemp–clay bricks types (L1–GGBS, L2–GGBS, and PC–GGBS) are presented in Table 18.5. It can be seen that the stabilized hemp–clay brick manufactured with the PC–GGBS system has the highest net present value while the lowest net present value was observed for stabilized hemp–clay brick manufactured with the LG1–GGBS system. Similar trends were observed for energy use. For the brick cost, the highest brick cost was observed for the stabilized hemp–clay brick manufactured with LG1–GGBS system, while the lowest brick cost was obtained for the stabilized clay–hemp brick manufactured with the PC–GGBS system. Since the simple payback analysis only gives the recovery period of an additional investment, it ignores the influence of discount rate and cost escalation. Net present value analysis is the correct approach for economic analysis as it takes into account the life period of the stabilized hemp–clay brick, time value of money (discount rate), and energy escalation cost. The net present value analysis shows that the stabilized hemp–clay brick manufactured with the LG1–GGBS system is the most effective of all the brick types as it has the lowest net present value of 61.17 £/m<sup>2</sup>.

**Table 18.5** The net present values of the stabilized hemp–clay bricks.

Brick type	$R$ (m <sup>2</sup> /K/W)	$D$ (degree-day)	$C$	$E$ (kWh/m <sup>2</sup> )	$BC$ (£/m <sup>2</sup> )	$NPV$ (£/m <sup>2</sup> )
L1–GGBS	0.3625	2,185	2.16	66.95	9.65	61.17
L2–GGBS	0.3471	2,185	2.16	69.92	9.35	63.16
PC–GGBS	0.3375	2,185	2.16	71.91	8.75	64.09

$R$ , the thermal resistance of the unfired clay bricks;  $D$ , degree-day;  $C$ , coefficient of thermal conductivity;  $E$ , energy used;  $BC$ , cost of the unfired clay bricks.

## 18.4 Conclusions

The results obtained so far suggest the following conclusions:

There is potential for using blended binders for the manufacture of unfired clay materials within the building construction industry. The lime–GGBS blends in

particular showed promise. Using Lower Oxford Clay and industrial hemp as the target stabilization materials, the cylinder test specimen made with PC–GGBS blends tended to achieve lower strength values compared with the different lime–GGBS blends. The strength characteristics of the unfired bricks were improved with the presence of the lime and GGBS, which act as a bond on the soil particles.

The lime and GGBS offer other benefits in enhancing the all-round performance with volume stability and overall durability. The expansive behavior upon moist curing and soaking in water of the stabilized hemp–clay mixture was within the acceptable limit for the durability of stabilized clay masonry units.

The outcome of the cost analysis shows that the stabilized hemp–clay bricks manufactured with the LG1–GGBS system is the most effective among the bricks studied as it has the lowest net present value.

## References

- Al Rim, A., Ledhem, O., Douzane, R. M., Dheilily, M., & Queneudec. (1999). Influence of the proportion of wood on the thermal and mechanical performances of clay-cement-wood composites. *Cement and Concrete Composites Journal*, 21(1999), 269–278.
- Al-Hadhrani, L. M., & Ahmad, A. (2009). Assessment of thermal performance of different types of masonry bricks used in Saudi Arabia. *Applied Thermal Engineering*, 29(2009), 1123–1130.
- Arrigoni, A., Grillet, A. C., Pelosato, R., Dotelli, G., Beckett, C. T., Woloszyn, M., & Ciancio, D. (2017). Reduction of rammed earth's hygroscopic performance under stabilisation: an experimental investigation. *Building and Environment*, 115, 358–367.
- Biswas, W. K. (2014). Carbon footprint and embodied energy consumption assessment of building construction works in Western Australia. *International Journal of Sustainable Built Environment*, 3(2), 179–186.
- Boardman, D. I., Glendinning, S., & Rogers, C. D. G. (2001). Development of stabilisation and solidification in lime–clay mixes. *Géotechnique*, 51(6), p533–p543.
- BS 1924-2. (1990). *Stabilised materials for civil engineering purposes - Part 2: Methods of test for cement-stabilised and lime-stabilised materials*. British Standards Institute.
- BS EN 15167-1. (1516). *Ground granulated blast furnace slag for use in concrete, mortar and grout. Part 1: Definitions, Specifications and Conformity Criteria*.
- BS EN 197-1. (2011). *Cement. Part 1: Composition, specifications and conformity criteria for common cements*.
- Dao, K., Ouedraogo, M., Millogo, Y., Aubert, J. E., & Gomina, M. (2018). Thermal, hydric and mechanical behaviours of adobes stabilized with cement. *Construction and Building Materials*, 158, 84–96.
- Esmeray, E., & Atus, M. (2019). Utilization of sewage sludge, oven slag and fly ash in clay brick production. *Construction and Building Materials*, 194, 110–121.
- Kariyawasam, K. D., & Jayasinghe, C. (2016). Cement stabilized rammed earth as a sustainable construction material. *Construction and Building Materials*, 105, 519–527.
- Khadka, B., & Shakya, M. (2016). Comparative compressive strength of stabilized and unstabilized rammed earth. *Materials and Structures*, 49(9), 3945–3955.
- Kinuthia, J. M., & Oti, J. E. (2012). Designed non-fired clay mixes for sustainable and low carbon use. *Applied Clay Science*, 59–60, 131–139.

- Labat, M., Magniont, C., Oudhof, N., & Aubert, J. E. (2016). From the experimental characterization of the hygrothermal properties of straw-clay mixtures to the numerical assessment of their buffering potential. *Building and Environment*, *97*, 69–81.
- Mazhoud, B., Collet, F., Pretot, S., & Lanos, C. (2017). Mechanical properties of hemp-clay and hemp stabilized clay composites. *Construction and Building Materials*, *155*, 1126–1137.
- McGregor, F., Heath, A., Fodde, E., & Shea, A. (2014). Conditions affecting the moisture buffering measurement performed on compressed earth blocks. *Building and Environment*, *75*, 11–18.
- Oti, J. E. (2010). PhD Thesis *The development of unfired clay building materials for sustainable building construction*. Pontypridd, UK: University of Glamorgan.
- Oti, J. E., & Kinuthia, J. M. (2012a). Stabilised unfired clay bricks for environmental and sustainable use. *Applied Clay Science*, *58*, 52–59.
- Oti, J. E., & Kinuthia, J. M. (2012b). Stabilised unfired clay bricks for environmental and sustainable use. *Applied Clay Science*, *58*, 52–59.
- Oti, J. E., Kinuthia, J. M., & Bai, J. (2008a). Using slag for unfired-clay masonry bricks. *Proceedings of ICE, Journal of Construction Materials*, *161*(CM4), 147–155. Available from <https://doi.org/10.1680/coma.2008.161.4.147>.
- Oti, J. E., Kinuthia, J. M., & Bai, J. (2008b). Developing unfired stabilised building materials in the UK. *Proceedings of ICE, Journal of Engineering Sustainability*, *161*(ES4), 211–218. Available from <https://doi.org/10.1680/ensu.2008.161.4.211>.
- Oti, J.E., Kinuthia, J.M., & Bai, J. (2008c). Development of Innovative low carbon clay bricks. In *Proceedings of the 2nd international conference on learning from earthen architecture in climate change (Kerpic'08), cyprus international university* (pp. 291–297). Lefkosa Northern Cyprus. ISBN: 978-975-6002-07-0.
- Oti, J. E., Kinuthia, J. M., & Bai, J. (2009). Engineering properties of unfired clay masonry bricks. *Engineering Geology*, *107*(3–4), 130–139.
- Oti, J. E., Kinuthia, J. M., & Bai, J. (2010). Unfired clay masonry bricks incorporating slate waste. *Proceedings of the Institution of Civil Engineers-Waste and Resource Management*, *163*(1), 17–27.
- Renouard, S., Hano, C., Doussot, J., Blondeau, J. P., & Lainé E, E. (2014). Characterization of ultrasonic impact on coir, flax and hemp fibers. *Materials Letters*, *129*, 137–141.
- Sutcu, M., Erdogmus, E., Gencel, O., Gholampour, A., & Ozbakkaloglu, T. (2019). Recycling of bottom ash and fly ash wastes in eco-friendly clay brick production. *Journal of Cleaner Production*, *233*, 753–764.
- UNEP. (2009). Buildings and climate change – summary for decision-makers. In *UNEP DTIE, sustainable consumption & production branch*. 15 Rue de Milan, 75441 Paris CEDEX 09, France.
- Venkatarama Reddy, V. B., & Jagadish, K. S. (2003). Embodied energy of common and alternative building materials and technologies. *Energy and Building*, *35*, 129–137.
- Webb, D. J. T. (1994). Stabilised soil and the built environment. *Renewable Energy*, *5*(5–8), 1066–1080.
- Worrell, E., Price, L., Martin, N., Hendriks, C., & Ozawa Media, L. (2001). Carbon dioxide emissions from the global cement industry. *Annual Review of Environment and Resource*, *26*(2001), 303–329.

# Innovative and sustainable concrete materials

19

*Antonella D'Alessandro and Filippo Ubertini*

Department of Civil and Environmental Engineering, University of Perugia, Perugia, PG, Italy

## 19.1 Introduction

The field of construction is a major consumer of natural resources (Tam et al., 2018), related to the consumption of energy, raw materials, or the production of dust pollutants, waste, and greenhouse gases. Among all the construction materials, concrete is one of the most diffuse ones, with a worldwide production of more than 10 billion tons per year (Meyer, 2009). As a matter of fact, concrete is very versatile for several types of structures, permitting complex and elaborate designs. It could be adopted also for infrastructures, for example, road pavements or important bridges and viaducts. Its use could determine a high impact on environment and health due to the production processes, the constructive phases, the maintenance, and the demolition. The first critical aspect to consider in order to decrease the environmental footprint is the use of raw materials; the main potential issues are related to the possible shortage of natural materials for clinker manufacturers, and to the impact that the uncontrolled supply of concrete components—mainly aggregates—could determine on the environment. A challenging factor related to the sustainability of concrete is also its great energy consumption, necessary for clinker calcination (which needs 1400°C–1450°C) and for the preparation and crushing of coal, clinker, aggregates, and additives. Moreover, the processes that request energy consumption are associated with gas emissions (Purnell, 2012). The average emission resulting from manufacturing each ton of clinker is around 0.9 tons of CO<sub>2</sub>, which contributes to about 8% of global CO<sub>2</sub> emissions. In particular, Portland cement production represents 74%–81% of the overall CO<sub>2</sub> emissions of concrete, and aggregate preparation produces 13%–20%; considering the emissions of the concrete industry, its contribution may be more than 10% of global anthropogenic CO<sub>2</sub> emissions (Flower & Sanjayan, 2007). As concerns high performance concretes, the effect could be also higher. The possible approaches for decreasing the impact of concrete industry on the environment can be pursued in different ways: in fact, the sustainability of the concrete can be enhanced by acting on resources, processes, or performance. Fig. 19.1 represents the set of possible solutions. The first approach concerns the recycling of the components, permitting to decrease both the use of raw materials during production, and the amount of waste after demolitions. Recycled materials could be aggregates (e.g., from construction and demolition—C&D, or recycled light materials), binders (kaolin, modified earth, etc.), additives (blast furnace slag, oils, and industrial waste), steel reinforcements, or a combination of them. The performance of the binders could be enhanced by using and

developing more effective materials, and their impact could be reduced by substituting part of them with more sustainable alternatives. The environmental footprint of the construction processes could be further limited by the use of local or recycled resources, and following lower impacting procedures. Moreover, the concept of sustainable design entails the selection of possible construction alternatives (Inyim & Zhu, 2013). Novel multifunctional materials for improving envelope thermo-energy efficiency through passive techniques are particularly promising. In this view, the integration of innovative materials, for example, phase change materials (PCMs), into cementitious composites shows interesting effects in enhancing the material thermal capacity while keeping proper constructive performance (Agyenim et al., 2010).



**Figure 19.1** Main approaches for achieving a sustainable concrete.

## 19.2 State-of-art concrete materials

Concrete is a composite material based on a cementitious paste matrix and an aggregate structure. The paste is a mix of cement and water, which constitute the binder of the composite. The aggregates are sand, gravel, or crushed stone of various granulometry. The main mixture could be integrated with supplementary materials or additives for increasing physical, chemical, or mechanical properties, such as fly ash, slag cement, or chemical admixtures. Concrete usually is composed as follows (Fig. 19.2): about 70% are aggregates, both fine and coarse; cement and water are about 8% and 15%, respectively; additives are usually added in the percentage of 1%–2%, and the residual volume is air content in air-entrained pores. The quality of the concrete depends upon the quality of the

paste and aggregates and the bond between them. Aggregates should consist of particles with adequate strength and resistance to exposure conditions and should not contain materials that could cause deterioration of the concrete. In properly made concrete, each particle of aggregate is fully coated with paste and all of the spaces between aggregate particles are completely filled with paste, as illustrated in Fig. 19.2. Cement could be natural or artificial. The former is obtained from rocks of sedimentary origin (i.e., marls) consisting mainly of clay, limestone, and iron oxide. Artificial cements, on the other hand, are obtained from silica, aluminum, and iron oxide according to preestablished quantities. Different types of cement are available in the market, depending on its performances: ordinary Portland cement (OPC), for all purposes, Portland Pozzolana cement (PPC), resistant to chemicals, rapid hardening cement, when a fast curing is needed, low heat cement, used in mass concrete, blast furnace slag cement, more cost-effective, high alumina cement, resistant at high temperatures, white cement, free from iron and oxide.

Chemical additives are adopted for (1) improving setting time or hardening, (2) reducing water, (3) increasing workability, (4) modifying the air content, and (5) adjusting other fresh or hardened concrete properties. Concretes components possess different dimensions from nano-metrical to macro-metrical (Fig. 19.3). In particular, the presence of voids at different scales allows the addition of fillers and a nanomodification for enhancing or adding multifunctional properties (Mehta & Monteiro, 2014; Brooks & Neville, 2019; Collepardi, 2010). The development and availability of nanomaterials determined the progress of novel smart concretes more performing than normal ones (Shah et al., 2015; D'Alessandro et al., 2020). From the previous discussion, it is clear that concrete technology is a great consumer of natural resources and energy, and its production processes are responsible for environmental impact and greenhouse gas emissions (Kusuma et al., 2015). As an example, the cement industry causes close to 7% of the global CO<sub>2</sub> emissions, while industrial waste product causes harmful consequences for the environment.

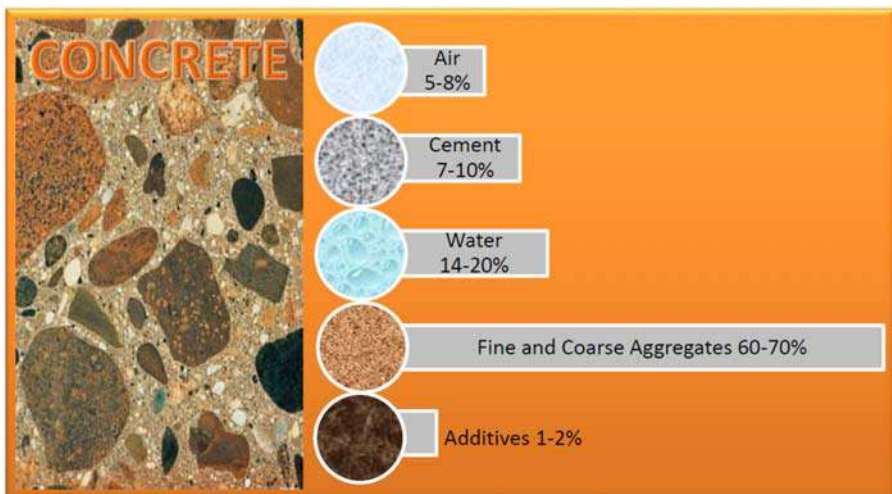


**Figure 19.2** Components of conventional concrete.

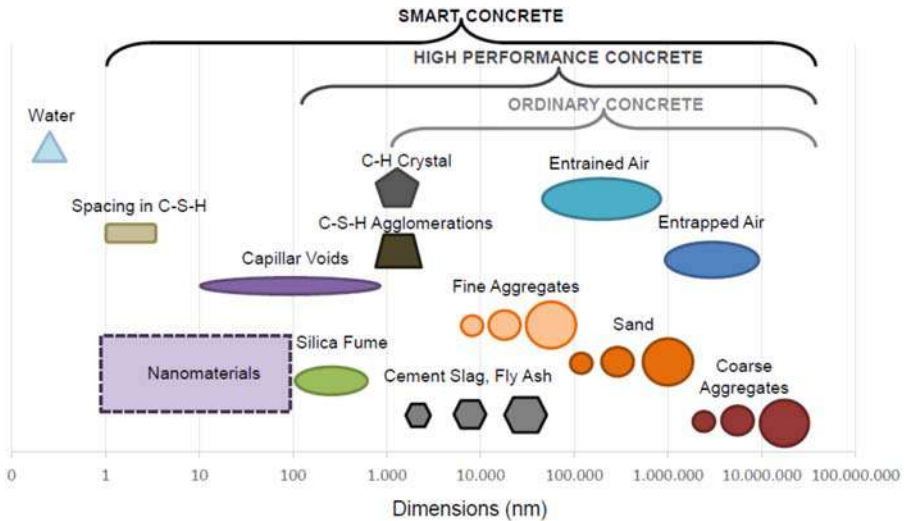


**Figure 19.3** Components' size of concretes.

By optimizing the packing of the combined aggregate gradations, concrete admixtures, and cementitious material, the cement paste content needed to make concrete can be reduced, improving sustainability, cost, performance, durability, and workability. The development of a sustainable concrete could be achieved with various synergic approaches: through decreasing the water/cement ratio, the mass, and the amount of cement, for enhancing the durability and the sustainability of the binder, increasing the compressive strength, the workability, or raising the performance of the material, thus reducing the sections of the structural elements and the amount of used material.

In the next sections, different approaches for increasing the sustainability of concrete and decreasing its environmental impact will be further discussed. The main solutions are as follows: (1) the adoption of novel more eco-friendly binders, (2) the recycling of concrete components, (3) the development of multifunctional materials, (4) the addition of novel performant admixtures, and (5) the improvement of production processes. The sustainable materials include reinforcing fibers (e.g., steel, polypropylene, and carbon fibers), recycled materials (e.g., tire rubber, crushed glass, plastic, and industrial waste), and organic and inorganic elements as concrete aggregates and reinforcement elements (Zamora-Castro et al., 2021).

## 19.3 New binders

The use of alternative binders to cement is one of the most promising strategies for decreasing the environmental impact of concrete (D'Alessandro et al., 2020). As a matter of fact, the production of cement determines a strong effect on environment. Approximately 3.6 billion tons of cement are produced globally every year. Considering

that 1 kg of cement produces 9 kg of carbon dioxide (Hendriks, 2004), 3.24 billion tons of CO<sub>2</sub> are dispersed every year. The adoption of eco-friendly binder for construction is gaining great interest in literature (Miller & Myers, 2020; Coppola et al., 2018). Among all the possible sustainable solutions, geopolymers, alkali-activated slag (AAS) cement, produced by mixing ground granulated blast furnace slag (GGBFS) with alkaline activators (Tataranni et al., 2018), and earth-concretes (Curto et al., 2020) appear particularly interesting because they are able to combine binding capabilities with an extremely low environmental impact in comparison to cement.

### **19.3.1 *Mixing ground granulated blast furnace slag (GGBFS) and geopolymers***

GGBFS is a by-product of the steel industry. It is the glassy granular material formed when molten blast furnace slag is rapidly chilled by immersion in water (Meyer, 2009). It is formed by calcium and magnesium aluminosilicates and may have pozzolanic properties. Reductions in CO<sub>2</sub> using GGBFS are important because the cement preparation process is less energy intensive, involving less heat to produce the calcination process (Imbabi et al., 2012). Due to its properties, it is also used as an aggregate for the concrete. GGBFS can enhance various mechanical properties of cementitious materials, for example, durability, and decrease the heat of hydration (Coppola et al., 2020). AAS cement, produced by mixing GGBFS with alkaline activators, are promising candidates in different construction applications, such as the restoration of existing structures, refractory systems, fire-retardant plasters, and concrete sewer pipes (Shi et al., 2006). Literature shows that the alkali content plays a crucial role in elasto-mechanical properties and durability of alkali-activated materials. As an example, the higher the alkali content, the higher the strength and the resistance in severe conditions (Fig. 19.4). Recent innovations allowed the development of a geopolymer foam concrete, which possesses lightweight performance benefits and emissions reduction (Zhang et al., 2014). A geopolymer is an aluminosilicate binder formed by the alkaline activation of solid alumina- and silica-containing precursor materials. Literature shows that a widespread application of this technology could be obtained with the deep investigation of factors including feedstock materials chemistry, microstructure, and control of engineering properties, as part of the process of broadening the uptake of this technology.

### **19.3.2 *Earth-concretes***

Ancient natural construction materials, such as rammed earth ones, are of growing interest in the field of civil engineering, due to their ecological implications (Pacheco-Torgal & Jalali, 2012). Various scientists agree that the choice of more sustainable construction materials and construction techniques represents a major contribution to the eco-efficiency of buildings. In this scenario, earth constructions allow an environmental advantage with respect to conventional materials and construction techniques. Current researches regard investigations on the seismic response of earth buildings, on the mechanical properties of earth masonry, and on thermal and hygrothermal performance



(Bruno et al., 2017). However, the earth needs a stabilization, which could be obtained through a deep compaction or the use of other binders (Guettala et al., 2006; Van Damme & Houben, 2017). Drawbacks connected to the mechanical performance or durability of compacted earth could be solved by stabilizing the material with cement, developing the so-called “earth-concrete.” New technologies of stabilized soil-concrete are based on the high-speed projection of a mix of earth, cement, aggregates, and water (shot-earth) (Curto et al., 2020). The preparation procedure foresees the dry mixing of the components, and the spraying process allows to decrease the water amount, in order to obtain a more compact and performing material (Fig. 19.5A).

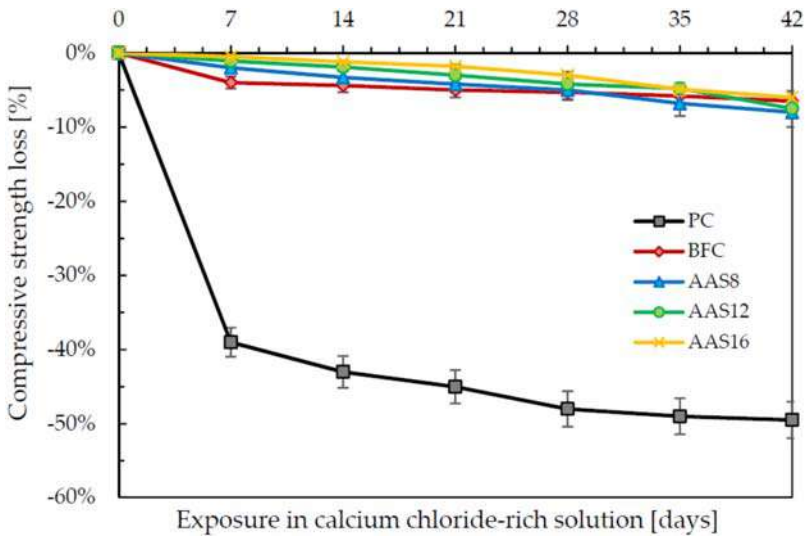
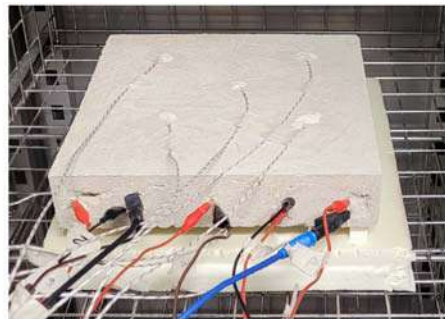


**Figure 19.4** Compressive strength loss of specimens exposed to solutions of  $\text{CaCl}_2$  (Coppola et al., 2020).



(A)



(B)

**Figure 19.5** Earth-concrete: (A) a detail of the materials; (B) an example of element made of smart-earth.

Shot-earth consists of a dry mix of soil, cement, and coarse sand (7 soil, 7 sand, and 2 cement) propelled through a nozzle. The size of the sand and the mix design are determined according to the composition of the available soil. The cohesion is obtained by adding a small amount of water during the spraying. The earth materials possess good mechanical properties, similar to the ones of low-strength concrete. This technology is also very flexible and could be applied to a wide range of structural and nonstructural applications (Fig. 19.5B).

### 19.3.3 Fine recycled fillers: fly ash and silica fume

Other interesting industrial by-products that can be successfully implemented in the concrete technology are silica fume (Helmuth, 1987), a by-product of the semiconductor industry, and fly ash (Demirboga, 2007), a by-product of coal-fired electric power plants.

Silica fume is a pozzolanic material, which is a by-product of the silicon smelting process, which improves both strength and durability of concrete, and it constitutes an important component for high-performance concrete mix designs. In literature, there are lots of papers, which document the benefits of silica fume both as a pozzolan and a filler material (ACI Committee 234, 2006; CANMET/ACI, 2004). Silica fume is also known as microsilica, which is obtained as a by-product of the production of silicon and silicon alloys in electric arc furnaces. Silica fume is known to produce a high-strength concrete, adopted in two different uses: as a cement replacement, in order to reduce the cement content (for economic and environmental purposes), and as an additive to improve concrete properties, both fresh and hardened.

Fly ash is widely used in blended cement. Two general classes could be distinct: low-calcium fly ash (LCFA: ASTM class F) produced by burning anthracite or bituminous coal, and high-calcium fly ash (HCFA: ASTM class C) produced by burning lignite or sub-bituminous coal.

Its beneficial effects, if added in concretes, are the decrease of the heat of hydration and the improvement of the durability when used as a cement replacement. It also contributes to concrete strength by pozzolanic and filler effects.

Recently, researchers are becoming interested in the use of a combination of the two by-products (Nochaiya et al., 2010). Available researches demonstrated that the addition of both silica fume and fly ash contributed to a significant increase in the fracture toughness of concretes at an early age (Golewski & Gil, 2021). Micrometrical investigations of the two types of fillers are visible in Fig. 19.6A and B, carried out by scanning electron microscopy (SEM). Moreover, some researchers (Yazici et al., 2008) are investigating the utilization of fly ash in combination with GGBFS in reactive powder concrete (RPC), demonstrating an increase in the strength of the obtained composite materials.

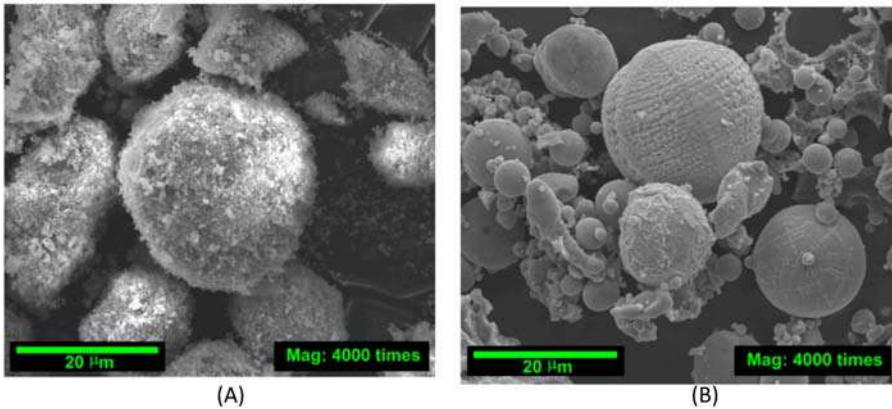


**Figure 19.6** SEM magnifications of (A) silica fume; (B) fly ash.

*Source:* From Golewski, G.L., & Gil, D.M. (2021). Studies of fracture toughness in concretes containing fly ash and silica fume in the first 28 days of curing. *Materials*, 14, 319. <https://doi.org/10.3390/ma14020319>.

### 19.3.4 New efficient cements

Another possible solution for decreasing the environmental impact of concrete is the development of new eco-efficient cements. Such cements could be produced through the improvement of cement manufacturing processes that use raw materials and a noticeable amount of energy. In this view, efficient cements would ideally use waste-derived fuels and raw materials (Mineral Products Association MPA, 2012). There are examples of low carbon cements in a few parts of the world, and not in a wide scale. For example, calcium sulfoaluminate cement (CSA) is starting to be implemented in China through the development of small start-up companies looking to build pilot plants. To mitigate the environmentally dangerous emissions, the main solution proposed by the International Energy Authority in 2009 was CO<sub>2</sub> capture and storage (CCS) (Scrivener et al., 2018). The proposal considered two clinker substitution technologies, that is, calcined clay plus limestone and engineered filler combined with dispersant, which could enhance the levels of possible replacement with respect to other previous solutions. As a matter of fact, the involved sources of raw materials are almost unlimited and available virtually everywhere.

## 19.4 Recycled components

### 19.4.1 Recycled aggregates

Industries and manufacturer factories are inevitable producers of high quantities of by-products and solid wastes. Moreover, the economic progress determines a worsening of the amount of solid waste that affects landfills, causing contamination of soil, water, and air with toxic substances. Possible contaminants are polychlorinated bi-phenyls, asbestos, construction chemicals, and heavy metals. The solution of a

not regulated environmental land occupation stays in the recycling and reutilization of wastes from C&D, and the development of a reassessment of the process procedures of such materials, in order to transform a waste into a resource (Meyer, 2009). The reuse of C&D in civil engineering constructions and infrastructures depends strongly on the quality of the original materials and their treatments. Possible treatment techniques for improving the materials' performances are carbonation, acetic acid immersion, acetic acid immersion with mechanical rubbing, acetic acid immersion with carbonation, and lime immersion (Kazmia et al., 2019). Moreover, the possible fields of employment of the different types of construction waste are several, with various levels of performance, from structural constructions, to not structural applications as stabilized conglomerate. In literature, the interest in the recycling of C&D is quickly increasing, proved by the great number of researches on the topic. The study of the characteristics (physical, chemical, mechanical, and technological) of recycled aggregates may be the most diffuse topic in the scientific panorama. Also, the sensitivity on the importance of the C&D reuse in novel construction is raising in many countries; detailed technical standards and recommendations could help the development of the market of recycled aggregate, and their integration into engineering project, toward a circular economy (Villagrán-Zaccardi et al., 2022). Fig. 19.7 represents the waste treatments of minerals from C&D in diverse European countries; it is clearly visible the different approaches of the administrations.

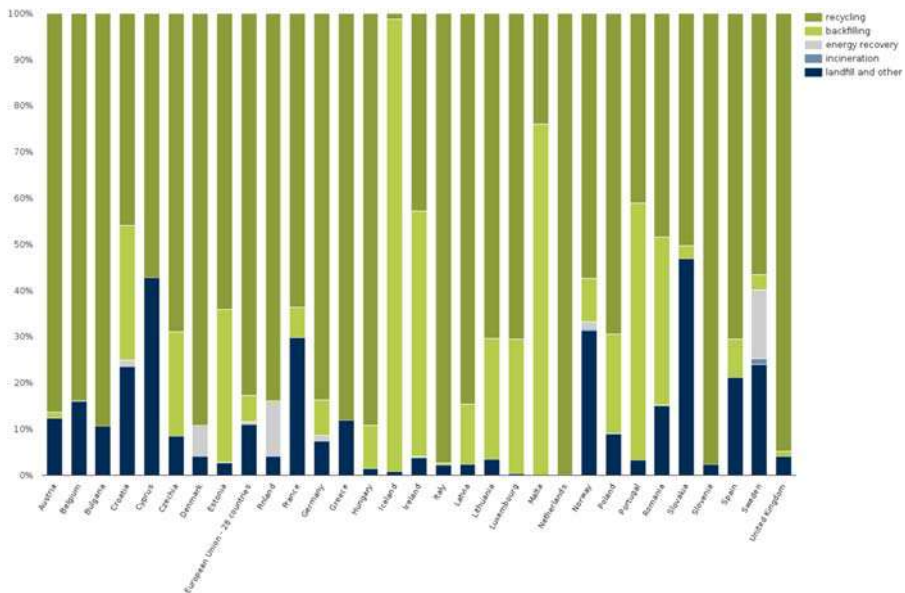


**Figure 19.7** Mineral waste from construction and demolition, waste treatment (EEA, 2020). Source: From European Environment Agency <https://www.eea.europa.eu/> (EEA, (2020). Mineral waste from construction and demolition, waste treatment. Available from: [https://www.eea.europa.eu/data-and-maps/daviz/mineral-waste-from-construction-and#tab-googlechartid\\_chart\\_13](https://www.eea.europa.eu/data-and-maps/daviz/mineral-waste-from-construction-and#tab-googlechartid_chart_13)).

Construction waste is produced by building interventions, excess or damage of construction materials, processing waste, or production of garbage during constructions. Demolition waste results from demolition or renovation of structures and infrastructures, also due to natural events or anthropic actions. C&D waste can be divided into six main typologies of materials: metal, concrete and mineral, bricks and ceramics, wood, miscellaneous, and unsorted. It could also contain glass, plastic, bituminous conglomerates, soils, insulation materials (including asbestos), gypsum materials (including plasterboard), electronics, chemicals, packaging materials, and other dangerous substances (Tam et al., 2018). Waste concrete is mainly used for producing recycled aggregates; however, its full recycling is still not practiced. Alternative uses include applications such as fine recycled aggregates, supplementary cementitious materials, filler, and feedstocks for clinker production (Villagrán-Zaccardi et al., 2022).

A large number of experimental campaigns has been carried out in the last 20 years on the possibility to use recycled concrete aggregates to produce novel structural concrete. In general, recycled concrete possesses lower properties than normal ones, such as lower elastic modulus, a more brittle postelastic behavior, lower workability, higher shrinkage, and creep, probably due to the content of mortar in recycled aggregates, which is difficult to remove at all (Liotta et al., 2016).

For obtaining a good performance of the recycled concrete, it is necessary to use good recycled concrete aggregate and follow specific design and production processes. Recycled concrete aggregate (RCA) is generally produced by two stages: crushing of demolished concrete, and screening and removal of contaminants such as reinforcement, paper, wood, plastics, and gypsum. Concrete made with such recycled concrete aggregate is called recycled aggregate concrete (RAC) (Malešev et al., 2010). Fine recycled aggregate usually is not adopted for preparing structural recycled concretes, because of their worsening effects on workability and resistance (RILEM, 1994; Khatib, 2005). In particular, the total replacement of the fine fraction by recycled fine aggregates presents some durability difficulties (Evangelista & de Brito, 2010).

Investigations on the fresh and hardened recycled concrete properties available in literature strongly differ for the quality of the adopted recycled aggregates. Some studies demonstrated that the bulk density is slightly lower with increasing quantities of recycled aggregate, and that the air content is not highly dependent on the amount of replacement (Fig. 19.8). All the studies underline that the compressive and tensile strengths depend on the quality of recycled aggregate (Zhou & Chen, 2017; Xiaoa et al., 2005). By varying the replacement percentage and adopting particular types of superplasticizers, it is possible to solve some weaknesses of the RAC, contributing to developing the use of this sustainable material (Matias et al., 2013). In particular, if the aggregates come from crushing of high strength concrete, the strength is not significantly affected (Fig. 19.9). The properties of high-strength concrete with coarse recycled aggregates were found significantly more variable than those of ordinary concrete, but the coefficient of variation and the standard deviation could match the limits of standards and codes (Pacheco et al., 2019). The two properties of RAC, which are generally lower than the ones of ordinary concretes, are the modulus of elasticity and shrinkage, so that some researchers suggest to avoid their use for structural elements for which large deformations are expected.

Moreover, RAC is not recommended for elements exposed to aggressive environment conditions because there are contrasting results from literature researches. Some experimental tests show a decrease in the stiffness of RAC with respect to normal concrete, especially for the mixes with higher percentages of recycled aggregates (Breccolotti et al., 2015).

In literature, there are also experimental tests on recycled concrete elements (Malešev et al., 2010); the presence of recycled coarse aggregates seems not to affect the crack paths, and in some cases, it increases the bending resistance.

Concrete mixture	Cement (kg/m <sup>3</sup> )	Total water (kg/m <sup>3</sup> )	Aggregate (kg/m <sup>3</sup> )	Water/cement ratio <sup>1</sup>	Aggregate/cement ratio	Slump <sup>2</sup> (cm)	Slump <sup>3</sup> (cm)	Air content (%)	Bulk density (kg/m <sup>3</sup> )
R0	352	181	1866	0.514	5.306	16	10	1.5	2,399
R50	352	200	1826	0.568	5.188	14.5	8.5	1.4	2,378
R100	348	216	1765	0.620	5.074	11	9	1.3	2,329

**Figure 19.8** Results of fresh concrete testing on normal and recycled concrete.

Source: From Malešev, M., Radonjanin, V., & Marinković, S. (2010). Recycled concrete as aggregate for structural concrete production. *Sustainability*, 2, 1204–1225. <https://doi.org/10.3390/su2051204>.

Concrete type	Concrete age (days)			Standard deviation (MPa)
	2	7	28	
R0 (MPa)	27.55	35.23	43.44	1.5769
R50 (MPa)	25.74	37.14	45.22	1.2089
R100 (MPa)	25.48	37.05	45.66	3.5016
R50/R0 (%)	93	105	104	
R100/R0 (%)	92	105	105	

**Figure 19.9** Results of compressive tests on normal and recycled concrete.

Source: From Malešev, M., Radonjanin, V., & Marinković, S. (2010). Recycled concrete as aggregate for structural concrete production. *Sustainability*, 2, 1204–1225. <https://doi.org/10.3390/su2051204>.

### 19.4.2 Recycled tires

About 1000 million of tires reach the end of their useful lives every year and 5000 million more are expected to be discarded by the year 2030 (Pacheco-Torgal et al., 2012). In particular, by the year 2030, the number of tires from motor vehicles is expect to be 1200 million.

Abandoned old tire dumps are dangerous for health hazards, as breeding grounds for mosquitoes as well as fire hazards (Taha et al., n.d.). Mainly, waste tire disposal areas contribute to the reduction of biodiversity, and also the tires hold toxic and soluble components. Some tire fires burn for months and even years (Dhir et al., 2001), so that the disposal of tires' landslides results not convenient for safety and for the environment, having the risk of contaminating soil, air, and water. However, illegal dumping is a growing

phenomenon. A possible solution to this environment issue could be the recycling of used tires and their reuse after retreading.

Old tires are already used for paving applications, but only a small amount of rubber waste can be recycled in this way. Other alternatives are artificial reef formation, but their validity has not been already confirmed by research investigations. Tire waste can also be used in cement kilns for energetic purposes and to produce carbon black by tire pyrolysis (Siddique & Naik, 2004).

One common treatment of old tires is a controlled burning for the production of steam, electricity, or heat. In fact, the transformation of old tires into alternative fuel for cement kilns is widespread throughout the United States and Europe (Meyer, 2009). The tire could be used also as an ingredient in cement composites, as shredded, chipped, ground, or crumb rubber, with sizes ranging from pieces of some centimeters, to powder particles. Rubber aggregates are obtained from old tires using generally two main technologies: mechanical grinding at ambient temperature or cryogenic grinding at a temperature below the glass transition temperature (Nagdi, 1993).

Rubber and cement matrix shows a great difference in Young's moduli, which results in a significant difference in the mechanical properties with respect to normal concrete composed only of natural aggregates. High difference could be the compressive and tensile strengths as well as the stiffness, which show a great decrease with increasing rubber content. The strength loss could reach the value of 80%. However, some literature works, which consider the use of old tires as aggregate replacement in recycled concrete, show that such an addition could enhance toughness and sound insulation properties, having a high energy absorption capacity (Sukontasukkul, 2009). In particular, the replacement of fine aggregates with recycled rubber would decrease the thermal conductivity of concrete. The replacement of up to 30% of material shows a reduction in thermal conductivity by more than 50% to a minimum of 0.241 W/m K.

Some researchers reported a reduction in the concrete workability for higher rubber content in self-compacting concretes, but the use of a superplasticizer could solve this issue (Guneyisi et al., 2004). Moreover, the authors assess that it is possible to produce a 40 MPa concrete replacing a volume of 15% of aggregates by rubber waste, even if for increasing amounts of crumb rubber, the strength of recycled concretes decreases (Guneyisi et al., 2004). A waste rubber volume of 15% leads to a 50% compressive strength decrease. When coarse aggregates are replaced by the tire particles, the compressive strength loss is much more significant with respect to the strength of concretes where fine aggregates were replaced by rubber particles (Aiello & Leuzzi, 2010).

The rubber aggregates have a preventive effect on crack path propagation, which results in a visible increase in strain capacity, ductility, and energy absorption capacity. Other potential positive effects of the rubber aggregates on recycled concretes are an improved sound absorption capacity as well as enhanced thermal properties.

### 19.4.3 Recycled glass

Glass is a material that could be recycled after its use into the packaging stream again, but an important quantity, which does not reach the suitable criteria for packaging novel glass, remains in the landfills and constitutes a waste. Some small

portions are recycled for other purposes, for example, a component for concretes (Shayan & Xu, 2004). Many studies have been carried out in the 1960s to investigate the effect of crushed waste glasses as aggregates for cement concrete (Schmidt & Saia, 1963). The addition of crushed glasses as aggregates for Portland cement concrete shows some negative effects on mechanical properties of the concrete, but a practical applicability of a complete replacement is possible. Some researchers demonstrated that it could be possible to produce a cementitious material using 100% crushed glasses as aggregates, 80% Portland cement, and 20% metakaolin as cementitious materials, adding a suitable quantity of superplasticizer, too (Bazant et al., 1998). The main concerns for the use of crushed glasses as aggregates for Portland cement concrete are the expansion and cracking caused by the glass aggregates. The pH of the system should be kept below 12, in order to prevent potential corrosion of glass aggregates and expansion of the concrete; this occurrence may be achieved by the replacement of Portland cement with pozzolanic materials, such as fly ash, silica fume, and metakaoline. Indeed, glass is unstable in an alkaline environment, as in the concrete, causing alkali–silica reaction (ASR) issues. For this reason, it is usually ground into a fine powder that possesses also pozzolanic properties. Thus, with some precautions, glass can be used as a cement replacement in Portland cement concrete (Shi & Zheng, 2007). As a matter of fact, if the waste glass is milled down to microsize particles, it demonstrates pozzolanic reactions with cement hydrates, due to the formation of secondary calcium silicate hydrate (C–S–H) (Sadiqul Islam et al., 2017). The compressive strength of concrete with small additions of recycled glass appears better than that one of normal cementitious materials. The replacement of 20% replacement of cement with waste glass is suitable for combining good performance, low costs, and low environmental impacts (Nassar & Soroushian, 2012). The substitution of up to 30% of cement in some concrete mixes determines satisfactory strength development. The use of waste glasses as concrete aggregates has a slight negative effect on the workability, strength, and freezing–thawing resistance of cement concrete. The drying shrinkage of recycled concrete with glass powder appears sufficient.

#### **19.4.4 Recycled plastic**

Plastic waste represents a great environmental issue in the world, due to the huge utilization in various fields and the still not advanced ecological attitude toward this material. Although degradable plastics are being introduced in packaging and disposable objects, the use of not biodegradable plastics is still prevailing. PET, polyethylene terephthalate, represents one of the most common polymeric wastes in solid urban waste (Mello et al., 2009). It is a not biodegradable plastic and could remain stable in nature for hundreds of years. The construction industry could represent a possible application field for the reuse of PET waste. Literature investigations confirmed the potential of PET waste in replacing aggregates in concrete. As a matter of fact, the addition of PET waste aggregates leads to an increase in the workability. This behavior is associated with the spherical and smooth shape of the aggregates adopted in the experimentations. Thus, the workability of PET concrete



is influenced by the treatments to which the PET materials are subjected before the reuse. PET fibers can also reduce shrinkage, even if the addition of PET fibers beyond 0.25% in volume shows very low reductions (Kim et al., 2008). Moreover, some researchers indicate that PET waste can be used to produce an unsaturated polyester resin in the presence of glycols and dibasic acid, which could act as a partial substitute for binder, producing polymer concrete with high mechanical performance (Rebeiz et al., 1994). Other authors (Jo et al., 2008) found out that this type of concrete can also be used to incorporate recycled concrete aggregates with a negligible strength loss, thus demonstrating that properly treated PET aggregates could perform similarly as natural aggregates. However, other authors observed a great compressive strength decrease (around 72%) for additions of 20% in volume of untreated PET waste. Other researchers (Silva et al., 2005) demonstrated that recycled monofilament PET fibers increased the toughness of cementitious composites, and that PET and polycarbonate wastes composites had a high energy absorbing performance. As an example, a replacement of 50% in volume of fine aggregates of PET wastes could determine a reduction of the thermal conductivity of PET recycled concretes by 46%, interesting thermal performance with respect to other insulation materials. However, for obtaining very low thermal conductivity coefficients, a great amount of recycled PET is required, conditions that could affect the mechanical performance of the composite. Literature works (Silva et al., 2005) also investigated the PET fibers degradation in alkaline environment, as that present in cementitious materials. The mechanism of PET degradation includes a depolymerization reaction that breaks the polymer chain splitting it into two groups (i.e., the aromatic ring and the aliphatic ester), resulting in a decrease in toughness capabilities of cementitious composites with time; those authors indicated a 20% loss between samples after 42 curing days and samples after 104 curing days.

Several other polymeric wastes have been investigated in literature for demonstrating their potentialities as recycled aggregates in cementitious composites: crumbled polystyrene waste and spherical blown polystyrene waste, ground thermosetting polymer (melamine) waste, thermosetting polymer (ground melamineformaldehyde), polyurethane wastes, polymeric waste, low-density polyethylene fibers, PVC wastes, and polyester and acrylic fibers. Some of them could show chemical degradation when immersed in the alkaline environment as cementitious materials (Pacheco-Torgal et al., 2012; Siddique et al., 2008). Other researchers investigated the combined effect of various hybrid replacements of concrete aggregates. As an example (Nematzadeh et al., 2022), combined nylon granules (0%, 10%, and 20%) as a replacement for fine aggregate, steel fibers (0%, 0.75%, and 1.25%), and zeolite (0%, 10%, 15%, and 20%) have been analyzed regarding the impact resistance and durability of concrete at different heating levels (20°C, 300°C, and 600°C). The results showed that the impact energy at the failure level declined considerably at high temperatures for concrete samples with nylon granules and steel fibers (by 46%–94% for 600°C).

Also, plastic components of electronic waste are available from circuit boards, body cabinets of a computer could be reused in concrete compounds after crushing. Investigations about the replacement of fine aggregate are available with percentages ranging between 0% and 20% (Veerabhadram et al., 2021). Results showed

that strength performance increases up to replacements of 15% thereafter there is a decreasing trend. The densities of the composites decreased with increasing additions of electronic plastic waste, which behave as lightweight materials.

#### 19.4.5 Organic waste

Waste unsustainable management involved different fields of the human activities. Organic waste has been rapidly growing in the last decades due to the rapid urbanization. Proper treatments of such a type of waste could solve environmental implications related to their disposal. Transforming such a waste could mitigate its impact on nature. A possible recycling activity of organic slugs could be in the production of auxiliary fuel. As an example, paper mill sludge is often incinerated for heat recovery and volume reduction. When it is burned, it produces paper mill sludge ash (PA), which could be adopted as a replacement for cement in concrete composites, showing a positive effect on the mechanical performance of the materials with additions below 10%, even if a higher amount of water is needed to guarantee the proper workability (Fava et al., 2011).

Waste paper sludge (WPS) is produced during the manufacturing of paper. This type of waste material may cause health environmental and economic issues, due to the presence of heavy metals and high disposal costs. Researchers demonstrated that WPS can be used as alternative building material if added to cementitious mixtures below tailored limits (Singh et al., 2022).

The wood manufacturing industry produced organic waste in the form of sawdust and pieces of side-cuts due to cutting, drilling, and milling operations; such wastes are usually kept in dust collectors. Studies demonstrated that wood by-products could be added to concrete for obtaining a more sustainable material (Corinaldesi et al., 2016). The addition of 5% could avoid an excessive loss of mortar mechanical strength, reducing the thermal conductivity by about 25%. Moreover, if a water reducing admixture is added, adequate mechanical performance can be obtained even with 10% wood by-products.

Due to the increase of urbanization, the treatment, recycling, or reuse of municipal solid waste (MSW) is becoming another critical topic. On average, out of 1.3 billion tons of municipal solid wastes generated per year, around 130 million tons are incinerated in the world. Incineration technology, with the benefit of volume and weight reduction as well as detoxification and energy recovery, is widely considered as the best and promising solution to reduce the environmental impact of MSW (Mambeli Barros, n.d.). Moreover, the residues coming from thermochemical processes for treating urban organic municipal solid waste could constitute solid waste ash, which could be introduced as a component of construction materials, as either fly ash or bottom ash (Joseph et al., 2018). As a matter of fact, the introduction of such materials in the chain of the cement industry as a binder and replacement is indicated in literature as a possible effective utilization option for large quantities of materials. The process parameters of incineration sites and pretreatment techniques need to be optimized for enhancing performance and recycling effectiveness of the residues (Ren et al., 2022). In available studies, MSW was pretreated with CO<sub>2</sub> via slurry carbonation (SC) and dry carbonation coupled with

subsequent water washing. The materials were then adopted as cement replacement in cementitious composites in the amounts of 10%, 20%, and 30% in weight. The investigation on the influence of the recycled material on hydration mechanisms, the physico-mechanical characteristics, and the leaching properties of the cement pastes demonstrated a very good behavior and foresaw its application as a supplementary cementitious material.

Possible sustainable replacements for cement in concretes could derive from agriculture waste (Mo et al., 2020). Huge amounts of solid wastes, originating from the agricultural industry, are an issue, for example, in the South East Asia. Examples of critical materials are as follows: oil palm shell, oil palm boiler clinker, and coconut shell. Researchers investigated the feasibility of adoption of these wastes as a potential substitute for conventional aggregate in cementitious materials. Recycled concrete produced by adding agriculture wastes generally shows acceptable quality in terms of water absorption, sorptivity, and chloride penetrability, while possible issues are in the performance related to strength, drying shrinkage, susceptibility toward severe chemical attack, and elevated temperature. Results demonstrated that in particular conditions, only a partial substitution of the aggregates is recommended.

Similar to the commonly used fly ash and municipal solid waste ash, rice husk ash (RHA) is a highly-reactive pozzolanic material and can constitute a replacement for cement in concretes. If used up to 30% of cement in concrete mix designs, it is able to enhance mechanical and durability properties of the construction material (Gursel et al., 2016). It results particularly suitable in combination with fly ash. As a matter of fact, literature results show that ternary and quaternary concrete mixes with RHA and fly ash exhibit a lower global warming potential while improving the durability of mixes without affecting design strength.

Advanced organic concrete replacements from waste are from various human activities and natural organic growth, such as animal bones and human hair (Petrounias et al., 2021). Such materials in general can be added to cementitious materials for preparing concretes. The use of bones with increased artificial microroughness and a defined amount of human hair with increased microtopography could be the ideal mixture for the replacement of natural aggregates for the production of concrete.

## 19.5 Multifunctional properties

The environmental impact of concretes and other cementitious construction materials on the nature could be limited by enhancing the capabilities of the materials themselves. As a matter of fact, more resistant concretes could allow a decrease in dimensions of the construction elements of structures and infrastructures, reducing the amount of concrete production. Consequently, the energy consumption for the production process and the construction activity, the waste, and the pollutant emission would be reduced. Possible approaches for enhancing the strength performance of concretes are the use of tailored fibers and fillers (Nalon et al., 2022). Examples are metal fibers, microfibers, and nanofibers (Belli et al., 2020). In particular, the

use of nanosized fillers could improve the fracture performance, acting at the beginning of the cracks. Studies present in literature investigate the effect of novel carbon nanoparticles, recently developed thanks to the progress of nanotechnology (Sobolev & Gutiérrez, 2005; Metaxa et al., 2009).

Another approach for increasing the enhancing the sustainability of concrete is the enhancement of its multifunctional properties (Han et al., 2014). For example, a construction material able to behave as a structural or environmental sensor, with self-healing and photocatalytic capability, or self-heating properties, could increase the durability, the safety, the maintenance time, the service life, and the ultimate resistance of a structure or an infrastructure (Espinoza-Moreno et al., 2021; Ubertini et al., 2016). This would result in a longer life of the material and consequently in a more rational and limited production of waste. Literature shows that such multifunctional properties could be obtained through the addition of smart fillers, such as carbon micro and nanosized ones (Faneca et al., 2018).

## 19.6 New additives

Thanks to emerging technologies and the progress in the chemical field, new advanced products, which are available in the market, or in phase of study, are able to enhance the concrete performance or mitigate possible issues arising from the addition of recycled materials (D'Alessandro et al., 2017; Kumar et al., 2006). As an example, the choice of the optimal tailored plasticizer could solve the issues connected to the loss of workability usually related to the presence of recycled aggregates (Matias et al., 2013). In the market, there are different types of chemical additives for particular purposes; however, the choice of the optimal one for the specific cementitious material should be done after a tailored experimental campaign.

## 19.7 Novel sustainable processes

The investigation on the processes related to the concrete production and applications, and their impact of air, soil, water, and environment is worth of investigation for enhancing the sustainability of this type of construction technology. Literature works explore alternative processing procedures and investigate their influence on the relevant physical and mechanical properties of the resulting aggregates and concrete mixtures (Pepe et al., 2014). Therefore, particle size distribution, bulk density attached mortar content, and associated water absorption capacity of recycled aggregates were monitored to evaluate the effectiveness of novel processes, for example, the “autogenous cleaning,” which removes surface impurities and reduces particle heterogeneities, typical of recycled aggregate matrices. The investigated cleaning procedure significantly reduces the gap between the performance of recycled aggregate concrete and normal one, in terms of workability at the fresh state and strength at the hardened state of the composites.

Aside from sustainable fuel, derived from recycled waste, which could be adopted for providing energy in the endothermic reactions during the cement and concrete preparation, or construction activity, other emerging technologies are developing in literature for energy saving (Hasanbeigi et al., 2012). Some examples are fluidized bed kiln, calcareous oil shale, the use of steel slag or no-carbonated raw materials, cement with low lime saturation factor, cement and construction materials based on magnesium oxide, geopolymer cement, capturing the CO<sub>2</sub> resulting from limestone precalcination, CO<sub>2</sub> sequestration in concrete curing technology, carbonate looping technology, biotechnological carbon capture, oxy-fuel technology, postcombustion carbon, capture using absorption technologies, the use of nanotechnology in cement and concrete production, and novel design methods (Muigai et al., 2016).

## 19.8 Conclusion

Concrete is a widespread construction material, due to its versatility, which permits the build of structures and infrastructures with various and diversified shapes and designs. However, the environmental impact of such a technology is high, due to the consumption of raw materials and energy during its preparation and utilization. The sensitivity, which is growing in several fields of industry and engineering for enhancing the sustainability of anthropic processes, allowed the development of multiple approaches for decreasing the impact of concrete constructions. Concrete, as a composite material with various types of porosity, appears particularly promising for an internal modification and for the additions of multiple recycled inclusions. Additives could act as partial or total replacement of cement and aggregates or enhance the physical, chemical, and mechanical performances of the concrete. Possible recycled additions could be rubber, steel slag, polymers and plastics, recycled concrete, fly ash, silica fume, ash from organic pyrolysis, glass, and other micro- and nano-size fillers. Literature results show in some cases issues in strength performance of the recycled materials if the replacements are beyond certain quantities, but with tailored precautions, the use of recycled additions is suitable for concrete components. Moreover, recycled materials could be used as more eco-friendly energy fuels for the preparation processes of cement and concrete. The critical literature review and the advance researches presented in this chapter demonstrated the feasibility of recycled concrete, but progress in standards or recommendations, and in the application to real cases are required for the widespread use of this type of construction material by designers, construction companies, and administrations.

## Funding

The authors acknowledge the funding by the European Union – Next Generation EU under the Italian Ministry of University and Research (MUR) National Innovation Ecosystem Grant ECS 00000041 – Vitality, and the support of the “Fondazione Cassa di Risparmio di Perugia” that funded this study through the project “LONG-LIFE: Innovative technoLOGies for enhanciNG LIFE-cycle sustainability of reinforced concrete structures” - Project Code: 21071 (2022.0400).

## References

- ACI Committee 234. (2006). Report 234R-06 *Guide for the use of silica fume in concrete*. Farmington Hills, MI: American Concrete Institute.
- Agyenim, F., Hewitt, N., Eames, P., & Smyth, M. (2010). A review of materials, heat transfer and phase change problem formulation for latent heat thermal energy storage systems (LHTESS). *Renewable and Sustainable Energy Reviews*, 14, 615–625.
- Aiello, M., & Leuzzi, F. (2010). Waste tyre rubberized concrete: Properties at fresh and hardened state. *Waste Manage*, 30, 1696–1704.
- Bazant, Z. P., Jin, W., & Meyer, C. (1998). In H. Mihashi, Mihashi, & K. Rokugo (Eds.), *Microfracturing caused by alkali-silica reaction of waste glass in concrete* (Vol. 3, pp. 1687–1694). Freiburg, Germany: Aadificatio Publishers.
- Belli, A., Mobili, A., Bellezze, T., & Tittarelli, F. (2020). Commercial and recycled carbon/steel fibers for fiber-reinforced cement mortars with high electrical conductivity. *Cement and Concrete Composites*, 109. Available from <https://doi.org/10.1016/j.cemconcomp.2020.103569>.
- Breccolotti, M., D'Alessandro, A., Roscini, F., & Bonfigli, M. F. (2015). Investigation of Stress - Strain Behaviour of Recycled Aggregate Concrete Under Cyclic Loads. *Environmental Engineering and Management Journal*, 14(7), 1543–1552.
- Brooks, J.J., & Neville, A.M. (2019). *Concrete technology*. Pearson India. ISBN-10: 9353436559.
- Bruno, A. W., Gallipoli, D., Perlot, C., & Mendes, J. (2017). Mechanical behaviour of hyper-compacted earth for building construction. *Materials and Structures*, 50, 160.
- CANMET/ACI. (2004). 8th CANMET/ACI international conference on fly ash, silica fume, slag, and natural Pozzolans in concrete. Farmington Hills, MI: American Concrete Institute; p. 963 [special publication SP-221].
- Colleparidi, M. (2010). *The new Concrete*, 436 p. Tintoretto, ISBN: 8890377720.
- Coppola, L., Coffetti, D., & Crotti, E. (2018). Pre-packed alkali activated cement-free mortars for repair of existing masonry buildings and concrete structures. *Construction and Building Materials*, 4, 677–686.
- Coppola, L., Coffetti, D., Crotti, E., Gazzaniga, G., & Pastore, T. (2020). The durability of one-part alkali-activated slag-based mortars in different environments. *Sustainability*, 12(9).
- Corinaldesi, V., Mazzoli, A., & Siddique, R. (2016). Characterization of lightweight mortars containing wood processing by-products waste. *Construction and Building Materials*, 123, 281–289. Available from <https://doi.org/10.1016/j.conbuildmat.2016.07.011>.
- Curto, A., Lanzoni, L., Tarantino, A. M., & Viviani, M. (2020). Shot-earth for sustainable constructions. *Construction and Building Materials*, 239.
- D'Alessandro, A., Fabiani, C., Pisello, A. L., Ubertini, F., Materazzi, A. L., & Cotana, F. (2017). Innovative concretes for low-carbon constructions: A review. *International Journal of Low-Carbon Technologies*, 12(3), 289–309. Available from <https://doi.org/10.1093/ijlct/ctw013>, September.
- D'Alessandro, A., Materazzi, A. L., & Ubertini, F. (2020). *Nanotechnology in cement-based construction*. Jenny Stanford Publishing, 424 p.
- D'Alessandro, A., Coffetti, D., Crotti, E., Coppola, L., Meoni, A., & Ubertini, F. (2020). Self-sensing properties of green Alkali-activated binders with carbon-based nano-inclusions. *Sustainability (Switzerland)*, 12(23), 1–13, art. no. 9916.
- Demirboga, R. (2007). Thermal conductivity and compressive strength of concrete incorporation with mineral admixtures. *Building and Environment*, 42, 2467–2471.

- EEA. (2020). Mineral waste from construction and demolition, waste treatment. Available from: [https://www.eea.europa.eu/data-and-maps/daviz/mineral-waste-from-construction-and#tab-googlechartid\\_chart\\_13](https://www.eea.europa.eu/data-and-maps/daviz/mineral-waste-from-construction-and#tab-googlechartid_chart_13).
- Espinoza-Moreno, C., Rodriguez-Rodriguez, M., Pellegrini-Cervantes, M. J., et al. (2021). Electrical percolation and fluidity of conductive recycled mortar cement: Graphite powder: Recycled sand with addition of industrial waste carbon fiber. *Carbon Letters*, 31, 707–720. Available from <https://doi.org/10.1007/s42823-020-00188-0>.
- Evangelista, L., & de Brito, J. (2010). Durability performance of concrete made with fine recycled concrete aggregates. *Cement & Concrete Composites*, 32, 9–14.
- Faneca, G., Segura, I., Torrents, J. M., & Aguado, A. (2018). Development of conductive cementitious materials using recycled carbon fibres. *Cement and Concrete Composites*, 92, 135–144. Available from <https://doi.org/10.1016/j.cemconcomp.2018.06.009>.
- Fava, G., Ruello, M. L., & Corinaldesi, V. (2011). Paper mill sludge ash as supplementary cementitious material. *Journal of Materials in Civil Engineering*, 23(6).
- Flower, D., & Sanjayan, J. (2007). Greenhouse gas emissions due to concrete manufacture. *International Journal of Life Cycle Assessment*, 2007(12), 282–288.
- Golewski, G. L., & Gil, D. M. (2021). Studies of fracture toughness in concretes containing fly ash and silica fume in the first 28 days of curing. *Materials*, 14, 319. Available from <https://doi.org/10.3390/ma14020319>.
- Guetta, A., Abibsi, A., & Houari, H. (2006). Durability study of stabilized earth concrete under both laboratory and climatic conditions exposure. *Construction and Building Materials*, 20(3), 119–127.
- Guneyisi, E., Gesoglu, M., & Ozturan, T. (2004). Properties of rubberized concretes containing silica fume. *Journal of Cement and Concrete Research*, 34, 2309–2317.
- Gursel, A. P., Maryman, H., & Ostertag, C. (2016). A life-cycle approach to environmental, mechanical, and durability properties of “green” concrete mixes with rice husk ash. *Journal of Cleaner Production*, 112, 823e836.
- Han, B., Yu, X., & Ou, J. (2014). Self-sensing concrete in smart structures, pp. 1–385. doi:10.1016/C2013-0-14456-X.
- Hasanbeigi, A., Price, L., & Lin, E. (2012). Emerging energy–efficiency and CO2 emission–reduction technologies for cement and concrete production: A technical review. *Renewable and Sustainable Energy Review*, 16, 6220–6238.
- Helmuth, R. (1987). *Fly ash in cement and concrete* (p. 203) Skokie, IL: Portland Cement Association.
- Hendriks, C. A. (2004). *Emission Reduction of Greenhouse Gases from the Cement Industry. Greenhouse gas control technologies conference paper*. California: IEA Greenhouse Gas and R&D Programme.
- Imbabi, M. S., Carrigan, C., & McKenna, S. (2012). Review Article. Trends and developments in green cement and concrete technology. *International Journal of Sustainable Built Environment*, 1, 194–216.
- Inyim, P., & Zhu, Y. (2013). Framework for integrated analysis of building designs using life cycle assessment and energy simulation. ICCREM 2013 ASCE. doi:10.1061/9780784413135.030.
- Jo, B., Park, S., & Park, J. (2008). Mechanical properties of polymer concrete made with recycled PET and recycled concrete aggregates. *Construction and Building Materials*, 22, 2281–2291.
- Joseph, A. M., Snellings, R., Van den Heede, P., Matthys, S., & De Belie, N. (2018). *The use of municipal solid waste incineration ash in various building materials:*

- A Belgian point of view. Materials* (11, p. 141). Switzerland: Basel (1). Available from <https://doi.org/10.3390/ma11010141>.
- Kazmia, S. M. S., Munira, M. J., Wub, Y.-F., Patnaikunib, I., Zhoua, Y., & Xing, F. (2019). Influence of different treatment methods on the mechanical behavior of recycled aggregate concrete: A comparative study. *Cement and Concrete Composites*, *104*, 103398.
- Khatib, J. M. (2005). Properties of concrete incorporating fine recycled aggregate. *Cement and Concrete Research*, *35*, 763–769.
- Kim, J., Park, C., Lee, S., Lee, S., & Won, J. (2008). Effects of the geometry of recycled PET fibre reinforcement on shrinkage cracking of cement-based composites. *Composites: Part B*, *39*, 442–450.
- Kumar, S., Kumar, R., & Bandopadhyay, A. (2006). Innovative methodologies for the utilization of wastes from metallurgical and allied industries. *Resources, Conservation and Recycling*, *48*, 301–314.
- Kusuma, G. H., Budidarmawan, J., & Susilowati, A. (2015). Impact of concrete quality on sustainability. *The 5th International Conference of Euro Asia Civil Engineering Forum (EACEF-5), Procedia Engineering*, *125*, 754–759.
- Liotta, M. A., Viviani, M., & Rodriquez, C. (2016). Structural concrete with recycled aggregate: Advances in mechanical properties, durability and sustainability. *Applied Mechanics and Materials*, *847*, 553–558. Available from <https://doi.org/10.4028/www.scientific.net/amm.847.553>.
- Malešev, M., Radonjanin, V., & Marinković, S. (2010). Recycled concrete as aggregate for structural concrete production. *Sustainability*, *2*, 1204–1225. Available from <https://doi.org/10.3390/su2051204>.
- Mambeli Barros, R. (2022). Municipal solid waste ash. In R. Siddique, R. Belarbi (Eds.), *Woodhead Publishing Series in Civil and Structural Engineering, Sustainable Concrete Made with Ashes and Dust from Different Sources* (pp. 93–177). Woodhead Publishing. <https://doi.org/10.1016/B978-0-12-824050-2.00008-5>.
- Matias, D., de Brito, J., Rosa, A., & Pedro, D. (2013). Mechanical properties of concrete produced with recycled coarse aggregates – Influence of the use of superplasticizers. *Construction and Building Materials*, *44*, 101–109.
- Mehta, P. K., & Monteiro, P. J. M. (2014). *Concrete: Microstructure, properties, and materials* (p. 704) McGraw Hill, ISBN-10: 0071797874.
- Mello, D., Pezzin, S., & Amico, S. (2009). The effect of post consumer PET particles on the performance of flexible polyurethane foams. *Polymer Test*, *28*, 702–708.
- Metaxa, Z. S., Konsta-Gdoutos, M. S., & Shah, S. P. (2009). *Carbon nanotubes reinforced concrete. American Concrete Institute* (pp. 11–20). ACI Special Publication. (267 SP).
- Meyer, C. (2009). The greening of the concrete industry. *Cement & Concrete Composites*, *31*, 601–605.
- Miller, S. A., & Myers, R. J. (2020). Environmental impacts of alternative cement binders. *Environmental Science & Technology*, *5*.
- Mineral Products Association (MPA) – Fact sheet 12, Novel cements: Low energy, low carbon cements. (2012). [http://cement.mineralproducts.org/downloads/fact\\_sheets.php](http://cement.mineralproducts.org/downloads/fact_sheets.php).
- Mo, K. H., Thomas, B. S., Yap, S. P., Abutaha, F., & Tan, C. G. (2020). Viability of agricultural wastes as substitute of natural aggregate in concrete: A review on the durability-related properties. *Journal of Cleaner Production*, *275*. Available from <https://doi.org/10.1016/j.jclepro.2020.123062>.
- Muigai, R., Alexander, M., & Moyo, P. (2016). A novel framework towards the design of more sustainable concrete infrastructure. *Materials and Structures*, *49*, 1127–1141.



- Nagdi, K. (1993). *Rubber as an engineering material: Guidelines for user*. Hanser Publication.
- Nalon, G. H., Santos, R. F., Soares de Lima, G. E., Rocha Andrade, I. K., Gonçalves Pedroti, L., Lopes Ribeiro, J. C., & Franco de Carvalho, J. M. (2022). Recycling waste materials to produce self-sensing concretes for smart and sustainable structures: A review. *Construction and Building Materials*, 325. Available from <https://doi.org/10.1016/j.conbuildmat.2022.126658>.
- Nassar, R. U. D., & Soroushian, P. (2012). Strength and durability of recycled aggregate concrete containing milled glass as partial replacement for cement. *Construction and Building Materials*, 29, 368–377.
- Nematzadeh, M., Nazari, A., & Tayebi, M. (2022). Post-fire impact behavior and durability of steel fiber-reinforced concrete containing blended cement–zeolite and recycled nylon granules as partial aggregate replacement. *Archives of Civil and Mechanical Engineering*, 22, 5. Available from <https://doi.org/10.1007/s43452-021-00324-1>.
- Nochaiya, T., Wongkeo, W., & Chaipanich, A. (2010). Utilization of fly ash with silica fume and properties of Portland cement–fly ash–silica fume concrete. *Fuel*, 768–774. Available from <https://doi.org/10.1016/j.fuel.2009.10.003>, ISSN 0016-2361.
- Pacheco, J., de Brito, J., Chastre, C., & Evangelista, L. (2019). Experimental investigation on the variability of the main mechanical properties of concrete produced with coarse recycled concrete aggregates. *Construction and Building Materials*, 201, 110–120.
- Pacheco-Torgal, F., Ding, Y., & Jalali, S. (2012). Review. Properties and durability of concrete containing polymeric wastes (tyre rubber and polyethylene terephthalate bottles): An overview. *Construction and Building Materials*, 30, 714–724.
- Pacheco-Torgal, F., & Jalali, S. (2012). Earth construction: Lessons from the past for future eco-efficient construction. *Construction and Building Materials*, 29, 512–519.
- Pepe, M., Toledo Filho, R. D., Koenders, E. A. B., & Martinelli, E. (2014). Alternative processing procedures for recycled aggregates in structural concrete. *Construction and Building Materials*, 69, 124–132. Available from <https://doi.org/10.1016/j.conbuildmat.2014.06.084>.
- Petrounias, P., Rogkala, A., Giannakopoulou, P. P., Lampropoulou, P., Xanthopoulou, V., Koutsovitis, P., Koukouzas, N., Lagogiannis, I., Lykokanellos, G., & Gofinopoulos, A. (2021). An innovative experimental petrographic study of concrete produced by animal bones and human hair fibers. *Sustainability*, 13, 8107. Available from <https://doi.org/10.3390/su13148107>.
- Purnell, P. (2012). Material nature versus structural nurture: The embodied carbon of fundamental structural elements. *Environmental Science & Technology*, 46(1), 454–461.
- Rebeiz, K., Fowler, D., & Paul, D. (1994). Mechanical properties of polymer concrete systems made with recycled plastic. *ACI Materials Journal*, 91, 40–45.
- Ren, P., Ling, T. C., & Mo, K. H. (2022). *Journal of Hazardous Materials*, 424, 127457.
- RILEM. (1994). Recommendation: Specifications for concrete with recycled aggregates. *Materials and Structures*, 27, 557–559.
- Dhir, R. K., Limbachiya, M. C., & Paine, K. A. (Eds.), (2001). *Recycling and use of used tyres*. London: Thomas Telford.
- Sadiqul Islam, G. M., Rahman, M. H., & Kazy, N. (2017). Waste glass powder as partial replacement of cement for sustainable concrete practice. *International Journal of Sustainable Built Environment*, 6, 37–44.
- Smidt, A., & Saia, W. H. F. (1963). Alkali-aggregate reaction tests on glass used for exposed aggregate wall panel work. *ACI Materials Journal*, 60, 1235–1236.
- Scrivener, K. L., John, V. M., & Gartner, E. M. (2018). Eco-efficient cements: Potential economically viable solutions for a low-CO<sub>2</sub> cement-based materials industry. *Cement and Concrete Research*, 114, 2–26. Available from <https://doi.org/10.1016/j.cemconres.2018.03.015>.

- Shah, S. P., Hou, P., & Konsta-Gdoutos, M. (2015). Nano-modification of cementitious material: Toward a stronger and durable concrete. *Journal of Sustainable Cement-Based Materials*, 5(1), 1–22.
- Shayan, A., & Xu, A. (2004). Value-added utilisation of waste glass in concrete. *Cement and Concrete Research*, 34(1), 81–89. Available from [https://doi.org/10.1016/S0008-8846\(03\)00251-5](https://doi.org/10.1016/S0008-8846(03)00251-5).
- Shi, C., Krivenko, P. V., & Roy, D. M. (2006). *Alkali-activated cements and concretes*. Abingdon: Taylor & Francis.
- Shi, C., & Zheng, K. (2007). A review on the use of waste glasses in the production of cement and concrete. *Resources, Conservation and Recycling*, 52(2), 234–247. Available from <https://doi.org/10.1016/j.resconrec.2007.01.013>.
- Siddique, R., Khatib, J., & Kaur, I. (2008). Use of recycled plastic in concrete: A review. *Waste Management*, 28(10), 1835–1852. Available from <https://doi.org/10.1016/j.wasman.2007.09.011>.
- Siddique, R., & Naik, T. (2004). Properties of concrete containing scrap-tyre rubber – An overview. *Waste Manage*, 24, 563–569.
- Silva, D., Betioli, A., Gleize, P., Roman, H., Gomez, L., & Ribeiro, J. (2005). Degradation of recycled PET fibers in Portland cement-based materials. *Cement and Concrete Research*, 35, 1741–1746.
- Singh, R., Patel, M., & Sohail, K. S. (2022). The potential use of waste paper sludge for sustainable production of concrete—A review. In B. Laishram, & A. Tawalare (Eds.), *Recent advancements in civil engineering. Lecture notes in civil engineering* (Vol. 172). Singapore: Springer. Available from [https://doi.org/10.1007/978-981-16-4396-5\\_33](https://doi.org/10.1007/978-981-16-4396-5_33).
- Sobolev, K., & Gutiérrez, M. F. (2005). How nanotechnology can change the concrete world. *American Ceramic Society Bulletin*, 84, 14–18. Available from <https://doi.org/10.1002/9780470588260.ch17>.
- Sukontasukkul, P. (2009). Use of crumb rubber to improve thermal and sound properties of pré-cast concrete panel. *Construction and Building Materials*, 23, 1084–1092.
- Taha, M.R., El-Dieb, A.S., & Nehdi, M. (n.d.). Recycling tire rubber in cement-based materials, concrete with recycled materials. ACI Committee 555, in preparation.
- Tam, V. W. Y., Soomro, M., & Evangelista, A. C. J. (2018). A review of recycled aggregate in concrete applications (2000–2017). *Construction and Building Materials*, 172, 272–292.
- Tataranni, P., Besemer, G. M., Bortolotti, V., & Sangiorgi, C. (2018). Preliminary research on the physical and mechanical properties of alternative lightweight aggregates produced by alkali-activation of waste powders. *Materials (Basel Switz.)*, 11, 1255.
- Ubertini, F., Laflamme, S., & D’Alessandro, A. (2016). Smart cement paste with carbon nanotubes. In K. J. Loh, & S. Nagarajaiah (Eds.), *Innovative developments of advanced multifunctional nanocomposites in civil and structural engineering* (pp. 97–120). Woodhead Publishing.
- Van Damme, H., & Houben, H. (2017). Earth concrete. *Stabilization revisited. Cement and Concrete Research*, 114, 90–102.
- Veerabhadram, K., Satya Bhavya, B. L., & Mani Bhaskar S. (2021). *IOP Conference Series: Materials Science and Engineering*, 1025, 012016.
- Villagrán-Zaccardi, Y. A., Marsh, A. T. M., Sosa, M. E., Zega, C. J., De Belie, N., & Bernal, S. A. (2022). Review. Complete re-utilization of waste concretes—Valorisation pathways and research needs. *Resources, Conservation & Recycling*, 177, 105955.
- Xiaoa, J., Lia, J., & Zhang, C. (2005). Mechanical properties of recycled aggregate concrete under uniaxial loading. *Cement and Concrete Research*, 35, 1187–1194.

- Yazici, H., Yigiter, H., Karabulut, A. S., & Baradan, B. (2008). Utilization of fly ash and ground granulated blast furnace slag as an alternative silica source in reactive powder concrete. *Fuel*, *87*, 2401–2407.
- Zamora-Castro, S. A., Salgado-Estrada, R., Sandoval-Herazo, L. Cs, Melendez-Armenta, R. A., Manzano-Huerta, E., Yelmi-Carrillo, E., & Herrera-May, A. L. (2021). Sustainable development of concrete through aggregates and innovative materials: A review. *Applied Sciences*, *11*, 629.
- Zhang, Z., Provis, J. L., Reid, A., & Wang, H. (2014). Geopolymer foam concrete: An emerging material for sustainable construction. *Construction and Building Materials*, *56*, 113–127.
- Zhou, C., & Chen, Z. (2017). Review. Mechanical properties of recycled concrete made with different types of coarse aggregate. *Construction and Building Materials*, *134*, 497–506.

# Index

*Note:* Page numbers followed by “*f*” and “*t*” refer to figures and tables, respectively.

## A

Abrasion resistance, 191–192, 236

Absorption test, 279

Acceleration carbonation, 347

Accelerators, 292

ACI. *See* American Concrete Institute (ACI)

Acid attack, 181

Acid resistance, 186

Activated carbon, 28–29

Adankwame (ADC), 281

ADC. *See* Adankwame (ADC)

Admixtures, 104, 292

- of superplasticizer, 52–54
  - mixing, handling, placing, and forming processes for upcycling of class F pulverized fuel ash, 53, 54*t*
  - relation between flowtime and superplasticizer dosage, 53*f*
  - test program, 53–54

Aggregates, 74, 291–292, 374–375

- gradation limits and design of aggregate gradation, 74*f*
- stack, 47

Aggressive species, 232

Aging, 286–287, 286*t*

- of selected blends, 163

Air permeability method, 136

Air pollution, 336

Air pollution control (APC), 335–336

Air pore

- of fresh mortar, 9–10
- measurement, 5–6

Air-entertaining agents, 292

Airport runways, 251–252

Albite, 340

Algerian NPs, 106–107

Alkali metal ions, 114

Alkali-activated materials, 377

Alkali-activated slag (AAS), 376–377

Alkali–aggregate reaction, 181

Alkaline cement, 144

Alkali–silica reaction (ASR), 114–116, 186–187, 384–385

Alternative recycled fillers

- environmental effect of municipal solid waste incineration ashes as road construction material, 345–347
- management practices of municipal solid waste incineration ashes, 337–339
- municipal solid waste incineration ashes as road construction material, 339–345

Alumina (Al<sub>2</sub>O<sub>3</sub>), 299

Aluminum (Al), 75, 148, 339–340

Aluminum oxide (Al<sub>2</sub>O<sub>3</sub>), 25–26, 84, 96, 339–340

American Concrete Institute (ACI), 18–19, 223

American Standard Testing and Material (ASTM), 126–127

ASTM 642–13, 261–262

ASTM C 39, 259

ASTM C 114–07 standard method, 71, 135

ASTM C128, 74

ASTM C136 standard, 71, 74

ASTM C150, 49–50

ASTM C 187–04 standard method, 132

ASTM C 191–19 standard method, 132–133

ASTM C 293, 72–73, 260

ASTM C311, 175

ASTM C496, 259

ASTM C 618, 134–135

ASTMC666/C666M standard, 72

ASTM C1202, 188

American Standard Testing and Material  
(ASTM) (*Continued*)

- ASTM C1365–18, 130
- ASTM C 1435, 258
- ASTM D 70–97, 156
- ASTM D1754/D1754M-20, 156
- Amorphous Al phase, 223
- Anaerobic digestion, 338–339
- Analcime ( $\text{NaAlSi}_2\text{O}_6 \cdot \text{H}_2\text{O}$ ), 148
- Anhydrite ( $\text{CaSO}_4$ ), 57–58, 340
- Anorthite, 340
- APC. *See* Air pollution control (APC)
- Arsenic (As), 339–340
- ASR. *See* Alkali–silica reaction (ASR)
- ASTM. *See* American Standard Testing and Material (ASTM)
- Atterberg limit, 279, 281, 281*t*

**B**

- BA. *See* Bottom ash (BA)
- Back-scattered electron (BSE), 50
- Barium (Ba), 339–340
- Batch leaching tests, 346
- BBMs. *See* Binder-based materials (BBMs)
- Beam flexing, 8–9
- Bending moment, 209–212, 210*f*, 211*f*
  - mathematical model for prediction of, 212–214
- Binary and ternary bitumen binder system
  - blend preparation, 279–280
  - hydrogen ion concentration (pH), 279
  - materials and method, 278–279
  - particle size distribution, 279
  - results, 281–284, 281*t*, 282*t*
- Binder-based materials (BBMs), 47
  - admixture of superplasticizer, 52–54
  - cement binder and types, 49–50
  - Class F pulverized fuel ash, 50–51
  - high-technology additive of graphite nanoparticles, 52
  - materials and methods, 48
  - properties related to strength, 55–61
    - compressive strength, 57–58
    - flexural strength, 56–57
    - splitting tensile strength, 55–56
    - strength gain index at early age, 58–59
    - strength variation in binders used commonly, 59–61
  - research methodology, 128–133

- tools and materials used, 128–129, 129*f*
  - research procedures, 129–133
    - chemical analysis of wastes sand new cement, 130
    - consistency of new cement paste, 132
    - density of new cement, 131–132
    - fineness of new cement, 131
    - setting time of new cement paste, 132–133
  - X-ray powder diffraction analysis of new cement manufactured, 130–131
  - results, 133–139
    - chemical composition of new cement, 135
    - chemical composition of wastes, 133–135
    - consistency and setting time of new cement, 138–139
    - density of new cement, 138
    - fineness of new cement, 136–138
    - physical properties, 136–139
    - X-ray powder diffraction analysis of new cement, 136
  - strength, 55–56
  - strength variation of BBMs made of different silos of cement in plant, 60*t*
- Binders
- strength variation in, 59–61
  - transforming of conventional binder into binder including graphite nanoparticles, 204–205
- Bitumen (B), 153, 164, 277–278
- Bitumen binder-based materials
- laboratory analysis, 155–156
    - flash point, 156
    - FTIR spectroscopy test, 156
    - kinematic viscosity, 155
    - penetration index and temperature susceptibility, 156
    - penetration point, 155
    - short-term aging test, 156
    - softening point temperature, 155
    - specific gravity, 156
  - materials and method, 155–156
    - bitumen-based binder, 155–156
  - natural rubber latex, 155
  - objective, 154
  - results, 159–164, 159*t*
    - flash point, aging, and viscosity of selected blends, 163, 163*t*

- Fourier-transform infrared analysis, 164  
penetration point, 159–160  
softening point temperature, 160–161, 160*f*  
specific gravity test, 162  
temperature susceptibility and penetration index, 162–163  
viscosity analysis, 161  
sample preparation, 155
- BL. *See* Blend (BL)
- Black pollution, 295
- Blast furnace slag, 221
- Blend (BL), 164  
Blocking ratio, 317–318
- Bogge chemical compounds, 131
- Bottom ash (BA), 127, 336  
application of bottom ash in bituminous mixtures, 340–342  
as mineral filler, 341–342  
properties of, 339–340
- Bragg's law, 131
- Brench method. *See* Wet chemistry
- British Standards (BS), 49–50, 79–80
- BS. *See* British Standards (BS); Burnt shale (BS)
- BSE. *See* Back-scattered electron (BSE)
- Bulk binder matrix, 47
- Bull moose Coal Mine, 256
- Burnt shale (BS), 49–50
- C**
- C-S-H. *See* Calcium silicate hydrate gel (C-S-H)
- C.A. *See* Coarse aggregates (C.A)
- Ca/Si. *See* Calcium-to-silica (Ca/Si)
- Cadmium (Cd), 339–340
- Calcareous sedimentary soils, 124
- Calcination process, 243
- Calcined clays, 67, 221, 230  
effect of combination of, 228–230  
combination of calcined clay with additions, 230  
durability properties, 232–236  
abrasion and skid resistance, 236  
absorption, porosity, and pore structure, 232–234  
fire resistance, 236  
general, 232  
permeability, chloride ingress, and carbonation, 234–235  
sulfate resistance, 235–236  
economic and environmental aspects, 236–237  
fresh concrete properties, 224–226  
consistency, 224, 224*t*, 225*f*  
setting time, 225, 225*f*  
workability, 226, 226*f*  
materials, 222–224  
chemical and physical requirements of pozzolanic materials, 223*t*  
various cases of calcined clay brick, 223*f*  
mechanical properties, 227–231  
compressive strength, 227–230  
elastic and dynamic moduli, 231  
splitting tensile and flexural strengths, 230–231  
effect of type and content of clay minerals, 227  
mix, 234  
shrinkage, 231–232  
waste, 143–144
- Calcined perlite powder (CPP), 114
- Calcite (CaCO<sub>3</sub>), 57–58, 95–96, 167, 293, 340
- Calcium (Ca), 339–340
- Calcium aluminosilicate hydrate, 223
- Calcium bicarbonate (Ca(HCO<sub>3</sub>)<sub>2</sub>), 124
- Calcium carbonate (CaCO<sub>3</sub>), 107, 124, 175–176, 186
- Calcium chloride (CaCl<sub>2</sub>), 292, 339–340
- Calcium hydro silicate (CHS), 181
- Calcium hydroxide (Ca(OH)<sub>2</sub>), 31, 47, 56–58, 61, 175–176, 178–180, 186–188, 207, 214–215
- Calcium oxide (CaO), 25–26, 56–57, 76, 79, 83–84, 95–96, 126–127, 134–135, 170, 192, 252–253, 299, 343, 365
- Calcium silicate hydrate gel (C-S-H), 61, 95–96, 107–108, 178, 223, 299
- Calcium sulfate (CaSO<sub>4</sub>), 112
- Calcium sulfoaluminate cement (CSA), 380
- Calcium-aluminum hydrate, 96
- Calcium-to-silica (Ca/Si), 115
- Calorimetry, 174
- Cantilever flexing, 8–9

- Capillarity coefficient, 146–147
- Capillary water absorption, 13–14,  
145–147  
measurement of, 7  
results of capillary water absorption of  
HPG, 146*t*
- Carbon dioxide (CO<sub>2</sub>), 31, 50, 67, 293
- Carbon-based nanomaterials, 203
- Carbonation, 107–110, 187–188  
calcined clay, 234–235  
influence of different parameters on  
carbonation resistance of RAC, 110*t*  
reactions, 107–108  
results of accelerated carbonation test on  
selected concrete mixtures, 108*t*
- Carbonic acid (H<sub>2</sub>CO<sub>3</sub>), 124
- Casted specimens, 259
- CBCMs. *See* Cement-based composite materials (CBCMs)
- CBMs. *See* Cement-based materials (CBMs)
- CBP. *See* Clay brick powder (CBP)
- CC. *See* Conventional concrete (CC)
- CDW. *See* Construction demolition waste (CDW)
- Cement, 67, 73–74, 127–128, 133, 235, 291–292  
based materials, 143–144  
binder and types, 49–50  
cement-based construction materials, 203–204  
cement-based mixture, 137–138  
chemical properties, 73*t*  
hydration, 37–38, 225  
making process, 126  
manufacture process, 117  
effect of marble powder on fresh properties of, 171–174  
paste  
consistency of new, 132  
setting time of new, 132–133  
production, 228  
setting time, 138
- Cement-based composite materials (CBCMs), 126–127
- Cement-based materials (CBMs), 1–2, 25–27
- Cementitious materials (CM), 108, 234, 258, 292, 309–310
- Cementitious systems, 236–237
- CH. *See* Calcium hydroxide (Ca(OH)<sub>2</sub>)
- Chemical admixtures, 12, 292
- Chemical analysis of wastes sand new cement, 130
- Chemical composition  
of MP, 170  
of new cement, 135, 135*t*  
of wastes, 133–135, 134*t*
- Chemical compounds, 84, 96
- Chemical separation, 347
- Chemical stabilization, 347
- Chloride, 232  
binding, 110  
diffusion coefficients, 189  
ingress, calcined clay, 234–235  
penetration for concrete, 189  
permeability, 188–189  
resistance to chloride attack, 110–112
- Chlorine (Cl), 339–340
- Chlorite, 222
- Chromium (Cr), 339–340
- Class C pulverized fuel ash, 31–32
- Class F pulverized fuel ash, 50–51  
BSE image of fuel ash in binder material, 50*f*  
mixing, handling, placing, and forming processes for upcycling of, 53  
properties of class FPFA and class C PFA used for comparison with properties of high-LOI PFA, 51*t*
- Class C fuel ash, 126–127
- Clay brick powder (CBP), 222
- Clayey bricks, 292  
WBP use in, 302–303
- Clays, 221–222, 278  
bricks, 222  
waste, 222  
samples, 278  
effect of type and content of clay minerals, 227
- CM. *See* Cementitious materials (CM)
- CO<sub>2</sub> capture and storage (CCS), 380
- Coal ash, 243–244
- Coal combustion products, 243–244
- Coal fly ash, 309–310
- Coal waste, 127
- Coal waste ash (CWA), 68–69
- Coal waste powder (CWP), 68–69

- Coal bottom ash (CBA). *See also* Oil shale ash (OSA); Wheat straw ash (WSA)  
 methodology, 244–246  
 preparation of concrete and testing, 246  
 preparation of raw materials, 244–245  
 result, 246–248  
   compressive strength, 247  
   splitting tensile strength, 248  
   workability, 246, 247*f*
- Coarse aggregates (C. A.), 258, 311–312
- Coefficient of capillarity, 147, 147*t*
- Column leaching tests, 346
- Combustion  
 process, 128  
 of raw material, 128  
 technologies, 335–336
- Compaction, 279, 282
- Composite, 25–26  
 cement, 127–128
- Composting, 338–339
- Compression force, 53  
 regression relationships between  
   compressive strength and nG/ASTM  
   type I cement, 39*f*  
 regression relationships between  
   compressive strength and nG/class C  
   PFA-cement, 40*f*  
 strength in, 37–40
- Compressive strength, 17–19, 48, 57–58, 227–230, 300–301  
 CBA, 247  
   result, 247*f*  
 combination of calcined clay with  
   additions, 230  
 effect of combination of limestone and  
   calcined clay, 228–230  
 GNP, 206–207  
   180th-day relative compressive strength  
   of mortar, GNP content, and control  
   mortar, 207*f*  
   28th-day relative compressive strength  
   of mortar, GNP content, and control  
   mortar, 206*f*  
 mathematical model for estimation of,  
   208–209  
 MP, 176, 177*t*  
 NP, 103–104  
 RCC, 259, 262–264  
   average compressive strength and  
   standard errors for RCC, 263*f*  
   compressive strength test results for  
   RCC mixes containing RCA, RAPA,  
   and SF, 262*t*  
   failure shape for RCC specimens under  
   load of compression, 264*f*  
   relationship between G/class F  
   PFA–binder and compressive  
   strength in binder-based materials,  
   55*f*  
   of self-compacting concrete mixture,  
   319–320  
   blended with fly ash, 321*f*  
   blended with GGBFS, 320*f*  
   blended with GGBFS and fly ash, 321*f*  
   test, 246  
   WSA, 9
- Compressive stress, 72–73, 82–85  
 after freezing–thawing cycle, 81–82  
 regression equations between  
   freezing–thawing cycle and, 81*f*
- Concrete, 25–26, 221, 243–244, 252, 291–295, 309–310, 373–375, 390  
 abrasion resistance, 191  
 durability properties of concrete made  
   with marble powder, 181–192  
 environmental hazards, 293  
 greenization, 293  
 ingredients, 292  
 effect of marble powder on fresh  
   properties of, 171–174  
 material, 67  
 mixing, casting, and curing, 258–259  
   cylindrical molds with specimens of  
   RCC, 259*f*  
   prism mold with specimen of RCC,  
   258*f*  
 permeability, 181  
 preparation of, 246  
   concrete mixture proportion, 246*t*  
 replacement of natural aggregates,  
   293–295  
 water absorption, 261–262, 270  
 WBP use in, 299–302
- Conservation of mass, 7–8
- Construction demolition waste (CDW), 251–252
- Conventional CBM, 16



Conventional binder transformation into binder and mortar, 204–205  
 Conventional concrete (CC), 117, 292, 375*f*  
 Conventional Portland cement, 73, 143–144  
 Copper (Cu), 339–340  
   slag, 293–294, 294*f*  
 Corn cub ash, 295, 295*f*  
 Corrosion, 181, 189–190  
 Cost–benefit analysis, 369–370  
 CPP. *See* Calcined perlite powder (CPP)  
 Crumb rubber, 252, 295–296, 296*f*  
 Crushing process, 255–256  
 CWA. *See* Coal waste ash (CWA)  
 CWP. *See* Coal waste powder (CWP)  
 Cylindrical steel mold, 71

## D

Daracem SP6RR, 255–256  
 Decomposition process, 227  
 Degradation, 189–190  
 Degree of hydration, 181  
 Degree of regression, 209, 213–214  
 Density  
   of fresh mixing, 76–77  
   of hardened specimens, 77–78  
     relationships between water content and dry density for different percentage of OSA in RCGC, 77*f*  
   of new cement, 131–132, 138  
   of RCC, 261, 272–273  
     average density of RCC with replacement percentages of RCA, RAPA, and SF, 272*f*

Differential thermal analysis (DTA), 175–176

Dolomitic soils, 124

Dry densities, 78, 261

Drying shrinkage, 184, 232

DTA. *See* Differential thermal analysis (DTA)

## Durability

evaluation test, 270

measurement, 72

NP, 106–116

  ASR, 114–116

  carbonation, 107–110

  permeability, 106–107

  resistance to chloride attack, 110–112

  resistance to sulfate attack, 112–114

properties of concrete made with marble powder, 181–192

  abrasion resistance, 191–192

  acid resistance, 186

  ASR, 186–187

  carbonation, 187–188

  chloride permeability, 188–189

  corrosion, 189–190

  fire resistance, 190

  permeability, 181–182

  porosity, 183–184

  resistance to freeze and thaw cycling, 191

  shrinkage, 184

  sulfate resistance, 185

  water absorption, 182–183

  of RCC mixtures, 252–253

Dust particles, 336

Dynamic moduli, 231

## E

E needles. *See* Ettringite needles (E needles)

EAF. *See* Electric arc furnace (EAF)

Eco-type cementitious materials, 221

Ecology-based sustainable green cement-based materials, 67–68

Elastic modulus, 105, 231

  of LC3 concrete, 231

Elasticity

  modulus of, 268–270

  static modulus of, 260–261

Electric arc furnace (EAF), 90–91, 252–253

Electrochemical technique, 347

Energy, 167

  recovery, 335–336

Energy power stations (EPSs), 124–126

Energy-dispersive X-ray fluorescence method (Energy-dispersive XRF method), 130

Energy-dispersive XRF method. *See* Energy-dispersive X-ray fluorescence method (Energy-dispersive XRF method)

Engineering-based composites, 233–234

Environmental assessment of usage of

  pulverized fuel ash in cement-based materials, 25–27

  carbon dioxide emission and energy consumption of constituent materials, 27*t*

- EPSs. *See* Energy power stations (EPSs)
- Ethylene–vinyl acetate, 277–278
- Ettringite needles (E needles), 178
- European Union, 221
- F**
- FA. *See* Fly ash (FA)
- FBD. *See* Fluidized bed combustion (FBD)
- Ferrite, 75
- Ferrite oxide, 84
- Fine aggregates (F.A.), 311–312  
replacement of, 340–341
- Fineness of new cement, 131, 136–138,  
137*f*, 137*t*
- Fire resistance, 190, 190*t*, 236
- Flash point, 156, 280, 286–287, 286*t*  
of selected blends, 163
- Flexural capacity, 148, 148*t*
- Flexural moment stress, 72–73, 88–91, 89*f*,  
90*f*
- Flexural strength, 16–17, 33–35, 48,  
56–57, 230–231  
NP, 103–105  
of RCC, 267  
RCC, 260, 266–268  
average and error bar of flexural  
strength for RCC, 268*f*  
flexural strength test with one-point  
loading method, 260*f*  
flexural strength test results for RCC  
mixes, 267*t*  
regression relationships between flexural  
strength and nG/ASTM type I  
cement, 33*f*  
of self-compacting concrete mixture, 324  
blended with fly ash, 325*f*  
blended with GGBFS, 324*f*  
blended with GGBFS and fly ash, 325*f*  
WSA, 8–9  
compressive strength, 9
- Flexural tensile strength, MP, 176
- Fluidized bed combustion (FBD), 335–336
- Fly ash (FA), 103–104, 143–144, 221, 252,  
310–311, 336, 380*f*  
application of fly ash in bituminous  
mixtures, 344–345  
chemical composition, 312*t*  
as mineral filler, 344–345  
properties, 342–344
- Fourier-transform infrared spectroscopy  
(FTIR spectroscopy), 154, 156, 164,  
164*f*
- Fourth-degree mathematical equations, 209,  
213–214, 217
- Freeze and thaw cycling, resistance to, 191
- Freezing process, 79–82
- Freezing–thawing cycle, 124  
change in weight after, 79–81  
compressive stress after freezing–thawing  
cycle, 81–82  
resistance, 72
- Freezing–thawing resistance of concrete,  
191
- Fresh and hardened densities, 300
- Fresh concrete results, 314–319, 315*t*  
J-ring test, 318  
L-box test, 317–318  
sieve segregation, 318–319  
slump flow, 315–316  
T50 flow, 316–317  
V-funnel, 316
- Fresh mixing, density of, 76–77, 76*f*
- Fresh mortars  
air pore of, 9–10  
results of fresh mortars tests, 103*t*  
unit weight of, 11–12
- Fresh properties of self-compacting concrete  
mixture, 313–314
- Frost damage, 181
- FTIR spectroscopy. *See* Fourier-transform  
infrared spectroscopy (FTIR  
spectroscopy)
- Fusion, 347
- G**
- Gas diffusion, 108
- Gasification, 338–339
- GCBC. *See* Ground clay brick calcined  
(GCBC)
- Geopolymers, 143–144  
geopolymer-based materials, 143–144,  
148
- GGBFS. *See* Ground granulated blast  
furnace slag (GGBFS)
- Ghana Highway Authority, 159
- Gilsonite, 277–278
- Glass powder, 252
- Glass-like particles, 311

- GNP. *See* Graphene nanoplates (GNP)
- GNPs. *See* Graphite nanoparticles (GNPs)
- Granulated blast furnace slag, 311
- Graphene, 203
- Graphene nanoplates (GNP), 31, 203
- Graphene oxide, 203
- Graphite (GRP), 211–212
- Graphite nanoparticles (GNPs), 47, 203
  - bending moment, 209–212
  - casting, mixing, and specimen preparation, 205
  - characterization, 206
  - class C pulverized fuel ash, 31–32
  - environmental assessment of usage of pulverized fuel ash in cement-based materials, 25–27
  - high-technology additive of, 52
  - materials and methods, 204–205, 204*t*
    - transforming of conventional binder into binder and mortar, 204–205, 205*t*
  - mathematical model for estimation of compressive strength, 208–209
  - mathematical model for estimation of splitting tensile strength, 216–217
  - mathematical model for prediction of bending moment, 212–214
  - nature of strength, 33–40
  - pulverized fuel ash-cement system, 25–27
  - results, 206–207
    - compressive strength, 206–207
    - splitting tensile strength, 214–215
  - synthetic graphite nanoparticles, 27–28
  - upcycling process and tests performed, 32–33
- Graphitic carbon, 28–29
- Gravimetric method, 133
- Green concrete, 293
- Greenhouse gas emissions, 309–310
- Greenization, 293
- Ground calcined bricks, 221
- Ground CBA, 244
- Ground clay brick calcined (GCBC), 235–236
- Ground granulated blast furnace slag (GGBFS), 47, 67, 144, 309–311, 358
  - chemical composition, 312*t*
  - materials and methods, 144
    - chemical composition of, 144*t*
    - mixing, handling, placing, and molding of HPG, 145
- methodology, 358–364
  - materials, 358–360
  - mix composition, sample preparation, and testing, 360–364
- methods, 145–146
- results, 146–149
  - capillary water absorption, 146–147
  - coefficient of capillarity, 147
  - cost analysis hemp–clay brick, 369–370
  - flexural capacity, 148
  - laboratory stabilized clay–hemp brick manufacture, 368
  - linear expansion, 365–368
  - PC–GGBS stabilized systems, 364–365
  - strength development of the lime–GGBS, 364–365
  - uniaxial compression strength, 148–149
- GRP. *See* Graphite (GRP)
- Gypsum, 133
- H**
- Halloysite, 222
- Hardened concrete results, 319–326
  - compressive strength of self-compacting concrete mixture, 319–320
  - flexural strength of self-compacting concrete mixture, 324
  - splitting tensile strength of self-compacting concrete mixture, 321–323
  - water penetration depth of self-compacting concrete mixture, 325–326
- Hardened properties of self-compacting concrete mixture, 314
- Hardening process, 205
- Heavy metals, 243–244
- Hematite (Fe<sub>2</sub>O<sub>3</sub>), 57–58
- Heterogeneous material, 339
- High-grade kaolinitic clays, 222
- High-loss-on-ignition, 51
- High-performance geopolymers (HPGs), 144, 146–147
  - mixing, handling, placing, and molding of, 145, 145*t*

- High-strength concrete, 230
- High-technology additive of graphite nanoparticles, 52
- High-volume fly ash (HVFA), 252
- High-volume fuel ash, 51
- High temperature resistance, 190
- HMA. *See* Hot mix asphalt (HMA)
- Hot mix asphalt (HMA), 335
- Household waste (HW), 123
- HPGs. *See* High-performance geopolymers (HPGs)
- HVFA. *See* High-volume fly ash (HVFA)
- HW. *See* Household waste (HW)
- Hydration heat, 174, 175*f*
- Hydration process, 49, 78, 116–117, 132, 181, 247, 252–253
- Hydration products, 96
- Hydraulic binder, 49–50
- research methodology, 128–133
  - tools and materials used, 128–129, 129*f*
  - research procedures, 129–133
  - chemical analysis of wastes sand new cement, 130
  - consistency of new cement paste, 132
  - density of new cement, 131–132
  - fineness of new cement, 131
  - setting time of new cement paste, 132–133
  - X-ray powder diffraction analysis of new cement manufactured, 130–131
- results, 133–139
- chemical composition of new cement, 135
  - chemical composition of wastes, 133–135
  - consistency and setting time of new cement, 138–139
  - density of new cement, 138
  - fineness of new cement, 136–138
  - physical properties, 136–139
  - X-ray powder diffraction analysis of new cement, 136
- Hydrogen ion concentration (pH), 279
- Hydrothermal solidification, 347
- Hydroxyl ions (OH<sup>-</sup>), 114
- I**
- IBA. *See* Incineration bottom ash (IBA)
- Illite, 222
- Incineration bottom ash (IBA), 340
- Incineration process, 124–126, 335–336
- Indirect test, 35
- Industrial byproducts, 49–50, 143–144
- Industrial hemp, 358–360, 360*t*
- Insoluble high-silicon-ratio crystalline matrix, 148
- Innovative and sustainable concrete materials
- alternative binders to cement, 376–377
  - earth-concretes, 377–379, 378*f*
  - fly ash and silica fume, 379
  - geopolymers, 377
  - ground granulated blast furnace slag, 377
  - new efficient cements, 380
  - multifunctional properties, 388–389
  - new additives, 389
  - novel sustainable processes, 389–390
  - recycled components, 380–388
  - organic waste, 387–388
  - recycled aggregates, 380–383
  - recycled glass, 384–385
  - recycled plastic, 385–387
  - recycled tires, 383–384
  - state-of-art concrete materials, 374–376
- Integrated waste management, 123
- Interfacial transition zone (ITZ), 47, 112, 209–210, 341–342
- Iron (Fe), 339–340
- powder, 294, 294*f*
- Iron oxide (Fe<sub>2</sub>O<sub>3</sub>), 25–26, 96, 299, 339–340
- ITZ. *See* Interfacial transition zone (ITZ)
- J**
- J-ring test, 313–314, 318
- K**
- Kaolinite, 222, 227
- Kaolinitic clays, 221–222, 278
- Kinematic viscosity, 155, 280, 284–285
- at 135°C for blends at different percentages of clay, 285*f*
- L**
- L-box test, 313–314, 317–318
- Laboratory analysis, 280
- Landfilling leachate, 337–338

- LC3-based concrete. *See* Limestone calcined clay cement-based concrete (LC3-based concrete)
- Leaching characteristics of municipal solid waste incineration ashes, 345–346
- Lead (Pb), 339–340
- Lignite, 126–127
- Lime (CaO), 57–58, 133
- Limestone (LS), 104
  - effect of combination of, 228–230
  - powder, 49–50, 67
  - soils, 124
- Limestone calcined clay cement-based concrete (LC3-based concrete), 228, 230
  - cement, 229
  - on elastic modulus, 231
- Linear regression equations, 56–58
- Linear variable differential transformer (LVDT), 260–261
- Lower Oxford Clay (LOC), 358–360, 359*t*
- LS. *See* Limestone (LS)
- LVDT. *See* Linear variable differential transformer (LVDT)
- M**
- Magnesium oxide (MgO), 25–26, 339–340
- Magnesium sulfate (MgSO<sub>4</sub>), 112
- Magnesium-silicate-hydrate, 96
- Magnetite (Fe<sub>3</sub>O<sub>4</sub>), 57–58
- Manufacturing process, 264
- Marble, 167–168
- Marble powder (MP), 67, 102, 143–144, 167, 184
  - advantages of, 167–168
  - applications of, 168
  - durability properties of concrete made with, 181–192
    - abrasion resistance, 191–192
    - acid resistance, 186
    - ASR, 186–187
    - carbonation, 187–188
    - chloride permeability, 188–189
    - corrosion, 189–190
    - fire resistance, 190
    - permeability, 181–182
    - porosity, 183–184
    - resistance to freeze and thaw cycling, 191
    - shrinkage, 184
    - sulfate resistance, 185
    - water absorption, 182–183
  - economic aspect, 192–193
  - effect on fresh properties of cement/mortar/concrete, 171–174
    - hydration heat, 174
    - rheological behavior, 173, 174*f*
    - setting time, 172–173, 173*t*
    - workability, 171–172, 172*f*
  - effect on hardened properties, 175–177
    - compressive strength, 176
    - flexural tensile strength, 176
    - modulus of elasticity, 177
    - SAI of mixtures incorporating marble powder, 175
    - splitting tensile strength, 176–177
    - thermal analysis of mixtures incorporating marble powder, 175–176
  - environmental performance, 193–194
  - microstructure, 178–180
    - micrographs of control mix and specimen, 179*f*
    - SEM analysis for paste samples containing marble powder, 178*f*
    - SEM morphology of mortar containing MP as replacement of cement, 180*f*
- MP-blended cement specimens, 178
- properties of, 168–170
  - chemical properties, 170, 170*t*
  - particle size, 168
  - physical properties, 169, 169*t*
  - specific gravity and fineness, 169
- Marl soils, 124
- Mass
  - burning, 335–336
  - change of, 14–15
  - measurement of change of, 7–8
- Mass burn (MB), 335–336, 338–339
- Mathematical equations, 9, 13, 15
  - of compressive strength, 208–209
  - of splitting tensile strength, 216
- Mathematical models, 216
  - for estimation of compressive strength, 208–209, 208*f*, 209*f*
  - for estimation of splitting tensile strength, 216–217, 216*f*
  - for prediction of bending moment, 212–214, 212*f*, 213*f*
  - for strength estimation, 9–19

- Maximum dry density (MDD), 281  
MB. *See* Mass burn (MB)  
MBT. *See* Mechanical-biological treatment (MBT)  
MDD. *See* Maximum dry density (MDD)  
Mechanical properties  
  OSA, 72–73  
  of RCC, 252–253  
Mechanical tests, 8–9  
  compressive strength, 9  
  flexural strength, 8–9  
Mechanical-biological treatment (MBT), 338–339  
Mechanics, 7–8  
Mechanistic empirical pavement design guide (MEPDG), 341–342  
Mediterranean Sea, 124  
Mediterranean soil, 123–126  
Melt blend techniques, 155  
Melting, 347  
MEPDG. *See* Mechanistic empirical pavement design guide (MEPDG)  
Metakaolin (MK), 40, 227  
Metal-based graphite, 52  
Methane (CH<sub>4</sub>), 67  
MFL Prüf-systeme Universal Testing Machine, 259  
Micrographs of control mix and specimen, 179f  
Microsilica, 379  
Microstructure  
  analysis with scanning electron microscopy, 93–94  
  SEM micrographs for RCC and RCGC, 94f  
  of concrete, 116–117, 234  
  of marble powder, 178–180  
  of natural pozzolan, 116–117  
  phase analysis, 73  
Mineral additions, 221  
Mineral admixtures, 103–104, 221  
Mineralogical phase analysis, 73  
  with X-ray diffraction, 95–96  
Minerals, 75  
Mix design, 256–257, 257t  
  of roller-compacted concrete and roller-compacted green concrete, 70–71, 70t  
Mixing materials  
  aggregate, 74  
  cement, 73–74  
  chemical and physical properties of, 71, 73–76  
  oil shale ash, 74–76  
Mixtures incorporating marble powder, thermal analysis of, 175–176  
MK. *See* Metakaolin (MK)  
Modulus of elasticity, 91–93  
  marble powder, 177, 178f  
  of RCC, 268–270  
    average and error bar of modulus of elasticity for RCC, 269f  
    mixes, 269t  
  stress–strain curves for RCC and RCGC, 92f  
Moisture content, 282  
Montmorillonite, 222, 278  
Mortars, 187, 207, 209–210, 214  
  bars, 187  
  graphite nanoparticles, 204–205  
  effect of marble powder on fresh properties of, 171–174  
  methods used for measuring physical and mechanical properties of, 5  
MP. *See* Marble powder (MP)  
MSW. *See* Municipal solid waste (MSW)  
MSWI. *See* Municipal solid waste incineration (MSWI)  
MSWI-BA. *See* Municipal solid waste incineration bottom ash (MSWI-BA)  
MSWI-FA. *See* Municipal solid waste incineration fly ash (MSWI-FA)  
Municipal solid waste (MSW), 335, 387–388  
Municipal solid waste incineration (MSWI), 335–336  
  MSWI-BA, 336–337  
  MSWI-FA, 336–337  
Municipal solid waste incineration ashes  
  management practices of, 337–339  
  as road construction material, 339–345  
  environmental effect, 345–347  
  leaching characteristics of municipal solid waste incineration ashes, 345–346  
  municipal solid waste incineration ash leaching reduction and treatments, 347

- Municipal solid waste incineration ashes  
(*Continued*)  
 municipal solid waste incineration  
 bottom ash, 339–340  
 municipal solid waste incineration fly  
 ash, 342–345
- Municipal solid waste incineration bottom  
 ash (MSWI-BA), 339–340  
 application of bottom ash in bituminous  
 mixtures, 340–342  
 properties of bottom ash, 339–340
- Municipal solid waste incineration fly ash  
 (MSWI-FA), 342–345  
 application of fly ash in bituminous  
 mixtures, 344–345  
 properties of fly ash, 342–344

## N

- NA. *See* Neutral axis (NA)  
 NAC. *See* Natural aggregate concrete (NAC)  
 Nanoclays (NC), 107, 278  
 Nanomaterials, 26–27, 203, 277–278  
 NAs. *See* Natural aggregates (NAs)  
 Natural aggregates (NAs), 68–69, 252–253,  
 335  
 copper slag, 293–294, 294*f*  
 corn cub ash, 295, 295*f*  
 iron powder, 294, 294*f*  
 replacement of, 293–295
- Natural pozzolan (NP), 55, 101  
 durability, 106–116  
 environmental and economical aspects,  
 117  
 mechanical properties, 103–105  
 compressive strength, 103–104  
 elastic modulus, 105  
 flexural strength, 104–105  
 shrinkage, 105  
 microstructure, 116–117  
 rheological properties, 101–103  
 fresh properties of SCC mixtures, 102*t*  
 results of fresh mortars tests, 103*t*
- Natural pozzolana, 221  
 Natural raw materials, 50  
 Natural rubber, 277–278  
 latex, 155, 278  
 Natural rubber latex-substituted-bitumen  
 binder  
 materials and method, 155–156

- bitumen-based binder, 155–156  
 objective, 154  
 results, 159–164, 159*t*  
 flash point, aging, and viscosity of  
 selected blends, 163, 163*t*  
 Fourier-transform infrared analysis,  
 164  
 penetration point, 159–160  
 softening point temperature, 160–161,  
 160*f*  
 specific gravity test, 162  
 temperature susceptibility and  
 penetration index, 162–163  
 viscosity analysis, 161
- Natural zeolite (NZ), 106  
 Natural aggregate concrete (NAC), 107  
 Natural resources, 243  
 NC. *See* Nanoclays (NC)  
 NCA. *See* Normal coarse aggregate (NCA)  
 Net present value (NPV), 369–370  
 Neutral axis (NA), 8–9  
 New cement  
 chemical composition of, 135  
 consistency and setting time of, 138–139,  
 138*t*  
 density of, 138  
 fineness of, 136–138  
 paste setting time of, 132–133  
 X-ray powder diffraction analysis of, 136
- Ni. *See* Nickel (Ni)  
 Nickel (Ni), 339–340  
 Nitrogen oxides (NO<sub>x</sub>), 67  
 Nongraphitizable carbon, 28–29  
 Normal coarse aggregate (NCA), 107  
 Novel sustainable processes, 389–390  
 NP. *See* Natural pozzolan (NP)  
 NZ. *See* Natural zeolite (NZ)

## O

- Oil shale ash (OSA), 67, 74–76. *See also*  
 Wheat straw ash (WSA); Coal  
 bottom ash (CBA)  
 analysis methods, 71–73  
 chemical and physical properties of  
 mixing materials, 71  
 density of fresh mixing, 71  
 density of hardened specimens, 72  
 durability measurement, 72  
 mechanical properties, 72–73

- microstructure and mineralogical phase analysis, 73
- porosity measurement, 72
- availability of data and materials, 97
- chemical composition of, 75*t*
- materials and methods, 70–73
  - mix design of roller-compacted concrete and roller-compacted green concrete, 70–71
  - preparation of roller compacted concrete and roller-compacted green concrete, 71
- OSA-substituted ASTM type I cement, 73 results, 73–96
  - chemical and physical properties of mixing materials, 73–76
  - durability properties of roller-compacted concrete and roller-compacted green concrete, 79–82
  - mechanical properties of roller-compacted concrete and roller-compacted green concrete, 82–93
  - microstructure analysis of roller-compacted concrete and roller-compacted green concrete, 93–96
  - physical properties of roller compacted concrete and roller-compacted green concrete, 76–79
- SEM micrograph and XRD analysis of OSA, 75*f*
- OMC. *See* Optimum moisture content (OMC)
- One-point loading method, flexural strength test with, 260*f*
- Optimum moisture content (OMC), 281
- Ordinary cementitious composites, 296
- Ordinary Portland cement (OPC), 374–375
- Organic waste, 387–388
- OSA. *See* Oil shale ash (OSA)
- Outdoor tiles, 126–127
- P**
- Particle size, 168
  - distribution, 279, 282
    - of clay samples, 282*f*
  - distributions of marble powder and cement, 168*f*
  - SEM analysis of marble powder, 169*f*
- Passing ability, 313–314
- Paste replacement method, 193–194
- PC. *See* Portland cement (PC)
- Penetration index, 156, 157*t*, 162–163, 163*t*
- Penetration point, 155, 159–160, 280, 283
  - for blends at different percentages of clay, 283*f*
  - penetration test results, 159*f*
- Periclase, 75
- Permeability, 106–107
  - calcined clay, 234–235
  - effect of natural zeolite on transport properties, 106*t*
- PFA. *See* Pulverized fuel ash (PFA)
- pH, 281, 281*t*
  - pH-static leaching tests, 346
- Phase change materials (PCMs), 373–374
- Physical properties of old concrete, 254–255
- Physical separation, 347
- Plasma arc gasification, 338–339
- Plastic viscosity, 173
- Plasticity, 279
- Plasticizers, 292
- Plastic materials, 168
- Plastic waste, 385–386
- Pollutants, 336
- Polycarboxylic ethers, 52
- Polymers, 153–154
  - materials application, 153–154
  - modification of bitumen, 153–154, 277–278
- Polynomial equations, 10–11, 14–15, 17–19, 37, 56–58, 213–214, 217
- Polynomial mathematical equations, 34–35, 40
- Polypropylene fiber (PPF), 254
- Polyvinyl chloride (PVC), 29
- Porosity, 78–79, 183–184
  - measurement, 72
  - values of concrete made with MP as partial replacement of cement, 183*f*
- Portland cement (PC), 1–2, 50, 114, 135, 137–139, 174, 203, 244, 309–310, 358–360, 384–385
  - chemical composition, 312*t*
  - composite concrete, 126–127
- Portland fly ash cement, 31
- Portland Pozzolana cement (PPC), 374–375
- Portland pozzolanic cement CEM II/B-P 42.5N, 255–256



- Portlandite ( $\text{Ca}(\text{OH})_2$ ), 1–2, 299  
 crystals, 93
- Potassium (K), 339–340
- Potassium oxide ( $\text{K}_2\text{O}$ ), 25–26, 339–340
- Potassium sulfate ( $\text{K}_2\text{SO}_4$ ), 112
- Power-type equations, 35
- Pozzolan materials, 49–50, 223
- PPF. *See* Polypropylene fiber (PPF)
- Present worth factor (PWF), 369–370
- Proctor Compaction tests, 361
- Production process, 221
- Pulverized fuel ash (PFA), 25–26, 67–68, 126–127  
 environmental assessment of usage of, 25–27
- PVC. *See* Polyvinyl chloride (PVC)
- Q**
- Quartz, 340
- Quinary cement, 230
- R**
- RAC. *See* Recycled aggregate concrete (RAC)
- RAPA. *See* Recycled asphalt pavement aggregate (RAPA)
- Raw materials, preparation of, 244–245  
 chemical composition of coal bottom ash, 245*t*  
 ground CBA, 245*f*  
 raw CBA, 245*f*
- RC. *See* Recycled concrete (RC)
- RCA. *See* Recycled concrete aggregate (RCA)
- RCC. *See* Roller-compacted concrete (RCC)
- RCCP. *See* Recycled coarse concrete pavement (RCCP)
- RCGC. *See* Roller-compacted green concrete (RCGC)
- RDF. *See* Refuse-derived fuel (RDF)
- Reactive powder concrete (RPC), 379
- Recycled aggregate concrete (RAC), 107, 382
- Recycled asphalt aggregate, 251–252
- Recycled asphalt pavement aggregate (RAPA), 68–69, 252, 254–255
- Recycled concrete (RC), 117
- Recycled concrete aggregate (RCA), 68–69, 117, 251–252, 382
- Recycled coarse concrete aggregates, 254–255
- Recycled coarse concrete pavement (RCCP), 252–253
- Recycled coarse concrete polluted in sea water (RRCC-Sw), 252–253
- Recycling of brick kiln dust and crumb waste rubber tires, 291–292  
 concrete, 292–295  
 rubberized concrete, 296–298  
 waste brick powder, 299–303  
 waste rubber tires, 295–296
- Refuse-derived fuel (RDF), 335–336, 338–339
- Regression equations, 3, 11, 14–16, 18–19, 79, 81–82
- Regression relationship degree ( $R^2$ ), 81
- Relative humidity (RH), 108
- Resistance to chloride attack, 110–112
- Resistance to freeze and thaw cycling, 191
- Resistance to sulfate attack, 112–114
- Retarders, 292
- RH. *See* Relative humidity (RH)
- RHA. *See* Rice husk ash (RHA)
- Rice husk ash (RHA), 67, 252–253, 309–310, 388
- Road pavement, 277–278
- Rocky soil. *See* Mediterranean soil
- Roller-compacted concrete (RCC), 16, 67–68, 251–252  
 durability properties of, 79–82  
 change in weight after  
 freezing–thawing cycle, 79–81  
 freezing and thawing, 79–82  
 mechanical properties of, 82–93  
 compressive stress, 82–85  
 flexural moment stress, 88–91  
 modulus of elasticity, 91–93  
 splitting tensile stress, 85–87  
 microstructure analysis of, 93–96  
 microstructure analysis with scanning electron microscopy, 93–94  
 mineralogical phase analysis with X-ray diffraction, 95–96  
 mix design of, 70–71  
 physical properties of, 76–79  
 density of fresh mixing, 76–77  
 density of hardened specimens, 77–78  
 porosity, 78–79

- preparation of, 71
  - casting and curing, 71
  - mixing, 71
- Roller-compacted green concrete (RCGC), 67
  - durability properties of, 79–82
    - freezing and thawing, 79–82
  - mechanical properties of, 82–93
    - compressive stress, 82–85
    - flexural moment stress, 88–91
    - modulus of elasticity, 91–93
    - splitting tensile stress, 85–87
  - microstructure analysis of, 93–96
    - microstructure analysis with scanning electron microscopy, 93–94
    - mineralogical phase analysis with X-ray diffraction, 95–96
  - mix design of, 70–71
  - physical properties of, 76–79
  - preparation of, 71
    - casting and curing, 71
    - mixing, 71
- RRCC-Sw. *See* Recycled coarse concrete polluted in sea water (RRCC-Sw)
- Rubber, 154, 277–278
  - aggregates, 384
  - powder as admixture, 298
- Rubberized concrete, 296–298
  - rubber powder as admixture, 298
  - treated rubber particles as replacement of fine aggregates, 298
  - untreated rubber particles as replacement of fine aggregates, 296–297, 297*f*
- S**
- SAI. *See* Strength activity index (SAI)
- Sample preparation, 279, 360–364
- SBS. *See* Styrene butadiene styrene (SBS)
- Scanning electron microscopy (SEM), 28–29, 71, 168, 343–344, 379, 380*f*
  - analysis of specimens, 179
  - microstructure analysis with, 93–94
  - morphology of mortar containing MP as replacement of cement, 180*f*
- Scanning electron microscopy with energy-dispersive X-ray analysis (SEM-EDX), 339–340
- SCC. *See* Self-compacting concrete (SCC)
- SCMs. *See* Supplementary cementitious materials (SCMs)
- Self-compacting concrete (SCC), 101–102, 309–310
  - chemical composition of GGBFS, FA, and PC, 312*t*
  - fresh properties of SCC mixtures, 102*t*
  - materials, 311–312
  - mix proportion, 312–313, 313*t*
  - physical properties of aggregates, 312*t*
  - results, 314–319
    - fresh concrete results, 314–319, 315*t*
    - hardened concrete results, 319–326
  - testing methods, 313–314
    - fresh properties of self-compacting concrete mixture, 313–314
    - hardened properties of self-compacting concrete mixture, 314
- SEM. *See* Scanning electron microscopy (SEM)
- SEM-EDX. *See* Scanning electron microscopy with energy-dispersive X-ray analysis (SEM-EDX)
- Setting process, 138–139
- SF. *See* Silica fume (SF)
- SGI. *See* Strength gain index (SGI)
- Short-term aging test, 156, 280
- Shrinkage, 105, 184, 231–232
- Sieve passing method, 136–138
- Sieve segregation test, 313–314, 318–319
- Silica, 293
- Silica fume (SF), 38–39, 47, 111, 221, 252, 379, 380*f*
- Silica oxide (SiO<sub>2</sub>), 25–26
- Silicate (Si), 148
- Silicon (Si), 339–340
- Silicon dioxide (SiO<sub>2</sub>), 84, 95–96, 311, 339–340
- Silicon oxide (SiO<sub>2</sub>), 79, 96
- Silicon–aluminum slag, 311
- Sintering, 347
- Skid resistance, 236
- Slag, 103–104, 143–144, 221, 311
- Slump flow, 313–316
- Slurry carbonation (SC), 387–388
- Sodium (Na), 75, 339–340
- Sodium chloride (NaCl), 339–340
- Sodium oxide (Na<sub>2</sub>O), 25–26, 339–340
- Sodium sulfate (Na<sub>2</sub>SO<sub>4</sub>), 112
  - durability test, 185
  - resistance of concrete, 185

- Softening point, 284  
 for blends at different percentages of clay, 284*f*  
 temperature, 280
- Soil compaction method, 70, 256
- Solid recovered fuel, 338–339
- Solid waste, 251–252
- Solidification, 347
- SP. *See* Superplasticizer (SP)
- Specific gravity, 156, 169, 280, 282, 285–287  
 and latex in modified bitumen binder, 162*f*  
 test, 162
- Specific surface method, 136–138
- Spectroscopic analysis, 339–340
- Spectroscopy test, 159
- Spherical shape particles, 51
- Splitting tensile strength, 48, 55–56, 230–231  
 CBA, 248, 248*f*  
 GNP, 214–215, 214*f*, 215*f*  
 MP, 176–177  
 RCC, 259, 264–266  
 average and error bar of splitting tensile strength for RCC, 266*f*  
 failure of cylinder after splitting load was applied, 260*f*  
 splitting tensile strength test results for RCC mixes, 265*t*  
 mathematical model for estimation of, 216–217  
 of self-compacting concrete mixture, 321–323  
 blended with fly ash, 323*f*  
 blended with GGBFS, 322*f*  
 blended with GGBFS and fly ash, 323*f*  
 test, 246
- Splitting tensile stress, 85–87  
 change in splitting tensile stress of RCC and RCGC, 85*f*  
 regression relationship between 28th-day splitting tensile stress and OSA-to cement ratio, 87*f*  
 regression relationship between 7th-day splitting tensile stress and OSA-to cement ratio, 86*f*  
 regression relationship between 90th-day splitting tensile stress and OSA-to cement ratio, 87*f*
- Splitting tension, strength in, 35–37, 36*f*, 36*t*, 37*f*
- Stabilization, 347
- Static modulus of elasticity, 260–261, 261*f*
- Steel, 252
- Stoichiometric methods, 133
- Stone, 252
- Strength activity index (SAI), 175  
 of mixtures incorporating marble powder, 175
- Strength gain index (SGI), 58  
 at early age, 58–59
- Stress gain process, 84–85
- Stress–strain curves of elasticity, 91
- Styrene butadiene styrene (SBS), 153–154, 277–278
- Sub-bituminous coal fuel ash, 126–127
- Substituted cement, 25–26
- Sulfate (SO<sub>3</sub>), 75, 229  
 attack, 181  
 resistance to, 112–114  
 ions, 232  
 resistance, 185, 235–236  
 salts, 112  
 solutions, 185
- Sulfated melamine formaldehyde, 52
- Sulfated naphthalene formaldehyde, 52
- Sulfur (S), 339–340
- Sulfuric acid (H<sub>2</sub>SO<sub>4</sub>), 114
- Superplasticizer (SP), 52  
 admixture of, 52–54
- Supplementary cementitious materials (SCMs), 1–2, 67, 107, 126–127, 299
- Surface absorption in concrete, 182
- Synthetic graphite nanoparticles, 27–28
- Synthetic nGs, 28–29
- T**
- T50 flow, 313–314, 316–317
- Technology in alkali-activated materials, 143–144
- TEM. *See* Transmission electron microscopy (TEM)
- Temperature susceptibility, 156, 157*t*, 162–163, 163*t*
- Terra Rossa Soil, 124
- Testing process, 144
- TGA. *See* Thermogravimetric analysis (TGA)

- Thawing, 79–82
- Theoretical equations of Bogue calculation, 131
- Theoretical shear equations, 254–255
- Thermal analysis of mixtures incorporating marble powder, 175–176
- Thermal treatment, 347
- Thermogravimetric analysis (TGA), 31, 175–176
- Thermosetting polymer, 386
- Tire rubber, 252
- Titanium, 75
- Titanium oxide (TiO<sub>2</sub>), 84, 339–340
- Trace elements, 57–58
- Transmission electron microscopy (TEM), 28–29
- Treated rubber particles as replacement of fine aggregates, 298
- Tricalcium silicate, 136
- U**
- Ultrasonic pulse velocity (UPV), 295
- quality of concrete, 301*t*
  - setup and sample, 301*f*
  - test, 301–302
- Unburned particles, 343
- Uniaxial compression strength, 148–149
- of HPG-600, 149
  - results of uniaxial compression strength at age 3, 7, 28 and 56 days, 149*t*
- Unit weight
- of CBM, 11
  - of fresh mortar, 11–12
  - measurement, 6
- United States Department of Agriculture, 1–2
- Unmodified bitumen binder, 161
- Untreated rubber particles as replacement of fine aggregates, 296–297, 297*f*
- Upcycling
- of class F pulverized fuel ash, mixing, handling, placing, and forming processes for, 53, 54*t*
  - experimental work, 255–262
  - materials, 255–259
  - process and tests performed, 32–33
  - results, 262–273
    - compressive strength, 262–264
    - density, 272–273
    - flexural strength, 266–268
    - modulus of elasticity, 268–270
    - splitting tensile strength, 264–266
    - water absorption, 270–272
- testing procedure, 259–262
- compressive strength, 259
  - density, 261
  - flexural strength, 260
  - splitting tensile strength, 259
  - static modulus of elasticity, 260–261
  - water absorption, 261–262
- UPV. *See* Ultrasonic pulse velocity (UPV)
- V**
- V-funnel, 313–314, 316
- VA. *See* Volcanic ash (VA)
- Vaporization, 347
- Vermiculite, 278
- Vinyl copolymers, 52
- Viscosity
- analysis, 161, 161*f*
  - of selected blends, 163
- Vitrification, 341–342, 347
- Vitrified municipal solid waste bottom ash (VMSW-BA), 341–342
- VMSW-BA. *See* Vitrified municipal solid waste bottom ash (VMSW-BA)
- Volcanic ash (VA), 110
- Volumetric method, 133
- W**
- Waste brick powder (WBP), 292, 299–303
- use in clayey bricks, 302–303, 302*t*
  - use in concrete, 299–302
    - compressive strength, 300–301
    - fresh and hardened densities, 300
    - ultrasonic pulse velocity test, 301–302, 301*f*
    - workability, 300, 300*f*
- Waste paper sludge (WPS), 387
- Waste to energy (WTE), 338–339
- Wastes, 123, 133, 168
- chemical composition of, 133–135
  - crumb rubber, 292
  - dumps, 337–338
  - fired ground brick, 227
  - materials, 192–193, 244
  - MP, 186
  - products, 335

- Wastes (*Continued*)
- recycling, 167
  - rubber tires, 295–296
    - crumb rubber, 295–296, 296*f*
    - sand new cement chemical analysis of, 130
  - Water absorption, 182–183
    - measurement in volume, 6–7
    - of RCC, 261–262, 270–272
      - average water absorption for RCA and RAPA mixtures, 271*f*
    - WSA, 12
  - Water penetration depth of self-compacting concrete mixture, 325–326
    - permeability of SCC mixture blended with fly ash, 327*f*
    - permeability of SCC mixture blended with GGBFS, 326*f*
    - permeability of SCC mixture blended with GGBFS and fly ash, 327*f*
  - Water-to-cement ratio, 10, 181
    - of mortar, 14–15
  - WBP. *See* Waste brick powder (WBP)
  - WCBPD. *See* White cement bypass dust (WCBPD)
  - Wet analysis. *See* Wet chemistry
  - Wet chemical analysis, 71
  - Wet chemistry, 133
  - Wet densities, 261
  - Wheat straw, 1–2
  - Wheat straw ash (WSA), 1–2, 309–310.
    - See also* Oil shale ash (OSA); Coal bottom ash (CBA)
    - materials and methods, 3–5
      - mixing, handling, placing, and forming, 3–5, 3*t*
      - methods used for measuring physical and mechanical properties of mortar, 5
      - physical tests, 5–8
      - results and mathematical models for strength estimation, 9–19
        - air pore of fresh mortar, 9–10
        - capillary water absorption, 13–14
        - change of mass, 14–15
        - compressive strength, 17–19
        - flexural strength, 16–17
        - unit weight of fresh mortar, 11–12
        - water absorption, 12
  - White cement bypass dust (WCBPD), 68–69, 254
  - Workability, 300, 300*f*
  - WSA. *See* Wheat straw ash (WSA)
  - WSA-SC. *See* WSA-substituted cement (WSA-SC)
  - WSA-substituted cement (WSA-SC), 4
  - WTE. *See* Waste to energy (WTE)
- X**
- X-ray diffractometer, 358–360
  - X-ray powder diffraction (XRD), 73, 75, 340
    - analysis of new cement manufactured, 130–131, 130*f*
    - analysis of new cement, 136
  - X-ray fluorescence (XRF), 128
  - X-ray diffraction, 170
    - mineralogical phase analysis with, 95–96
  - XRD. *See* X-ray powder diffraction (XRD)
  - XRF. *See* X-ray fluorescence (XRF)
- Z**
- Zinc (Zn), 339–340
  - Zinc oxide (ZnO), 1–2

## WOODHEAD PUBLISHING SERIES IN CIVIL AND STRUCTURAL ENGINEERING

*This book provides state-of-the-art research on upcycling of by-products for use in hydraulic binder and binder-based construction materials.*

Hydraulic binders are essential components that are widely used in construction materials. Cement manufacture consumes large amounts of nonrenewable raw materials and energy, so many efforts are now being undertaken to develop "greener" binders. *Advance Upcycling of By-products in Binder and Binder-based Materials* focuses on recent research trends in this important research field.

The chapters look at the properties of these materials, both physical and mechanical, and the durability as well as the inner structure both at the micro and nanoscale. The reuse of by-products within binder systems is also discussed as well as new innovative approaches and advanced solutions for making cost-, ecology-, and environment-friendly hydraulic binder and binder-based materials from the upcycling of by-products.

Because of the popularity of additive manufacturing, various by-product materials, in terms of constructional applications are also identified. These include latent hydraulic supplements, activators of transport properties, and increase in inner strength and durability. The book also looks at additive manufacturing and explains the effects of by-products on the properties of binder and binder-based materials. It monitors inter-reactions between by-products and binders, reveals hydration products in the inner structure of binder-based materials containing by-products, and presents new and current results to help readers better understand the properties and potential of these new innovative materials. The book will be an essential reference resource for academic and industrial researchers, materials scientists, and civil engineers and all those who are working in the development of "greener" construction materials and utilization of waste and other fine by-products in the production of environment-friendly concrete.

### Key Features

- Provides a detailed review of recent research on upcycling of by-products for use in binder and binder-based materials
- Presents innovative approaches and advanced solutions for making environment-friendly hydraulic binders and binder-based materials from the upcycling of by-products
- Includes mathematical models for strength estimation

### About the Editor

**Mehmet Serkan Kirgiz** is currently working as a professor at Istanbul University-Cerrahpaşa, Turkey. He was also previously a professor at Gazi University in Turkey and served as a vice dean and an active member of the Faculty Management Board and the Department Management Board in both aforementioned institutions. He has published several peer-reviewed articles in highly reputable journals indexed in SCI, SCI-E, and Scopus. He also has a national patent on cement manufacturing through the burning of marble powder and brick powder as farina. He has worked as an active chair, reviewer, and board member for several educational and technical committees for both degree and graduate education, conferences, journals, and workshops. His major research interests are in the broad field of ecology-based construction materials, raw minerals and by-products, and upcycling of by-products for sustainable development.



**WP**  
WOODHEAD  
PUBLISHING

An imprint of Elsevier  
[elsevier.com/books-and-journals](http://elsevier.com/books-and-journals)

ISBN 978-0-323-90791-0



9 780323 907910